



Technical Report

revised edition (July 2009)

Authors:

Ivo OFFENTHALER ¹
Rodolfo BASSAN ²
Claudio BELIS ³
Ingrid GARO-STACH ¹
Stefania GANZ ²
Saverio IOZZA ⁴
Gert JAKOBI ⁵
August KAISER ⁶
Manfred KIRCHNER ⁵
Wilhelm KNOTH ⁷
Norbert KRÄUCHI ⁸
Walkiria LEVY ⁵
Wolfgang MOCHE ¹
Johanna NURMI-LEGAT ¹
Stefano RACCANELLI
Karl-Werner SCHRAMM ⁵
Peter SCHRÖDER ⁵
Isabella SEDIVY ⁸
Primož SIMONČIČ ⁹
Michael STAUDINGER ⁶
Gerhard THANNER ¹
Maria UHL ¹
Urša VILHAR ⁹
Peter WEISS ¹

Lead Partner ¹⁰:

Thomas JAKL

Compilation, graphs, layout:

Ivo OFFENTHALER

Statistics:

Ivo OFFENTHALER, Peter WEISS

Project management ¹:

Peter WEISS, Maria UHL

1. Umweltbundesamt GmbH, Spittelauer Lände 5, 1090 Wien (Austria), 2. Regional Agency for Environmental Prevention and Protection of Veneto. Via F. Tomea 5, I-32100 Belluno (Italy), 3. Regional Agency for Environmental Protection of Lombardia. Via Stelvio 35, I-23100 Sondrio (Italy), 4. EMPA Materials Science and Technology. Überlandstrasse 129, CH-8600 Dübendorf (Switzerland), 5. Helmholtz-Zentrum München. Ingolstädter Landstraße 1, 85764 Neuherberg (Germany), 6. Central Institute for Meteorology and Geodynamics. Hohe Warte 38, 1190 Wien (Austria), 7. Umweltbundesamt (Federal Environment Agency). Wörlitzer Platz 1, 06844 Dessau-Roßlau (Germany), 8. Swiss Federal Institute for Forest, Snow and Landscape Research. Zürcherstrasse 111, CH-8903 Birmensdorf (Switzerland), 9. Slovenian Forestry Institute. Večna pot 2, 1000 Ljubljana (Slovenia), 10. Federal Ministry of Agriculture, Forestry, Environment and Water Management. Stubenring 1, 1012 Wien (Austria)

Editors:

Umweltbundesamt GmbH, Spittelauer Lände 5, 1090 Wien (Austria) • Austrian Ministry for Agriculture, Forestry, Environment and Water Resources. Stubenring 1, 1012 Wien (Austria) • Bavarian State Ministry for Environment, Public Health and Consumer Protection. Rosenkavalierplatz 2, 81925 München (Germany) • Federal Office for the Environment. 3003 Bern (Switzerland) • EMPA Materials Science and Technology. Überlandstrasse 129, CH-8600 Dübendorf (Switzerland) • Helmholtz-Zentrum München. Ingolstädter Landstraße 1, 85764 Neuherberg (Germany) • Organic Analytical Chemistry. St. Johannis-Ring 19, CH-4056 Basel (Switzerland) • Regional Agency for Environmental Protection of Lombardia. Via Stelvio 35, I-23100 Sondrio (Italy) • Regional Agency for Environmental Prevention and Protection of Veneto. Via F. Tomea 5, I-32100 Belluno (Italy) • Slovenian Forestry Institute. Večna pot 2, 1000 Ljubljana (Slovenia) • Swiss Federal Institute for Forest, Snow and Landscape Research. Zürcherstrasse 111, CH-8903 Birmensdorf (Switzerland) • Umweltbundesamt (Federal Environment Agency). Wörlitzer Platz 1, 06844 Dessau-Roßlau (Germany)

Publisher:

Federal Ministry of Agriculture, Forestry, Environment and Water Management
Stubenring 1, 1012 Wien, Austria. Europe

ISBN 3-902338-93-8

All rights reserved

Preface

The load of persistent organic pollutants (POPs) in the environment represents one of the major challenges in environmental protection. Their long-range transport to remote areas, their accumulation, toxicological properties and impact have attracted international attention. The global dimension is well expressed by the multilateral UN “Stockholm Convention on POPs” and the “POPs-Protocol” under the UN-ECE “Convention on long-range transboundary air pollution”. The European dimension is covered by the Regulation (EC) 850/2004 on POPs. Austria has recently submitted its National Implementation Plan (NIP) and National Action Plan (NAP) both to the Secretariat of the Stockholm Convention and the European Commission. Currently, 162 countries are parties to the Stockholm Convention, among them the EU and most Alpine countries.

The Stockholm Convention entered into force in 2004 during the term of project MONARPOP within the European INTERREG-Programme. In other words, this important project to assess the load of the Alps with POPs was ahead of time. Its results were ready then to contribute – as one of very few international projects – to the process of the effectiveness evaluation according to Article 16 of the “Stockholm Convention”. The MONARPOP data represent the baseline for the Alpine region in the first Global Monitoring Report.

Beside its relevant contribution to that international environmental regulation and control instrument, MONARPOP made it for the first time possible to broadly assess the load of POPs in the Alps in a trans-boundary manner. Therefore, the results of this project will be used as an important basis for international, national and regional measures of environmental protection of the unique Alpine area from POPs pollution.

I am proud that my ministry was lead partner of that important European and international project. I am very happy that several partners from our neighbouring countries Germany, Italy, Slovenia and Switzerland participated in MONARPOP so that the project could cover a large part of the Alps and attained a broad international dimension. The success of the project was only possible with the generous support of the funding organisations and regions as listed in the acknowledgements and due to the excellent work of the project management, the project partners and the subcontractors as listed in the previous pages. I would like to thank all of them for their great support and contribution. I hope that the results of the project compiled in this report will become a milestone for environmental protection, control and science.



Niki Berlakovich

Austrian Federal Minister of Agriculture, Forestry, Environment and Water Management
Vienna, December 2008



Acknowledgements

The project MONARPOP was funded by the European Union within the [Interreg III B programme “Alpine Space”](#). It received generous financial and administrative support, graded up by strong personal commitment on the part of Thomas Jakl, Aline Berthold, Barbara Perthen-Palmisano, Helga Schrott, Susanna Eberhartinger-Tafill of the [Austrian Federal Ministry for Agriculture, Forestry, Environment and Water Management](#) as Lead Partner, Dieter Heublein of the [Bavarian State Ministry for Environment, Public Health and Consumer Protection](#) and Georg Karlaganis, David Schmid and Fabio Wegmann of the [Swiss Federal Office for the Environment](#). Substantial financial support was also granted by the Austrian provinces of [Kärnten](#), [Niederösterreich](#), [Oberösterreich](#), [Steiermark](#), [Vienna](#) and [Vorarlberg](#).

The project became successful through the joint contribution of funds, expertise and labour of the involved institutions (in alphabetical order): [Central Institute of Meteorology and Geodynamics](#) (Austria), [Consorzio I.N.C.A](#) (Italy), [Federal Environment Agency](#) (Germany), [Helmholtz-Zentrum München](#), [Regional Agency for Environmental Protection of Lombardia](#), [Organic Analytical Chemistry](#) (Basel University), [Regional Agency for Environmental Prevention and Protection of the Veneto](#), [Slovenian Forest Institute](#) (Slovenia), [Swiss Federal Institute for Forest, Snow and Landscape Research](#), [Umweltbundesamt](#) (Austria).

Air and deposition measurements on the mountains Weissfluhjoch, Zugspitze and Sonnblick relied on the excellent support provided by the staff of the respective observatories.

Site selection and extensive sampling in sensitive mountainous forest ecosystems would not have been possible without the consent and practical support of the land owners, private and institutional, who without exception aided the field staff in the most cooperative manner. Valuable help for the selection of Austrian sites came from the [Research and Training Centre for Forests, Natural Hazards and Landscape](#) (Austria). Valuable editorial support was given by Alexandra Freudenschuss.

Summary

The Alps represent a significant sink and a barrier for long-range transported persistent organic pollutants (POPs). This is the most prominent finding of the project MONARPOP¹.

POPs are bioaccumulating, hardly degradable chemicals of problematic toxicological properties. MONARPOP gave a first time survey of alpine POP pollution with comprehensive geographical coverage. Horizontal and vertical variation was examined with a network of 40 sites in Austria, Germany, Italy, Slovenia and Switzerland, including seven altitude profiles of up to six plots, stretching from valleys to the top of alpine summits. Remote forests were chosen as an ecosystem widespread enough for such large scale screening, offering Norway spruce needles, humus and mineral soil as proven pollution indicators. In addition to the screening of environmental matrices, semi-permeable membrane devices (SPMD) were used as passive samplers at some altitude profiles. Active air samplers and bulk deposition collectors were installed at three Alpine summits (Sonnblick in AT, Weissfluhjoch in CH and Zugspitze in D) to study atmospheric POP loads. Both active air and deposition samplers are innovations of the project to allow continuous sampling of POPs under the extreme climatic conditions of high mountains. The construction of the active air samplers permits, as a novelty, a separate sampling of air from different source regions. Meanwhile, both sampler types perform in routine operation.

The following compounds were analysed in all or some of the sampled media: polychlorinated dibenzodioxins and -furans (PCDD/F), polychlorinated biphenyls (PCBs), DDT and metabolites (DDX), hexachlorobenzene (HCB), hexachlorocyclohexans (HCH), aldrin, dieldrin, endrin, heptachlor, mirex, pentachlorophenol, polybrominated diphenylether (PBDE), polycyclic aromatic hydrocarbons (PAHs), chlorinated paraffins (CP), perfluorooctane sulfonate and related compounds (PFOS), nonylphenol, nitrophenols and several short chain chlorinated compounds. This selection includes, beside others, all² POPs listed in the UN “Stockholm Convention” on POPs and the UN-ECE “POPs Protocol”, two important instruments to reduce POPs in the environment. The dioxin-like activity of samples was tested with the EROD bioassay, and enzymatic reactions of needle extracts were measured to study biological effects.

The procedural aspects of sample harvest, distribution, preparation and analysis were optimised for comparability of results among the participating countries. This report compiles and describes a total of 28 000 single data. An in-depth discussion of the findings can be found in numerous existing and scheduled contributions to journals and congresses.

Nearly all of the analysed POPs were detected in the environmental samples. This is particularly remarkable for compounds like Mirex that have never been used in Central Europe or, like DDT, were banned in Europe decades ago. More astonishing still was the detection of these substances in matrices that indicate current pollution (air, deposition or conifer needles). Such findings evince an ongoing long-range transport of POPs to the Alps. So do mass balances based on project data (not included in this report; Belis et al., in press) which

¹ Monitoring network in the Alpine region for persistent and other organic pollutants)

² except toxaphene which was not found in humus samples

show an unexplainable discrepancy between the masses of several POPs bound in the forests of the Alps on one hand, and the emissions in this region on the other hand. In other words, the Alps import and accumulate POPs emissions from outside their area. Considering the sensitive ecosystems of the Alps and the important resources they supply, like drinking water, high quality agricultural products or recreational environment, this fact deserves the attention of the decision makers. The mass balances may also serve the validation and tuning of EMEP models for European POP emissions and inputs.

POP concentrations in the Alps have been found to lie within a range that is typical for remote regions. Nevertheless, the detected loads are frequently higher than those in very remote parts of the world like the Arctic. In some cases, they approach the concentration ranges of regions that are closer to sources. This is remarkable since site selection focused on remoteness from polluters. A precondition, however, that was partly violated at single sites: in some cases there was evidence of local influence, particularly for compounds of unintentional release by combustion processes and traffic like PCDD/F and PAHs. Some outliers, i. e. exceptionally high concentrations could be also explained by local sources. Obviously, local use and emission can dramatically change the load to the surroundings and the exposure to such compounds even at otherwise remote environments. So, beside international action, local measures are another key contribution to reduce the POP pollution in the Alps.

A comparison of the concentration ranges of individual POPs lead to some remarkable findings. For instance, even despite their long time ban, DDT and metabolites belong to those POPs with higher soil concentrations. Nonylphenol and chlorinated paraffins show humus concentrations even close to the mg kg^{-1} range which is comparable to PAH concentrations. This is a notable result for compounds which are assumed to be emitted during production and use mainly (and not, like PAHs, unintentionally), even the more in remote regions.

Nevertheless, the current concentrations of some compounds are clearly lower than those detected some years earlier. Some MONARPOP sites were already part of an Austrian study ten years ago. A comparison suggests, particularly for dioxin loads, a significant decrease during the last ten years. Emission reduction measures seem to have been successful.

The most significant finding of the project were the regional concentration differences across the Alpine region. Generally, higher POP concentrations were found in the peripheral zones of the Alps while the central or middle³ part of the Alps was less polluted. Frequently, the northern part of the Alps showed higher concentrations, particularly in the humus layer, which indicates a long-time accumulation driven, *inter alia*, by the pollutant input (e.g., of PCDD/F, PCBs, PBDEs, PAHs, γ -HCH, Aldrin, Dieldrin, Mirex). Some compounds showed higher concentrations in the South of the Alps (DDX, α -HCH in needles) or at least had another southern peak in addition to their high levels in the North (PCDD/F, some PCBs in needles, lower brominated PBDEs in humus). Also longitudinal differences were observed: for instance, some PCBs (in needles or humus) and the more volatile PAHs (in needles) showed higher concentrations in the West, while higher levels of the heavier PAHs (needles) and higher brominated PBDEs (humus) occurred in the East of the Alps. PCDD/F concentrations in the

³ “central” and “middle” referring to latitude and longitude, resp.

needles were higher in the West and East than in the middle region of the Alps. As can be expected already from these findings, the concentration differences across the Alpine region were also associated with distinct variations in the pollutant patterns (e.g. the composition of the PCDD/F, PBDEs, PAHs and certain groups of pesticides like the DDX and HCH). Obviously, differences between Alpine regions were not only quantitative but also qualitative. Moreover, corresponding spatial gradients lead to positive correlations of different compounds, especially so in humus samples. In other words, increased levels of a certain POP indicated a multiple contamination. So far, the impact of a mixture of various POPs is hardly understood.

The gathered evidence clearly demonstrates the specific role of the Alps as a barrier for long-range transboundary air pollution. The barrier intercepts further pollutant transport across Europe and provides relatively clean central Alps. On the other hand, the barrier effect causes higher pollutant loads in the border regions of the Alps (limestone Alps). These border regions receive significantly more precipitation than the central parts and are closer to areas with higher anthropogenic emissions. Both factors likely have contributed to the observed regional differences in POP pollution.

The concentrations of the heavier PCDD/F homologues, several PCBs, PAHs, PBDEs, Dieldrin and Mirex in the humus layer were significantly and positively correlated with average precipitation. Higher concentrations of tetra- and pentachlorinated dioxins in the humus layer were associated with lower average temperature. Needle contamination, too, was significantly correlated with climate: several PAHs negatively with precipitation, several PCBs, PCDD/F homologues and β -HCH positively with precipitation, lighter PCDD/F homologues positively with temperature. Climate thus partly explains the local concentration of these compounds. Since the correlations were not very high, other than climatic factors must be considered, though. As a Central European mountain range, the Alps are surrounded by regions and countries with different histories of POPs emission and use. The varying pollutant concentrations and patterns across the Alps seem to reflect that fact. An excellent example that supports this assumption is the humus concentration of PBDE 183: contrary to other PBDE congeners it was not correlated with precipitation but showed clearly higher concentrations in the East of the Alps. A likely cause are substantially higher emissions in the East of the Alps or its neighbouring countries.

Although barrier effects have been detected, POPs are transported across the Alps nonetheless, as could be shown with active air sampling at three Alpine summits. For the first time in the Alps, POPs were measured in the ambient air of high mountain tops. Atmospheric concentrations and deposition at these remote high altitude sites partly even reached values that have been reported from sites closer to sources. For some compounds seasonality has been observed, with higher concentrations in the cold season (PCDD/F, heavier PAHs) or in the summer (some pesticides). These observations are in agreement with literature, among the more obvious causes are increased domestic heating in winter (additional PAH and PCDD/F emissions) and heavier pesticide use and/or higher revolatilisation during the vegetation period. However, longer time series would be necessary to confirm the observed trends. Observed concentration differences between the three summits coincide, in cases, with the regional variation indicated by humus layer and needle samples. For instance, Mt. Zugspitze in the northern Alps showed higher average PCDD/F concentrations in air than the two central alpine summits Mt. Sonnblick and Mt. Weissfluhjoch, while PCBs tended towards higher atmospheric levels at western Mt. Weissfluhjoch and decreased towards eastern Mt. Sonnblick. Again, the short observation period and deviating results for deposition (e.g., higher PCDD/F deposition at Mt. Sonnblick compared to the two other

sites) would require a continuation of monitoring to substantiate the found correspondence. For the 1.5 years observed so far, source specific sampling did not reveal, for any of the Alpine summits or compounds, a source region for elevated concentrations that would prevail over the course of sampling periods. For single sampling periods and compounds, however, a particular source region could dominate at all three sites.

Seven height profiles were investigated to see whether the altitudinally increasing predisposition (by temperature, precipitation and wind speed) for POPs input and accumulation would indeed be reflected by higher POP concentrations at greater elevations. This was not generally the case. The concentration peaks along the altitudinal gradients varied from one altitude profile to the next, from compound to compound and between soil and needle samples. Obviously, various influences favouring or constraining POPs accumulation are like pieces of a jigsaw which combine to the detected altitudinal gradients. However, some more or less general trends were observed. At all altitude profiles of the central and northern Alps, pesticides showed higher concentrations in the humus layer at the higher located sites. Of the studied compounds, pesticides belong to the more volatile ones. For these and the humus layer reflecting the long-time accumulation, meteorological conditions seem to have a predominating impact on the altitudinal gradient. Nevertheless, the Italian and Slovenian altitude profiles located in the southern part of the Alps showed no or even the opposite trend. At five of seven height profiles dioxin-like activity of humus extracts tended to increase with height. Single altitude profiles showed very consistent trends for almost all compounds or media: concentration increases with altitude were generally observed at the easternmost altitude profile “Wechsel” and occurred frequently at the “Rauris” altitude profile in the Central Alps. At least at these two height profiles, and for humus pesticide concentrations also at most other profiles, vertical concentration gradients indicate a higher exposure to POPs at the more remote and sensitive higher mountain regions. However, some compounds and some altitude profiles closer to sources behaved in the opposite manner: PCDD/F and PAHs frequently reached higher concentrations close to the valley ground, a likely impact of local sources (domestic heating and traffic). The whole range of factors is well demonstrated by the Klosters altitude profile which ascended – due to a lack of alternatives – above a village. Humus levels of banned pesticides were higher at the upper plots, while currently and locally emitted PCDD/F and PAHs peaked close to the valley. Different from the former, higher concentrations of PBDEs were often detected at an intermediate altitude suggesting an influence of the inversion layer.

EROD bioassays indicated dioxin-like activity in extracts of forest humus and soil – as expected even for the relatively low contamination of remote sites. A strong correlation between the toxic equivalent concentrations of PCDD/F and PCBs on one hand and the dioxin-like activity on the other hand was observed. However, the response of the bioassay was stronger than explainable by the total content of PCDD/F and dioxin-like PCBs only. This indicates the presence of further dioxin-like agents in the samples.

Beside the survey of POPs loads in the Alps, MONARPOP also aimed at a broad dissemination of this survey, at informing policy makers and contributing to key implementation steps against POP pollution. All three aims have been reached. So far, approximately 50 publicity measures were taken, including presentations, posters and papers at scientific conferences and policy meetings, or contributions to important political processes like the Stockholm Convention. Dissemination of results further encompassed three regional conferences for the public, local experts and decision makers, a scientific symposium gathering all international experts for POPs in mountains, from the Himalayas to the Rocky Mountains. Folders and press releases were issued. MONARPOP

provided, among very few other international monitoring programmes⁴, the first “Global Monitoring Report” for the “Effectiveness Evaluation” of the UN Stockholm Convention with European results. In this way, MONARPOP contributed significantly to the international key monitoring process to combat POP pollution.

Outlook

MONARPOP provides an excellent set of data containing a wealth of information that still awaits further elaboration, for example to link measurements with large scale models of POP distribution. Many more questions were raised by the evidence collected. Particularities of regional and altitudinal patterns need clarification to allow an improvement of the situation, even more because the Alps very likely reflect the conditions for a still larger part Europe. Identified incidences of local release need to be examined for their frequency and relevance on a larger scale.

Gaps in the regional coverage should be closed by further monitoring activities (the French and, partly, Italian Alps were not captured by the present study).

Although the project gives a good quantitative and qualitative overview, other key issues of POP contamination, e. g. accumulation along Alpine food chains could not be addressed at all.

Last but maybe most important, the contribution of MONARPOP to the “Effectiveness Evaluation” of the “Stockholm Convention” depends on the continuation of air and deposition monitoring at the selected Alpine summits to survey time trends. Prolongation is also needed to back up preliminary conclusions on geographic origin and seasonality of atmospheric POP levels in the Alps.

⁴ e.g., AMAP (Arctic Monitoring and Assessment Program) and EMEP (European Monitoring and Evaluation Programme under the UN-ECE “Convention on Long-range Transboundary Air Pollution”)

Introduction

The contamination of ecosystems with POPs (Persistent Organic Pollutants) is a global environmental concern.

POPs are mainly anthropogenic chemicals which are toxic, resist degradation and accumulate along food chains. International protocols were adopted to control and reduce POP emissions (UN-ECE Protocol and UNEP Stockholm Convention on POPs).

To examine the extent of pollution, monitoring has to be done at regional scale at least. The Alpine region, with its rich natural heritage, offering recreation, protecting alpine wildlife and human welfare, seems particularly susceptible to POP contamination for geographical and climatic reasons. Earlier studies suggested that the Alps might be an important sink for POPs, although major emissions occur outside the Alps. Nevertheless there was insufficient data to assess the gravity of this problem.

Within the framework of the European Union Community Initiative “Alpine Space” project MONARPOP was launched. Several institutions⁵ from five countries (Austria, Germany, Italy, Slovenia, and Switzerland) established a network to assess the POP load of the Alps. Main goals of the project were to identify (i) long-range transport of POPs to remote alpine regions, (ii) prevalent European source regions, (iii) POP loads in the Alpine range, including regional differences, (iv) altitudinal variations, (v) stocks present in forests of the Alpine region, and (vi) possible biological effects of the detected loads.

⁵ see acknowledgements

Table of Contents

1	Methods	1
1.1	Site selection	1
1.1.1	General considerations	1
1.1.2	Country-specific considerations	2
1.1.3	Site maps	3
1.2	High altitude sites	5
1.3	Meteorology	7
1.4	Trajectory forecasts and evaluation	8
1.5	Sampling	8
1.5.1	Needles, mineral soil, humus	8
1.5.2	Active air sampling	9
1.5.3	Deposition	10
1.5.4	SPMD type passive air sampling	11
1.6	Sample preparation	12
1.6.1	Needles	12
1.6.2	Humus, mineral soil	13
1.6.3	Air	13
1.6.4	SPMD	13
1.7	Chemical analysis	14
1.7.1	Polychlorinated dibenzodioxins and -furans (PCDD/F) and polychlorinated biphenyls (PCB)	14
1.7.2	Chlorophenols	15
1.7.3	Nitrophenols	16
1.7.4	Short chain chlorinated hydrocarbons (CHCs) and trichloroacetic acid (TCA)	17
1.7.5	Chloropesticides	18
1.7.6	Polycyclic aromatic hydrocarbons (PAH)	19
1.7.7	Polybrominated diphenyl ethers (PBDE)	20
1.7.8	Chlorinated paraffins	21
1.7.9	Enzyme assays	24
1.7.10	Micro-EROD bioassay	25
1.8	Data processing and statistical analysis	27
1.8.1	Longitudinal and latitudinal grouping	27
1.8.2	Treatment of low values	28
1.8.3	Correlations between different compound groups	28
1.8.4	Averaging atmospheric pollutant concentrations	28
2	Abbreviations	29
3	Results	30
3.1	How to interpret the graphs	30
3.1.1	Boxplots	30
3.1.2	Spatial variation	30
3.1.3	Longitudinal and latitudinal differences	31
3.1.4	Wind roses	31

3.1.5	Combined atmospheric / deposition data.....	32
3.2	Organochloropesticides (OCP).....	32
3.2.1	Characterization.....	32
3.2.2	Overview of results.....	35
3.2.3	Summary statistics.....	36
3.2.4	Spatial variation.....	46
3.2.5	Altitudinal variation.....	77
3.3	Chlorophenols	104
3.3.1	Characterization.....	104
3.3.2	Overview of results.....	106
3.3.3	Summary statistics.....	107
3.3.4	Spatial variation.....	107
3.3.5	Longitudinal, latitudinal and altitudinal variation	108
3.4	Polycyclic aromatic hydrocarbons (PAH)	108
3.4.1	Characterization.....	108
3.4.2	Overview of results.....	109
3.4.3	Summary statistics.....	110
3.4.4	Spatial variation.....	119
3.4.5	Altitudinal variation.....	132
3.5	Polybrominated diphenylethers (PBDE)	135
3.5.1	Overview of results.....	135
3.5.2	Characterization.....	136
3.5.3	Summary statistics.....	137
3.5.4	Spatial variation.....	144
3.5.5	Altitudinal variation.....	158
3.6	Polychlorinated dibenzodioxins and -furans (PCDD/F).....	160
3.6.1	Characterization.....	160
3.6.2	Overview of results.....	162
3.6.3	Summary statistics.....	162
3.6.4	Spatial variation.....	168
3.6.5	Altitudinal variation.....	179
3.7	Polychlorinated biphenyls (PCB)	184
3.7.1	Characterization.....	184
3.7.2	Overview of results.....	185
3.7.3	Summary statistics.....	186
3.7.4	Spatial variation.....	196
3.7.5	Altitudinal variation.....	205
3.8	Nitrophenols	212
3.8.1	Characterization.....	212
3.8.2	Summary statistics.....	213
3.8.3	Spatial variation.....	214
3.8.4	Altitudinal variation.....	214
3.9	Short chain chlorinated hydrocarbons (CHCs) and trichloroacetic acid (TCA)	215
3.9.1	Characterization.....	215

3.9.2	Summary statistics.....	216
3.9.3	Spatial variation.....	217
3.9.4	Longitudinal variation	218
3.9.5	Latitudinal variation	218
3.9.6	Altitudinal variation.....	218
3.10	Chlorinated paraffins (CP).....	219
3.10.2	Summary statistics.....	220
3.10.3	Altitudinal variation.....	220
3.11	Perfluorinated tensides (PFT).....	221
3.11.1	Physicochemical properties	222
3.11.2	Emissions and use.....	222
3.11.3	Environmental behaviour and bioaccumulation	222
3.11.4	Toxicology.....	222
3.11.5	Summary statistics.....	223
3.11.6	Longitudinal variation	223
3.11.7	Altitudinal variation.....	223
3.12	Nonylphenol	227
3.12.1	Characterisation	227
3.12.2	Altitudinal variation.....	228
3.13	Physiological parameters.....	228
3.13.1	Micro-EROD Bioassay	228
3.13.2	Enzyme activity	230
3.14	Correlations between different pollutants / effect parameters	232
3.14.1	Needles	233
3.14.2	Humus	235
3.14.3	Air.....	240
3.15	Correlations between concentrations of the same substance in different media.....	245
3.15.1	Humus and needle concentrations	245
3.15.2	Needle and SPMD concentrations	246
3.16	General descriptives	248
3.16.1	Humus	248
3.16.2	Needles	250
3.17	Meteorology	251
3.18	Correlations between pollutant concentrations and climatic parameters.....	252
3.18.1	Needles	252
3.18.2	Humus	253
4	Appendix	254
4.1	Accuracy of trajectory prognoses	254
5	Literature	257

1 Methods

1.1 Site selection

1.1.1 General considerations

1.1.1.1 Screening criteria

As a first step, each participating country screened for favourable sampling areas according to the following requirements:

- Sites had to be remote, i. e. far away from settlements, factories, public roads and other potential sources (Table 1-1). Because in mountainous terrain the transport of polluted air masses is likely to be channelled along valleys, the required minimum distances were further assessed with regard to the local conditions: potential pollution sources in the same valley would require to select the site further off, while a source in a neighbouring valley might effectively be shielded by the intersecting ridge even at a shorter distance. Site selection therefore accounted for all available geographical, meteorological and environmental information to avoid influences of local/regional sources of the investigated pollutants.
- Sites were distributed to obtain a balanced geographical representation of the study area.
- All sites, except the additional plots of altitude profiles, had to lie within the standard altitude band (1300-1600 m above sea level).
- Seven altitude profiles consisted of 4-5 plots (including that at standard height) lined up along a slope to investigate vertical pollution gradients. Three of these profiles (Mt. Sonnblick / AT, Mt. Weissfluhjoch / CH, Mt. Zugspitze / DE) included an air sampling plot well above the tree line.
- Sites had to be accessible by car (to ensure rapid collection of samples) via restricted or weakly frequented roads to avoid traffic influence.
- Where possible, sites were chosen close to existing monitoring locations to take advantage of scientific and infrastructural synergisms).

Table 1-1: Minimum distances from potential sources for level ground (adapted from EMEP-Guidance for the European Air Quality Directive)

source type	distance (km)	comments
Large pollution sources (cities, power plants, waste incineration plants, industrial plants, major motor ways)	> 50	Depending on prevailing wind directions (see general comments above).
Small scale domestic heating with coal, fuel oil or wood	> 0.5	A maximum of only one emission source at minimum distance
Minor roads (up to 50 vehicles per day)	> 0.5	
Larger roads (up to 500 vehicles per day), villages	> 5	
Application of relevant agri- or silvicultural chemicals (arable land, vineyards, orchards, tree nurseries, Christmas tree cultures, timber yards, application of sewage sludge)	> 5	Application in the forests can be avoided by the forest age (by selecting sites with a tree age >60 years) and/or studying of the past and present national/regional/local forest management practices and respective national/regional regulations

1.1.1.2 Local selection

The actual plots were chosen by inspecting the preselected areas on site for the following preconditions:

- Sites had to provide at least 0.5 hectare (ha; e.g. 100 × 50 m) of homogenous Norway spruce stand, accepting a maximum admixture of 20 % other species. Trees had to be at least 60 years (at least 30 years if former or recent pesticide use could be excluded). The actual sampling area (approx. 5 × 25 m for soil and two dominant Norway spruce) had to lie in the centre of the selected 0.5 ha and 100 m off from the nearest forest edge.
- Avoided were sites with evidence of: thinning during the last 5 years, soil tillage, regular forest litter use in the past 50 years, nearby forest fires or wind throws during the last decades.
- Sites for parallel SPMD measurements had to be outside the lee and at least three tree heights off the edge of the sampled stand.

1.1.2 Country-specific considerations

1.1.2.1 Austria

Apart from the general selection criteria described above (1.1.1), Austrian sites were located to coincide with existing surveys where possible. These surveys were:

- the Austrian “Waldschadensbeobachtungssystem” (forest damage monitoring system), which is linked to the EU ICP-Forests survey and maintained by the Federal Research and Training Centre for Forests, Natural Hazards and Landscape (www.bfw.ac.at)
- earlier studies on the organic pollution of remote Austrian forest sites (WEISS et al. 2000)

1.1.2.2 Germany

The four Bavarian sites lie on the Northern Alpine fringe, representing the situation of the “Allgäuer Alpen” (Sonthofen), “Werdenfelser Alpen” (height profile Eschenlohe), “Inn” valley (Kiefersfelden) and “Berchtesgadener Alpen” (height profile Berchtesgaden). The Sonthofen and Berchtesgaden sites were located near so called 'forest climate stations', which are part of a climate monitoring net of the Bavarian Forest Institute (LWF) installed in 1995.

1.1.2.3 Italy

Val Visdende (location of the Italian height profile) was assumed to be among the least contaminated Dolomite valleys: the only potential emitter is a mountain cabin at the valley bottom. Together with Prampera (in the center of Belluno province) and Monte Grappa (Padana valley), the three sites were thought to represent the main geographic landscape types of Veneto.

1.1.3 Site maps

The origins of the needle samples, and the subsets of sites, where humus and mineral soil were sampled are shown in Figure 1-1-Figure 1-3. Additional material is available from

http://www.monarpop.at/methods/geographical_scope.php. Overlays for use with Google Earth® can be

downloaded from http://www.monarpop.at/downloads/MONARPOP_sampling_sites.kml and

http://www.monarpop.at/downloads/MONARPOP_height_profiles.kml

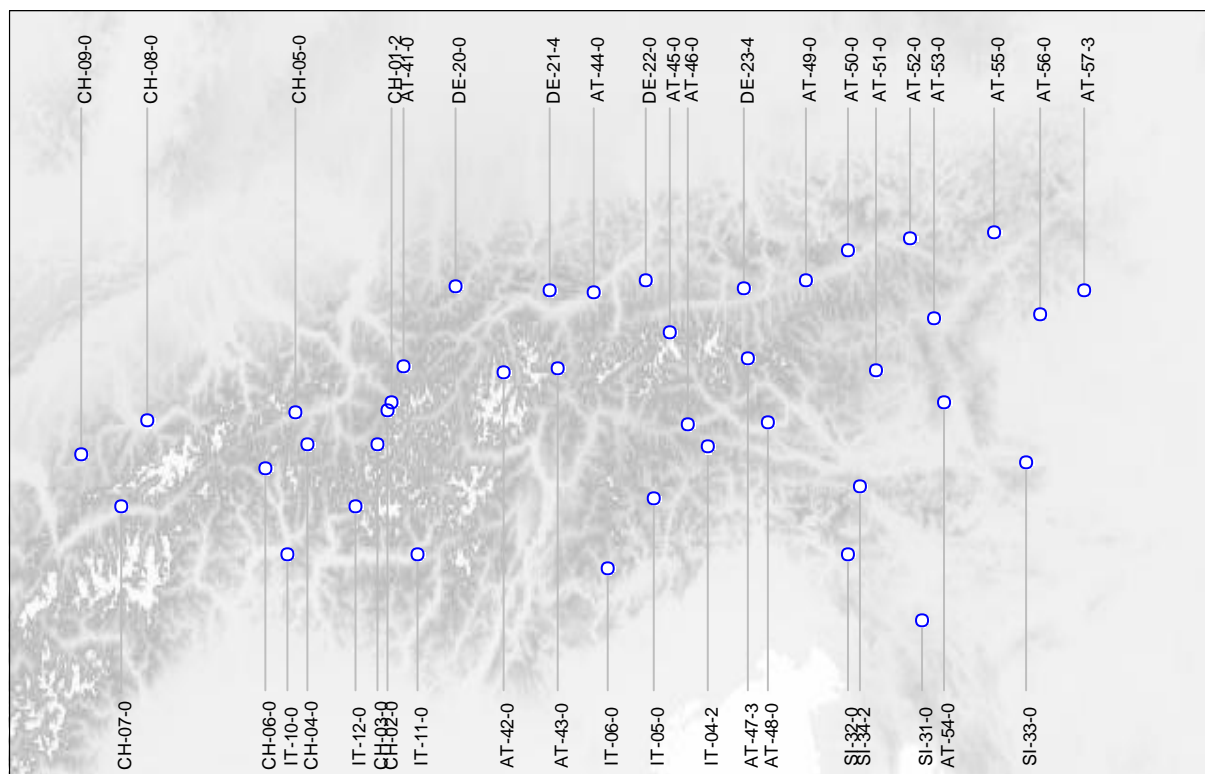


Figure 1-1: Origin and site codes of needle samples.

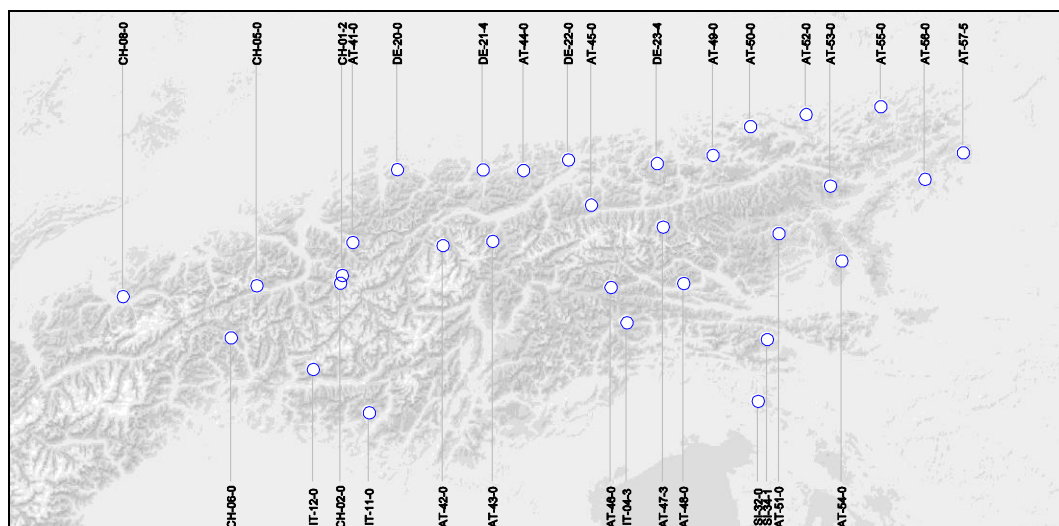


Figure 1-2: Origin and site codes of humus samples.

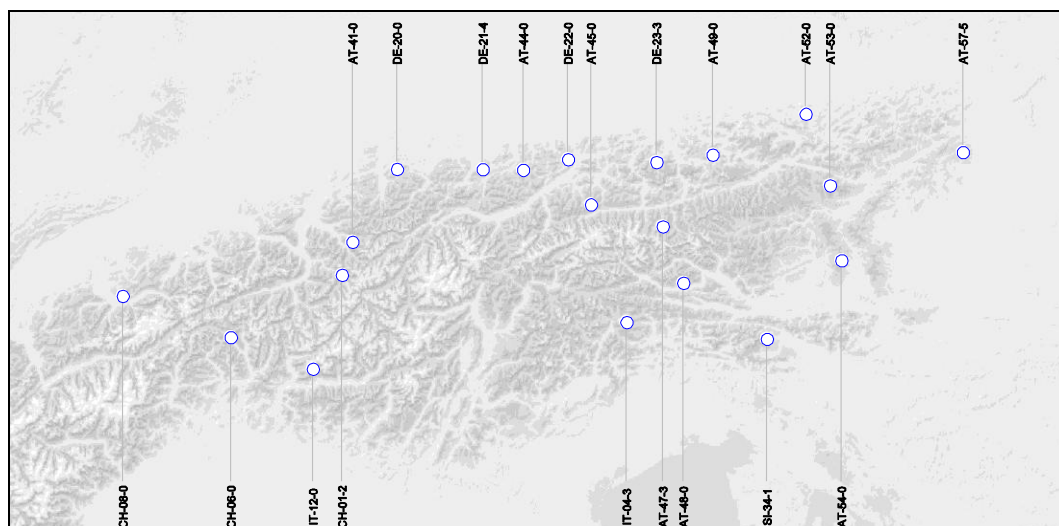


Figure 1-3: Origin and site codes of mineral soil samples.

Table 1-2: Site coordinates (west to east)

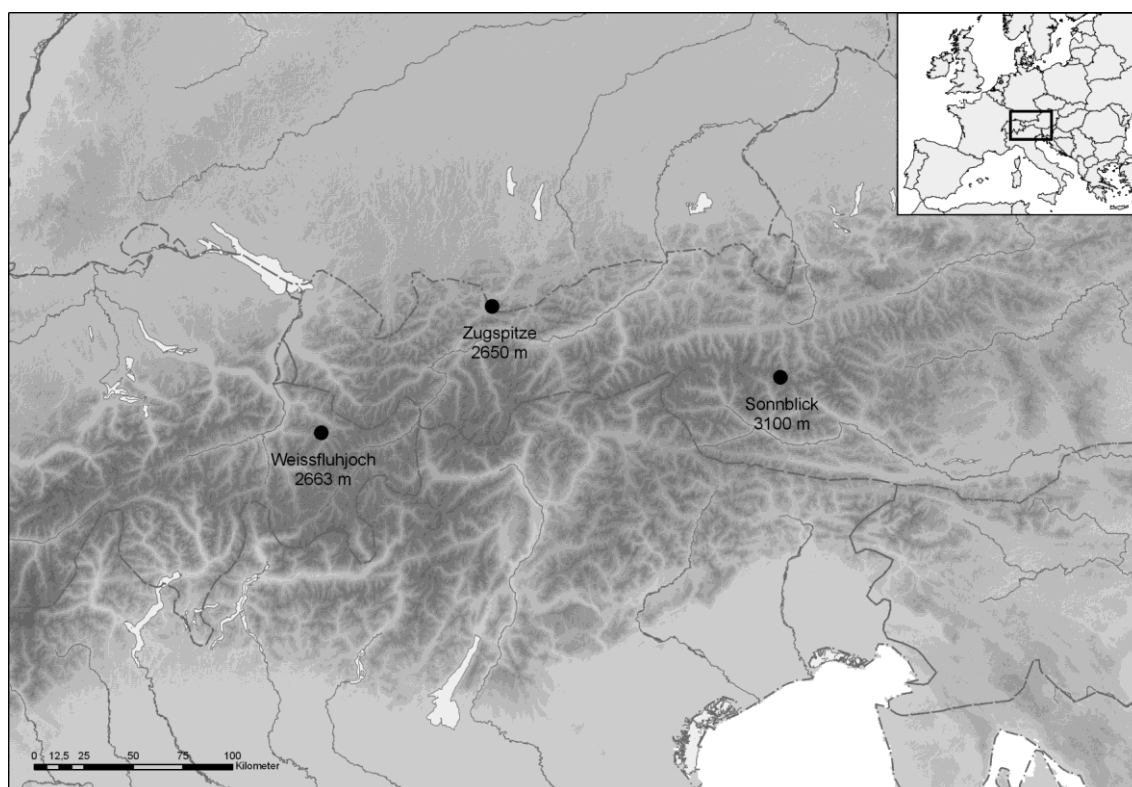
site *	name	longitude (°E)	latitude (°N)	altitude (m a. s. L)
CH-09-0	Rougemont	7.21598	46.4759	1310
CH-07-0	Grimentz	7.58369	46.1819	1390
CH-08-0	Beatenberg	7.76356	46.7021	1540
CH-06-0	Chironico	8.81009	46.446	1400
IT-10-0	Alpe Gotta	9.02178	45.9417	1451
CH-05-0	Brigels	9.04942	46.7931	1580
CH-04-0	Vals	9.16652	46.6024	1530
IT-12-0	Bagni di Masino	9.5984	46.2428	1176
CH-03-0	Bergün	9.76316	46.6145	1590
CH-02-0	Davos	9.85586	46.8153	1650
CH-01-6	Klosters	9.86039	46.8636	1700
CH-01-5	Klosters	9.86843	46.8614	1600
CH-01-4	Klosters	9.87016	46.8647	1520
CH-01-2	Klosters	9.87397	46.8649	1410
CH-01-1	Klosters	9.87788	46.8671	1300
AT-41-0	Schrüns	9.97526	47.0841	1324
IT-11-0	Giovetto di Palline	10.1314	45.9572	1200
DE-20-0	Sonthofen	10.4103	47.5653	1405
AT-42-0	Pitztal	10.8485	47.0596	1460
DE-21-5	Eschenlohe	11.2294	47.555	1650
DE-21-3	Eschenlohe	11.2342	47.5619	1230
DE-21-4	Eschenlohe	11.25	47.5575	1450
DE-21-2	Eschenlohe	11.2744	47.5731	1030
DE-21-1	Eschenlohe	11.2981	47.5706	830
AT-43-0	Pinnisalm	11.3329	47.0828	1494
AT-44-0	Achenkirch	11.6458	47.5475	1426

site *	name	longitude (°E)	latitude (°N)	altitude (m a. s. l.)
IT-06-0	Mte. Grappa	11.7758	45.8935	1345
DE-22-0	Kiefersfelden	12.0883	47.6103	1405
IT-05-0	Val Prampera	12.1566	46.3127	1486
AT-45-0	Mühlbach	12.299	47.3068	1406
AT-46-0	Tessenberg	12.4626	46.7576	1402
IT-04-1	Val Visdende - Val Frison	12.5908	46.5471	1123
IT-04-4	Val Visdende - Val Frison	12.591	46.6414	1656
IT-04-3	Val Visdende - Val Frison	12.6037	46.5201	1553
IT-04-2	Val Visdende - Val Frison	12.6256	46.6258	1305
DE-23-1	Berchtesgaden	12.9272	47.5964	805
DE-23-2	Berchtesgaden	12.9439	47.5917	1005
DE-23-3	Berchtesgaden	12.9531	47.5717	1210
DE-23-4	Berchtesgaden	12.9558	47.5661	1420
AT-47-1	Buchebeben	12.9745	47.1352	1134
AT-47-2	Buchebeben	12.9841	47.1475	1381
AT-47-3	Buchebeben	12.9898	47.1442	1470
AT-47-4	Buchebeben	12.9949	47.1476	1614
AT-47-5	Buchebeben	12.9994	47.1594	1779
AT-48-0	Greifenburg	13.165	46.765	1424
AT-49-0	Rußbach	13.5069	47.6037	1404
SI-32-0	Smrecje	13.8151	45.9628	1038
AT-50-0	Ebensee	13.8882	47.781	1365
SI-34-4	Pokljuka	13.9298	46.3769	1638
SI-34-3	Pokljuka	13.9325	46.3736	1532
SI-34-2	Pokljuka	13.9388	46.3674	1354
SI-34-1	Pokljuka	13.9903	46.3342	1194
AT-51-0	St. Lorenzen	14.1087	47.0628	1404
AT-52-0	Zöbelboden	14.4422	47.8394	930
SI-31-0	Velika Padeznica	14.4464	45.5554	1122
AT-53-0	Gaal	14.6355	47.3566	1433
AT-54-0	Wolfsberg	14.7001	46.8559	1409
AT-55-0	Ötscher	15.1819	47.8583	1439
SI-33-0	Kladje	15.3923	46.4738	1268
AT-56-0	Plankogel	15.5609	47.3558	1415
AT-57-1	Wechsel	15.9186	47.4642	732
AT-57-2	Wechsel	15.9478	47.4796	898
AT-57-3	Wechsel	15.953	47.4858	1117
AT-57-5	Wechsel	15.9548	47.511	1510
AT-57-4	Wechsel	15.9679	47.4926	1282

* the first two letters of the site code indicate the country (AT...Austria, CH...Switzerland, DE...Germany, IT...Italy, SI...Slovenia)

1.2 High altitude sites

Ambient air was measured at three high altitude sites: Weissfluhjoch (Switzerland, 2663 m a. s. l.), Zugspitze (Germany, 2650 m) and Sonnblick (Austria; 3100 m): Figure 1-4.



Map by Christian Ansorge, Umweltbundesamt

Figure 1-4: Location of the high altitude sites.

Each of these sites hosted one low volume sampler (“LoVol”, flow rate: $3 \text{ m}^3 \text{ h}^{-1}$), one high volume sampler (“HiVol”, $8 \text{ m}^3 \text{ h}^{-1}$), seven deposition samplers (for different pollutant classes) and one SPMD type passive sampler, taking advantage of the facilities provided by the meteorological stations on these summits. Figure 1-5 shows the installation at Mt. Zugspitze.

The selection of high altitude sites considered the following criteria:

- remoteness within the investigated region of the Alps
- availability of electricity for pumps, heating devices and control units of the active air samplers
- reliable internet access for remote control of active air samplers
- permanent attendance of technical staff for maintenance and repair of equipment
- availability of supplementary monitoring data (various air pollutants like NO_x , SO_2 , PM) and information about their origin (determined by backward air trajectory)



1...low volume sampler, 2...high volume sampler, 3...deposition samplers, 4...SPMD passive sampler

Figure 1-5: Sampling site at Mt. Zugspitze

1.3 Meteorology

The setup of meteorological stations at all of the large number of sites was not feasible. Furthermore, pluriennial data of meteorological parameters seemed to be more useful for the interpretation of humus concentration data than short time measurements. Not only organic substance (e. g., carbon content in soil) but also POP content in humus are the result of several years of pollutant accumulation. Therefore we used averaged temperature and precipitation data from the climate periods of 1961–1990 or 1971–2000, collected at meteorological stations in the climatically corresponding region (defined from general climatological considerations).

This was also necessary because data from climatological maps may be inappropriate for the interpolation of single sites in mountains due to the low spatial resolution of such maps. To assess the vertical variation of meteorological parameters at the height profiles we took data from proximate stations at different altitudes and modelled the linear dependency of parameters on height. Due to the low horizontal and very low vertical density of meteorological stations within each climate region, barrier effects, temperature inversion layers and local influences on meteorological parameters such as slope exposition could not be studied in detail. Similarly, the estimated altitudinal dependency of meteorological parameters should be interpreted with caution.

As an alternative approach we also considered gridded precipitation data from EFTHYMIADIS et al. (2006).

1.4 Trajectory forecasts and evaluation

Meteorological services were provided by the Austrian Central Institute for Meteorology and Geodynamics. Trajectories were predicted daily at a resolution of one hour. Forecasts combined expert meteorological prognosis with the predictions of two numerical trajectory models (global: ECMWF¹, alpine range: ALADIN-Austria²; Figure 1-6).

The accuracy of forecasts was evaluated by *post hoc* inspection of the trajectories of air actually collected by each filter unit, i. e. air masses passing the site when the respective filter was operative.

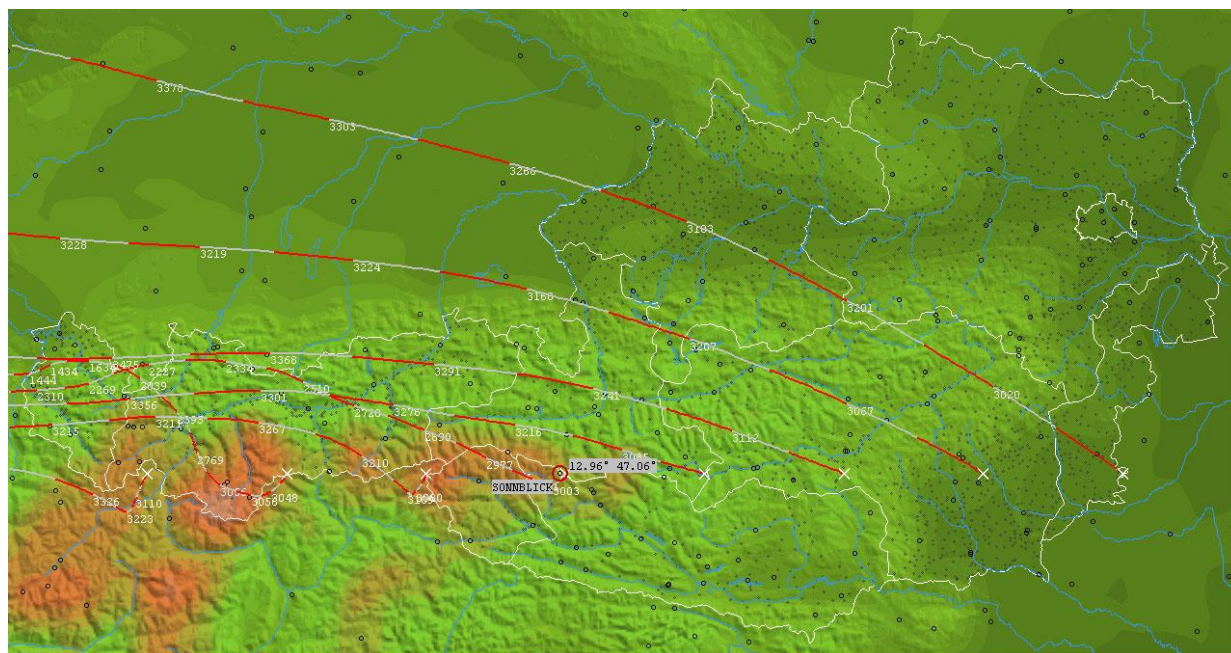
Map: August Kaiser (www.zamg.ac.at)

Figure 1-6: Trajectories (isentropic lines) arriving at the latitude of the sampling site Mt. Sonnblick (AT) as predicted by the mesoscale model ALADIN-Austria.

1.5 Sampling

1.5.1 Needles, mineral soil, humus

1.5.1.1 Needles

Needles were sampled between late September and October 2004 for the main campaign. Sampling was repeated at a subsample of sites between September and October 2005 and between May and June 2006. Three to five branches with different orientations were cut from the top 7th whirl of two dominant, vital adult trees. Six months old twigs of the current year (or 18 months old twigs in the case of the spring campaign 2006) were collected, pooled, transferred to the lab in airtight pre-cleaned glass jars. After sampling the jars were immediately sealed

¹ ECMWF (European Centre for Medium-Range Weather Forecasts): <http://www.ecmwf.int/>

² ALADIN (Numerical Weather Prediction Project): <http://www.cnrm.meteo.fr/aladin>

and the samples were frozen by storage under dry ice. These were also the conditions during transport to the laboratory. At the laboratory the samples were stored frozen at -20°C until freeze drying.

1.5.1.2 Humus

Samples were taken at the 2×5 points of a rectangular sampling grid. At each point, the entire humus layer within a 0.09 m² square was collected into airtight glass jars, transferred to the lab and stored at -20 °C like the needle samples.

1.5.1.3 Mineral soil

After removing all humus down to the mineral soil surface, 10 cm mineral soil cores were extracted from each pit, transported and stored like the needle and humus samples.

Supplementary information about sites and sampling at <http://www.monarpop.at>

1.5.2 Active air sampling

Existing sampling techniques for POP (Standard VDI 3498 Part 1: 2002-07 and standard VDI 4300 Part 2: 1997-12) were modified to avoid the overlay of trajectories during the necessarily long measurement periods. The air flow was distributed between four separate filter cartridges which were assigned to one of three predefined source regions (plus one cartridge for air of undefined origin). These source regions were selected according to their potential influence on the Alps (as expectable from long-term monitoring data for NO_x, SO₂, PM (see criteria for selection of high altitude sites: p. 5), namely the industrial regions of (i) Germany, Great Britain, Belgium, The Netherlands in the Northwest of the Alps, (ii) the Czech Republic, Slovakia and Poland in the North East of the Alps and (iii) the Po basin in Italy. (iv) Air masses with less than two days residence time over a particular region (prior to arrival at the station) were loaded onto the filter cartridge for “undefined origin”). The appropriate filter cartridges were activated through remote (internet) control based on daily meteorological trajectory forecasts. A technical drawing of the sampling equipment is shown in 1-7.

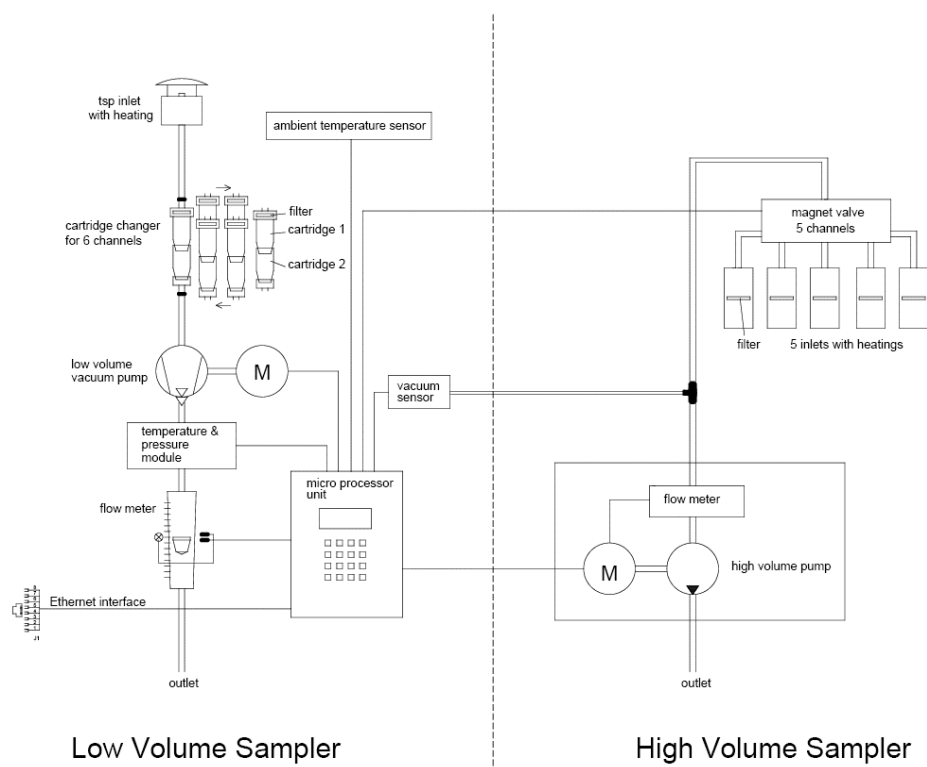


Figure 1-7: Ambient air sampling equipment.

The cartridges for the low volume sampler contained a glass fibre filter (GF8, Ø=45mm) and XAD-2 resin, the cartridges for the high volume sampler a glass fibre filter (GF8, Ø=100mm) and two PU-foam plugs.

Samplers were installed in spring 2005. A series of technical failures delayed the start of the sampling program until December 2005. Five consecutive sampling periods then lasted until July 2007. Every sampling period took approximately three months to collect enough air volume for each cartridge. The detailed sampling schedule is shown in the following table

Table 1-3: Active air sampling schedule.

sampling period		Weissfluhjoch (CH)	Zugspitze (DE)	Sonnblick (AT)
I	winter 2005/6	05/12/02-06/03/16	05/12/03-06/03/14	05/12/04-06/03/16
II	spring-early summer 2006	06/03/16-06/07/06	06/03/14-06/07/11	06/03/16-06/07/19
III	early summer-late autumn 2006	HiVol	06/07/06-06/11/10	06/07/19-06/11/07
		LoVol	06/07/14-06/11/10	06/07/26-06/11/07
IV	late aut. 2006-late winter 2007	06/11/10-07/03/07	06/11/07-07/02/21	06/11/07-07/03/09
V	spring 2007	07/03/07-07/06/25	07/02/21-07/06/20	07/03/09-07/06/20

Note that period III of low volume sampling started with some delay.

1.5.3 Deposition

Also deposition sampling made use of a modified existing method: bulk deposition samplers according to DIN 19739-1 were equipped with heated glass funnels to melt snow, and heated cartridge chambers to avoid frost shattering (Figure 1-8). The filter cartridges were filled with XAD-2 resin.

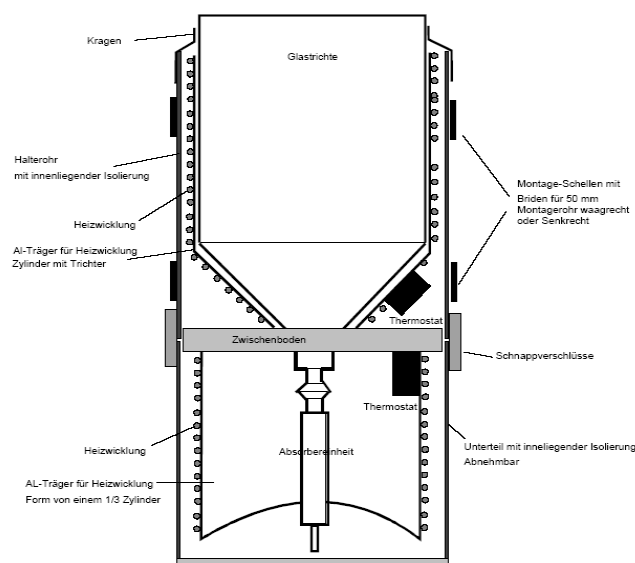


Figure 1-8: Deposition sampler.

Deposition samplers were installed in spring 2005. There were six consecutive sampling periods (Table 1-4). From the third period on, sampling intervalls lasted approximately three months and corresponded to those of active air sampling (p. 10). The first and second period, however, have no parallel active sampling data, due to the technical difficulties mentioned earlier (p. 9).

Table 1-4: Deposition sampling schedule

sampling period	Weissfluhjoch (CH)	Zugspitze (DE)	Sonnblick (AT)
A spring-late summer 2005	2005/04/20-2005/09/09	2005/05/23-2005/09/06	2005/05/02-2005/09/08
B late summer 2005-late winter 2006	2005/09/09-2006/03/15	2005/09/06-2006/03/13	2005/09/09-2006/03/16
C late winter-summer 2006	2006/03/15-2006/07/14	2006/03/13-2006/07/11	2006/03/15-2006/07/20
D summer-autumn 2006	2006/07/14-2006/11/10	2006/07/11-2006/11/07	2006/07/20-2006/11/08
E autumn 2006-late winter 07	2006/11/17-2007/03/07	2006/11/07-2007/02/20	2006/11/15-2007/03/09
F late winter-spring 2007	2007/03/06-2007/06/25	2007/02/20-2007/06/20	2007/03/08-2007/06/19

1.5.4 SPMD type passive air sampling

SPMD type passive sampling has been chosen as a novel technology especially suited for areas with little infrastructure (e.g. lack of electric power supply).

Passive air sampling was performed with semipermeable membrane devices (SPMD). These consisted of LDPE (low density polyethylene) membranes (length=23cm, width=0.25 cm, thickness ca. 67.5µm), filled with 0.7 ml 99% triolein solution (Sigma-Aldrich, Taufkirchen, Germany) and heat sealed. SPMD were then placed into clean glass vials which were sealed hermetically and stored at -20°C until deployment at the sampling sites. All manipulations were done in a glove chamber in inert nitrogen atmosphere to avoid contamination.

On site, SPMD were removed from the vials and exposed 2.5 m above ground in wooden meteorological cabins for a period of six months (corresponding to a double sampling period of the low and high volume air samplers

and to the exposition period of the Norway spruce needles). Four metal frames were installed inside the cabin, each of which held four SPMD tubes (Figure 1-9).

Cabins were equipped with a set of eight SPMDs per sampling period. At the end of each period the exposed SPMDs were released from the clamps, coiled up and stored in the corresponding glass vials for transport (all manipulations done with clean tweezers and protective gloves). To obtain blank values, SPMDs in closed glass bottles were exposed at Weissfluhjoch, CH (2663 m a.s.l.).



Figure 1-9: Meteorological cabin for SPMD exposure.

Different gas-particle partitioning and dry deposition between summer and winter seems to influence the uptake of compounds into SPMD. The strong selectivity of SPMD for the gas phase might be an asset for nanoaerosol research and fine particles, since a combination of SPMD and active air sampling could distinguish between gas phase and aerosol.

1.6 Sample preparation

1.6.1 Determination of dry mass

Humus and mineral soil: 1–2 g of each site's freeze dried material were oven dried at 105 °C until no further weight loss was observed (EN 12880). The ratio of oven-dry and lyophilised mass was used to calculate dry mass concentrations from the analytical values for the lyophilised material.

Needles: 1–2 g of each sample were dried at 105 °C for four hours to obtain the dry mass : fresh mass ratio (VDLUF 2007).

1.6.2 Needles

To avoid contamination in the laboratory, twigs were deneedled in a glove box under protective N₂ atmosphere. After flushing the box with N₂, the glass jars were opened and the shoots immersed in liquid nitrogen. After about five minutes needles could easily be removed by stirring. The defoliated twigs were removed with

tweezers, needles were skimmed off with a filter and filled in precooled bottles standing in a dry ice bath. The bottles were stored and transported under permanent dry ice cooling.

1.6.3 Humus, mineral soil

To avoid any contamination by glassware or ambient laboratory conditions, handling of the samples was minimized. For the transport, the storage, the freeze drying and the storage after freeze drying the samples remain in the same jars they have been filled at the sampling sites. During lyophilisation, the material remained in the glass jars which were then sealed again and stored at room temperature. The lyophilised humus was ground to a particle size < 0.5 mm in a cooled device, pooled per site and homogenised. The freeze dried mineral soil was sieved to use the fraction < 2 mm for analysis.

1.6.4 Air

1.6.4.1 High volume sampling

The filter cartridges for high volume air sampling contained two polyurethane-foam (PUF) plugs and a glass fibre filter (GF). PUF plugs were precleaned by Soxhlet extraction with toluene and subsequently acetone for 24 hours each. After extraction, PUF plugs were dried in an exsiccator under vacuum and a gentle stream of nitrogen. Glass fibre filters were heated 12 h @ 250 °C. Precleaned PUF plugs and GFs were wrapped in aluminium foil and stored in airtight polyethylene bags in a refrigerator at app. 4 °C until cartridge assembly. Before assembling the filter cartridge, GFs were spiked with ¹³C isotopes of 1,2,3,4-TCDD and PCB 47. Filter cartridges were sealed with end caps and stored under cool conditions until sampling.

1.6.4.2 Low volume and deposition sampling

Glass cartridges were filled with XAD (low volume: 50 g, deposition: 25 g) and glass wool was placed on the top to reduce blank values. These cartridges were Soxhlet extracted with a 3:1 n-hexane/acetone mixture for 24 hours and 3 µl ¹³C-PCB was added as a sampling standard. Cartridges were sealed hermetically and transported to the deployment sites.

After exposition, filters were extracted at Umweltbundesamt GmbH (Austria) and GSF (Germany). The extracts were then distributed among the different laboratories.

1.6.5 SPMD

LDPE (low density polyethylene) membranes (length: 23cm, width: 2.5cm, thickness: approx. 67.5µm) were filled with 0.7 ml triolein 99 % (Sigma-Aldrich, Taufkirchen, Germany) and heat-sealed in inert N₂ atmosphere in a glove chamber. SPMD then were transferred into clean glass vials under nitrogen atmosphere to avoid contaminations and stored at -20 °C. These hermetic vials were used to transport the SPMDs between field sites and the laboratory.

1.7 Chemical analysis

To ensure comparability of results, chemical analyses were distributed between the laboratories per analyte. Thus, concentrations of a given pollutant have been determined at the same laboratory, regardless of matrix (e. g. air, humus) or contributing country¹.

1.7.1 Polychlorinated dibenzodioxins and -furans (PCDD/F) and polychlorinated biphenyls (PCB)

1.7.1.1 Chemicals

Humus, mineral soil, needles

The ¹³C-labelled standards (PCB, PCDD/F) and all solvents (Picograde) used were purchased from LGC Promochem (Wesel, Germany). The cleanup columns were purchased from Fluid Management Systems (Waltham, MA, USA), the Celite and sulphuric acid from Merck (Darmstadt, Germany).

SPMD

¹³C-PCDD/F and ¹³C-PCB mixtures were purchased from Cambridge Isotope Laboratories (USA).

1.7.1.2 Extraction and clean-up

Humus, mineral soil, needles, XAD cartridges (deposition sampling), filter cartridges (active air sampling)

Delivered needles were stored at -20°C until freeze drying. After freeze drying the needle samples were stored at room temperature until analysis. All sample material (freeze dried whole needles, freeze dried and ground humus, freeze dried and sieved mineral soil samples, XAD resin from deposition samplers, glass fibre filters and PUF plugs from active air samplers) were spiked with 17 ¹³C-labelled PCDD/F congeners, twelve ¹³C-labelled dioxin-like PCBs and six ¹³C-labelled indicator PCBs. The extraction was carried out in a soxhlet extractor with toluene for the humus and needle samples, and in an ASE (Dionex Corporation, Sunnyvale, CA, USA) using toluene for the mineral soil samples. The further clean-up comprised treatment with concentrated sulphuric acid adsorbed on Celite followed by a multilayer silica column and an alumina column. The latter was also used to separate PCB from PCDD/F. For recovery calculation one ¹³C-labelled standard was added to each fraction prior to injection.

SPMD

Two membranes were combined to a single sample, due to the low concentrations of PCDD/F and PCB in this passive sampler. The membrane devices were cut into slices and spiked with the ¹³C-PCDD/F and ¹³C-PCB mixtures. Then they were extracted for 24 hours with 100 ml cyclohexane each by use of a rotating shaking machine. After that, water was removed with anhydrous sodium sulphate. The sandwich column for the clean-up consisted of Na₂SO₄, silica, H₂SO₄ treated silica, silica, NaOH treated silica and Na₂SO₄ layers (from top to

¹ Except PCDD/F and PCB concentrations in SPMD type passive samplers which were determined by GSF Germany.

bottom). The sandwich column was followed by an active carbon column. The samples were eluted with 200 ml hexane followed by 30 ml hexane/dichloromethane 9:1. The eluate was concentrated and eluted with ACN on a C18 column. This eluate was concentrated to 0.2 ml under a nitrogen stream at 45 °C. The extracts were transferred into vials and spiked with ^{13}C -1,2,3,4-TCDD as recovery standard before PCB analysis. To obtain the PCDD/F retained in the active carbon column, the column was eluted upside down with 100 ml toluene. Another elution was performed with a Na_2SO_4 , alumina B and Na_2SO_4 column. A first fraction eluted with 35 ml hexane/chloroform 88:12 was discarded, and the second fraction eluted with 50 ml CH_2Cl_2 was concentrated. The extracts were transferred into vials and spiked with ^{13}C -1,2,3,4-TCDD as recovery standard before the PCDD/F analysis.

1.7.1.3 Detection

Humus, mineral soil, needles, XAD cartridges (deposition sampling), filter cartridges (active air sampling)

The PCDD/F and PCB analysis was performed with a high resolution mass spectrometer finnigan MAT 95 (Thermo Electron GmbH, Bremen, Germany) coupled to a Agilent 6890 gas chromatograph (Agilent Technologies, Waldbronn, Germany) equipped with a cool injection system by Gerstel GmbH (Mühlheim/Ruhr, Germany). PCDD/F have been analysed using a J&W (Agilent Technologies) DB5 column and a DBDIOXIN column, PCBs using a DB5ms column. The mass spectrometer was operated in single ion mode at a mass resolution of 8000 to 10000. The identification and quantification was done by isotope dilution method according to EPA 1613.

Table 1-5: Detection limits for PCDD/F and PCB in various media.

	PCDD/F	dl-PCB	indicator PCB
humus, mineral soil [$\text{ng kg}^{-1} \text{ d.m.}$]	0.02-0.3	0.09-5	0.08-22
needles [$\text{ng kg}^{-1} \text{ d.m.}$]	0.01-0.2	0.07-30	0.5-110
ambient air [fg m^{-3}]	0.09-23	0.13-50	1-172
deposition [$\text{pg m}^{-2} \text{ m}^{-1}$]	0.03-1.13	0.09-30	0.55-201

SPMD

The compounds were determined by high resolution gas chromatography (HRGC) using a Rtx-Dioxin2 column for PCDD/F and a Rtx-CLPesticides2 column for PCB (Restek, Germany). The GC was coupled to a high resolution mass spectrometer MAT95s (Thermo Electron GmbH, Germany) operating in single ion monitoring mode.

1.7.2 Chlorophenols

1.7.2.1 Chemicals

The isotope labelled chlorophenols (4-chlorophenol $^{13}\text{C}_6$, 2,4-dichlorophenol $^{13}\text{C}_6$, 2,4,5- and 2,4,6-trichlorophenol $^{13}\text{C}_6$, 2,3,4,5-tetrachlorophenol $^{13}\text{C}_6$ and pentachlorophenol $^{13}\text{C}_6$) were purchased at Cambridge Isotope Laboratories (USA) whereas the chlorophenol mix and the chlorophenol acetate mix were supplied by Dr. Ehrenstorfer (Augsburg, Germany). All organic solvents used for sample preparation were

residue analysis grade. Acetic anhydride was redistilled in the laboratory immediately before it was used as a derivatization reagent.

1.7.2.2 Extraction and clean-up

The samples were spiked with isotope labelled chlorophenols as a surrogate standard. Soxhlet extraction with acetone/n-hexane was carried out under acidic conditions. After pH adjustment the organic phase was extracted by the liquid/liquid extraction with an aqueous Na_2CO_3 solution. The organic phase was evaporated gently by a rotary evaporator. Na_2CO_3 solution and petroleum ether were added to the aqueous phase for the first cleanup step. After discarding the organic phase the samples were derivatized with freshly distilled acetic anhydride. After a liquid/liquid extraction with petroleum ether the organic phase was introduced to a silica gel column. The analytes were eluted by a mixture of dichloromethane and n-hexane and evaporated to a final volume of 1 ml. After the addition of an internal standard the extracts were separated and measured by a GC-MS.

1.7.2.3 Detection

The gas chromatographic system used was an Agilent 5890 II Plus containing a split/splitless injector, an autosampler and finally a mass spectrometric detector. Separations were performed with a 60m DB5-MS (0,25 mm ID, 0,25 μm film thickness) obtained from J&W. Following temperature programme was used: starting with a temperature of 60 °C (hold time 2 min), raising to 150 °C (by 2 °C min^{-1}), afterwards to 270 °C in 20 min (hold time nine minutes) and finally to 300 °C (by 20 °C min^{-1} and a hold time of two minutes).

1.7.3 Nitrophenols

1.7.3.1 Chemicals

All solvents (Picograde) were purchased from LGC Promochem (Wesel, Germany). Silica, Florisil, sodium sulphate and sulphuric acid were purchased from Merck (Darmstadt, Germany), nitrophenol and nitroanisole standards from Sigma Aldrich (St. Louis, USA). Some not commercially available nitroanisole standards were synthesized at the University of Vienna.

1.7.3.2 Extraction and clean-up

Needles were stored at -20 °C until analysis. 10 g of the whole needles were extracted twice with a mixture of 40 ml dichloromethane and 20 ml acidified water (100 ml ultra pure water mixed with 1 ml of conc. H_2SO_4) in an ultrasonic bath for 15 min. After filtration, the needles were washed with 20 ml dichloromethane. The combined extracts were transferred into a separation funnel for the separation of the organic phase. The aqueous phase was extracted three times with 50 ml of dichloromethane. The combined dichloromethane extracts were dried with sodium sulphate and evaporated to approx. 2 ml.

The further clean-up was done by treating the sample with conc. H_2SO_4 adsorbed on silica and eluting with 150 ml of dichloromethane. After evaporation to less than 1 ml, 1 ml methanol was added. The remaining dichloromethane was evaporated under a gentle nitrogen stream. The sample was derivatised twice (reaction time 1 hour) after adding 1,5 ml etheric diazomethane solution.

Derivatisation was followed by a final clean-up step on a Florisil column and by an elution with 250 ml n-hexane/toluene (8/2). The organic layer was dried with sodium sulphate and evaporated to 1 ml. 50 ng of octachlorostyrene was added as internal standard before the analysis. A blank and a recovery sample were analyzed with each sample batch.

1.7.3.3 Detection

The GC-MS analysis was carried out by a Thermoquest Trace GC/MS system with electron impact ionisation using selected ion monitoring (SIM) mode (Thermo Electron, USA). A crosslinked DB-5 (J&W, USA) fused silica capillary column (60 m, 0.25 mm i.d., 0.25 µm film thickness) was used.

Table 1-6: Ions (m/z) used for SIM recording and quantification

analyte	m/z
mononitro anisoles	153, 154, 123
dinitroanisoles	168, 198, 199
methyl-nitroanisoles	137, 150, 167, 168
methyl-dinitroanisoles	182, 212, 213
dimethyl-nitroanisoles	166, 181, 182
Dinoseb	225, 254, 255

1.7.4 Short chain chlorinated hydrocarbons (CHCs) and trichloroacetic acid (TCA)

1.7.4.1 Chemicals

Standards were purchased from: Riedel-de Haën (Seelze, Germany: trichloromethane, 1,1,1-trichloroethane, trichloroethene, tetrachloromethane and tetrachloroethene), Sigma-Aldrich (Steinheim, Germany: trichloroacetic acid), Promochem (Wesel, Germany: n-hexane), and Aldrich (Steinheim, Germany: carbon disulfide).

1.7.4.2 Extraction

Needles

For CHC analysis 5 g needles were added to 125 ml deionised water (Milli-Q, degassed) and 5 ml n-hexane. The solvent was extracted using a modified Nielsen-Kryger steam-distillation apparatus.

For TCA analysis 5 g needles were added to 100 ml deionised water (Milli-Q) and degassed with nitrogen (N₂ 5.0) for 2 h to remove contaminating CHCs. 25 ml deionised water and 5 ml n-hexane were added. The solvent was extracted using a modified Nielsen-Kryger steam-distillation apparatus. Thermal decarboxylation of trichloroacetic acid to trichloromethane occurs during this procedure.

Air samples

Air diffuses into the passive sampling tube filled with activated charcoal, where the substances are collected. The desorption is performed using carbon disulfide.

1.7.4.3 Detection

Needles and deposition

The CHCs were analysed in needle samples, and TCA in both needle and deposition samples. The hexane extract was analysed with a HP 6890 gas chromatograph (Agilent Technologies, Waldbronn, Germany) equipped with an automatic sampling injection system and a mass selective detector MSD 5973 using a HP-5 column (Agilent Technologies). The mass spectrometer was operated in a single ion mode.

Air samples

The eluate was analysed with an Agilent 6890 gas chromatograph (Agilent Technologies, Waldbronn, Germany) equipped with an automatic sampling injection system and an electron capture detector (ECD) using a CP-SIL 5 CB column (Chrompack).

1.7.5 Chloropesticides

1.7.5.1 Chemicals

Needles

¹³C-Chloropesticide standards (Cambridge Isotope Laboratories, USA) were used for spiking the samples.

1.7.5.2 Extraction and clean-up

Needles

The needle samples were spiked with ¹³C-chloropesticide standards and extracted for 24 hours with cyclohexane using a rotating shaking machine. The extracts were reduced and eluted with a 1:1 *n*-hexane/dichloromethane mixture on a mixed column filled with 10 g silica gel, 5 g Al₂O₃ and 2 g Na₂SO₄ from bottom to top. After that, the extracts were eluted through a C18 modified silica column with ACN and reduced to 0.2 ml under a nitrogen stream at 45°C. The extracts were transferred into vials and spiked with 2,3,4,5,6-pentachlorotoluene (PCT) as a recovery standard. Finally, the eluates were reduced to 20 µL, and the vials were stored at -20 °C until analysis.

Active air samples

Exposed XAD cartridges were Soxhlet-extracted after spiking with a mixture of ¹³C labelled PAH and chloropesticide standards (Cambridge Isotope Laboratories, USA). The extracts were reduced and split in four parts. One quarter was stored at -20 °C until further delivery, while another quarter was stored at -20 °C as a backup sample. The rest was eluted with a 1:1 *n*-hexane/dichloromethane mixture on a mixed column. The further clean-up and sample preparation proceeded as described above for the needle samples.

Deposition samples

Exposed XAD cartridges were Soxhlet-extracted after spiking with ¹³C-chloropesticide standards. The extracts were reduced and split in two halves. One half was stored at -20 °C until further delivery. The other half was eluted with a 1:1 *n*-hexane/dichloromethane mixture on a mixed column. The further clean-up and sample preparation proceeded as described above for the needle samples.

SPMD

The exposed membrane devices were cut into slices and spiked with ^{13}C -chloropesticide standards. They were extracted for 24 hours with 100 ml cyclohexane each with a rotating shaking machine. The further clean-up and sample preparation for the SPMD samples was the same as for needle, active air and deposition samples (see above).

1.7.5.3 Detection

The compounds were determined by high resolution gas chromatography (HRGC) using a Rtx-Dioxin2 column (Restek, Germany). The GC was coupled to a high resolution mass spectrometer MAT95 (Thermo Electron GmbH, Germany) operating in single ion monitoring mode.

1.7.6 Polycyclic aromatic hydrocarbons (PAH)

1.7.6.1 Chemicals

All solvents (n-hexane, dichloromethane, acetone, toluene, ethyl acetate) were Picograde[®] reagent grade (Promochem GmbH, Wesel, Germany). Native PAH standards were purchased from Supelco (Belfonte, PA, USA), deuterated (Acenaphthylene-D8, Benzo[e]pyrene-D12) and $^{13}\text{C}_{12}$ -labelled PAH standards were purchased from Cambridge Isotope Laboratories (Woburn, MA, USA) and the hydroscopic Sample Dispersing Agent (Speed Matrix) from Applied Separation, Inc (Allenton, PA, USA).

1.7.6.2 Extraction and clean-up

All glassware was washed with basic detergent, rinsed with distilled water, treated with a solution of ammonium persulphate 350 g l⁻¹ in sulphuric acid (98%) and rinsed twice with distilled water and acetone. Subsequently, the cleaned glassware was treated with dimethyldichlorosilane 5% in toluene, rinsed twice with distilled water and acetone, heated to 300 °C for three hours, and covered with an aluminium foil.

The homogenised, freeze-dried and grinded humus, soil and needle samples were firstly spiked with a series of 16 $^{13}\text{C}_{12}$ -Labelled PAH (ES4087-US EPA Cocktail) as internal standards and mixed with a Speed Matrix. The extraction was performed by ASE 200 (DIONEX Sunnyvale, CA) with acetone/dichloromethane 50/50 at 150 °C, 1500 psi, 7 min heat-up and 2 cycles of 10 min static time. The extracts were transferred to hexane before the clean up using the Dioxin Prep (Fluid Management System Inc.) automatic system with pre-packed disposable columns containing multilayer silica and sodium sulphate.

1.7.6.3 Detection

The HRGC/HRMS analyses were performed using a HP 6890 plus gas chromatograph coupled to a Micromass Autospec Ultima mass spectrometer operating in EI mode at 35 eV and with a resolution of 10.000 (5% valley).

Sample injections were performed in the splitless mode on a 30 m Rtx 5 ms column (J&D DB5-MS 30m, 0.25 mm ID, 0.25 µm film). The column program was as follows: 60 °C for 1 min, 15 °C min⁻¹ to 140 °C, 6 °C min⁻¹ to 300 °C, 4 °C min⁻¹ to 325 °C, and finally 325 °C for 4 min. Helium (1.0 ml min⁻¹) was used as the carrier gas.

The injector and transfer line temperatures were 290 °C and 300 °C, respectively. Mass spectral data was acquired in selected ion monitoring mode. The quantitative determination of PAH was performed by an isotope dilution method using relative response factors previously obtained from three standard solution injections (ST1, ST2, ST3).

GC/MS system performance and calibration were verified for all PAH and labelled compounds with the ST2 calibration verification standard at the beginning of each analysis day.

Two deuterated PAH (Acenaphthylene-D8, Benzo[e]pyrene-D12) were added to the extract before injection for the recovery calculations. Corrected response for an analyte varied by more than 15% from the calibration standard of the analysis sequence. The recovery ranged between 40% and 110%. Reproducibility was 20% for lower value or better. The laboratory blanks, repeated twice a week, were lower than 10 % with respect to the minimum concentration found in the samples.

The concentrations of PAHs in soil samples were calculated on a dry weight basis. The moisture content of each sediment sample was determined by drying a separate subsample overnight at 105°C.

1.7.7 Polybrominated diphenyl ethers (PBDE)

1.7.7.1 Chemicals

Humus and needles

Table 1-7: Chemicals and suppliers.

chemical	supplier
all solvents (residue analysis grade)	LGC Standards (Wesel)
alumina (B-super I for dioxin analysis) silica (63-200 µm, 60 Å)	MP Biomedicals (Eschwege)
bio-beads S-X3	Bio-Rad (München)
sodium hydroxide (pellets)	Merck (Darmstadt)
sodium sulfate (anhydrous extra fine powder)	
sulphuric acid (95-97%)	
silane treated glass wool	Alltech (Macherey-Nagel, Düren)
¹³C₁₂-labelled extraction and clean-up standard solution/mixture:	Wellington Laboratories (Campro Scientific, Berlin)
¹³ C ₁₂ -2,4,4'-Tribromodiphenylether (¹³ C ₁₂ -BDE 28)	
¹³ C ₁₂ -2,2',4,4'-Tetrabromodiphenylether (¹³ C ₁₂ -BDE 47)	
¹³ C ₁₂ -2,2',4,4',5-Pentabromodiphenylether (¹³ C ₁₂ -BDE 99)	
¹³ C ₁₂ -2,2',4,4',5,5'-Hexabromodiphenylether (¹³ C ₁₂ -BDE 153)	
¹³ C ₁₂ -2,2',4,4',5,6'-Hexabromodiphenylether (¹³ C ₁₂ -BDE 154)	
¹³ C ₁₂ -2,2',3,4,4',5',6-Heptabromodiphenylether (¹³ C ₁₂ -BDE 183)	
¹³ C ₁₂ -Decabromodiphenylether (¹³ C ₁₂ -BDE 209)	
injection standard solution:	
¹³ C ₁₂ -2,2',3,4,4',5'-Hexabromodiphenylether (¹³ C ₁₂ -BDE 138)	

Glass fibre extraction thimbles, glass filter and wool and Pasteur pipettes were heated to 450°C and then cooled down immediately. All other laboratory glassware, silica and sodium sulfate used for the clean-up were heated for 16 h @ 450°C. After cooling, the glassware was immediately capped with aluminium foil or stored in metal boxes until use. Sodium hydroxide water solution for the preparation of SiO₂-NaOH was extracted thrice with hexane. The vapour tubes of the rotary evaporators were changed after each sample to avoid cross contamination.

1.7.7.2 Extraction and clean-up

Humus and needles

20 g freeze-dried humus or 10 g fresh spruce needles were spiked with the $^{13}\text{C}_{12}$ -BDE standard solution/mixture (1 ng BDE 28, 47, 99; 2 ng BDE 153, 154, 183, and 5 ng BDE 209) and Soxhlet-extracted (Knöfler-Böhm hot extractor). Residual water was simultaneously distilled with a Dean-Stark water separator with toluene. The extract was cleaned with a four column clean-up (1. Multilayer $\text{SiO}_2\text{-H}_2\text{SO}_4$, NaOH, 2. Macro alumina, 3. GPC bio-beads S-X3, 4. Mini alumina). The cleaned extract was spiked with the injection standard solution (1 ng $^{13}\text{C}_{12}$ -BDE 138) and reduced to 50 μl .

SPMD

Semipermeable membrane devices (SPMD) were cut and shaken with cyclohexane in an Erlenmeyer flask for 16 h @ 200 rpm. The extract was cleaned up and analysed as described for humus and needle samples.

1.7.7.3 Detection

1 μl of spiked extract was injected on-column (guard column 2 m \times 0.32 mm, uncoated, deactivated) and analysed by GC-SIM(EI+)-HRMS (TRACE GC-MS MAT 95 XP, Thermo Scientific, Bremen) using a DB-5MS column (15 m \times 0.25 mm, 0.1 μm). The two most intense masses of the bromine cluster (Tri- and TeBDE: M^+ . Te- to DeBDE: M^+-2Br) were measured for each homologue group. The identification of PBDE was based on retention time and correct isotope ratio for both fragments recorded. Quantification was performed by means of the $^{13}\text{C}_{12}$ -labelled internal standards. All congeners except BDE 100 were quantified based on their corresponding $^{13}\text{C}_{12}$ -labelled analogues used as internal standards. BDE 100 was quantified using the $^{13}\text{C}_{12}$ -BDE 99 as an internal standard (CEN 2007). Eight relevant congeners were determined for the three commercial PBDE formulations: the sum of six BDE (28, 47, 99, 100, 153, 154) for the PeBDE formulation, BDE 183 for OcBDE and BDE 209 for DeBDE.

After every fourth sample, a plug of glasswool in a Soxhlet extraction thimble was spiked with the method blanks and extracted and cleaned up. Blank concentrations were calculated for an assumed mean sample weight of 18.3 (humus) or 9.5 (needles) gram dry mass. The method detection limit (MDL) was determined as the mean concentration in the blank plus three times the standard deviation of 21 measurements.

1.7.8 Chlorinated paraffins

1.7.8.1 Chemicals

Cyclohexane, dichloromethane and *n*-hexane for residue analysis were obtained from Biosolve (Vallenswaard, Netherlands). Acetone for gas chromatography was purchased from Merck KGaA (Darmstadt, Germany). $^{13}\text{C}_{10}$ -*trans*-chlordane (100 ng μl^{-1} , solution in *n*-nonane, purity 99%) was supplied by Cambridge Isotope Laboratories (Andover, USA) and $^{13}\text{C}_{12}$ -PCB118 (crystalline, purity 99.4%) by Promochem (Wesel, Germany). Reference SCCP (C_{10-13} , chlorine contents of 51.5, 55.5 and 63.0%) and reference MCCP mixtures (C_{14-17} , chlorine contents of 52.0 and 57.0%) with concentrations of 100 ng μl^{-1} in cyclohexane as well as ϵ -hexachlorocyclohexane (ϵ -HCH, solution in cyclohexane, 10 ng μl^{-1}) were purchased from Dr. Ehrenstorfer

GmbH (Augsburg, Germany). Silica gel for column chromatography (230-400 mesh, 0.045-0.063 mm) and sulphuric acid (98%) were obtained from Merck KGaA. Florisil®PR (60-100 mesh) and anhydrous sodium sulphate (Pestanal®) were purchased from Fluka (Buchs, Switzerland). Florisil®, sodium sulphate, and silica gel were dried overnight at 220 °C.

1.7.8.2 Extraction and clean-up

Extreme care was taken to minimize the background and cross contamination. All glassware was washed in a glassware washer and immersed in a detergent bath (5% RBS®35 concentrate, Fluka) for 12 hours. Then, glassware and glass fiber thimbles (30 × 100 mm, 603G, Wathman®, Schleicher & Schuell, Meidsone, England) were rinsed with dichloromethane and *n*-hexane, and heated at 450 °C overnight. Prior to use, glassware was rinsed with the same solvents.

Humus and mineral soil

20 g of dried and homogenised samples filled in a glass fiber thimble were spiked with the internal standards (ISTDs: 10 ng of ¹³C₁₀-*trans*-chlordan and 9.4075 ng of ¹³C₁₂-PCB118) and Soxhlet extracted with 200 ml of dichloromethane and *n*-hexane (1:1, v/v) for 8 h. Activated copper powder was added to eliminate sulphur. Extracts were concentrated to 1 ml using a Turbo Vap 500 (Zymark, Hutchinson, USA).

Deposition

Deposition samples were transferred in a Soxhlet apparatus layered with 1 cm glass wool, spiked with the ISTDs and extracted with 200 ml of acetone and *n*-hexane (1:1, v/v) for 24 h. Extracts were concentrated to 1 ml using a Turbo Vap 500.

Needles

20 g fresh needle sample were placed in a 250 ml Schott® glass bottle. The needles were spiked with the ISTDs and cold extracted with 150 ml of dichloromethane and *n*-hexane (1:1, v/v) by shaking for 16 h. The extract solution was decanted over a funnel filled with a glass wool directly into a Turbo Vap flask. Another portion of dichloromethane and *n*-hexane (30 ml) was added to the needles. After shaking and decanting this procedure was repeated. The combined extract solutions were concentrated to 1 ml using a Turbo Vap 500.

The following clean-up method was applied to all sample extracts, independently of the matrix. After solvent evaporation, sample matrix not persistent to sulphuric acid was removed by column chromatography on 20 g of silica gel impregnated with concentrated sulphuric acid (44%). The column was conditioned with dichloromethane and *n*-hexane (1:1, v/v). After transferring the extract to the column, toxaphenes and CPs were eluted with 70 ml of dichloromethane and *n*-hexane (1:1, v/v). The eluate was evaporated to 0.5 ml with a Turbo Vap 500, diluted with 10 ml of *n*-hexane and reduced to 0.5 ml, each twice.

The further clean-up step was performed in a deactivated Florisil® column (16 g, 1.5% water content; conditioned with *n*-hexane). This column was eluted with 75 ml of *n*-hexane and 5 ml of dichloromethane (first fraction) and 60 ml of dichloromethane (second fraction). The first fraction containing toxaphenes was concentrated to 0.5 ml, then diluted with 10 ml of cyclohexane and reduced to 100 µl with a Turbo Vap 500, each twice. The remaining solvent was concentrated and transferred to a GC vial containing the recovery

standard (10 ng of ϵ -HCH in 10 μ l of cyclohexane). The second fraction containing all CPs was concentrated to 0.5 ml, and the solvent was also changed to cyclohexane. Finally, 10 ng of ϵ -HCH in 10 μ l of cyclohexane was added as a recovery standard prior to analysis.

1.7.8.3 Detection

Instrumental analysis was performed on a gas chromatograph CP-3800 coupled to a 1200L triple quadrupole mass spectrometer (Varian, Walnut Creek, USA) using electron ionisation tandem mass spectrometry (EI-MS/MS) and negative ion chemical ionisation mass spectrometry (ECNI-MS). The gas chromatograph was equipped with a split/splitless injector and a DB5-MS (J&W Scientific, Folsom, USA) fused silica capillary column (15 m \times 0.25 mm, 0.25 μ m crosslinked methylphenylpolysiloxane coating). The injector temperature was set to 275 °C, the transfer line to 280 °C and the ion source to 200 °C. Splitless injections (3.0 min) of 2.5 μ l were carried out with a Combi Pal autosampler (CTC Analytics, Zwingen, Switzerland).

The temperature program for the GC-EI-MS/MS analysis was as follows: 3 min isothermal at 100 °C, 50 °C min⁻¹ to 300 °C, then isothermal for 3 min. Helium (99.996%, Sauerstoffwerk Lenzburg, Lenzburg, Switzerland) was employed as carrier gas at a constant flow of 2 ml min⁻¹. The EI mass spectra were acquired at 70 eV electron energy with a filament emission current of 150 μ A and a scan time of 0.25 s scan⁻¹. CID gas pressure (argon, 99.5%, Sauerstoffwerk Lenzburg) was set to 0.13 Pa. The mass spectrometer was regularly tuned to optimal performance using perfluorotributylamine for both quadrupoles at m/z 69, 219, and 502. The fragmentation masses were slightly modified for the determination of the total CP amount: m/z 91 \rightarrow m/z 53 (collision energy: -10 eV), m/z 102 \rightarrow m/z 67 (-10 eV) and m/z 104 \rightarrow m/z 67 (-10 eV). The precursor ion m/z 383 and the product ion m/z 276 were selected for the detection of the internal standard ¹³C₁₀-*trans*-chlordanes (-28 eV). The recovery standard ϵ -HCH was determined with the fragmentation masses m/z 180.9 \rightarrow m/z 144.9 (-16 eV).

The temperature program for the GC-ECNI-MS analysis was as follows: 2 min isothermal at 100 °C, 15 °C min⁻¹ to 280 °C and isothermal for 4 min, 50 °C min⁻¹ to 300 °C and isothermal for 1.6 min. The mass spectrometer was employed in the ECNI mode with methane (99.995%, Carbagas, Rümlang, Switzerland) as reagent gas at an ion source pressure of 730 Pa. The transfer line temperature was set to 280 °C, the ion source to 200 °C. The ion source was tuned to optimum performance using perfluorotributylamine at m/z 283, 452 and 633. The most abundant isotopes of the [M-Cl]⁻ ions of CPs with 5-13 chlorine atoms and of the [M]⁻ ion (m/z 419.8) of ¹³C₁₀-*trans*-chlordanes were recorded in the selected ion monitoring (SIM) mode (dwell time 0.250 s per cycle). The most abundant isotope of the [M-Cl]⁻ ion (m/z 254.9) was selected for the recovery standard ϵ -HCH. Identification of the CP congener groups was performed by comparison of retention time, signal shape and correct isotope ratio according to Reth and Oehme (2004). The applied quantification procedure was described by Reth et al. (2005). Using this method, a reliable quantification can be achieved even if the degree of chlorination of the samples and the reference standards are different. For this purpose, three SCCP (51%, 55%, and 63% Cl) and two MCCP references (52% and 57% Cl) from Ehrenstorfer were used as described by Reth and Oehme.

1.7.9 Enzyme assays

1.7.9.1 Sampling

The experiments were performed with protein extracts of needles of *Picea abies* (L.) Karst. sampled at the given MONARPOP sites. Freshly cut branches were immediately immersed into liquid nitrogen at the sampling site, and frozen needles were stripped off the branches into aluminium foil envelopes. The samples were transferred to the laboratory in liquid nitrogen and stored at -80 °C.

1.7.9.2 Chemicals

Bovine serum albumin (BSA), CDNB (1-chloro-2,4-dinitrobenzene), DCNB (1,2-dichloronitrobenzene), reduced glutathione (GSH), Nonidet P40, PVP K 30 (polyvinylpyrrolidone) were obtained from Sigma Fluka Chemie (Steinheim, Germany). All other chemicals used were research grade commercial materials.

1.7.9.3 Enzyme purification

The work up procedures followed established methods (SCHRÖDER et al. 1990, 1997). Frozen needles were ground to a fine powder in liquid nitrogen with mortar and pestle. The powder was added to ten volumes (v/w) of 100 mM potassium phosphate buffer (pH 7.8), containing 10 mM dithioerythritol, 5 mM EDTA, 1 % Nonidet P40 and 10 mg ml⁻¹ soluble polyvinylpyrrolidone. The mixture was allowed to incubate for 10 min under gentle stirring before it was filtered through two layers of Miracloth (Calbiochem) and centrifuged at 30 000 G for 30 minutes.

Solid ammonium sulfate was added to the supernatant (designated as crude extract) to yield a saturation of 40 %. After stirring for 30 min, the precipitated proteins were removed by centrifugation at 48 000 G for 25 min. The supernatant was decanted and adjusted to 80 % ammonium sulfate saturation, stirred for 30 min and centrifuged as described previously. The resulting pellet was resuspended in 2 ml 20 mM Tris-HCl (pH 7.8; buffer A). The extract was desalted by gel filtration (PD 10, Pharmacia). All fractions collected from the gel filtration columns were analyzed for GST (Glutathione S-transferase) activity and for protein contents.

1.7.9.4 Detection

Enzyme Assays and protein determination

Glutathione S-transferase activity in protein extracts derived from the needles was determined spectrophotometrically using CDNB (1-chloro-2,4-dinitrobenzene) as a model substrate according to HABIG et al. (1974) and with DCNB (1,2-dichloro-4-nitrobenzene) and p-NBC (p-nitrobenzyl chloride) following the assay methods described by SCHRÖDER et al. (1990). The reaction was started by the addition of varying amounts of enzyme extract to give a final volume of 0.6 ml. Product formation was calculated using the published extinction coefficients: CDNB ($\epsilon_{340 \text{ nm}} = 9.6 \text{ mM}^{-1}\text{cm}^{-1}$), DCNB ($\epsilon_{345 \text{ nm}} = 8.5 \text{ mM}^{-1}\text{cm}^{-1}$), p-NBC ($\epsilon_{310 \text{ nm}} = 1.8 \text{ mM}^{-1}\text{cm}^{-1}$), and p-nitrobenzoyl-chloride (p-NBOC, $\epsilon_{310 \text{ nm}} = 1.9 \text{ mM}^{-1}\text{cm}^{-1}$). All measurements were corrected for nonenzymatic conjugation rates.

Catalytic properties of the enzymes, e.g. Michaelis constants for CDNB and GSH, respectively, were determined from Lineweaver-Burk plots. The measurements were performed according to the standard assay procedures mentioned above. The concentrations of the respective substrates were varied in a range of 0.0625 to 2 mM. GST activity was measured in triplicate at five different substrate concentrations. Protein contents were determined by the method of Bradford (1976) using bovine serum albumin as standard.

From selected samples, GST isoenzymes were further purified by affinity chromatography on epoxy-activated agarose beads with S-bound GSH as a ligand (Sigma-Aldrich). Combined isoenzyme fractions from Mono P runs were desalted by gel filtration and centrifuged as described above. Extracts were loaded onto GSH agarose columns pre-equilibrated with 20 mM Tris-HCl (pH 7.0), 1 mM dithioerythritol (buffer C). After sample application, the column was washed with five volumes of buffer C. Bound GST was eluted by a step gradient of 0 to 20 mM GSH dissolved in buffer C. To concentrate the protein in fractions (0.5 ml) containing GST activity, buffer C was replaced with water by gel filtration on Sephadex G25, and the proteins were lyophilized over night.

Gel electrophoresis

GST isoenzymes molecular mass and purity were estimated by SDS-PAGE using 8 to 25% gradient gels (Phast System, Pharmacia LKB). A low molecular weight marker kit (Sigma-Aldrich) was used as a standard for determination of GST subunit molecular weights. Lyophilized proteins were resuspended in small volumes of water (20 to 50 µl), diluted 1:1 with loading buffer and proteins were denatured by boiling for seven minutes. Gels were silver stained to visualize protein bands.

HPLC-determination of glutathione

Reduced (GSH) and oxidized glutathione (GSSG) were measured according to SILLER-CEPEDA et al. (1991). Briefly, 0.5 g of cells were homogenized in 10 % perchloric acid and 1 mM bathophenanthroline-disulfonic acid and centrifuged (5 min, 6000 G). The supernatant was collected and mixed with 50 µl of 100 mM iodoacetic acid and 0.2 mM m-cresol-purple for S-carboxy-methylation. Addition of 480 µl of 2 M KOH and 2.4 M KHCO₃ increased pH to 9. Derivatization occurred overnight at 4°C after addition of 1 ml of 1% 2,4-difluoro-1-fluorobenzene solution. Incubations were terminated by centrifugation (5 min, 6000 G) and filtration (0.45 µm). Aliquots of filtrate (up to 100 µl) were injected into a 3-aminopropyl-Spherisorb column and thiols were separated within 20 min in a linear solvent gradient of 80% MeOH (solvent A) to 64% MeOH, 0.5 M sodium acetate and 10 % acetic acid (solvent B). Detection was carried out at 365 nm in an UV-vis detector.

1.7.10 Micro-EROD bioassay

The method targets persistent planar halogenated hydrocarbons or other structurally similar compounds which can bind to the aryl hydrocarbon receptor (AhR), and thus induce the cytochrome CYP1A1 synthesis. This induction can be measured indirectly with the 7-Ethoxyresorufin-o-deethylase (EROD) bioassay. The ability to elicit a cytochrome CYP1A response makes this bioassay a suitable screening tool for persistent chemicals that can bind to AhR in environmental samples.

1.7.10.1 Extraction and clean-up

Soil

50 g were Soxhlet-extracted with toluene for 24 hrs. The extract was concentrated to 4 ml, and a clean-up step was carried out on a sandwich column, consisting of 10 g active silica gel, 20 g silica gel (44 % H₂SO₄), 40 g silica gel (4 % H₂O), 10 g Na₂SO₄ from bottom to top. The sample was eluted with *n*-hexane.

Needles

50 g were extracted with cyclohexane for 16 hours at 200 rpm. The needle extracts were filtered through Na₂SO₄ to eliminate possible water remains. The sample was concentrated almost to dryness and 1 ml hexane was added. The clean-up procedure was followed as described above.

SPMD

SPMDs were weighted and cut into slices without exterior cleaning. The extraction was performed with 100 ml cyclohexane per SPMD for 16 hours at 200 rpm. The SPMD extracts were filtered through Na₂SO₄ to eliminate possible water remains. The sample was concentrated almost to dryness and 1 ml hexane was added. The clean-up was done through a sandwich column that contains from bottom to top: 4 g silica gel (4 % H₂O), 10 g silica gel (44 % H₂SO₄), 2 g silica gel (4 % H₂O) and 1 cm layer of Na₂SO₄. *n*-hexane was used as an elution solvent. This step eliminates triolein and other compounds that interfere in the bioanalytical procedure.

The eluates of the different matrices were concentrated and transferred to 200 µl DMSO (dimethyl sulfoxide) under N₂ stream at 45 °C. The carrier solvent for the bioassay was a mixture of DMSO/ Isopropanol 4:1.

Micro EROD bioassay

The EROD bioassay was carried out to evaluate the overall AhR disrupting potential of the complex mixture extracted from humus and mineral soil. The lypophilic extracts were pre-treated to select persistent bioaccumulative compounds (PBT) from the complex mixture. The bioassay was also performed for the needle and SPMD matrices but in those the bioanalytical values were below the limit of quantification.

The rat liver cell line (HII4E) expressing the cytochrome P450 was cultured to perform the ethoxyresorufin-*O*-deethylase (EROD) bioassay based on DONATO ET AL. (1993) with modifications as described in SCHWIRZER ET AL. (1996). H4IIE cells were incubated in culture flasks at 37 °C and 7.5 % CO₂. The hepatic cells were trypsinised, counted (Neubauer cell counter) and diluted in supplemented medium (DMEM) to achieve a cell concentration of 1×10⁵ ml⁻¹. This H4IIE cell suspension was seeded onto 96 well plates and incubated for 24 hours. Subsequently, cells were exposed to 2,3,7,8-TCDD standards, sample extracts or blanks for 24 and 72 hours.

1.7.10.2 Detection

After incubation, the medium was substituted with a 7-ethoxyresorufin solution (8 µM) and the resorufin produced was measured by fluorescence (excitation 535 nm, emission 590 nm) after 30 min incubation. The protein determination was performed according to Pierce (Micro BCA Protein Assay Kit). The EROD induction of the sample after incubation was compared to the 2,3,7,8-TCDD response used as a standard in this assay. The

induction values were interpolated with a fourth order logistic function. The results are given in WHO toxicity equivalents to 2,3,7,8-TCDD.

1.8 Data processing and statistical analysis

1.8.1 Longitudinal and latitudinal grouping

Standard sites were divided into longitudinal groups („west“, „middle“ and „east“: Figure 1-10) or latitudinal groups („north“, „central“, „south“: Figure 1-11) to test for geographical differences. Groups were established *a priori* by simple visual partitioning of sites. Differences between all groups were tested for significance (Kruskal-Wallis test or, after positive testing for normal distribution and homogeneity of variances, one-way ANOVA). In case of significant differences in the whole sample, the origin of these difference(s) was tested by pairwise group comparisons (Wilcoxon test or Student t-test, where appropriate) with Bonferroni's correction of significance.

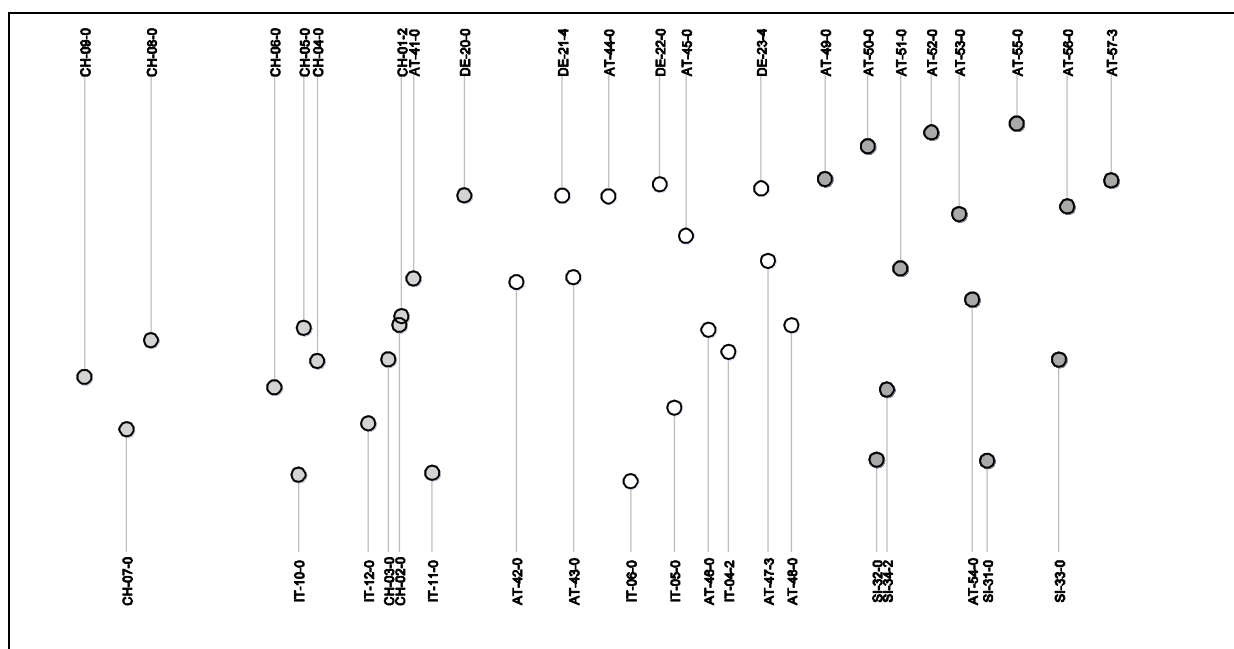


Figure 1-10: Longitudinal site groups (east / middle / west).

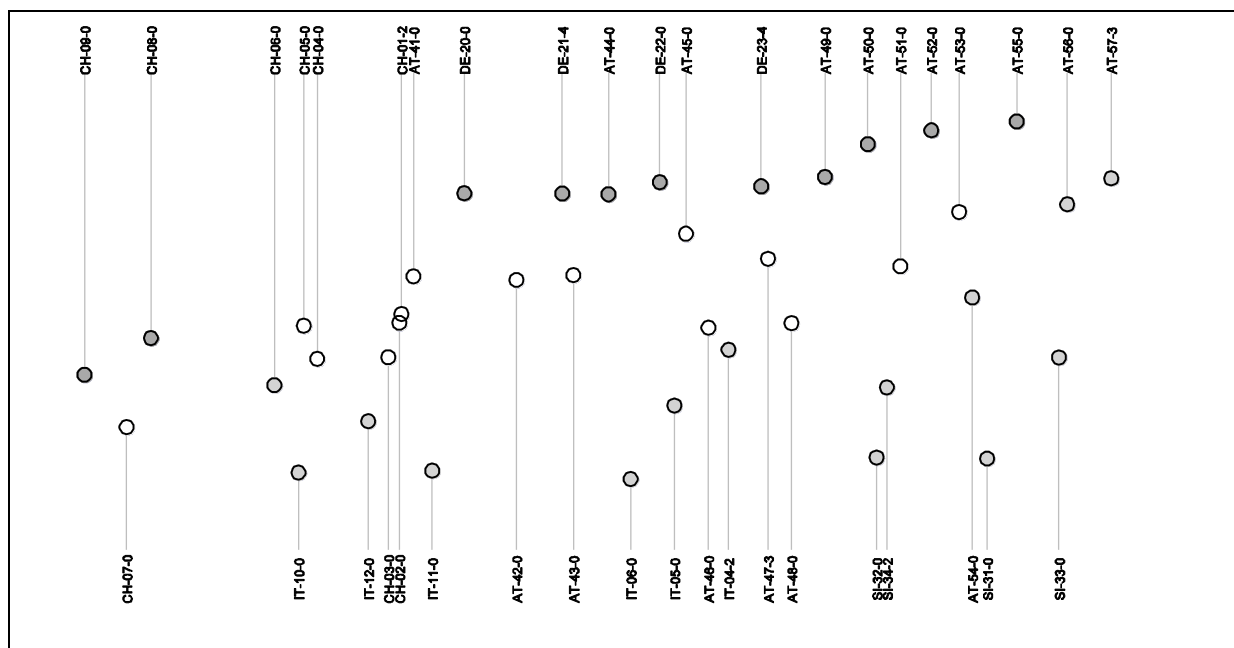


Figure 1-11: Latitudinal site groups (north / centre / south)

1.8.2 Treatment of low values

For all summary statistics and graphics, concentrations below the detection limit (LOD) have been treated as zero, values above LOD but below the quantification (LOQ) have been replaced by half the LOQ.

1.8.3 Correlations between different compound groups

To maintain an overview over the most important associations between different structural pollutant groups (e. g., PAH, PCDD/F, OCP...), only significant ($p \leq 0.05$) and high (absolute value of correlation coefficient ≥ 0.6) correlations are reported in section 3.14 (p. 232 ff). Where necessary (i. e. Shapiro-Wilks test rejecting normal distribution at $p \leq 0.05$), parameters were ¹⁰log-transformed. If either parameter still failed to attain normal distribution after transformation, Spearman's non-parametric instead of Pearson's correlation coefficient was reported.

1.8.4 Averaging atmospheric pollutant concentrations

Concentration data were collected for separate trajectories, corresponding to predefined source regions (p. 9). As source regions changed during a measurement period, an average concentration for the site was estimated by weighing the concentration of each source region with its relative incidence.

1.8.5 Software

For statistics and graphs, the "R" computing environment was used (R DEVELOPMENT CORE TEAM 2008), within which particularly the lattice and ggplot2 (WICKHAM 2008) packages proved extremely helpful.

2 Abbreviations

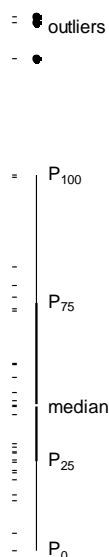
2,4-DNP...2,4-Dinitrophenol	DBaI...dibenzo(a,i)anthracene	PCB...polychlorinated biphenyl(s)
2-NP...2-Nitrophenol	DBaH...dibenzo(a,h)anthracene	PCDD/F...sum of PCDD and PCDF
3-M-2-NP...3-Methyl-2-Nitrophenol	DBaL...dibenzo(a,l)anthracene	PCDD...sum of polychlorinated(p)dibenzodioxins
3-M-4-NP...3-Methyl-4-Nitrophenol	dl-PCB...PCB with dioxin-like activity	PCDF...sum of polychlorinateddibenzofurans
4-M-2,6-NP...4-Methyl-2,6- Dinitrophenol	EPA-PAH...16 PAH classified as „priority pollutants“ by the US Environmental Protection Agency	PCP...pentachlorophenol
4-M-2-NP...4-Methyl-2-Nitrophenol	EROD...ethoxyresorufin-O-deethylase	PHEN...phenanthrene
6 BDE...six BDE (congeners no. 28, 47, 99, 100, 153, 154)	FLA...fluoranthene	p _L ...vapour pressure of liquid
6 PCB...six PCB used for routine screening (congeners no. 28, 52, 101, 138, 153, 180)	FLU...fluorene	P _n ...n th percentile
6-M-2,4-NP...6-Methyl-2,4- Dinitrophenol	IND...indeno(1,2,3-c,d)pyrene	p _S ...vapour pressure of solid substance
Ah...aryl hydrocarbon (substrate for Ah-receptor)	k _{OA} ...octanol/air partition coefficient	PYR...pyrene
ANA...acenaphthene	k _{OW} ...octanol/water partition coefficient	SPMD...semipermeable membrane device
ANT...anthracene	LOD...detection limit	sd...standard deviation
ANY...acenaphthylene	LOQ...quantification limit	T/Pe/Hx/Hp/OCD/F...sum of tetra- /penta-/hexa-/hepta- /octochlorinated (p) dibenzodioxins/furans
BaA...benz(a)anthracene	LRTAP...long-range transboundary air pollution	TCA...trichloroacetic acid
BaP...benz(a)pyrene	m...mean	TCE...1,1,1-trichloroethane
BbF...benzo(b)fluoranthene	max...maximum	TCM...trichloromethane (chloroform)
BeP...benz(e)pyrene	med...median	TEQ _{WHO} ...WHO toxic equivalents for mammals
BghiP...benzo(g,h,i)perylene	min...minimum	TETRA...tetrachloromethane
BkF...benzo(k)fluoranthene	MW...molecular weight	TETRE...tetrachloroethene
CHR...chrysene	n...sample size	TRI...trichloreth(yl)ene
COR...coronene	n.d...not detectable (below LOD)	
d.m...dry mass	PAH...polycyclic aromatic hydrocarbon(s)	
DBaE...dibenzo(a,e)anthracene	PBDE...polybrominated diphenylethers	

3 Results

3.1 How to interpret the graphs

3.1.1 Boxplots

The boxplots inform about spread and distribution of the data (see example on the left). Indicated are the values of minimum (P_0), first quartile (P_{25}), median, third quartile (P_{75}), maximum without outliers (P_{100}), and outliers. Considered outliers are values with at least 1.5 box lengths distance from the “box” (thick line between first and third quartile). The “rug” (small marks on the left margin) marks the single observations.



3.1.2 Spatial variation

The spatial variation of a given parameter has been illustrated as in Figure 3-1: sampling locations are shown as dots on the map of the study area, the dot diameter being proportional to the parameter value (indicated in the top and bottom map margins). Dots bearing an exclamation sign represent outlier values.

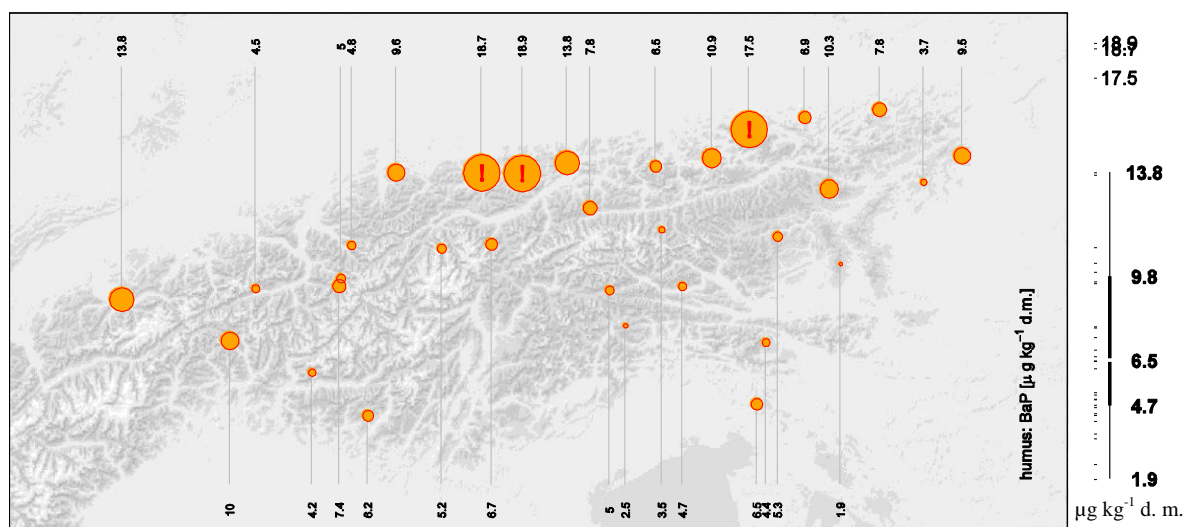


Figure 3-1: Example graph for spatial variation.

3.1.3 Longitudinal and latitudinal differences

To investigate the longitudinal and latitudinal variation of data, sampling locations were divided into groups (see pp. 27 f). The corresponding sample distributions are illustrated with juxtaposed boxplots (Figure 3-2). In these graphs, the sequence of boxplots follows the cartographic conventions (left-right = west-east, top-bottom = north-south).

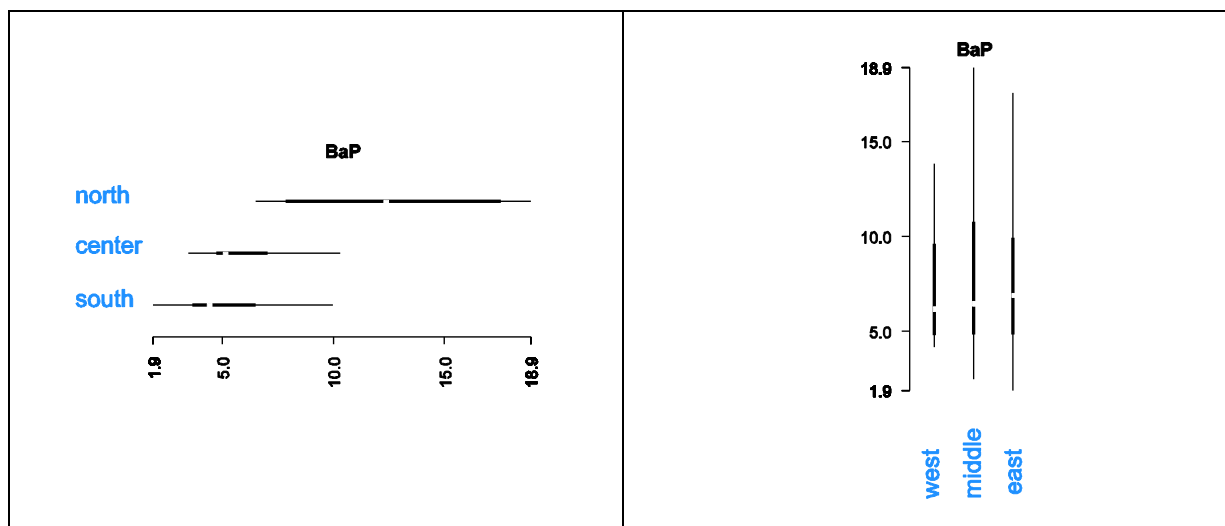


Figure 3-2: Example illustration of latitudinal (left) and longitudinal (right) variations.

3.1.4 Wind roses

Atmospheric pollutant concentrations at three high altitude sites were attributed to predefined source regions (p. 9). Values for each source region are indicated by length and direction of the radii in the plotted wind roses, together with the corresponding numbers. Values for air of undefined origin are depicted with grey circles. Unusually high or low concentrations at a given site or sampling period were rescaled; scales are indicated in the top right corner of each panel (Figure 3-3).

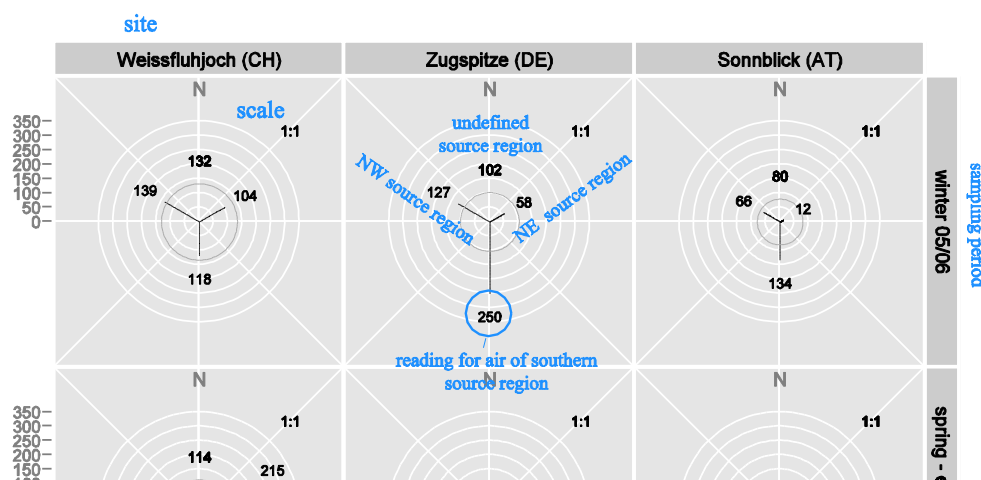


Figure 3-3: Example graph for region-specific pollutant concentrations in air.

3.1.5 Combined atmospheric / deposition data

Some plots combine the concentration of a pollutant in ambient air and in bulk deposition at three alpine summits (p. 9). Blue solid bars indicate the average concentrations (p. 28) in air, black dashed bars those in deposition. The horizontal extent of the bars shows the duration of the sampling period, their vertical position (separate scaling for air and deposition) indicates the concentration whose value is also denoted beside the bars (facing the appropriate y-axis, i.e.: left=deposition, right=atmospheric concentration).

It is important to bear in mind that in these plots atmospheric concentrations for a given sampling period are averages of four separate (direction-specific) measurements, weighted by the actual incidence of air masses arriving from each of the four directions. One might thus discern a sector with high atmospheric concentrations in the wind rose plots (see above section 3.1.4), while the average concentration is much lower, owing to the relatively rare occurrence of wind blowing from that sector.

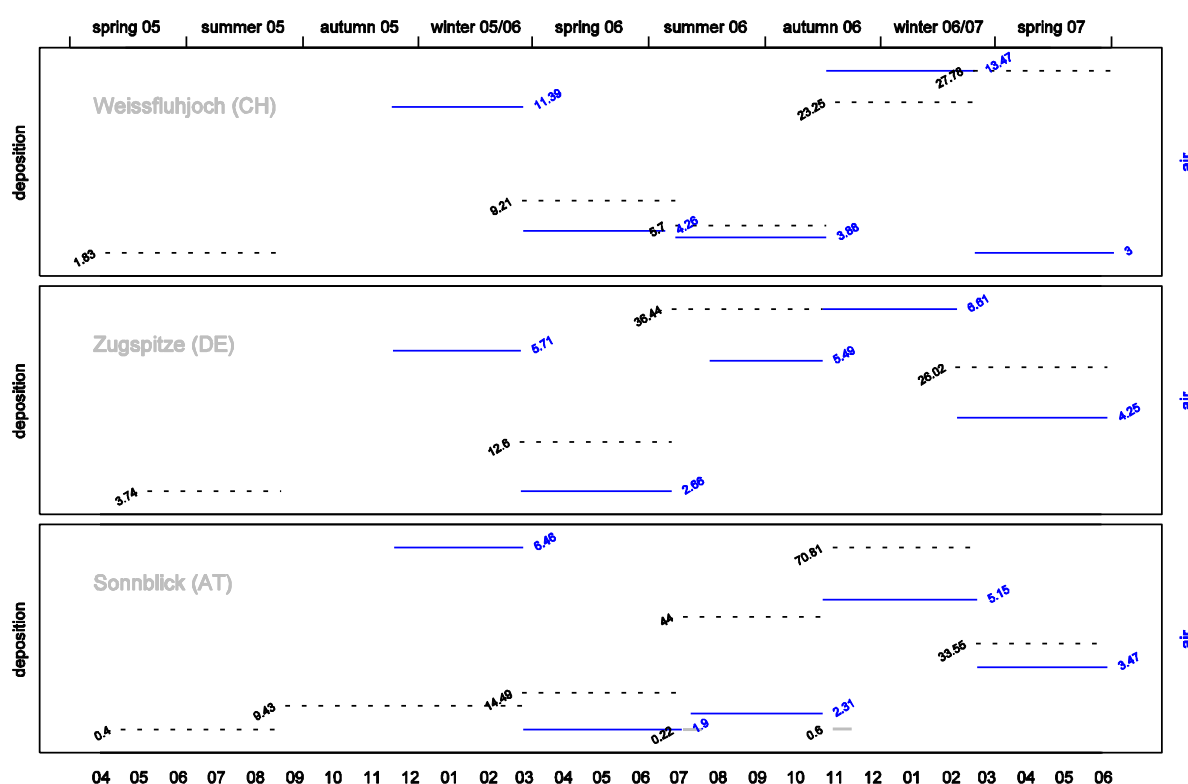


Figure 3-4: Example graph for atmospheric concentration and deposition data.

3.2 Organochloropesticides (OCP)

3.2.1 Characterization

All compounds of this group except HCH are listed in the Stockholm Convention. They include HCH isomers, DDT and metabolites, the structurally very similar cyclodiene insecticides (Aldrin, Dieldrin, Endrin and Heptachlor), the insecticide and flame retardant Mirex and Hexachlorobenzene (HCB).

3.2.1.1 Physicochemical properties

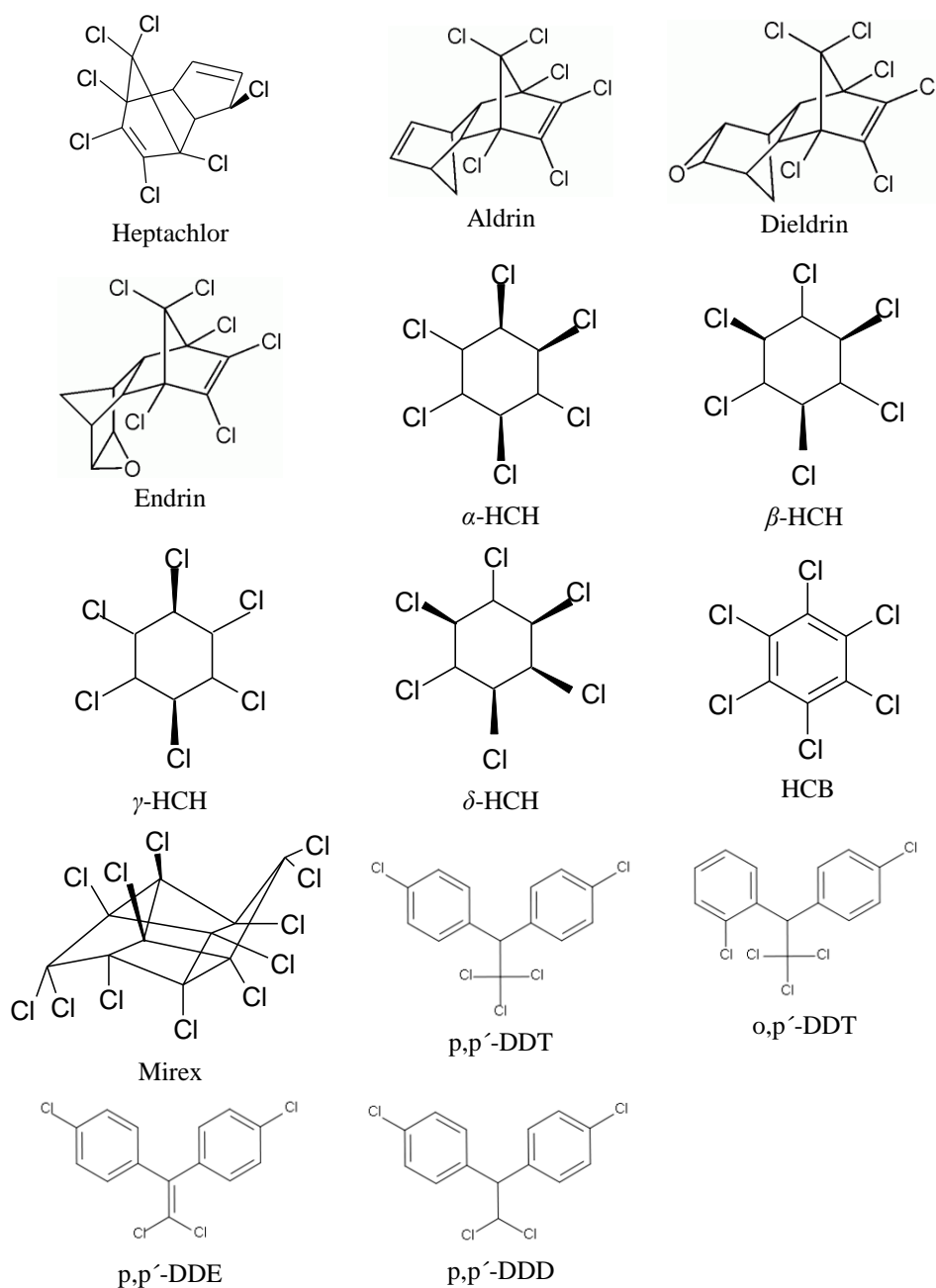


Figure 3-5: Molecular structure of various organochloropesticides

Hexachlorocyclohexane (HCH) isomers

This group consists of five hexachlorocyclohexane (HCH) configurational isomers. These isomers are not planar and their reactivity is determined by the amount of the chlorine substituents in axial or equatorial orientation around the ring. γ -HCH has three, α -HCH two and δ -HCH one axial chlorine(s). The β -isomer has all its chlorines in the equatorial orientation. The γ -conformation is the most reactive isomer. Lindane is the commercial name of the insecticide that has 99 % of the γ -isomer (KEITH 1997).

DDT family

Standard technical mixtures of the pesticide consist of around 70 % p,p'-DDT and 15 % o,p'-DDT. The mixtures also contain DDE, as an impurity. DDD and DDE are also biodegradation products of DDT (KEITH 1997).

3.2.1.2 Emissions and use

The industrial production of organochlorine chemicals started around 1946 and reached maxima between 1960 and 1970; due to growing concern about their persistence, bioaccumulative and toxic properties, most compounds have been restricted or banned worldwide.

HCH isomers are produced commercially. BHC is the standard name for the isomers mixture. Such “technical mixtures” contain around 60-70 % α , 5-12 % β , 10-12 % γ , 6-10 % δ and 3-4 % ϵ isomer (SITTIG 1985). The insecticide Lindane is almost pure (> 99%) γ -HCH and was applied to fruit and vegetable crops, for seed treatment, in forestry and veterinary medicine. In Europe the use of γ -HCH decreased from about 25 000 tons in 1970 to 671 tons in 1990; it has been banned in 2000 (except as a medical treatment against lice: WHO, 2003).

DDT was used since 1946 for agricultural purposes. The world-wide production reached a maximum of 81 154 tons in 1963. In 1970 it was banned in Sweden, 1972 in the United States and later in most countries worldwide, except the use against malaria vectors. Within the alpine region Austria, Germany, Switzerland and Italy 3 861 tons were used in 1970; in 1980 the usage had decreased to 107 tons in these countries (WHO, 2003).

HCB sources are not limited to its past use as a fungicide: it is a by-product of the chemical industry and occurs as impurity in diverse chemicals. In 1972, the unintended creation of HCB as a by-product was estimated at 1 124-2 225 tons (IARC, 1979). HCB is also formed during waste incineration. It is still used in developing countries to fumigate grain.

The use of Heptachlor (HC) as an insecticide is currently restricted to ant control in power transformers. As a pesticide, Endrin is mainly used in cotton and grain production. It has also been used as a rodenticide.

3.2.1.3 Environmental behaviour and bioaccumulation

Organochloropesticides generally resist degradation and they bioaccumulate. They are transported in air and water and adsorb to soil and sediments. Lindan (γ -HCH) can be isomerized by microorganisms and plants to α - and δ -conformers. The analysed DDT isomers (DDT, DDD and DDE in their double ortho and ortho/para forms) adsorb strongly to soil and can resist degradation for more than thirty years (ATDSR, 2002). HCB has an estimated atmospheric half-life of two years and is usually present in the vapour phase. It is also strongly absorbed in soils and sediments. Aldrin is rapidly transformed to Dieldrin, so Dieldrin measurements indicate the immission of either. Dieldrin persists more than seven years in soils. Endrin, a stereoisomer of Dieldrin, persists in soil up to 14 years (KEITH, 1997). The hydrolysis of Heptachlor in soils seems to be substantial. Heptachlor degrades to 1-hydroxychlorde, Heptachlorepoxyde (HCE) and an unidentified metabolite. HCE is a persistent metabolite and bioconcentrates along the food chain (KEITH, 1997).

3.2.1.4 Toxicology

OCP belong to the chemicals that cause long range transboundary air pollution (LRTAP). Their persistence and bioaccumulation pose health risks to humans, mainly via long-time oral uptake. They are highly toxic chemicals with partly carcinogenic, immunotoxic and neurotoxic properties; several substances act as endocrine disruptors.

HCH: Animal studies in mice have revealed neurotoxic, hepatic and reproductive effects and immunotoxicity. β -HCH, the isomer with the strongest bioaccumulation, is known to be a poor agonist for the estrogen receptor (ER). HCH is considered a possible health risk through LRTAP (WHO, 2003).

DDT: The critical issues for human health concern the potential carcinogenicity of DDT, damage to the nervous, reproductive and immune system, and endocrine disruption.

HCB has been shown to cause death, systemic (e.g., liver, skin, bone, and thyroid), neurological, developmental, endocrine, and immunological toxicity in humans. Animal studies have demonstrated that HCB has reproductive toxicity and increases the risk for cancer formation (ATDSR, 2002).

The insecticides Aldrin and Dieldrin (also a breakdown product of Aldrin) are highly toxic and suspected endocrine disruptors. Mirex, a carbamate compound, is possibly carcinogenic and a suspected endocrine disruptor.

Table 3-1: Properties of various organochloropesticides

	MW	vapour pressure [mPa]	at (°C)	solubility in water	at (°C)	log K _{OW}
α -HCH	290.8	5.92	20	10 ppm		3.80
β -HCH	"	4.74×10^{-2}	25	5 ppm		3.78
γ -HCH	"	5.53	20	17 ppm		3.72
δ -HCH	"	4.61	25	10 ppm		4.14
p,p'-DDT	354.5	2.1×10^{-2}	20	0.025 mg l ⁻¹	25	6.91
p,p'-DDE	318.0	7.89×10^{-1}	25	0.12 mg l ⁻¹	25	6.51
p,p'-DDD	320.1	1.78×10^{-1}	25	0.09 mg l ⁻¹	25	6.02
HCB	284.8	1.45	20	0.005 mg l ⁻¹	20	5.50
Heptachlor	373.4	39.5	25	0.056 mg l ⁻¹	25	5.44
Aldrin	364.9					
Dieldrin	380.9			0.19 mg l ⁻¹	25	3.69
Mirex	545.6					

MW...molecular weight

3.2.2 Overview of results

The investigated OCP were nearly ubiquitous, i. e. they could be detected at three alpine summits (except Aldrin) and throughout mountainous forest ecosystems at 1400 m elevation. However, the OCP cocktail varied between the different media. HCB, HCH, DDT and Dieldrin were the most abundant organochloropesticides, whether on alpine summits (measured in air and bulk deposition) or in mountainous forests (Norway spruce needles, forest humus, mineral soil). HCB was the main component of the OCP mix found in air and the second largest fraction in mineral soil, while only ranking third or fourth in the other media. HCH dominated in needles and bulk deposition, especially the γ -isomer at twice the concentration of the α -isomer (the isomer ratio was shifted towards the α - and β -isomers in humus and particularly in mineral soil). In contrast to needles, forest soil (humus and mineral soil layer) was primarily contaminated with members of the DDX family. While p,p'-DDT

prevailed in humus, the *p,p'*-DDE reached twice the concentration of its precursor DDT in mineral soil. Looking at the OCP concentration in needles vs. humus often delivered different, even contrasting images of the geographic distribution of OCP pollution. Usually, needle contamination was highest in the south, while humus pollution peaked in the north. Similarly, average concentrations of a given pollutant (HCB) in needles would show a continuous increase towards the east, while the same substance was most abundant in humus samples from the west. With only few exceptions, the highest contamination was found in one of the lateral zones (north or south, east or west), not in the central part of the study region.

Vertical concentration gradients varied between height profiles, regardless whether concentrations in needles, humus or (extending the profile beyond the treeline) SPMD passive samplers were considered. However, with the exception of the two southern height profiles (Val Vissdende in Italy, Pokljuka in Slovenia), pesticide concentrations in humus tended to increase with height. Different OCP could exhibit similar altitudinal trends at the same profile.

The atmospheric import of OCP into the alpine region - as indicated by air and deposition on three summits - was not constant over the sampling periods but changed, sometimes markedly. The quarterly sampling periods were roughly synchronised with the calendaric change of the seasons. Atmospheric concentrations dropped in the wintertime (except those of Heptachlor). OCP concentrations in air and deposition did not always go in parallel, however. While there was rather good agreement between both media for HCH and DDX, HCB levels for instance increased in air but decreased in deposition from spring to summer. There were also qualitative differences between source regions: air from a particular European region could bear markedly higher concentrations of a given pesticide. Moreover, the source region of highest atmospheric levels could change between seasons and sampling site. As an example, during summer and autumn 2006 Mt. Weissfluhjoch (and the two other sites) received highest atmospheric *p,p'*-DDT concentrations from the northwest, while during winter and spring the maximum contamination arrived from the northeastern source region. Compounds like HCB, Dieldrin, Mirex and Heptachlorine were characterized by at least two major source regions. Particularly HCB - the dominant OCP measured in air - was usually found at similar concentrations in air from all source directions, including air which was not attributable to any European source region.

3.2.3 Summary statistics

3.2.3.1 Needles and soil

OCP concentrations in needles and soil ranged between ppm and ppb (w/w). Generally, concentrations were highest in the humus layer, followed by mineral soil and needles. Humus concentrations could be two orders of magnitude higher than those in the needles (Figure 3-6). The most important OCP (by concentration) in needles were γ -HCH, HCB and *p,p'*-DDT. In soil, however, *p,p'*-DDT or its breakdown product *p,p'*-DDE were the most prominent OCP, followed by Dieldrin or (in humus but *not* mineral soil) γ -HCH. Anyhow, HCB also ranked among the top OCP in soil. The ratio between total HCH and DDX content shifted from needles over humus to mineral soil: while needles contained more HCH than DDX, DDX concentrations were twice as high as those of HCH in humus and 3.6 times as high in mineral soil.

Remarkably, Aldrin was detected in almost all soil samples, while there were no traceable amounts in air or deposition at three alpine summits (p. 38) and only half the needle samples were positive for this substance. Needles and half of the mineral soil samples were also free of Endrin, which was present in the humus layer nonetheless. The OCP mixture in mineral soil differed conspicuously from that in needles or humus, e. g. by a considerably lower ratio of γ -HCH and its breakdown α - and β -isomers and a markedly lower p,p'-DDE : p,p'-DDT ratio.

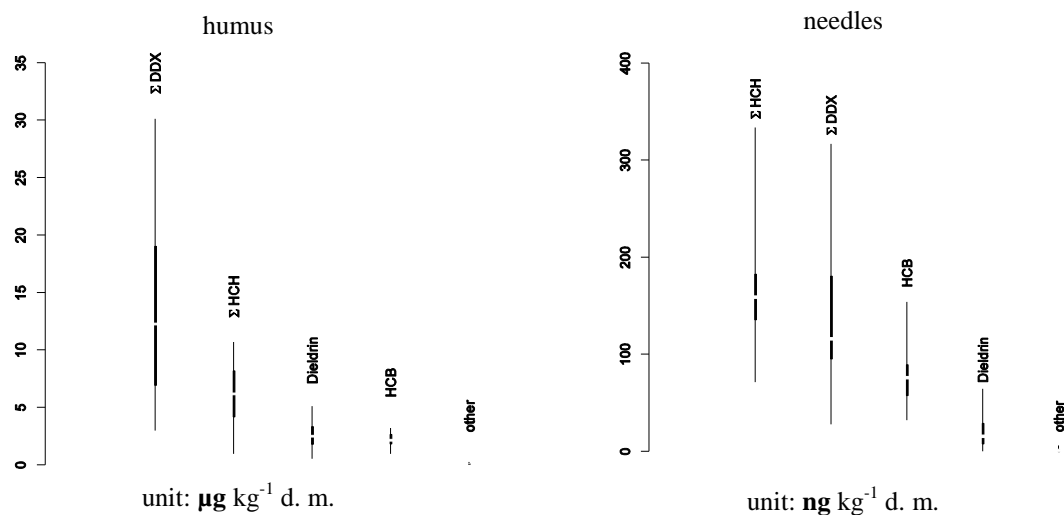


Figure 3-6: Concentration of various OCP in forest humus and 0.5 year old Norway spruce needles.

Table 3-2: Concentration of various OCP in 0.5 year old Norway spruce needles

	n < LOD	mean	sd	min	P ₁₀	P ₂₅	median	P ₇₅	P ₉₀	max
α -HCH	0	50.8	17.9	22.4	30.8	39.6	46.9	60.2	71.9	109
β -HCH	2	5.1	2.1	< LOD	3.3	3.8	5.1	6.4	8.1	9.7
γ -HCH	0	107.9	38.4	29.7	69.2	81.8	105	116	160.2	211
δ -HCH	14	2.4	2.6	< LOD	< LOD	< LOD	1.9	3.5	6	9.8
ϵ -HCH	33	0.3	0.9	< LOD	< LOD	< LOD	< LOD	< LOD	0.6	4.1
Σ HCH		165.5	53.8	71.3	110.5	136.1	159.4	182.5	234.5	333.6
p,p'-DDT	0	67	35.7	20	37.6	43.8	53	81.4	113.2	174
o,p'-DDT	2	19.8	9.4	< LOD	10.4	13.9	18.7	27.4	30.0	40.9
p,p'-DDD	11	1.5	1.4	< LOD	< LOD	< LOD	1.2	2.8	3.7	4.2
o,p'-DDD	16	0.9	1.2	< LOD	< LOD	< LOD	0.5	1.2	3.1	3.8
p,p'-DDE	1	47.9	31.6	< LOD	12	23.4	44.8	67.7	94.6	117
o,p'-DDE	9	2.8	2.6	< LOD	< LOD	1	2.5	3.3	6.4	11.2
Σ DDX		136.9	63.9	27.7	71.8	96.8	116.4	179.9	222.0	316.7
Aldrin	19	0.8	1	< LOD	< LOD	< LOD	< LOD	1.4	1.9	3.8
Dieldrin	2	19.7	15	< LOD	4.3	8.1	16.1	28.9	36.3	64.4
Endrin	36 (sic)									4.3
Mirex	29	0.3	0.6	< LOD	< LOD	< LOD	< LOD	< LOD	1.2	1.9
HCB	0	75.9	25.5	32.1	46.4	57.6	75.7	83.3	109.2	154
Heptachlor	29	0.2	0.5	< LOD	< LOD	< LOD	< LOD	< LOD	1.1	2

unit: ng kg⁻¹ dry mass; LOD...detection limit; sample size n=37

Table 3-3: Concentration of various OCP in forest humus

	n < LOD	mean	sd	min	P ₁₀	P ₂₅	median	P ₇₅	P ₉₀	max
α -HCH	0	1372	770.6	380.2	653.3	826.2	1147	1531	2459	3625
β -HCH	0	1588	1047	211.3	667.0	837.1	1441	2341	3023	4164
γ -HCH	0	3053	1288	349.1	1887	2116	2754	4118	4780	5607
δ -HCH	0	109.8	69.7	8.1	44.4	60.1	97.5	145.6	178.4	306
ϵ -HCH	0	61.9	43.3	4.0	24.3	37.0	50.6	73.9	102.7	213.6
Σ HCH		6184	2440	953	3223	4200	6206	8197	9129	10681
p, p'-DDT	0	8399	5207	1158	2753	4174	6674	12009	15783	19915
o, p'-DDT	0	1888	1091	448.5	927.3	1101	1518	2282	3536	4668
p, p'-DDD	9	47.6	51.1	< LOD	< LOD	< LOD	44.4	68.35	111	183.2
o, p'-DDD	14	16.5	30.2	< LOD	< LOD	< LOD	7.4	20.4	33.5	154.4
p, p'-DDE	0	3611.3	1802	1194	1393	2363	3082	4671	6205	7803
o, p'-DDE	0	65.0	31.2	17.9	29	41.2	60	81.25	111.7	137.4
Σ DDX		14027	7757	2979	6327	6964	12288	19049	27080	30111
Aldrin	0	10.78	6.46	3.1	3.50	5.55	9.00	16.70	19.60	23.8
Dieldrin	0	2558	1027	527.3	1593	1833	2515	3353	3767	5115
Endrin	1	45.6	36.0	< LOD	18.4	20.6	36.0	62.0	80.4	178.4
Mirex	0	53.4	20.4	16.3	38.1	41.1	52.3	58.5	80.8	117.6
HCB	0	2212	587.8	943.7	1353	1835	2173	2667	2900	3187
Heptachlor	3	4.69	2.91	< LOD	2.1	3.1	4.2	5.8	8.9	12.1

unit: ng kg⁻¹ dry mass; LOD...detection limit; sample size n=31**Table 3-4: Concentration of various OCP in forest mineral soil**

	n < LOD	mean	sd	min	P ₁₀	P ₂₅	median	P ₇₅	P ₉₀	max
α -HCH	0	152.3	163.1	13.1	18.1	46.4	80.8	202.5	330.7	611.0
β -HCH	0	294.4	408.2	8.7	21.2	35.0	82.5	401.7	673.7	1624
γ -HCH	0	224.7	258.1	22.2	26.7	59.6	96.7	293.3	564.5	1010
δ -HCH	0	12.2	15.0	0.9	1.2	2.1	4.8	15.4	31.0	51.5
ϵ -HCH	3	4.1	5.2	< LOD	< LOD	1.1	1.8	5.4	8.3	19.2
Σ HCH		688	825	47	69	157	393	993	1332	3312
p, p'-DDT	0	1802	2270	83.0	171.3	254.5	428.0	2288	5635	7132
o, p'-DDT	0	458.2	531.1	39.5	70.6	136.2	255.2	593.3	1058	2021
p, p'-DDD	0	15.2	21.1	0.7	1.7	2.3	4.9	17.7	51.9	72.5
o, p'-DDD	1	4.9	5.6	< LOD	0.8	1.4	2.7	7.8	9.4	21.8
p, p'-DDE	0	1246	1194	176.2	227.5	297.4	830.6	2016	2997	3672
o, p'-DDE	0	16.6	18.2	2.3	2.8	3.4	8.8	20.8	46.3	61.9
Σ DDX		3543	3906	343	462	770	1402	5904	8810	12956
Aldrin	3	7.6	9.8	< LOD	< LOD	1.8	3.4	10.0	25.1	32.6
Dieldrin	0	633.8	647.6	95.3	134.9	176.5	385.7	758.8	1540	2239
Endrin	12	5.3	9.8	< LOD	< LOD	< LOD	< LOD	7.1	20.3	34.4
Mirex	2	12.1	10.4	< LOD	1.2	4.8	11.1	14.3	25.8	38.0
HCB	0	735.0	700.6	87.2	138.8	238.0	479.2	837.7	1798	2441
Heptachlor	9	1.0	1.4	< LOD	< LOD	< LOD	0.7	1.6	2.5	5.3

unit: ng kg⁻¹ dry mass; LOD...detection limit; sample size n=19

3.2.3.2 Deposition and air

HCH levels at Mt. Sonnblick and summer-autumn 2006 DDX levels at Mt. Zugspitze were exceedingly high. At least at Mt. Sonnblick, these values are very probably due to a local source and should therefore not be regarded as background concentrations.

Daily OCP deposition ranged (in orders of magnitude) between 10⁰ and 10³ (where locally influenced: 10⁴) picogram per square metre, atmospheric concentrations between 10⁻² and 10² picogramm per cubic metre.

All investigated OCP were detected in both ambient air and bulk deposition at three alpine summits (except Aldrin, which was found in neither air nor deposition). However, their abundance varied between air and bulk

deposition. Mirex and Heptachlor, for example, seldom reached detectable concentrations in deposition but were routinely found in air samples. On the contrary, Endrin was more frequently detected in deposition.

In air, HCB was clearly the most prominent OCP, followed by HCH (sum of α - ϵ isomers) which in turn amounted to about five times the total DDX concentration. This ratio is higher than in needles and opposite to that found in humus and mineral soil of mountainous spruce forests (p. 36). Like in spruce needles and forest soil, Dieldrin was the most abundant cyclodien.

Atmospheric concentrations of most OCP (HCH, DDX, HCB, Dieldrin, Mirex) concentrations were lowest in the wintertime and typically rose during spring and summer. Endrin, however showed some atypical highs during winter 2005/6, apart from the conspicuously high values in spring 07 (Figure 3-13).

In contrast to air, OCP deposition was clearly dominated by HCH concentrations which were several times higher than those of DDT related compounds, the secondmost abundant OCP class. Dieldrin was the most prominent cyclodien, while HCB – unlike in air, needles and forest soil – contributed only little to OCP bulk deposition.

Table 3-5: Deposition of various OCP on three alpine summits

	Period	α -HCH	β -HCH	γ -HCH	δ -HCH	ϵ -HCH	Σ -HCH	p,p'-DDT	o,p'-DDT	p,p'-DDD	o,p'-DDD	p,p'-DDE	o,p'-DDE	Σ -DDX
Weissfluh	A	939.8	86.58	2878	54.26	18.99	3978	156.1	32.56	7.65	4.44	56.24	1.87	258.9
	B	157.8	10.02	352	13.65	2.13	536	70.0	13.78	3.76	2.38	18.79	0.75	109.5
	C	339.8	48.26	1565	38.91	23.79	2016	164.1	39.59	8.50	3.74	55.90	2.04	273.9
	D	712.8	71.06	2218	40.64	20.43	3063	148.9	28.83	11.58	2.95	51.76	2.27	246.3
	E	127.8	13.16	276	20.02	2.52	439	80.9	16.10	0.87	8.96	20.72	1.54	129.1
	F	424.7	33.24	1241	22.33	11.42	1732	171.2	26.86	13.93	4.87	59.43	1.44	277.8
Zugspitze	A	2173	257.9	5971	129.1	69.41	8601	126.9	40.33	9.69	6.57	66.59	4.69	254.8
	B	583.6	53.22	1584	80.47	9.26	2310	671.0	192.31	26.22	19.03	194.1	10.80	1114
	C	592.6	92.15	3446	74.96	25.48	4231	349.6	99.55	19.56	9.48	144.9	7.11	630.2
	D*	1010	128.2	3413	69.42	29.02	4650	10290	3854	401.7	152.3	6956	355.2	22010
	E**													
	F	735.4	95.78	3043	85.11	< LOD	3959	723.6	205.80	34.40	15.72	326.20	14.23	1320
Sonnblick	A***	1235	103.6	12625	74.21	28.39	14066	149.2	45.07	16.68	8.47	73.21	3.49	296.1
	B	647.3	64.01	4132	66.53	8.27	4918	137.0	48.19	15.46	11.87	105.01	5.39	322.9
	C	714.6	83.13	7505	57.45	< LOD	8361	149.0	42.50	8.87	4.34	74.73	3.13	282.6
	D***	860.0	87.29	10311	51.17	19.35	11329	125.1	40.85	13.33	7.31	67.94	3.61	258.2
	E	743.4	122.8	6328	121.7	17.29	7333	217.2	87.48	46.34	50.14	108.6	7.26	517.0
	F	287.6	50.33	5687	39.91	8.92	6074	101.4	33.22	11.90	8.18	58.51	3.22	216.4

unit: $\text{pg m}^{-2} \text{d}^{-1}$; * high DDX concentrations during summer-autumn 06 at Mt. Zugspitze perhaps due to local influence; ** sample destroyed; *** high γ -HCH values probably due to local influence; sampling periods: A...spring-late summer 2005, B...late summer 2005-late winter 2006, C...late winter-summer 2006, D...summer-autumn 2006, E...autumn 2006-late winter 2007, F...late winter-spring 2007

Table 3-5 (continued): Deposition of various OCP on three alpine summits

		Dieldrin	Endrin	Mirex	HCB	Heptachlor
Weissfluhjoch	A	352.7	11.59	< LOD	57.72	< LOD
	B	182.8	10.65	< LOD	13.78	< LOD
	C	300.8	13.59	< LOD	91.59	3.74
	D	290.6	14.53	1.04	54.48	< LOD
	E	130.1	8.54	0.50	10.36	< LOD
	F	240.1	60.61	1.24	95.19	< LOD
Zugspitze	A	315.8	24.07	< LOD	96.29	< LOD
	B	938.4	68.90	< LOD	55.79	< LOD
	C	530.4	69.92	< LOD	119.70	4.15
	D	515.5	28.56	< LOD	69.19	2.32
	E*					
	F	646.5	262.74	< LOD	27.87	0.83
Sonnblick	A	1008.5	38.35	< LOD	85.91	< LOD
	B	992.5	69.05	< LOD	67.97	< LOD
	C	616.5	26.15	1.63	131.71	2.62
	D	537.5	28.38	1.42	76.54	< LOD
	E	902.5	71.23	4.15	95.44	< LOD
	F	451.2	81.56	2.31	57.76	< LOD

unit: $\text{pg m}^{-2} \text{d}^{-1}$; * sample destroyed; LOD... detection limit; sampling periods: A...spring-late summer 2005, B...late summer 2005-late winter 2006, C...late winter-summer 2006, D...summer-autumn 2006, E...autumn 2006-late winter 07, F...late winter-spring 2007

Table 3-6: Atmospheric concentrations of various OCP at three alpine summits

	period	α -HCH	β -HCH	γ -HCH *	δ -HCH	ϵ -HCH	Σ HCH *	p, p'-DDT	o, p'-DDT	p, p'-DDD	o, p'-DDD	p, p'-DDE	o, p'-DDE	Σ DDX
Weissfluh	I	5.81	0.03	4.19	0.05	< LOD	10.10	0.70	0.44	0.01	0.01	1.13	0.13	2.43
	II	10.67	0.18	18.73	0.10	0.07	29.75	2.36	1.37	0.10	0.03	1.51	0.15	5.53
	III	18.96	0.16	16.85	0.05	0.06	36.10	2.62	1.49	0.13	0.02	2.10	0.19	6.55
	IV	6.99	0.06	4.65	0.05	0.02	11.78	1.13	0.63	0.02	0.09	1.12	0.16	3.15
	V	11.40	0.18	13.93	0.02	< LOD	25.62	2.01	1.15	0.07	0.04	1.54	0.17	4.99
Zugspitze	I	2.73	< LOD	2.64	< LOD	< LOD	5.70	< LOD	0.03	< LOD	0.01	0.47	0.05	0.78
	II	5.78	0.12	13.15	0.07	0.07	19.22	0.41	0.47	0.01	0.01	0.68	0.10	1.69
	III **	20.42	0.33	31.84	0.14	0.12	52.86	7.69	4.64	0.04	0.72	9.53	0.76	23.38
	IV	5.03	0.04	4.42	0.04	0.01	9.56	0.63	0.68	0.01	0.02	1.47	0.21	3.01
	V	13.94	0.30	24.55	0.14	< LOD	38.96	1.90	1.81	0.04	0.06	3.76	0.46	8.03
Sonnblick	I	5.59	0.02	38.08	0.07	0.01	43.82	0.32	0.29	0.03	0.12	0.96	0.12	1.84
	II	11.06	0.19	405.91	0.13	0.03	417.38	0.46	0.51	< LOD	< LOD	0.81	0.07	1.87
	III	14.11	0.19	375.90	0.11	0.05	390.42	0.42	0.60	0.05	0.03	1.05	0.10	2.26
	IV	6.80	0.05	73.90	0.04	0.02	80.84	0.19	0.33	< LOD	0.01	0.92	0.11	1.57
	V	12.27	0.23	383.88	0.05	< LOD	396.46	0.49	0.55	0.01	0.02	1.57	0.13	2.78

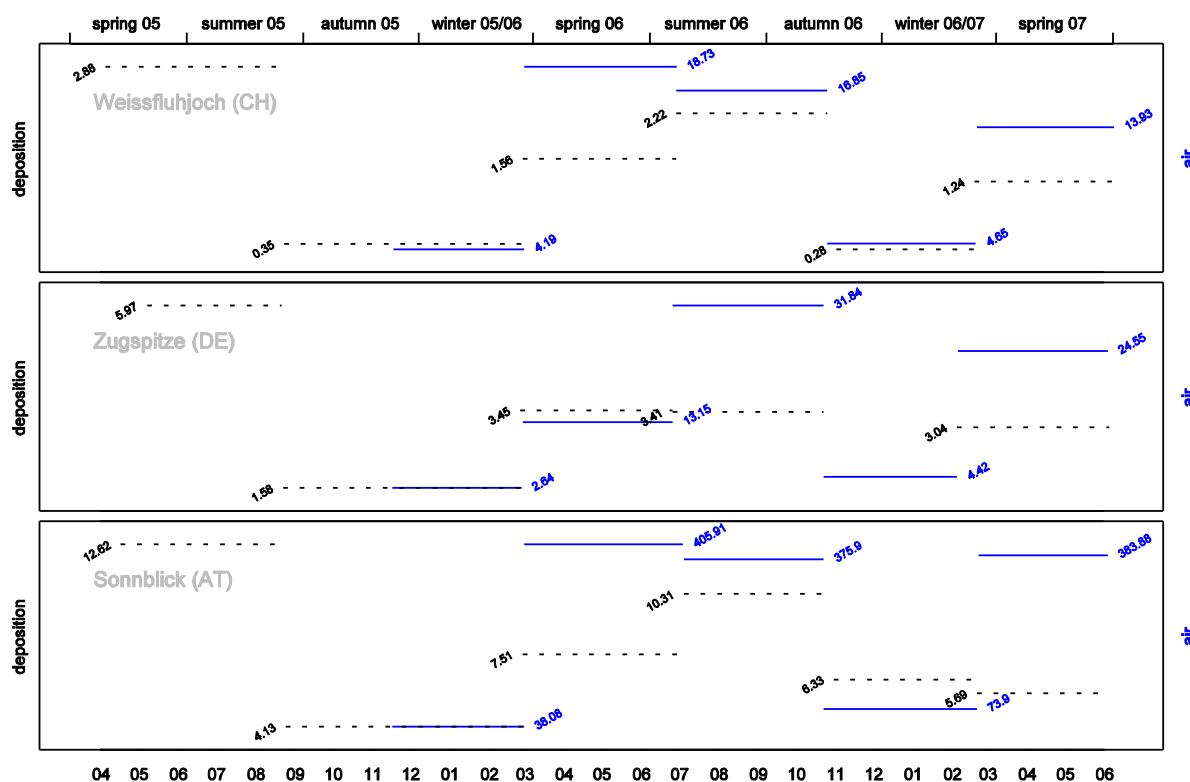
unit: pg m^{-3} at 0 °C and 1013 hPa; LOD...detection limit; * **High γ -HCH concentrations at Mt. Sonnblick probably stem from a local source.** ** **Elevated DDX levels at Mt. Zugspitze perhaps influenced locally.** Sampling periods: I...winter 2005/6, II...spring-early summer 2006, III...early summer-late autumn 2006, ..., IV...late aut. 2006-late winter 2007, V...spring 2007

Table 3-6 (continued) Atmospheric concentrations of various OCP at three alpine summits

	period	Dieldrin	Endrin	Mirex	HCB	Hepta-chlorine
Weissfluh-joch	I	1.25	< LOD	0.04	54.81	0.07
	II	2.88	< LOD	0.10	84.51	0.06
	III	3.45	0.08	0.13	120.10	0.06
	IV	1.32	0.10	0.08	77.15	0.07
	V	2.32	0.33	0.09	80.85	0.04
Zugspitze	I	0.15	< LOD	0.08	71.90	< LOD
	II	0.96	< LOD	0.02	35.77	0.01
	III	4.04	0.18	0.12	108.92	0.07
	IV	0.83	0.04	0.06	54.22	0.04
	V	2.50	0.22	0.09	97.64	0.05
Sonnblick	I	1.06	< LOD	0.06	52.91	0.04
	II	1.64	< LOD	0.05	63.18	0.03
	III	1.87	0.06	0.08	75.63	0.03
	IV	1.19	0.11	0.08	65.09	0.05
	V	1.18	0.12	0.07	84.00	0.03

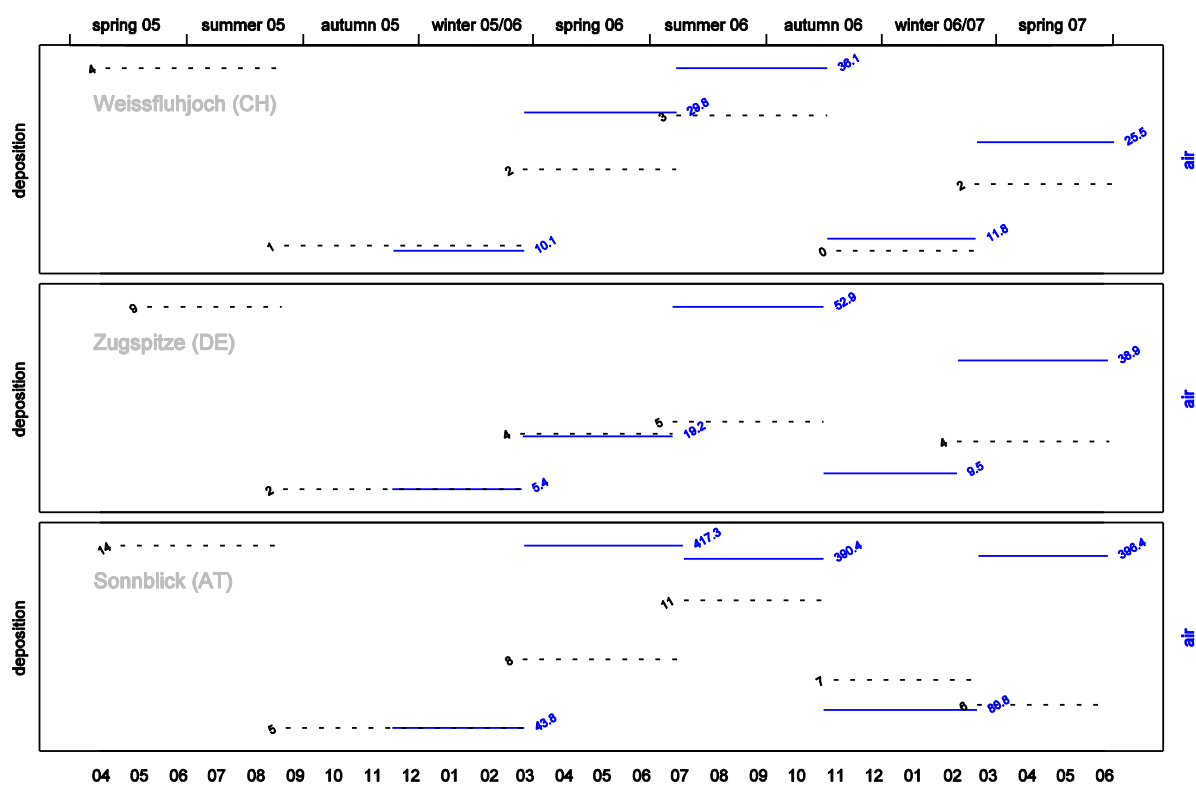
unit: pg m^{-3} at 0 °C and 1013 hPa; LOD...detection limit

The following figures illustrate OCP concentrations in air and deposition at three alpine summits. An instruction to interpret the graphs can be found on page 32.



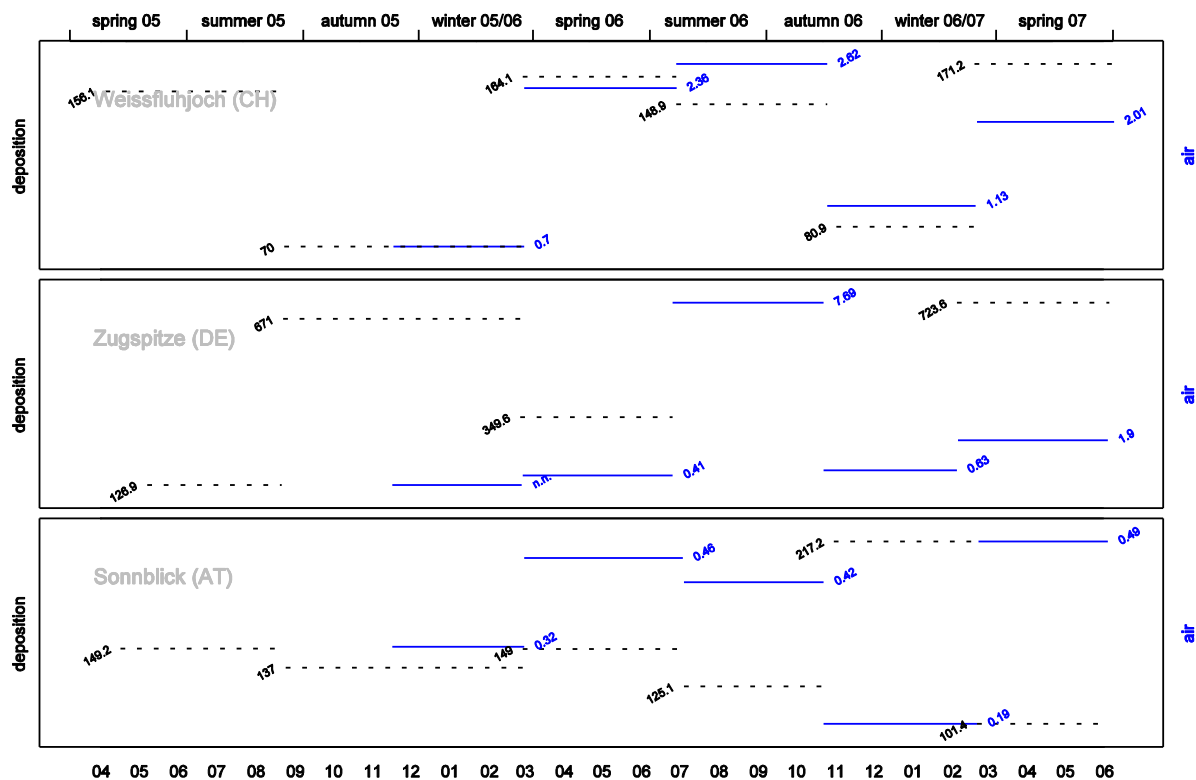
units: deposition: $\text{ng m}^{-2} \text{d}^{-1}$, air: pg m^{-3}

Figure 3-7: Concentration of γ -HCH in deposition (---) and ambient air (—) on three alpine summits.



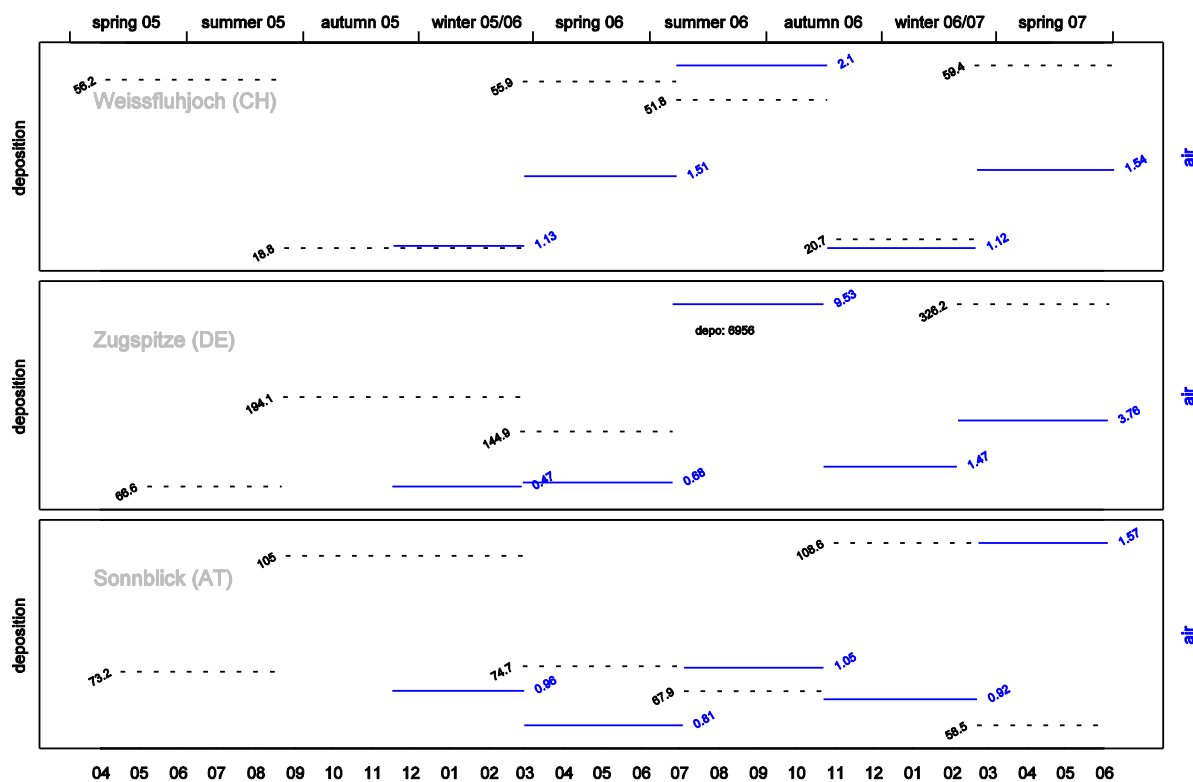
units: deposition: ng m⁻² d⁻¹, air: pg m⁻³

Figure 3-8: Total HCH concentration (sum of α - ϵ -isomers) in deposition (---) and ambient air (—) on three alpine summits.



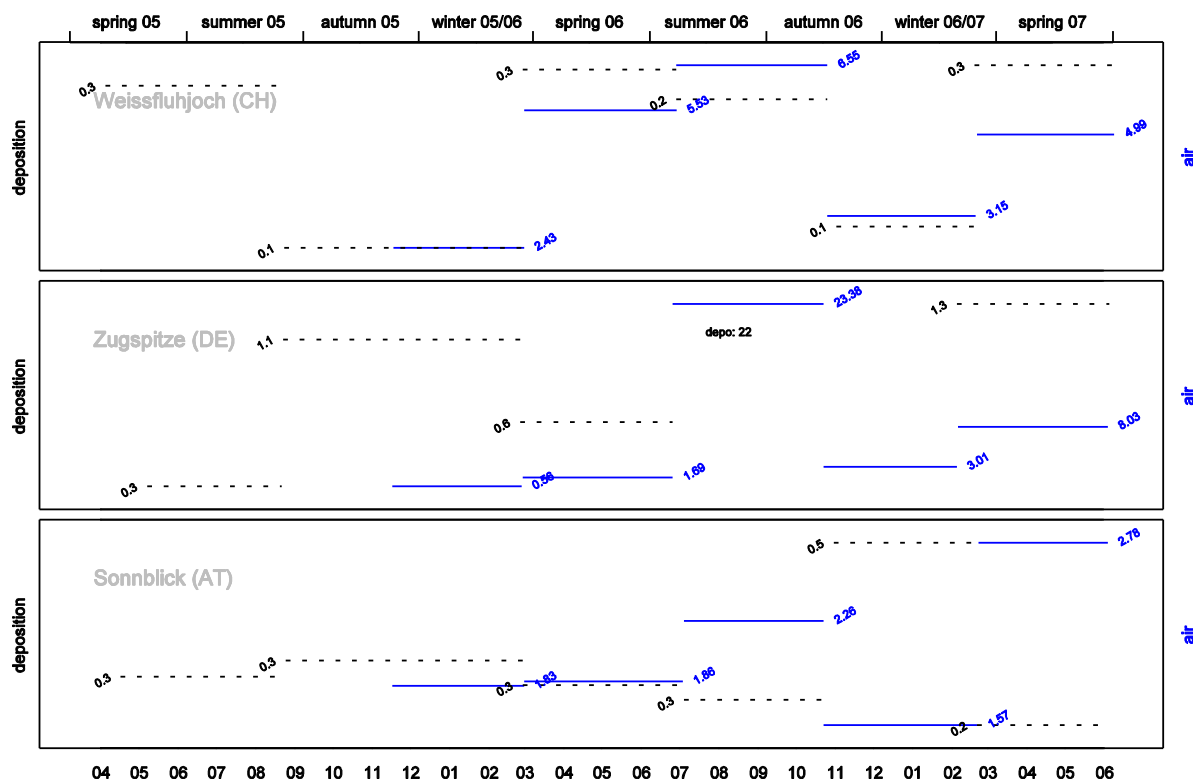
units: deposition: pg m⁻² d⁻¹, air: pg m⁻³

Figure 3-9: Concentration of p,p' -DDT in deposition (---) and ambient air (—) on three alpine summits.



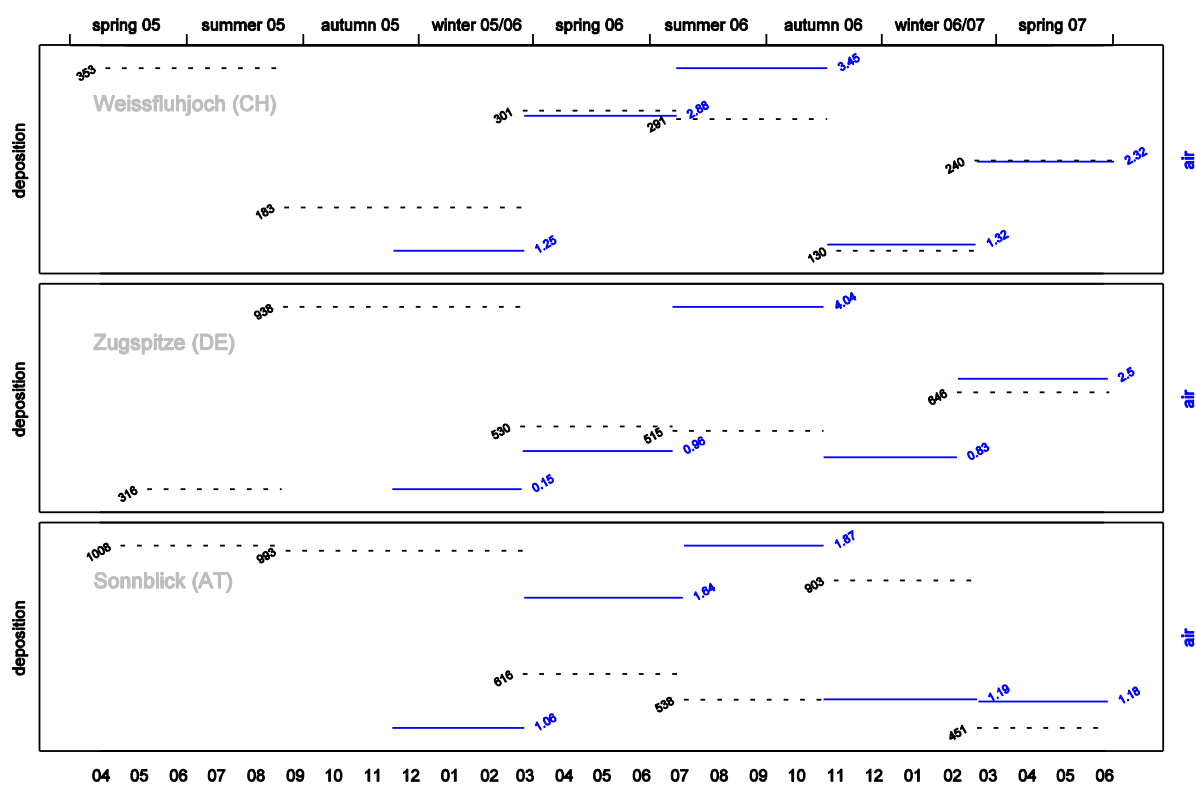
units: deposition: $\text{pg m}^{-2} \text{d}^{-1}$, air: pg m^{-3}

Figure 3-10: Concentration of *p,p'*-DDE in deposition (---) and ambient air (—) on three alpine summits. Note extremely high deposition rates ($6.96 \text{ ng m}^{-2} \text{d}^{-1}$) at Mt. Zugspitze during summer–autumn 2006.



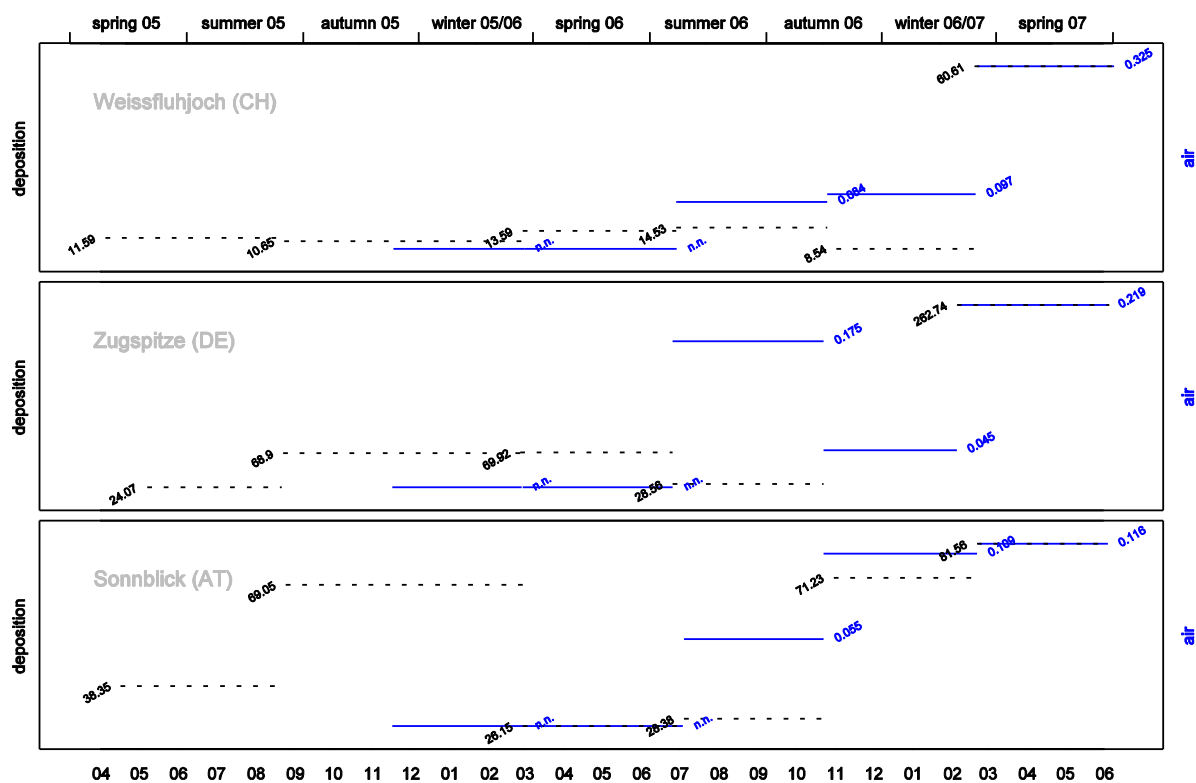
units: deposition: $\text{ng m}^{-2} \text{d}^{-1}$, air: pg m^{-3}

Figure 3-11: Total DDX content of deposition (---) and ambient air (—) on three alpine summits. Note extremely high deposition rates ($22 \text{ ng m}^{-2} \text{d}^{-1}$) at Mt. Zugspitze during summer–autumn 2006.



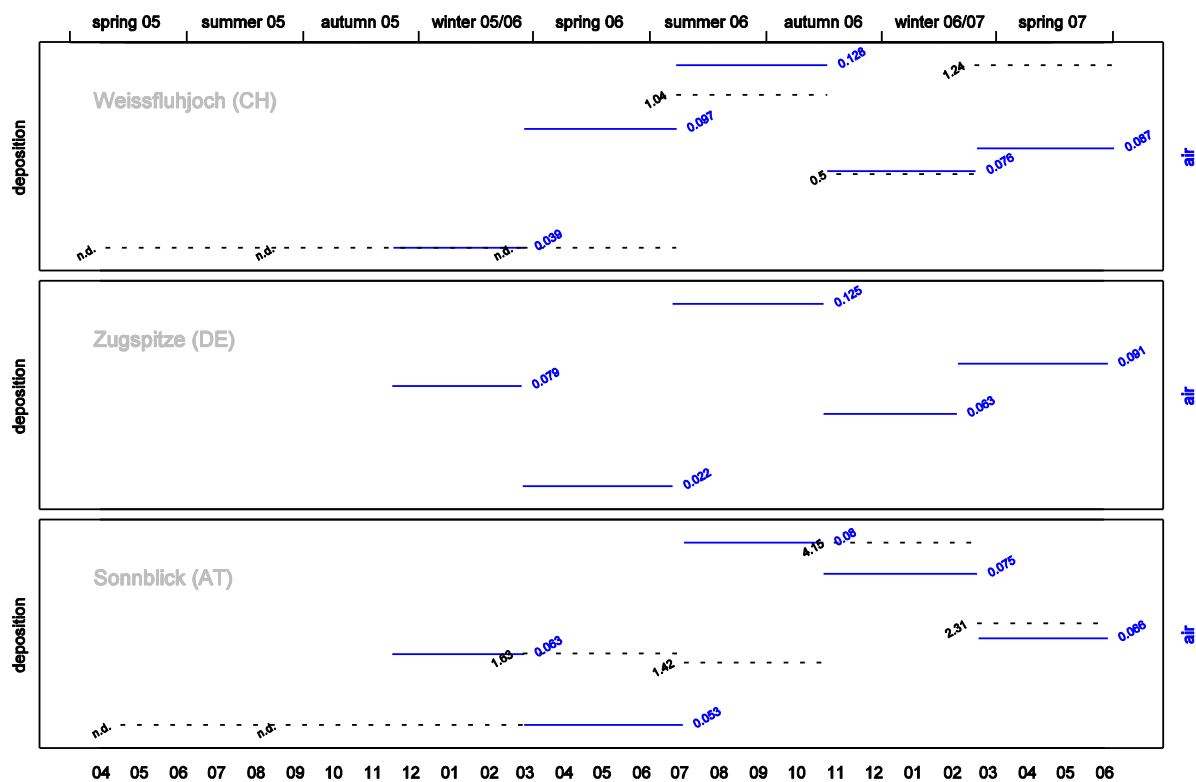
units: deposition: $\text{pg m}^{-2} \text{d}^{-1}$, air: pg m^{-3}

Figure 3-12: Dieldrin concentration in deposition (---) and ambient air (—) on three alpine summits.



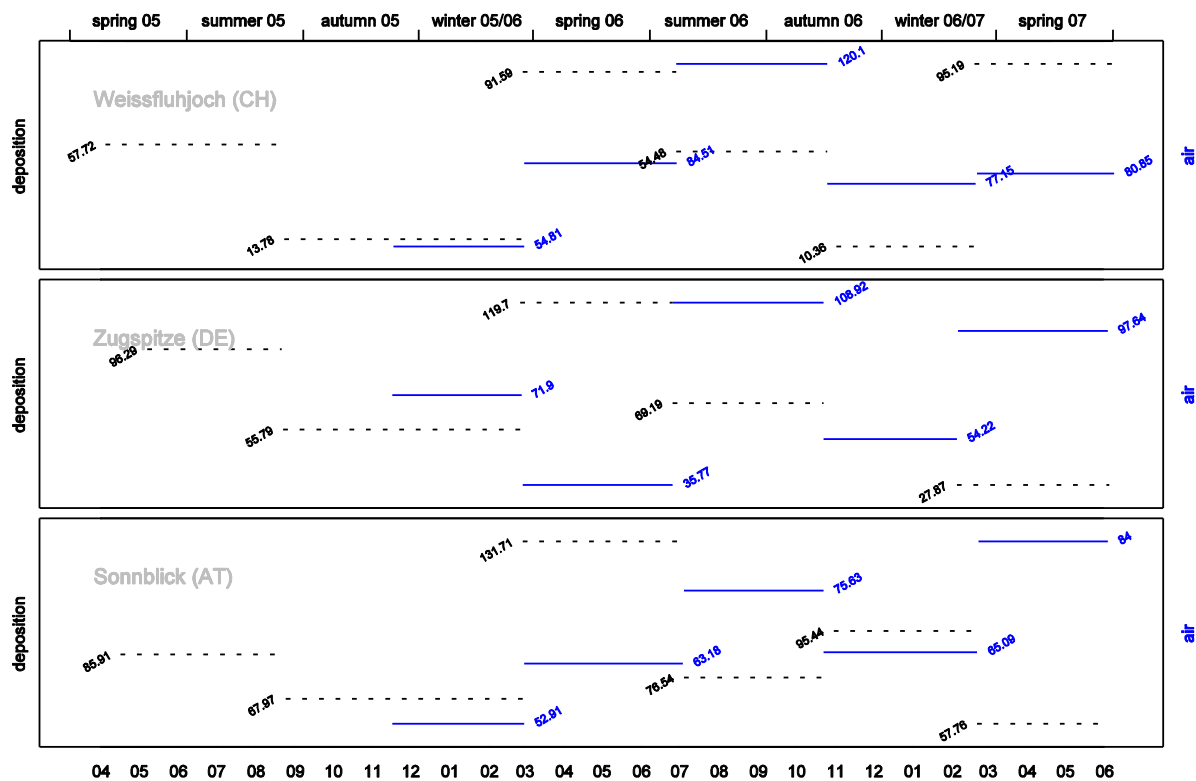
units: deposition: $\text{pg m}^{-2} \text{d}^{-1}$, air: pg m^{-3}

Figure 3-13: Endrin concentration in deposition (---) and ambient air (—) on three alpine summits.



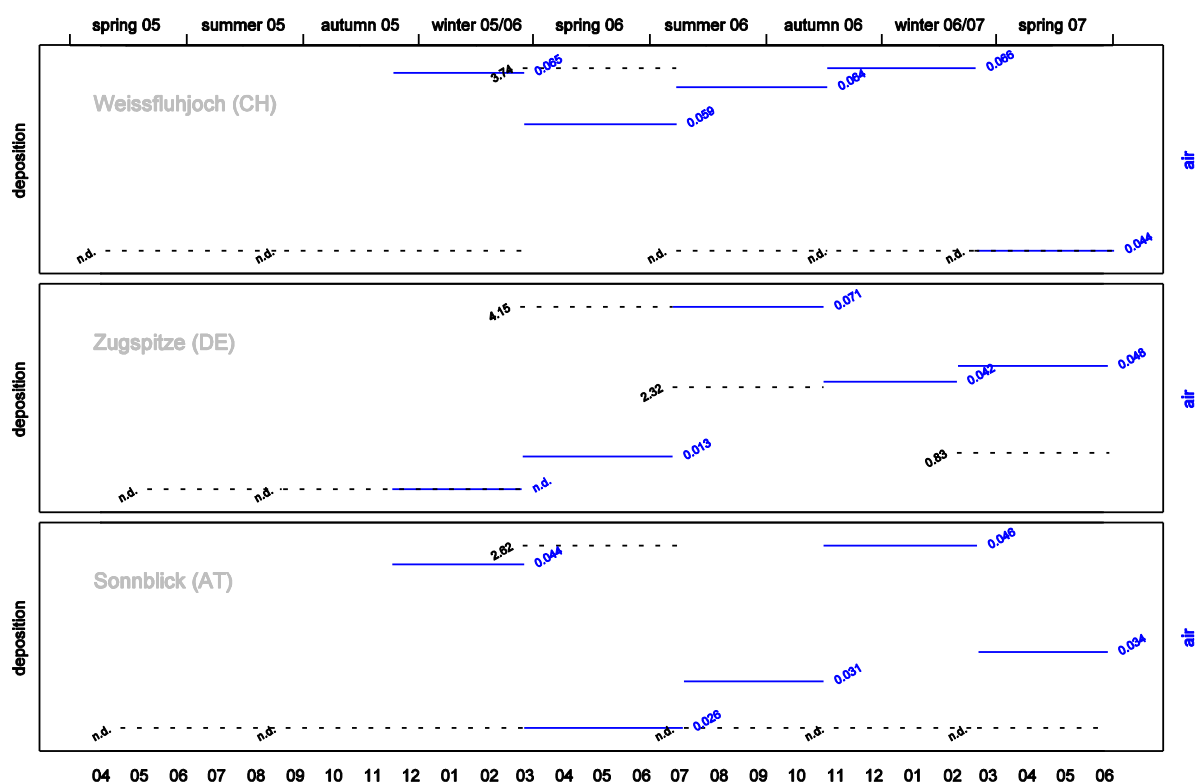
units: deposition: pg m⁻² d⁻¹, air: pg m⁻³

Figure 3-14: Mirex concentration in deposition (---) and ambient air (—) on three alpine summits.



units: deposition: pg m⁻² d⁻¹, air: pg m⁻³

Figure 3-15: HCB concentration in deposition (---) and ambient air (—) on three alpine summits.



units: deposition: $\text{pg m}^{-2} \text{d}^{-1}$, air: pg m^{-3}

Figure 3-16: Heptachlor concentration in deposition (---) and ambient air (—) on three alpine summits.

3.2.4 Spatial variation

As a general pattern with few exceptions, the highest OCP contamination was always found in the eastern or western zone of the study region. The middle zone was the least polluted, at least regarding the most prominent OCP (total HCH, DDX, Dieldrin). The strongest longitudinal contrasts were found for needles DDX concentrations. Accordingly, differences between longitudinal zones turned out statistically significant for DDX and Dieldrin in needles but not for the corresponding concentrations in humus where longitudinal concentration gradients were less pronounced. Total DDX as well as Dieldrin content in needles were highest in the west, and minimal in the middle.

As observed for the longitudinal differences, the highest OCP concentrations were usually found in one of the lateral zones, i. e. in the north or the south of the study area - regardless of the investigated matrix. Total DDX content of needles was far higher in the south but in humus DDX sums of the northern and southern band were similar. Top γ -HCH levels in humus were found in the north, however the latitudinal gradient was much steeper in humus than in needles. Altogether, OCP contamination was more severe in the south for needles but in the north for humus.

3.2.4.1 Needles

To recapitulate, HCB, γ -HCH and p,p'-DDT were the most abundant OCP found in spruce needles. The spatial distribution of HCB in needles did not exhibit a strong gradient, but concentrations in the centre were higher than in the north or south of the study region. This pattern is exceptional not only among the OCP but all investigated

pollutants which usually tended to peak in either of the lateral zones of the investigated area. In this context it is interesting that even at the low average temperatures at mountain tops, deposition was poor in HCB (p. 38) which nonetheless constituted a major fraction of airborne OCP at these summits.

Higher γ -HCH (and total HCH) concentrations appeared in the eastern part of the study region, although there were no significant longitudinal differences. Latitudinal trends varied between HCH isomers: while average α -HCH levels were highest in the south, the β - and particularly the δ -isomers peaked in the north.

Strong and significant differences between the western, middle and eastern third of the study region were observed for DDX, with the highest DDT concentrations found in the West.

Of the remaining OCP, the spatial distribution of Aldrin differed from the common pattern (highest concentrations in one of the lateral zones) because Aldrin levels were elevated in the middle part of the study region. Interestingly, humus samples showed the opposite pattern (p. 56).

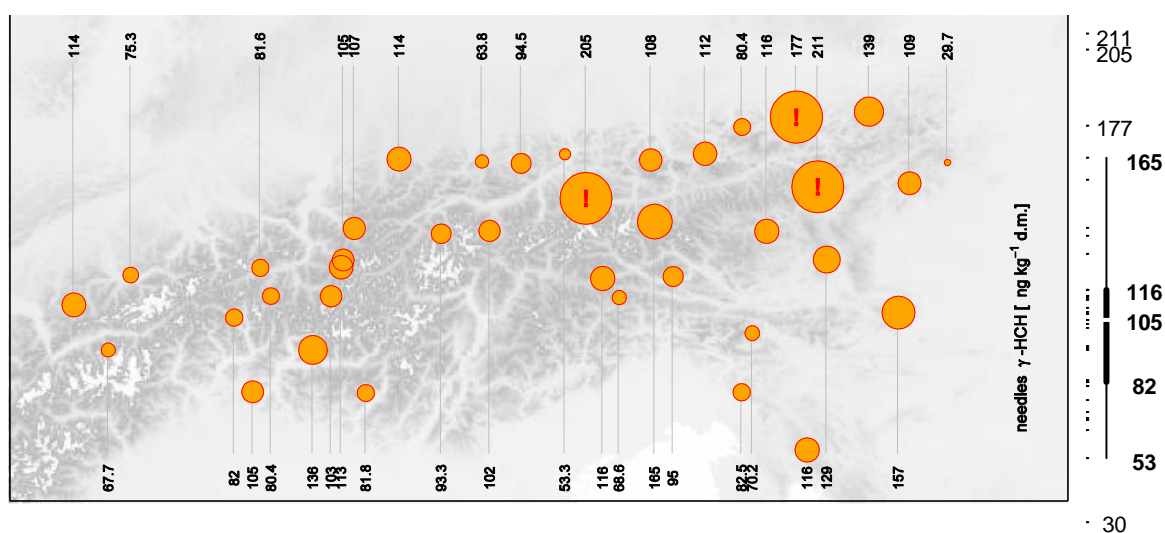


Figure 3-17: Needle γ -HCH content

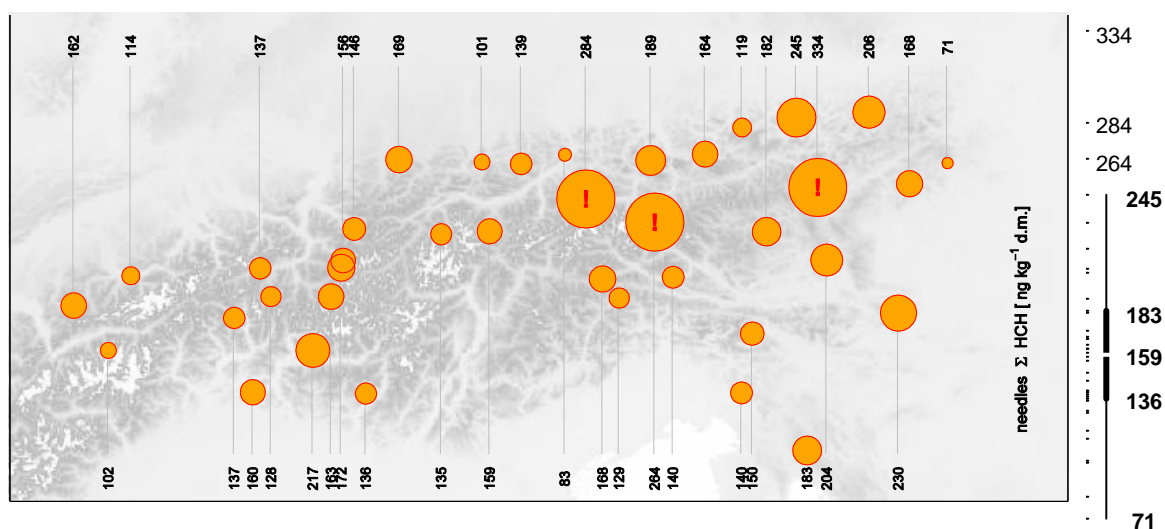


Figure 3-18: Needle total HCH content (sum of α - ϵ isomers)

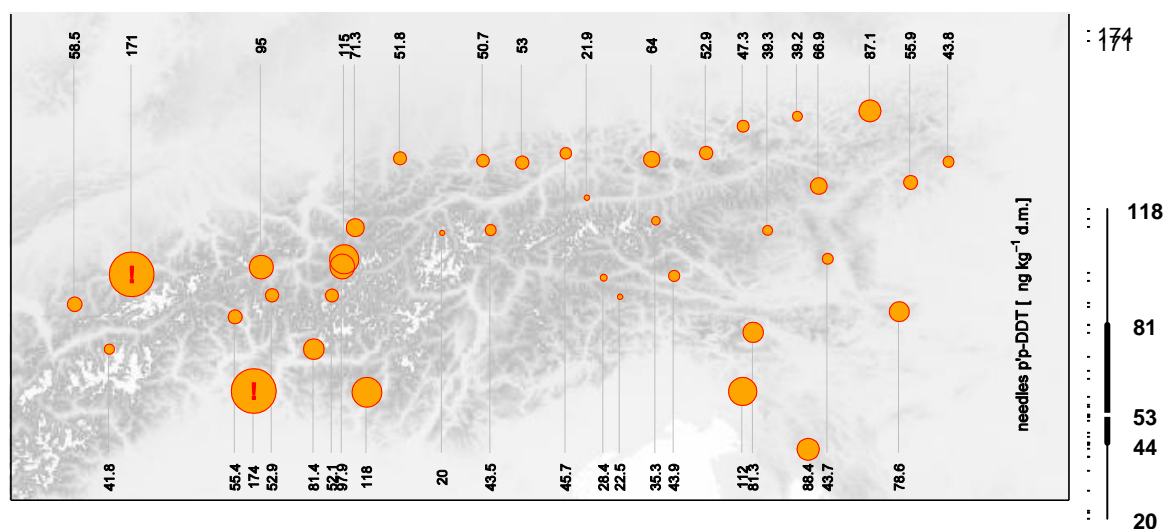


Figure 3-19: Needle *p,p'*-DDT content

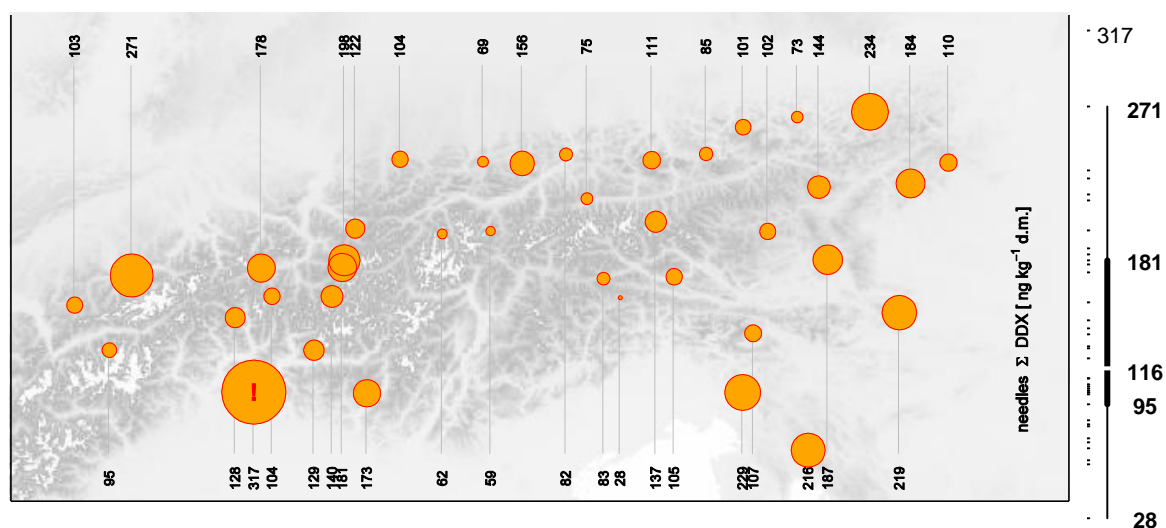


Figure 3-20: Needle DDX content (sum of DDT, DDD and DDE isomers)

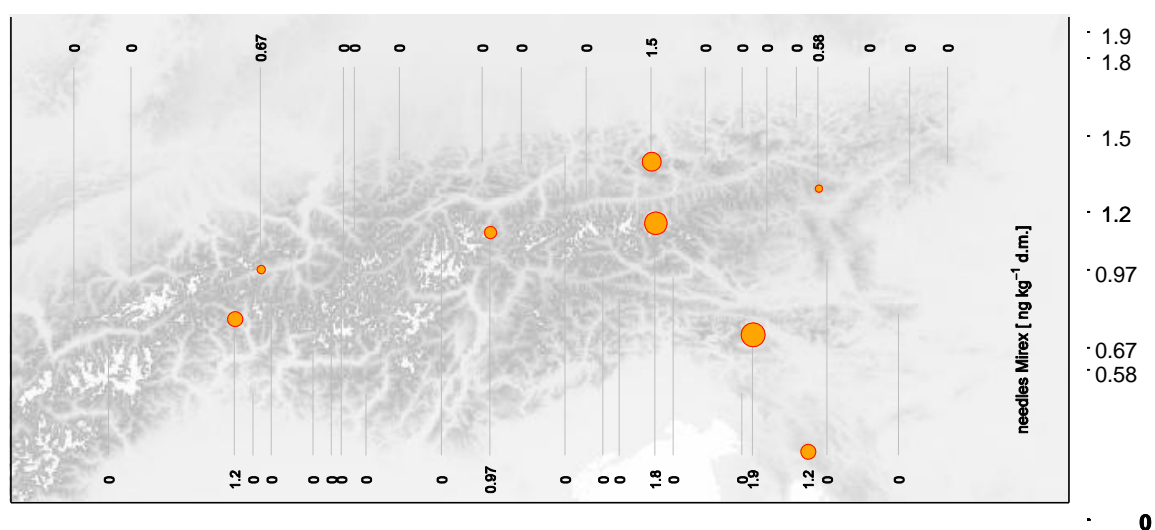


Figure 3-21: Needle Mirex content

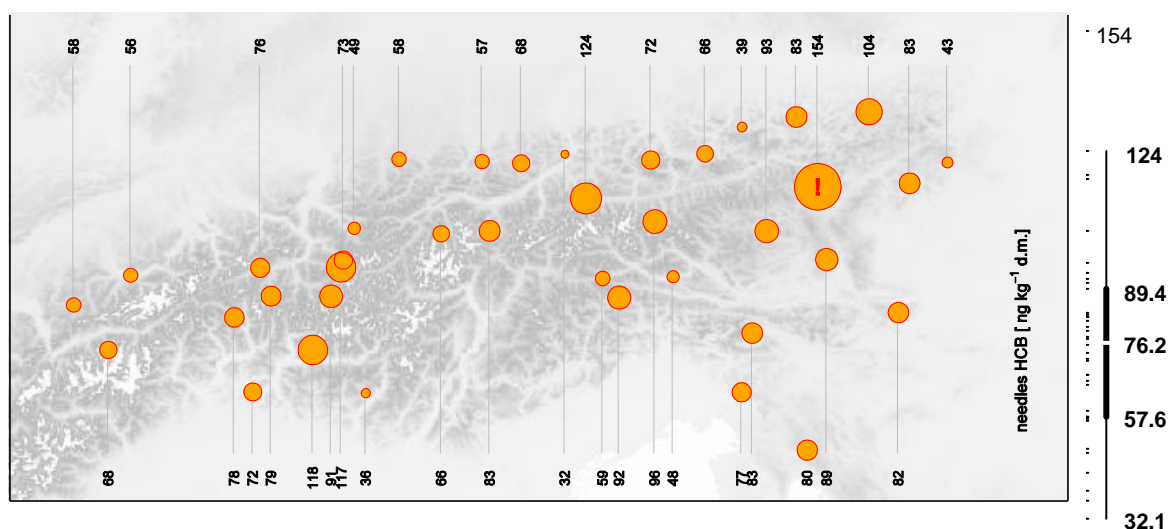


Figure 3-22: Needle HCB content

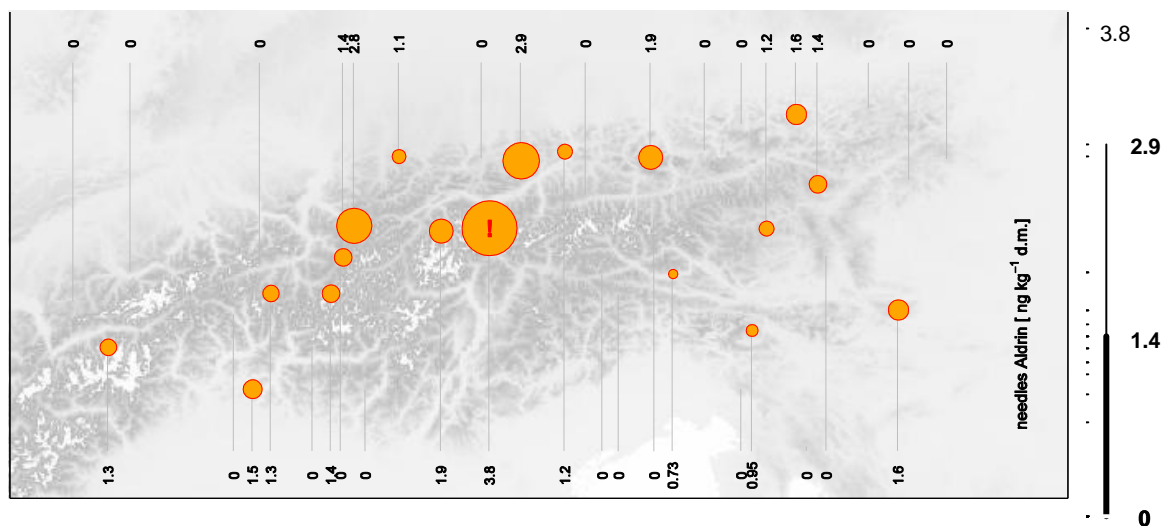


Figure 3-23: Needle Aldrin content

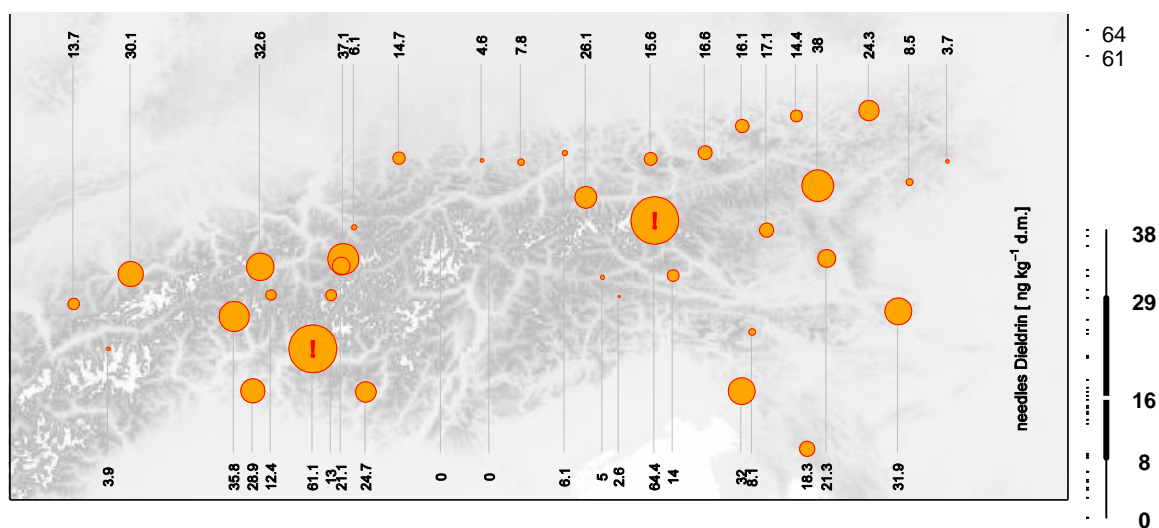


Figure 3-24: Needle Dieldrin content

Endrin was only detected in needles from site AT-43-3 at a concentration of 4.3 ng kg⁻¹ d. m.

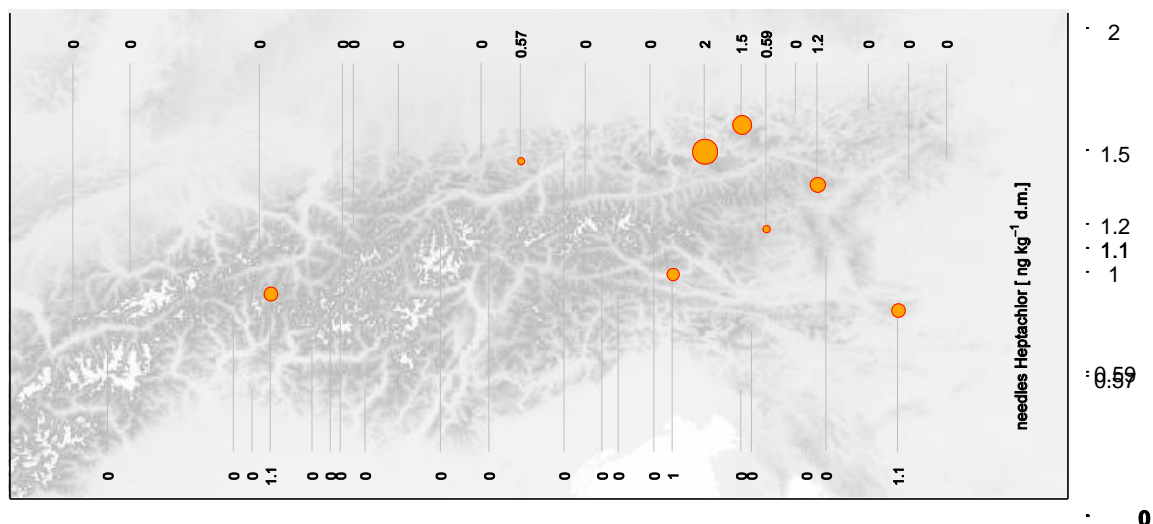


Figure 3-25: Needle Heptachlor content.

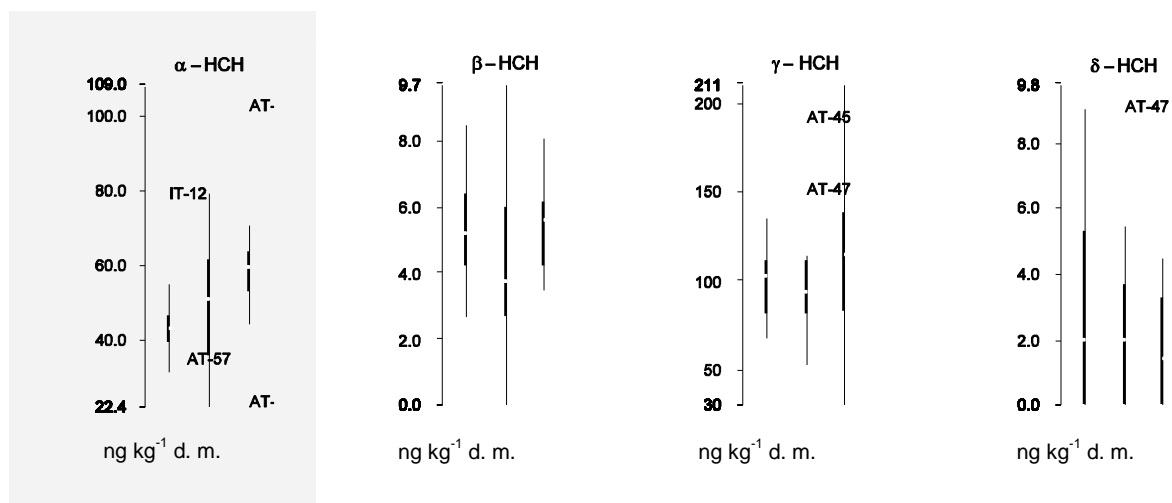
Longitudinal differences

Significant longitude related differences (Kruskal-Wallis test) for the whole study region were discovered for DDX isomers (p,p' -DDT: $p=0.001$, o,p' -DDT: $p=0.019$, p,p' -DDD: $p<0.001$), total DDX content ($p=0.006$) and Dieldrin ($p=0.047$).

Groupwise comparison confirmed significant differences (Mann-Whitney test, $p<0.05$) between:

- west and middle for both DDT isomers, p,p' -DDD, total DDX content and Dieldrin
- middle and east for both DDT isomers, p,p' -DDD, total DDX content and Dieldrin
- west and east for α -HCH and p,p' -DDD

The magnitude of the longitudinal differences can be estimated from Figure 3-26 (a grey background indicates significant differences either over the whole study region or between two site groups).



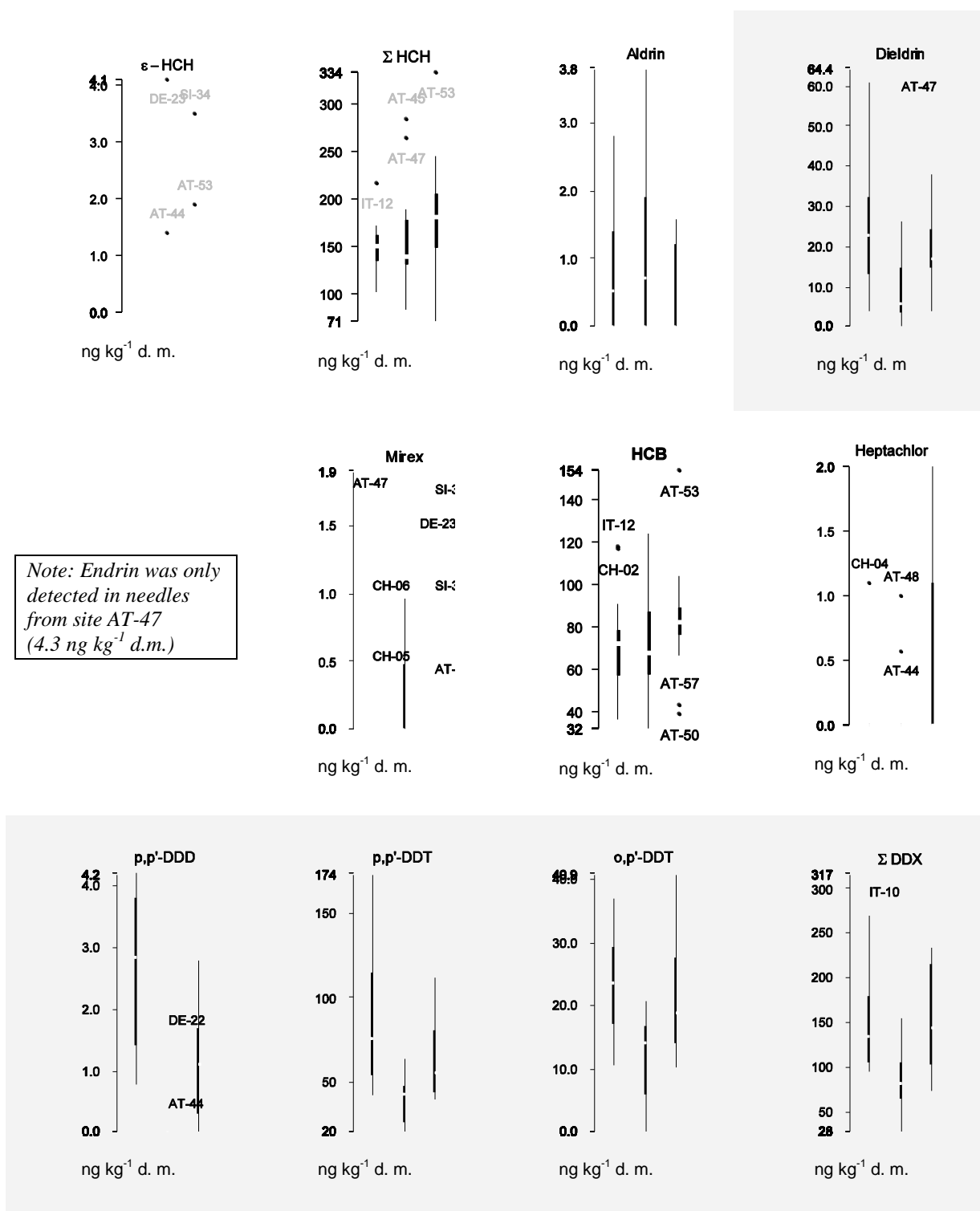


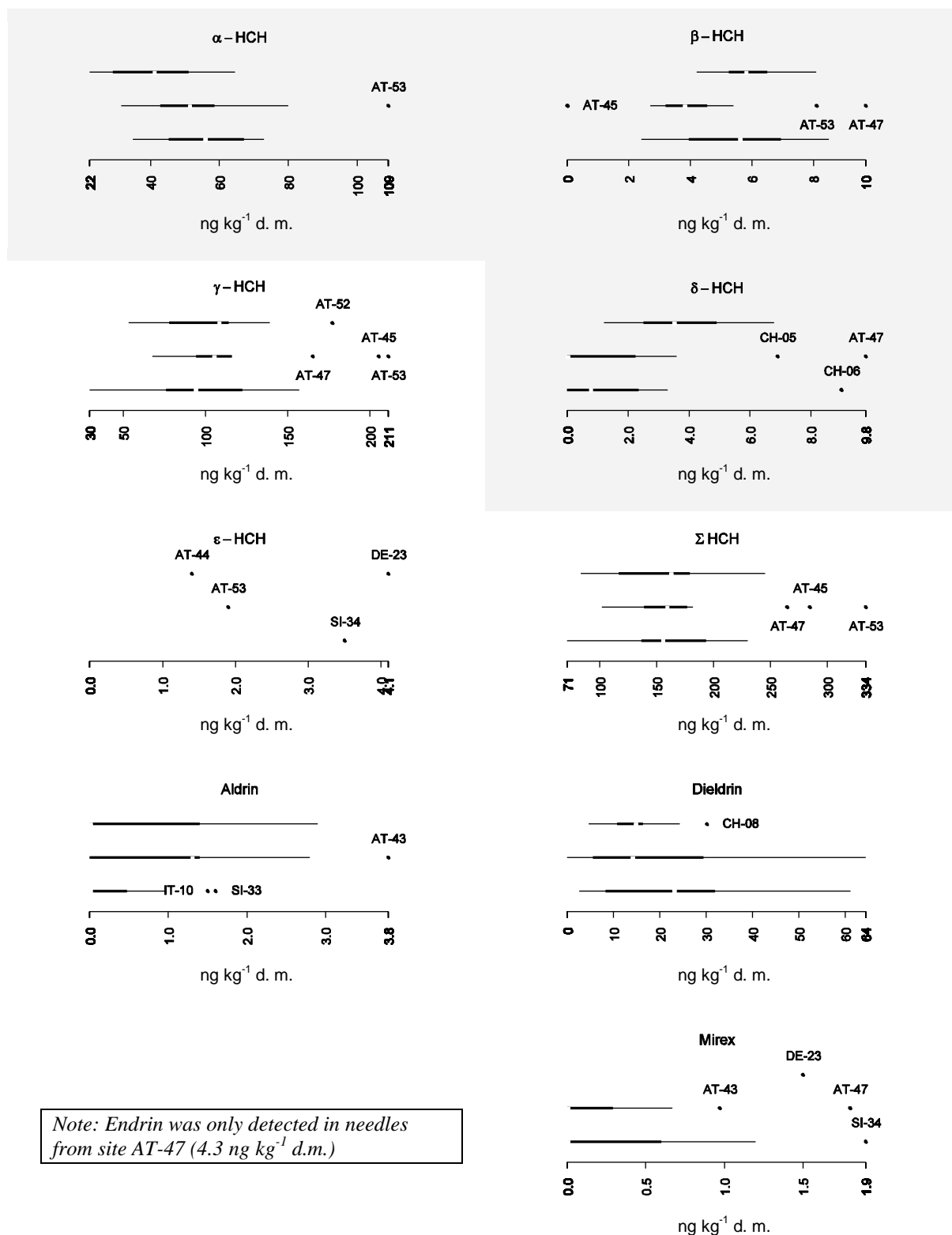
Figure 3-26: Longitudinal pollution trends of various OCP in needles.

Latitudinal differences

Significant latitude related differences (Kruskal-Wallis test) for the whole study region were found for the HCH isomers β -HCH ($p=0.018$) and δ -HCH ($p=0.010$). The latitudinal trends varied between pesticides and even between isomers of the same substance (cf. α - and δ -HCH in Figure 3-27). HCB showed the highest range of concentrations in the central zone (Figure 3-27).

Pairwise comparison of latitudinal groups showed significant (Mann-Whitney test, $p \leq 0.05$) differences between:

- north and centre for β -HCH, δ -HCH and HCB
- centre and south for total DDX content
- north and south for α -HCH and δ -HCH, sum DDX



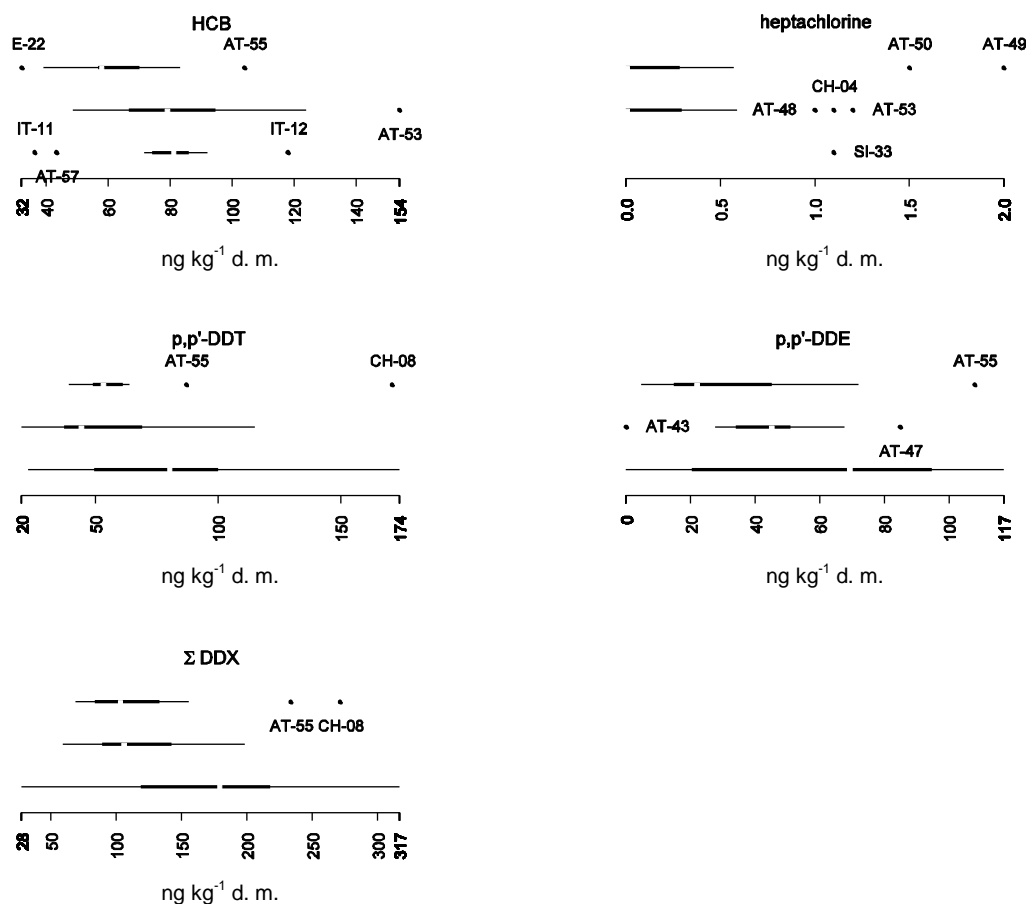


Figure 3-27: Latitudinal pollution trends of various OCP in needles.

3.2.4.2 Humus

The highest average OCP concentrations were generally found in the peripheral zones of the study region (the exceptions were HCH other than the γ -isomer and Heptachlor). Humus OCP content was dominated by DDT and DDE, γ -HCH and Dieldrin. While the DDX were most abundant in the south, almost all OCP (except the non- γ HCH isomers) peaked in the northern part of the study region – including HCB, which in needle samples prevailed in the centre (p. 53). Total DDX content and p,p'-DDT were highest in the east, unlike the maximum concentrations of the DDT breakdown product p,p'-DDD which occurred in the west. Also γ -HCH (and some of the other isomers) increased towards the east. Dieldrin and Aldrin, in turn, were more abundant in the western third of the investigated region.

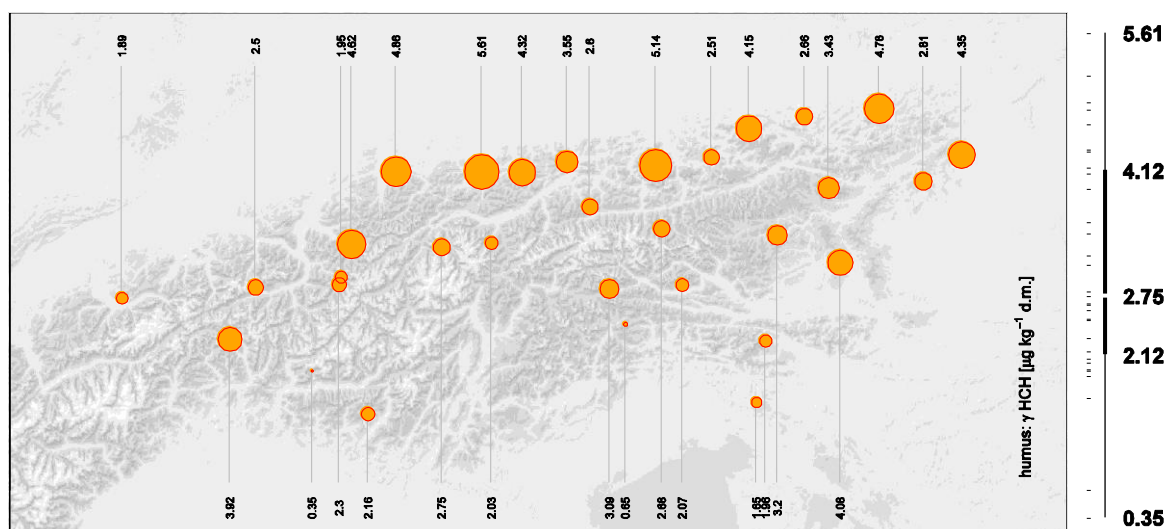
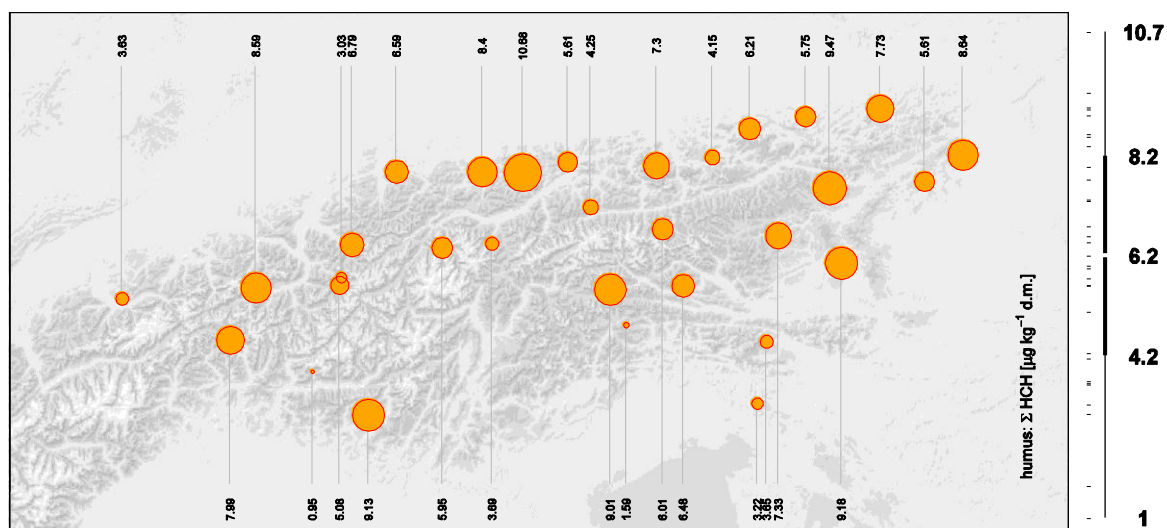
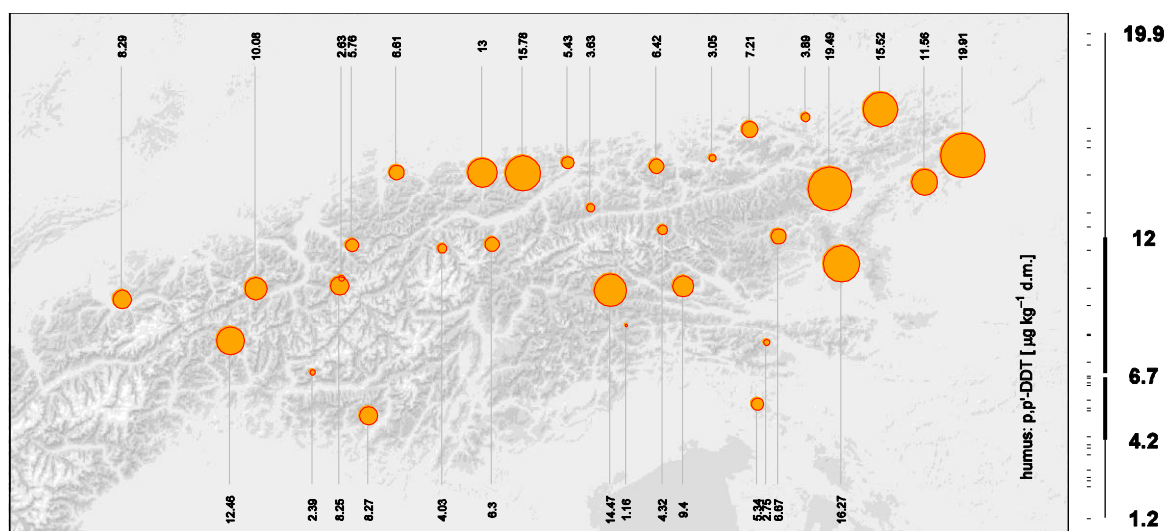
Figure 3-28: Humus γ -HCH contentFigure 3-29: Total humus HCH content (sum of α - ϵ isomers)

Figure 3-30: Humus p,p'-DDT content

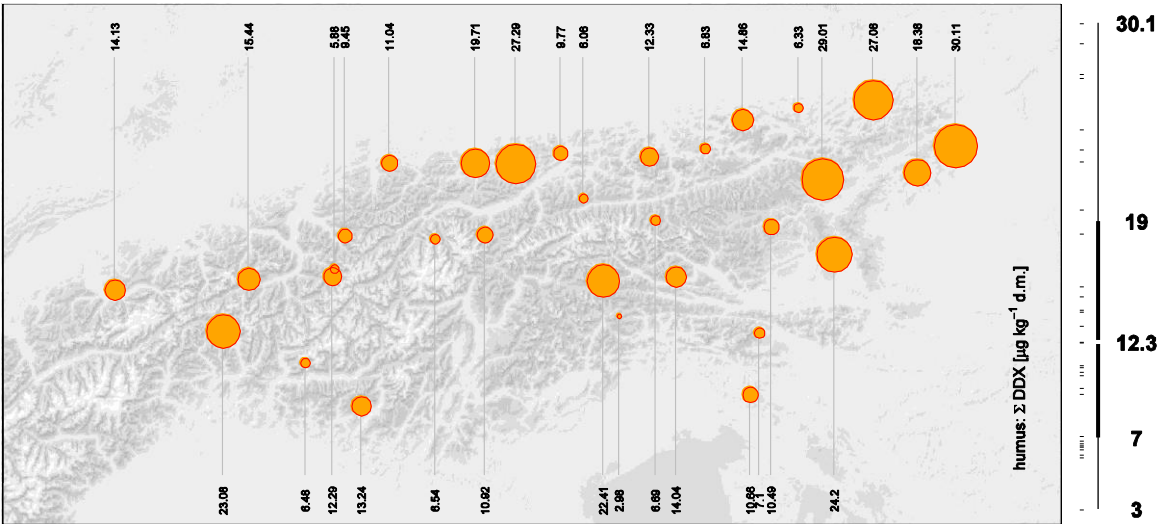


Figure 3-31: Humus DDX content (sum of DDT, DDD and DDE isomers)

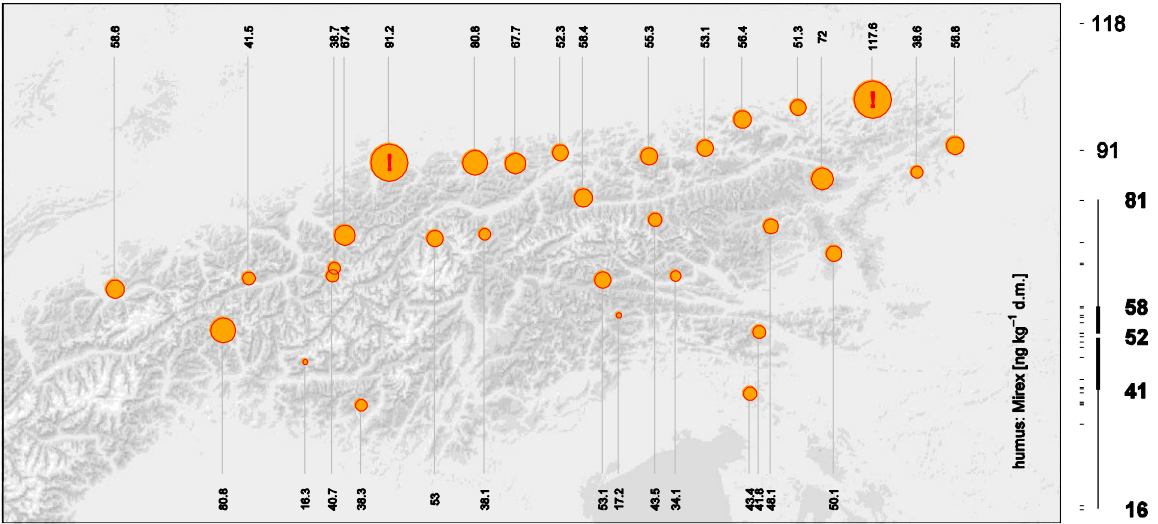


Figure 3-32: Humus Mirex content

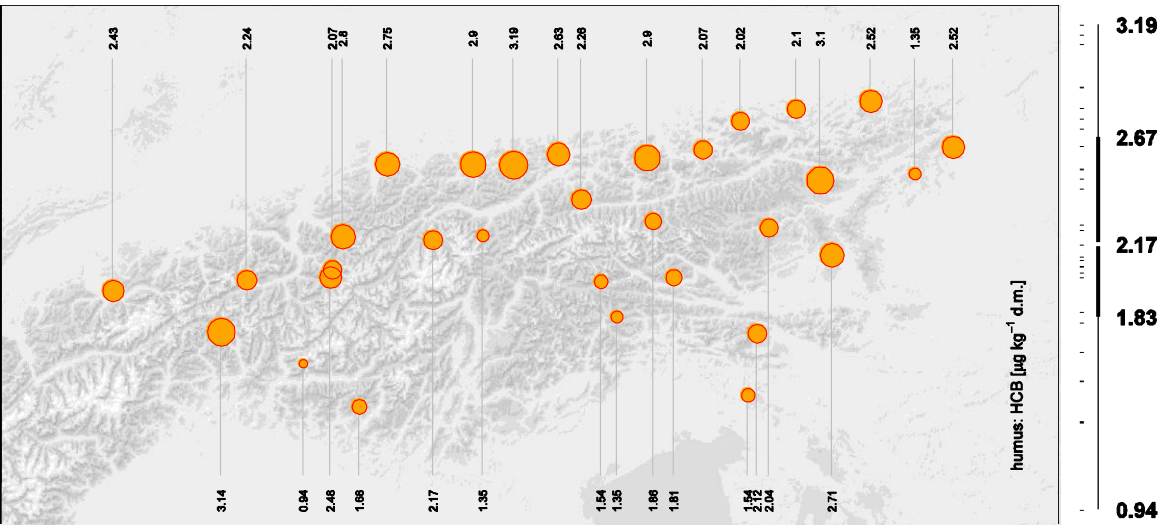


Figure 3-33: Humus hexachlorobenzene (HCB) content

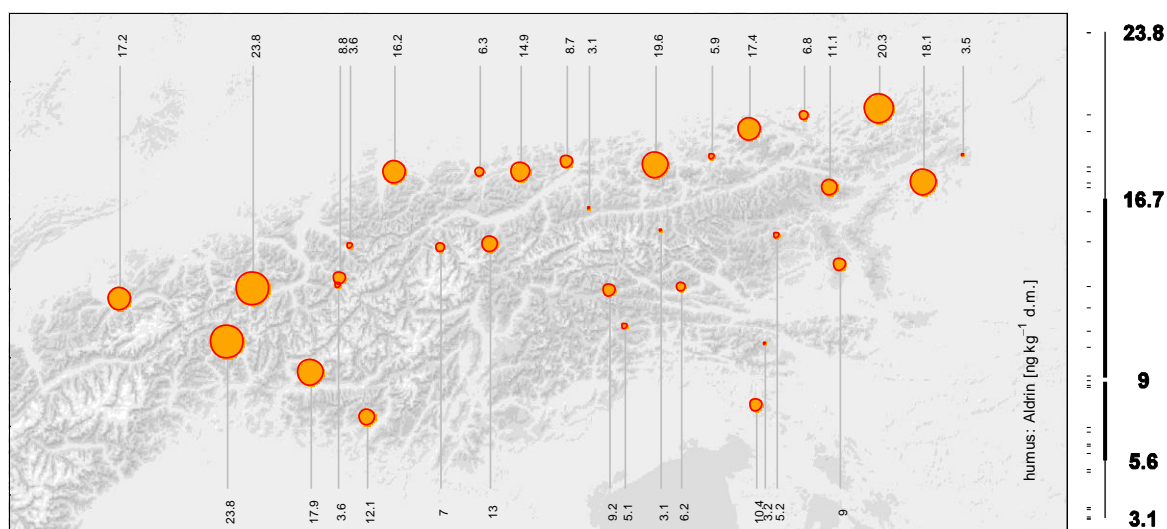


Figure 3-34: Humus Aldrin content

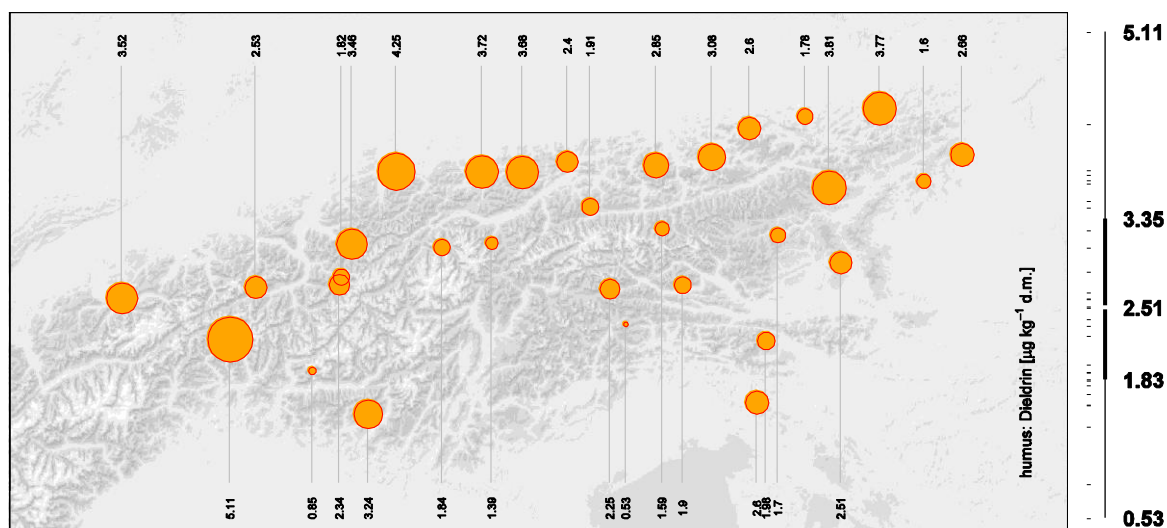


Figure 3-35: Humus Dieldrin content

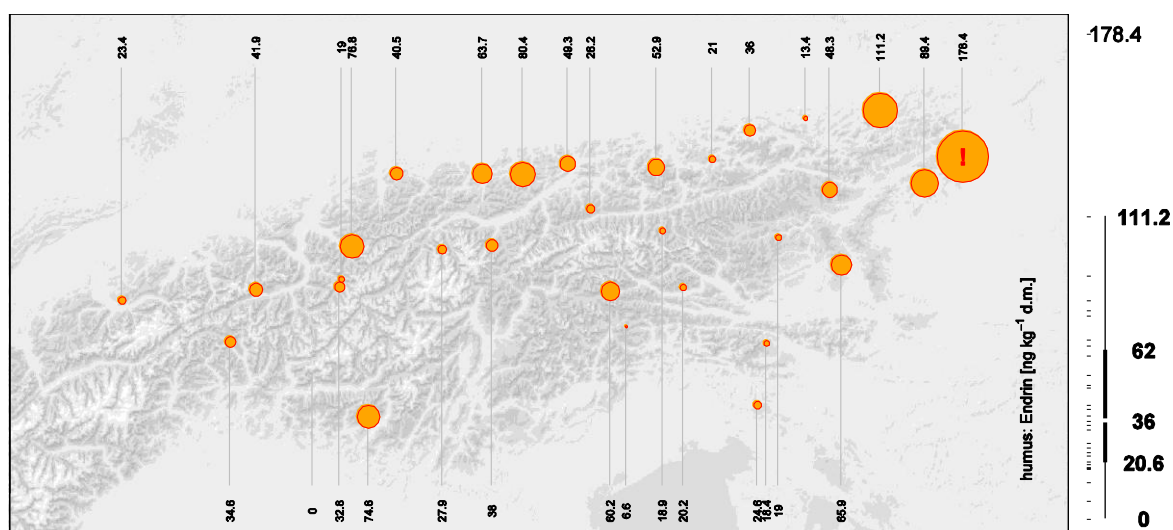


Figure 3-36: Humus Endrin content

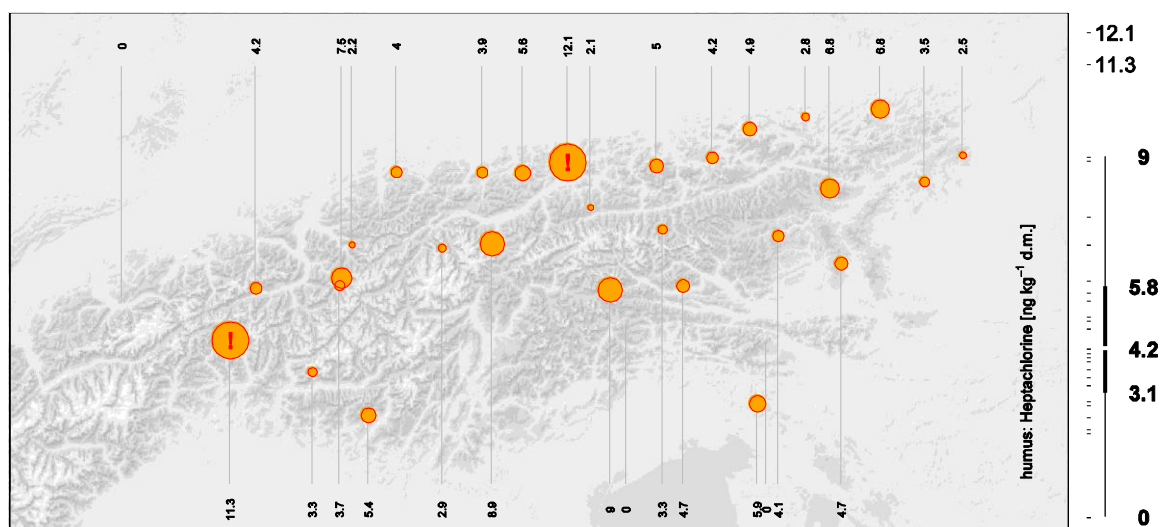
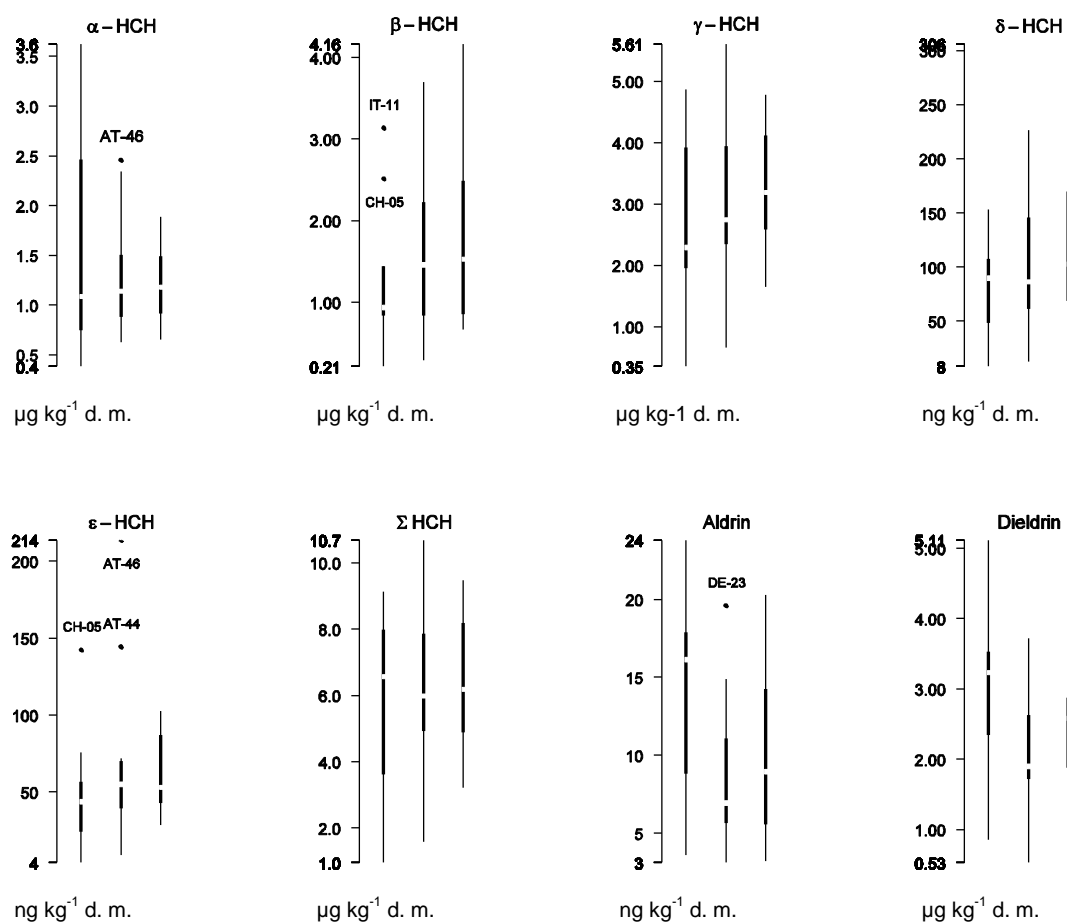


Figure 3-37: Humus Heptachlor content

Longitudinal differences

There was no significant influence of longitudinal group membership on pollutant content: the differences across the study region as a whole could still be random variation. However, longitudinal trends were apparent (Figure 3-38). Differences between groups were also insignificant (Mann-Whitney's test), with the exception of p,p'-DDD.



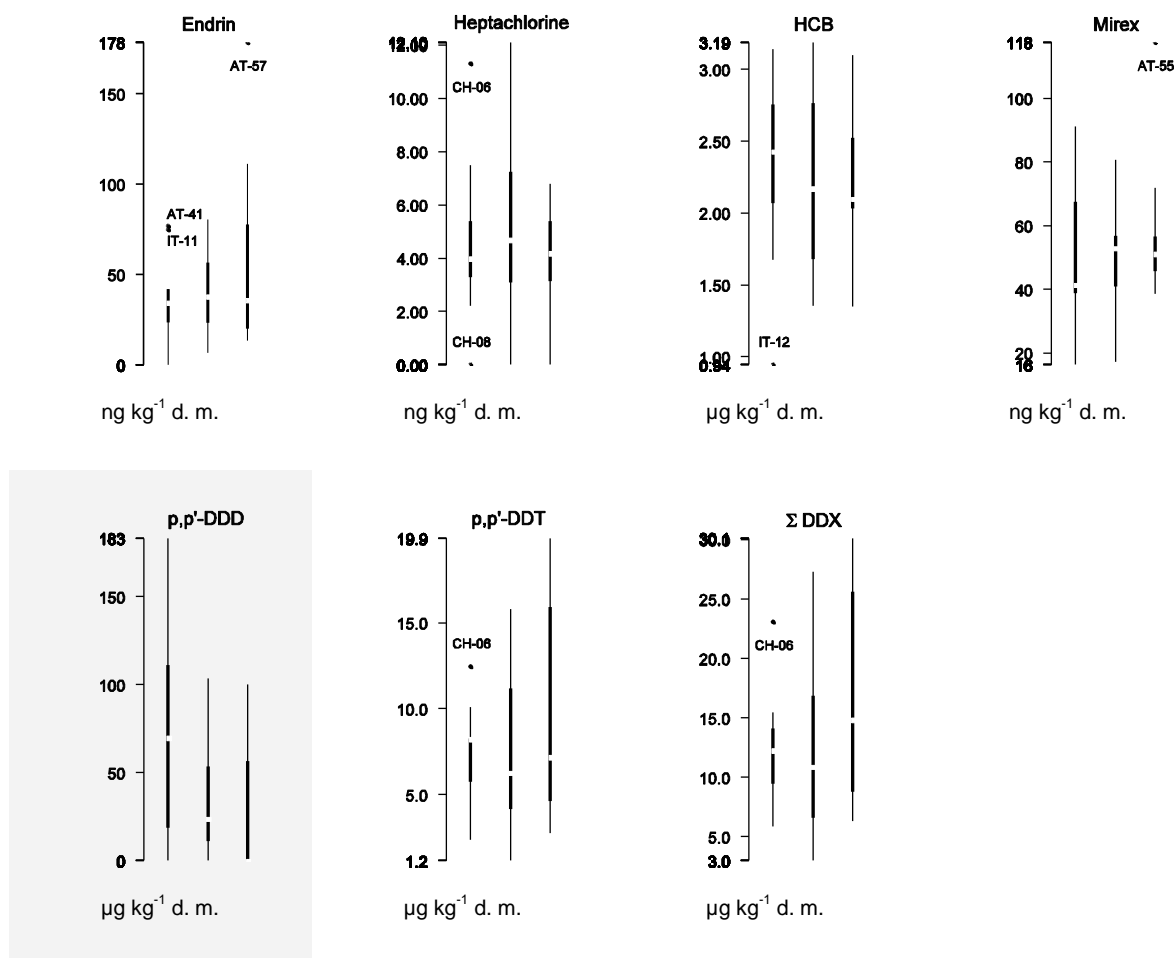
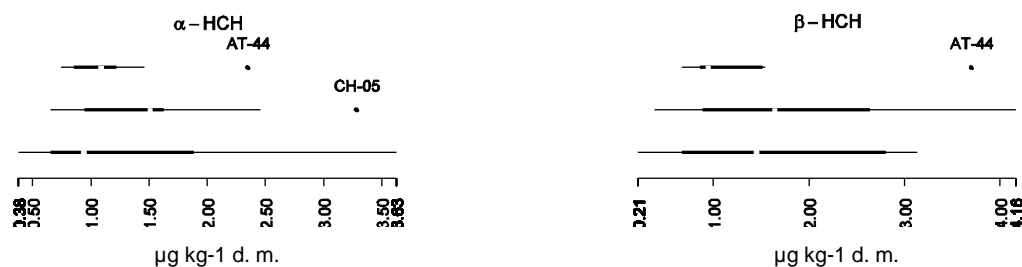


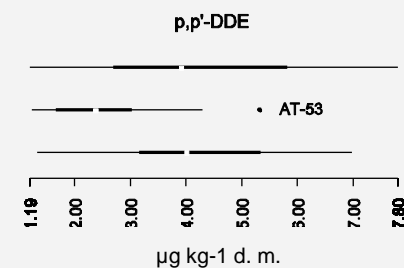
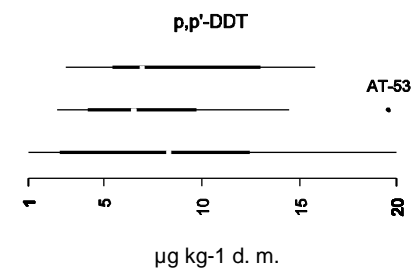
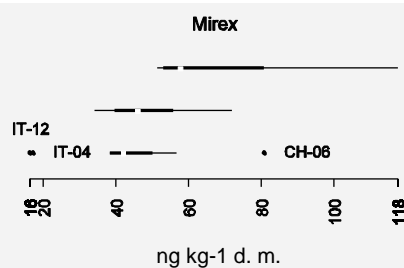
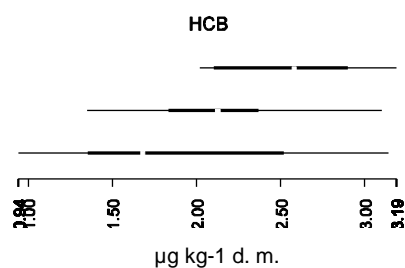
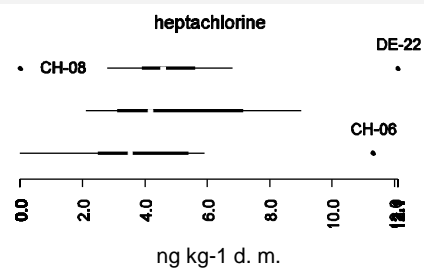
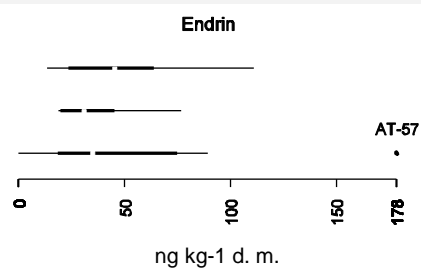
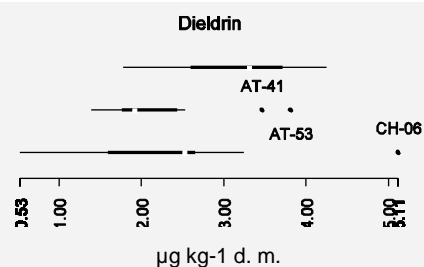
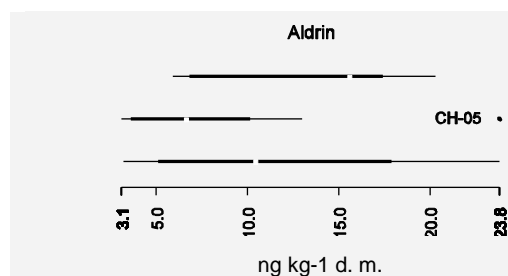
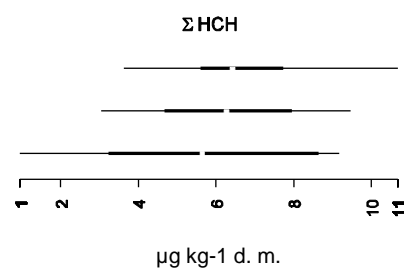
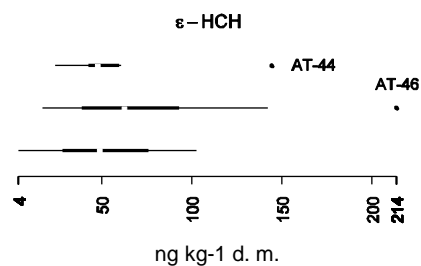
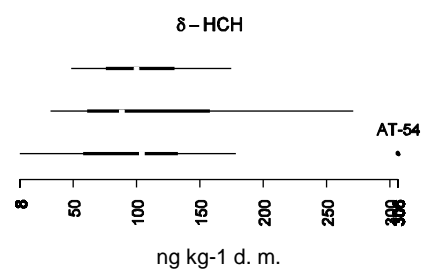
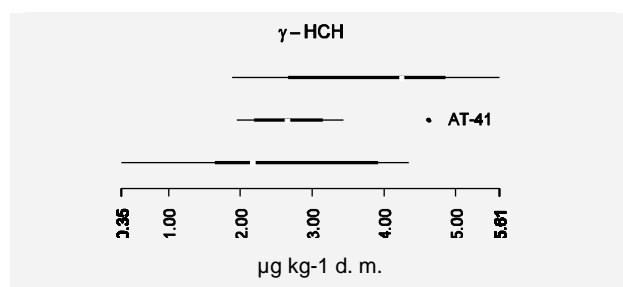
Figure 3-38: Longitudinal pollution trends of various OCP in humus.

Latitudinal differences

Latitude related differences across the whole study region were significant (Kruskal-Wallis) for Mirex, Dieldrin, γ -HCH and p,p'-DDE (error probabilities: .010, .039, .044 and .047). Pairwise investigation of the latitudinal site groups revealed significant differences (Mann-Whitney test, $p \leq .05$) between:

- north and centre for Aldrin, Dieldrin, Mirex and γ -HCH
- centre and south for p,p'-DDE
- north and south for γ -HCH and Mirex





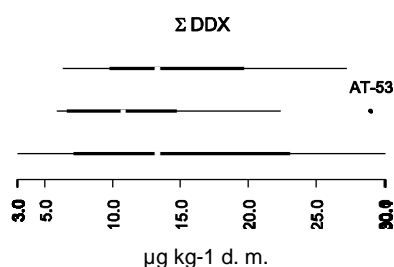


Figure 3-39: Latitudinal pollution trends of various OCP in humus.

3.2.4.3 Air

Generally, the monitoring stations at Weissfluhjoch, Zugspitze and Sonnblick recorded similar geographic origins of arriving atmospheric pesticide loads. It has already been mentioned that the seasonal concentration changes were similar for all three research stations (p. 38). Usually the influence of different source regions on atmospheric concentrations at the three sites was similar, too. The strongest deviations between sites were found for members of the DDX group.

Repeatedly, atmospheric OCP contamination showed pronounced differences between source regions. However, the origin of highest contamination (by pollutant concentration, not necessarily by mass flow) sometimes changed between source regions from one sampling period to the next. For example, the highest β -HCH concentrations were found in air from the northwestern source region during early summer-late autumn 2006, while in spring 2007 air from southeast was most contaminated (Figure 3-41 on p. 62). There were also remarkable correspondencies between the prevailing source regions for different OCP, for instance γ -HCH and p,p'-DDT (pp. 63 and 66).

HCB, the most abundant OCP in air samples, hardly showed a cardinal provenience. Concentrations from different source regions were comparable and were usually similar to those in fast travelling air masses from the Atlantic or Arctics (marked “not attributable” in Figure 3-40-Figure 3-54).

Despite similar patterns for geographic origin, a given station as well as a particular sampling period could show conspicuous pollution levels. During the warmer sampling periods, ambient air at Mt. Weissfluhjoch (Switzerland), for instance, contained much more DDT and DDE than at the other mountain peaks. Filters from Mt. Sonnblick, in turn, bore comparably low DDT but exceedingly high γ -HCH levels, *the latter very probably being due to a local source and not representative for background sites*. The transient local character of the northwesternly DDX peaks at Mt. Zugspitze during winter 2005/6 (Figure 3-44 ff.) *should be interpreted with equal caution*.

Atmospheric pesticide concentrations were tendentially higher in the warmer sampling periods, although for HCB and Mirex variations were small and irregular. Especially HCH isomers showed pronounced changes from low concentrations during the winter periods to high levels in spring and summer (Figures 3-40 ff). Corresponding variations were also found for the DDT isomers and, to a lesser extent, their DDD and DDE derivatives.

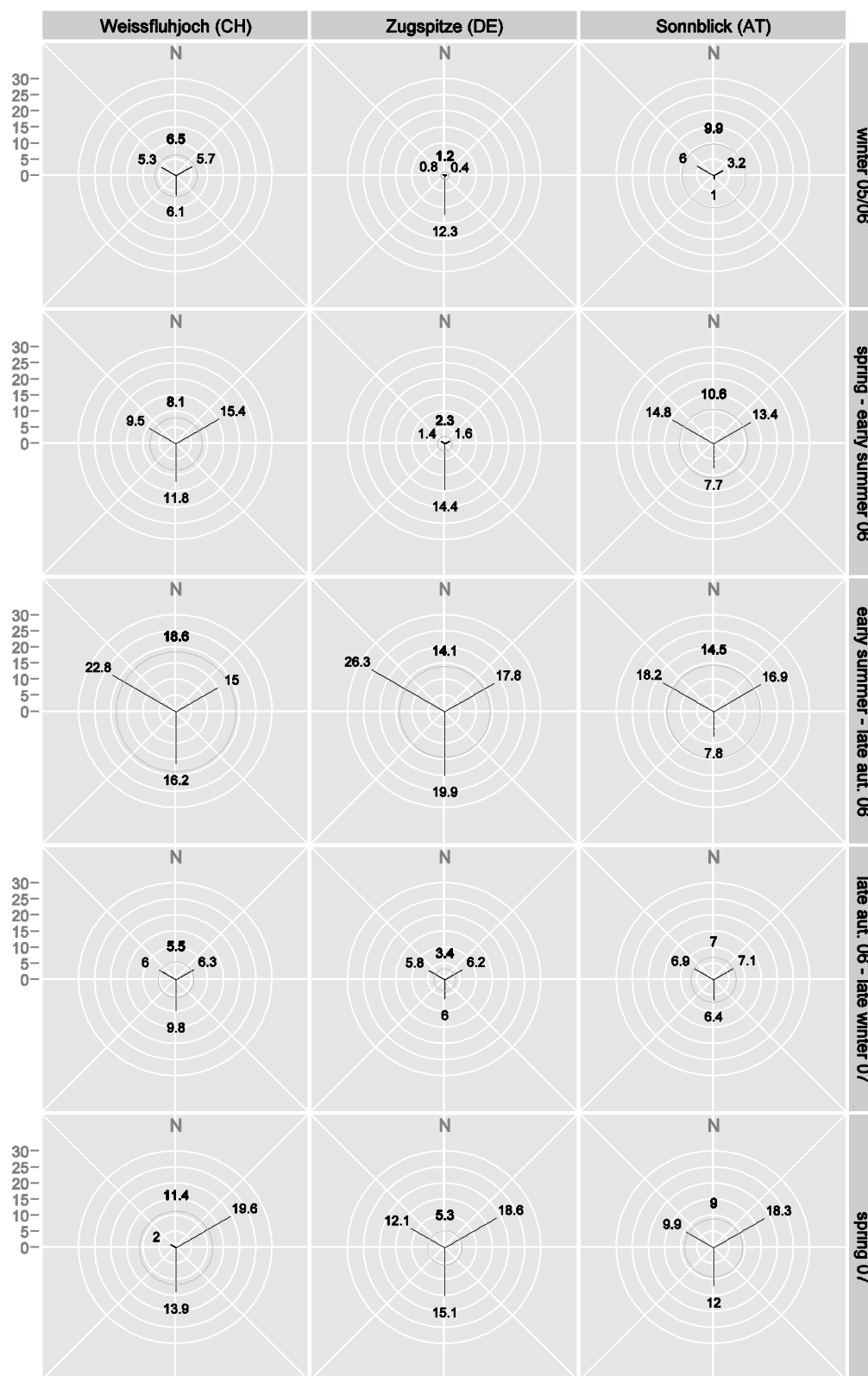


Figure 3-40: Concentration [pg m^{-3}] of α -HCH in air from NW, NE and S (circle: trajectory not attributable to a particular source region).

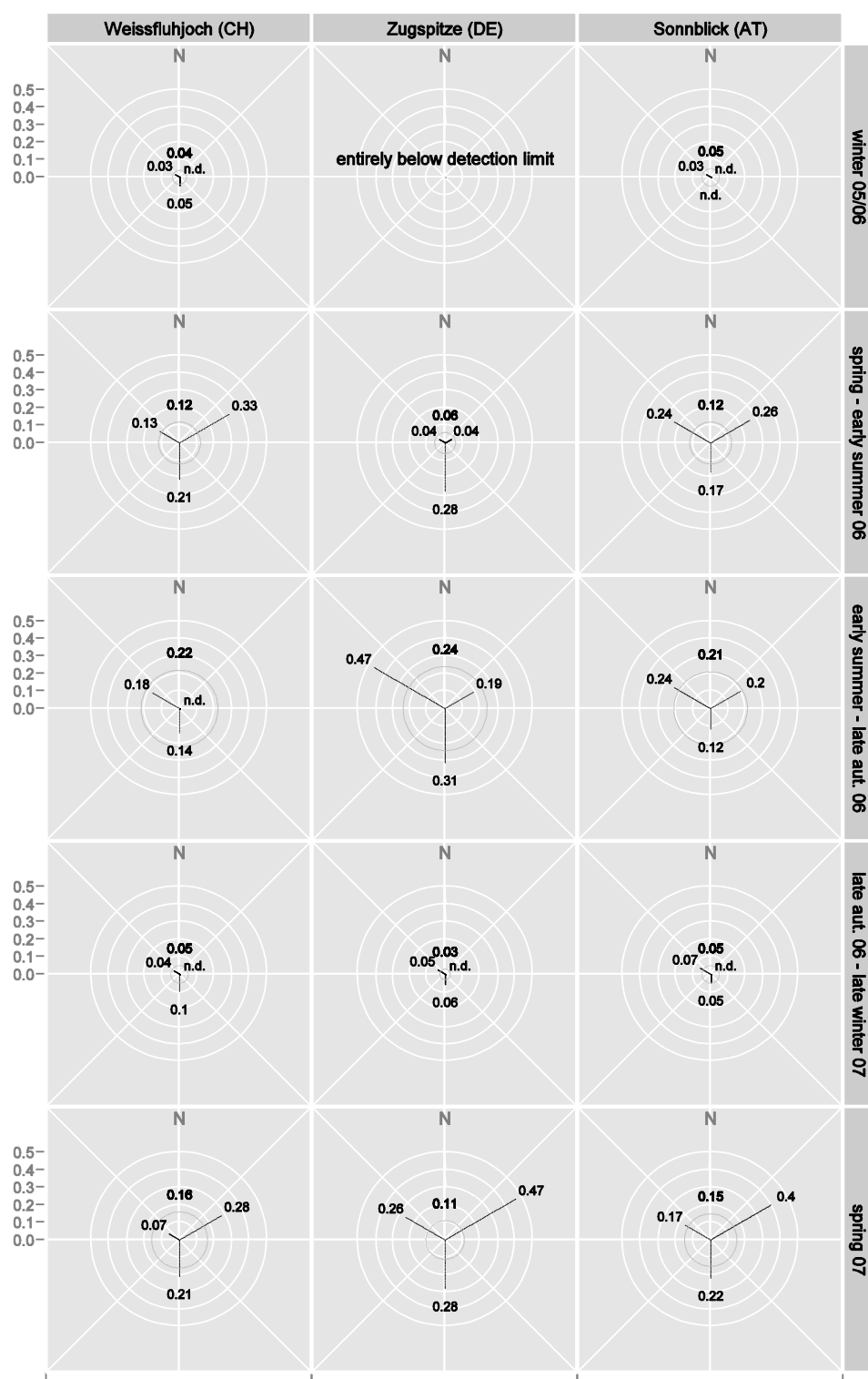
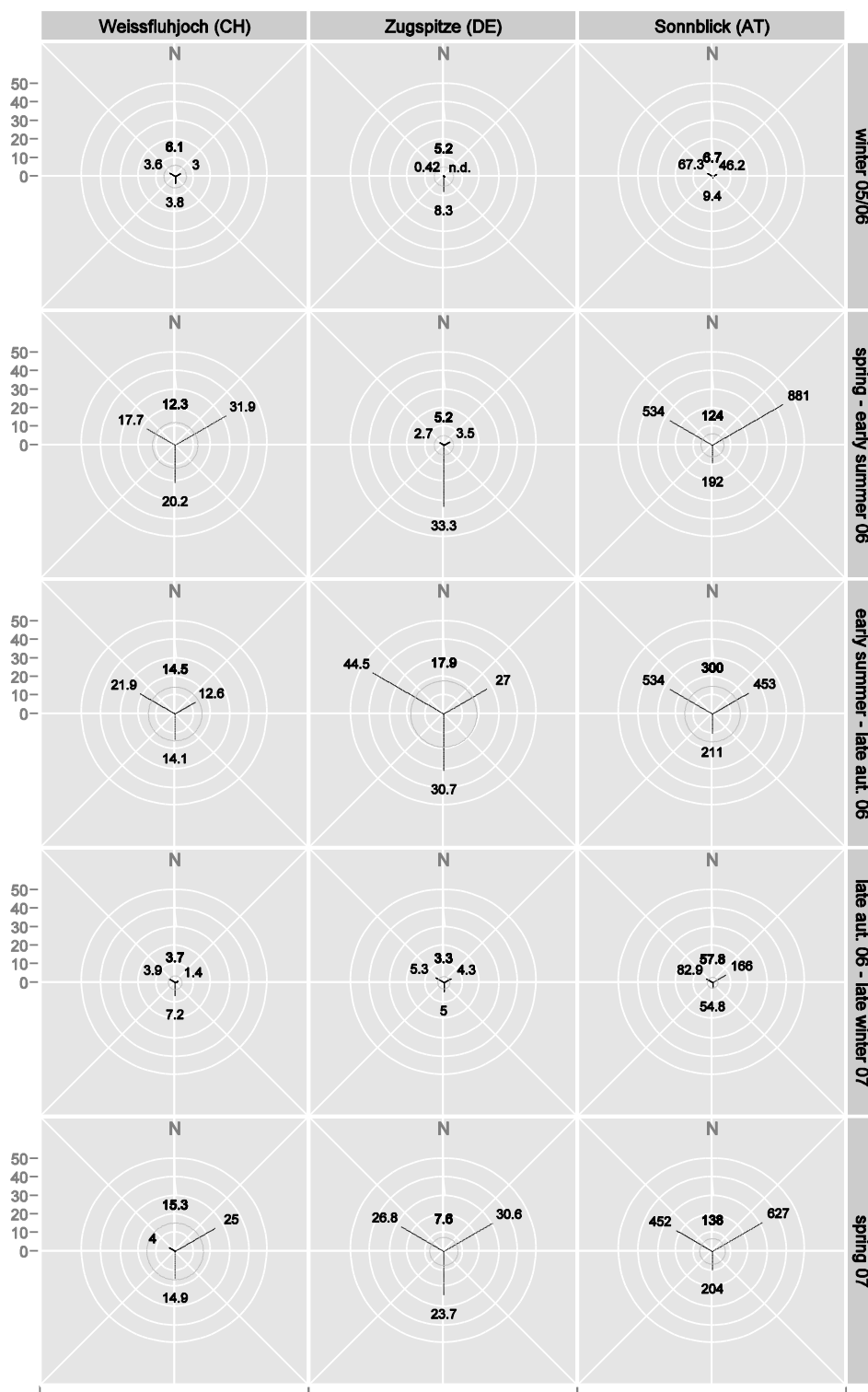


Figure 3-41: Concentration [pg m^{-3}] of β -HCH in air from NW, NE and S (circle: trajectory not attributable to a particular source region).



Note the reduced ($f=0.05$ [!]) scale for values from Mt. Sonnblick

Figure 3-42: Concentration [pg m^{-3}] of γ -HCH in air from NW, NE and S (circle: trajectory not attributable to a particular source region).

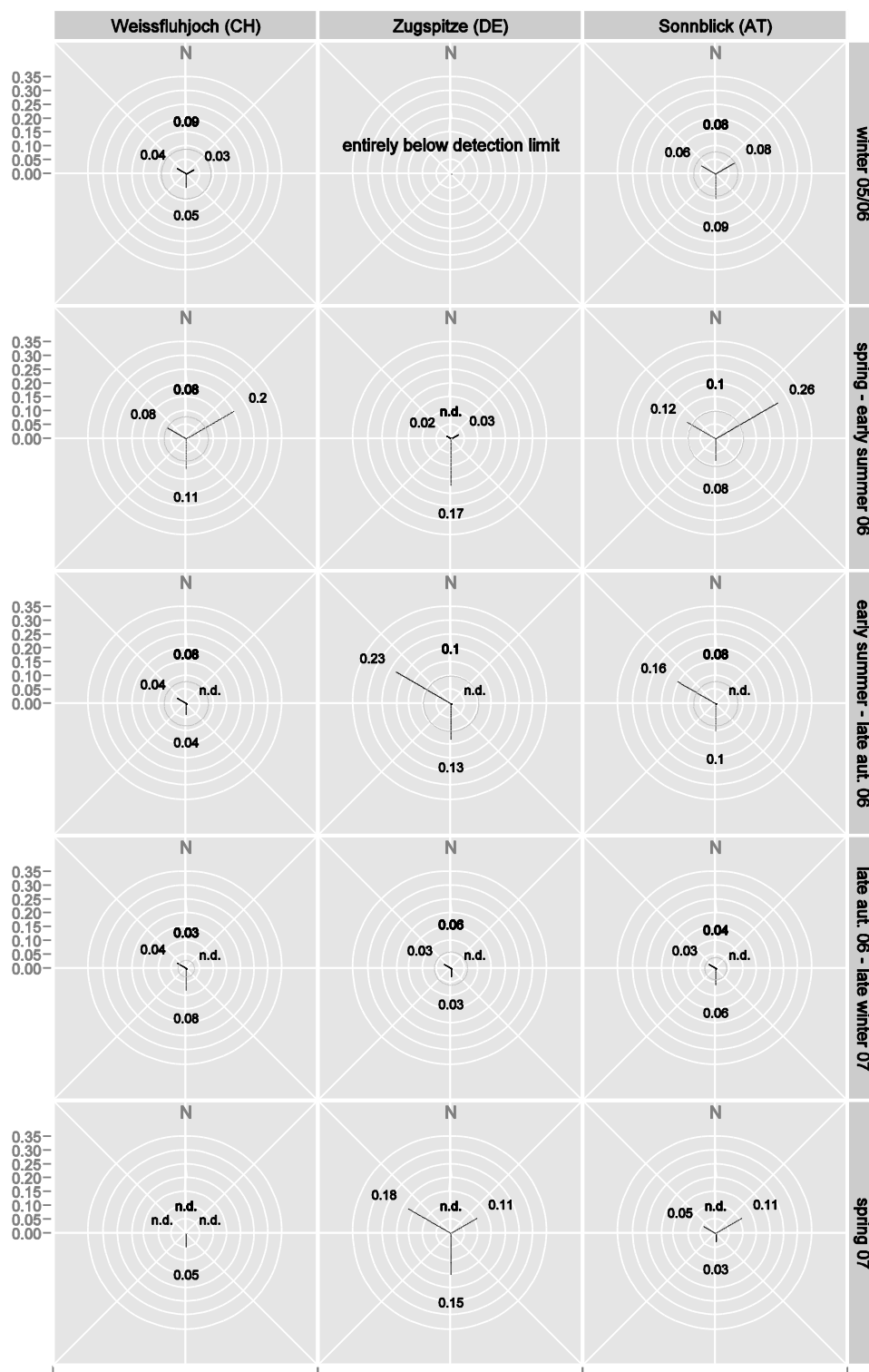


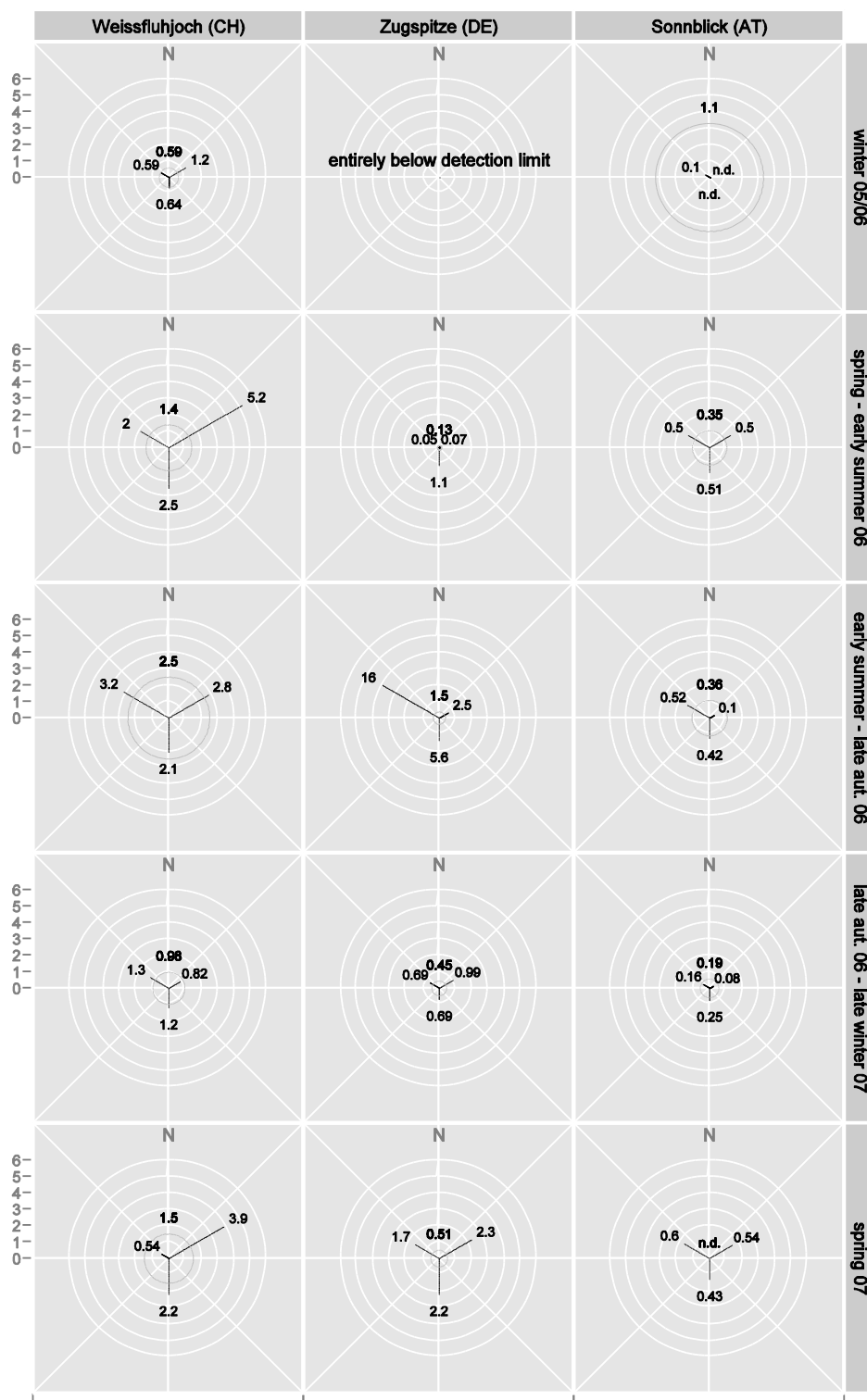
Figure 3-43: Concentration [pg m^{-3}] of δ -HCH in air from NW, NE and S (circle: trajectory not attributable to a particular source region).

Concentrations of ε -HCH were frequently below the detection limit. Complete observations (per site and period) are too few for a meaningful graphic display; instead values are given in Table 3-7 below.

Table 3-7: Concentrations of ε -HCH in ambient air

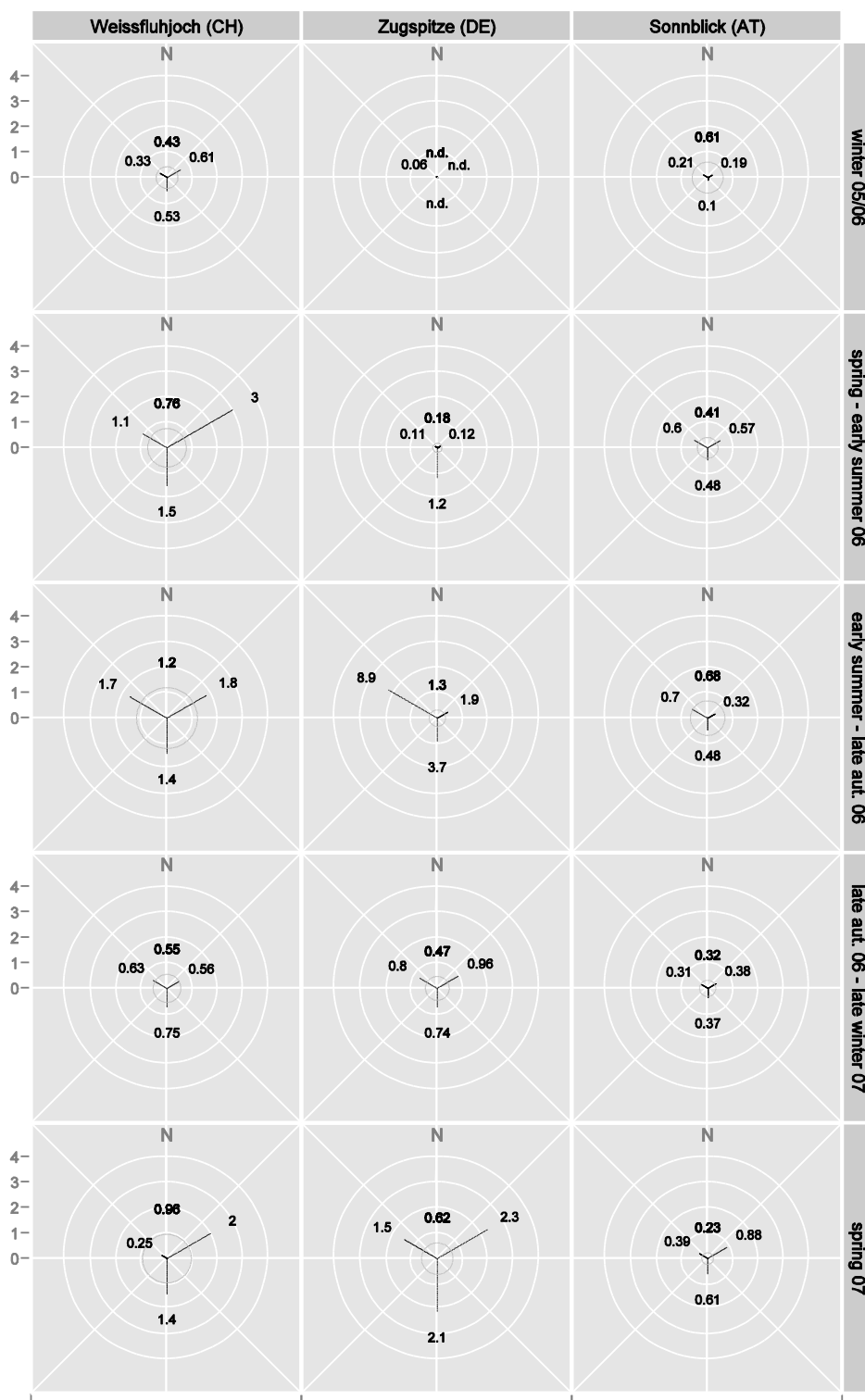
sampling period	sector	Weissfluhjoch (CH)	Zugspitze (DE)	Sonnblick (AT)
I	NW	0.01	< LOD	< LOD
	NE	< LOD	< LOD	< LOD
	S	< LOD	< LOD	< LOD
	undef.	< LOD	< LOD	0.03
II	NW	0.08	0.05	0.11
	NE	0.21	< LOD	< LOD
	S	0.04	0.17	< LOD
	undef.	0.06	< LOD	< LOD
III	NW	0.07	0.18	0.13
	NE	< LOD	0.08	< LOD
	S	0.05	0.10	< LOD
	undef.	0.06	0.09	< LOD
IV	NW	< LOD	0.02	0.04
	NE	< LOD	< LOD	< LOD
	S	0.03	0.03	0.03
	undef.	0.02	< LOD	< LOD
V	NW	< LOD	< LOD	< LOD
	NE	< LOD	< LOD	< LOD
	S	< LOD	< LOD	< LOD
	undef.	< LOD	< LOD	< LOD

sampling periods: I...winter 2005/6, II...spring-early summer 2006, III...early summer-late autumn 2006, ..., IV...late aut. 2006-late winter 2007, V...spring 2007



Note the reduced scale ($f=25$) for values from Mt. Weissfluhjoch and early summer-late autumn 2006 values from Zugspitze, and the enlarged ($f=3$) scale for values from Mt. Sonnblick.

Figure 3-44: Concentration of p,p' -DDT [pg m^{-3}] in air from NW, NE and S (circle: trajectory not attributable to a particular source region).



Note the reduced scale (1:4) for values from Mt. Weissfluhjoch and early summer-late autumn 2006 values from Zugspitze.

Figure 3-45: Concentration of *o,p'*-DDT [pg m^{-3}] in air from NW, NE and S (circle: trajectory not attributable to a particular source region).

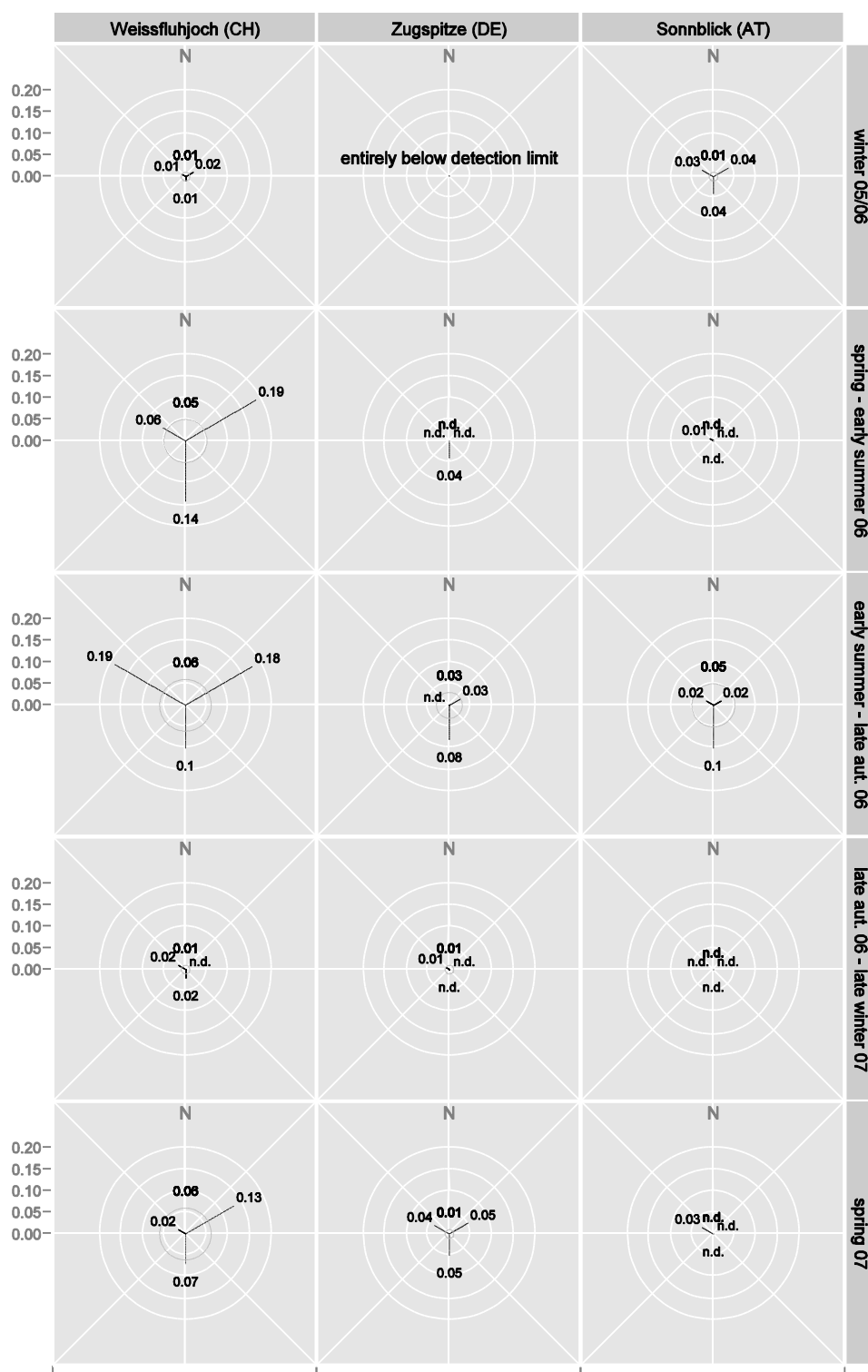
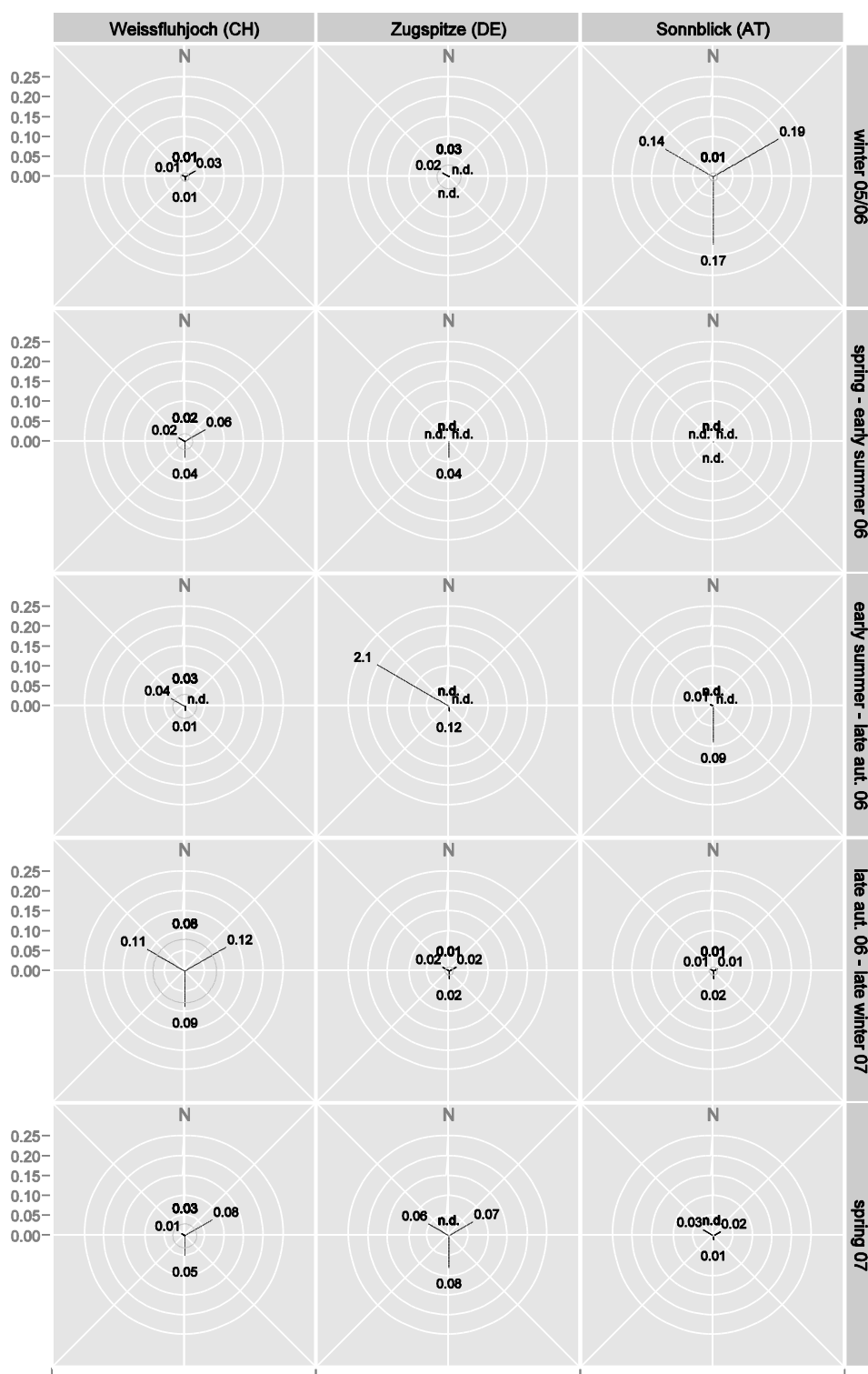
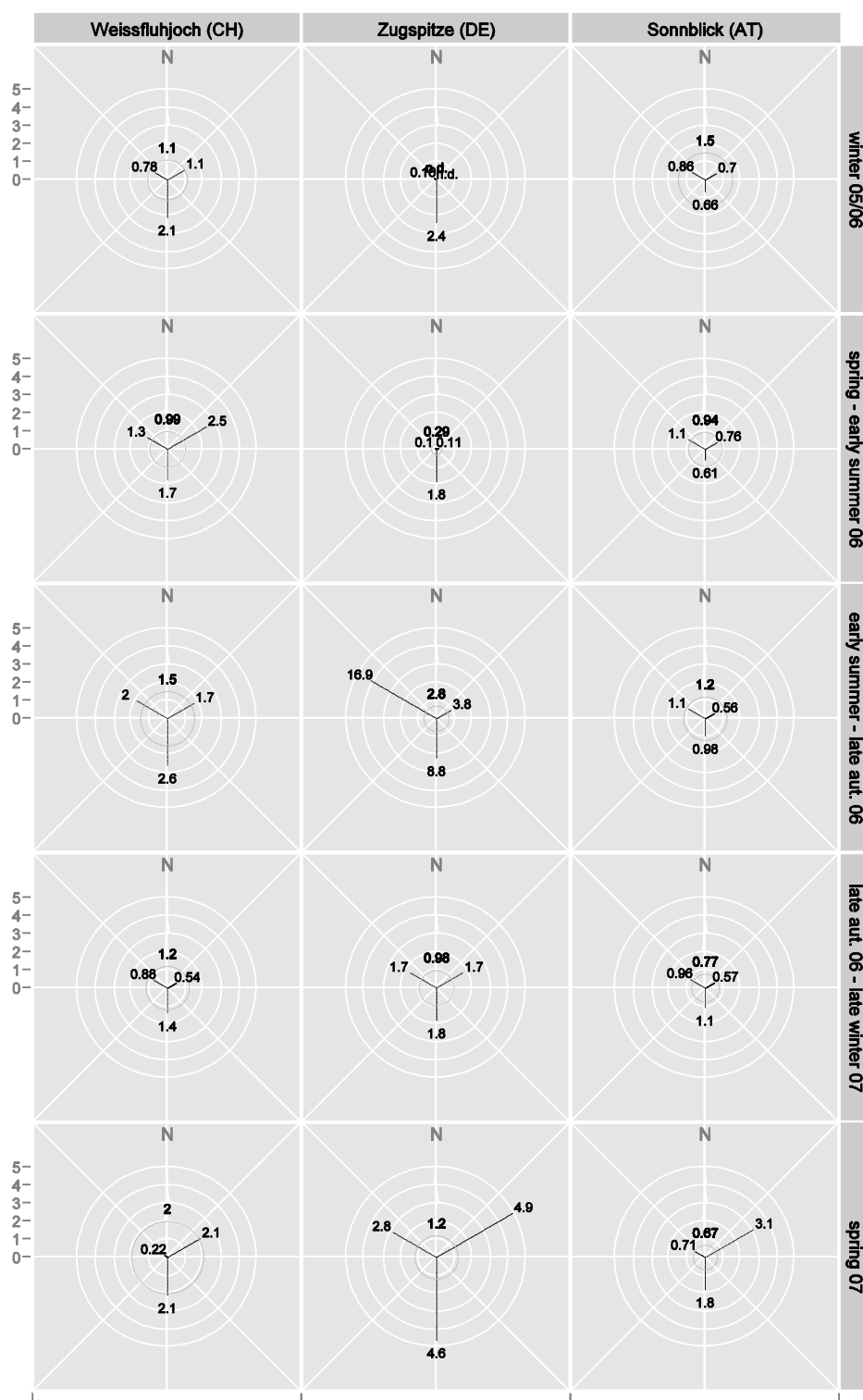


Figure 3-46: Concentration of p,p' -DDD [pg m^{-3}] in air from NW, NE and S (circle: trajectory not attributable to a particular source region).



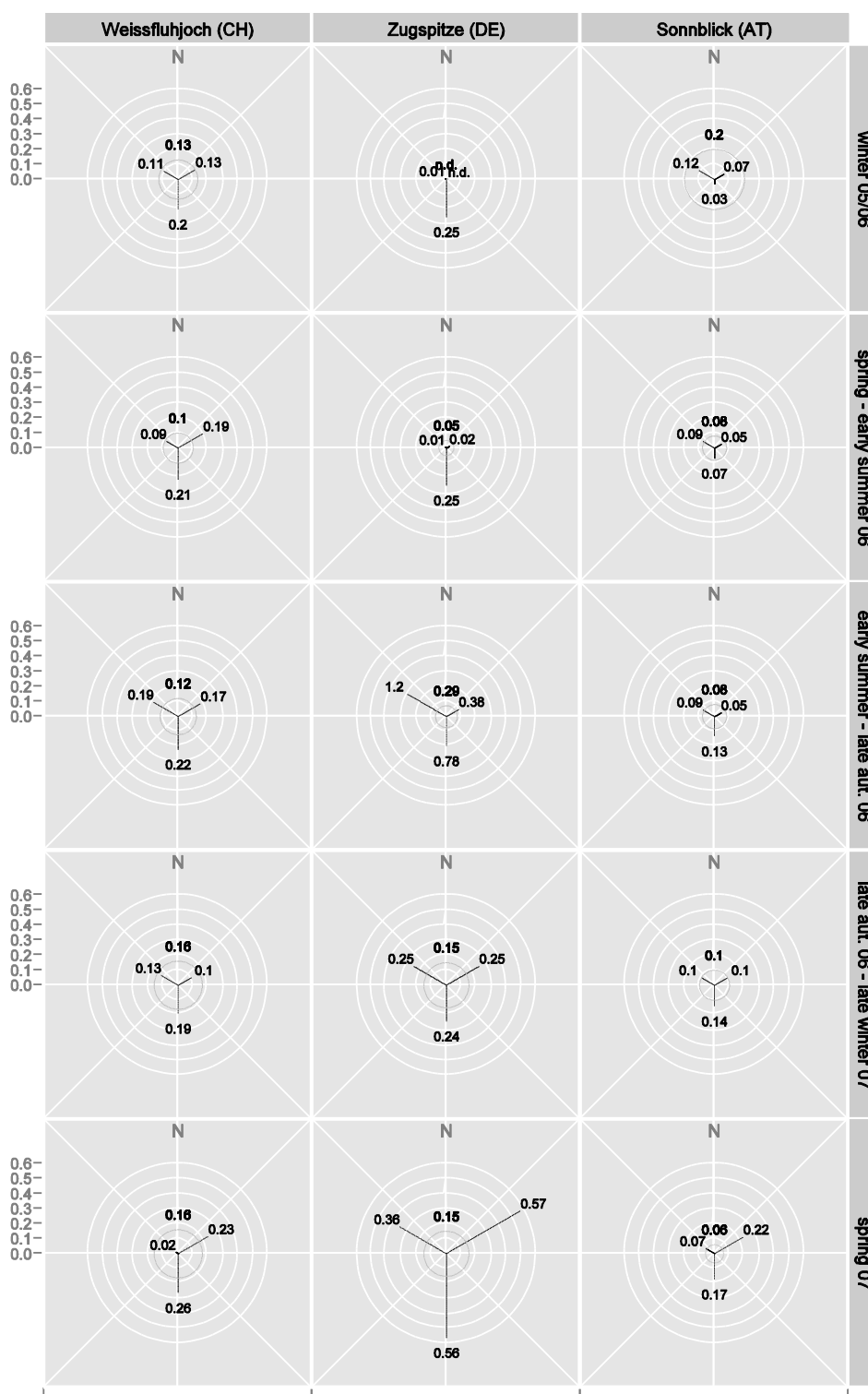
Note the reduced scale (1:10) for early summer-late autumn 2006 values from Mt. Zugspitze.

Figure 3-47: Concentration of *o,p'*-DDD [pg m^{-3}] in air from NW, NE and S (circle: trajectory not attributable to a particular source region).



Note the reduced scale (1:4) for early summer-late autumn 2006 values from Mt. Zugspitze.

Figure 3-48: Concentration of p,p' -DDE [pg m^{-3}] in air from NW, NE and S (circle: trajectory not attributable to a particular source region).



Note the reduced scale (1:4) for early summer-late autumn 2006 values from Mt. Zugspitze.

Figure 3-49: Concentration of *o,p'*-DDE [pg m^{-3}] in air from NW, NE and S (circle: trajectory not attributable to a particular source region).

Atmospheric Aldrin concentrations were entirely below the detection limit.

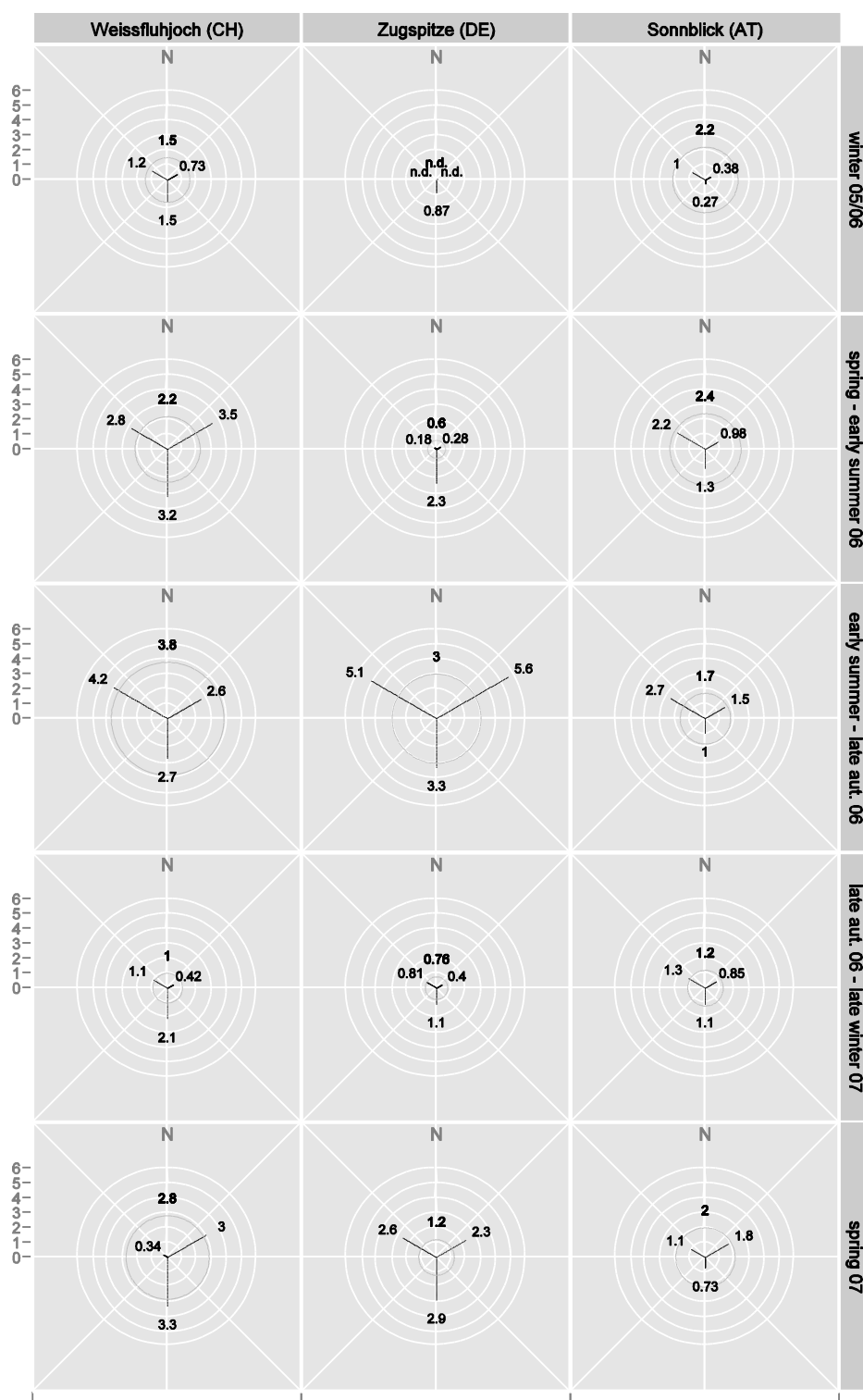


Figure 3-50: Concentration of Dieldrin [pg m^{-3}] in air from NW, NE and S (circle: trajectory not attributable to a particular source region).

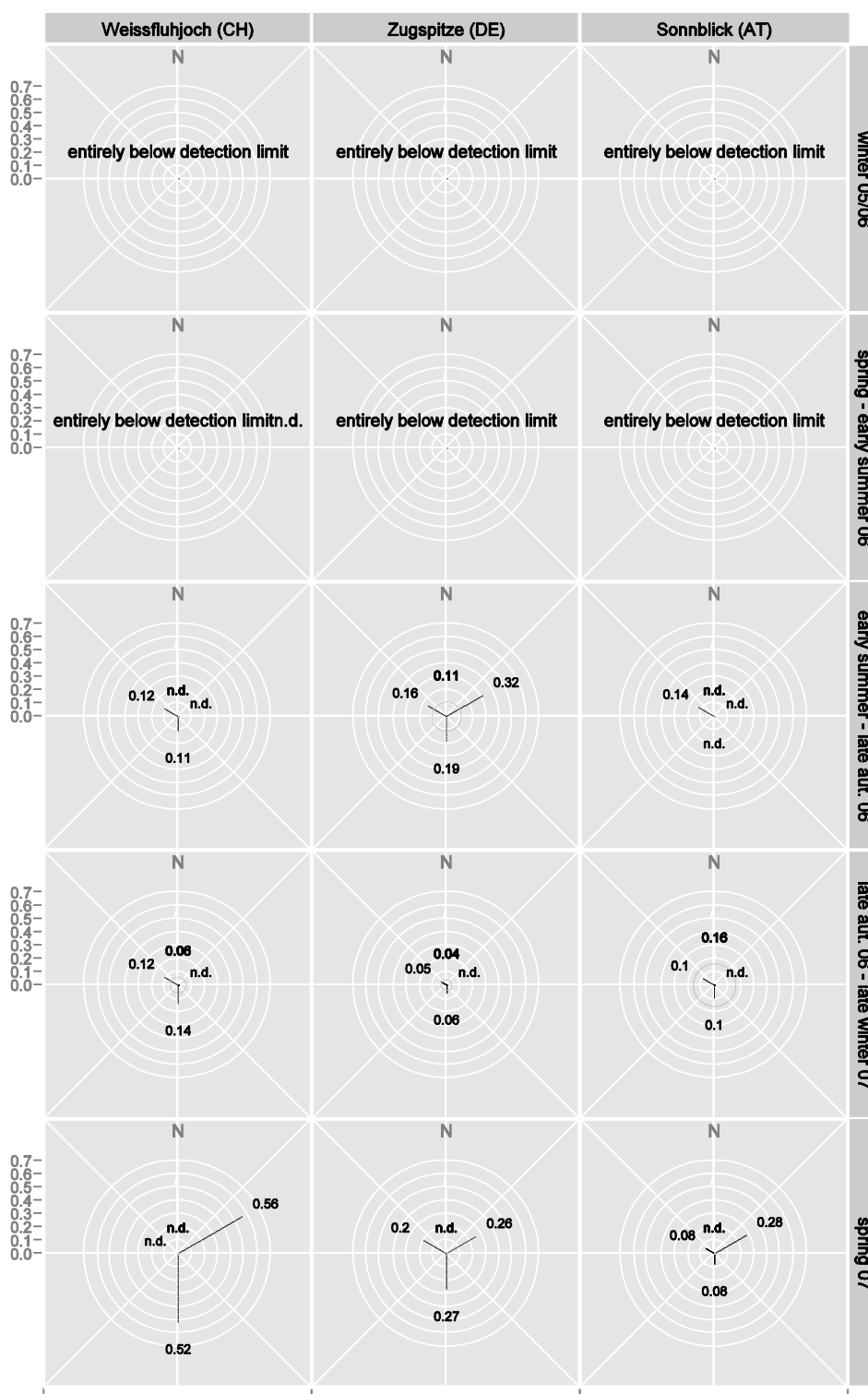
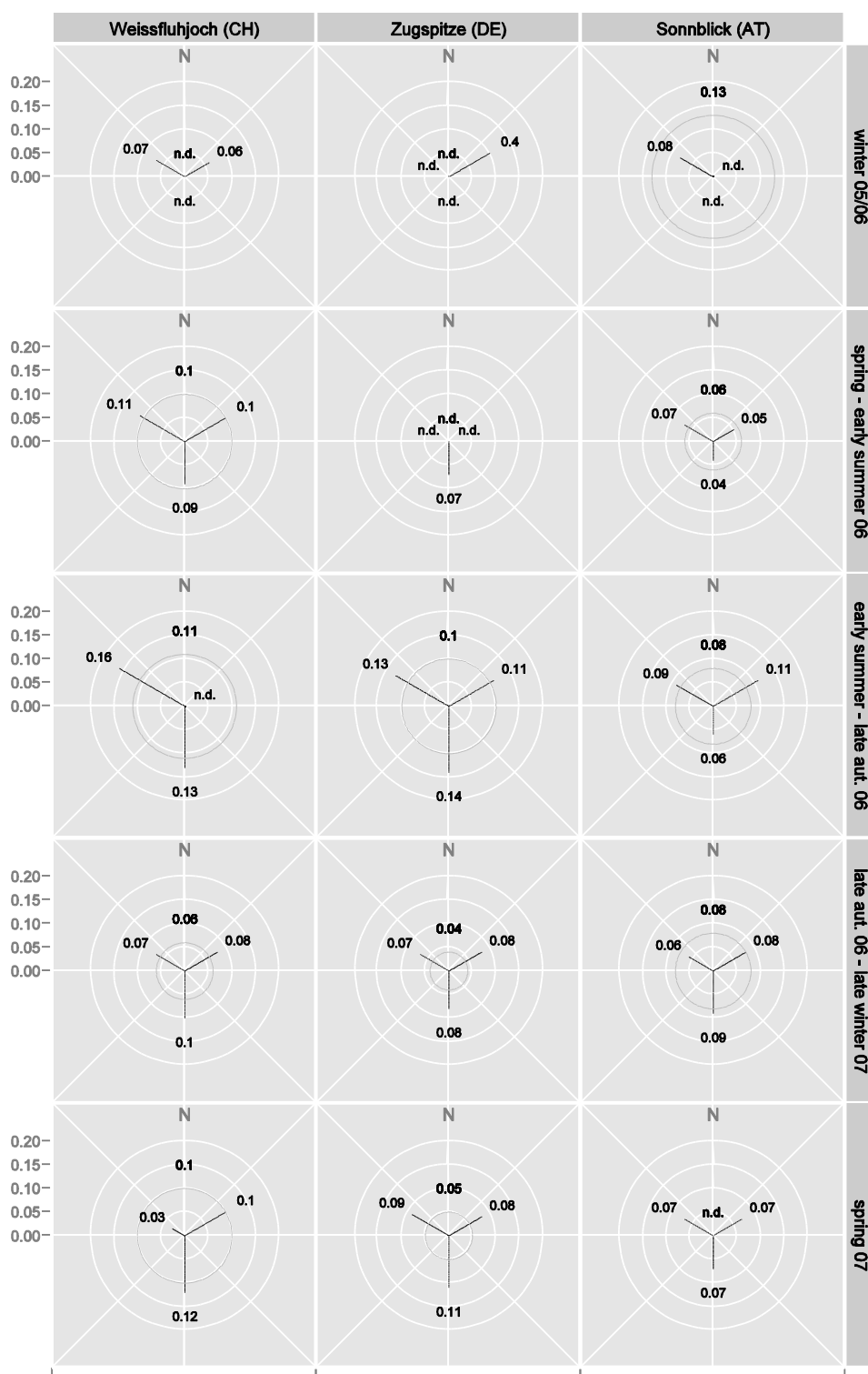
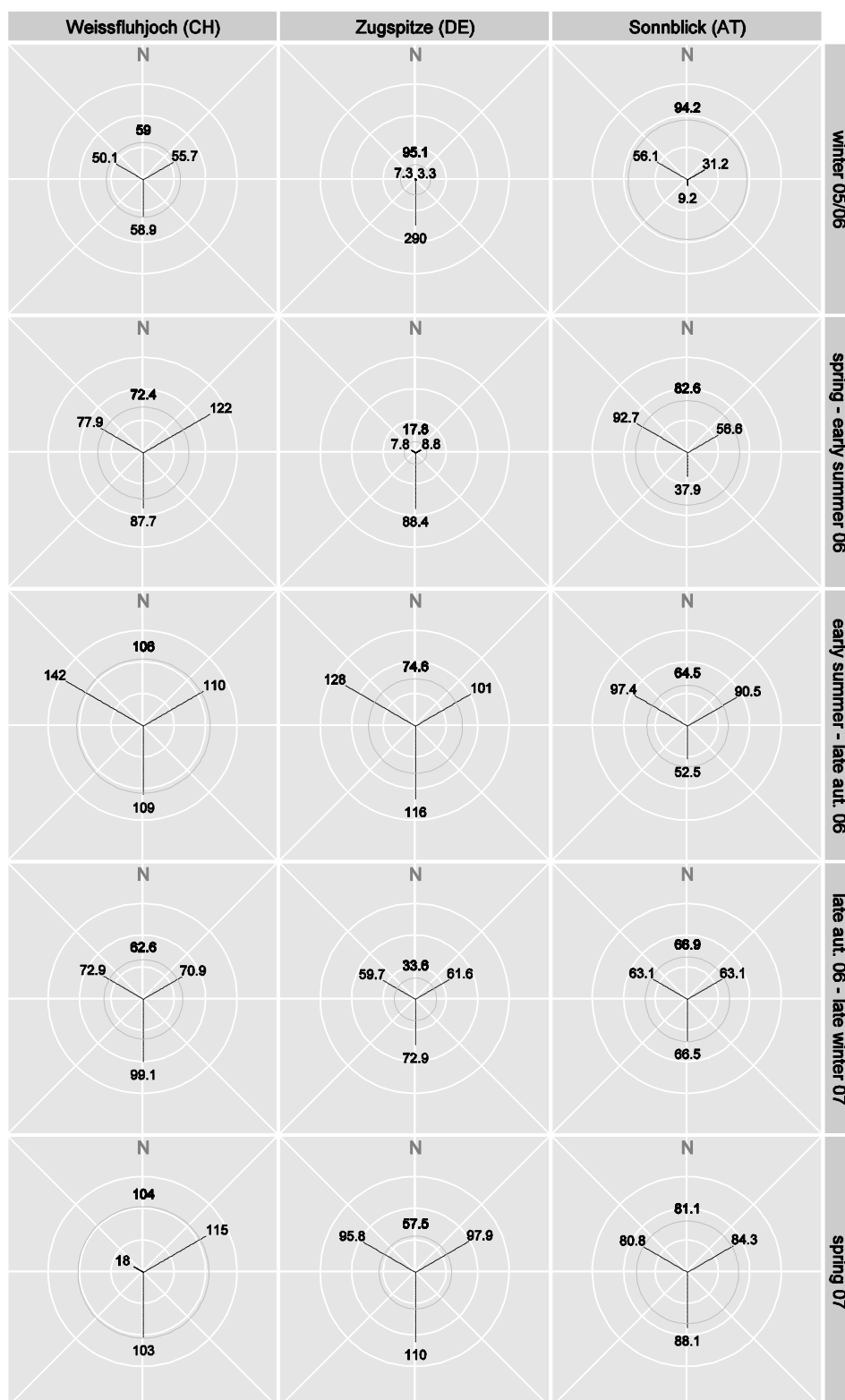


Figure 3-51: Concentration of Endrin [pg m^{-3}] in air from NW, NE and S (circle: trajectory not attributable to a particular source region).



Note the reduced scale (1:4) for winter 2005/06 values from Mt. Zugspitze.

Figure 3-52: Concentration of Mirex [pg m^{-3}] in air from NW, NE and S (circle: trajectory not attributable to a particular source region).



Note the reduced scale (1:4) for winter 2005/06 values from Mt. Zugspitze.

Figure 3-53: Concentration of HCB [pg m^{-3}] in air from NW, NE and S (circle: trajectory not attributable to a particular source region).

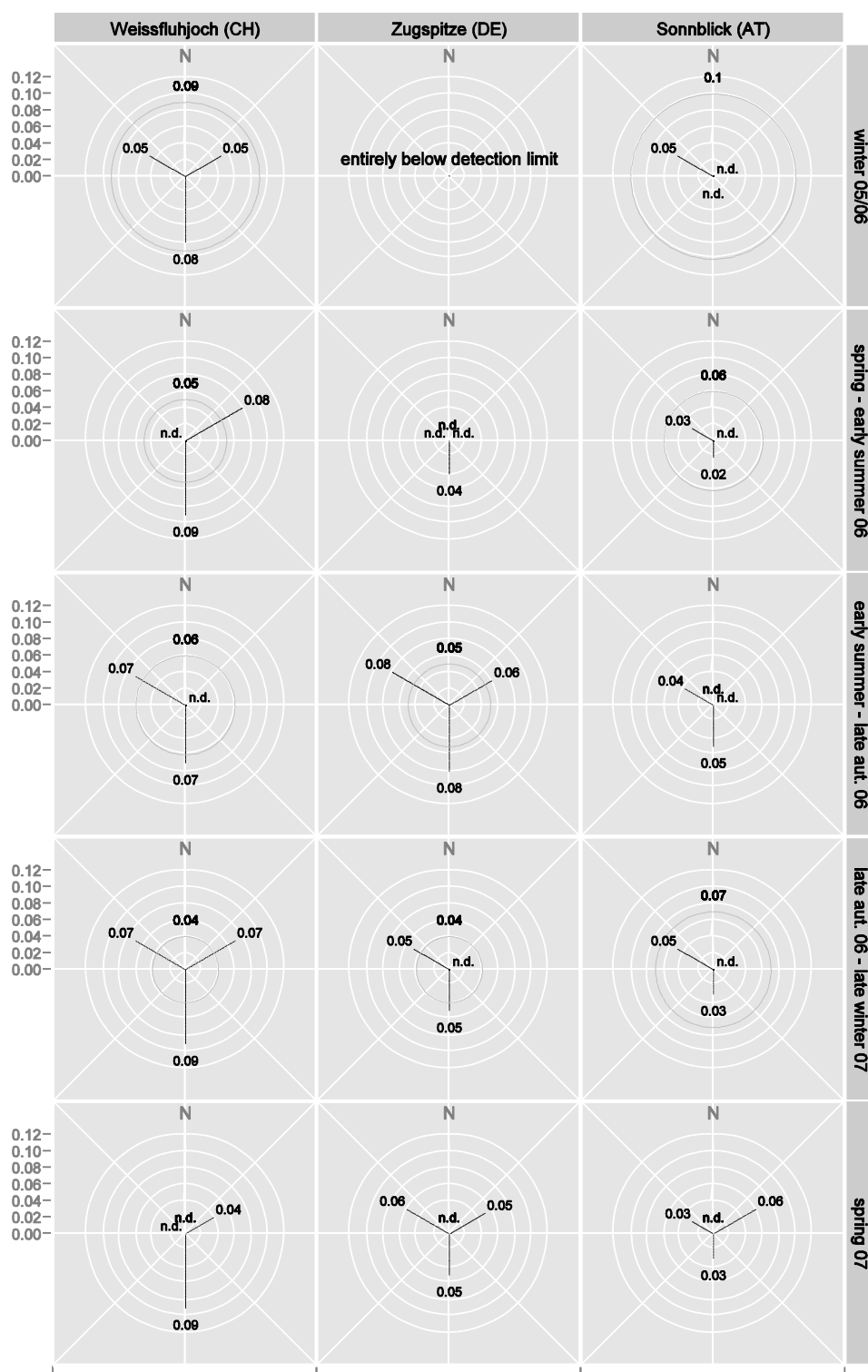


Figure 3-54: Concentration of Heptachlor [pg m^{-3}] in air from NW, NE and S (circle: trajectory not attributable to a particular source region).

3.2.5 Altitudinal variation

3.2.5.1 Needles

Altitudinal trends of OCP contamination of 0.5 year old Norway spruce needles were highly variable between profiles. A continuous vertical trend was only observed in a minority of cases. Depending on the particular substance, concentrations could either rise or fall with elevation. Also, a given parameter could exhibit opposite trends along different height profiles (see DDT:DDE-ratio at Wechsel and Rauris on p. 82).

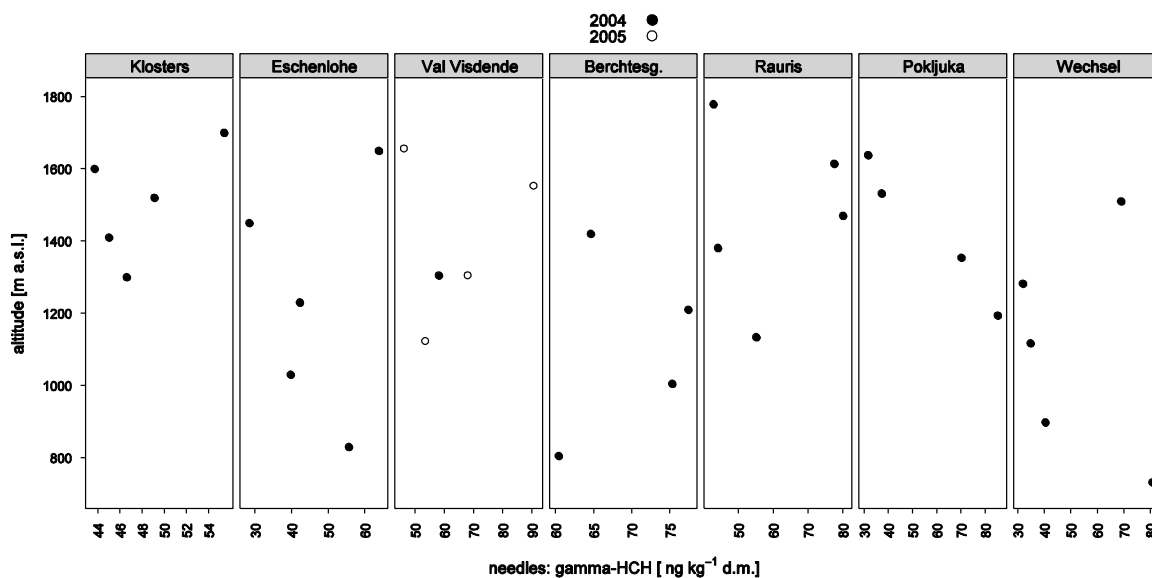


Figure 3-55: Altitudinal variation of the α -HCH concentration in 0.5 year old Norway spruce needles

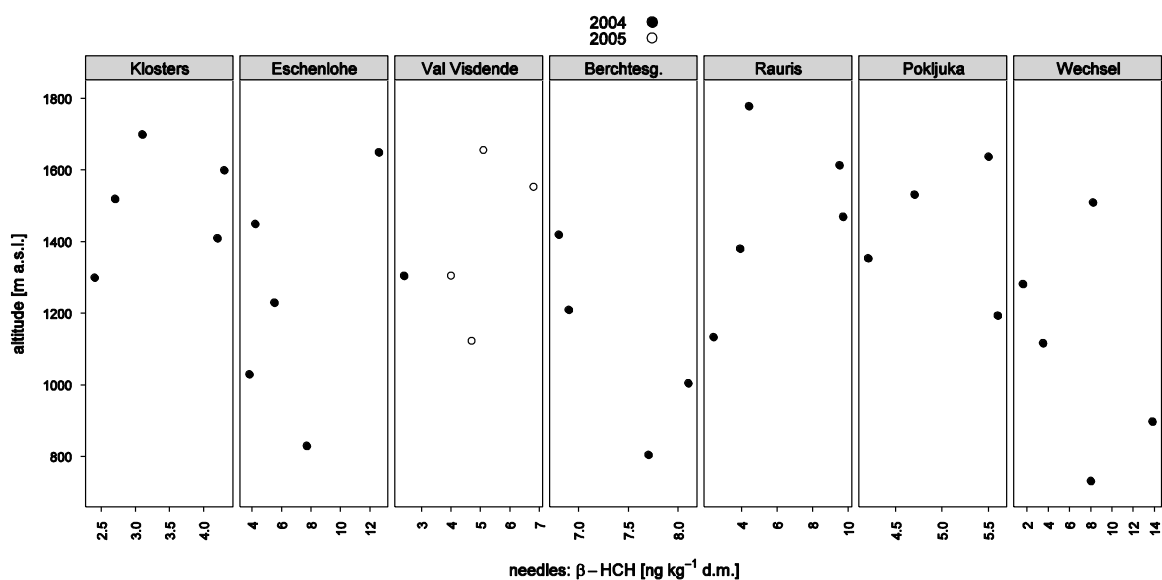


Figure 3-56: Altitudinal variation of the β -HCH concentration in 0.5 year old Norway spruce needles

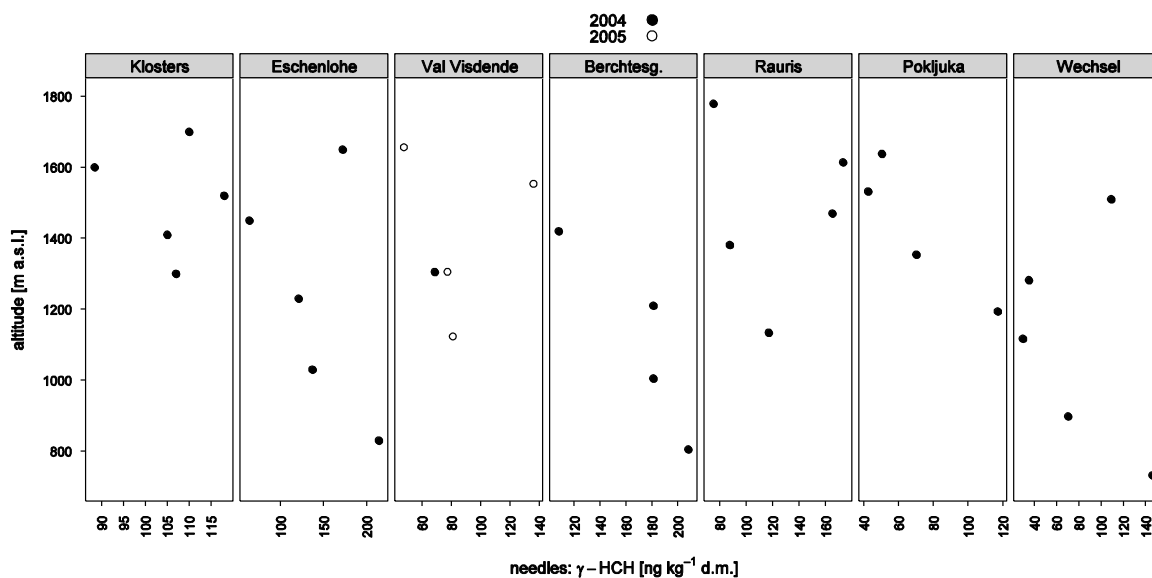


Figure 3-57: Altitudinal variation of the γ -HCH concentration in 0.5 year old Norway spruce needles

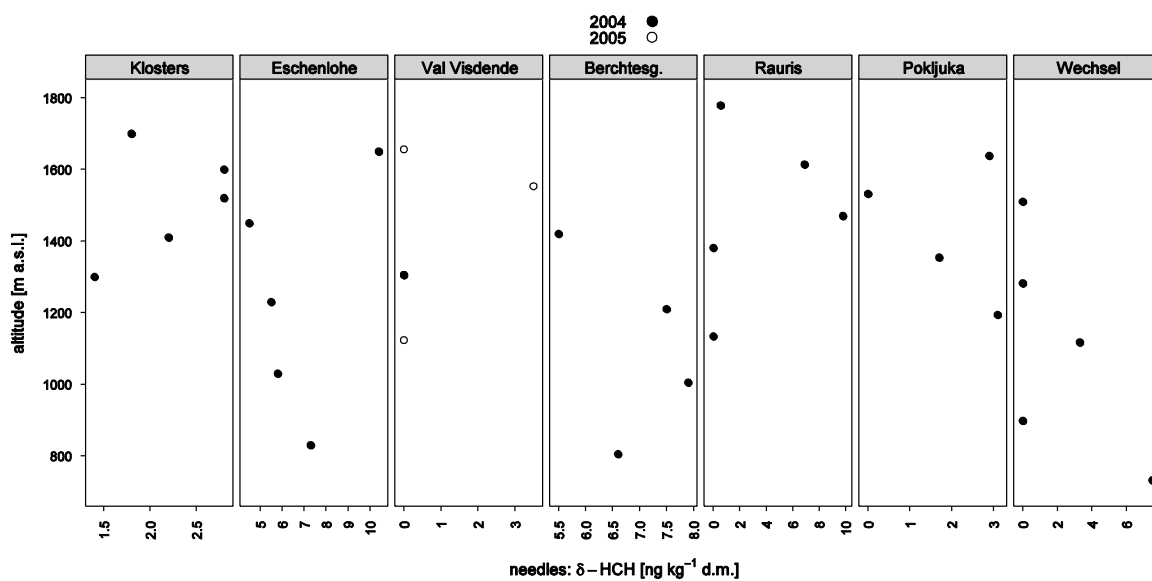


Figure 3-58: Altitudinal variation of the δ -HCH concentration in 0.5 year old Norway spruce needles

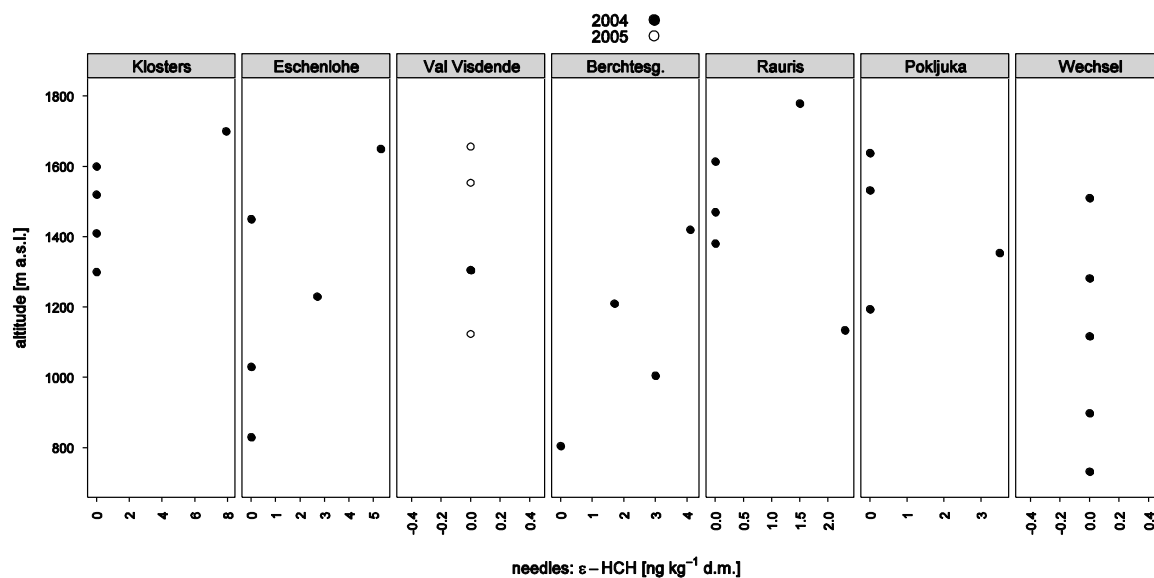


Figure 3-59: Altitudinal variation of the ϵ -HCH concentration in 0.5 year old Norway spruce needles

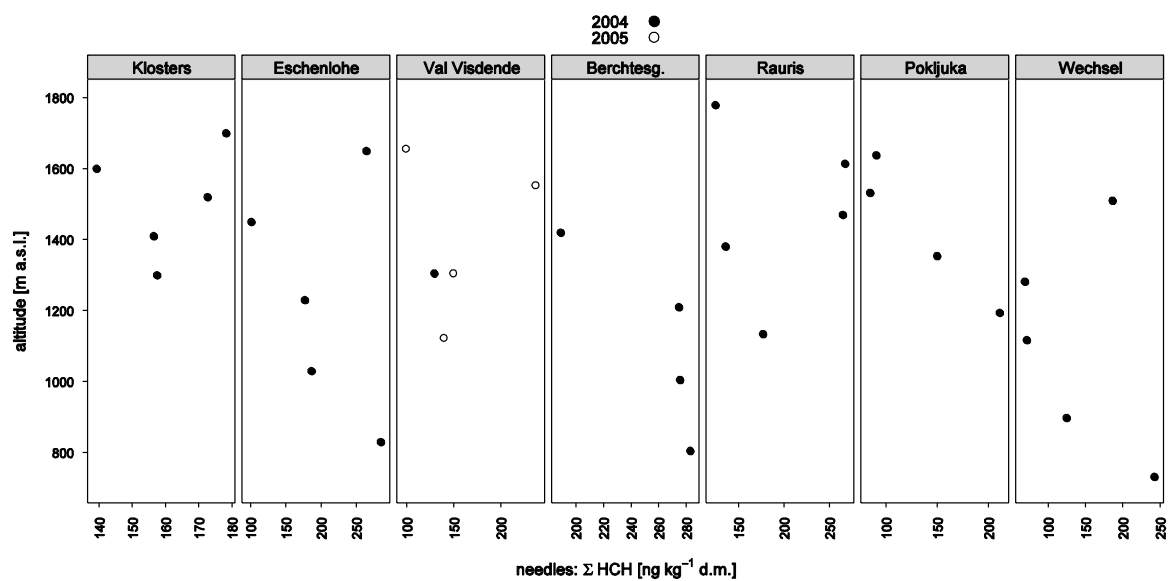


Figure 3-60: Altitudinal variation of total HCH content of 0.5 year old Norway spruce needles

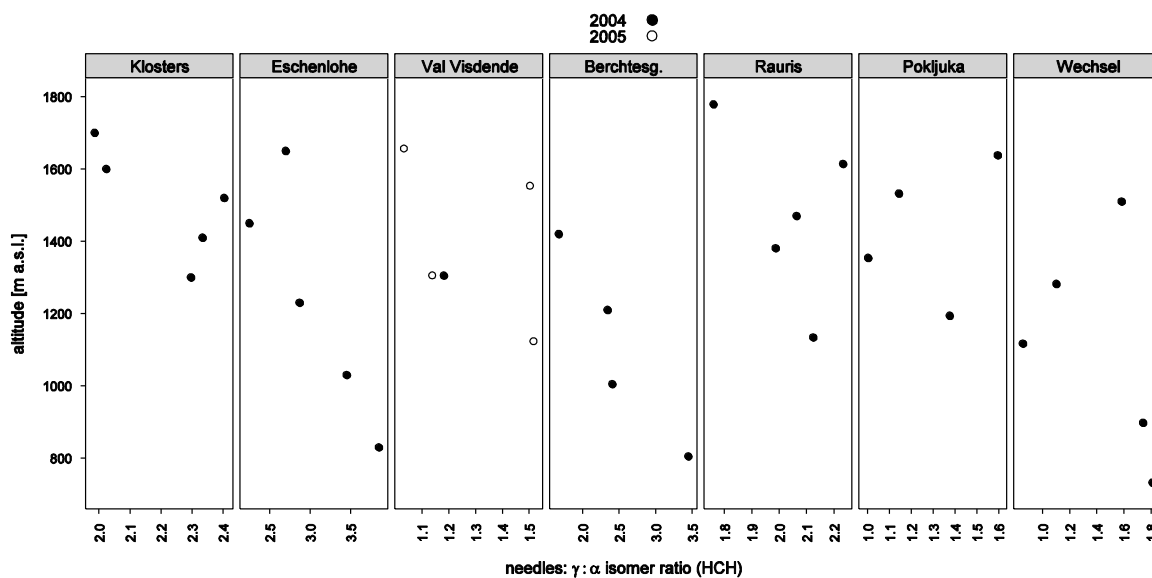


Figure 3-61: Altitudinal variation of the $\alpha : \gamma$ isomer ratio of HCH in 0.5 year old Norway spruce needles

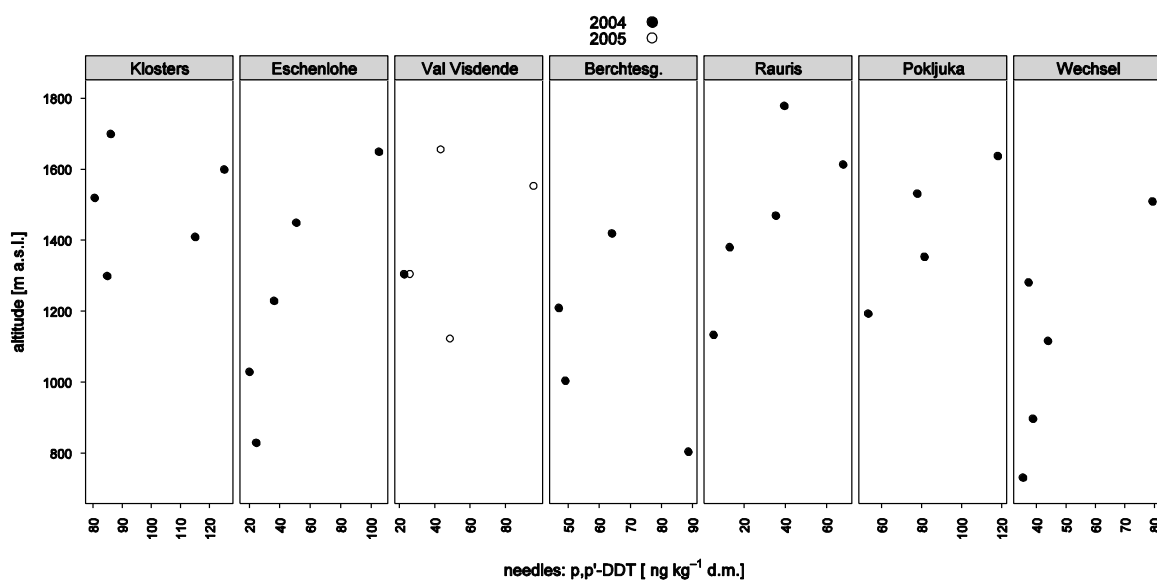


Figure 3-62: Altitudinal variation of the p,p' -DDT concentration in 0.5 year old Norway spruce needles

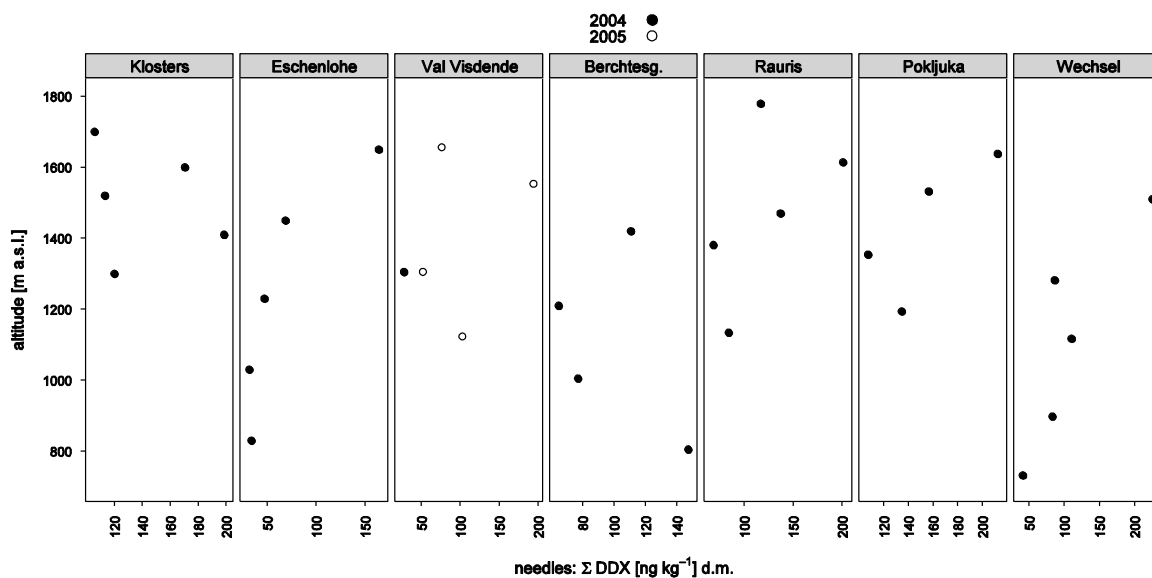


Figure 3-63: Altitudinal variation of total DDX content of 0.5 year old Norway spruce needles

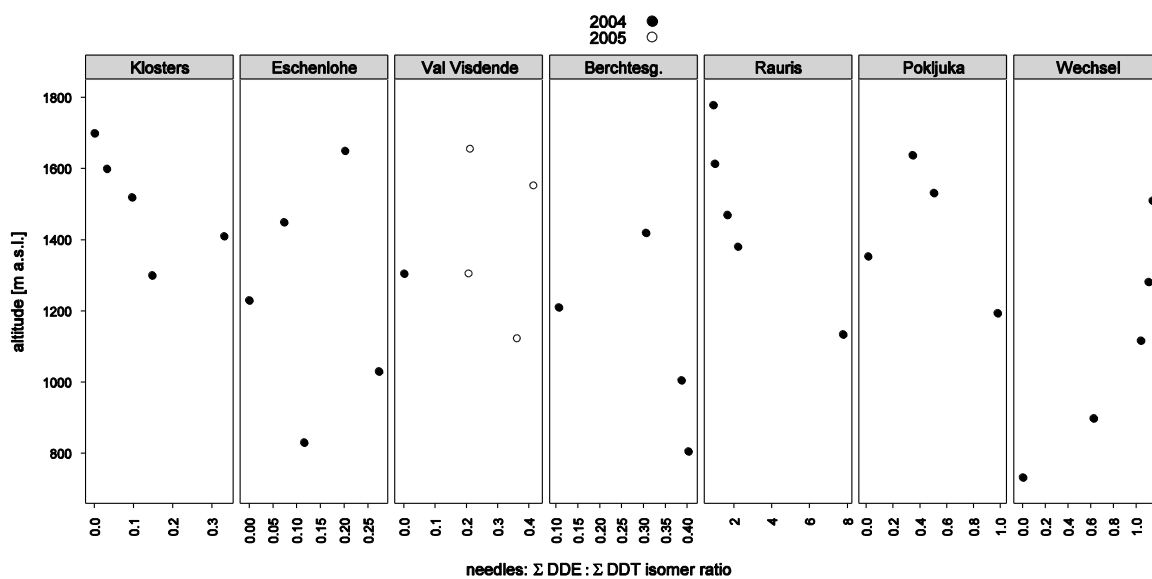
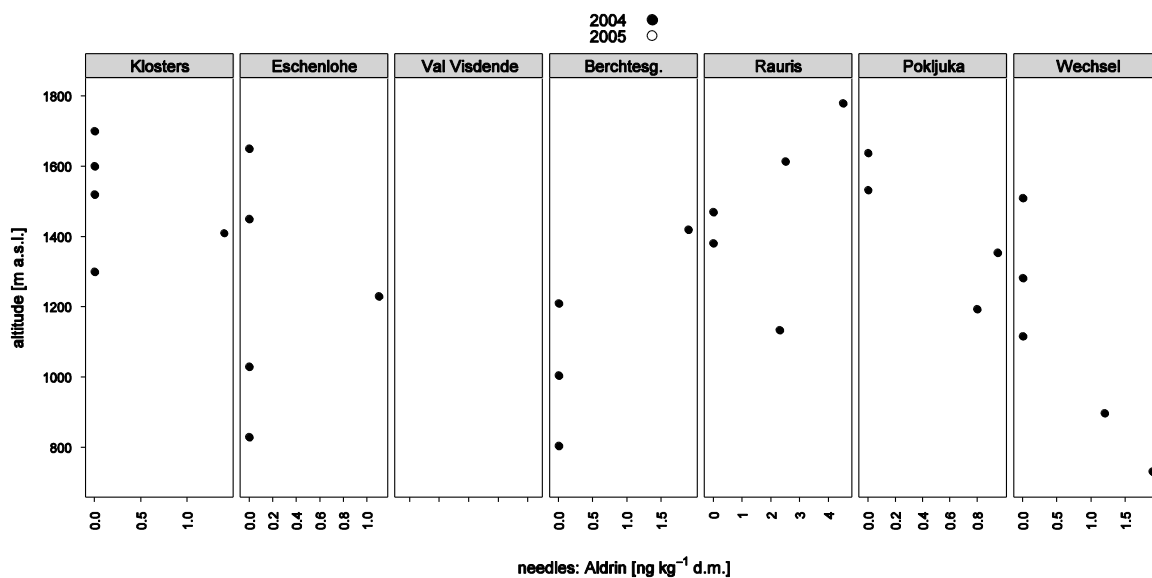


Figure 3-64: Altitudinal variation of the p,p' -DDE : p,p' -DDT ratio in 0.5 year old Norway spruce needles



No Aldrin was found in needles from height profile Val Visdende.

Figure 3-65: Altitudinal variation of the Aldrin concentration in 0.5 year old Norway spruce needles

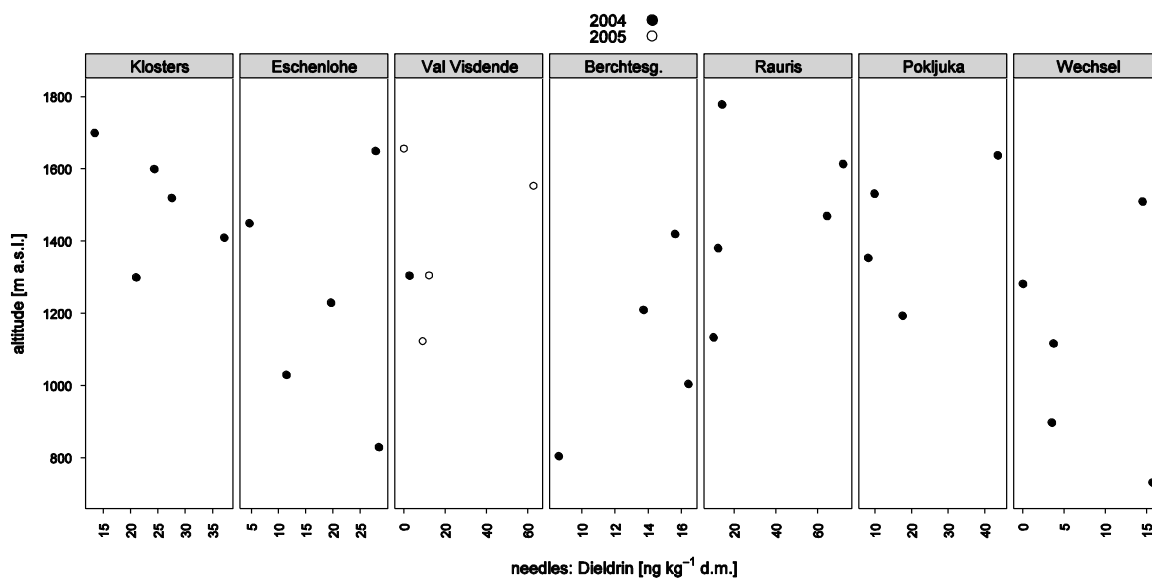


Figure 3-66: Altitudinal variation of the Dieldrin concentration in 0.5 year old Norway spruce needles

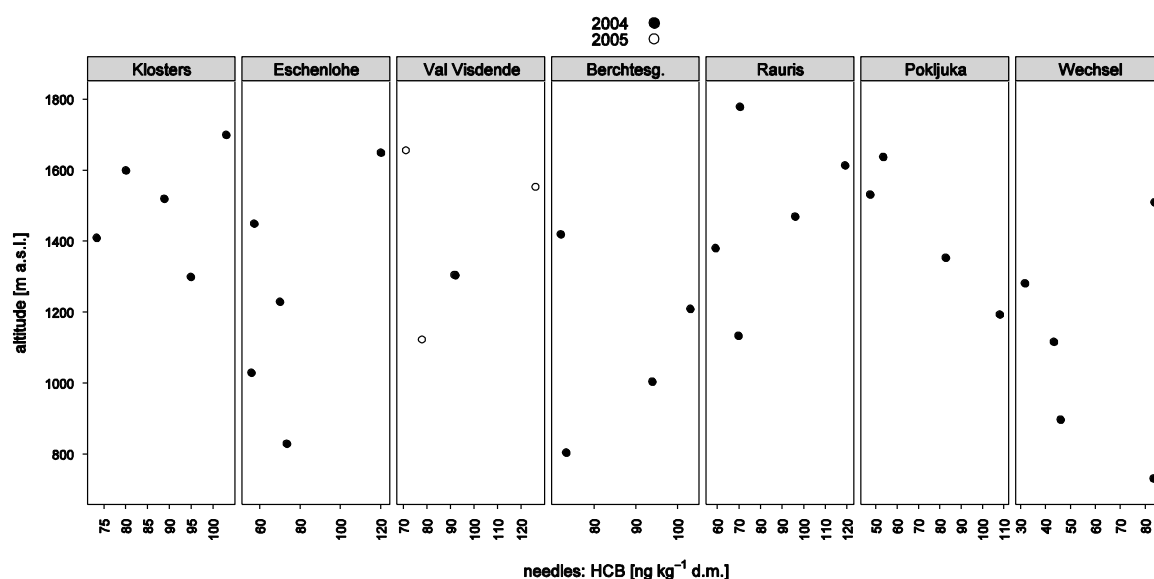
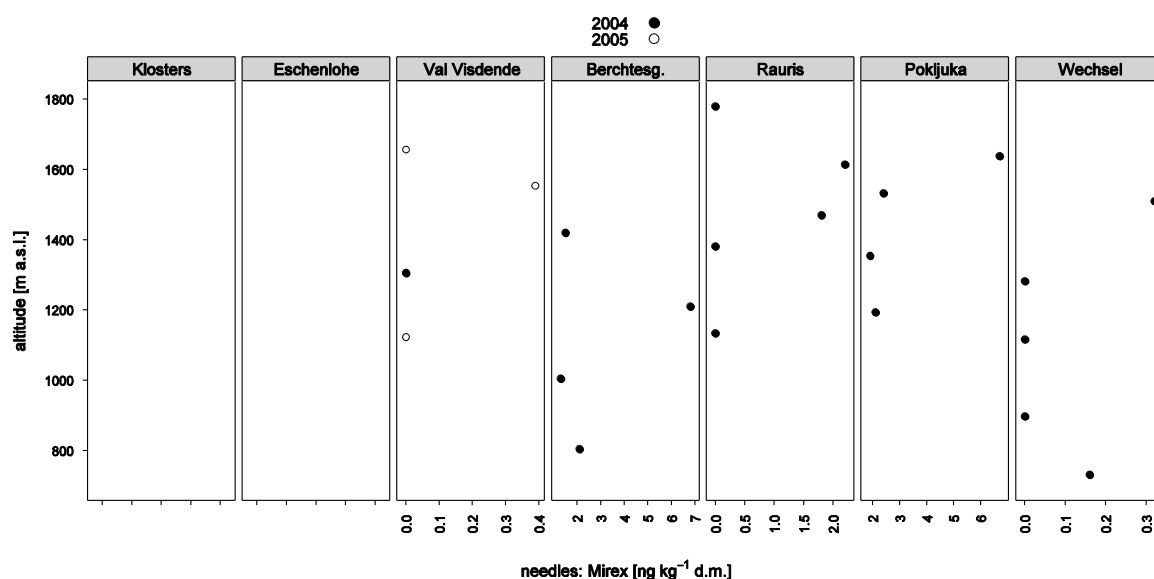


Figure 3-67: Altitudinal variation of the HCB concentration in 0.5 year old Norway spruce needles

Heptachlor was not detected in needles from any height profile.



No Mirex was found in needles from the height profiles Klosters and Eschenlohe.

Figure 3-68: Altitudinal variation of the Mirex concentration in 0.5 year old Norway spruce needles

3.2.5.2 Humus

As observed with needle samples, vertical concentrations gradients - where present - varied between height profiles. While there were height profiles of similar behaviour (e. g. an increase of γ -HCH content with elevation at the profiles Klosters, Rauris and Wechsel), the same substance could exhibit an opposed trend at another profile (e. g. γ -HCH decrease towards the top of Val Visdende profile). However, at a given profile different OCP could show remarkable analogies. For instance, all analysed pesticides except Aldrin and Heptachlor

showed an upwards increase at the profiles Wechsel and Rauris. The profiles in the northern and central Alps showed higher concentrations of nearly all OCP at the highest plots – opposite to the two profiles (Val Visdende, Pokljuka) in the South of the Alps.

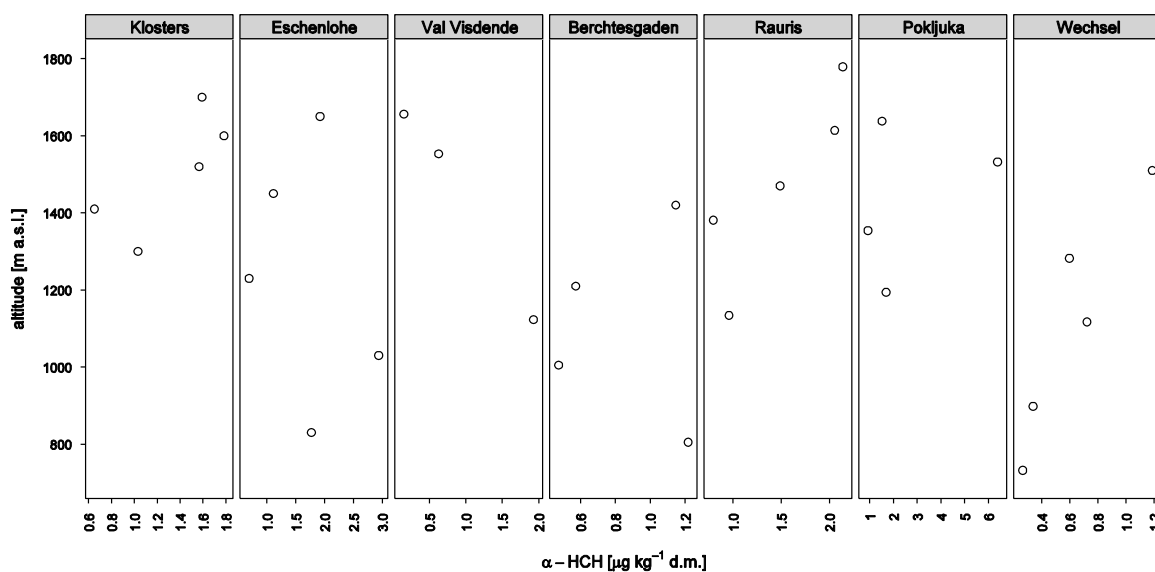


Figure 3-69: Altitudinal variation of the α -HCH concentration in humus from Norway spruce stands

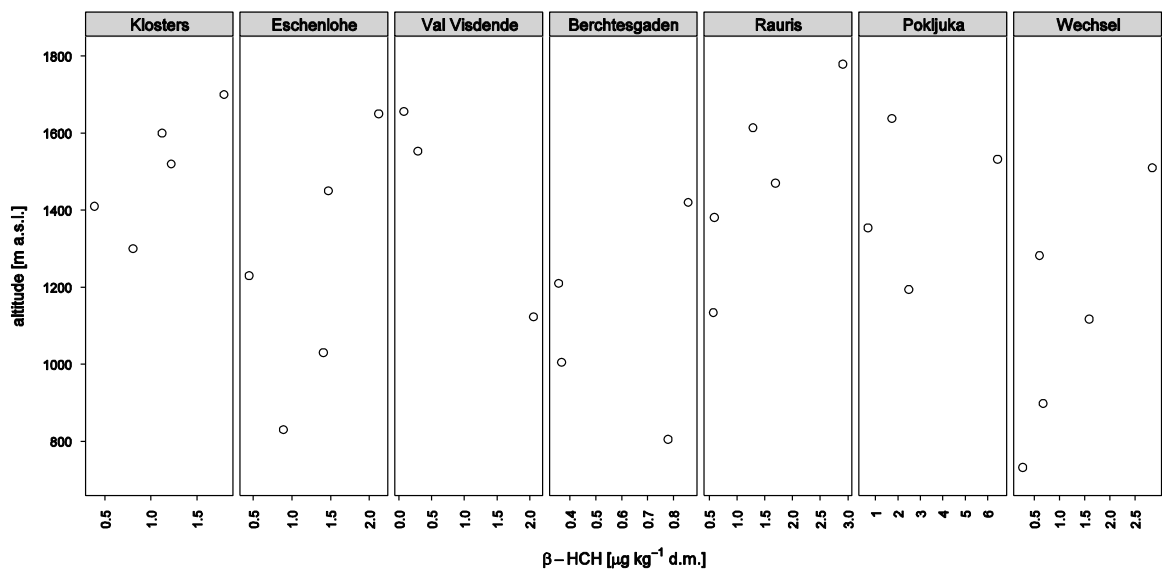


Figure 3-70: Altitudinal variation of the β -HCH concentration in humus from Norway spruce stands

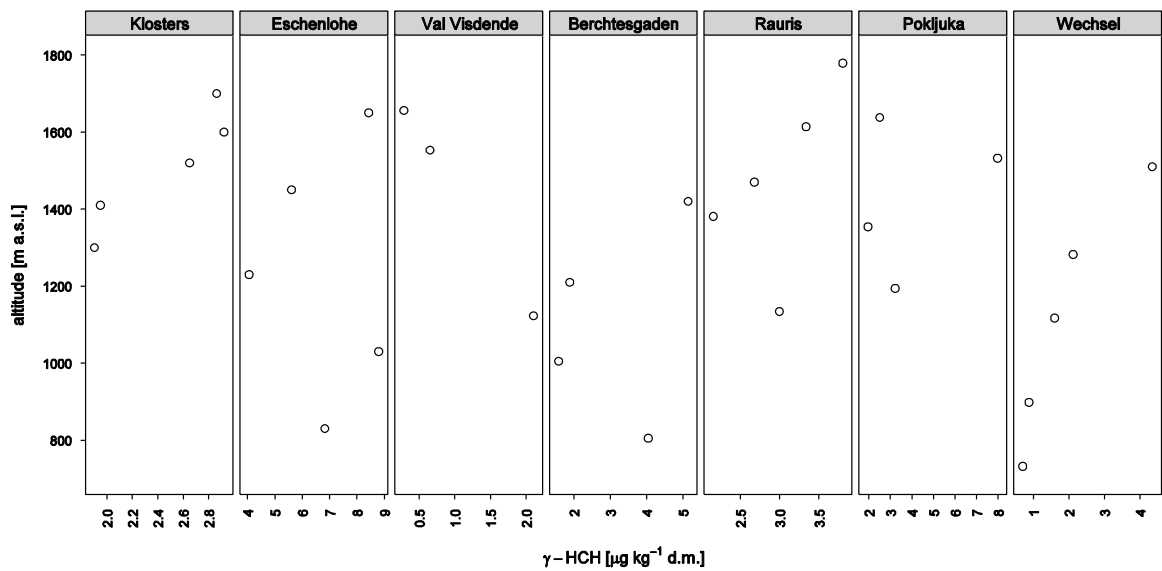


Figure 3-71: Altitudinal variation of the γ -HCH concentration in humus from Norway spruce stands

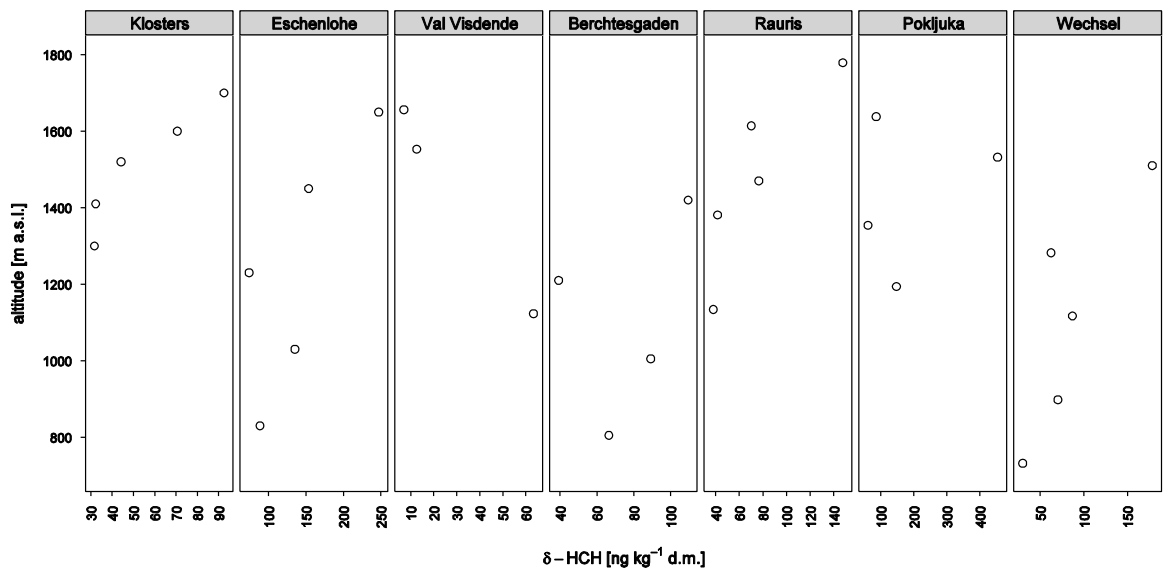


Figure 3-72: Altitudinal variation of the δ -HCH concentration in humus from Norway spruce stands

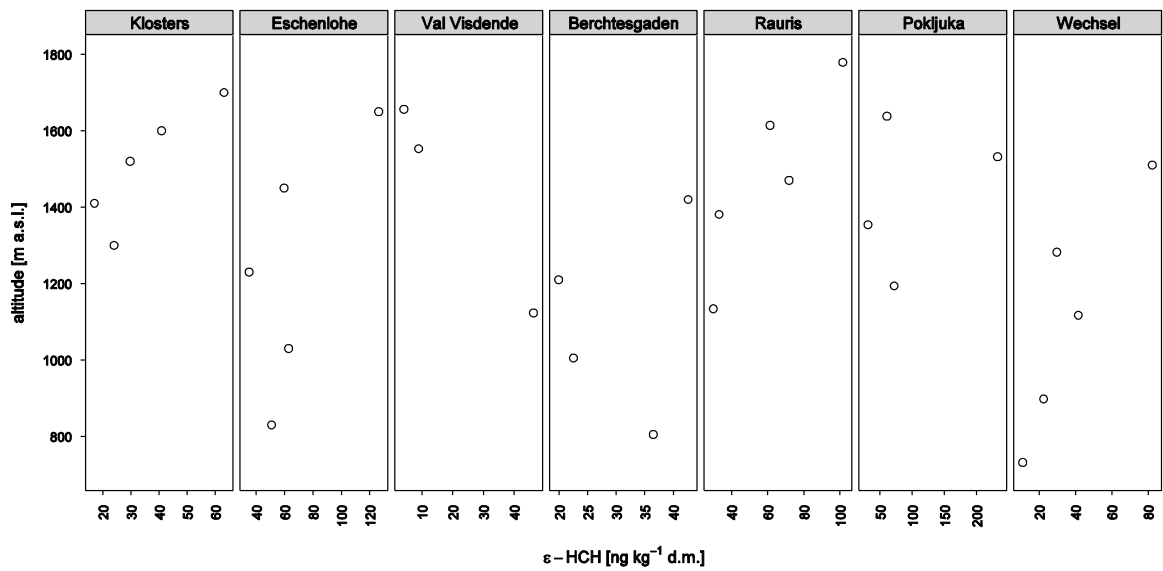


Figure 3-73: Altitudinal variation of the ϵ -HCH concentration in humus from Norway spruce stands

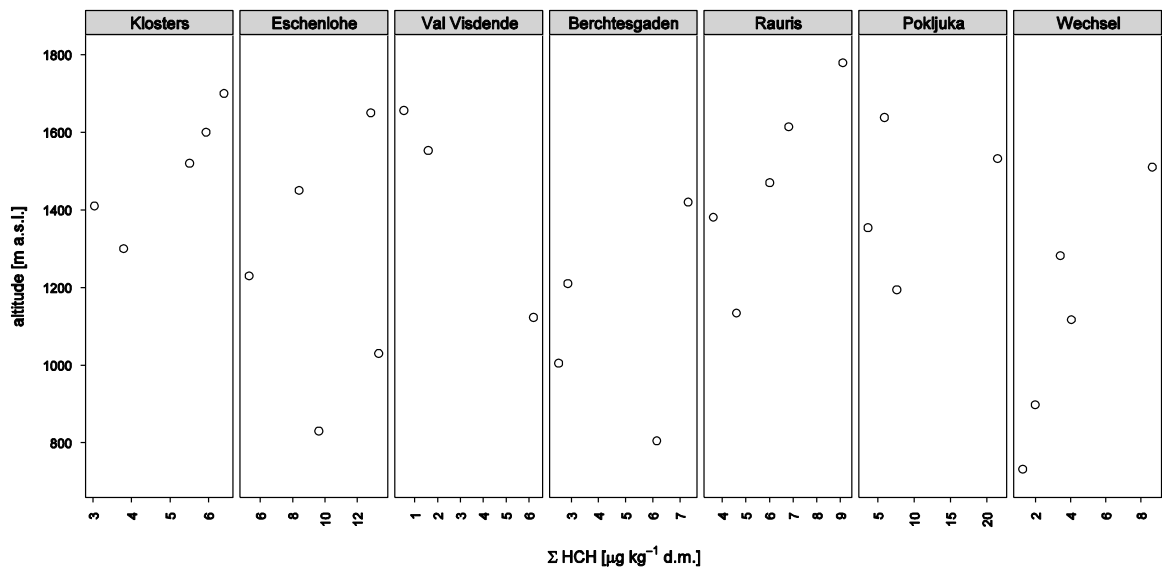


Figure 3-74: Altitudinal variation of total HCH content of humus from Norway spruce stands

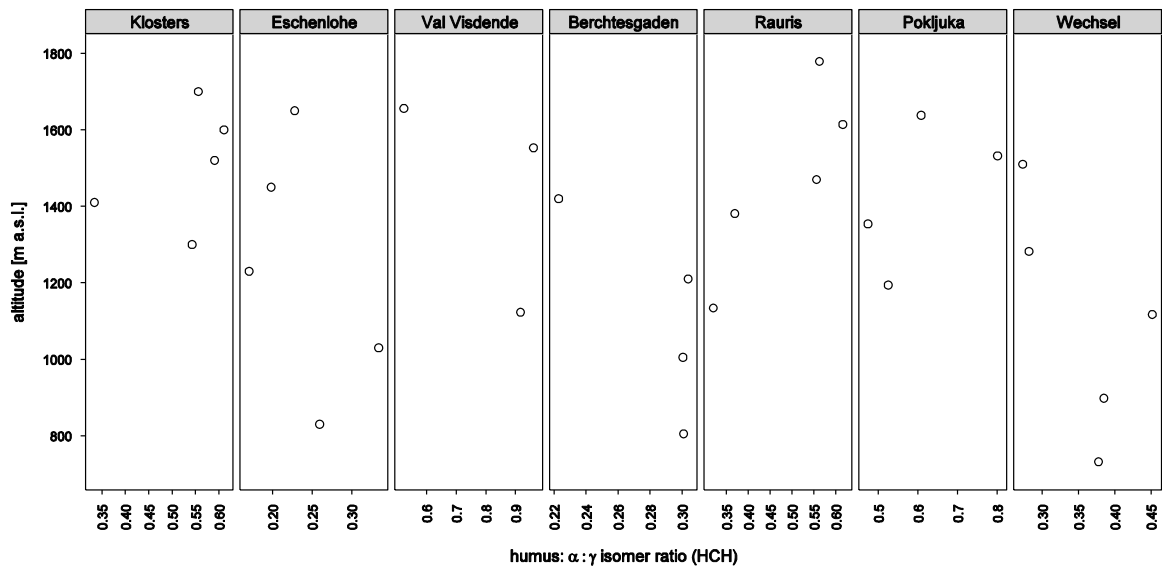


Figure 3-75: Altitudinal variation of the α : γ isomer ratio of HCH in humus from Norway spruce stands

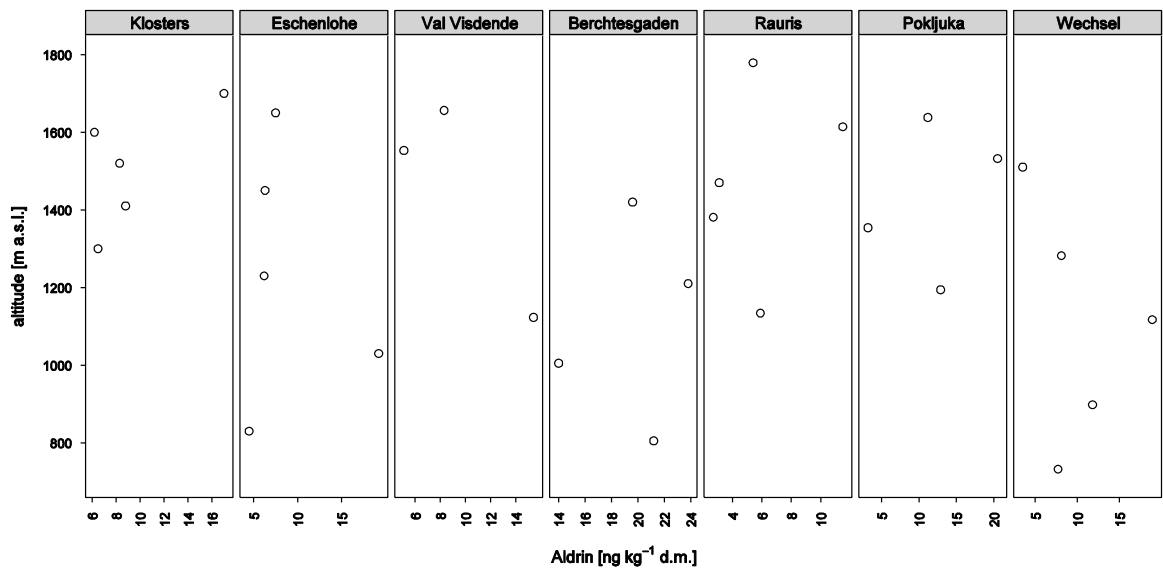


Figure 3-76: Altitudinal variation of the Aldrin concentration in humus from Norway spruce stands

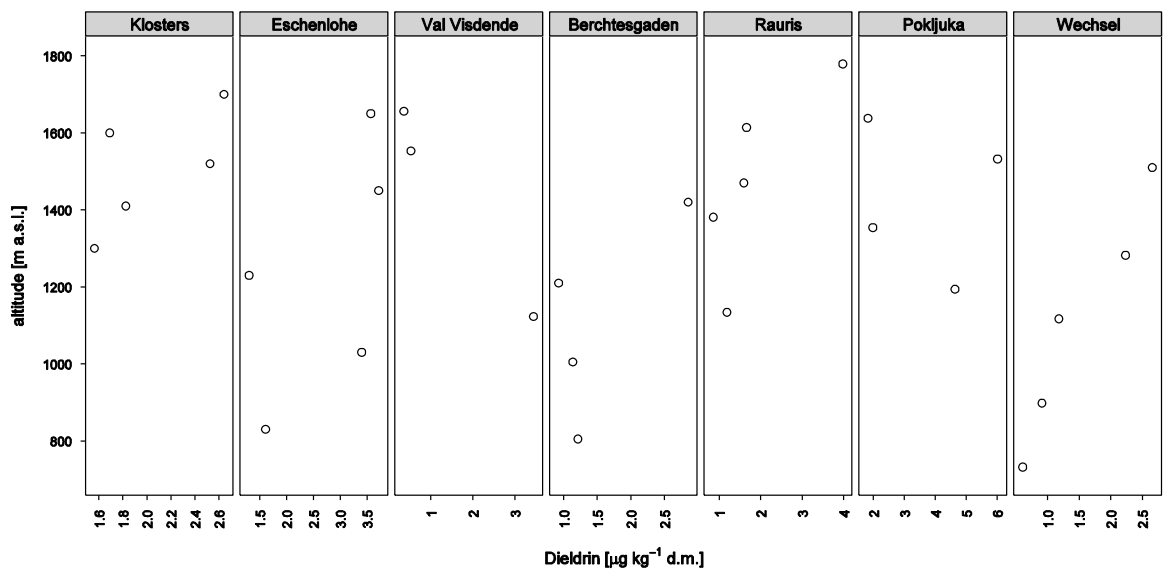


Figure 3-77: Altitudinal variation of the Dieldrin concentration in humus from Norway spruce stands

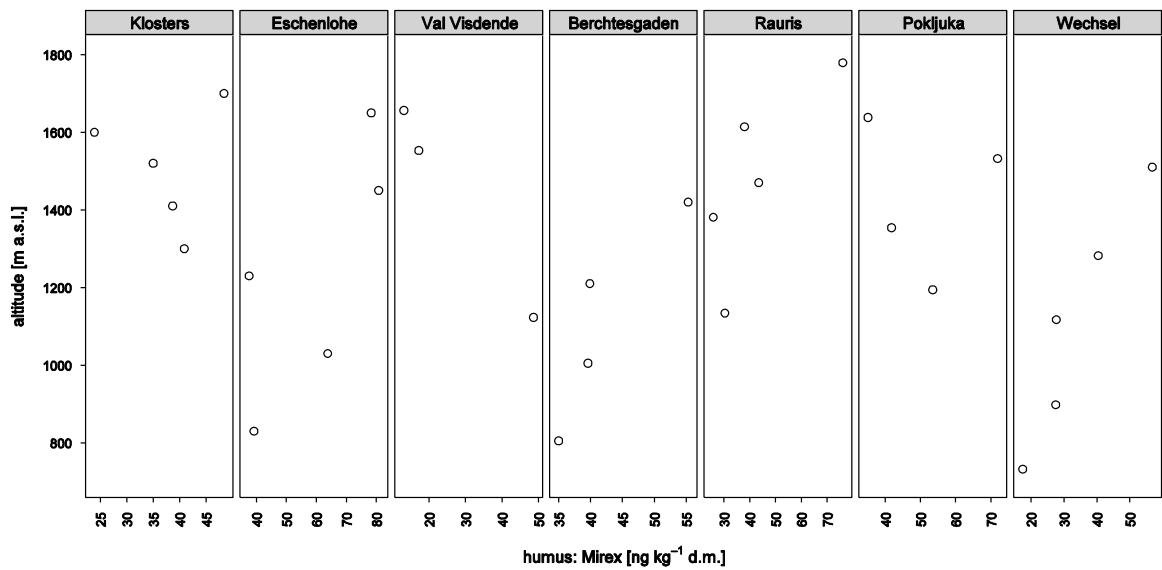


Figure 3-78: Altitudinal variation of the Mirex concentration in humus from Norway spruce stands

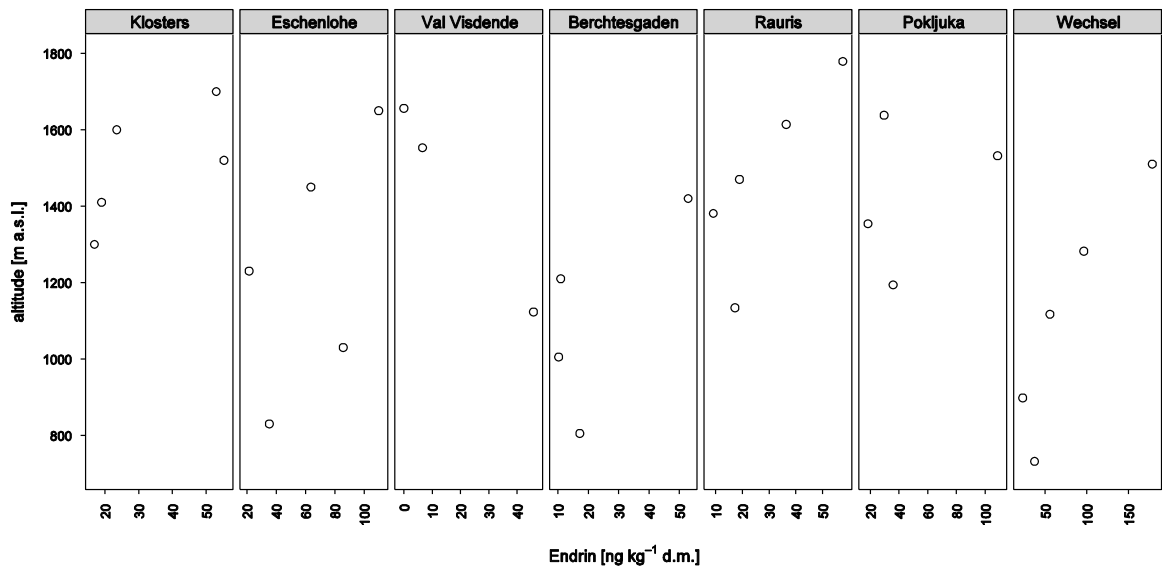


Figure 3-79: Altitudinal variation of the Endrin concentration in humus from Norway spruce stands

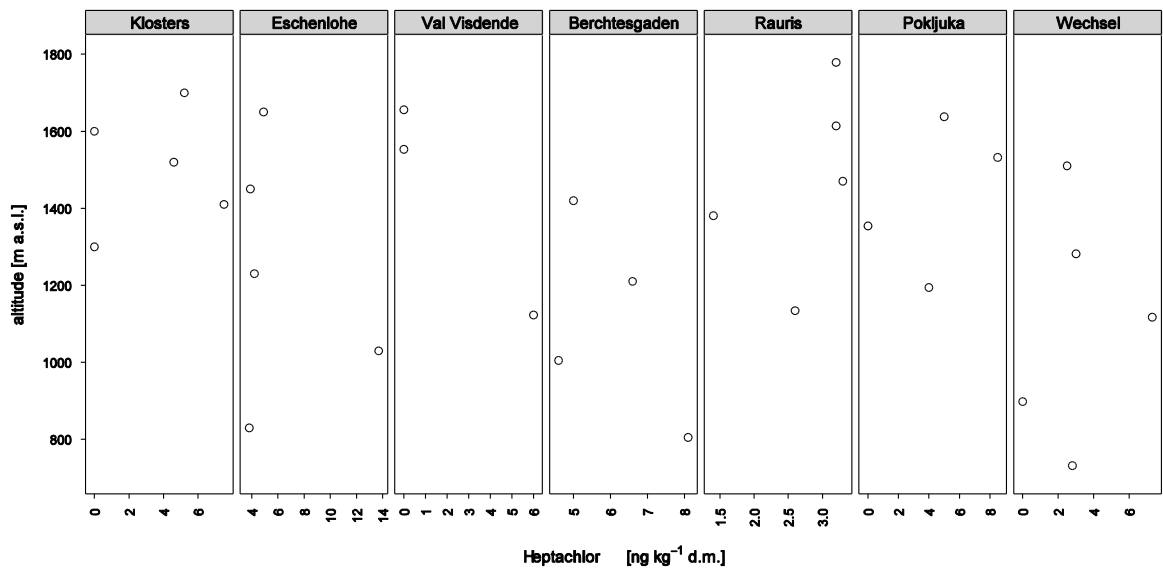


Figure 3-80: Altitudinal variation of the Heptachlor concentration in humus from Norway spruce stands

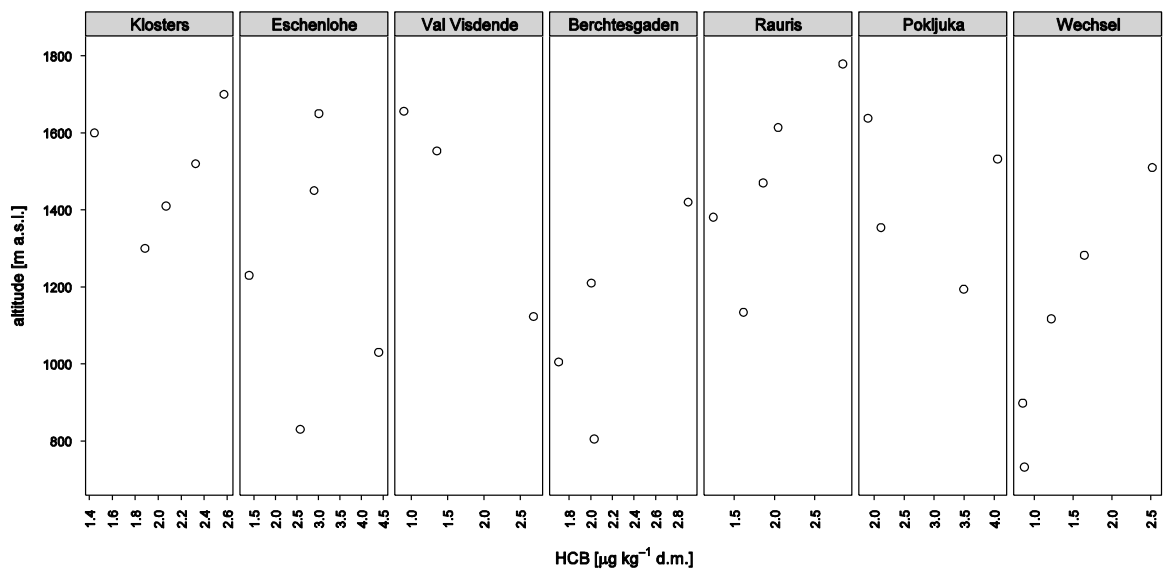


Figure 3-81: Altitudinal variation of the HCB concentration in humus from Norway spruce stands

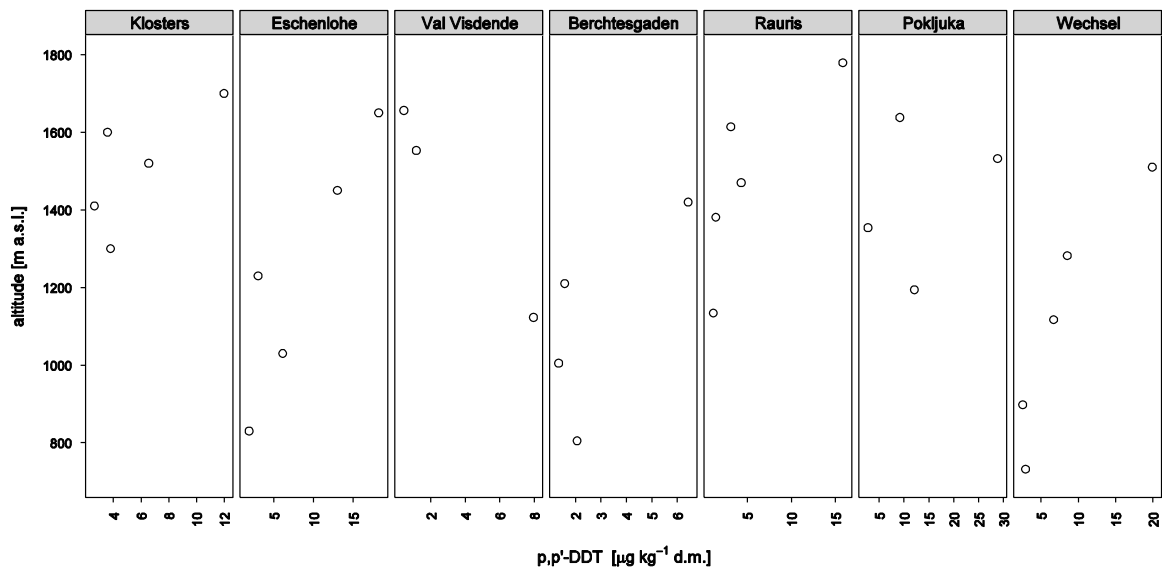


Figure 3-82: Altitudinal variation of the p,p' -DDT concentration in humus from Norway spruce stands

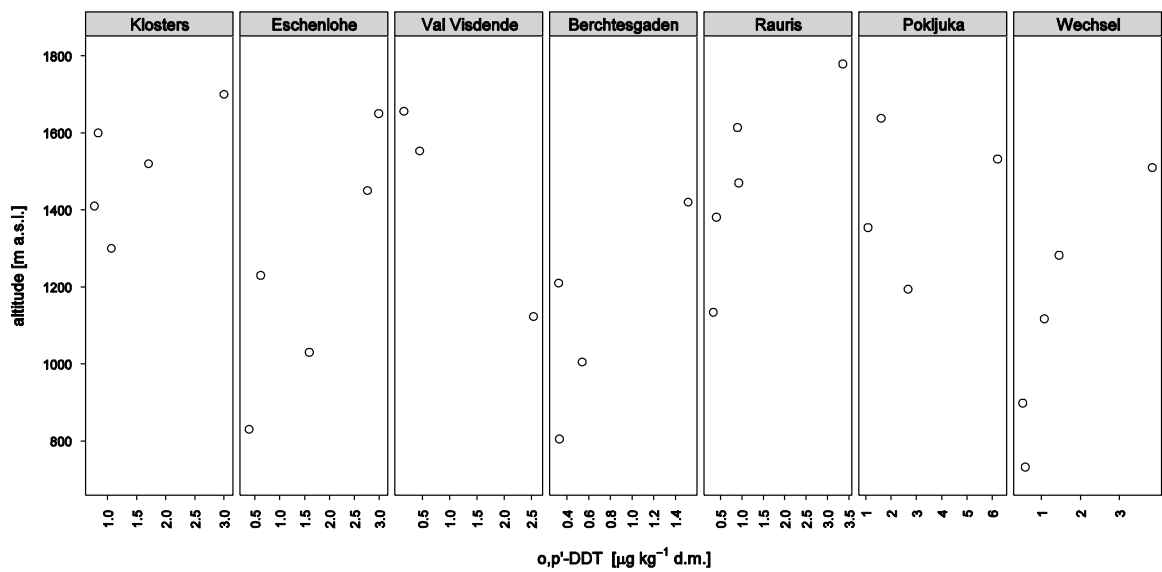


Figure 3-83: Altitudinal variation of the o,p' -DDT concentration in humus from Norway spruce stands

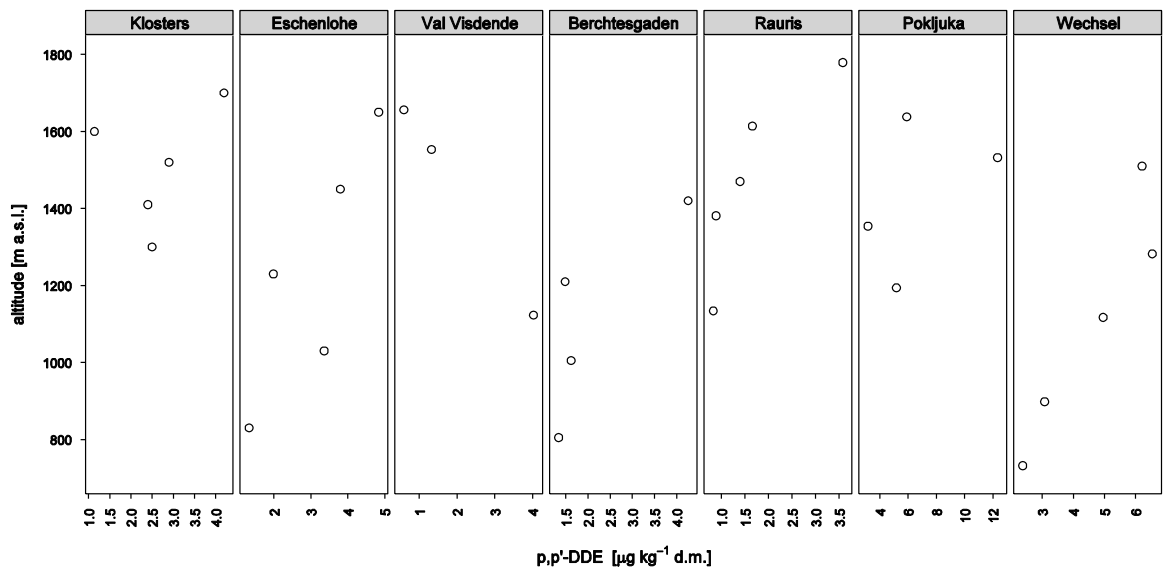


Figure 3-84: Altitudinal variation of the *p,p'*-DDE concentration in humus from Norway spruce stands.

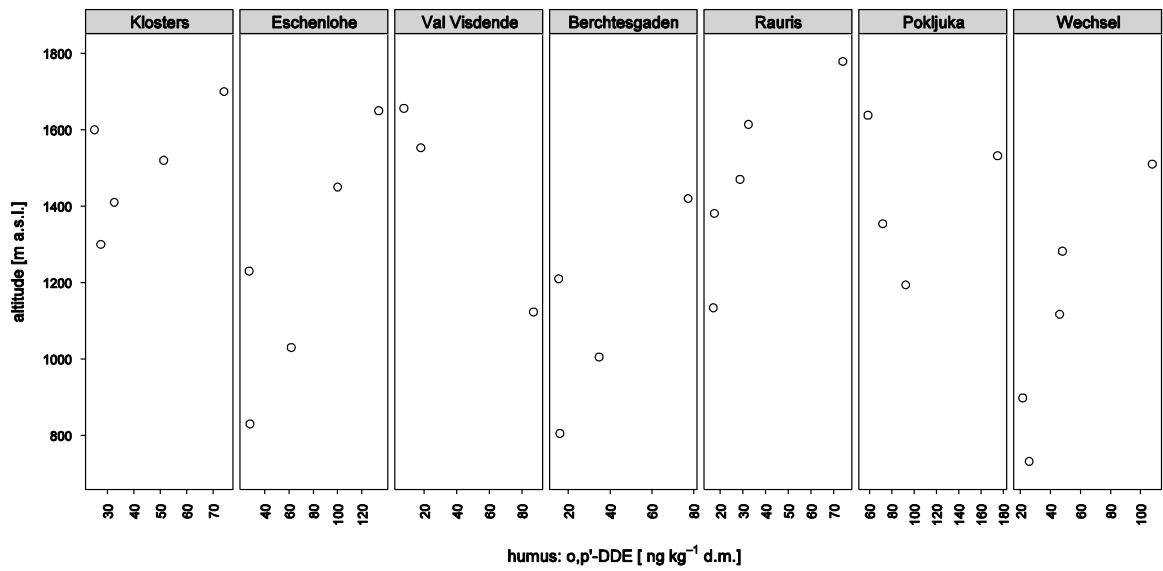


Figure 3-85: Altitudinal variation of the *o,p'*-DDE concentration in humus from Norway spruce stands

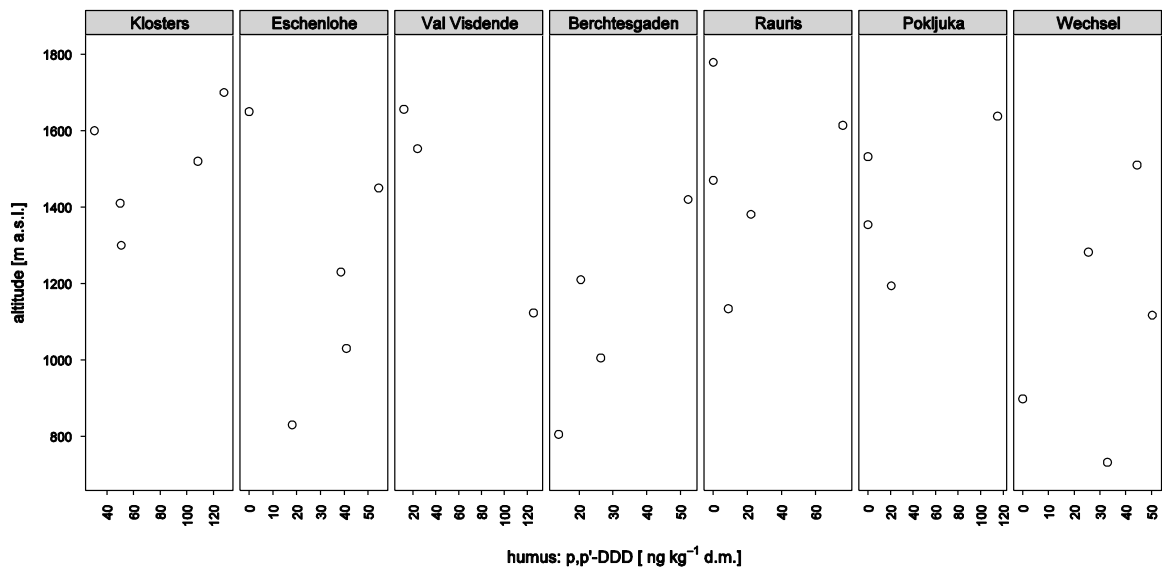


Figure 3-86: Altitudinal variation of the *p,p'*-DDD concentration in humus from Norway spruce stands.

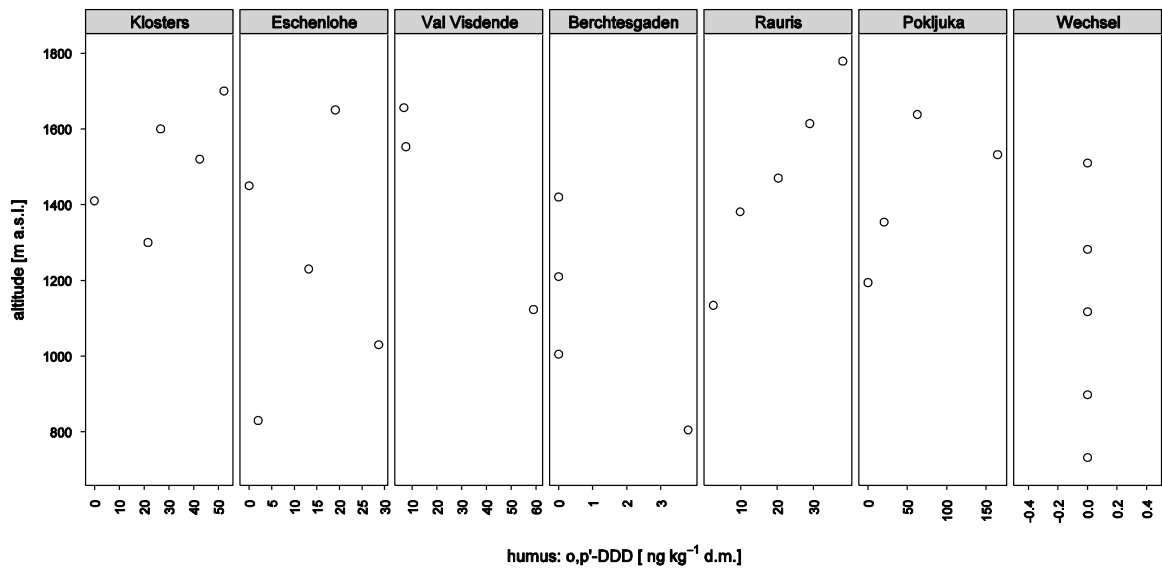


Figure 3-87: Altitudinal variation of the *o,p'*-DDD concentration in humus from Norway spruce stands

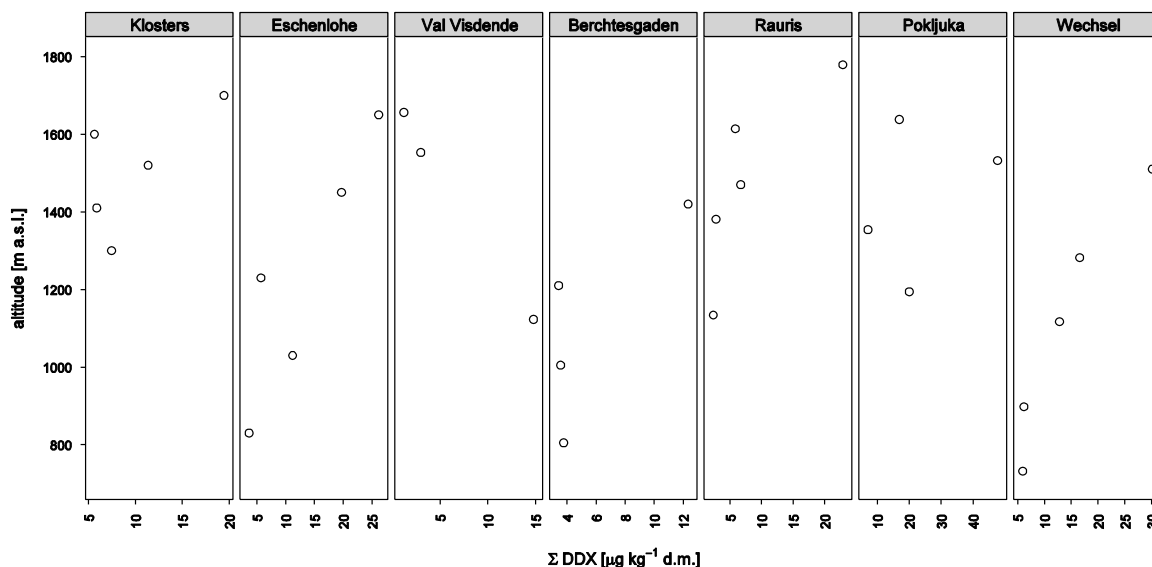


Figure 3-88: Altitudinal variation of total DDX content of humus from Norway spruce stands.

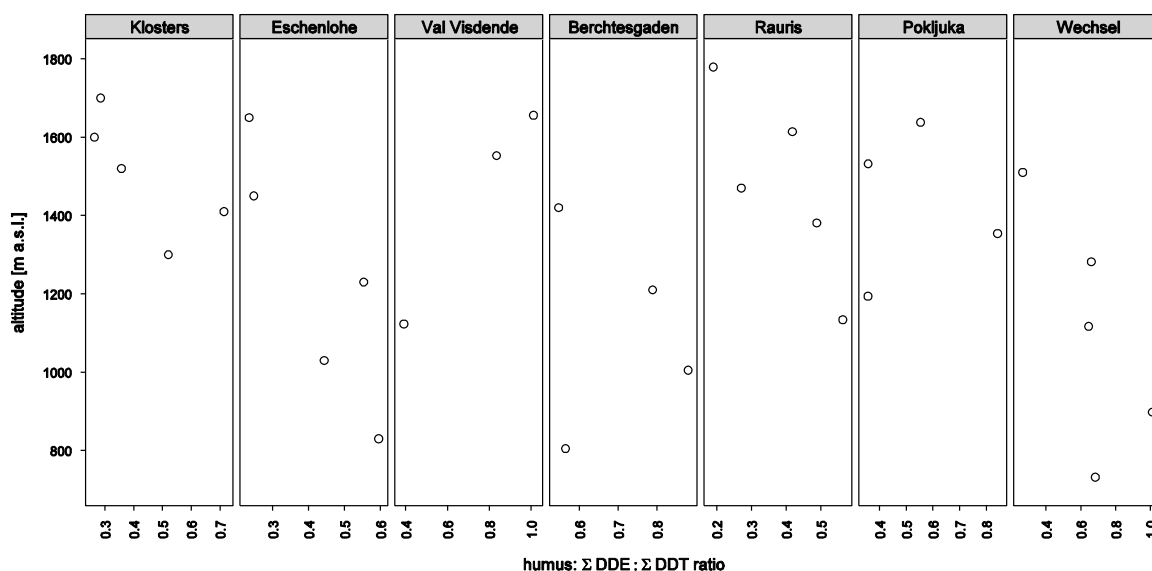
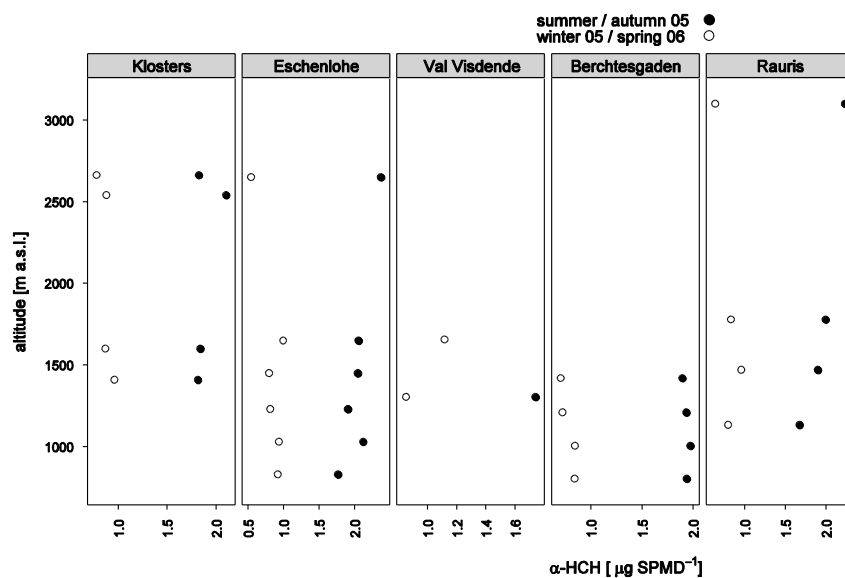
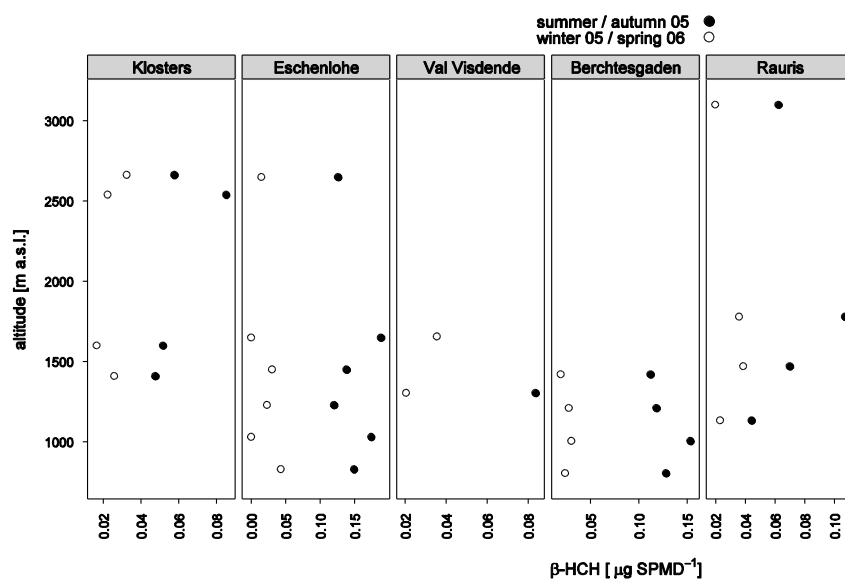
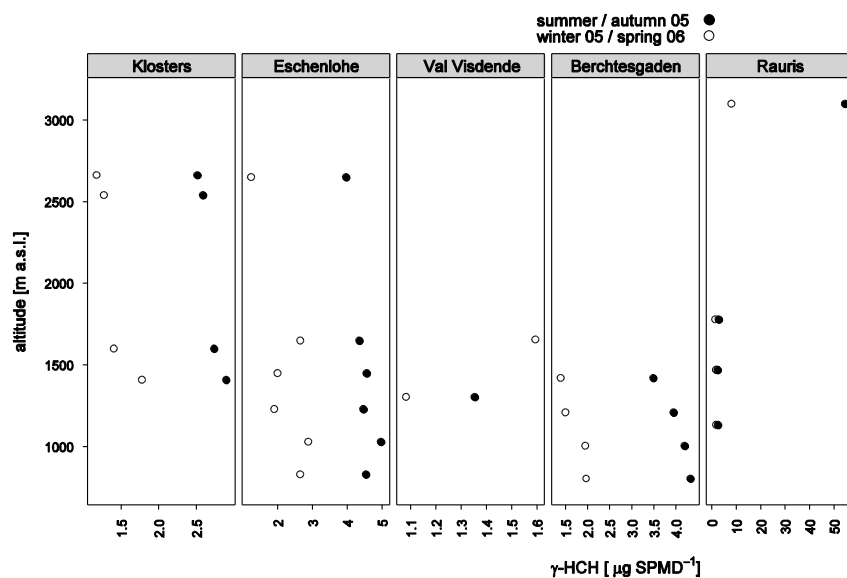
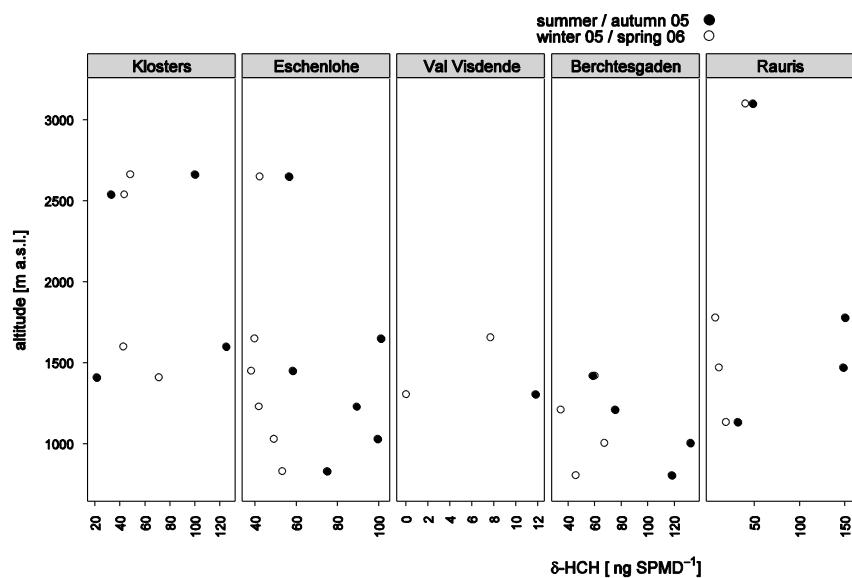


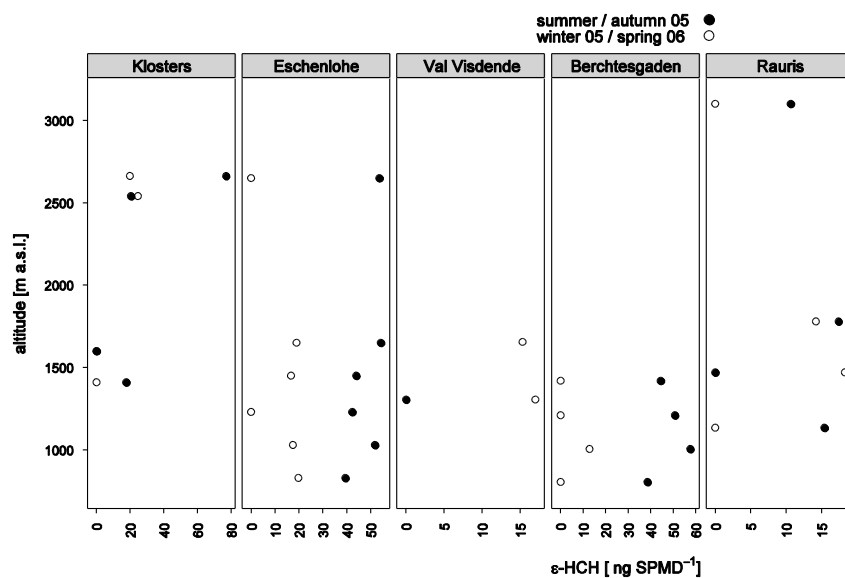
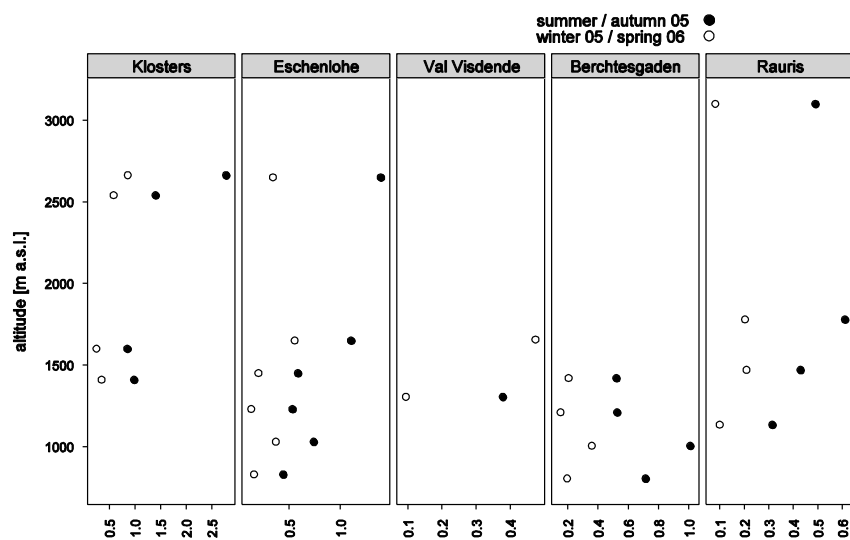
Figure 3-89: Altitudinal variation of the DDE :DDT isomer ratio in humus from Norway spruce stands.

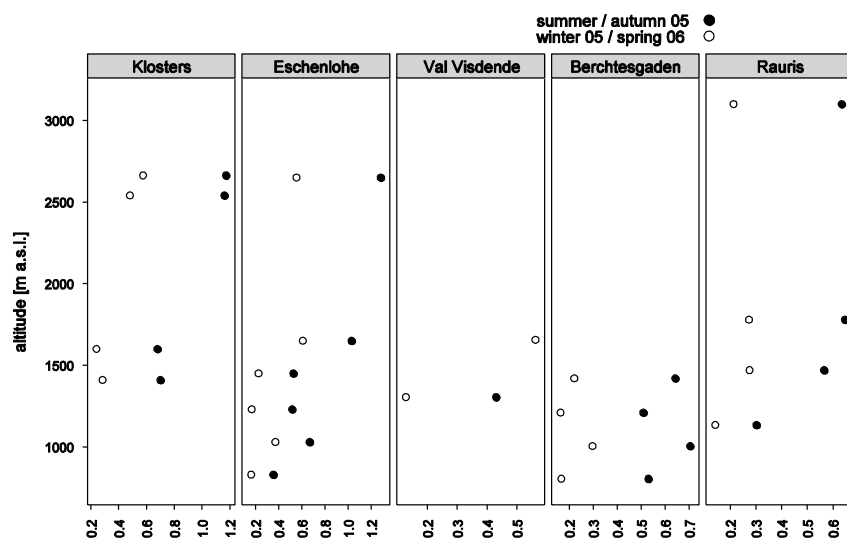
3.2.5.3 SPMD

Vertical trends of OCP concentrations in SPMD passive samplers were not uniform across the different height profiles, although for some OCP the majority of sites displayed an increase of concentrations with height. Furthermore, along a given profile, vertical trends of different OCP could exhibit striking similarities, e. g. in the case of Dieldrin and total DDX content. Pesticide contents of the samples exposed during the warmer period (summer-autumn 2005) were usually higher than those exposed during winter 2005-spring 06, with the notable exception of the comparably high concentrated HCB which showed little difference between both periods.

Figure 3-90: Altitudinal variation of α -HCH in SPMDFigure 3-91: Altitudinal variation of β -HCH in SPMD

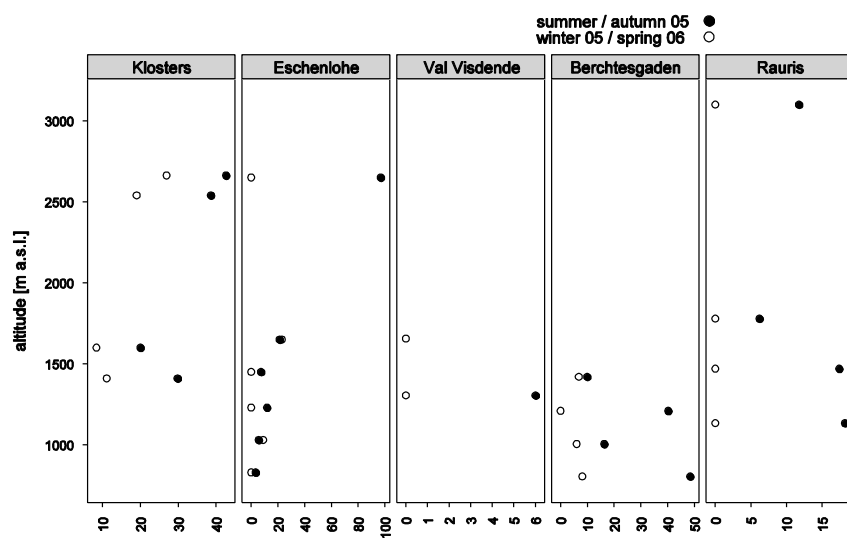
Figure 3-92: Altitudinal variation of γ -HCH in SPMDFigure 3-93: Altitudinal variation of δ -HCH in SPMD

Figure 3-94: Altitudinal variation of ϵ -HCH in SPMDunit: ng SPMD⁻¹Figure 3-95: Altitudinal variation of p,p' -DDT in SPMD



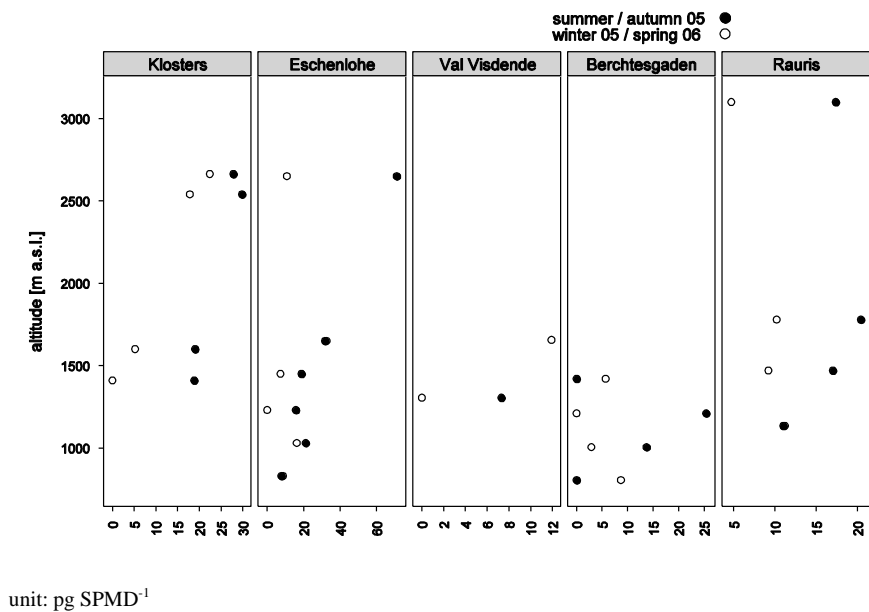
unit: ng SPMD⁻¹

Figure 3-96: Altitudinal variation of *o,p'*-DDT in SPMD



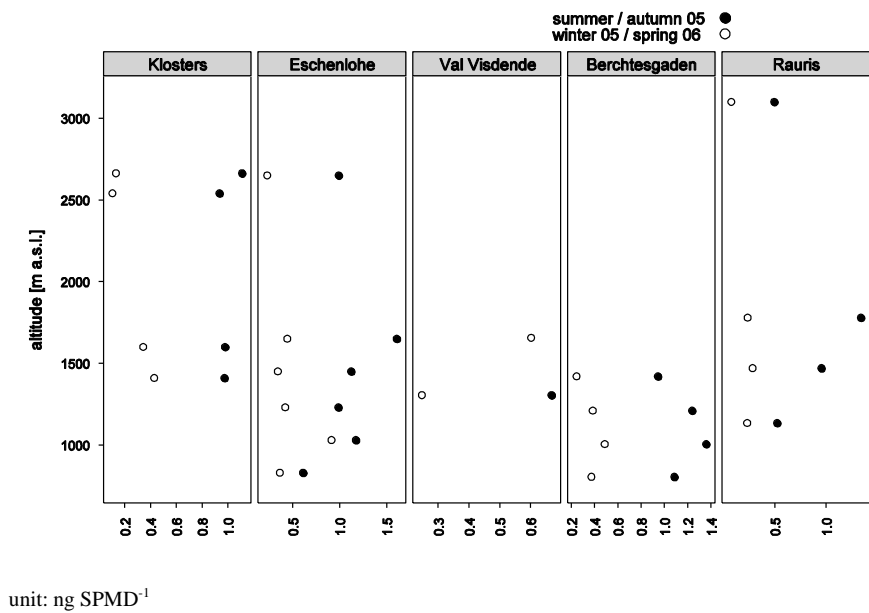
unit: pg SPMD⁻¹

Figure 3-97: Altitudinal variation of *p,p'*-DDD in SPMD



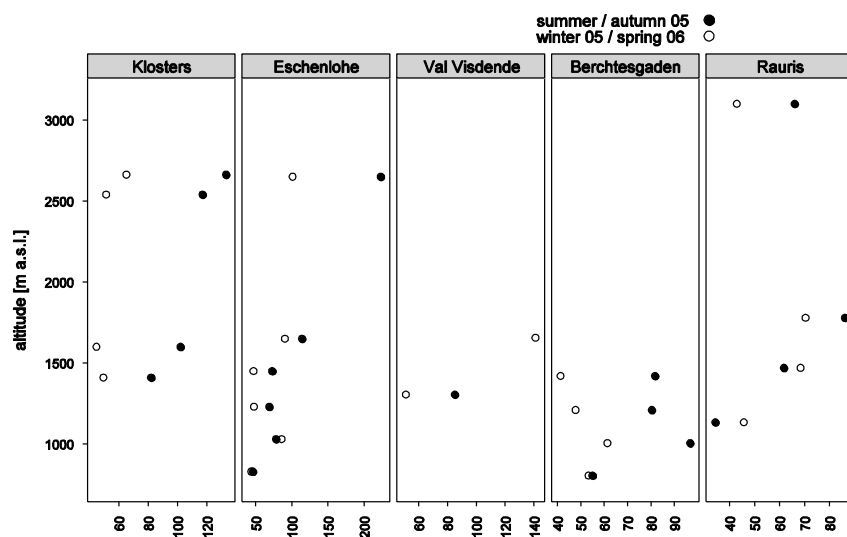
unit: pg SPMD⁻¹

Figure 3-98: Altitudinal variation of *o,p'*-DDD in SPMD



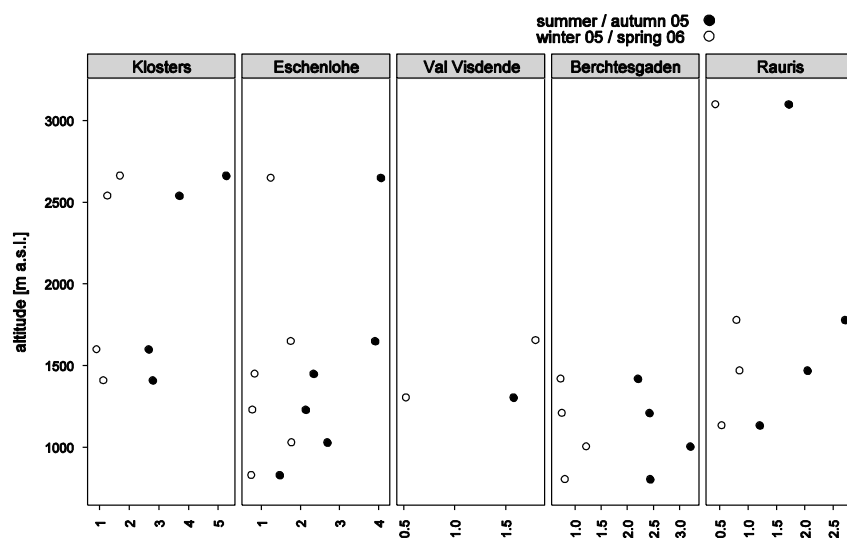
unit: ng SPMD⁻¹

Figure 3-99: Altitudinal variation of *p,p'*-DDE in SPMD



unit: pg SPMD⁻¹

Figure 3-100: Altitudinal variation of *o,p'*-DDE in SPMD



unit: ng SPMD⁻¹

Figure 3-101: Altitudinal variation of total DDX content of SPMD

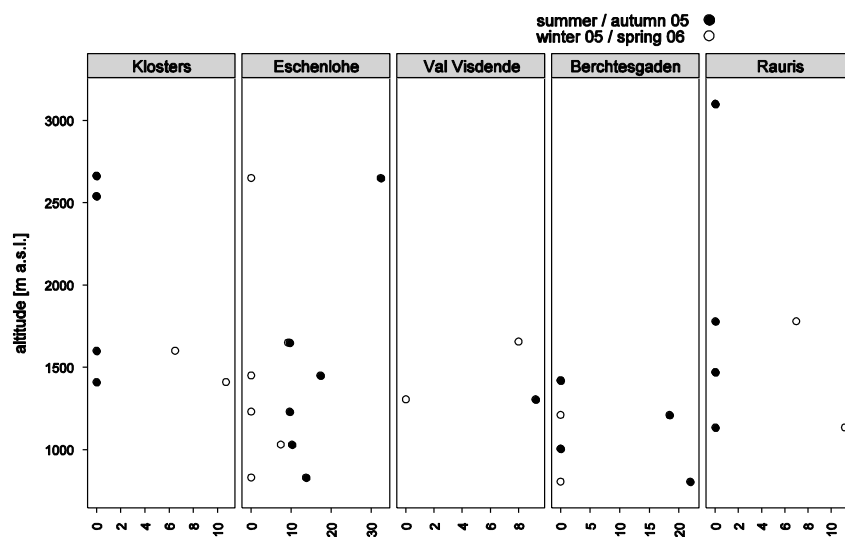
unit: pg SPMD⁻¹

Figure 3-102: Altitudinal variation of Aldrin content of SPMD

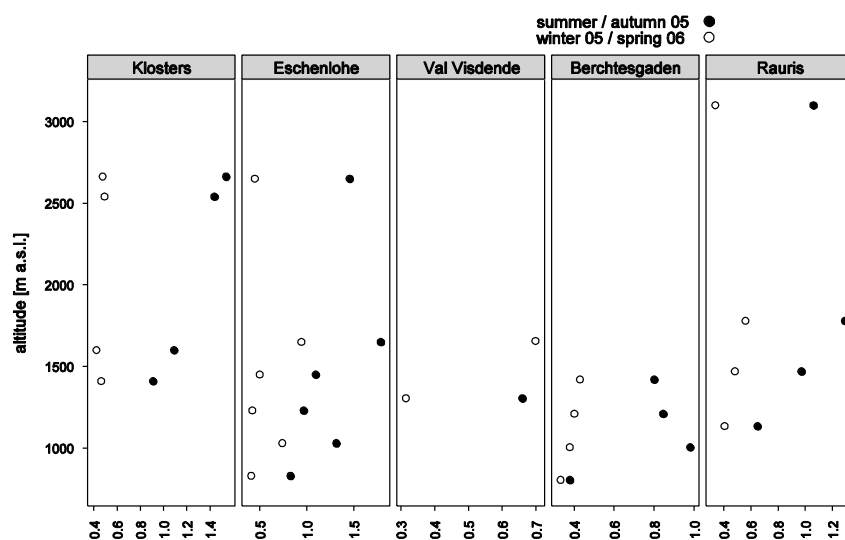
unit: ng SPMD⁻¹

Figure 3-103: Altitudinal variation of Dieldrin in SPMD

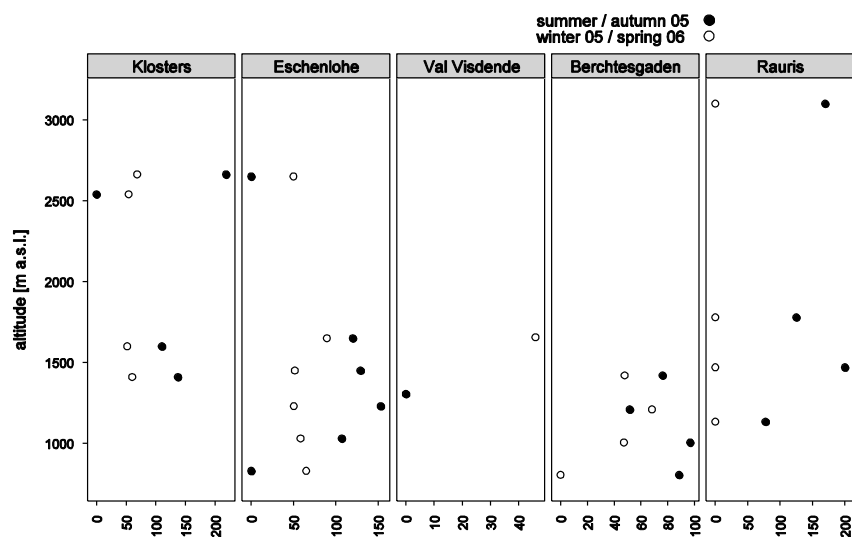
unit: pg SPMD⁻¹

Figure 3-104: Altitudinal variation of Endrin in SPMD

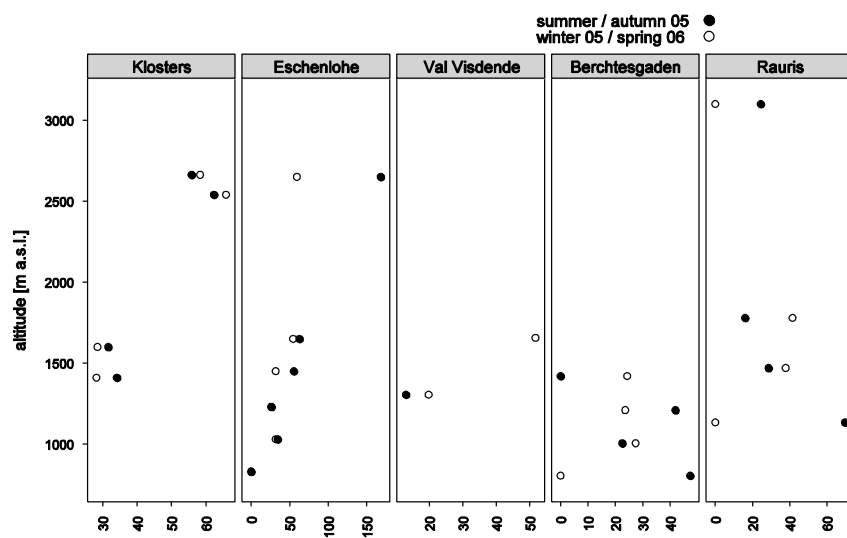
unit: pg SPMD⁻¹

Figure 3-105: Altitudinal variation of Mirex in SPMD

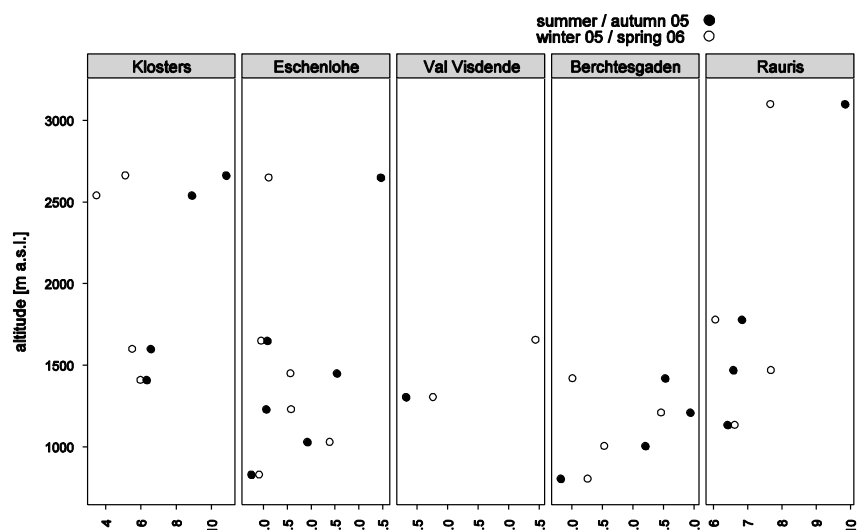
unit: ng SPMD⁻¹

Figure 3-106: Altitudinal variation of HCB in SPMD

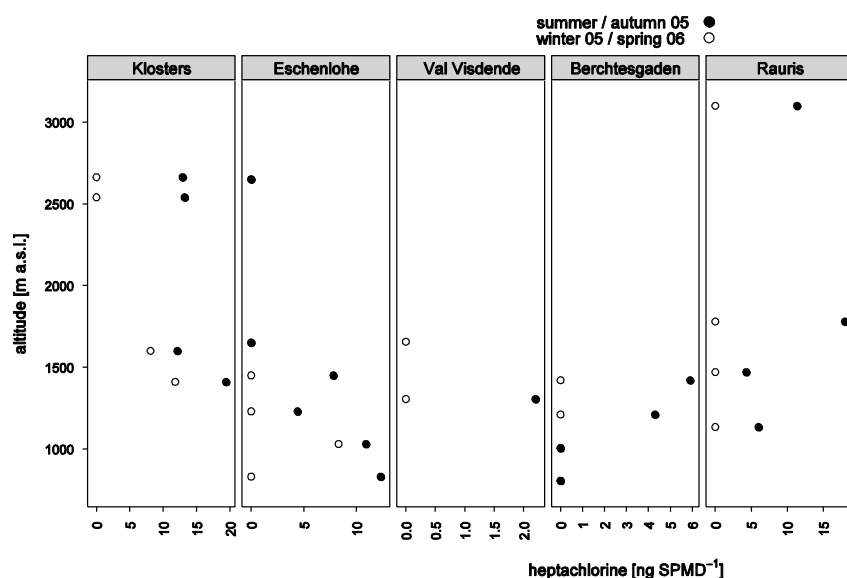
unit: pg SPMD⁻¹

Figure 3-107: Altitudinal variation of Heptachlor in SPMD

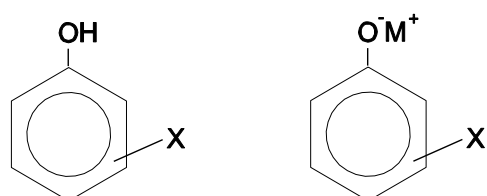
3.3 Chlorophenols

3.3.1 Characterization

3.3.1.1 Physicochemical properties

Chlorophenols are organic chemicals formed from phenol by substitution in the phenol ring with one or more chlorine atoms. Nineteen congeners are possible, ranging from monochlorophenols to the fully chlorinated pentachlorophenol (PCP). All chlorophenols are solids at room temperature, except for 2-monochlorophenol,

which is a liquid. The solubility of chlorophenols in water is poor, but they readily dissolve in a number of organic solvents. In contrast, the sodium or potassium salts of chlorophenols (most commonly Na-trichlorophenol, -tetrachlorophenol, and -pentachlorophenol) are up to four orders of magnitude more soluble in water than the parent compounds. The acidity of chlorophenols increases with the number of chlorine substitutions. The *n*-octanol/water partition coefficients of chlorophenols ($\log K_{ow}$) increase with chlorination, indicating a propensity for the higher chlorophenols to bioaccumulate. Technical grade chlorophenols are heterogeneous mixtures of chlorophenol congeners. (WHO 1989)



X...1-5 chlorine atoms, M⁺...cation

Figure 3-108 Molecular structure of chlorophenol congeners (left) and their salts (right) (WHO 1989)

Table 3-8 Physical properties (range) of chlorophenols

	2-chlorophenol	pentachlorophenol
MW (g mol ⁻¹)	128.56 ^a	266.4 ^b
boiling point (°C)	174.9 ^a	310 ^b
water solubility at 20 °C (mg l ⁻¹).....	14 ^b	14 ^b
vapour pressure (Pa).....	133 @ 12.1°C ^a	0.002 @ 20°C ^b
log K _{ow}	2.15 ^a	3.32 ^b

^a WHO (1989) ^b WHO (1987)

3.3.1.2 Emissions and use

The majority of chlorophenol wastes (other than PCP) are released in spills and leaching from treated lumber and as contaminants or breakdown products of agricultural pesticides. Substantial amounts of chlorophenol wastes are released from sawmills, planer mills, and the incineration of wood wastes. Significant amounts of chlorophenols can be formed and subsequently released into the environment from the chlorine bleaching process in pulp- and papermills, the chlorination of waste- and drinking water, and the incineration of municipal waste (WHO 1989).

Higher chlorophenols are used in pressure treatment in the wood preservation industry. Lower chlorophenols serve as intermediates in the production of pesticides. The use of 2,4,5-trichlorophenol has been discontinued in a number of countries (WHO 1989).

PCP can be formed during the incineration of waste containing chlorine. PCP and its salts were previously mainly used as wood preservatives, herbicides and biocides in several applications. Because of its toxicity the production of PCP has been prohibited in the European Union since 1992 (WHO 2003).

3.3.1.3 Environmental behaviour and bioaccumulation

Chlorophenols adsorb strongly on acidic soils, especially those of high organic content. Leaching is more significant in basic and mineral soils. Adsorption appears to play an important role in surface waters. Chlorophenols that are not degraded in the water body may adsorb into the sediment particulates and persist in sediments for years. While a large part of the chlorophenols entering natural waters is probably degraded, they are nonetheless fairly persistent and, thus, may be transported considerable distances by water. Although chlorophenols are principally water and soil contaminants, some atmospheric movement of chlorophenols occur, and low levels of PCP have been found in rain, snow, and outdoor air (WHO 1989).

PCP is widespread in the environment. The photolytic dechlorination of PCP in water is a significant process largely dependent on the pH. The ionized form is more sensitive to photodegradation than the protonated form, which means that the degradation increases with the increasing pH (WHO 2003). High organic matter, humidity, high pH, and mediate temperatures enhance the microbial breakdown of PCP in soil. Low oxygen conditions are generally unfavourable for the biodegradation of PCP, allowing it to persist in soil (half-life = 10-70 days under flooded conditions), water (half-life = 80-192 days in anaerobic water), and sediments (10% decomposition within five weeks to almost no degradation) (WHO 1987).

Bioconcentration factors of 100-1000 for PCP in aquatic organisms have been reported by several authors (WHO 2003). Bioaccumulation factors of other chlorophenols range mostly between 100 and 1000. The bioconcentration factor is usually a positive function of the chlorine number, and there are no obvious relationships to the type of organism (WHO 1989).

3.3.1.4 Toxicology

Toxicity generally increases with the degree of chlorination of the phenol ring, however chlorophenols with chlorine in the 3 and 5 positions (“meta chlorophenols”) are especially toxic. The very few animal studies concerning exposure to various tri- and tetrachlorophenols have identified exposure related changes in the weight or histology of the liver and, in some instances, of the spleen or kidney; also haematological or immunological effects have been detected. Studies on mutagenicity were mostly negative, carcinogenic effects were unclear due to impurities of the compounds and/or promoting effects (IPCS, 1989). PCP induced significant decreases in thyroxine levels and an increase in serum insulin. PCP affects fertility; reproductive effects are discussed controversially. PCP has been classified as possibly carcinogenic to humans (IARC group 2B). The outcome of an epidemiological study in Canada suggests that high plasma PCP concentrations are related to an altered thyroid status in newborns which could affect neural development of infants (WHO 2003).

3.3.2 Overview of results

While only few of the numerous chlorophenol congeners were detected in forest humus, the concentration of these (4-chlorophenol, sum of 2,4- and 2,5-chlorophenol) was relatively high, exceeding that of other organic chloropesticides (p. 36) and equalling a number of PAH species (p. 111). Across the study region, there were no contingent spatial pollution patterns. The detection limits were much higher than those for the other OCP. Pentachlorophenol concentrations in the humus layer likely are similar to those of other OCPs.

3.3.3 Summary statistics

Only few out of the numerous chlorophenols were detected in forest humus. The concentration of these, however, exceeded that of organic chloropesticides (p. 36) and equalled a number of PAH species (p. 111).

3.3.3.1 Humus

Table 3-9: Chlorophenol content of forest humus

	n < LOD	n < LOQ	LOQ	mean	sd	min	median	max
2-CP	30	0		1.10		< LOD	< LOD	34
3-CP	27	4	48				< LOD	< 33
4-CP	6	20	34	21.0		< LOD	16.5	85
2,6-DCP	28	2	17			< LOD	< LOD	24
2,4-DCP and 2,5-DCP	13	13	16			< LOD	< 16	45
2,3	30	0				< LOD	< LOD	18
3,5	30	0				< LOD	< LOD	21
2,4,6	26	3	15	3.4		< LOD	< LOD	55
2,3,6	30	0				< LOD	< LOD	20
2,3,4	30	1	15			< LOD	< LOD	< 15
3,4,5	30	1	15			< LOD	< LOD	< 15
2,3,4,5	30	1	15			< LOD	< LOD	< 15
PCP	30	1	22			< LOD	< LOD	< 22

sample size: n=31; unit: $\mu\text{g kg}^{-1}$ d.m. None of the following chlorophenols was detected in humus samples: 3,4-DCP; 2,3,5-TriCP 2,4,5-TriCP; 2,3,5,6-TetraCP and 2,3,4,6-TetraCP.

3.3.4 Spatial variation

Chlorophenols were only detected in humus from few sites. Figure 3-109 shows these sites together with the corresponding chlorophenol (labelled with chlorine positions). 4-chlorophenol, as an exception, was detected in most samples (Figure 3-110), although two thirds of the values were below the limit of reliable quantification.

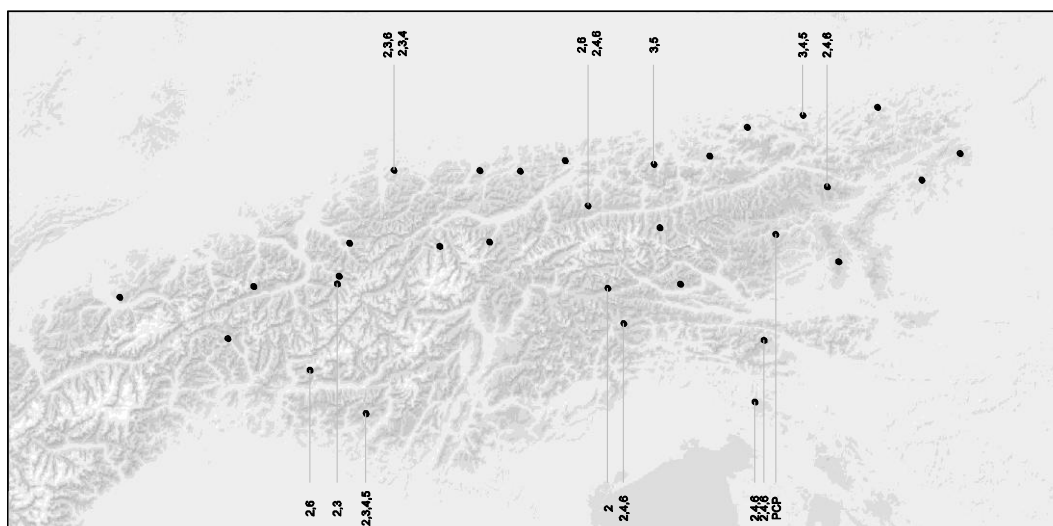


Figure 3-109: Sites with conspicuous chlorophenol concentrations in humus

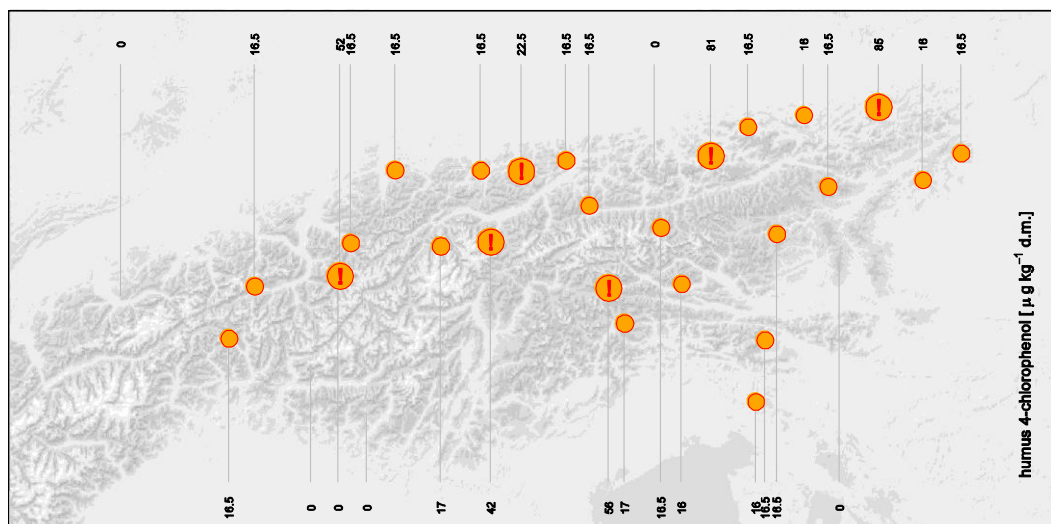


Figure 3-110: Humus concentration of 4-chlorophenol

3.3.5 Longitudinal, latitudinal and altitudinal variation

With the exception of 4-chlorophenol, there were not enough observations to conclude on spatial gradients.

3.4 Polycyclic aromatic hydrocarbons (PAH)

3.4.1 Characterization

3.4.1.1 Physicochemical properties

Polycyclic aromatic hydrocarbons (PAH) are a group of compounds with two or more fused aromatic rings. The chemical and physical properties of the individual PAH vary due to the number and position of rings. Specific physical and chemical properties of the analysed compounds are summarized in Table 3-10.

Table 3-10: Physical properties of PAH at 25 °C

		MW	S_w [$\mu\text{g l}^{-1}$]	p [Pa]	$\log K_{ow}$
ANA	Acenaphthene	154.2	3.93×10^{-3}	2.9×10^{-1}	3.92
ANY	Acenaphthylene	152.2		8.9×10^{-1}	4.07
ANT	Anthracene	178.2	73	8.0×10^{-4}	4.5
BaA	Benz[a]anthracene	228.3	14	2.8×10^{-5}	5.61
BbF	Benzo[b]fluoranthene	252.3	2.0		5.75
BkF	Benzo[k]fluoranthene	252.3	0.76	1.3×10^{-8}	6.84
BghiP	Benzo[ghi]perylene	276.3	0.26	1.4×10^{-8}	7.10
BaP	Benzo[a]pyrene	252.3	3.8	7.3×10^{-7}	6.50
CHR	Chrysene	228.3	14	8.4×10^{-5}	5.91
DBahA	Dibenz[a,h]anthracene	278.4	0.5 (27°C)	1.3×10^{-8} (20°C)	6.50
FLA	fluoranthene	202.3	260	1.2×10^{-3}	5.22
FLU	fluorene	166.2	1.98×10^{-3}	9.0×10^{-2}	4.18
INCcdP	Indeno[1,2,3-cd]pyrene	276.3	62	1.3×10^{-8}	6.58
NAPH	Naphthalene	128.2	3.17×10^{-4}	10.4	3.4
PHEN	Phenanthrene	178.2	1.29×10^{-3}	1.6×10^{-2}	4.6
PYR	Pyrene	202.3	135	6.0×10^{-4}	5.18

MW...molecular weight; S_w ...solubility in water @ 25 °C; p ...vapour pressure @ 25 °C; source: WHO, 1998

3.4.1.2 Emissions and use

PAH are produced during pyrolytic processes and incomplete combustion and released to the atmosphere by human activity, forest fires and volcanoes. Residential burning of wood is the largest source of atmospheric PAH. Other important sources include industrial power generation, incineration, production of coal tar and coke, petroleum catalytic cracking and primary aluminium production. Mobile sources of PAH are exhausts from gasoline and diesel powered vehicle engines (WHO 2003).

3.4.1.3 Environmental behaviour and bioaccumulation

Due to the semivolatile properties of some PAHs the lighter PAH species are highly mobile throughout the environment. Heavier species are, in the atmosphere, mostly associated with particulate matter, in the aquatic environment with sediments or suspended particles. PAHs in soil can volatilize, undergo abiotic degradation (photolysis and oxidation) biodegrade, accumulate in plants or enter the groundwater and be transported within an aquifer (WHO 2003).

3.4.1.4 Toxicology

The most serious health concern of PAH exposure is cancer. Some PAH (i.e. BaP) are classified as known human carcinogens (group 1), some PAHs and derivatives as probable (2A) or possible (2B) human carcinogens. Data obtained from epidemiological studies on occupational exposure suggest an association with lung cancer. Some PAHs (i.e. the reference compound BaP) are teratogenic and toxic to reproduction and the immune system.

3.4.2 Overview of results

Norway spruce needles contained ca. 5–45, forest humus 80–500 and mineral soil 60–1900 µg PAH (sum of 16 EPA-PAH) per kg dry mass. The high levels of PAH in mineral soil (as compared to humus and needles) are remarkable, since for other pollutants (and in other studies) humus was the most contaminated matrix. The PAH mixture in needles was dominated by NAPH > PHEN > FLA; that of humus by FLA > BbF > CHR. Mineral soil was characterised by Bbf >> CHR > PHEN > FLA. The PAH mix in needles was dominated by the lighter PAH species whereas the spectrum in humus and mineral soil was shifted towards the heavier PAH.

The concentration of PAH in needles and humus changed markedly from the west to the east of the investigated alpine region; in the case of needles, the differences between the western, the middle and the eastern zone were often statistically significant. Needle samples showed contrasting trends: while the lighter PAH reached their maxima in the western part, the highest levels of the heavier species were found in needles from the east. This contrast was not as pronounced in the humus samples. Anyhow, the highest PAH levels were always (except needle BghiP content) found in one of the lateral geographic regions. Concerning the latitudinal variation, humus PAH contamination showed significant differences among the northern, central and southern zone of the study region. The highest pollution levels were always found in the north. In contrast, latitudinal differences of needle PAH contamination were insignificant. Remarkably, the two light PAH species naphthalene and phenanthrene, attained highest levels in the central part of the Alps.

As observed for other pollutants, altitudinal trends of PAH levels could differ between sites and media (needles, humus, SPMD).

NAPH, FLA and PHEN were the most important PAH in air and deposition. Much of the time, the prevailing source region for higher atmospheric PAH concentrations on three alpine summits could vary between sites and PAH species. However, there was a remarkable consistence for the cold period from late autumn 2006 to late winter 2007, during which the most abundant atmospheric PAH (together with BaP) mainly arrived from northwestern Europe.

3.4.3 Summary statistics

3.4.3.1 Needles

PAH levels at the second plot of the Val Visdende height profile (Italy) were at least ten times as high as at the remaining 39 sites of the study. This site has been excluded from the descriptive statistics in Table 3-11.

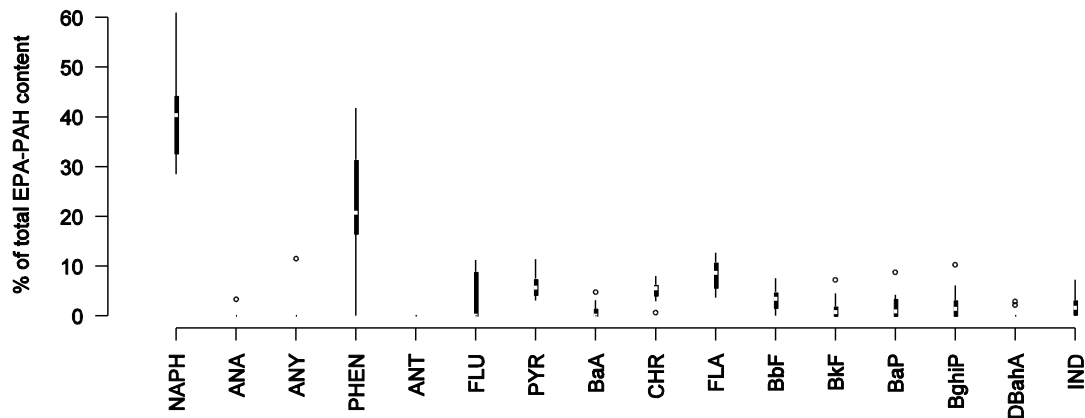
NAPH and PHEN were the most abundant PAHs in needles, followed by FLA, FLU, and PYR (Table 3-11, Figure 3-111). Some light PAHs, like ANA, ANY and ANT, and a heavy one, DbahA, fell below the detection limit in most of the samples. Total PAH concentration in this matrix was on average one tenth of that in the humus and one twentieth of that in the mineral layer.

Table 3-11: PAH concentrations in six month old Norway spruce needles

	n < LOD	mean	sd	min	P ₁₀	P ₂₅	median	P ₇₅	P ₉₀	max
ANA	37	< LOD	< LOD	< LOD	< LOD	< LOD	< LOD	< LOD	< LOD	1.61
ANY	36	< LOD	< LOD	< LOD	< LOD	< LOD	< LOD	< LOD	< LOD	2.02
ANT	39	< LOD	< LOD	< LOD	< LOD	< LOD	< LOD	< LOD	< LOD	0.00
BaA	18	0.17	0.20	< LOD	< LOD	< LOD	0.13	0.27	0.39	0.85
BbF	1	0.61	0.42	< LOD	0.20	0.24	0.44	0.86	1.20	1.60
BkF	12	0.25	0.24	< LOD	< LOD	< LOD	0.18	0.46	0.59	0.81
BghiP	7	0.52	0.49	< LOD	< LOD	0.18	0.26	0.88	1.31	1.59
BaP	13	0.32	0.31	< LOD	< LOD	< LOD	0.23	0.61	0.76	1.05
CHR	0	0.83	0.36	0.16	0.34	0.57	0.83	1.00	1.30	1.66
DBahA	29	0.08	0.15	< LOD	< LOD	< LOD	< LOD	0.08	0.35	0.48
FLA	0	1.62	0.92	0.24	0.65	0.92	1.42	2.26	2.89	4.02
FLU	18	1.14	1.26	< LOD	< LOD	< LOD	1.20	2.03	2.89	3.95
IND	6	0.40	0.32	< LOD	< LOD	0.16	0.27	0.58	0.86	1.16
NAPH	0	7.19	4.22	1.98	3.55	4.12	5.93	8.60	14.28	17.23
PHEN	1	5.06	3.53	0.00	2.18	2.78	3.88	7.42	8.67	17.19
PYR	0	1.25	0.67	0.36	0.54	0.71	1.14	1.64	2.20	3.34
Σ 16 PAH	0	19.63	9.16	5.27	10.45	12.76	17.72	23.69	31.34	45.13

unit: $\mu\text{g kg}^{-1}$ d.m.; sample size n=39; LOD...detection limit. DBaPYR, DBaePYR, DBaiPYR and DBahPYR were only detected at the second plot of Val Visdende height profile.

Figure 3-111 illustrates the typical PAH pattern in spruce needles (PAH arranged from left to right by increasing ring count). The dominance of the light species NAPH and PHEN is obvious.



(Subsample of the 16 standard sites for which also PAH data of humus and mineral soil are available).

Figure 3-111: PAH pattern in 0.5 year old Norway spruce needles.

3.4.3.2 Humus, mineral soil

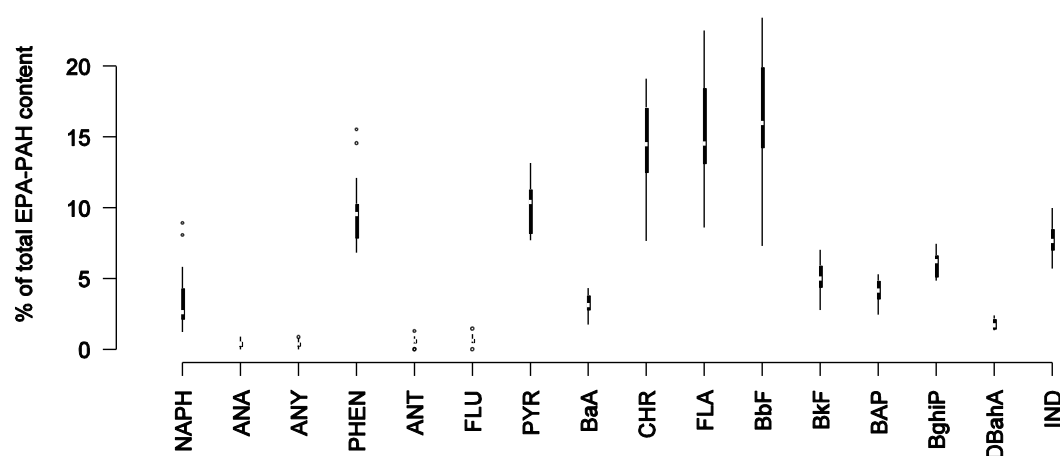
The most abundant PAHs in the humus were BbF, FLA and CHR (Table 3-12, Figure 3-112). Like in the needles, ANA, ANY and ANT reached only low concentrations. Also DBahA and FLU were among the least abundant. Noteworthy are the considerable levels of DBalPYR, one of the four analyzed isomers which are not included in the EPA list.

Table 3-12: PAH concentrations in forest humus

	n < LOD	mean	sd	min	P ₁₀	P ₂₅	median	P ₇₅	P ₉₀	max
ANA	8	0.70	0.50	< LOD	< LOD	0.27	0.78	1.04	1.20	1.97
ANY	5	0.81	0.51	< LOD	< LOD	0.58	0.83	1.12	1.43	1.91
ANT	5	1.35	0.93	< LOD	< LOD	0.64	1.27	1.95	2.75	3.02
BaA	0	6.63	3.67	1.35	3.30	4.24	5.68	8.28	11.60	15.36
BbF	0	35.84	23.55	5.64	14.30	17.76	28.84	46.15	65.31	117.28
BkF	0	10.22	6.34	2.13	4.39	5.87	8.97	11.48	19.77	26.24
BghiP	0	12.51	6.58	4.68	5.67	7.31	10.46	16.61	22.87	25.23
BaP	0	7.85	4.57	1.90	3.67	4.75	6.51	9.79	13.84	18.89
CHR	0	30.81	16.75	5.98	16.44	20.38	25.89	36.71	54.22	73.07
DBahA	0	3.53	2.16	1.12	1.57	1.85	2.53	4.67	6.97	9.27
FLA	0	32.44	15.75	10.03	15.52	18.86	30.46	44.89	50.64	69.11
FLU	3	1.35	0.78	-	0.55	0.76	1.38	1.76	2.34	3.22
IND	0	16.61	9.66	4.99	7.46	9.30	13.59	22.12	28.27	47.66
NAPH	0	5.62	2.16	1.66	3.08	4.01	5.59	6.98	9.09	9.62
PHEN	0	20.27	8.88	7.82	9.52	12.32	19.90	26.22	32.20	39.05
PYR	0	22.58	11.98	8.98	10.09	13.20	19.00	29.20	34.95	61.29
Σ 16 PAH		209.1	104.5	77.2	107.9	127.3	184.8	258.4	362.0	500.7
DBalPYR	0	12.03	7.20	3.88	5.36	5.89	9.56	17.75	21.46	28.43
DBaePYR	0	4.58	2.96	1.22	1.69	2.21	3.93	6.71	7.61	12.68
DBaiPYR	15	0.76	0.94	< LOD	< LOD	< LOD	0.64	1.23	1.88	3.34
DBahPYR	24	0.21	0.41	< LOD	< LOD	< LOD	< LOD	< LOD	0.91	1.27

unit: $\mu\text{g kg}^{-1}$ d.m.; sample size n=31; LOD...detection limit.

Figure 3-112 illustrates how the PAH spectrum in the humus samples is, other than that of needles (Figure 3-111), shifted towards the heavier species (PAH are arranged by increasing ring count from left to right).



(Subsample of the 16 standard sites for which also PAH data of needles and mineral soil are available).

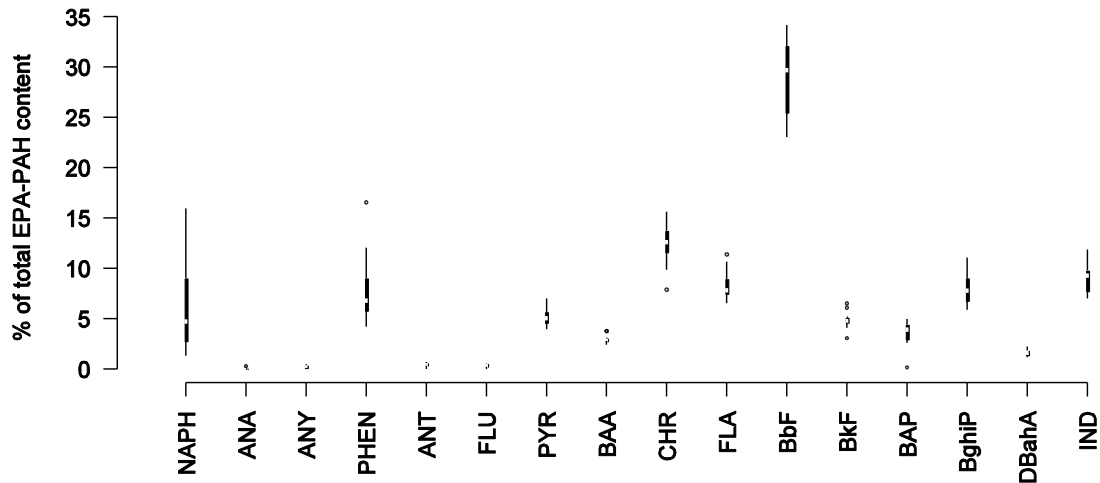
Figure 3-112: PAH pattern in forest humus

BbF was by far the most abundant PAH in the mineral layer, followed by CHR, IND, BghiP and FLA (Table 3-13, Figure 3-113). Remarkably, total PAH content of the mineral soil (median 202 $\mu\text{g kg}^{-1}$ d. m.) was higher than in humus (median 184.8). Like in the previous matrices ANA, ANY and ANT had the lowest concentrations.

Table 3-13: PAH concentrations in forest mineral soil.

	n < LOD	mean	sd	min	P ₁₀	P ₂₅	median	P ₇₅	P ₉₀	max
ANA	13	0.42	0.69	< LOD	< LOD	< LOD	< LOD	0.68	1.64	2.17
ANY	6	1.23	1.46	< LOD	< LOD	< LOD	0.64	1.44	3.80	4.45
ANT	4	1.99	2.43	< LOD	< LOD	0.84	0.99	2.16	5.59	8.46
BaA	0	13.88	17.28	1.32	1.57	3.85	5.38	14.78	42.94	57.70
BbF	0	147.9	190.2	14.0	17.8	31.4	58.6	153.9	467.8	605.5
BkF	0	24.75	32.90	1.85	2.81	6.04	9.35	26.62	82.63	115.1
BghiP	0	39.73	53.99	3.87	4.72	10.35	13.68	40.53	116.2	181.7
BaP	0	18.21	23.97	0.10	1.81	4.23	6.61	17.75	55.49	78.49
CHR	0	61.32	76.29	6.94	7.71	12.17	26.23	69.53	213.0	239.8
DBahA	0	8.24	11.01	0.69	0.77	1.96	2.81	9.53	21.98	41.94
FLA	0	36.48	41.96	4.19	4.73	9.79	17.45	41.22	104.1	140.0
FLU	4	1.18	1.17	< LOD	< LOD	0.68	0.79	1.30	2.94	4.46
IND	0	47.11	62.64	4.36	5.52	11.67	15.61	57.38	121.3	225.5
NAPH	0	16.73	12.04	2.77	5.29	7.70	13.39	22.93	35.43	44.99
PHEN	0	27.41	25.89	3.76	7.76	10.30	18.97	30.75	72.59	91.06
PYR	0	22.81	26.97	2.64	2.95	6.99	10.25	25.62	64.54	91.95
Σ 16 PAH	0	469	573	56	66	130	202	513	1417	1899
DBalPYR	0	16.07	17.32	1.32	2.56	5.20	8.34	18.62	41.96	66.52
DBaePYR	6	6.59	8.65	0.69	0.96	1.57	2.46	6.34	15.66	33.31
DBaiPYR	17	< LOD	< LOD	< LOD	< LOD	< LOD	0.71	1.61	6.05	6.83
DBahPYR	13	0.28	0.70	< LOD	< LOD	< LOD	< LOD	< LOD	1.36	2.49

unit: $\mu\text{g kg}^{-1}$ d.m.; sample size n=20; LOD...detection limit.



(Subsample of the 16 standard sites for which also PAH data of needles and humus soil are available).

Figure 3-113: PAH pattern in forest mineral soil.

3.4.3.3 Deposition and air

Atmospheric PAH concentrations on all three summits could show very similar trends, for instance in the case of BaP. BaP levels peaked during the cold and leveled off during the warm seasons (Figure 3-119). BaP concentrations varied, to the greatest part, correspondingly in air and deposition. In contrast, air and deposition trends of NAPH – the most abundant PAH species in ambient air and deposition – could develop into opposite directions as observed on Mt. Sonnblick (Figure 3-115). Spring–summer total PAH deposition tended to increase from 2005 to 2007.

In ambient air - contrarily to solid matrices - PAHs with low molecular weight dominated the PAH spectrum. Naphthalene was by far the most abundant PAH, and FLU, PHEN and ANA reached high concentrations, compared to the heavier PAH (Table 3-14). DBahA, on the other hand, was the least abundant component of the PAH mixture.

The total concentration of carcinogenic PAHs in air followed a seasonal pattern with higher levels in the cold season while in the warm season atmospheric PAH concentrations were lower and the provenience of the air masses fluctuated more strongly (Figure 3-120).

Table 3-14: Atmospheric PAH concentrations at three alpine summits

site	period	ANA pg m ⁻³	ANY pg m ⁻³	ANT pg m ⁻³	BaA pg m ⁻³	BbF pg m ⁻³	BkF pg m ⁻³	BghiP pg m ⁻³	BaP pg m ⁻³	CHRY pg m ⁻³
Sonnblick	I	99.0	8.1	14.2	3.7	23.6	5.4	10.2	6.5	14.0
	II	53.9	5.8	1.8	0.0	7.4	1.5	3.8	1.9	5.2
	III	87.4	10.2	4.8	2.0	8.6	2.0	3.9	2.3	6.3
	IV	54.8	6.7	0.0	4.1	16.0	4.6	7.6	5.2	10.8
	V	34.8	0.0	0.0	1.6	11.0	3.2	4.9	3.5	7.7
Weissfluh	I	*	*	*	8.8	48.7	10.7	26.4	11.4	29.7
	II	148.5	27.4	5.6	2.1	14.4	3.1	8.8	4.3	11.3
	III	208.8	0.0	2.5	2.3	15.0	3.7	8.0	3.9	12.1
	IV	179.9	172.0	19.4	8.5	33.6	10.6	51.2	13.5	23.5
	V	94.1	0.0	1.9	1.3	20.1	5.1	10.3	3.0	14.2
Zugspitze	I	0.0	0.0	9.0	2.5	20.9	4.2	10.4	5.7	9.6
	II	*	*	0.0	1.3	9.9	2.1	5.3	2.7	6.9
	III	432.1	0.0	4.8	4.6	14.0	4.1	7.3	5.5	12.1
	IV	255.8	39.2	10.2	5.6	24.9	6.7	12.2	6.6	18.1
	V	*	*	7.3	3.1	14.0	4.0	11.1	4.2	14.1

* too low recovery of standards for meaningful calculation of concentrations; sampling periods: I...winter 2005/6, II...spring-early summer 2006, III...early summer-late autumn 2006, ..., IV...late aut. 2006-late winter 2007, V...spring 2007

Table 3-14 (continued): Atmospheric PAH concentrations at three alpine summits

site	period	DBaA pg m ⁻³	FLA pg m ⁻³	FLU pg m ⁻³	IND pg m ⁻³	NAPH ng m ⁻³	PHEN pg m ⁻³	PYR pg m ⁻³	Σ EPA-PAH ng m ⁻³
Sonnblick	I	0.9	105.8	879.7	11.0	10.25	493.5	38.5	11.96
	II	0.0	59.8	229.0	4.2	3.124	259.8	62.9	3.82
	III	0.0	74.6	336.1	3.7	3.974	270.4	112.5	4.90
	IV	0.6	67.1	347.6	8.0	4.930	308.8	44.5	5.82
	V	0.0	40.4	281.6	5.0	*	167.5	28.8	2.35
Weissfluh	I	1.3	196.9	*	20.6	*	572.7	101.2	5.84
	II	0.0	118.1	486.6	7.5	8.579	469.1	73.9	9.96
	III	0.0	106.1	412.5	7.3	*	420.3	51.6	6.00
	IV	0.7	153.5	564.2	24.4	10.42	561.5	147.8	12.38
	V	0.0	111.0	443.7	10.0	4.924	353.7	60.5	6.05
Zugspitze	I	0.0	86.6	1034.1	10.6	3.261	588.9	41.6	5.08
	II	0.0	59.3	*	5.1	*	340.0	25.2	0.97
	III	0.0	133.0	660.4	6.4	7.106	598.4	63.4	9.05
	IV	0.9	102.5	577.6	11.7	9.093	518.8	55.0	10.74
	V	0.0	124.5	832.1	8.2	*	605.5	65.7	9.30

* too low recovery of standards for meaningful calculation of concentrations; sampling periods: I...winter 2005/6, II...spring-early summer 2006, III...early summer-late autumn 2006, ..., IV...late aut. 2006-late winter 2007, V...spring 2007

PAH deposition was dominated by NAPH, followed by FLA and PHEN. (Table 3-15, Figure 3-114). DBa,hPYR was not detected in deposition. Average PAH deposition was higher on Mt. Sonnblick than on Mt. Zugspitze while Weissfluhjoch was the summit with the lowest deposition rates. Mt. Sonnblick was also the site at which the deposition trend of many PAH, including the more abundant species except NAPH was similar.

Little can be said about the seasonality of PAH depositions, because of the incomplete time series for Mt. Zugspitze and Mt. Weissfluhjoch. Besides, even at comparable sampling periods, deposition could vary considerably: for example, springtime NAPH deposition was low in the years 2005 and 2007 but reached a maximum in 2006 (Figure 3-115).

The highest deposition rates of NAPH were observed on Mt. Sonnblick around spring 2006 (Figure 3-115). At this site, NAPH deposition was highest during the cold season (autumn-spring) 2006. On Mt. Zugspitze naphthalene deposition peaked in spring 07.

Highest BaP depositions were observed during autumn-winter 2006/7 at Mt. Sonnblick and Mt. Weissfluhjoch (winter data from Mt. Zugspitze missing: Figure 3-119).

Table 3-15: PAH deposition at three alpine summits

	period	ANA	ANY	ANT	BAA	BBF	BKF	BGHIP	BAP	CHR	DBAHA
Weissfluh	A	< LOD	< LOD	< LOD	1.46	3.76	1.54	2.96	1.83	4.39	0.55
	B	*									
	C	n.a.	n.a.	0.74	5.87	23.92	6.76	10.63	9.21	17.62	1.39
	D	1.03	1.26	1.50	10.59	3.90	7.31	6.10	5.70	14.42	0.87
	E	2.33	0.96	2.85	18.20	37.09	17.64	17.02	23.25	43.65	5.16
	F	2.02	6.49	3.41	19.93	42.88	15.12	22.59	27.78	35.64	4.29
Zugspitze	A	1.13	< LOD	< LOD	3.13	8.21	3.32	6.15	3.74	8.38	0.98
	B	*									
	C	< LOD	< LOD	1.47	8.07	36.77	10.63	18.83	12.60	27.10	3.47
	D	9.53	4.55	110.71	68.76	31.80	48.07	6.24	36.44	93.03	47.41
	E	*									
	F	2.00	5.82	2.58	18.35	55.20	19.78	36.47	26.02	52.42	4.43
Sonnblick	A	< LOD	< LOD	< LOD	0.37	0.96	0.26	0.60	0.40	0.70	0.14
	B	0.72	1.04	2.34	11.62	26.60	5.87	8.52	9.43	17.21	1.46
	C	0.90	1.70	1.84	11.76	38.25	11.53	16.65	14.49	27.70	2.30
	D	2.11	2.02	5.14	32.77	90.32	23.80	39.30	44.00	49.69	5.98
	E	4.72	4.82	16.95	86.25	142.89	42.88	60.35	70.81	95.75	11.67
	F	< LOD	2.60	3.07	28.91	84.35	24.87	44.89	33.55	50.17	6.89

unit: ng m⁻² d⁻¹ at 0 °C and 1013.3 hPa; LOD...detection limit; * sample destroyed; n.a....not available; ** w/o NAPH, ANA and ANY; sampling periods: A...spring-late summer 2005, B...late summer 2005-late winter 2006, C...late winter-summer 2006, D...summer-autumn 2006, E...autumn 2006-late winter 07, F...late winter-spring 2007

Table 3-15 (continued) PAH deposition at three alpine summits

	period	FLA	FLU	IND	NAPH	PHEN	PYR	Σ EPA-PAH	DB(a,l)PYR	DB(a,e)PYR	DB(a,i)PYR
Weissfluh	A	9.15	1.97	2.86	37.73	9.97	6.93	85	< LOD	< LOD	< LOD
	B	*									
	C	23.98	4.03	11.07	n.a.	21.40	17.32	154 **	1.80	1.19	< LOD
	D	20.32	3.01	6.76	285.5	17.06	20.13	405	< LOD	< LOD	< LOD
	E	64.20	3.18	18.42	28.6	34.13	46.45	363	4.91	3.04	1.02
	F	53.46	5.91	24.94	31.6	48.25	40.86	385	7.12	4.16	1.08
Zugspitze	A	16.32	4.13	5.13	44.1	18.26	12.04	135	2.26	1.13	< LOD
	B	*									
	C	54.30	5.03	17.17	339.6	42.63	34.00	612	2.93	2.27	< LOD
	D	88.35	77.21	6.72	< LOD	6.20	41.60	677	4.47	1.65	< LOD
	E	*									
	F	84.27	16.55	37.28	59.1	88.22	59.63	568	8.68	5.57	0.90
Sonnblick	A	1.24	< LOD	0.57	1.5	1.04	1.05	9	< LOD	< LOD	< LOD
	B	39.09	2.77	10.02	59.3	25.16	24.85	246	< LOD	< LOD	< LOD
	C	52.47	4.85	17.42	323.4	39.39	37.54	602	2.69	1.76	< LOD
	D	88.95	6.43	37.30	65.3	45.98	67.91	607	6.99	4.41	0.97
	E	173.35	12.02	63.86	52.5	117.51	139.84	1096	11.91	6.65	1.93
	F	83.50	5.01	49.28	29.6	60.93	62.68	570	12.80	6.31	< LOD

unit: ng m⁻² d⁻¹ at 0 °C and 1013.3 hPa; LOD...detection limit; * sample destroyed; n.a....not available; ** w/o NAPH, ANA and ANY; sampling periods: A...spring-late summer 2005, B...late summer 2005-late winter 2006, C...late winter-summer 2006, D...summer-autumn 2006, E...autumn 2006-late winter 07, F...late winter-spring 2007

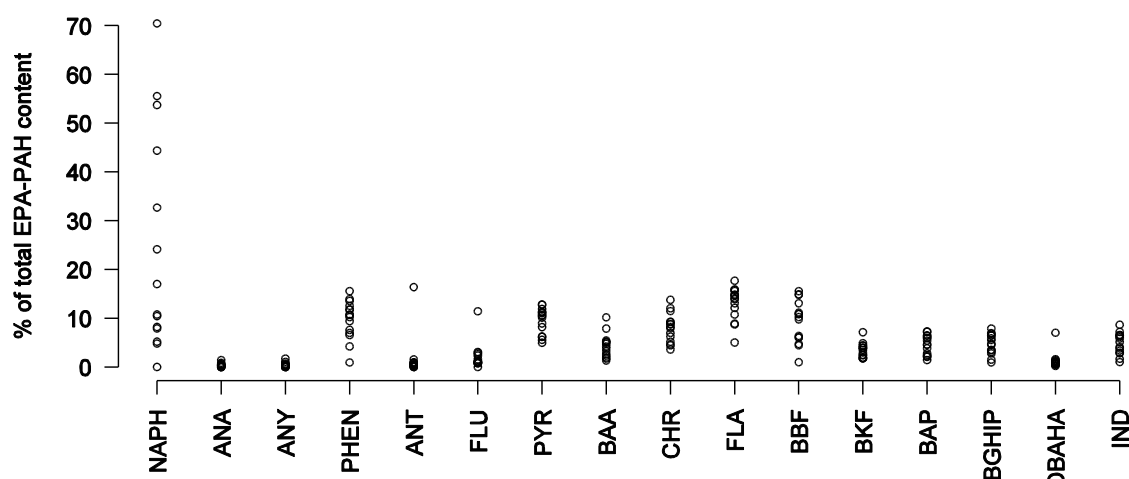
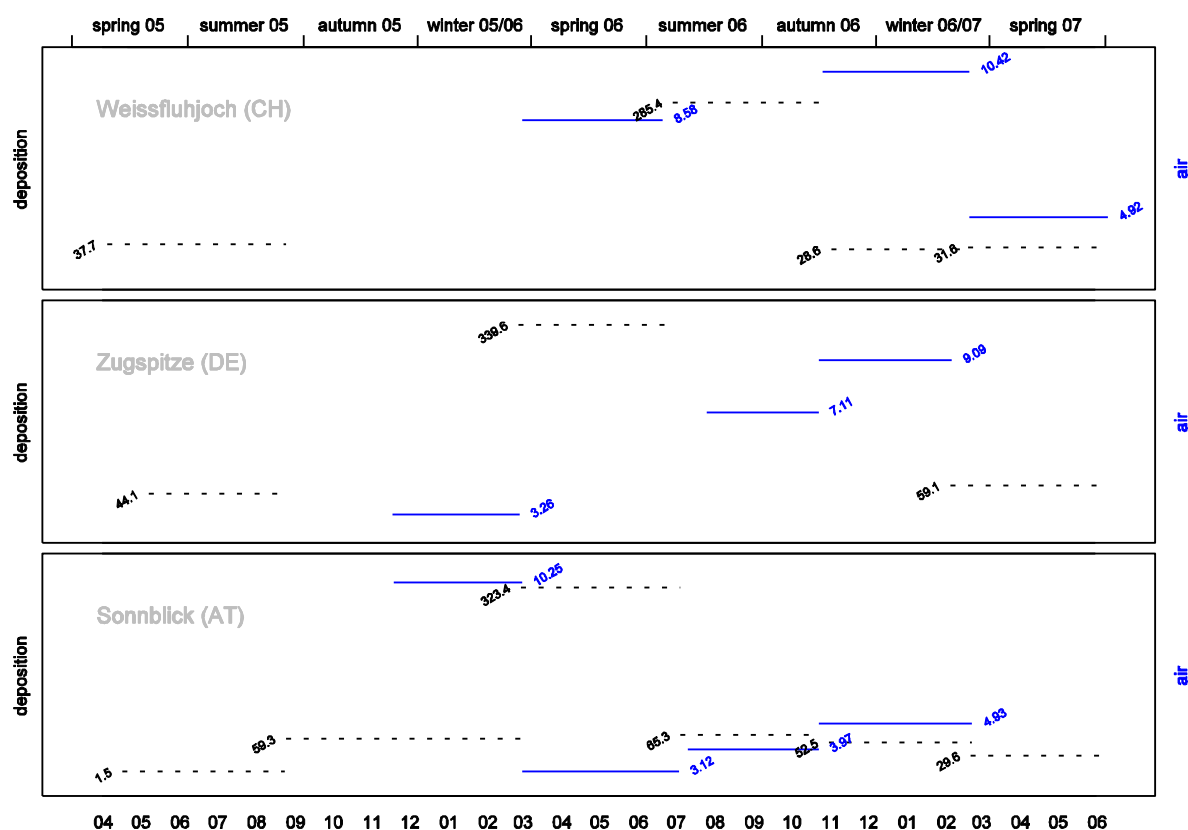


Figure 3-114: PAH pattern of deposition on three alpine summits

Figure 3-114 gives an impression of the PAH pattern found in deposition. Note that the illustration contains pooled data of different summits and sampling periods. For more detailed information, e.g. differences between the seasons covered by the consecutive sampling periods, see the following figures.

Sample loss lead to missing observations for the following periods: autumn-winter 2005 (Weissfluhjoch, CH) and autumn-winter 2005 and late autumn-winter 2006 (Zugspitze, DE). These periods do not appear in the following graphs.



Units: deposition: $\text{ng m}^{-2} \text{d}^{-1}$, atmospheric concentration: ng m^{-3} .

Figure 3-115: Naphthalene in ambient air and deposition on three alpine summits

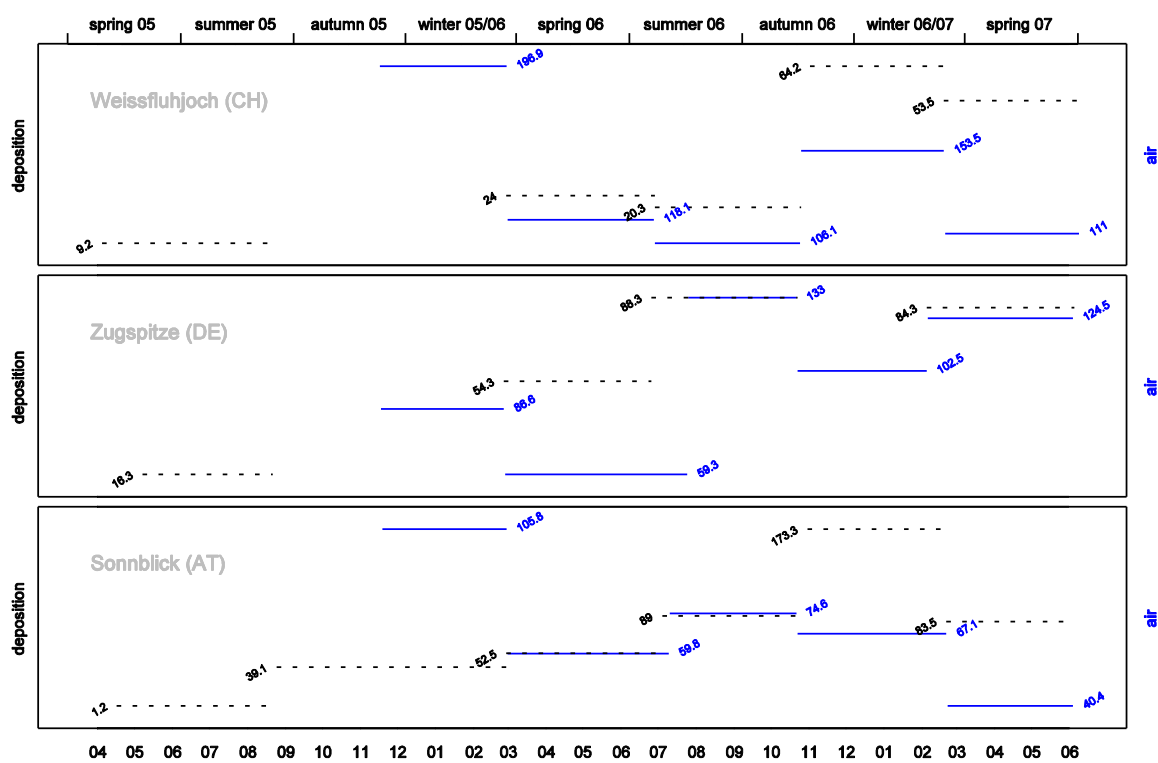


Figure 3-116: Fluoranthene in ambient air and deposition on three alpine summits

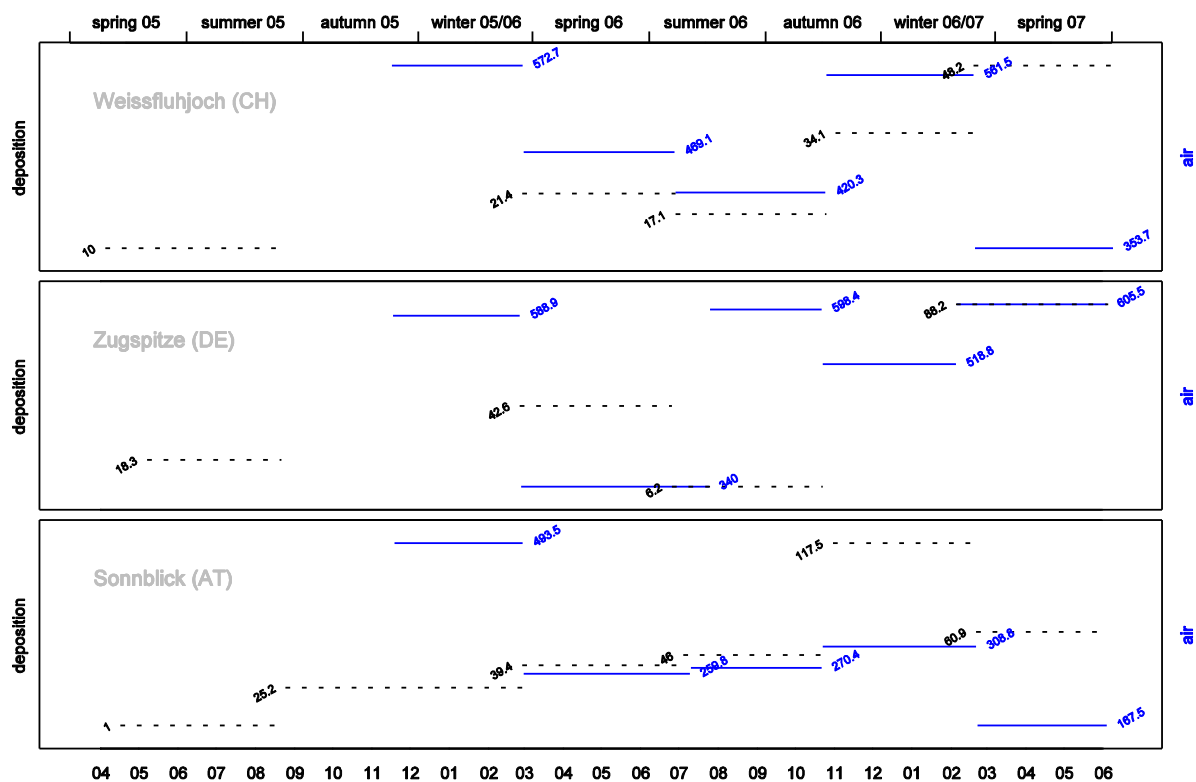
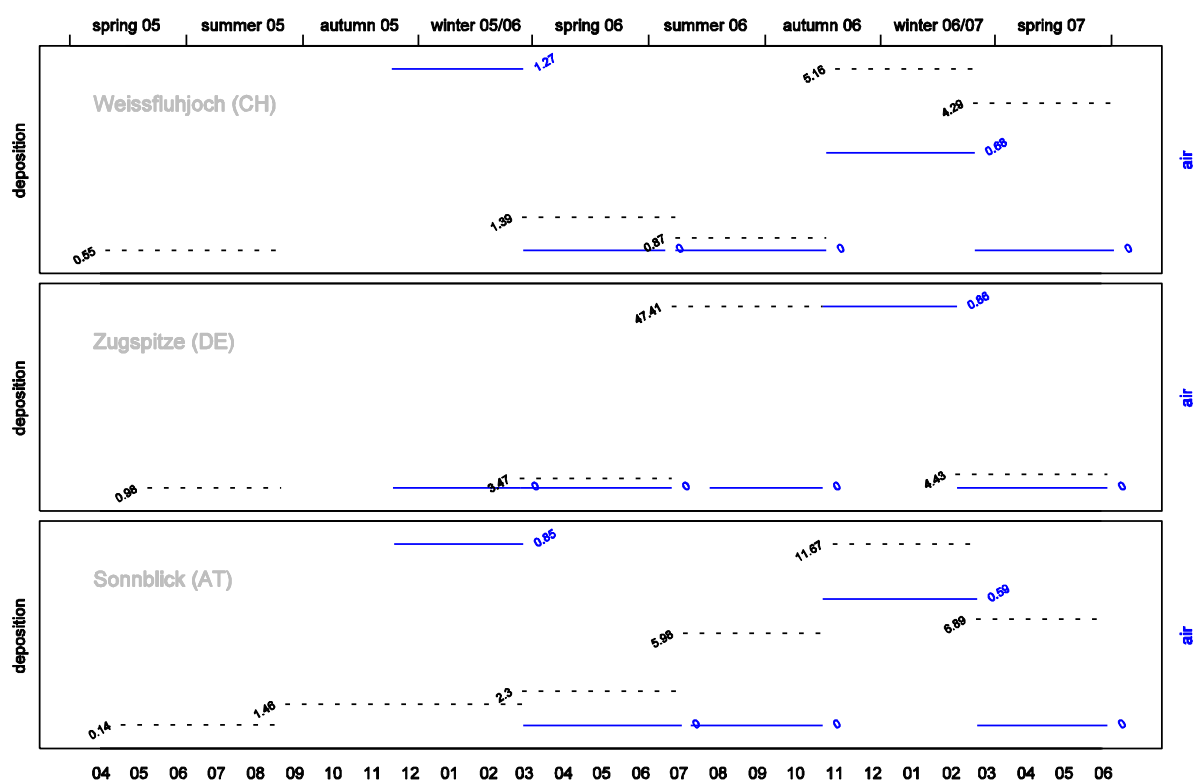
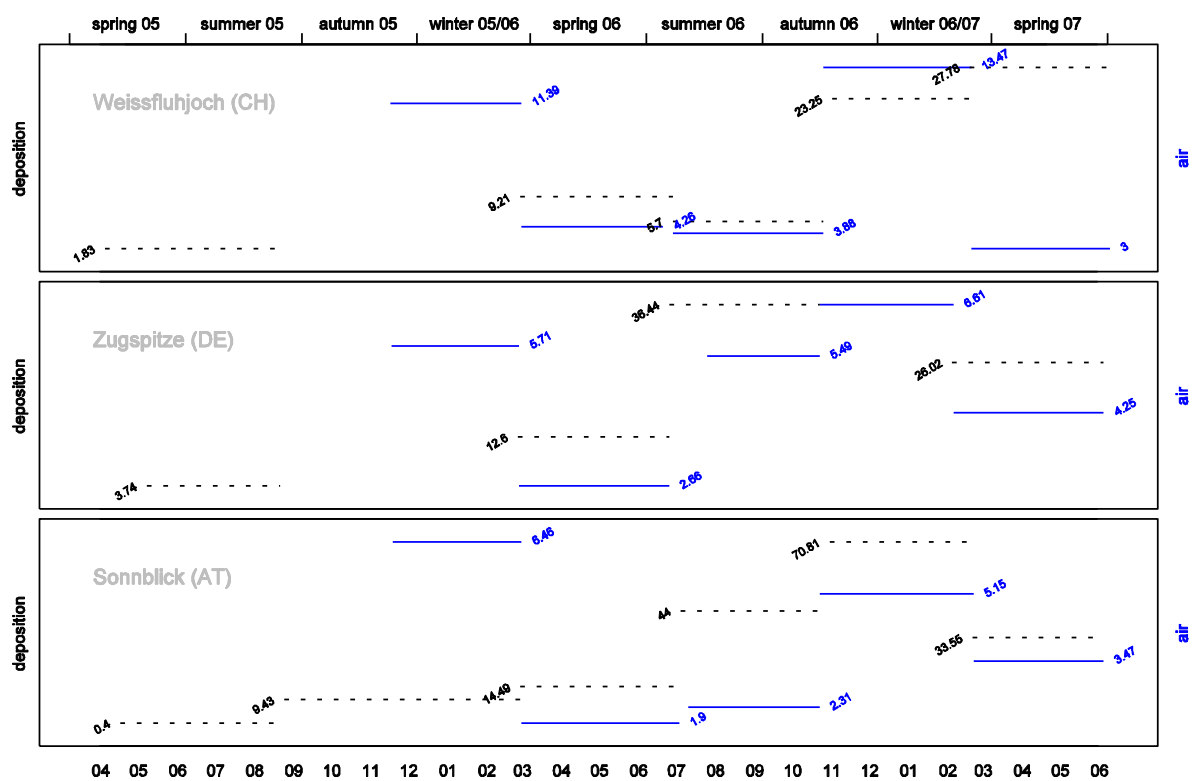


Figure 3-117: Phenanthrene in ambient air and deposition on three alpine summits



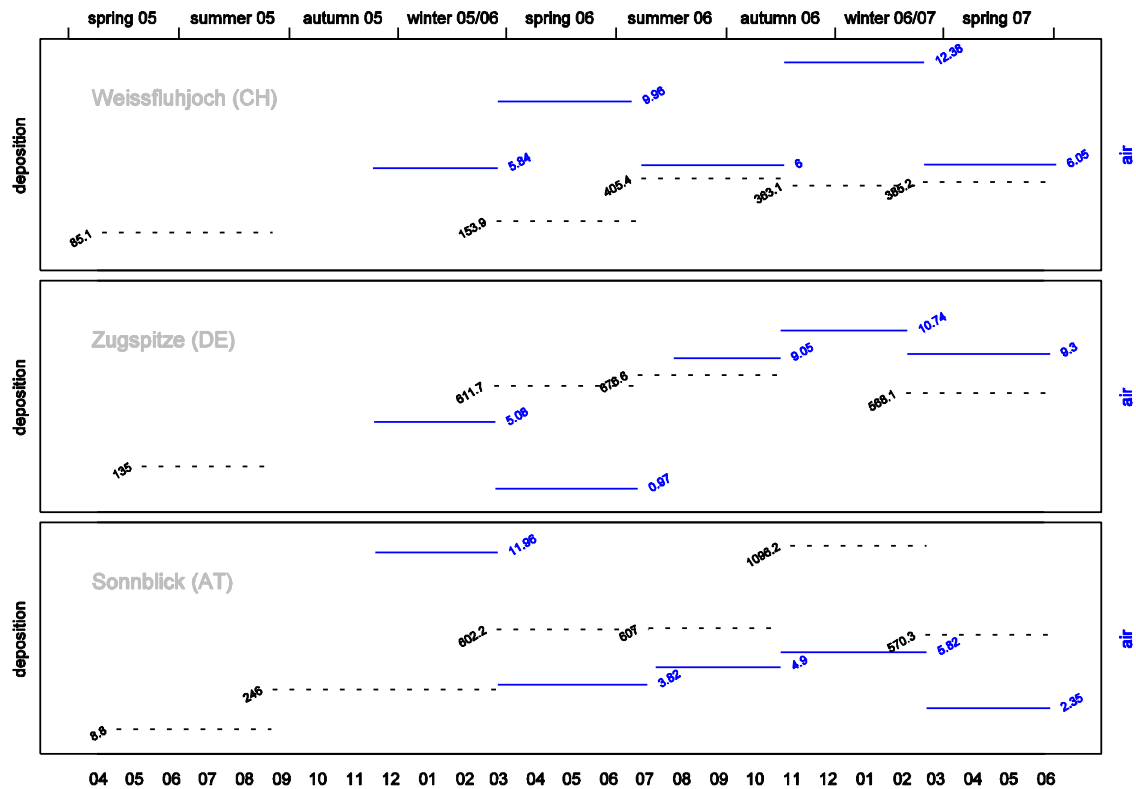
Units: deposition: ng m⁻² d⁻¹, atmospheric concentration: pg m⁻³.

Figure 3-118: Dibenzo(a,h)anthracene in ambient air and deposition on three alpine summits



Units: deposition: ng m⁻² d⁻¹, atmospheric concentration: pg m⁻³.

Figure 3-119: Benzo(a)pyrene in ambient air and deposition on three alpine summits



Units: deposition: $\text{ng m}^{-2} \text{d}^{-1}$, atmospheric concentration: ng m^{-3} . Acenaphthene and Acenaphthylene concentrations are not known for the spring 2006 deposition at Mt. Weissfluhjoch, the actual Σ EPA-PAH deposition might thus be 2-9 $\text{ng m}^{-2} \text{d}^{-1}$ higher.

Figure 3-120: Deposition and atmospheric concentration of 16 EPA-PAH (sum) on three alpine summits

3.4.4 Spatial variation

The total concentrations of 16 PAHs in the needles decreased from west to east: levels at Klosters and Griments (CH) were much higher than the rest of the sites (indicated by exclamation marks in Figure 3-121). However if only the heavier and most toxic compounds are considered (e.g. BaP), the gradient is opposite with higher levels in the East and North of the Alps (see 3.4.4.3, p. 126).

PAH levels of both humus and mineral soil were higher at the northern fringe of the Alps. Much higher than average PAH concentrations were found in humus from Rougemont (CH) and in mineral soil from Beatenberg (CH) and Berchtesgaden (DE).

3.4.4.1 Needles

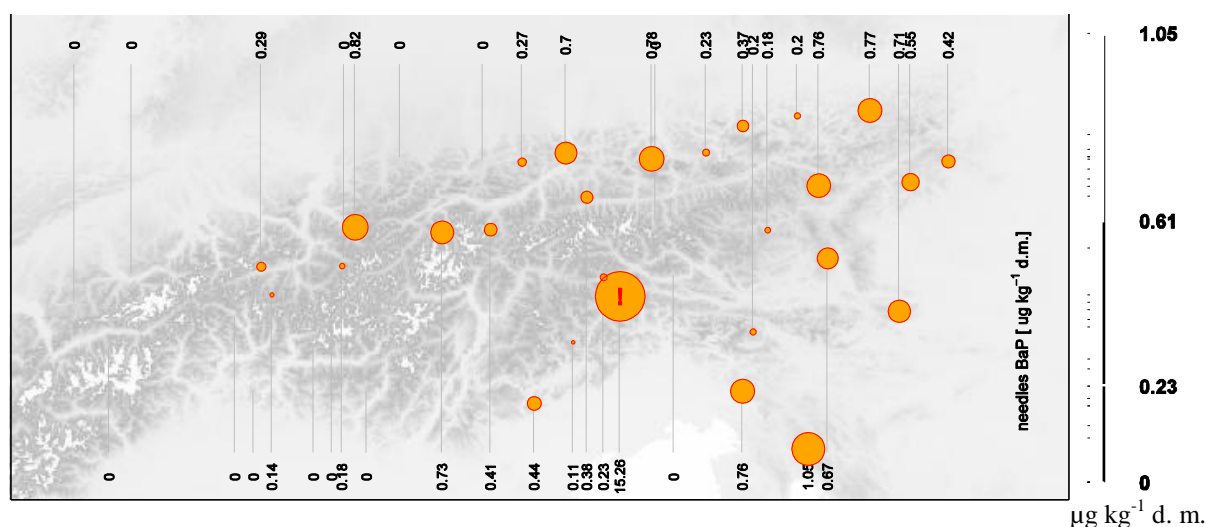


Figure 3-121: BaP content of in 0.5 year old Norway spruce needles

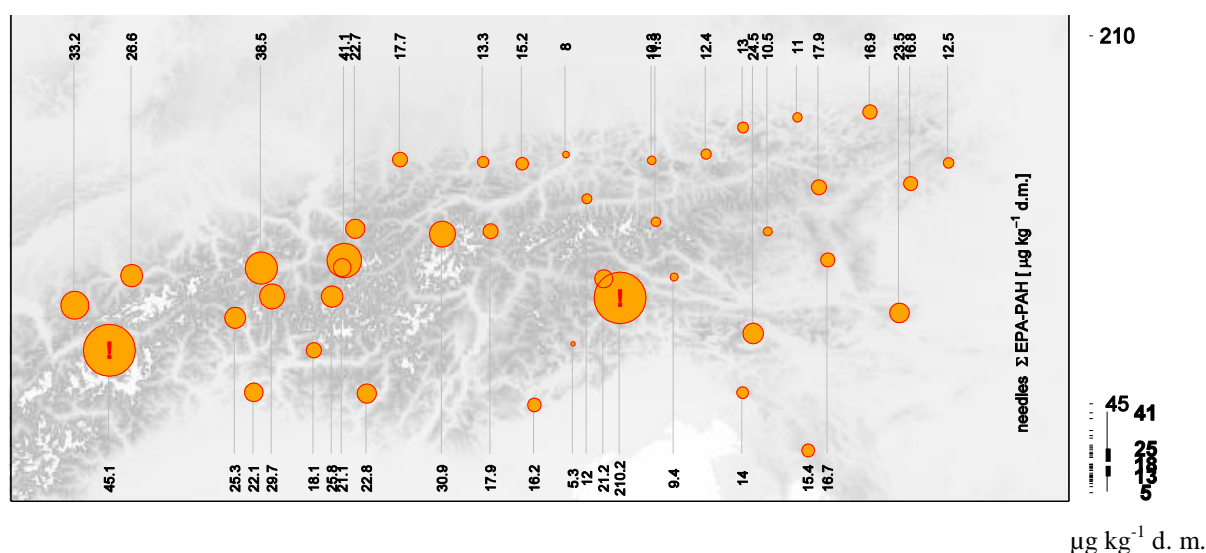


Figure 3-122: Total concentration of 16 EPA-PAH in 0.5 year old Norway spruce needles

Longitudinal differences

The PAH concentrations at the Italian site IT-04-2 (part of the height profile Val Viscdende) were usually several times higher than those of the remaining sites. Site IT-04-2 has therefore been omitted from the following boxplots.

Significant longitude related differences (Kruskal-Wallis test, $\alpha \leq 0.05$) for the whole study region were discovered for the majority of the 16 EPA-PAH (exceptions: ANA, ANY, DBahA, CHR, ANT) and for total EPA-PAH content. Note that the heavy and toxic PAHs (BaA, BbF, BkF, BghiP, BaP and IND) reach higher levels in the east (and in some cases central) part of the Alps while the lighter and more volatile ones (vapour pressure of the solid ≥ 0.6 mPa: NAPH, PHEN, FLU, FLA and PYR) peak at the western side of the study area (Figure 3-123).

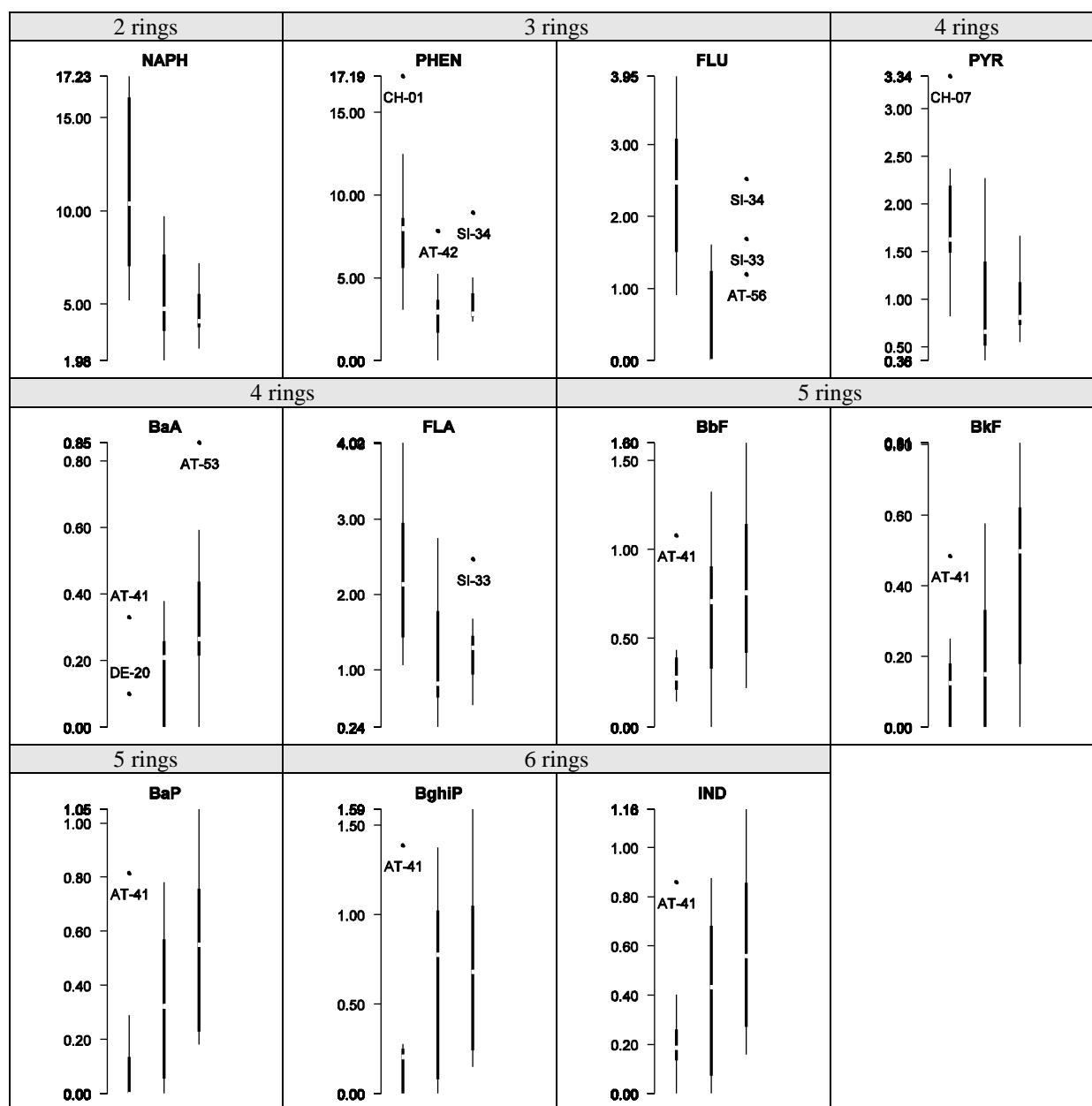


Figure 3-123: Longitudinal pollution trends of various PAH in 0.5 year old Norway spruce needles

Latitudinal differences

There were no significant latitude related differences (Kruskal-Wallis test, $\alpha \leq 0.05$) for the whole study region. However, differences were almost significant for the two most volatile PAH (naphthalene: $\alpha = 0.054$, phenanthren: $\alpha = 0.057$). Remarkably, these two PAH have the highest median value in the central zone of the study region.

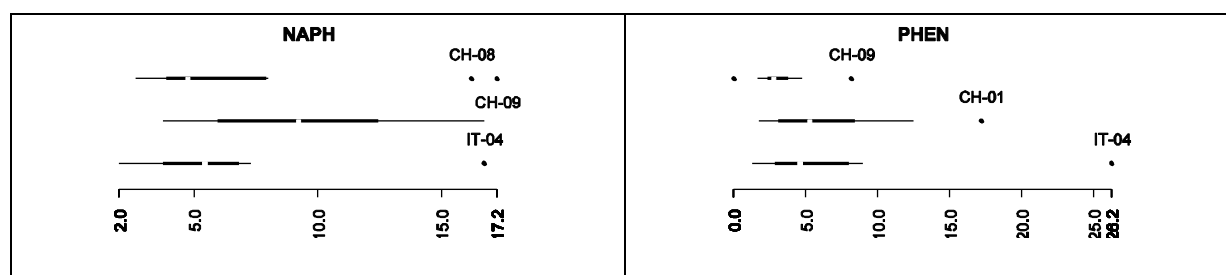


Figure 3-124: Latitudinal pollution trends of PAH in 0.5 year old Norway spruce needles

3.4.4.2 Humus

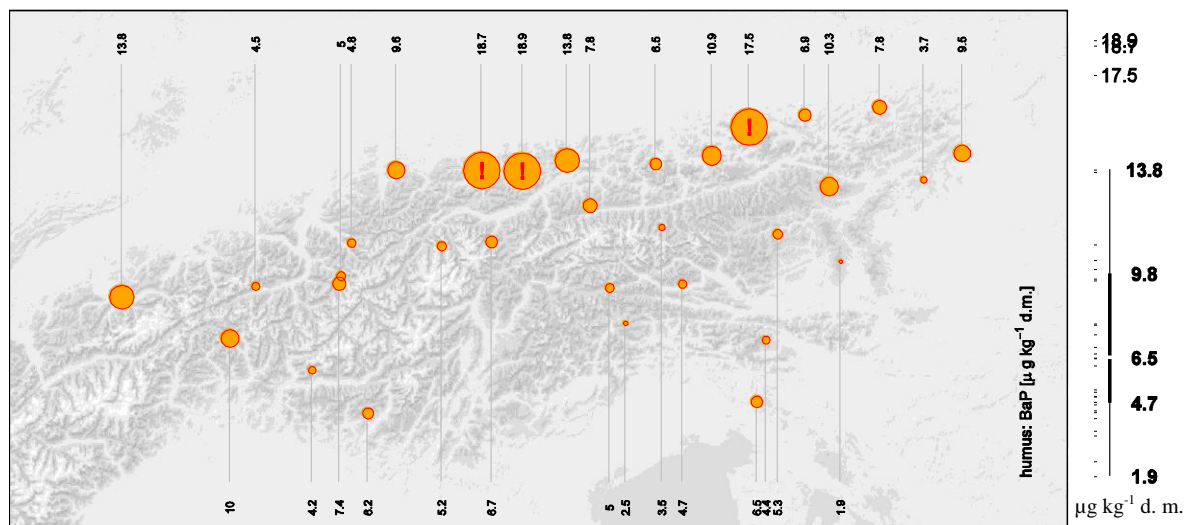


Figure 3-125: BaP concentration in forest humus

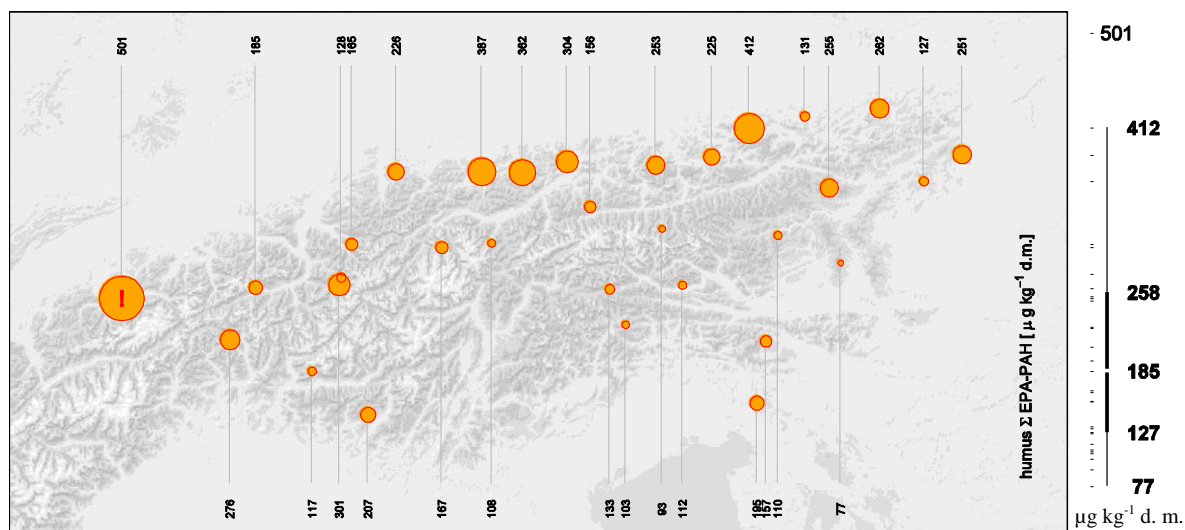
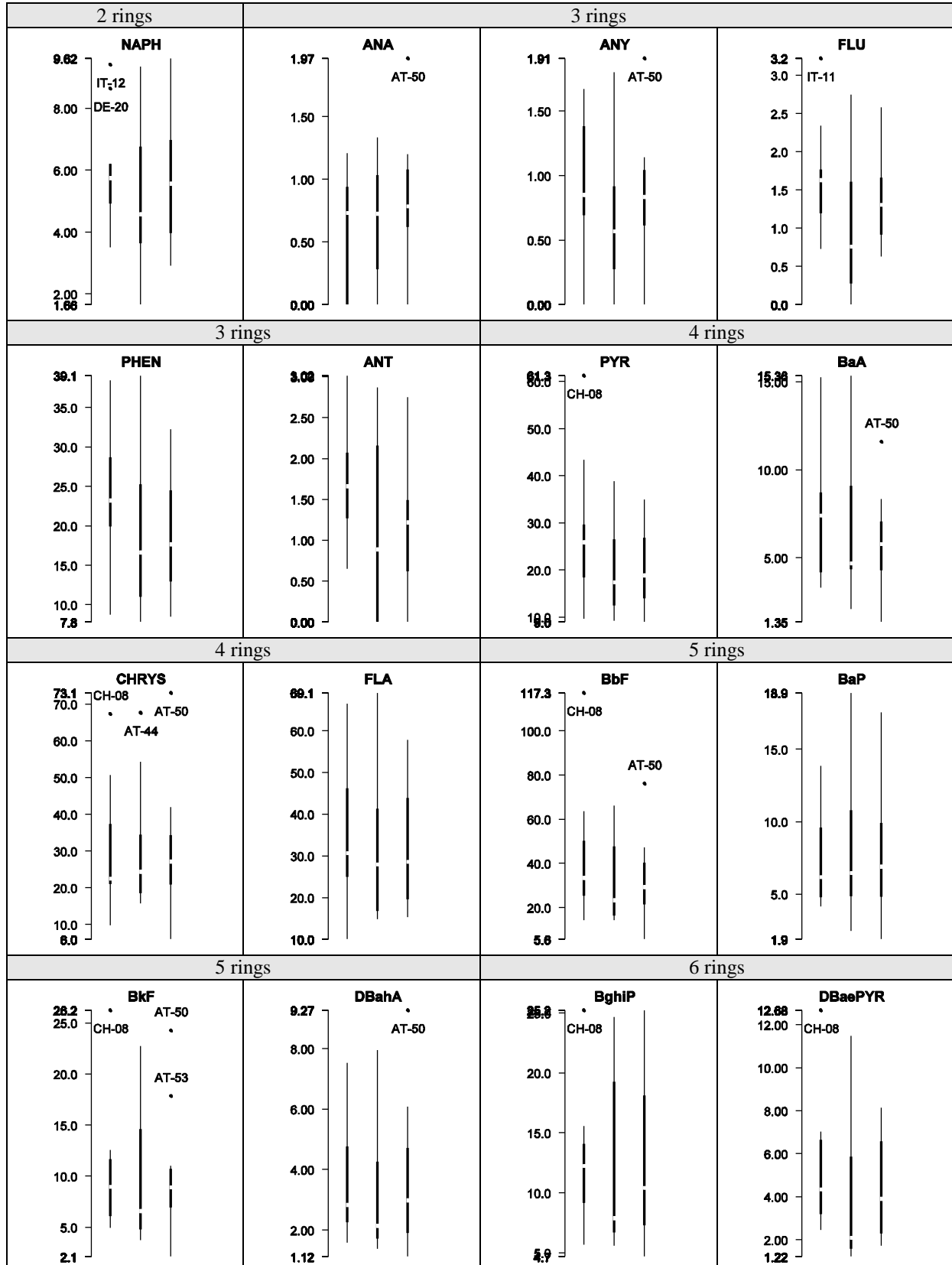
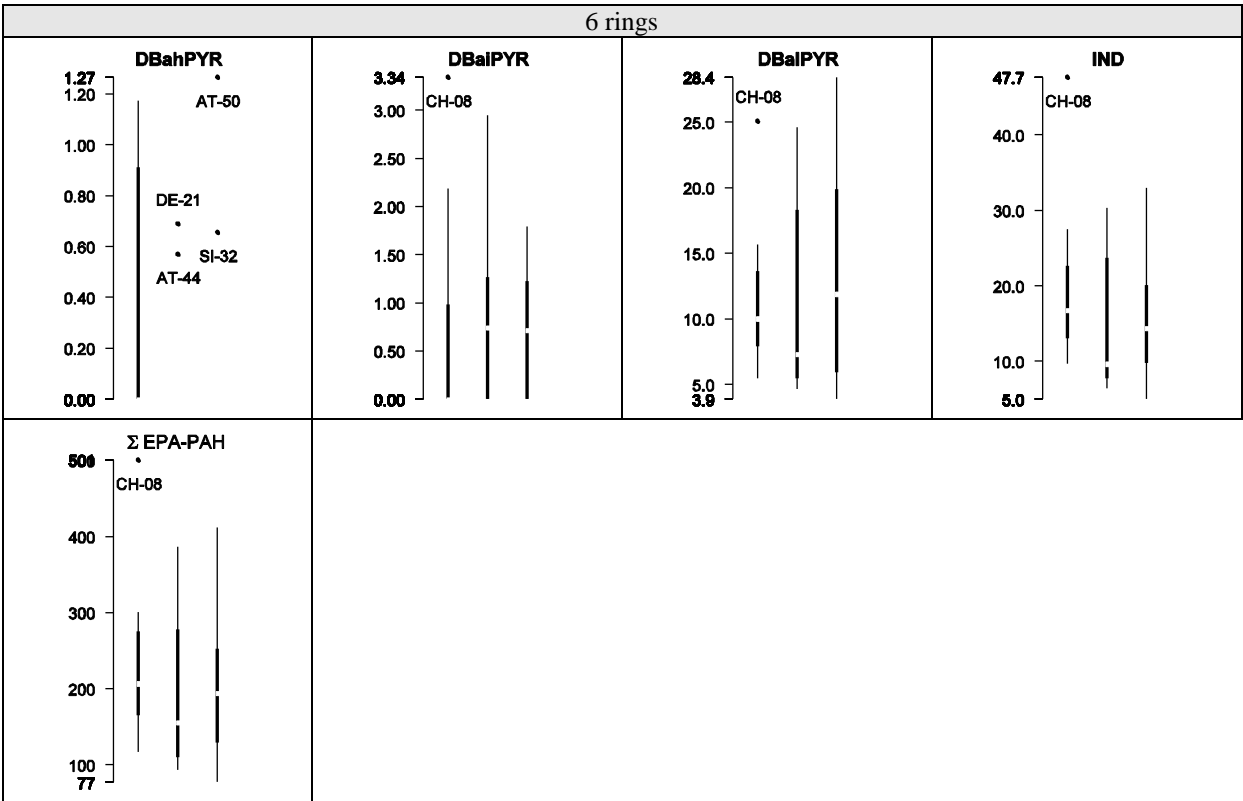


Figure 3-126: Total content of 16 EPA-PAH of forest humus

Longitudinal differences

No significant concentration differences were detected among the longitudinal site groups. The longitudinal band of highest pollution varied from one PAH to the next. However, the middle zone never showed the highest median concentration, except for BaP and DBaPYR (Figure 3-127).



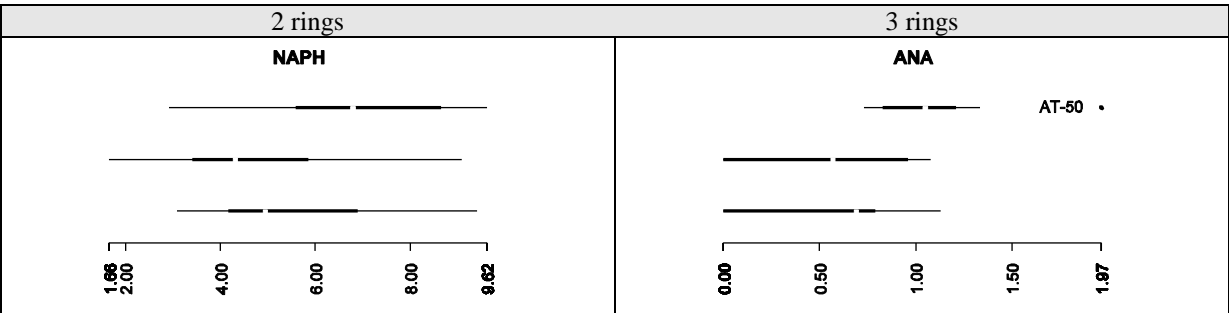


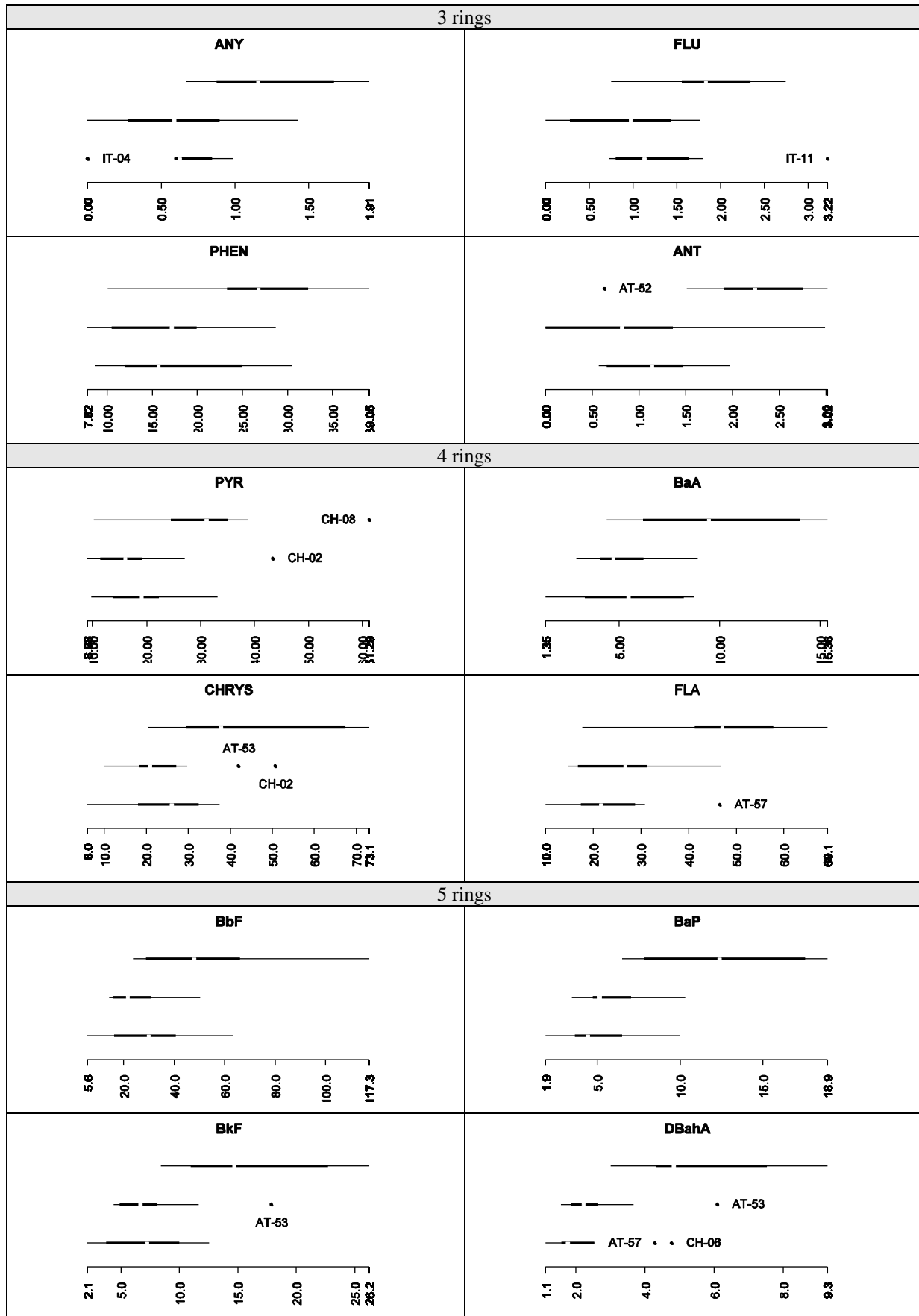
unit: µg kg⁻¹ d.m.

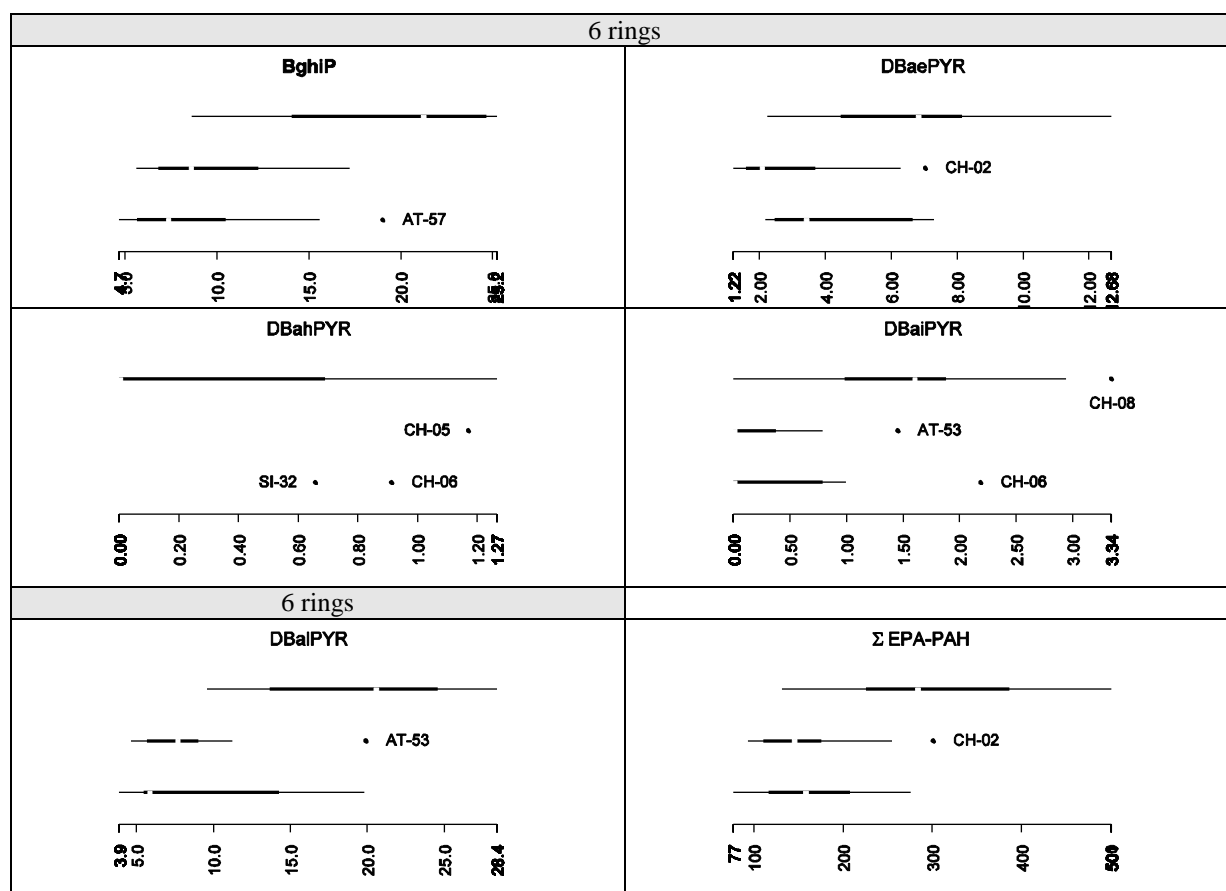
Figure 3-127: Longitudinal pollution trends of various PAH in forest humus

Latitudinal differences

Contrary to the longitudinal differences, all PAH except DBahPYR showed significant (Kruskal-Wallis, $\alpha \leq 0.05$) or highly significant (including the sum of 16 EPA-PAH; $\alpha \leq 0.01$) concentration differences among the latitudinal site groups. Highest PAH medians were, without exception, in the north and never in the central part of the study region (Figure 3-128).







unit: $\mu\text{g kg}^{-1} \text{ d.m.}$

Figure 3-128: Latitudinal pollution trends of various PAH in forest humus.

3.4.4.3 Air

The prevailing source region for atmospheric PAHs could vary between sampling periods, sites and PAH species. However, during the cold season (late autumn 06-late winter 07), air from the northwest had the highest concentrations of the most abundant species NAPH, PHEN and FLU as well as for BaP.

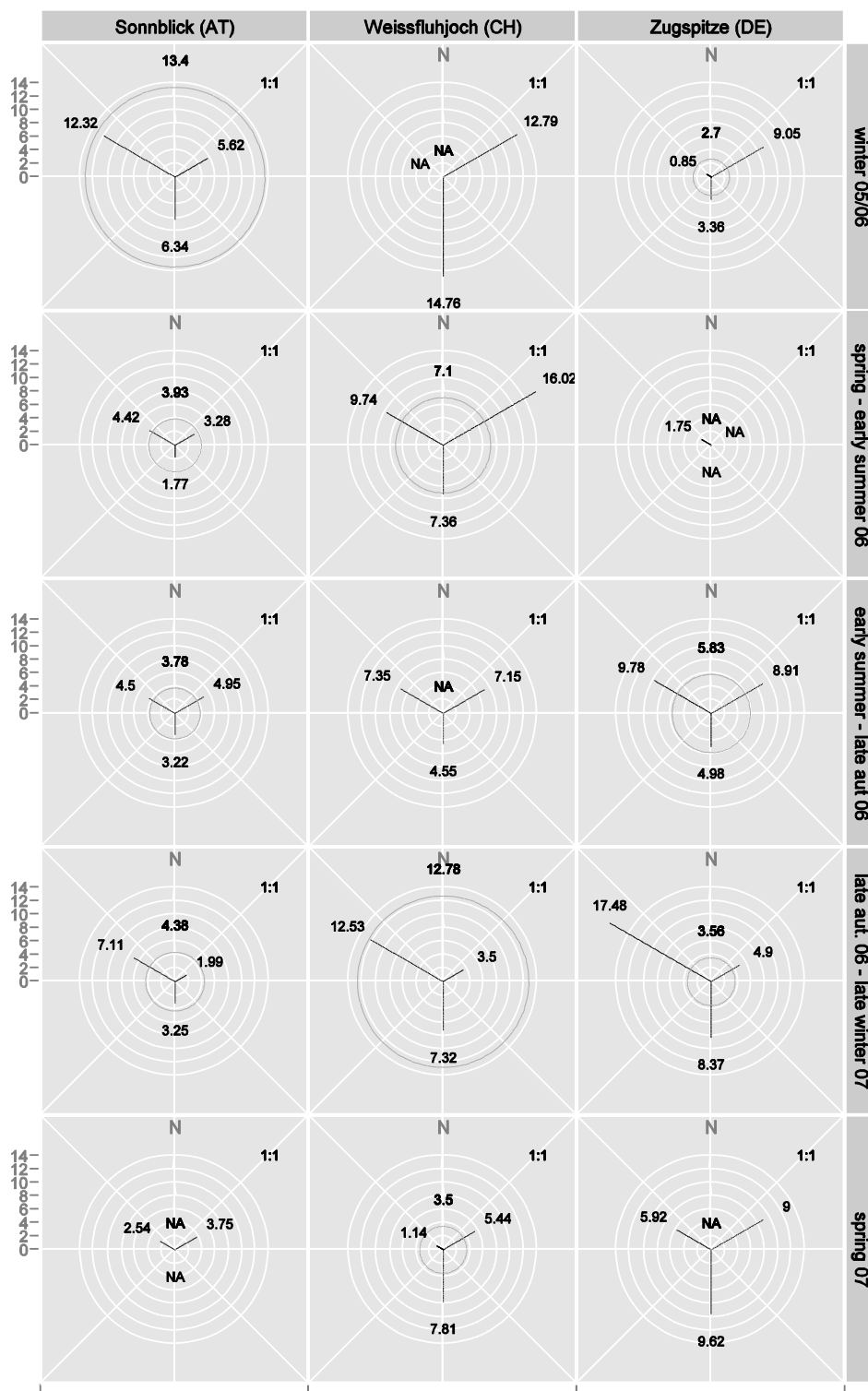


Figure 3-129: Concentration [ng m^{-3}] of naphthalene in air from NW, NE and S (circle: trajectory not attributable to a particular source region)

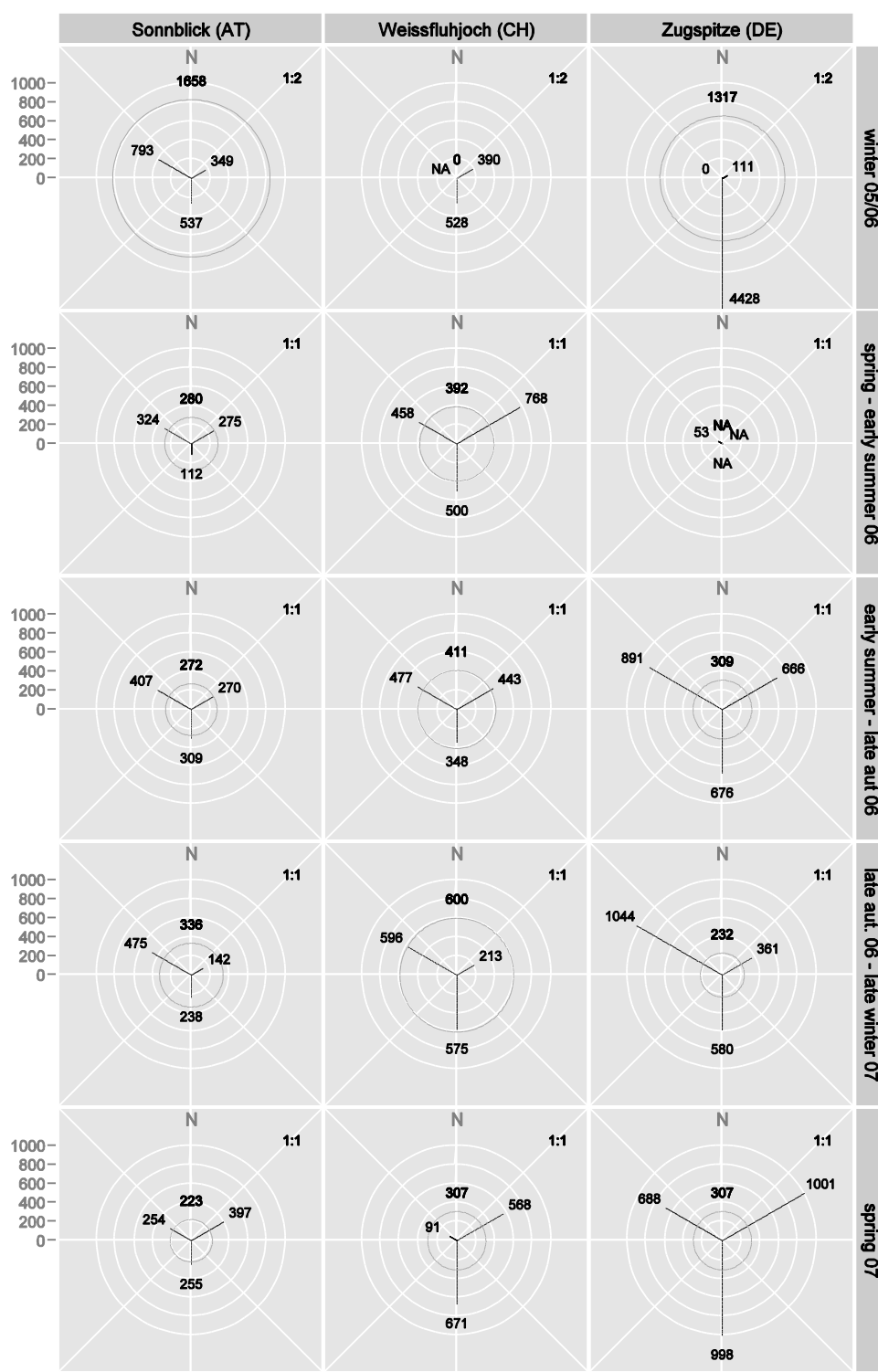


Figure 3-130: Concentration [pg m^{-3}] of fluorene in air from NW, NE and S (circle: trajectory not attributable to a particular source region); note the different scaling of winter 05/06 values.

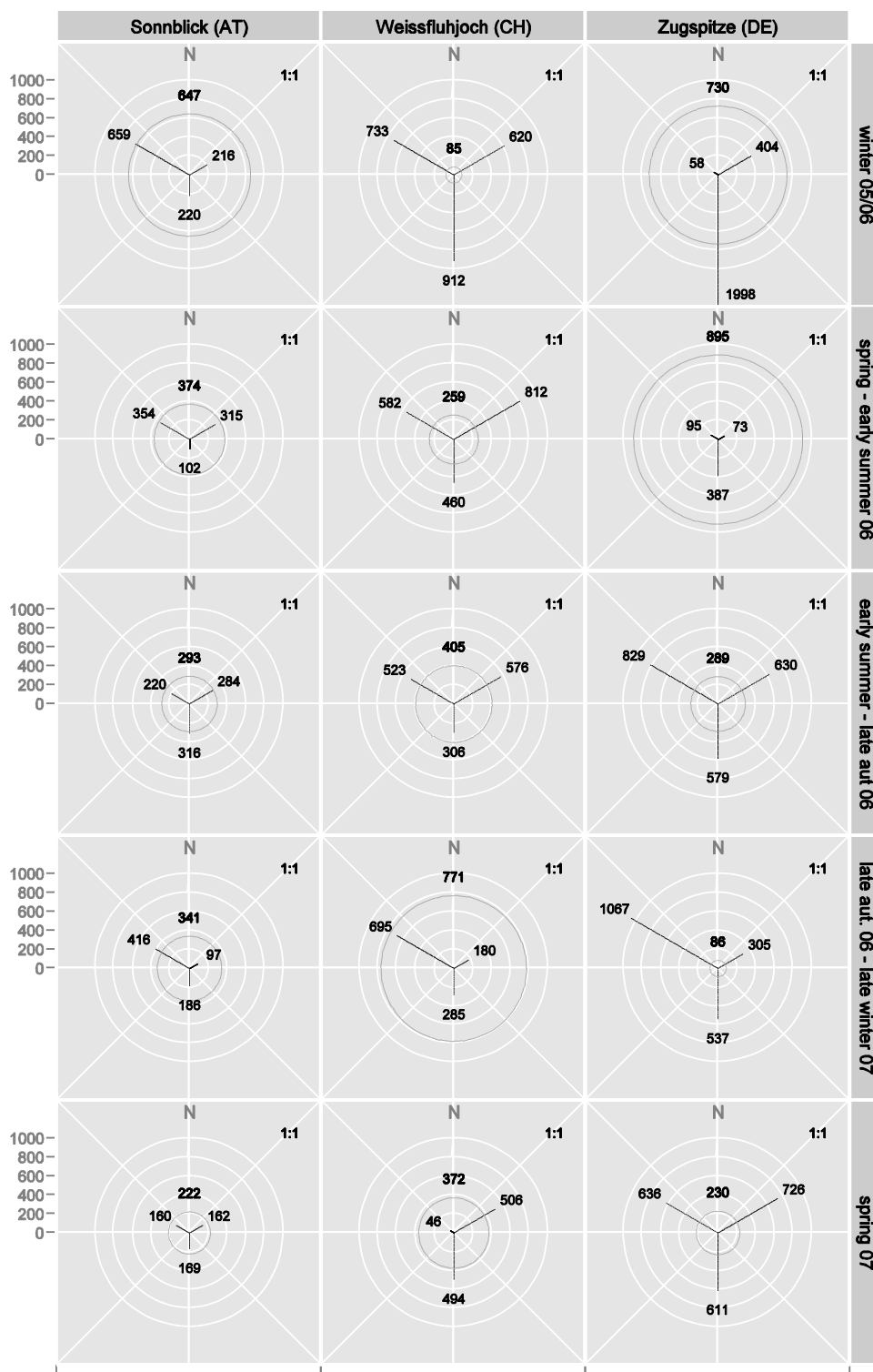


Figure 3-131: Concentration [pg m^{-3}] of phenanthrene in air from NW, NE and S (circle: trajectory not attributable to a particular source region)

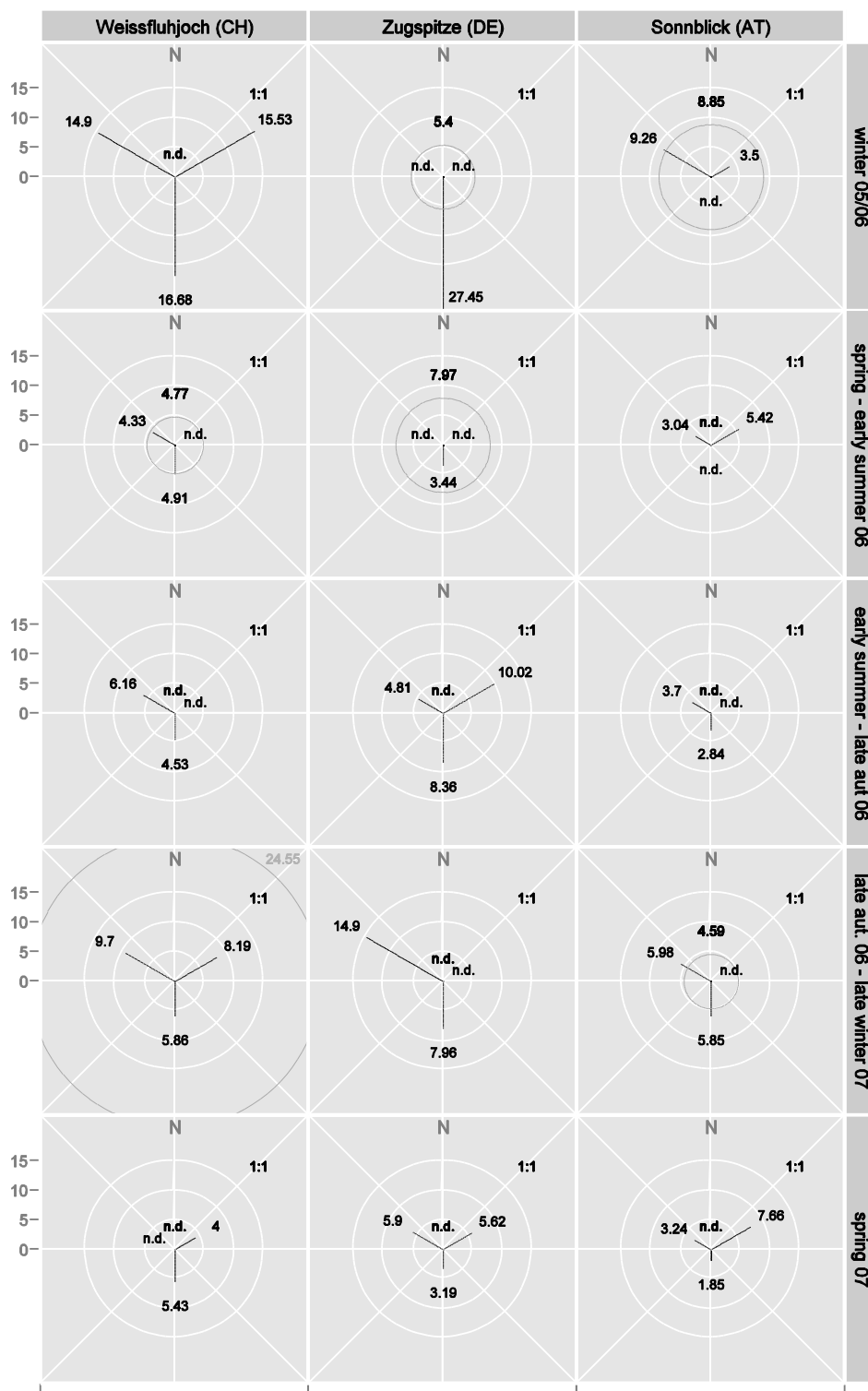


Figure 3-132: Concentration [pg m^{-3}] of BaP in air from NW, NE and S (circle: trajectory not attributable to a particular source region)

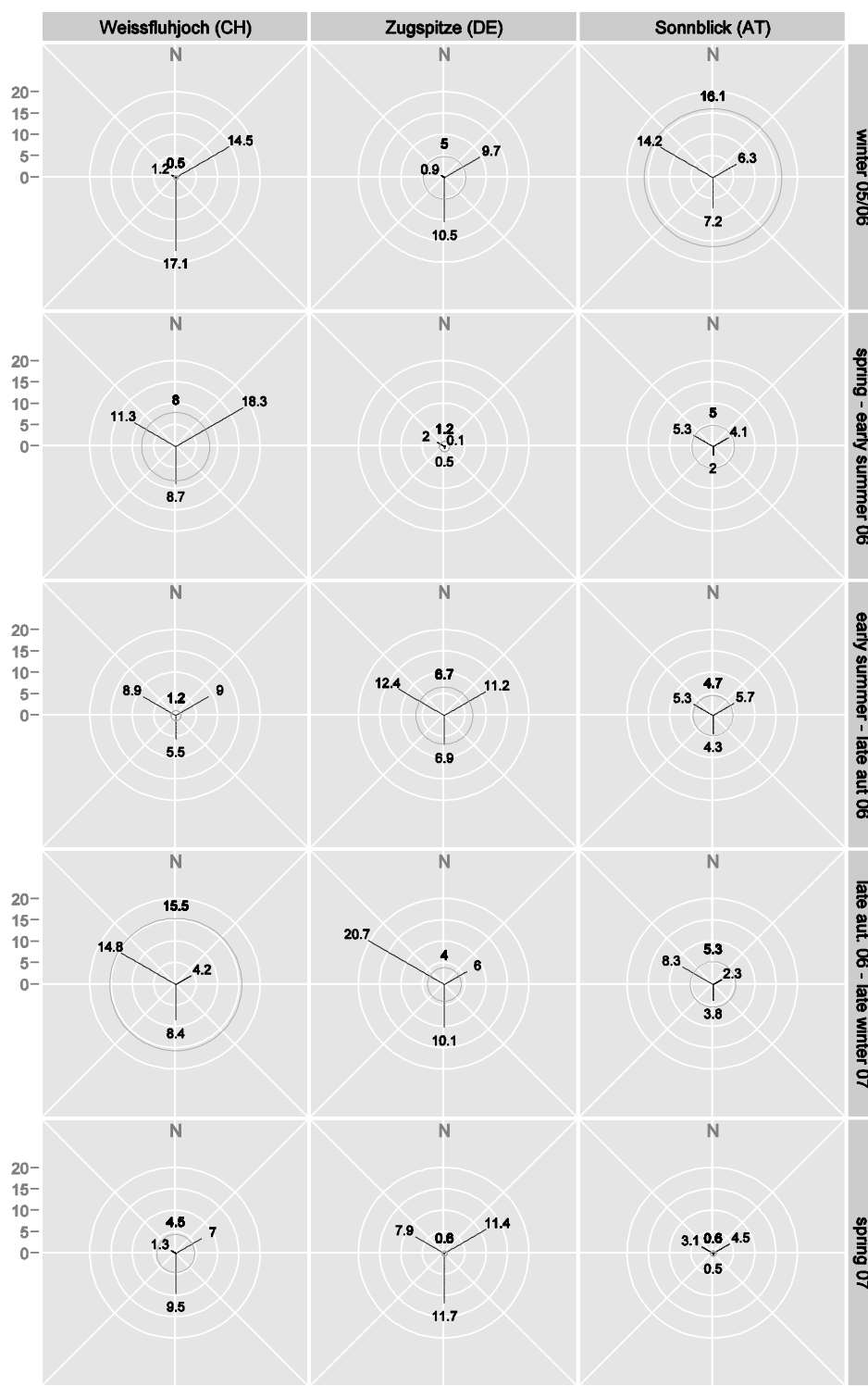


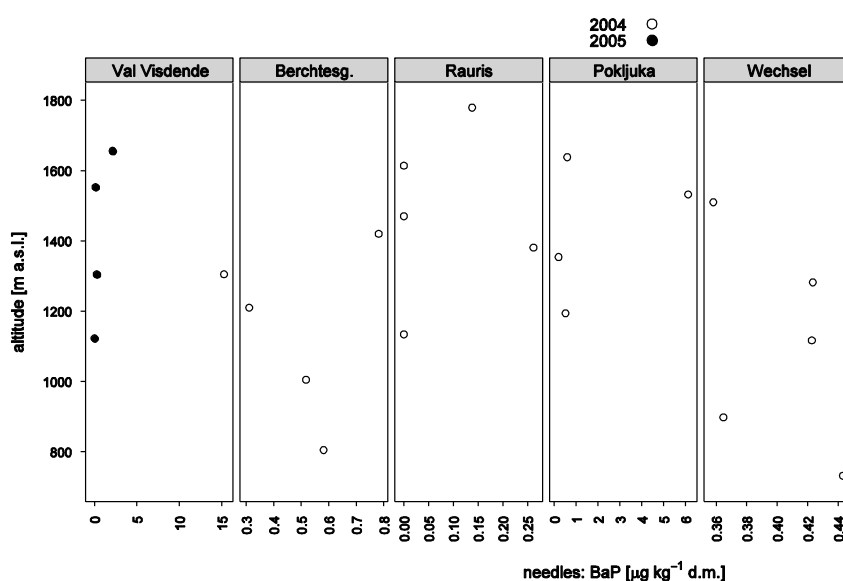
Figure 3-133: Concentration [ng m^{-3}] of 16 EPA-PAH in air from NW, NE and S (circle: trajectory not attributable to a particular sector)

3.4.5 Altitudinal variation

3.4.5.1 Needles

Note that the needle PAH dataset of the Italian height profile Val Viscende is from autumn 2005, except one additional sample at 1305 m a. s. l. from 2004 (shown in the following plots for comparison with the other profiles).

Most altitude profiles showed higher PAH concentrations closer to the bottom of the valley, a likely impact of nearby local emissions.



BaP was not found in needles from the height profiles Klosters and Eschenlohe.

Figure 3-134: Altitudinal variation of the BaP concentration in 0.5 year old Norway spruce needles

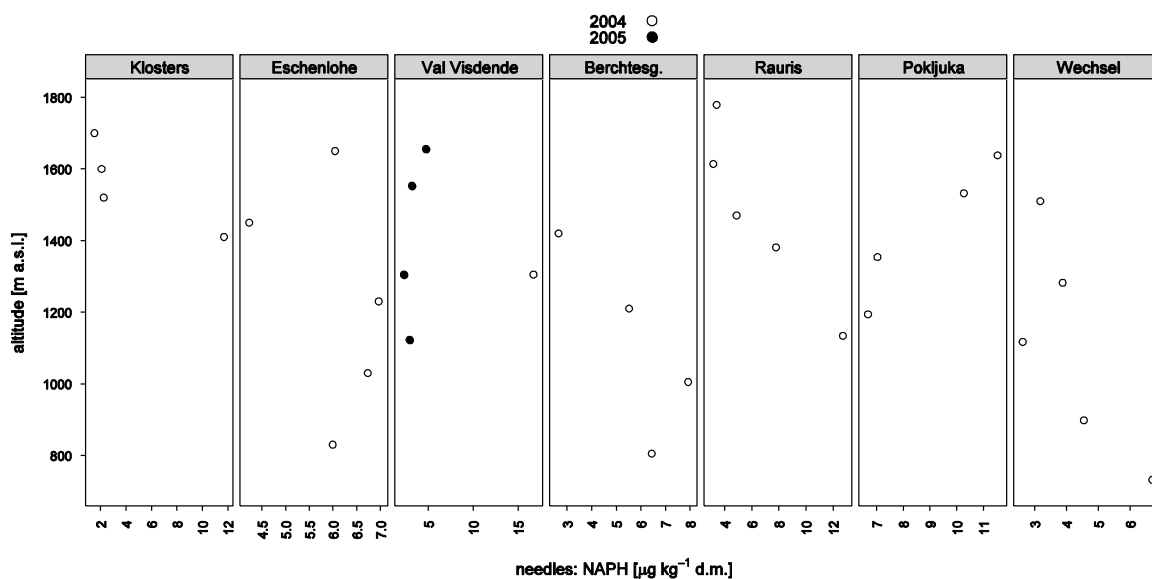


Figure 3-135: Altitudinal variation of the naphthalene concentration in 0.5 year old Norway spruce needles

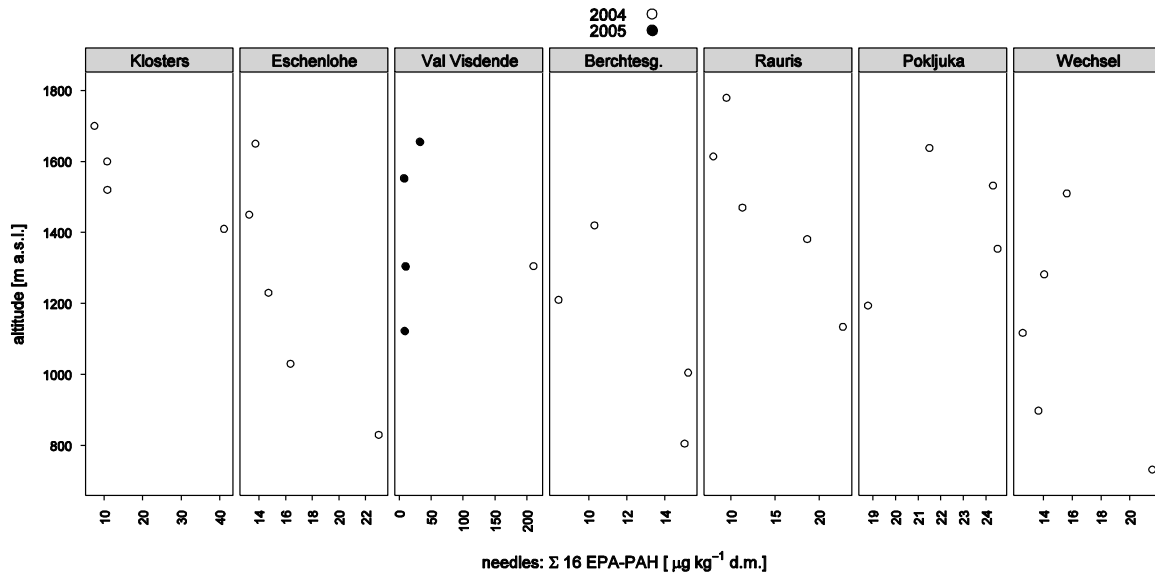


Figure 3-136: Altitudinal variation of the sum of 16 EPA-PAH in 0.5 year old Norway spruce needles

3.4.5.2 Humus

Particularly at the Wechsel and Rauris height profiles, PAH levels increase with altitude, indicating a lack of nearby sources. At profile Klosters, which is located above a village, PAH peaked at the lower plots closer to the village.

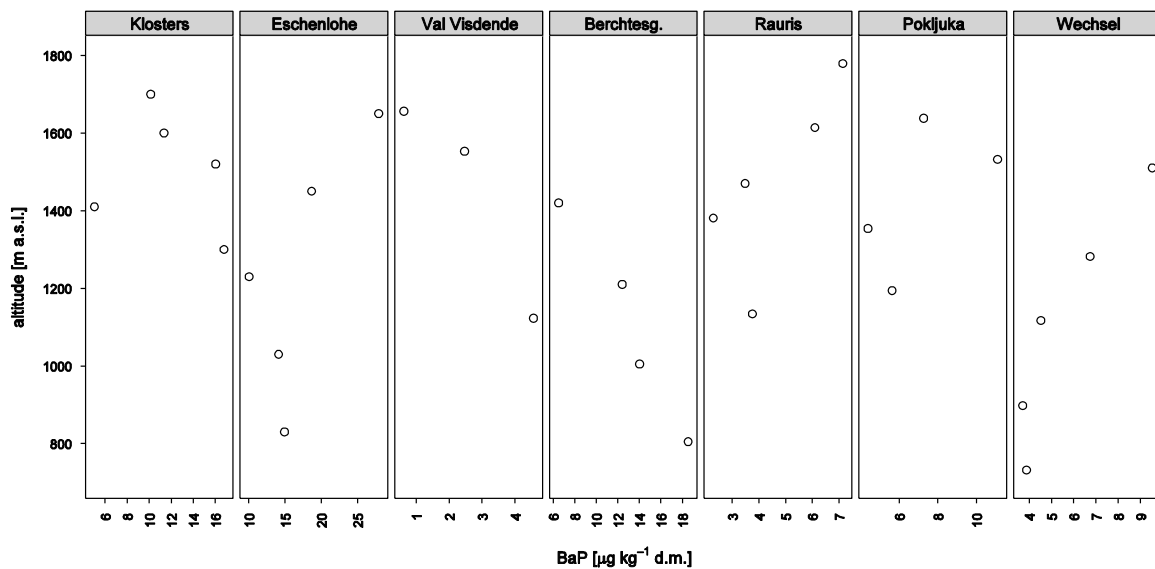


Figure 3-137: Altitudinal variation of humus BaP concentrations

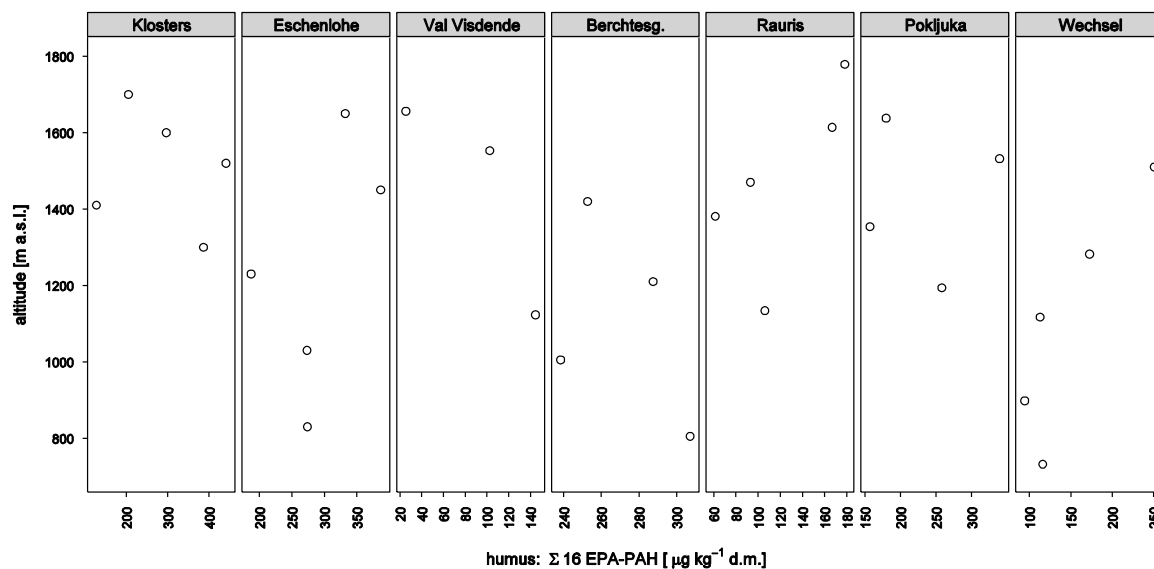


Figure 3-138: Altitudinal variation of the sum of 16 EPA PAH in humus

3.4.5.3 SPMD

Benz(a)pyren was only detected in four SPMD samples of different height profiles.

The vertical variation detected with SPMD measurements resembles that deduced from needle sampling. Higher PAH concentrations were found close to the bottom of the valleys.

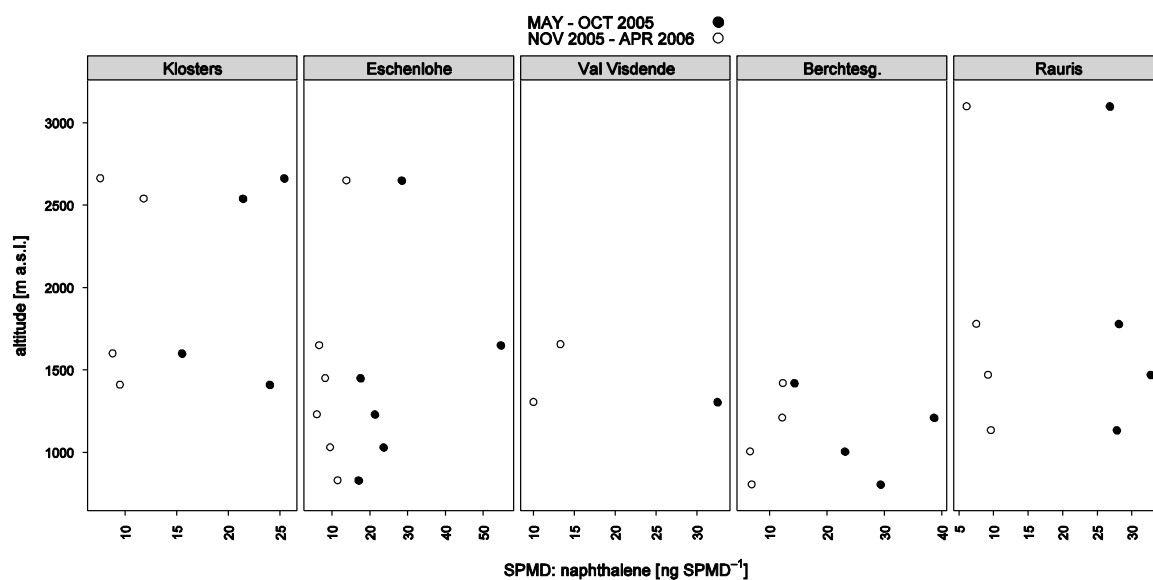


Figure 3-139: Altitudinal variation of naphthalene in SPMD

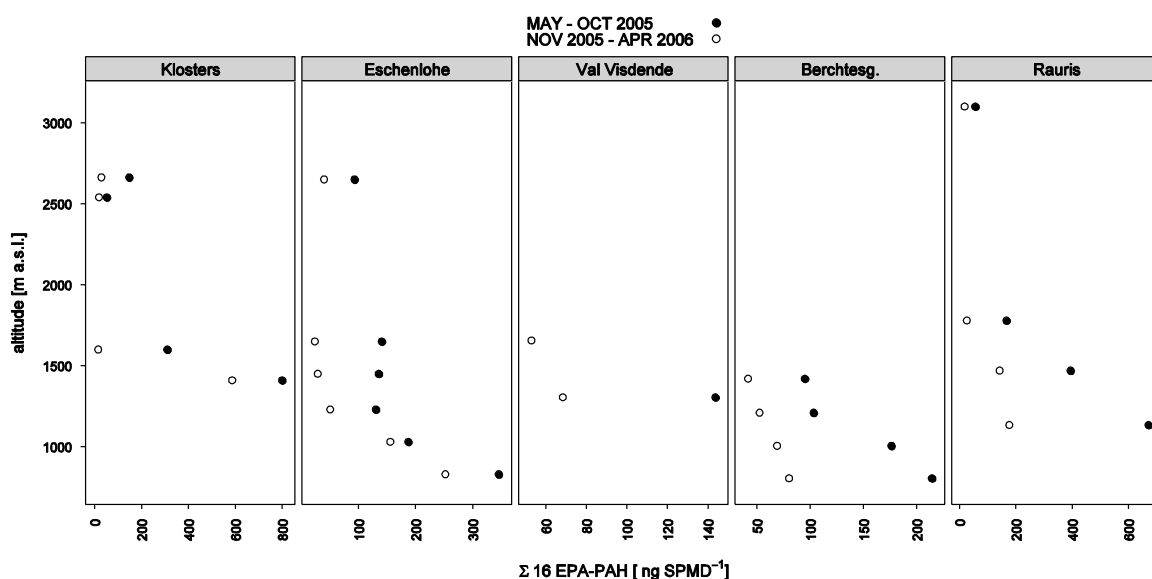


Figure 3-140: Altitudinal variation of 16 EPA-PAH in SPMD

3.5 Polybrominated diphenylethers (PBDE)

3.5.1 Overview of results

Polybromo-diphenylether flame retardants reach the alpine region by long-range air transport. While the concentrations in needles were near the detection limit, PBDE accumulated in humus up to 2–5 times the levels found in needles. The concentrations of several PBDE in humus varied significantly between the western, middle and eastern part of the study region with maximum loads in the East. For this pollutant group, too, the highest concentrations always occurred in a lateral part of the study area. The levels of most PBDE culminated at the northern fringe of the alpine range, near potential sources. The main congener of the commercial OcBDE formulation – BDE 183 – dominated in the northeastern Alps, possibly because of a higher usage of the product in this area. The dominating congeners in humus were BDE 209, followed by BDE 183, BDE 47 and BDE 153. In most environmental samples, however, BDE 183 contributes little to total BDE content. Its higher share in the humus samples from this study may be due to revolatilisation of the congeners with less than seven bromine substituents or slower deposition via atmosphere and litter fall.

The main congeners of commercial DecaBDE (BDE 209) and PentaBDE (BDE 47 and 99) dominated air and deposition congener profiles. On three alpine summits, air arriving from the Northeast usually bore the highest PBDE levels, irrespective of sampling period or site. Within the limited duration of active air sampling, the seasonal variation of atmospheric PBDE levels at the three mountain peaks showed no common trend, and the variation between years appeared to be more influential than the course of seasons. Seasonal deposition changes at the three summits were remarkably coherent for the sum of six BDE, despite a probable local release at one of the stations.

No consistent altitudinal trend was found for humus PBDE levels. However, the particlebound congeners BDE 183 and BDE 209 repeatedly showed a maximum at some intermediate height level. This is possibly an effect of increased atmospheric concentrations below the thermal inversion layer.

3.5.2 Characterization

3.5.2.1 Physicochemical properties

Polybrominated diphenylethers (PBDE) are bicyclic aromatic ethers (Figure 3-141). PBDE isomers cover a wide range of chemical and physical properties which depend on the bromine content. 209 positional isomers are possible, but as they are synthesized by electrophilic substitution of diphenylether, eight 2,2',4,4'-PBDE isomers dominate in the commercial formulations (Table 3-16).

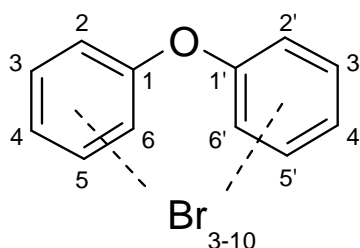


Figure 3-141: Molecular structure of PBDEs.

Table 3-16: Physical properties of PBDEs at 25°C (Wania 2003)

BDE ^a	position of bromine substituents	Formula	MW [g mol ⁻¹]	T _M [°C]	P _L [Pa]	S _S ng l ⁻¹	log K _{OA}	log K _{OW}
28	2,4,4'-	C ₁₂ H ₇ Br ₃ O	406.90	64.25	1.96E-03	7.08E+04	9.5	5.53
47	2,2',4,4'	C ₁₂ H ₆ Br ₄ O	485.80	84	2.66E-04	1.30E+04	10.53	6.11
99	2,2',4,4',5	C ₁₂ H ₅ Br ₅ O	564.69	92.5	4.57E-05	5.87E+03	11.31	6.61
100	2,2',4,4',6	C ₁₂ H ₅ Br ₅ O	564.69	100.5	3.99E-05	8.92E+03	11.13	6.51
153	2,2',4,4',5,5'	C ₁₂ H ₄ Br ₆ O	643.59	161.5	7.58E-06	8.69E+02	11.82	7.13
154	2,2',4,4',5,6'	C ₁₂ H ₄ Br ₆ O	643.59					
183	2,2',3,4,4',5',6	C ₁₂ H ₃ Br ₇ O	722.49	172	4.68E-07	1.50E+03	11.96	7.14
209	2,2',3,3',4,4',5,5',6,6'	C ₁₂ Br ₁₀ O	959.17	302.5	2.95E-09	4.00E+00		9.97

^a BDE numbering according to IUPAC nomenclature of PCB

MW...molecular mass, T_M...melting point, P_L...supercooled liquid vapour pressure, S_S...solubility in water, log K_{OA}...n-octanol/air partition coefficient, log K_{OW}...n-octanol/water partition coefficient

3.5.2.2 Use and emissions

PBDE are widely used as additive flame retardants for plastics and textile back coatings. For this purpose the polymer material is blended with amounts from 10-30 % w/w. PBDE are not chemically bound to the polymer and can therefore evaporate, separate or leach from the surface of treated products into the environment.

Three commercial formulations exist: pentabromo-diphenylether (PeBDE), octabromo-diphenylether (OcBDE) and decabromo-diphenylether (DeBDE), named after their average bromine content. The three PBDE formulations have different product applications: PeBDE for polyurethane foam (soft furnishings, mattresses, car seating, insulation), OcBDE for acrylnitril-butadiene-styrene (ABS) casings and DeBDE for hard plastic (electronic equipment components and casings, rubber, textile backcoatings).

Bromine flame retardants interrupt the radical chain mechanism of the combustion process in the gas phase: the energy-rich H· and OH· radicals released by burning hydrocarbons are neutralised by HBr emitted by the decomposing brominated flame retardant: the flame is extinguished (Troitzsch 2004).

PBDE are not synthesized in Europe but imported as formulation or in products. In 2001, the world market demand of penta / octa / decaBDE was 7 500 / 3 790 / 56 100 tons. Europe: 150 / 610 / 7 700 tons, i. e. 3 / 16 / 14 % of the global demand (BSEF 2008). In 2004 the decaBDE usage in Europe was 8 010.8 t, and in the single EU countries Belgium: 934 t (12%), France: 1 006.6 t (13%), Germany: 1 837 t (23%), Italy: 1 813.2 t (23%) and UK: 2 214.8 t (28%) (EBFRIP 2005).

Pe- and OcBDE preparations have been banned in the EU since August 15, 2004 (EU, 2003) and are under review for Stockholm Convention. DeBDE was exempt from this ban because it was believed to be hardly subject to long-range transport and have a low bioaccumulation potential. Possible degradation of DeBDE under anaerobic conditions or in biota into more toxic forms was not considered (EU 2004). The European Court of Justice recently annulled the exemption from the EU Restriction of Hazardous Substances (RoHS) directive (ECJ). Effective from July 1, 2008 the use of DeBDE in electrical and electronic equipment is also restricted.

3.5.2.3 Environmental behaviour and bioaccumulation

PBDE are persistent and bioaccumulate and biomagnify in the food web. Their widespread use made them ubiquitous in abiotic and biotic samples. Increasing levels were analysed in sewage sludge, sediments, human plasma and milk (DE WIT 2002, LETCHER 2003, HITES 2004, HALE 2006, WANG 2007).

3.5.2.4 Toxicology

PBDE are structurally similar to PCB. Animal experiments have indicated that technical PBDE products are able to induce liver toxicity by the increased activity of liver microsomal ethoxyresorufin-O-deethylase (VON MEYERINCK, 1990; see also section 1.7.10, pp. 25 ff), that long-term exposure to PBDEs was found to induce thyroid hyperplasia and thyroid adenomas, and that they also induce neurotoxicity when administered at a sensitive period of brain growth (DE WIT, 2002).

3.5.3 Summary statistics

3.5.3.1 Needles

Table 3-17: Concentration of PBDE in 0.5 year old Norway spruce needles

	n<LOD	mean	sd	min	10%	25%	median	75%	90%	max
BDE 28	1	5.01	3.67	2.28	3.04	3.28	3.97	4.84	5.36	18.98
BDE 47	7	176.6	412.0	< LOD	< LOD	< LOD	109.2	130.0	142.2	2114
BDE 99	10	52.12	122.75	< LOD	< LOD	< LOD	32.52	41.29	62.18	621.60
BDE 100	12	9.48	15.01	< LOD	< LOD	< LOD	9.70	11.50	14.55	64.96
BDE 153	15	2.72	4.60	< LOD	< LOD	< LOD	< LOD	3.69	6.02	16.14
BDE 154	6	3.62	4.46	< LOD	< LOD	2.16	2.61	3.56	5.03	19.69
Σ 6 BDE	7	252.9	557.2	< LOD	< LOD	< LOD	161.3	190.6	221.5	2856
BDE 183	23	< LOD	< LOD	< LOD	< LOD	< LOD	< LOD	< LOD	< LOD	15.90
BDE 209	17	229.0	397.8	< LOD	< LOD	< LOD	< LOD	276.8	782.1	1347

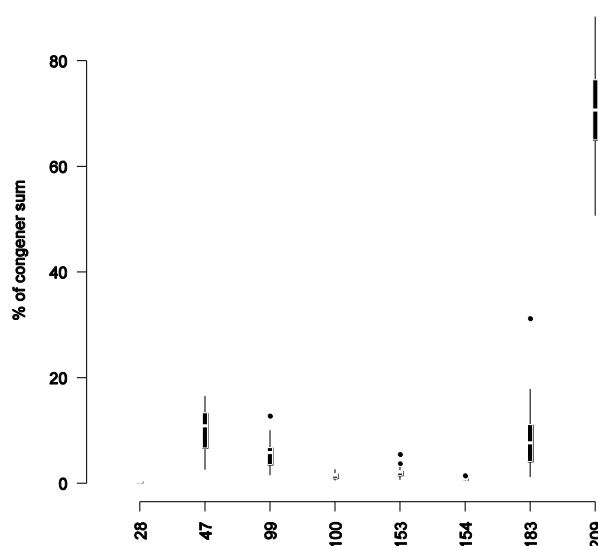
unit: ng kg⁻¹ d.m.; sample size n=25; LOD...detection limit

3.5.3.2 Humus

Table 3-18: Concentration of PBDE in forest humus

	n<LOD	mean	sd	min	10%	25%	median	75%	90%	max
BDE 28	0	6.82	4.00	2.05	2.94	4.32	6.12	8.56	10.87	19.14
BDE 47	0	304.4	179.6	93.36	111.6	171.8	256.7	408.2	558.1	745.1
BDE 99	0	176.8	125.8	45.80	56.68	84.63	129.9	247.6	390.8	462.7
BDE 100	0	46.29	29.88	13.43	15.72	24.39	36.37	63.66	95.64	109.8
BDE 153	0	68.23	57.96	7.18	21.46	31.45	43.59	81.38	165.3	214.1
BDE 154	0	25.49	17.41	6.52	8.42	11.52	19.18	37.26	53.24	63.01
Σ 6 BDE	0	628.0	380.3	209.7	223.3	326.4	523.8	836.7	1157	1472
BDE 183	0	295.4	321.6	13.60	47.89	96.75	156.1	376.8	939.5	1143
BDE 209	0	2858	2868	611	877	1102	1436	3897	7357	11382

unit: ng kg⁻¹ d.m.; sample size n=31; LOD...detection limit



(boxplot of 31 observations)

Figure 3-142: PBDE congener pattern in forest humus.

3.5.3.3 Deposition and air

At Mt. Zugspitze, exceedingly high PBDE (and PCDD/F and PCB) contents appeared to accumulate in the filter cartridge reserved for air masses from NW-Europe during autumn and winter 2006/07. However, a series of instrument failures during this period suggests that also the volume readings underestimated the actual filtered volume by far (60 m³ at an average volume of 1000 m³ for the other filters), resulting in calculation of unusually high air concentrations. Some atmospheric concentration data from Mt. Weissfluhjoch (sectors NE and “undefined” in early summer-late autumn 2006, and from Mt. Sonnblick (sector NW for spring-early summer 06) are missing due to sample loss. For the summary statistics, implausible or missing data mentioned earlier were replaced, per site, with the missing sector’s average of the wholly functional periods.

It is suspected that the elevated PBDE deposition at Sonnblick is due to emissions from the adjacent building and should thus not be considered representative for regional PBDE immissions. For Mt. Zugspitze, there are no data for the first two measurement periods (spring 05-winter 05/06) because cartridges broke during retrieval / processing.

Atmospheric concentrations of several PBDE were markedly higher at Mt. Weissfluhjoch (Switzerland) than on the other two summits (Table 3-19, Figures 3-143- 3-151). In contrast to PBDE atmospheric concentrations, deposition was up to two orders of magnitude higher at the Austrian site Mt. Sonnblick (Table 3-20) - probably due to a local source (see introductory remark).

Table 3-19: Atmospheric PBDE concentration at three alpine summits

	period	BDE 28	BDE 47	BDE 99	BDE 100	BDE 153	BDE 154	Σ 6 BDE	BDE 183	BDE 209
Weissfluh.	I	0.16	5.76	2.50	0.54	1.66	0.28	10.90	9.27	40.73
	II	0.22	4.24	1.87	0.32	0.23	0.25	7.14	1.01	72.68
	III *	0.27	5.10	2.08	0.43	0.00	0.00	7.51	0.00	0.00
	IV	0.13	2.73	1.13	0.22	1.55	0.27	6.04	5.94	13.21
	V	0.28	1.07	0.00	0.00	0.00	0.00	1.34	0.00	0.00
Zugspitze	I	0.17	3.10	1.36	0.27	1.55	0.24	6.68	7.97	27.74
	II	0.23	4.34	1.86	0.33	0.00	0.15	6.91	0.62	36.13
	III	0.12	1.91	0.89	0.21	0.32	0.08	3.53	1.41	0.00
	IV	0.13	2.54	0.91	0.21	0.00	0.06	3.74	0.91	24.11
	V	0.14	0.88	0.40	0.05	0.00	0.02	1.48	0.00	4.87
Sonnblick	I	0.10	2.52	1.51	0.27	0.23	0.11	4.75	0.73	21.78
	II *	0.15	2.65	1.04	0.24	1.38	0.16	5.58	6.74	0.00
	III	0.08	2.09	4.23	0.53	1.05	0.54	8.52	0.35	5.87
	IV	0.07	1.78	0.95	0.17	0.00	0.08	3.05	0.00	23.88
	V	0.08	0.29	0.56	0.12	0.00	0.02	1.06	0.00	8.72

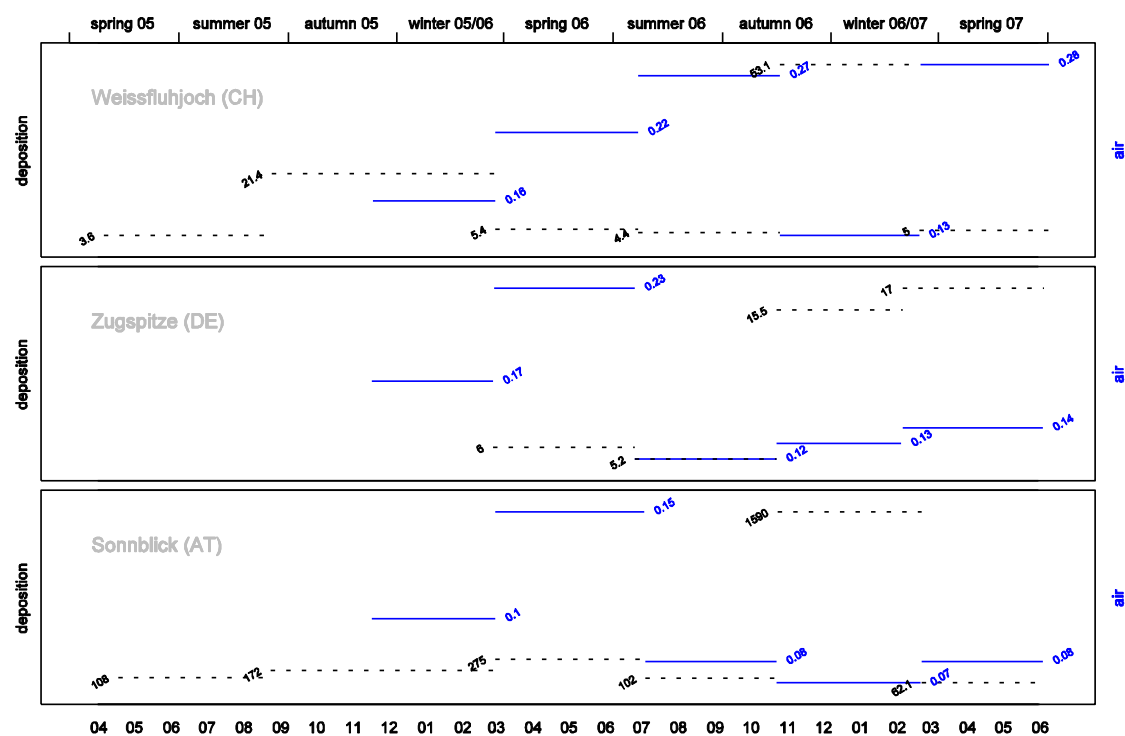
unit: pg m^{-3} at 0 °C and 1013.3 hPa; * interpolated values (see introduction of this section); sampling periods: I...winter 2005/6, II...spring-early summer 2006, III...early summer-late autumn 2006, IV...late aut. 2006-late winter 2007, V...spring 2007

Table 3-20: PBDE deposition at three alpine summits

site	period	BDE 28	BDE 47	BDE 99	BDE 100	BDE 153	BDE 154	Σ 6 BDE	BDE 183	BDE 209
Weissfluhj.	A	3.6	136	78.3	15.7	20.2	10.4	264	48.9	2490
	B	21.4	253	67.1	14.7	7.6	5.7	369	16.4	5620
	C	5.4	153	119	26.8	179	292	775	887	232000
	D	4.4	163	57.7	< 11.9	6.4	5.9	238	16.6	2860
	E	53.1	823	286	54.9	21.9	19.1	1259	21.7	16800
	F	5.0	< 135	80.7	17.9	19.7	11.2	135	40.8	34400
Zugspitze	A *									
	B *									
	C	6.0	175	99.7	22.0	15.3	13.3	331	34.2	11000
	D	5.2	< 135	116	21.5	16.4	14.7	174	45.1	15200
	E	15.5	368	293	58.5	54.1	43.1	832	89.2	102000
	F	17.0	209	137	35.7	41.1	25.0	465	76.7	45100
Sonnblick **	A	108	8870	11500	1640	1010	648	23777	83.8	17500
	B	172	20800	26200	4070	2270	1610	55122	167	75500
	C	275	36900	52100	6350	3950	2520	102095	172	64800
	D	102	12000	15900	2350	1590	1080	33022	113	173000
	E	1590	244000	343000	45300	29500	20600	683990	764	212000
	F	62.1	6250	8330	1420	1030	619	17711	129	201000

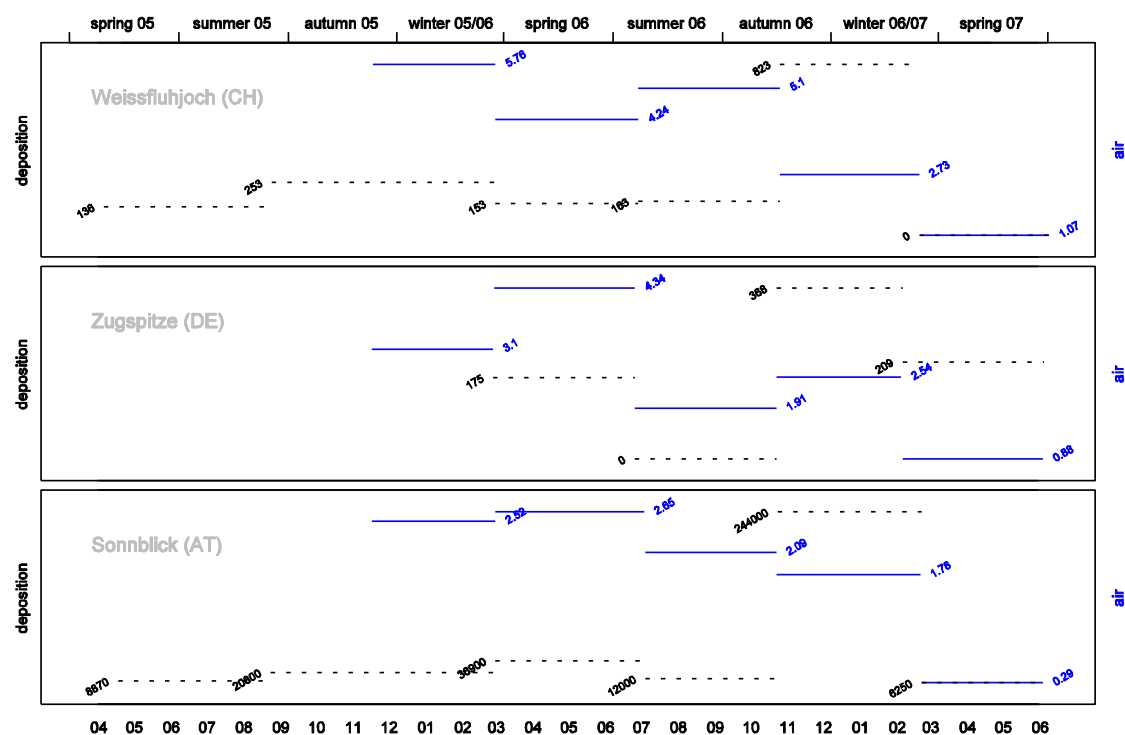
unit: $\text{pg m}^{-2} \text{d}^{-1}$; * missing data (cartridges broken); ** values influenced by local emissions; sampling periods: A...spring-late summer 2005, B...late summer 2005-late winter 2006, C...late winter-summer 2006, D...summer-autumn 2006, E...autumn 2006-late winter 07, F...late winter-spring 2007

The seasonal pattern of lower brominated congeners was similar to that of the BDE 183 and 209 – except the spring 2006 peak values at Weissfluhjoch (Figures 3-143– 3-151).



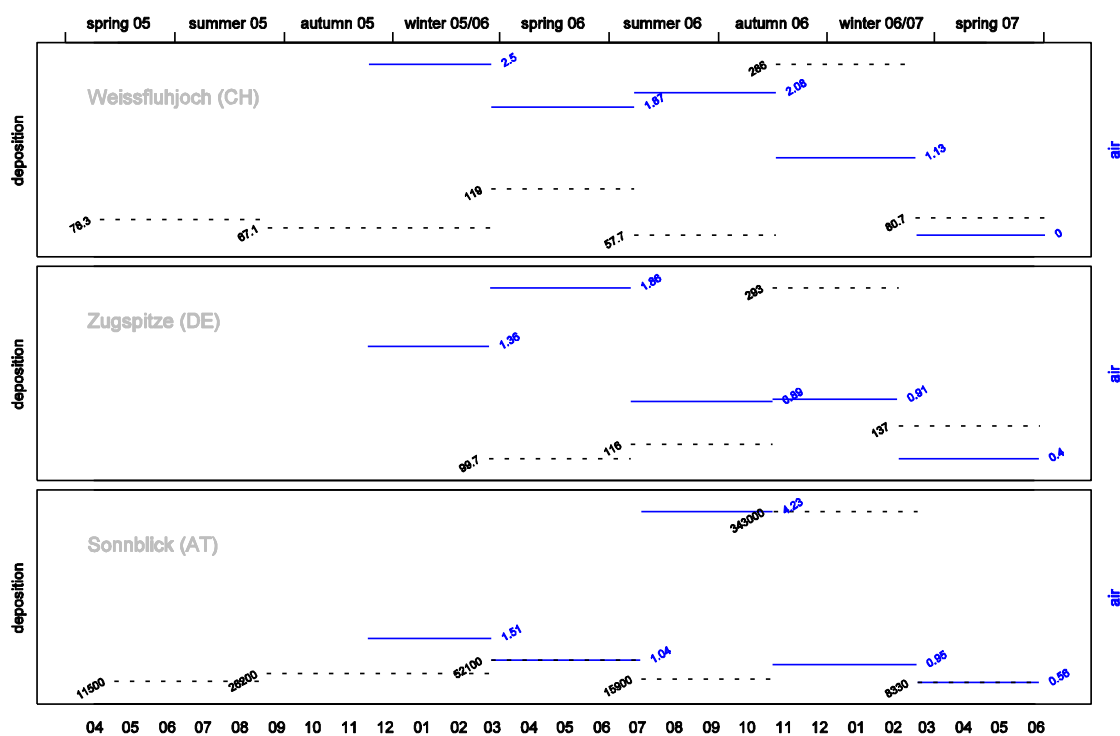
units: deposition: $\text{pg m}^{-2} \text{d}^{-1}$, ambient air: pg m^{-3}

Figure 3-143: Concentration of BDE 28 in deposition and ambient air on three alpine summits



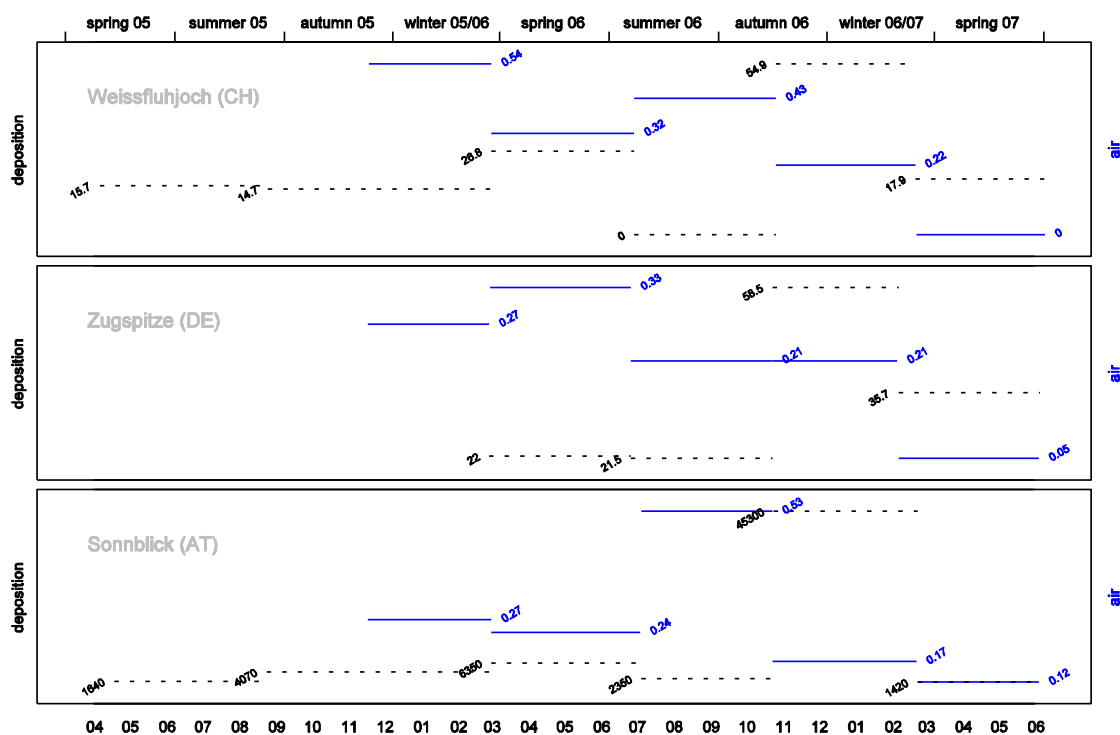
units: deposition: $\text{pg m}^{-2} \text{d}^{-1}$, ambient air: pg m^{-3}

Figure 3-144: Concentration of BDE 47 in deposition and ambient air on three alpine summits



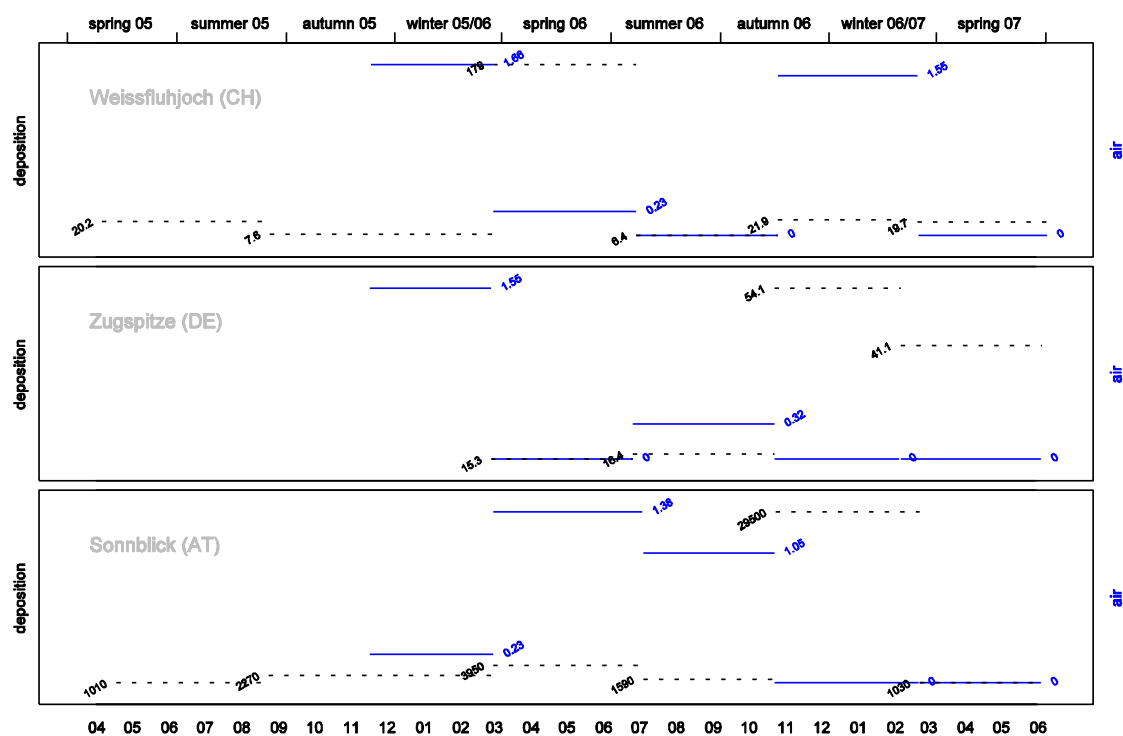
units: deposition: pg m⁻² d⁻¹, ambient air: pg m⁻³

Figure 3-145: Concentration of BDE 99 in deposition and ambient air on three alpine summits



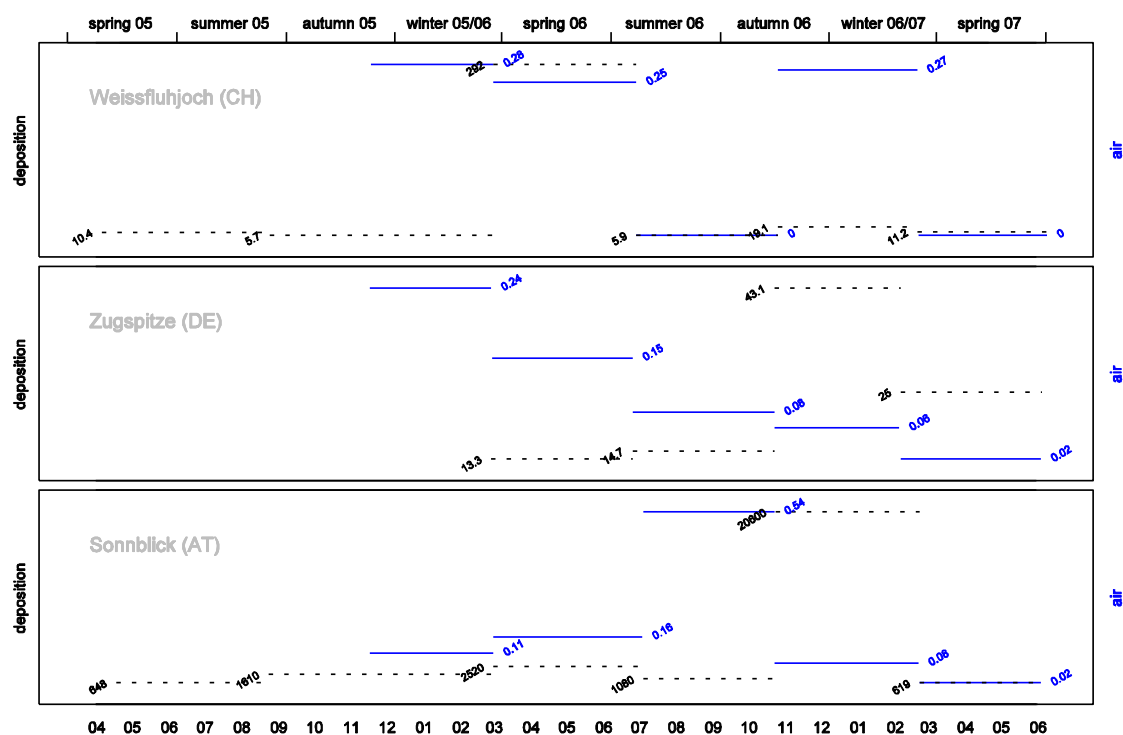
units: deposition: pg m⁻² d⁻¹, ambient air: pg m⁻³

Figure 3-146: Concentration of BDE 100 in deposition and ambient air on three alpine summits



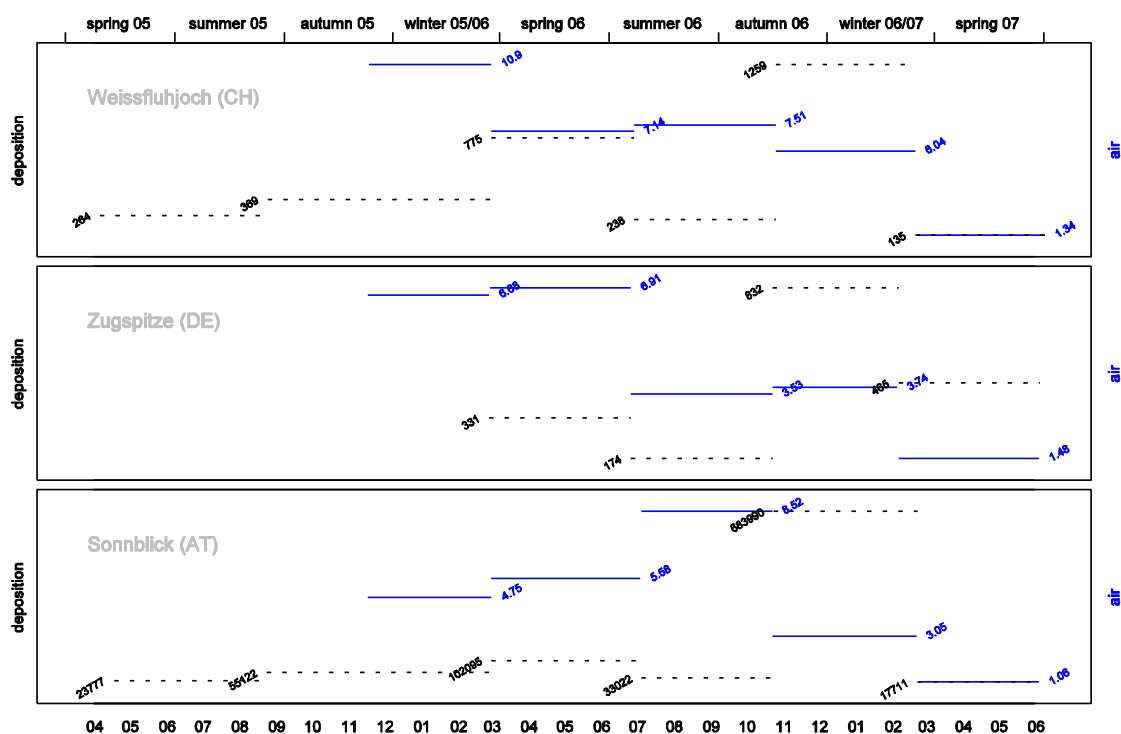
units: deposition: $\text{pg m}^{-2} \text{d}^{-1}$, ambient air: pg m^{-3}

Figure 3-147: Concentration of BDE 153 in deposition and ambient air on three alpine summits



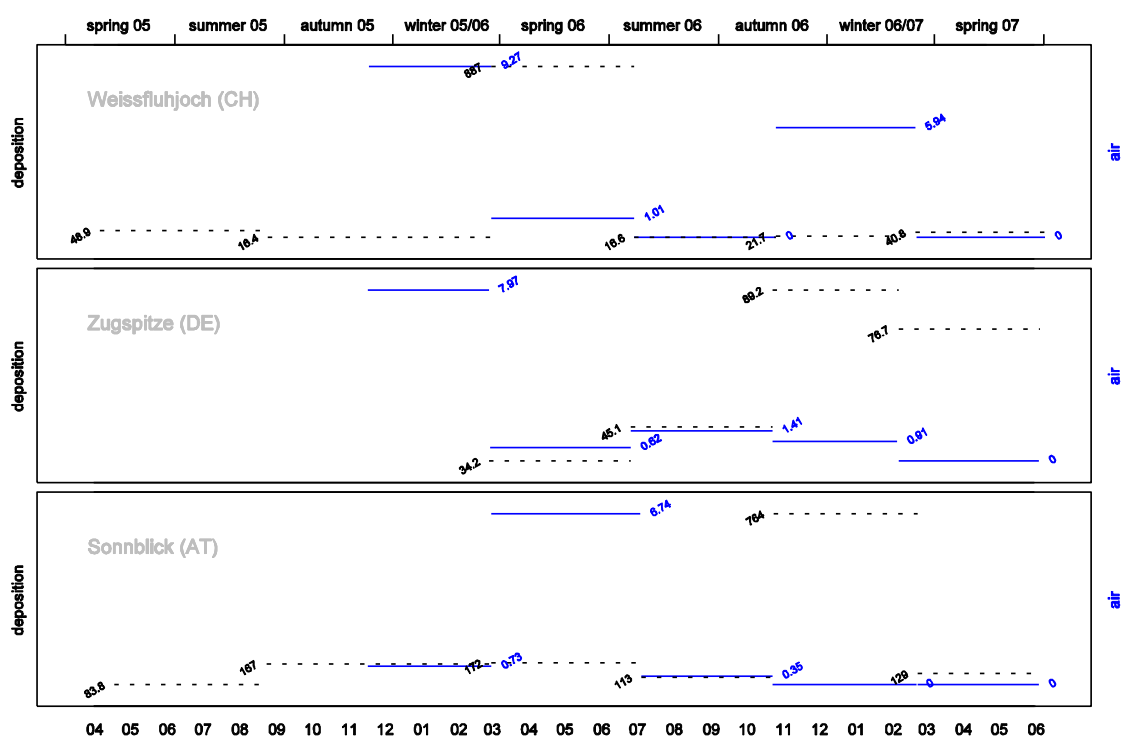
units: deposition: $\text{pg m}^{-2} \text{d}^{-1}$, ambient air: pg m^{-3}

Figure 3-148: Concentration of BDE 154 in deposition and ambient air on three alpine summits



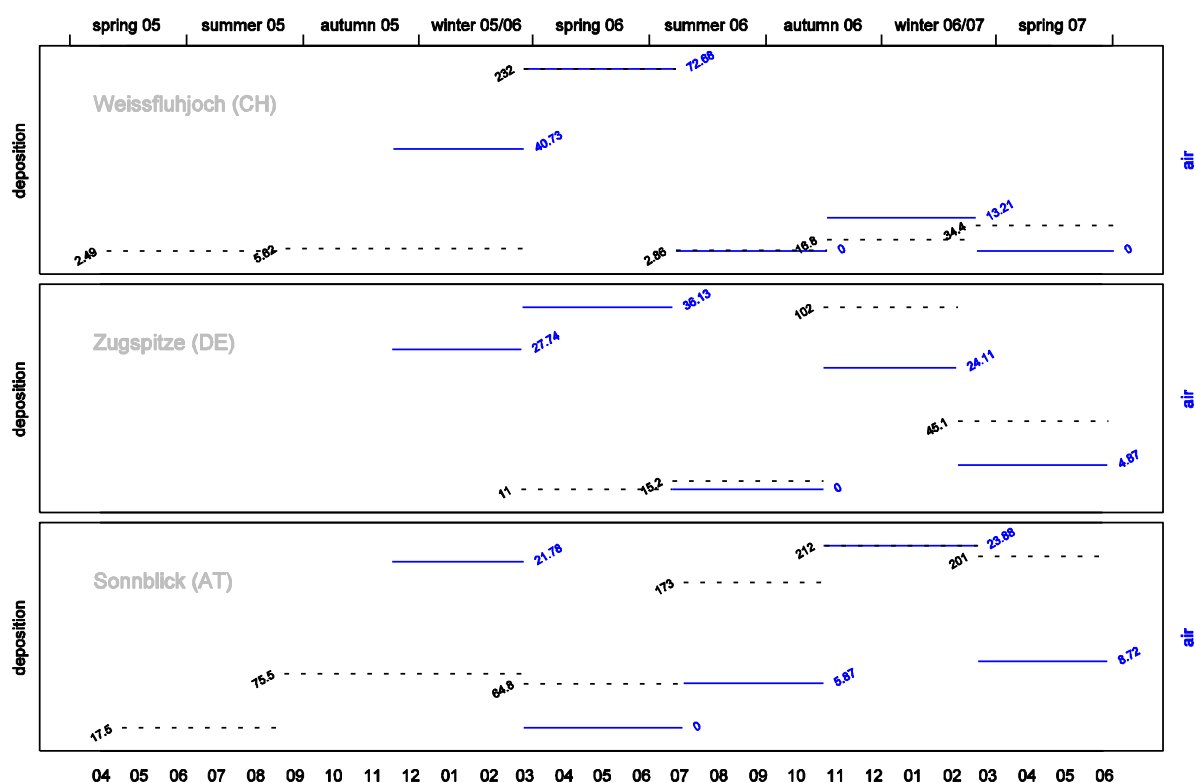
units: deposition: $\text{pg m}^{-2} \text{d}^{-1}$, ambient air: pg m^{-3}

Figure 3-149: Total concentration of 6 BDE in deposition and ambient air on three alpine summits



units: deposition: $\text{pg m}^{-2} \text{d}^{-1}$, ambient air: pg m^{-3}

Figure 3-150: Concentration of BDE 183 in deposition and ambient air on three alpine summits



units: deposition: $\text{ng m}^{-2} \text{d}^{-1}$, ambient air: pg m^{-3}

Figure 3-151: Concentration of BDE 209 in deposition and ambient air on three alpine summits

3.5.4 Spatial variation

3.5.4.1 needles

Needle samples were analysed starting from the west. After most PBDE congeners had been detected in only few samples, analysis was discontinued. Spatial analysis is therefore confined to the western part of the study region. Figure 3-152 shows the distribution of the BDE 28 which was found in most of the samples, and Figure 3-153 depicts $\sum 6 \text{ BDE}$. One Italian and one Swiss plot had BDE concentrations (of all analysed congeners) much higher than the rest of the sample.

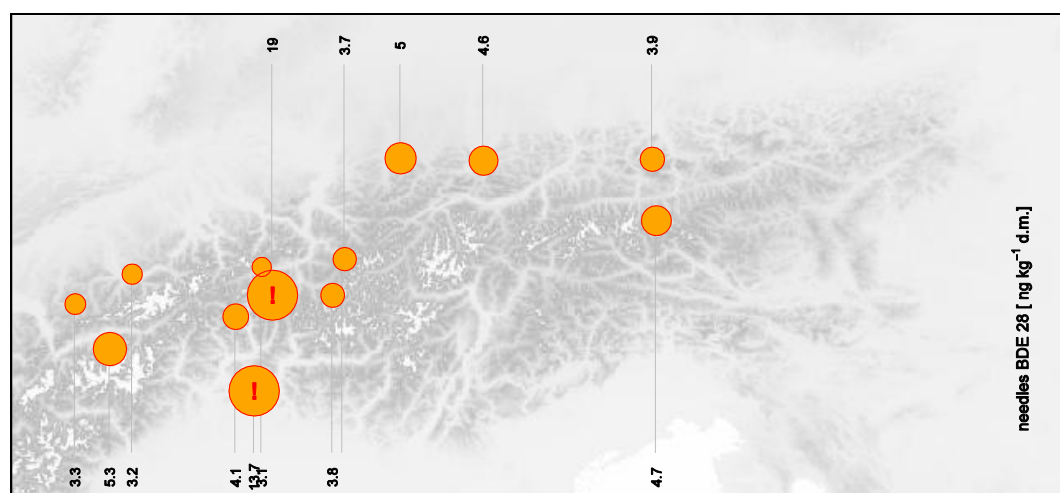


Figure 3-152: Spatial distribution of BDE 28 in a subsample of 0.5 year old Norway spruce needles

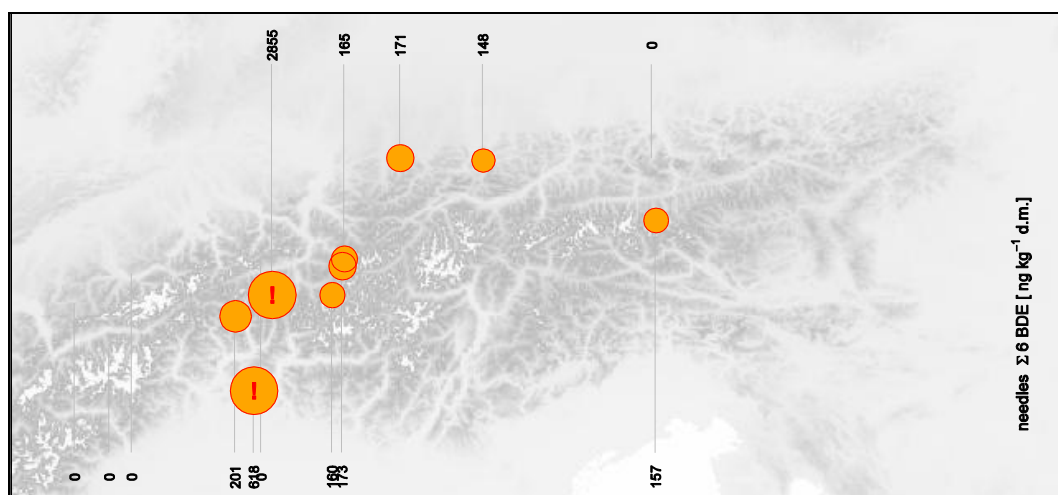


Figure 3-153: Spatial distribution of $\Sigma 6$ BDE in a subsample of 0.5 year old Norway spruce needles

Longitudinal differences

Longitudinal differences were not examined, because all analysed samples except three belonged to the western site group.

Latitudinal differences

Among the analysed samples were only two from the southern site group. Comparison of the northern and central site group did not show any significant latitude related differences (Mann-Whitney test; $n = 5$ and 7 , resp.).

3.5.4.2 Humus, mineral soil

The higher brominated congeners BDE 209, especially BDE 183, and also BDE 153 (but *not* BDE 154) showed a conspicuous cluster of high concentrations in the northeast (Figure 3-156, Figure 3-157). This geographic pattern is unique among the various compounds described in this report.

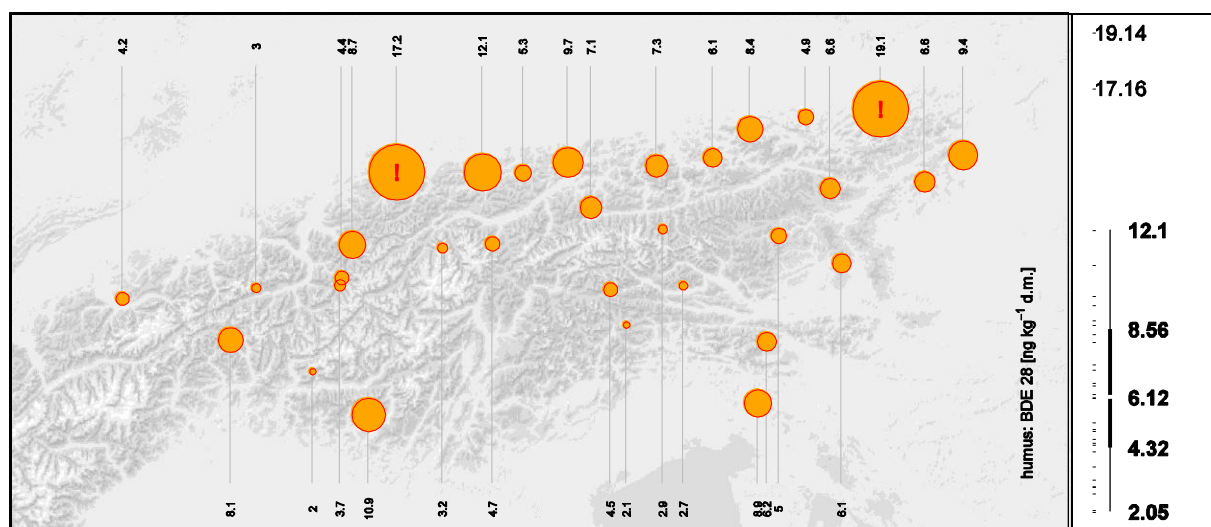


Figure 3-154: Spatial distribution of BDE 28 in forest humus

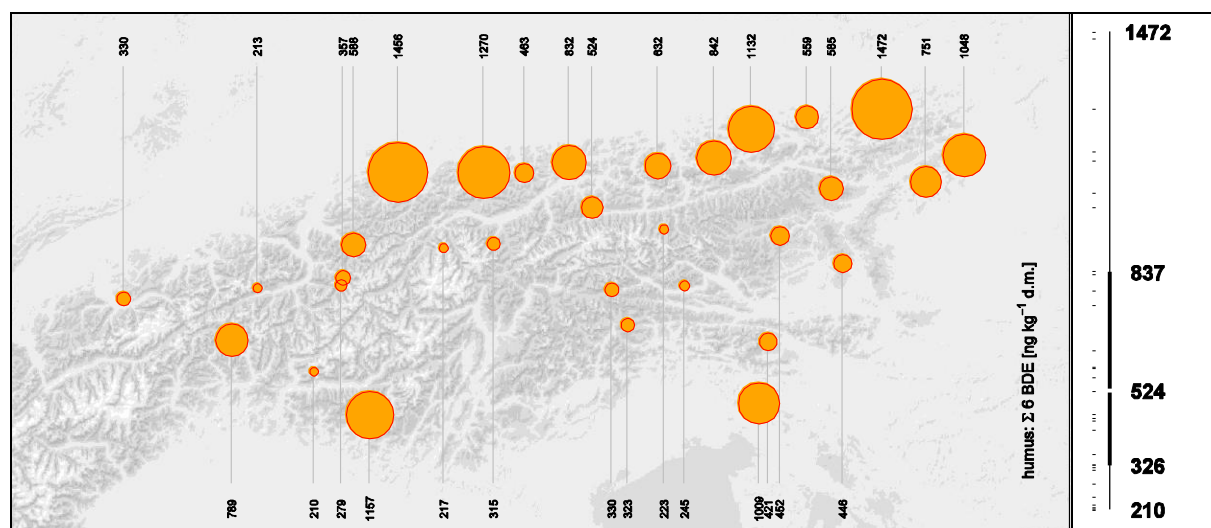


Figure 3-155: Spatial distribution of Σ 6 BDE in forest humus

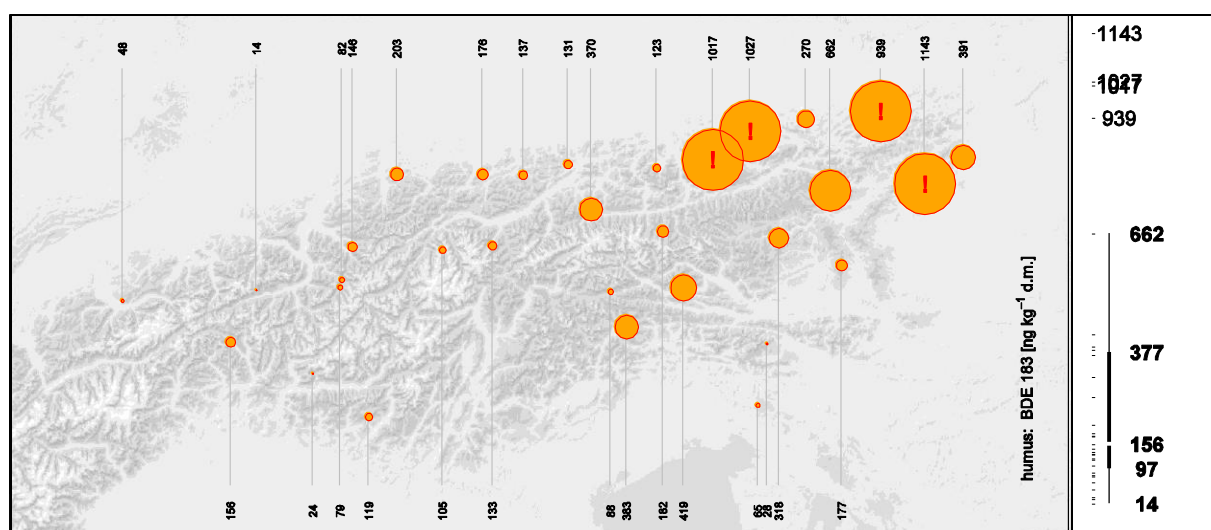


Figure 3-156: Spatial distribution of BDE 183 in forest humus

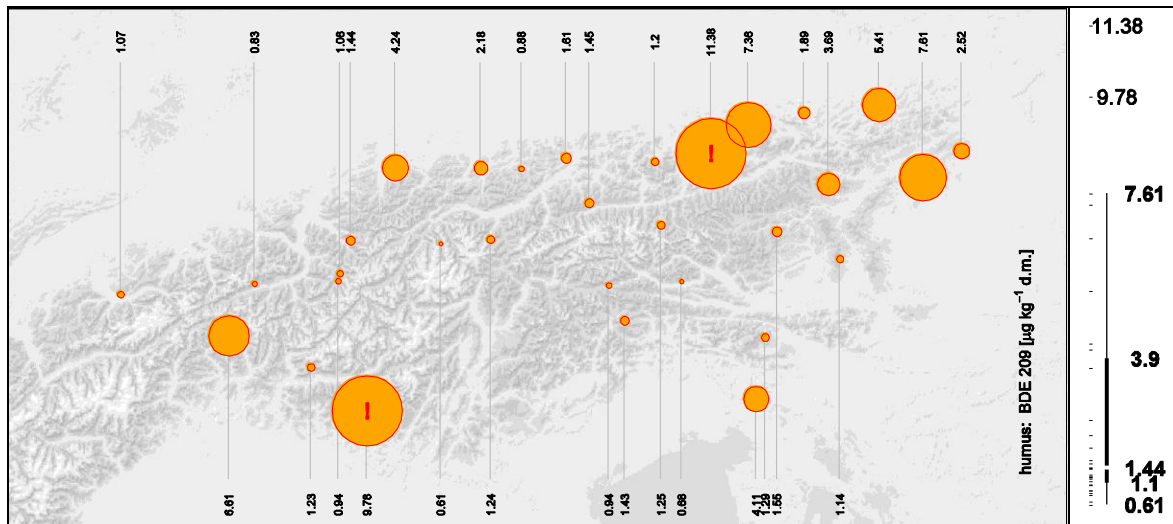


Figure 3-157: Spatial distribution of BDE 209 in forest humus (note the high concentrations in the $\mu\text{g kg}^{-1}$ range)

Longitudinal differences

The BDE congeners 153, 183, 209 showed significant (Kruskal-Wallis, $\alpha \leq 0.05$) differences among longitudinal site groups. Differences were almost significant ($\alpha = 0.051$) for BDE no. 154.

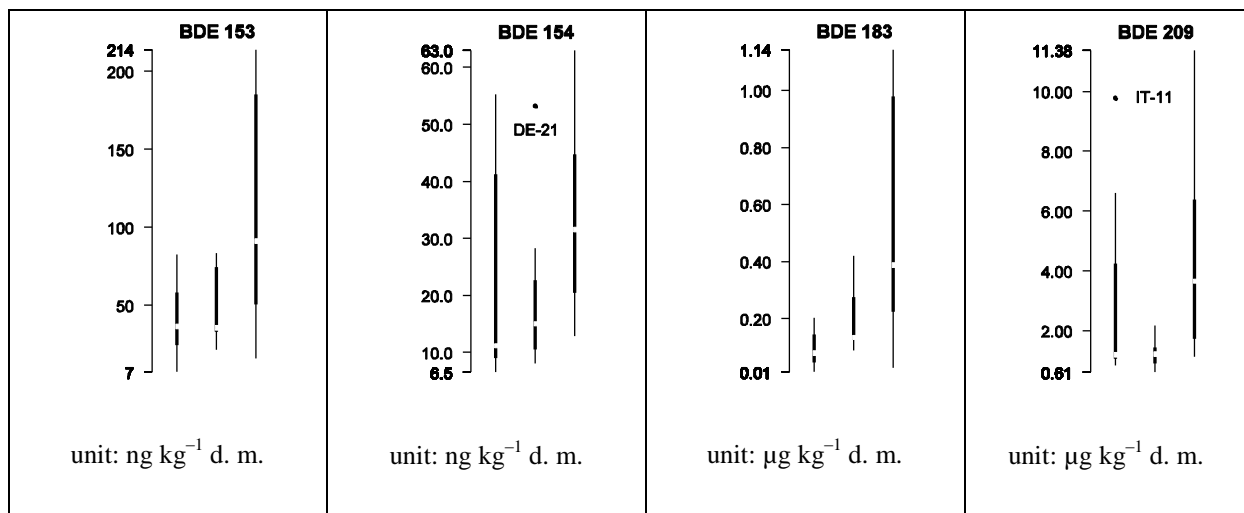
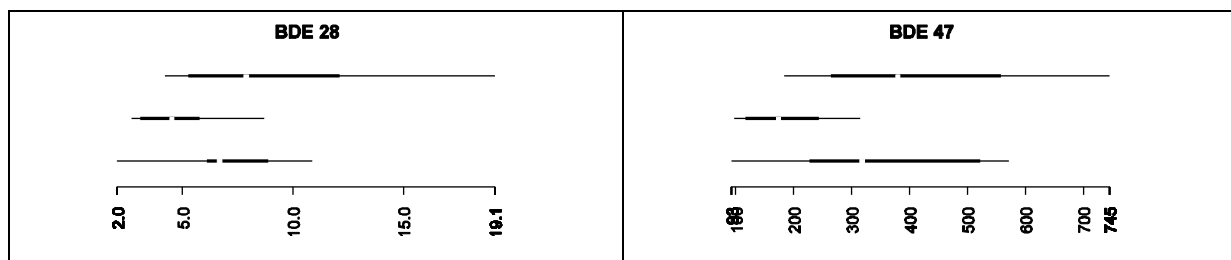


Figure 3-158: Longitudinal pollution trends of PBDE in forest humus.

Latitudinal differences

With the exception of BDE 153 and BDE 183, all analysed PBDE as well as $\Sigma 6$ BDE showed significant differences (Kruskal-Wallis, $\alpha \leq 0.05$) between latitudinal site groups. For the BDE 47, 99, 100, 154 and $\Sigma 6$ BDE, differences were highly significant ($\alpha \leq 0.01$). Median PBDE concentrations were highest in the north and lowest in the center of the study region (exception: BDE 209 with the highest median in the south).



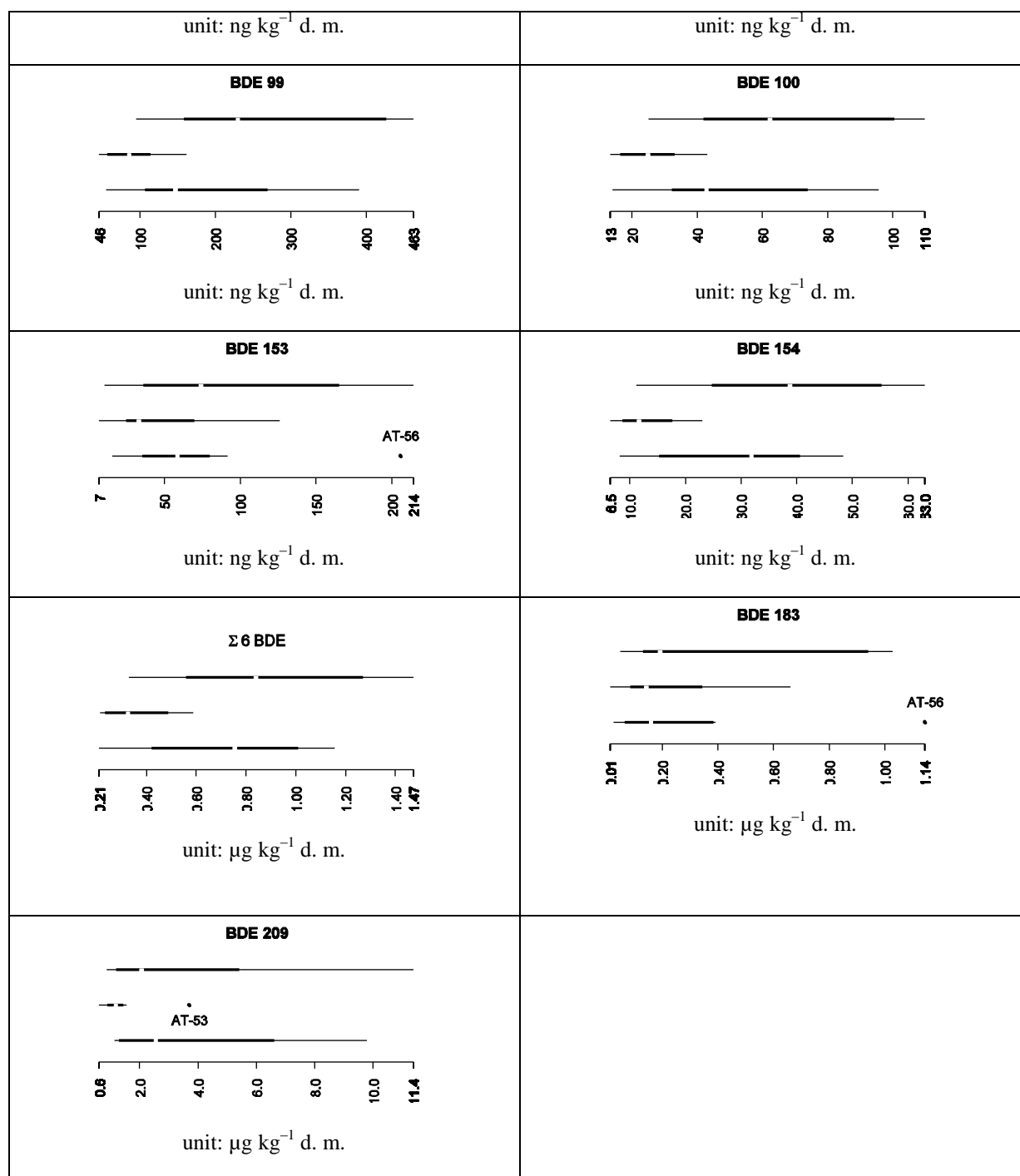


Figure 3-159: Latitudinal pollution trends of PBDE in forest humus

3.5.4.3 Air

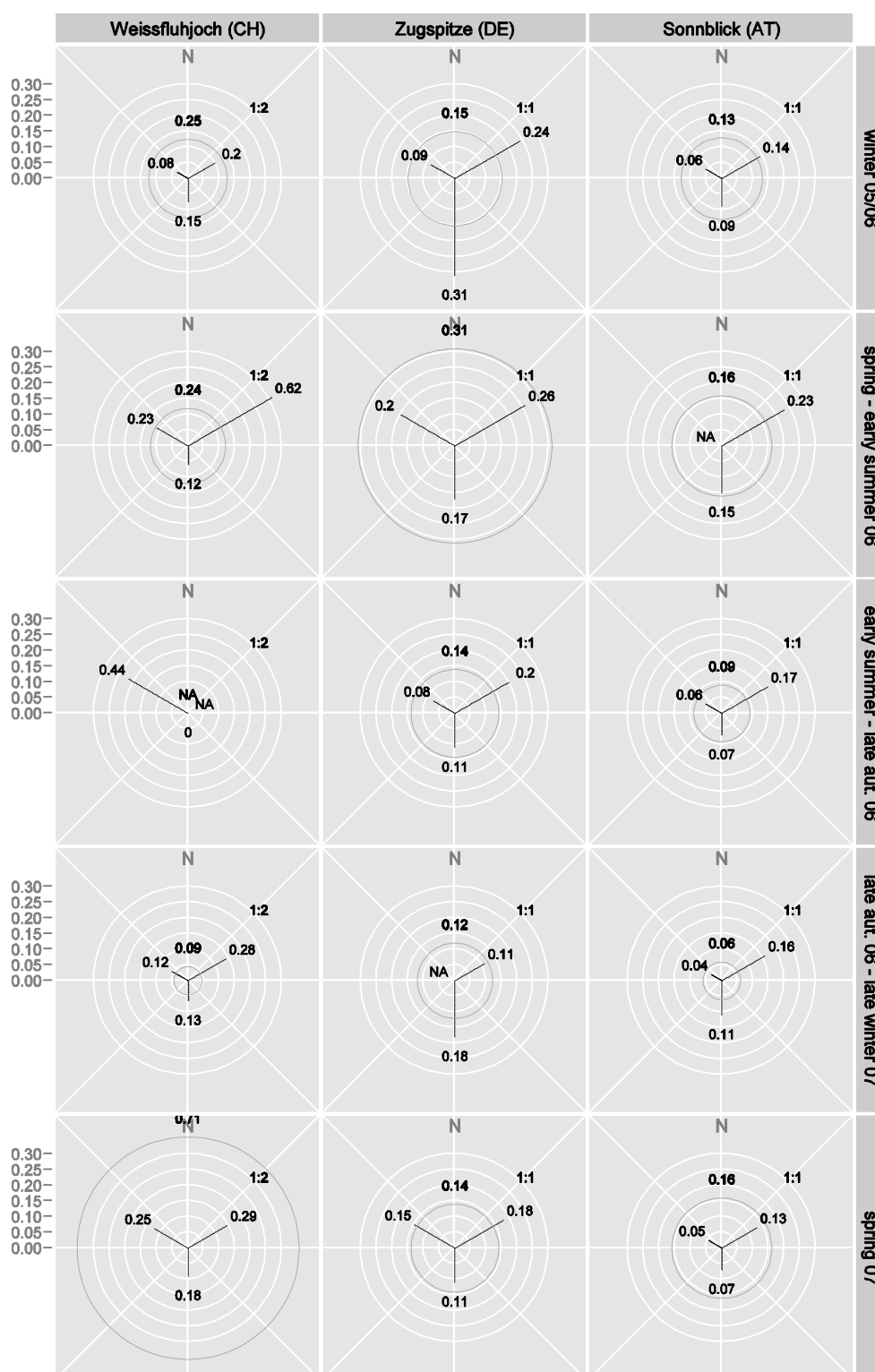
As explained in 3.5.4.3 (p.148), there were implausibly high PBDE concentrations in air from NW-Europe arriving at Mt. Zugspitze during autumn and winter 2006/07. These are probably artefacts (due to inaccurate volume readings of the device) and have thus been omitted in the following plots.

Some data from Mt. Weissfluhjoch (sectors NE and “undefined” in early summer–late autumn 2006, and from Mt. Sonnblick (sector NW for spring–early summer 06), are missing due to sample loss. These are indicated with “NA” in the plots below.

PBDE measurements on the three mountain peaks showed a prevailing source region, regardless of measuring site or period: the highest air concentrations were usually found in air arriving from the northeast. This

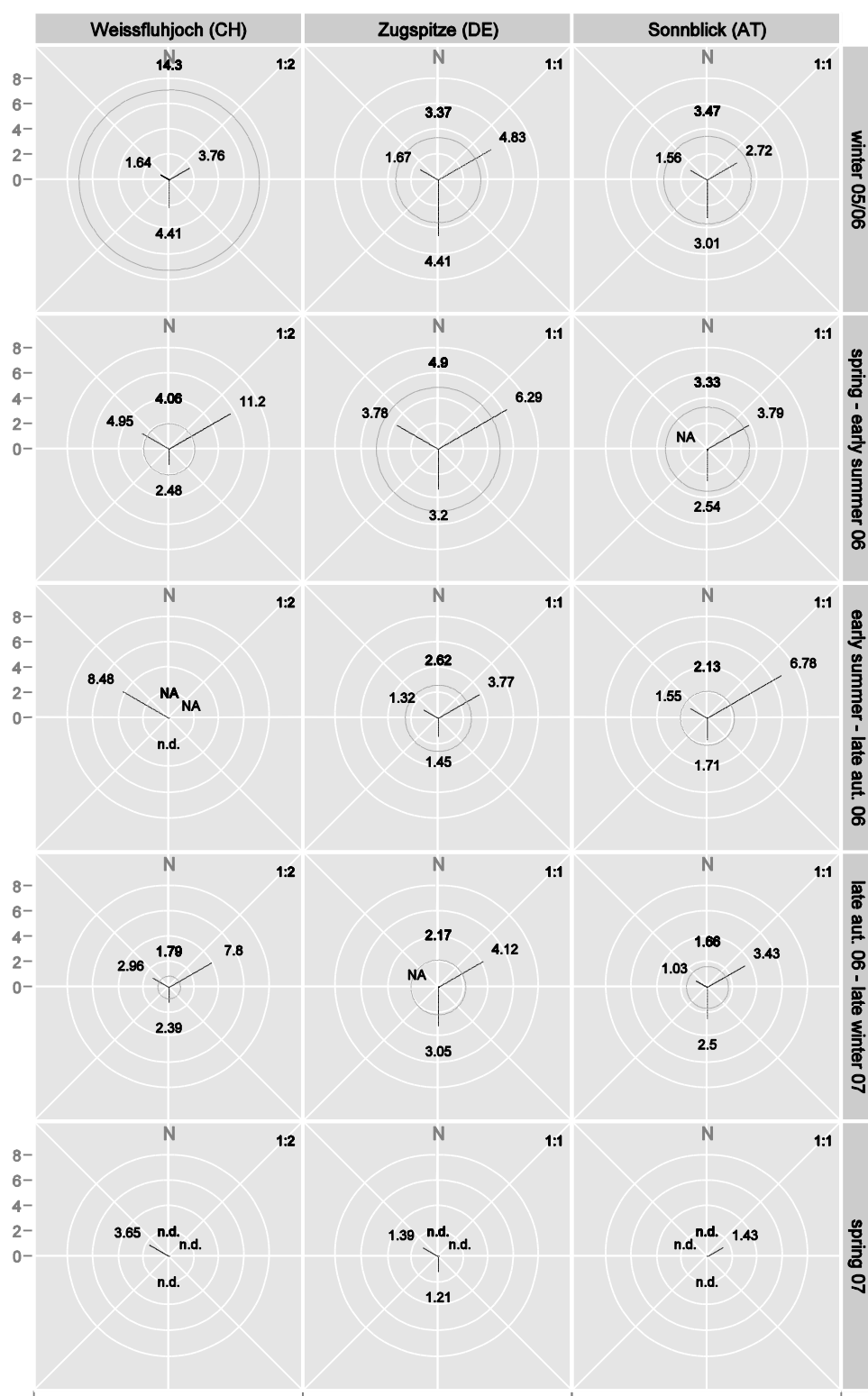
corresponds to the finding that the highest PBDE concentrations in humus occurred in the eastern site group of the study area.

Although there were marked differences between the sampling periods, the existing time series is too short to conclude about immission seasonality. However, the association between air concentrations and deposition rates is noteworthy (compare, e. g. the generally low air concentrations and deposition rates of $\Sigma 6$ BDE in spring 2007: Figure 3-149 on p. 143).



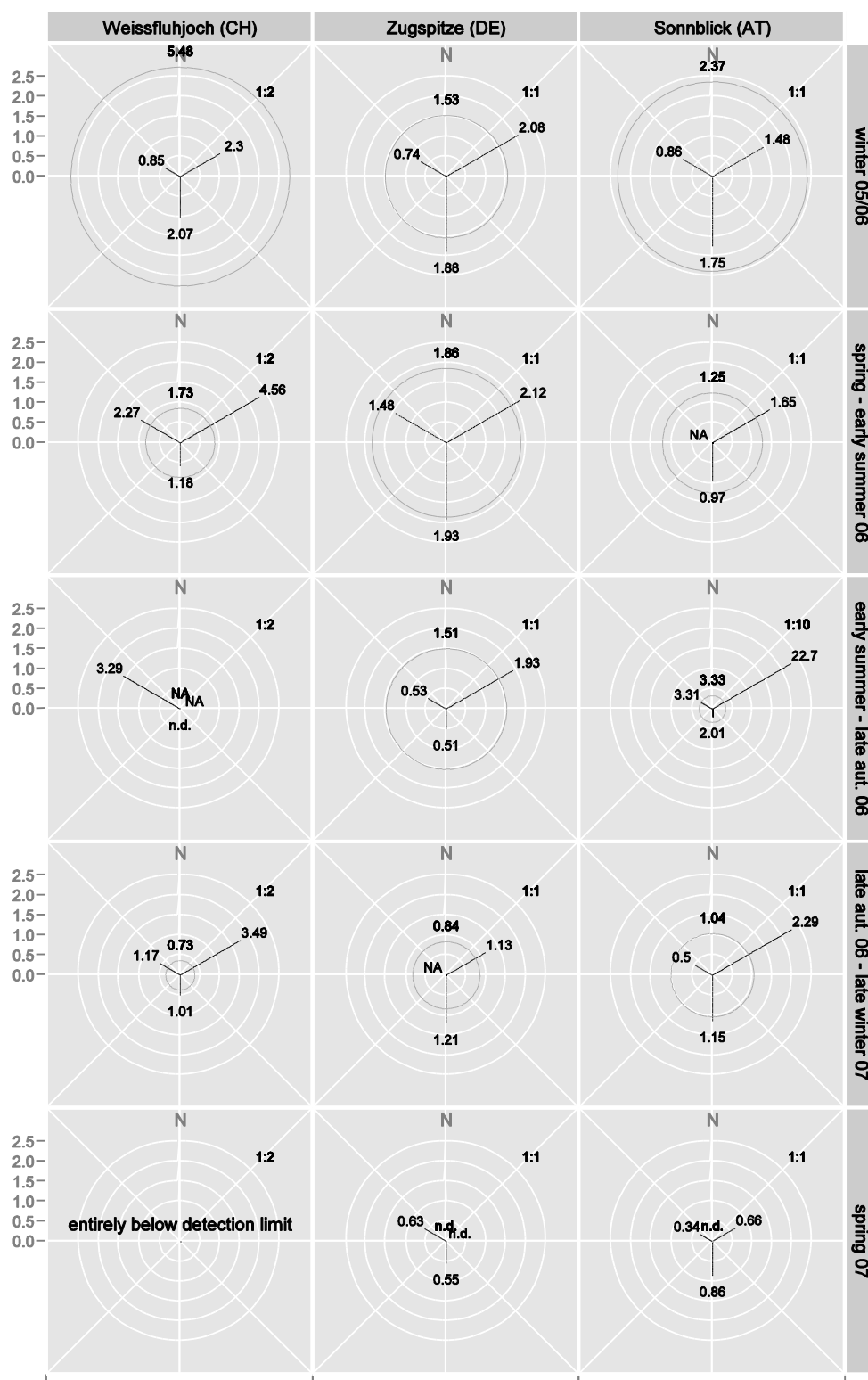
Note reduced scale ($f=.5$) for values from Mt. Weissfluhjoch

Figure 3-160: Concentration [pg m^{-3}] of BDE 28 in air from NW, NE and S (circle: trajectory not attributable to a particular sector)



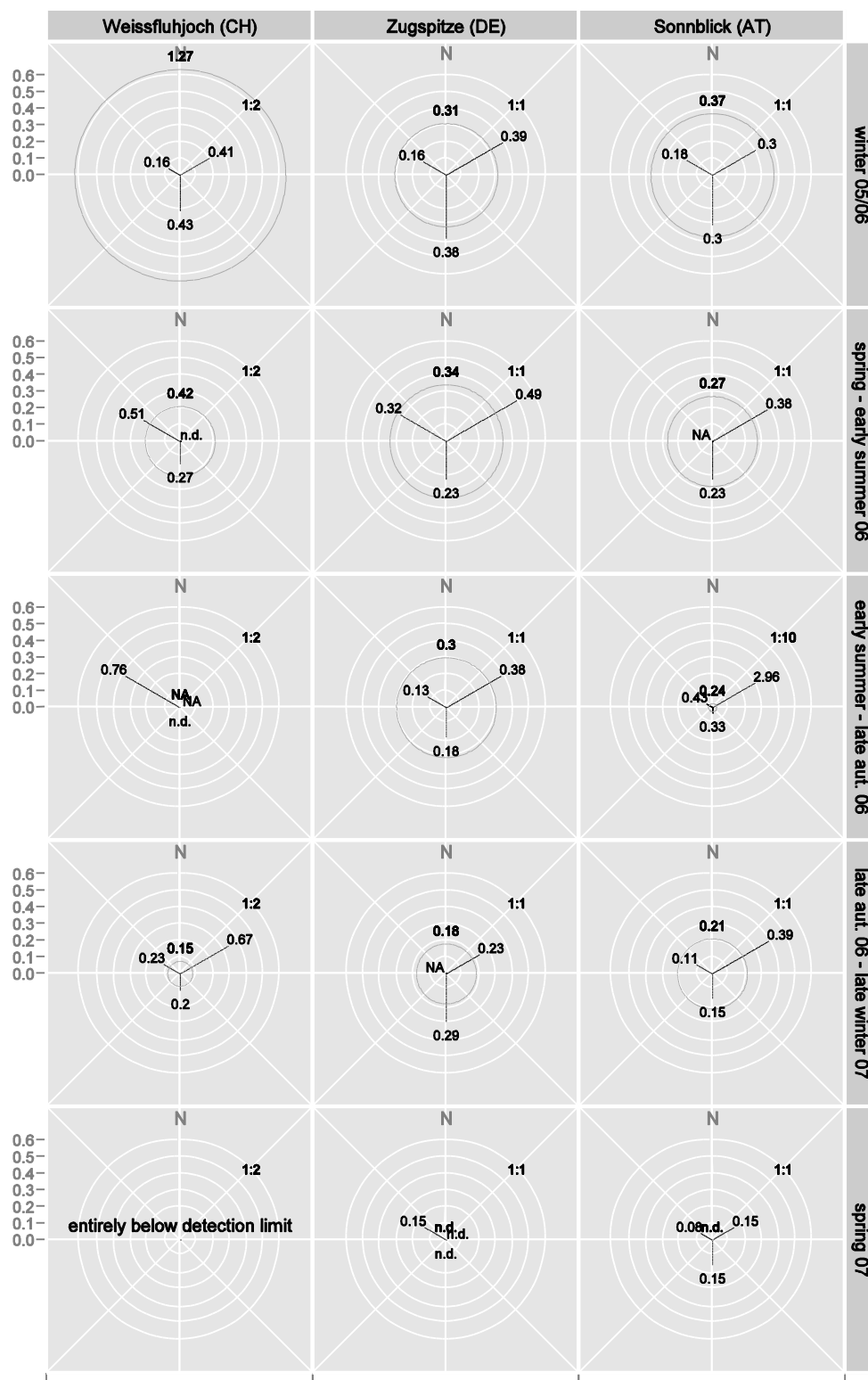
Note reduced scale ($f=.5$) for values from Mt. Weissfluhjoch.

Figure 3-161: Concentration [pg m^{-3}] of BDE 47 in air from NW, NE and S (circle: trajectory not attributable to a particular sector)



Note reduced scales for values from Mt. Weissfluhjoch ($f=.5$) and early summer–late autumn 2006 values from Mt. Sonnblick ($f=.1$).

Figure 3-162: Concentration [pg m^{-3}] of BDE 99 in air from NW, NE and S (circle: trajectory not attributable to a particular sector)



Note reduced scales for values from Mt. Weissfluhjoch ($f=.5$) and early summer–late autumn 2006 values from Mt. Sonnblick ($f=.1$).

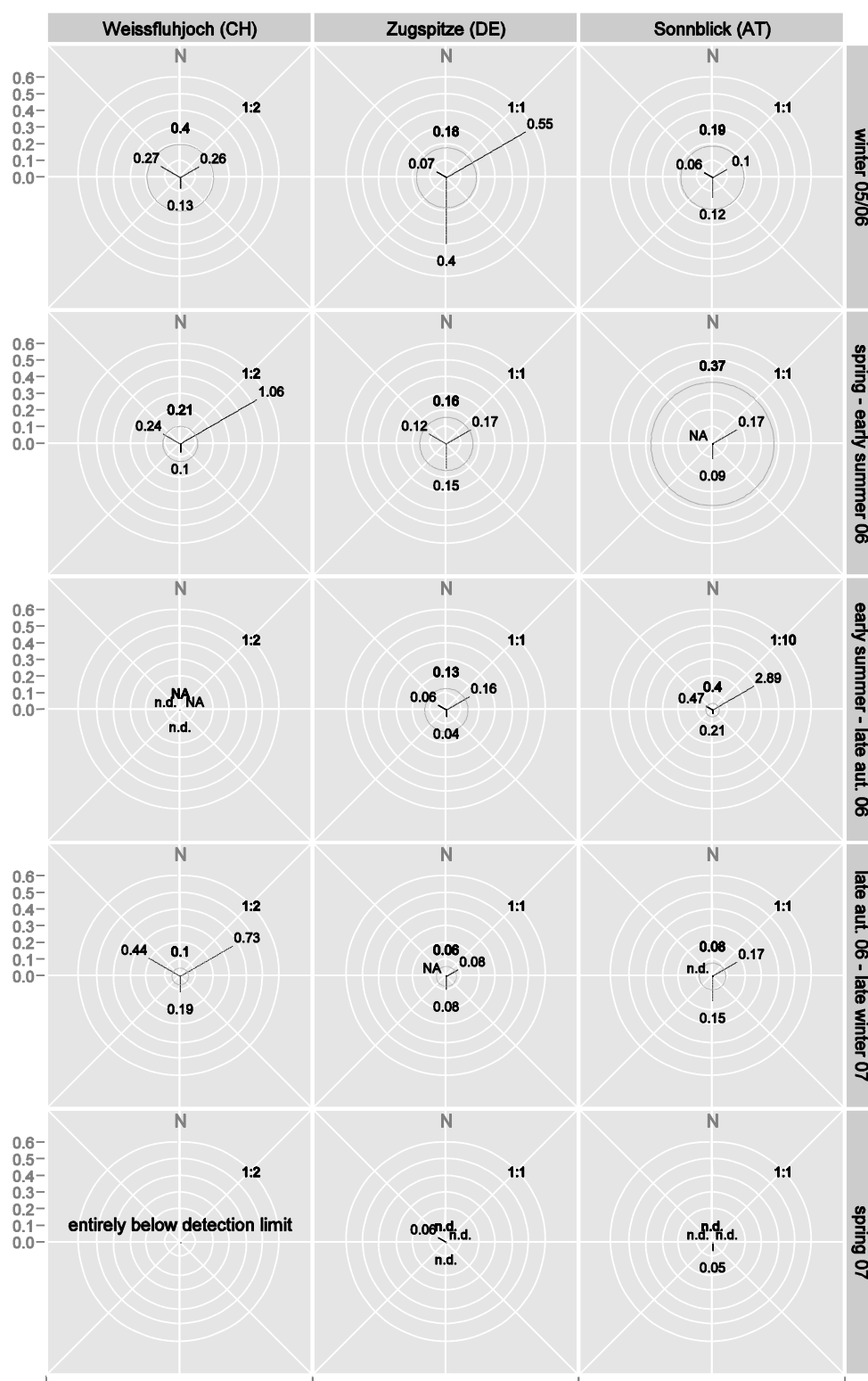
Figure 3-163: Concentration [pg m^{-3}] of BDE 100 in air from NW, NE and S (circle: trajectory not attributable to a particular sector)

Concentrations of BDE 153 frequently remained below the detection limit, so there are too few complete (per site and period) observations for a meaningful chart. Instead, values are therefore given in Table 3-21 below.

Table 3-21: Atmospheric concentrations of BDE 153

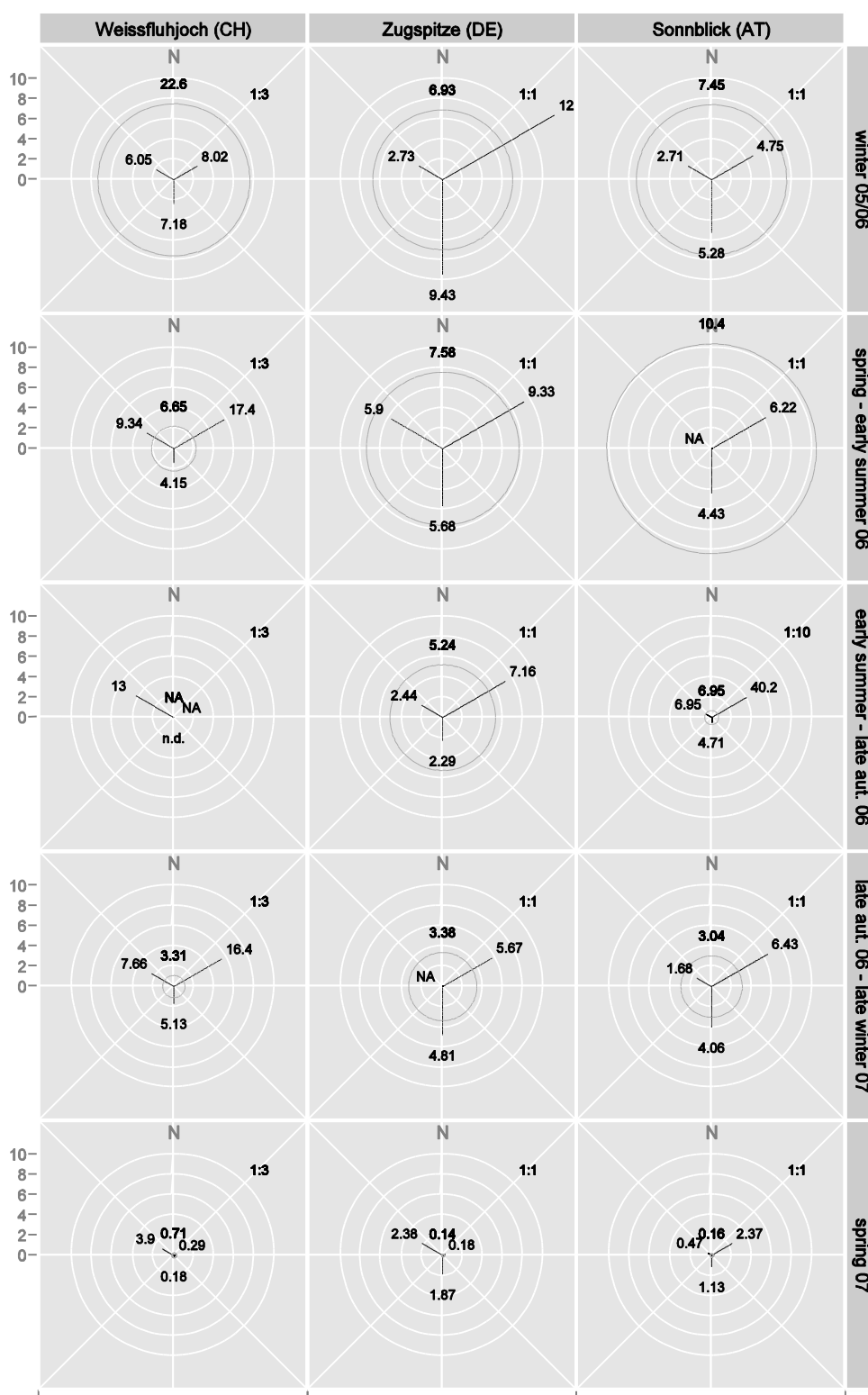
period	sector	Weissfluhjoch (CH)	Zugspitze (DE)	Sonnblick (AT)
I	NW	3.04	< LOD	< LOD
	NE	1.09	4.67	< LOD
	S	< LOD	2.05	< LOD
	undef.	0.91	1.39	0.91
II	NW	1.15	< LOD	n. a.
	NE	< LOD	< LOD	< LOD
	S	< LOD	< LOD	0.44
	undef.	< LOD	< LOD	4.98
III	NW	< LOD	0.32	1.13
	NE	n. a.	0.72	4.74
	S	< LOD	< LOD	0.38
	undef.	n. a.	0.55	0.76
IV	NW	2.74	n. a.	< LOD
	NE	3.41	< LOD	< LOD
	S	1.21	< LOD	< LOD
	undef.	0.45	< LOD	< LOD
V	NW	< LOD	< LOD	< LOD
	NE	< LOD	< LOD	< LOD
	S	< LOD	< LOD	< LOD
	undef.	< LOD	< LOD	< LOD

unit: pg m^{-3} ; n. a....data not available (cartridge loss); LOD...detection limit; sampling periods: I...winter 2005/6, II...spring–early summer 2006, III...early summer–late autumn 2006, IV...late aut. 2006–late winter 2007, V...spring 2007



Note reduced scales for values from Mt. Weissfluhjoch ($f=.5$) and early summer–late autumn 2006 values from Mt. Sonnblick ($f=.1$).

Figure 3-164: Concentration [pg m^{-3}] of BDE 154 in air from NW, NE and S (circle: trajectory not attributable to a particular sector)



Note reduced scales for values from Mt. Weissfluhjoch ($f=1/3$) and early summer–late autumn 2006 values from Mt. Sonnblick ($f=.1$).

Figure 3-165: Concentration [pg m^{-3}] of $\Sigma 6$ BDE in air from NW, NE and S (circle: trajectory not attributable to a particular sector)

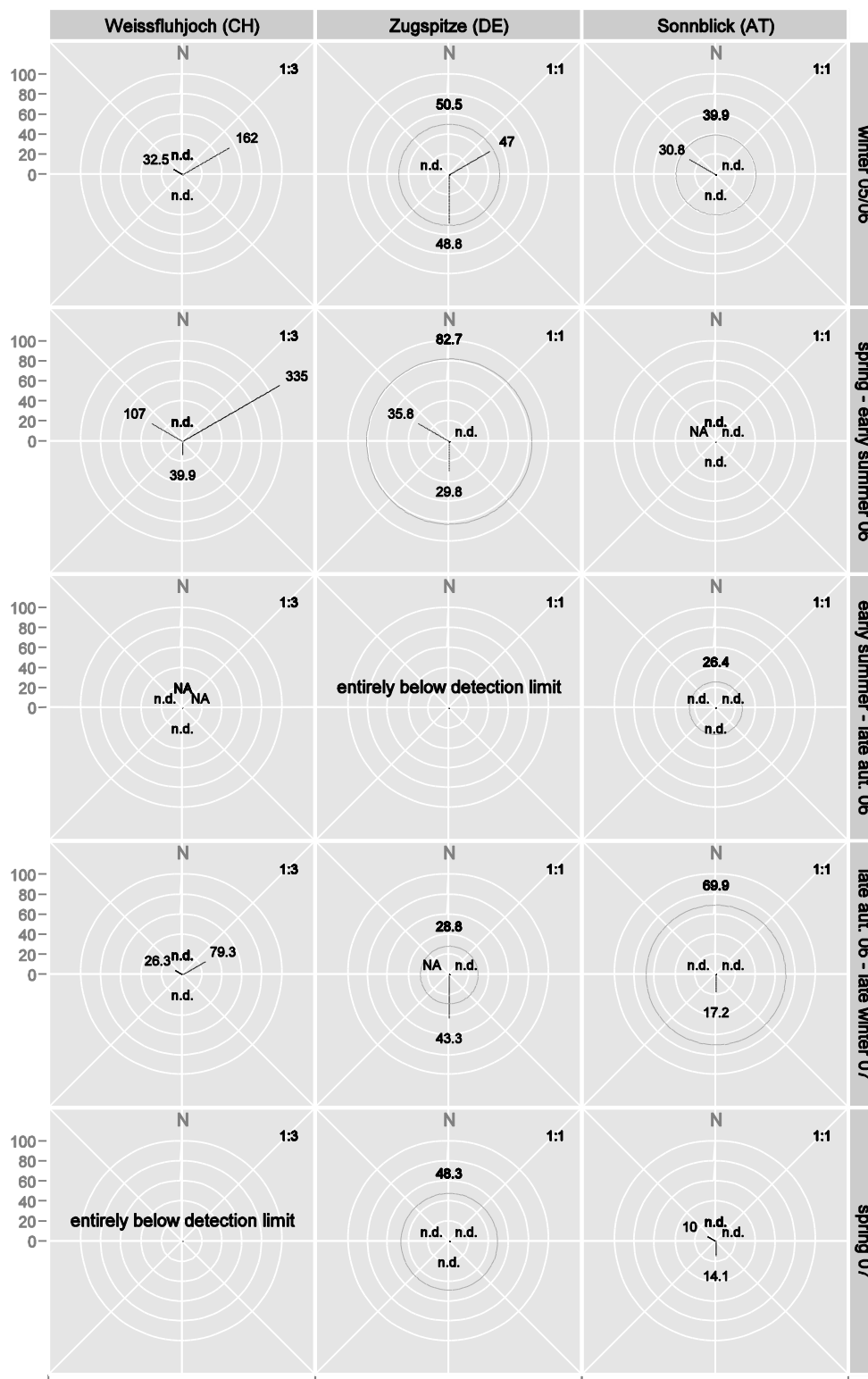
Similar to BDE 153, BDE 183 concentrations remained below the detection limit in numerous cases. Moreover, there were drastic concentration differences between sites and sampling periods. The values are tabulated below.

Table 3-22: Atmospheric concentrations of BDE 183

period	sector	Weissfluhjoch (CH)	Zugspitze (DE)	Sonnblick (AT)
I	NW	19.0	1.26	< LOD
	NE	4.59	24.8	< LOD
	S	< LOD	8.66	< LOD
	undef.	2.93	5.38	2.87
II	NW	4.95	< LOD	n. a.
	NE	< LOD	< LOD	< LOD
	S	< LOD	< LOD	1.67
	undef.	< LOD	2.86	21.7
III	NW	< LOD	1.83	0.89
	NE	n. a.	2.49	< LOD
	S	< LOD	< LOD	< LOD
	undef.	n. a.	1.99	< LOD
IV	NW	10.4	n. a.	< LOD
	NE	11.9	1.17	< LOD
	S	4.77	1.81	< LOD
	undef.	1.89	0.73	< LOD
V	NW	< LOD	< LOD	< LOD
	NE	< LOD	< LOD	< LOD
	S	< LOD	< LOD	< LOD
	undef.	< LOD	< LOD	< LOD

unit: pg m^{-3} ; n. a....data not available (cartridge loss); sampling periods: I...winter 2005/6, II...spring–early summer 2006, III...early summer–late autumn 2006, IV...late aut. 2006–late winter 2007, V...spring 2007

Atmospheric concentrations of BDE 209, the heaviest among the analysed BDE, were below the detection limit in many cases.



Note the reduced scale ($f=1/3$) for values from Mt. Weissfluhjoch.

Figure 3-166: Concentration [pg m^{-3}] of BDE 209 in air from NW, NE and S (circle: trajectory not attributable to a particular sector).

3.5.5 Altitudinal variation

3.5.5.1 Needles

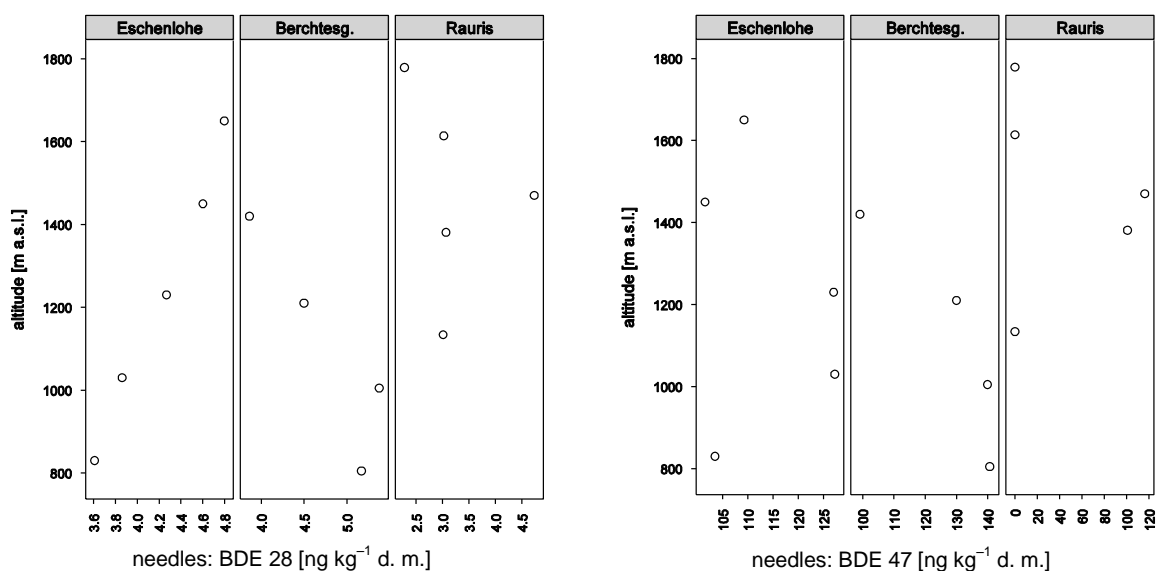


Figure 3-167: Altitudinal variation of the total concentration of BDE 28 (left) and BDE 47 (right) in 0.5 year old Norway spruce needles.

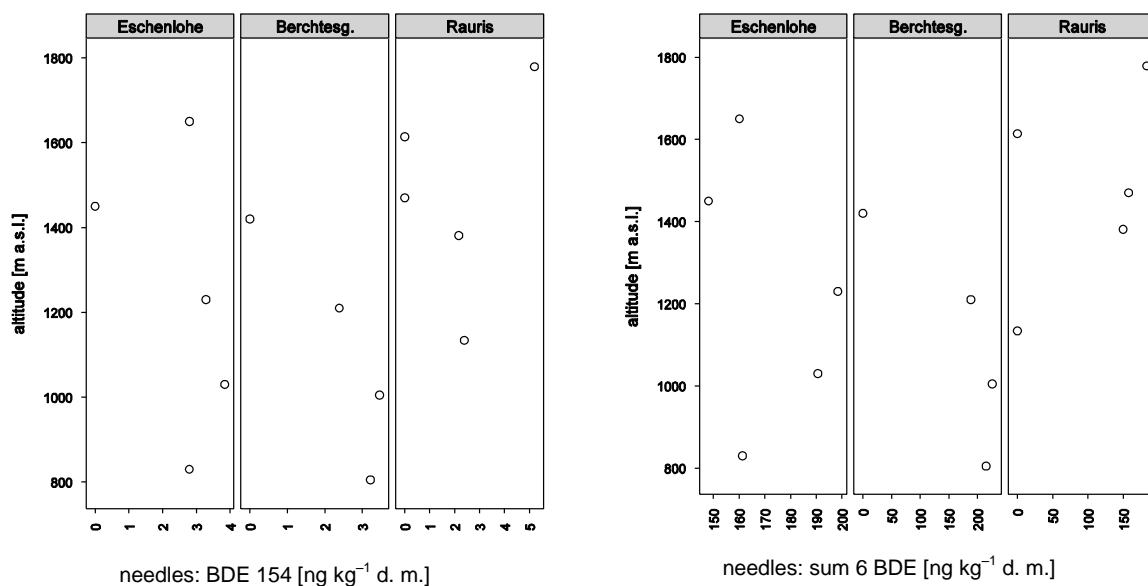
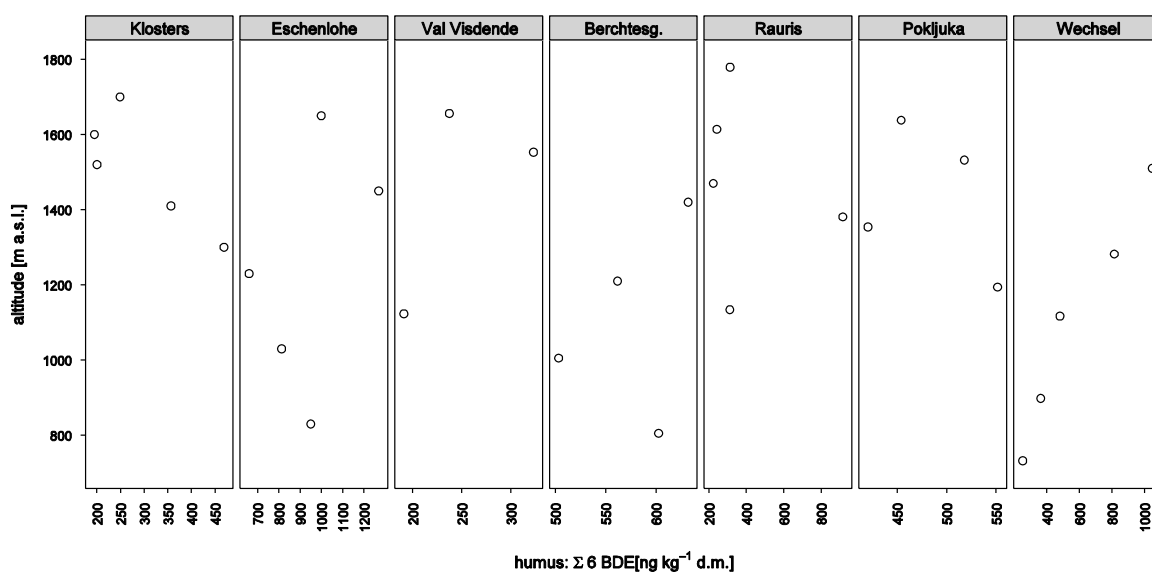


Figure 3-168: Altitudinal variation of the concentration of BDE 154 (left) and Σ 6 BDE (right) in 0.5 year old Norway spruce needles.

3.5.5.2 Humus



The high value at the second plot of the Austrian height profile Rauris is caused by the BDE 153 and 154.

Figure 3-169: Altitudinal variation of $\sum 6$ BDE in forest humus.

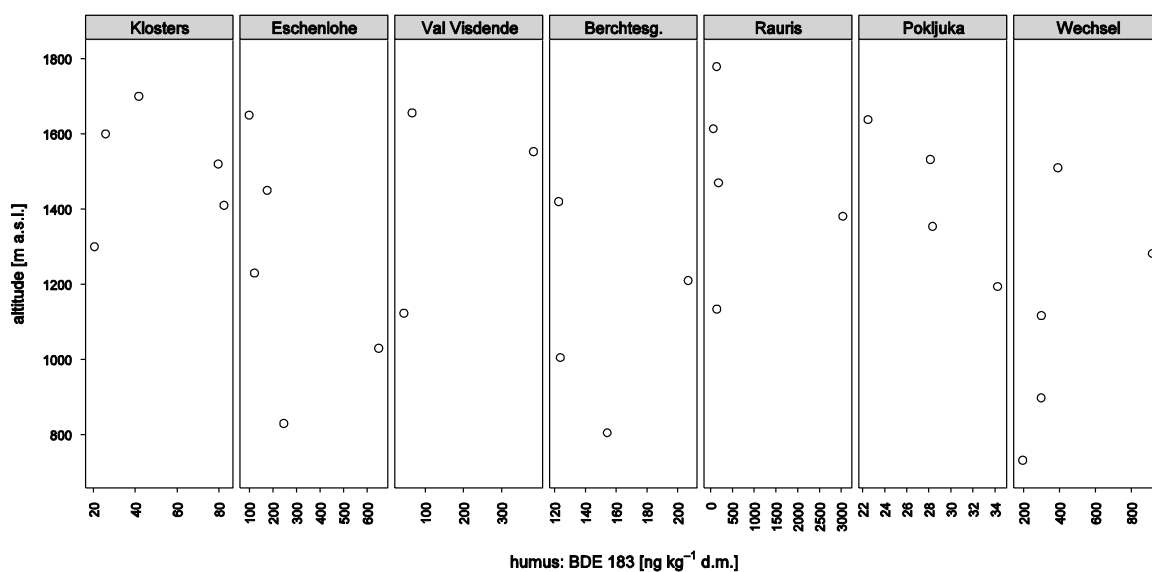


Figure 3-170: Altitudinal variation of BDE 183 in forest humus.

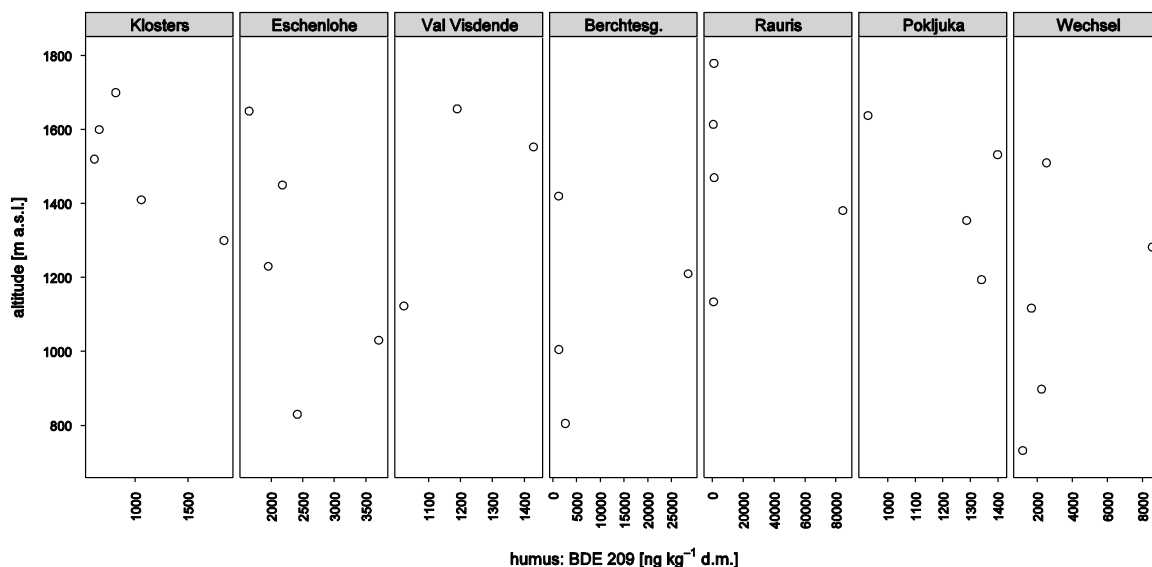


Figure 3-171: Altitudinal variation of the BDE 209 in forest humus.

3.5.5.3 SPMD

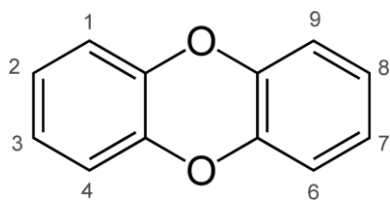
In an initial analysis of SPMD from the Eschenlohe height profile, 25 out of 37 concentrations (78 %) were less than the double blank values: further analysis of PBDE in SPMD was stopped.

3.6 Polychlorinated dibenzodioxins and -furans (PCDD/F)

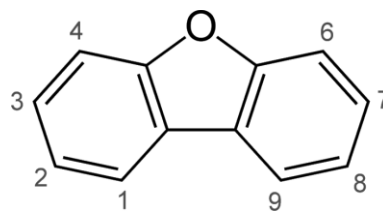
3.6.1 Characterization

3.6.1.1 Physicochemical properties

Polychlorinated dibenzo-*p*-dioxins (PCDDs) and polychlorinated dibenzofurans (PCDFs), often simply called “dioxins”, consist of two groups of tricyclic aromatic compounds with similar structure and varying chemical and physical properties, depending on the number of chlorine atoms in the molecule (Figure 3-172). Dioxins have 75 and furans 135 positional isomers.



polychlorinated dibenzo-*p*-dioxin (PCDD)



polychlorinated dibenzofuran (PCDF)

Figure 3-172: Molecular structure of PCDDs and PCDFs. Each of the numbered positions can hold a chlorine substituent.

Table 3-23: Physical properties of PCDDs and PCDFs at 25 °C.

	2,3,7,8-TCDD	OCDD	2,3,7,8-TCDF	OCDF
molecular weight (g mol ⁻¹)	322	460	306	443.8
boiling point (°C)	446.5	510	464.7	537
water solubility (ng l ⁻¹)	19.3	0.074	419	1.16
vapour pressure (Pa)	2.0×10^{-7}	1.10×10^{-10}	2.0×10^{-6}	5.0×10^{-10}
log K _{ow}	6.8	8.2	6.1	8.0

source: Mackay et al. (1992b)

3.6.1.2 Emissions and use

Neither dioxins nor furans are produced commercially. They form unwanted byproducts in many industrial and combustion processes. The most important PCDD and PCDF emission sources are: incineration of municipal, hazardous, and clinical wastes, and of sewage sludges; metal industry, such as steel mills and sintering plants (WHO 2003).

3.6.1.3 Environmental behaviour and bioaccumulation

Dioxins and furans are very persistent compounds, adsorbing to particles in air, soil and sediment, which means that their mobility in the ground is very low. The air is probably the most significant compartment for the environmental distribution and fate of these compounds. PCDD/Fs are lipophilic and hardly dissolve in water. Because of their persistence and lipophilicity, they remain in the environment for a long time. A half-life of 10–12 years in soil has been reported for TCDD. Highly chlorinated PCDD/Fs seem to be more resistant to degradation than those with few chlorine atoms.

The high lipid solubility and the low water solubility lead to the retention of PCDD/Fs and their metabolites in fat-containing tissues of living organisms. The accumulation rate in organisms varies with species, duration and concentration of exposure, and environmental conditions (WHO 2003). A bioconcentration factor of 26.7×10^3 has been reported for 2,3,7,8-TCDD in rainbow trout (*Salmo gairdneri*) (IOMC 1995).

3.6.1.4 Toxicology

2,3,7,8-substituted PCDD/PCDFs and coplanar PCBs trigger an identical toxicological response (via mediated by Ah-receptors). The concept of *toxic equivalents* assumes that the toxic response differs between congeners, with the unit response (=1) elicited by 2,3,7,8-TCDD (WHO, 2003). The toxic responses observed in several animal species include body weight loss, enzyme induction/modification, hepatotoxicity, porphyria, dermal toxicity, gastric lesions, thymus atrophy and immunotoxicity, teratogenicity, reproductive effects, and carcinogenicity. The most characteristic toxic effects observed in all laboratory animals are body weight loss, thymus atrophy, and immunotoxicity. Chloracne and related dermal lesions are the most frequently noted signs of 2,3,7,8-TCDD toxicosis in humans. (IPCS, INCHEM, 1989). Epidemiological studies on the cohorts most highly exposed to 2,3,7,8-TCDD produced the strongest evidence of increased risks for all cancers combined; along with less strong evidence of increased risks for cancers of particular sites. Studies of non-cancer effects in children have indicated neurodevelopmental delays and neurobehavioural effects, including neonatal hypotonia (WHO, 2003).

In 2001, the European Commission and the Scientific Committee for Food proposed a temporary tolerable weekly intake (TWI) of 14 pg kg⁻¹ body weight for PCDD, PCDF and dioxin-like PCB.

3.6.2 Overview of results

Again, there were strong concentration differences between humus, mineral soil and needles. Humus contained about twice as much PCDD/F as mineral soil, both of which exceeded needle PCDD/F contamination by two orders of magnitude. Qualitative differences were observed as well: the PCDD/F homologue pattern of mineral soil, with its high fraction of furans, deviated from that of humus and needles. Pronounced contrasts were also found between the homologue patterns in ambient air and deposition at three alpine summits. Within the limitations set by the low number of sampling periods, differences between years were much larger than between seasons regarding the PCDD/F levels in air and deposition. Two of the three summits showed similar time trends of PCDD/F in air and deposition. PCDD/F loads, but not the PCDD/F homologue profiles, differed considerably between stations. Although it occurred repeatedly that one of four source regions stood out by particularly high PCDD/F concentrations in corresponding air masses, the origin of high atmospheric concentrations could change from one sampling period to the next and, during the same period, between sites.

Needle and humus samples show pronounced geographical gradients of PCDD/F loads. Concentrations are highest at the margins of the investigated range. While needle samples show an enrichment of dioxins in the North and of furans in the South, humus samples indicate highest loads of both dioxins and furans in the North. The significantly highest needle levels (median) of dioxins and dioxin+furans occurred in the East, while concentrations in humus peaked in the West, though not statistically significant. Again, needle and humus samples gave a contrasting impression of the geographical pollution gradient. Consistent vertical concentration trends, where observable, could develop in both directions (increase or decrease with altitude), depending on the particular height profile.

3.6.3 Summary statistics

Similar to other pollutant groups, the dioxin and furan content differed drastically between compartments of the investigated forests. Total PCDD/F concentration in humus was roughly twice as high as in the underlying mineral soil whose PCDD/F content still exceeded that of 0.5 year old needles by two orders of magnitude. There were qualitative differences, too: the homologue pattern of mineral soil deviated from that of needles and humus, mainly for its dominant furan component. Humus was characterised by a particularly high share of OCDD. Pronounced contrasts were also observed between the PCDD/F patterns of deposition and ambient air at three alpine summits. Air samples had a higher share of furanes on total PCDD/F content than deposition. The PCDD/F pattern in deposition was characterised by a distinct OCDF peak. Despite similar homologue profiles in air and deposition, the three high altitude stations were exposed to different PCDD/F levels. Atmospheric concentrations varied widely between sampling periods which makes a comparison of stations difficult. PCDD/F levels in deposition were clearly lowest at Mt. Weissfluhjoch, followed by Mt. Zugspitze and Mt. Sonnblick. At Mt. Weissfluhjoch with its low PCDD/F levels, deposition and air PCDD/F contamination showed similar time trends. During sampling periods of relatively high PCDD/F loads on Mt. Sonnblick, levels in deposition and air varied independently from each other.

3.6.3.1 Needles

Table 3-24: Concentrations of polychlorinated dibenzodioxins and -furans (PCDD/F) in 0.5 year old Norway spruce needles

	n < LOD	mean	sd	min	P ₁₀	P ₂₅	median	P ₇₅	P ₉₀	max
TCDD	24	0.094	0.166				< LOD	0.130	0.290	0.79
PeCDD	27	0.084	0.163				< LOD	0.115	0.291	0.66
HxCDD	16	0.240	0.269			< LOD	0.145	0.455	0.521	1.10
HpCDD	1	0.778	0.702	< LOD	0.279	0.360	0.590	0.748	1.650	3.20
OCDD	4	0.903	1.263	< LOD	0.180	0.328	0.495	0.830	1.710	6.00
TCDF	6	0.563	0.733		< LOD	0.140	0.315	0.703	1.610	3.30
PeCDF	14	0.310	0.523			< LOD	0.125	0.375	0.807	2.20
HxCDF	17	0.127	0.192			< LOD	0.047	0.168	0.383	0.74
HpCDF	4	0.217	0.345	< LOD	0.053	0.083	0.140	0.225	0.332	2.20
OCDF	27	0.041	0.078				< LOD	0.043	0.151	0.31
Σ PCDD	1	2.100	1.980	< LOD	0.688	0.800	1.425	2.650	3.828	8.57
Σ PCDF	1	1.257	1.540	< LOD	0.168	0.376	0.658	1.523	3.424	6.99
Σ PCDD/F	1	3.357	2.888	< LOD	0.918	1.249	2.139	4.635	8.090	10.72
TEQ _{WHO}	1	0.034	0.045	< LOD	0.002	0.005	0.011	0.048	0.094	0.174

unit: ng kg⁻¹ d.m.; sample size n=40; LOD...detection limit (0.19)

3.6.3.2 Humus, mineral soil

Table 3-25: Concentrations of polychlorinated dibenzodioxins and -furans in humus

	mean	sd	min	P ₁₀	P ₂₅	median	P ₇₅	P ₉₀	max
TCDD	4.49	3.04	0.48	1.30	2.35	3.8	6.05	8	12
PeCDD	10.73	6.91	1.5	3	4.90	9.6	14	22	28
HxCDD	23.39	15.36	7.2	7.6	12	20	30.5	48	57
HpCDD	43.55	33.31	12	14	17.5	34	56.5	97	140
OCDD	76.68	60.46	18	24	30.5	54	100	160	250
TCDF	43.84	22.01	13	20	26	39	60	75	91
PeCDF	49.13	26.69	13	20	27	40	77.5	87	93
HxCDF	26.84	17.10	7.9	10	13.5	23	32	56	65
HpCDF	19.73	12.21	5.6	8.3	11	15	26.5	40	45
OCDF	15.48	10.61	3.5	6.5	7.15	11	22.5	29	41
Σ PCDD	158.83	116.15	43.3	53.48	65.2	119	206.75	344.1	477
Σ PCDF	155.01	80.44	63	66.7	91.25	132.6	211.5	280	311
Σ PCDD/F	313.84	188.47	115.7	122.36	155.85	262.3	404.55	632	758
TEQ _{WHO}	4.44	2.79	1.37	1.62	2.55	3.70	5.21	8.94	10.81

unit: ng kg⁻¹ d.m.; sample size n=31; all concentrations were above the below detection limit (0.09)

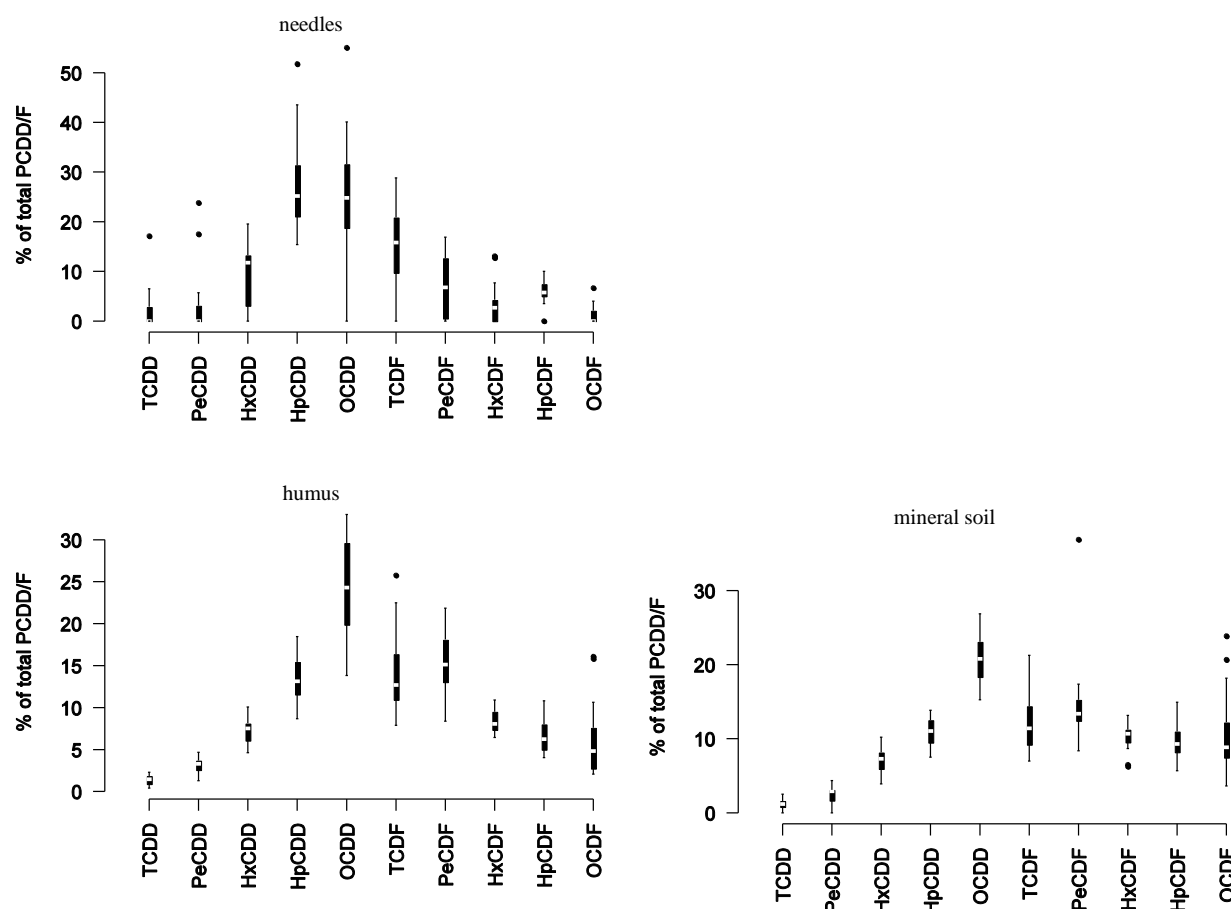
Table 3-26: Concentrations of polychlorinated dibenzodioxins and -furans in forest mineral soil

	n < LOD	mean	sd	min	P ₁₀	P ₂₅	median	P ₇₅	P ₉₀	max
TCDD	1	2.87	3.05	< LOD	0.43	0.70	1.7	3.75	8.34	9.9
PeCDD	1	5.95	6.26	< LOD	0.64	1.00	3.65	8.78	17.1	19
HxCDD	0	16.03	16.44	1.1	3.03	3.63	9.05	23	47.3	50
HpCDD	0	23.66	22.80	1.6	5.77	6.10	14	31.75	62.3	75
OCDD	0	44.83	43.48	3	9.61	12.75	26.5	63.75	121	140
TCDF	0	25.38	23.72	1.3	5.38	7.30	17	35.25	57.6	91
PeCDF	0	28.99	27.42	2.7	5.07	10.08	23.5	29.25	78.1	100
HxCDF	0	22.43	21.64	1.1	4.97	6.10	15.5	28.25	65.1	69
HpCDF	0	18.94	16.93	2.6	3.53	6.90	15	20.5	50.5	57
OCDF	0	18.57	15.93	2.3	4.06	8.58	14.5	20.25	48.6	55
Σ PCDD	0	93.33	91.60	5.7	20.75	25.83	55.15	125.08	261.06	291.7
Σ PCDF	0	114.30	103.11	11.9	29.83	47.53	77.5	127.75	312.5	358
Σ PCDD/F	0	207.62	193.51	17.6	47.49	74.79	131.15	252.83	579.94	625.9
TEQ _{WHO}	0	3.20	3.21	0.14	0.62	0.84	2.01	3.96	9.35	10.15

unit: ng kg⁻¹ d.m.; sample size n=20; LOD... below detection limit (0.06)

Figure 3-173 shows that the needles, in contrast to humus and mineral soil, contained a relatively high amount of heptachlorinated dioxins. The PCDD/F pattern in the ground was dominated by OCDD. Mineral soil was characterised by the high contribution of furans (particularly the highly chlorinated ones) to total PCDD/F

content, actually resembling the atmospheric pattern at alpine summits (PCDD/F patterns of air and deposition samples are shown on p. 168).



Boxplots of relative homologue concentrations at 20 sites from which needles, humus and mineral soil data were available.

Figure 3-173: PCDD/F pattern in 0.5 year old Norway spruce needles, forest humus and –mineral soil

3.6.3.3 Deposition and air

At Mt. Zugspitze, exceedingly high dioxin and furan (and PBDE and PCB) contents appeared to accumulate in the filter cartridge reserved for air masses from NW-Europe during autumn and winter 2005/06. However, a series of instrument failures during this period suggests that also the volume readings underestimated the actual filtered volume by far (60 m³ at an average volume of 1000 m³ for the other filters), resulting in calculation of unusually high air concentrations. These data have therefore been omitted in the corresponding plots (row 4 column 2 in figures 3-191 to 3-193).

On all three summits, deposition of dioxins was much higher than that of furans (Table 3-27) – a strong contrast to the relatively furan-rich samples of ambient air (Table 3-28). The variation of deposition rates between different periods was quite similar on all three summits, except a deposition peak on Mt. Sonnblick during winter 2006/7 (Figure 3-176). Mt. Sonnblick experienced the highest PCDD/F deposition, while the Swiss station Weissfluhjoch did not only have the lowest deposition rates but also showed a different temporal development: most notably, it lacked the deposition peak observed at the two other stations during Nov. 06–February 07.

Table 3-27: PCDD/F deposition on three alpine summits

	period**	TCDF	PeCDF	HxCDF	HpCDF	OCDF	TCDD	PeCDD	HxCDD	HpCDD	OCDD	PCDF	PCDD	PCDD/F	TEQWHO
Sonnblick	I	13.0	13.0	15.0	19.0	18.0	0.8	3.4	15.0	87.0	170.0	78.0	276.2	354.2	2.3
	II	38.0	32.0	15.0	26.0	21.0	8.3	13.0	31.0	90.0	190.0	132.0	332.3	464.3	4.8
	III	16.0	12.0	5.3	2.3	6.6	*	1.2	14.0	29.0	52.0	42.2	96.2	138.4	2.1
	IV	*	1.1	5.8	2.5	16.0	*	*	5.4	87.0	310.0	25.4	402.4	427.8	2.6
	V	62.0	61.0	83.0	130.0	130.0	16.0	27.0	78.0	650.0	2800.0	466.0	3571.0	4037.0	19.7
	VI	26.0	19.0	14.0	15.0	10.0	1.1	4.3	18.0	55.0	130.0	84.0	208.4	292.4	4.1
Weissfluhj.	I	4.1	3.9	2.9	2.8	1.7	*	0.4	1.8	14.0	24.0	15.4	40.2	55.6	0.4
	II	2.9	2.6	1.1	2.3	2.5	*	0.6	3.8	25.0	64.0	11.4	93.4	104.8	0.5
	III	6.4	4.7	1.7	2.3	1.7	*	*	1.2	7.5	10.0	16.8	18.7	35.5	0.5
	IV	*	*	*	2.3	*	*	*	*	3.8	12.0	2.3	15.8	18.1	0.1
	V	*	*	*	0.9	*	*	*	*	4.1	9.1	0.9	13.2	14.1	0.1
	VI	6.8	2.9	1.8	3.6	*	*	*	0.8	13.0	28.0	15.1	41.8	56.9	0.5
Zugspitze	I	7.0	8.8	6.5	5.2	2.8	*	1.5	5.8	36.0	25.0	30.3	68.3	98.6	1.1
	II	12.0	14.0	9.1	18.0	9.6	2.2	6.1	23.0	83.0	97.0	62.7	211.3	274.0	2.7
	III	5.0	6.4	3.7	3.9	2.6	*	*	11.0	41.0	92.0	21.6	144.0	165.6	1.1
	IV	*	*	0.8	0.4	2.9	*	*	0.6	11.0	33.0	4.1	44.6	48.8	0.2
	V	5.1	17.0	31.0	28.0	9.5	13.0	29.0	69.0	77.0	90.0	90.6	278.0	368.6	6.7
	VI	8.2	8.7	13.0	12.0	5.1	*	1.2	17.0	36.0	56.0	47.0	110.2	157.2	3.3

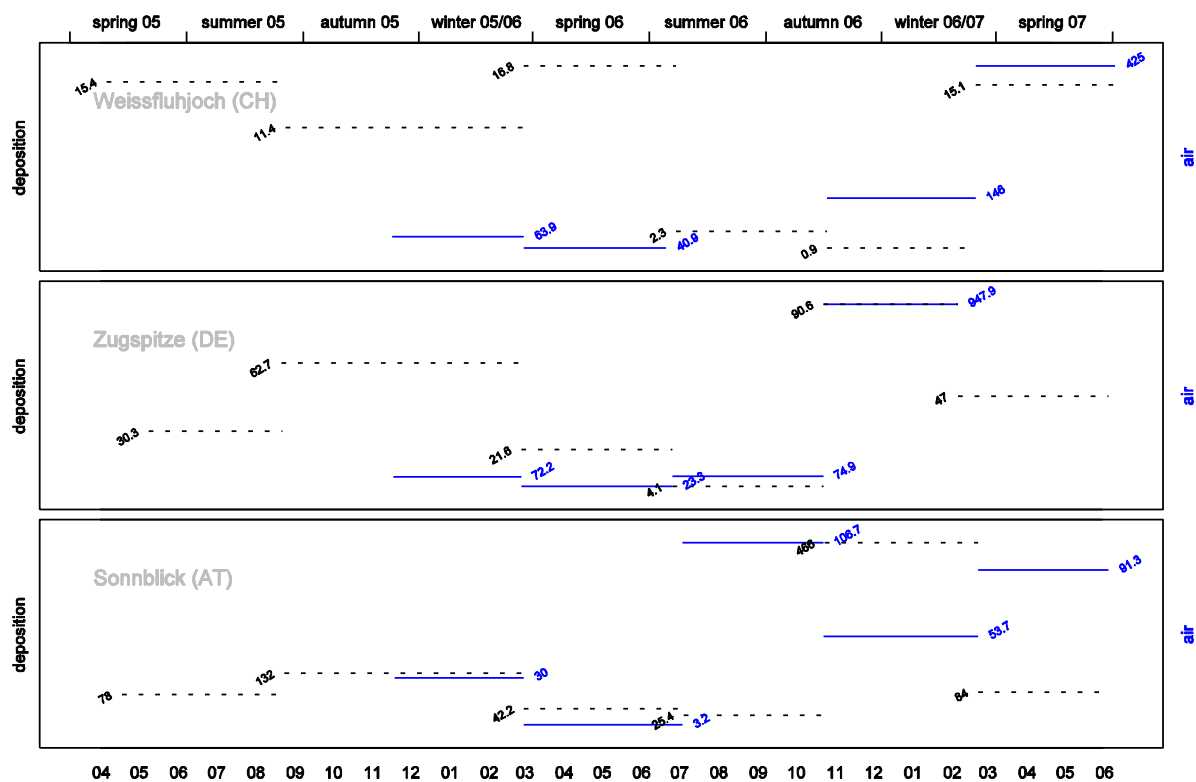
unit: $\text{pg m}^{-2} \text{d}^{-1}$; * value below detection limit; ** sampling period: I=spring–late summer 2005, II=late summer 05–late winter 06, III=spring–early summer 06, IV=early summer–late aut. 06, V=late aut. 06–late winter 07, VI=spring 07

The seasonal course of atmospheric PCDD/F concentrations was similar at the three sites although the loss of single samples and, most important, the short duration of active sampling makes it difficult to generalize. The results at hand suggest that the differences between years are more important than those between seasons (compare, e.g. the small drop between already low levels from winter 2005/6 to spring 2006 with the much higher PCDD/F levels in winter 2006 which still increase in spring 2007: Figure 3-176).

Table 3-28: PCDD/F concentrations in ambient air at three alpine summits

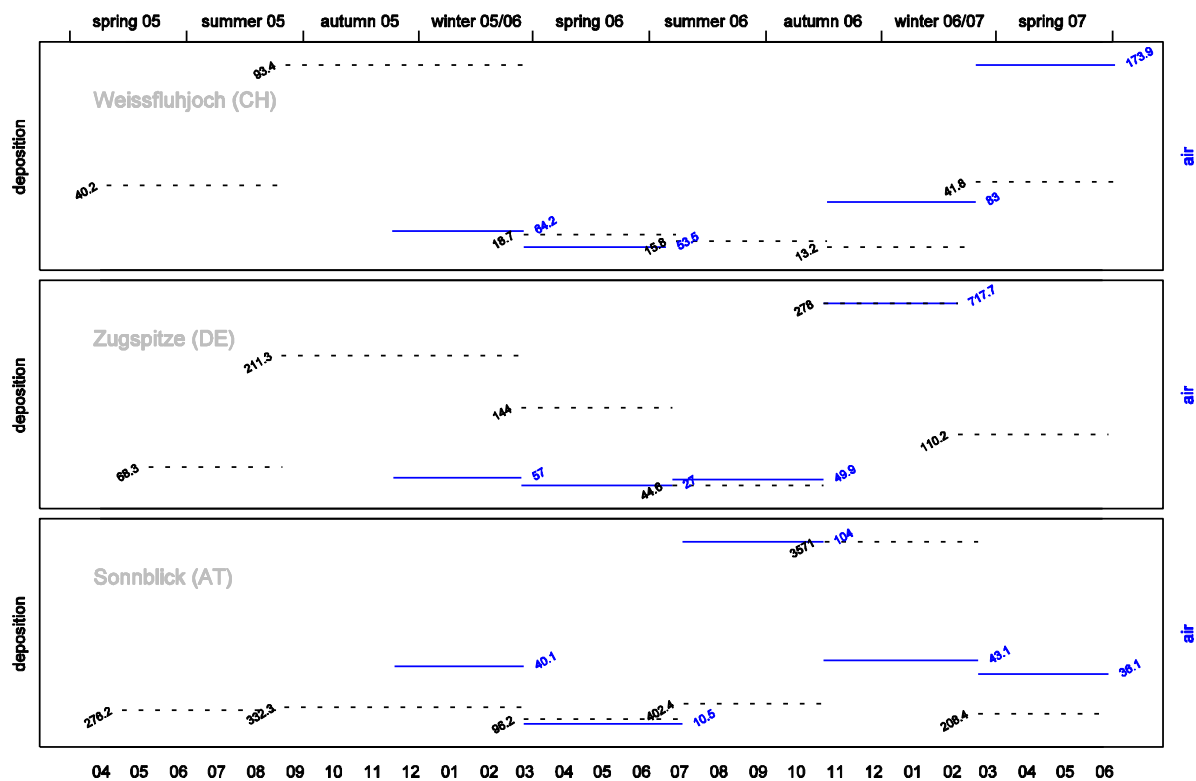
	period **	TCDF	PeCDF	HxCDF	HpCDF	OCDF	TCDD	PeCDD	HxCDD	HpCDD	OCDD	PCDF	PCDD	PCDD/F	TEQ WHO
Sonnblick	I	14.5	5.2	3.9	5.3	1.2	0.5	0.6	7.6	14.0	17.3	30.0	40.1	70.1	0.86
	II	0.0	0.0	0.0	3.2	0.0	0.0	0.0	0.0	1.4	9.1	3.2	10.5	13.7	0.05
	III	29.0	34.4	33.1	7.7	2.4	2.6	14.6	36.8	35.2	14.9	106.7	104.0	210.7	4.19
	IV	8.8	12.4	16.5	12.4	3.5	0.0	0.0	5.4	17.8	19.9	53.7	43.1	96.8	2.18
	V	38.1	20.4	18.8	11.4	2.7	3.1	2.3	6.6	13.4	10.7	91.3	36.1	127.4	2.35
Weissfluh.	I	32.9	14.8	9.5	6.8	0.0	5.0	1.4	12.6	20.6	24.5	63.9	64.2	128.1	1.79
	II	13.4	1.5	1.8	22.0	2.2	0.0	0.0	0.0	22.1	31.3	40.9	53.5	94.4	1.74
	III	*	*	*	*	*	*	*	*	*	*	*	*	*	*
	IV	36.5	36.2	43.4	25.2	4.8	1.9	5.0	21.8	32.0	22.3	146.0	83.0	229.0	5.06
	V	128.2	103.7	108.7	72.6	11.8	2.2	5.5	35.9	70.0	60.2	425.0	173.9	598.9	12.25
Zugspitze	I	33.3	17.9	10.5	7.3	3.2	1.9	0.0	11.9	19.7	23.6	72.2	57.0	129.1	1.41
	II	12.2	0.0	1.2	9.8	0.0	0.0	0.0	0.0	9.6	17.4	23.3	27.0	50.3	0.72
	III	18.6	25.3	18.6	10.4	2.0	0.0	6.2	10.4	19.8	13.4	74.9	49.9	124.8	2.61
	IV	204.9	264.0	287.9	167.1	24.0	26.4	96.1	176.8	265.1	153.4	947.9	717.7	1665.6	37.13
	V	*	*	*	*	*	*	*	*	*	*	*	*	*	*

unit: fg m^{-3} at 0 °C and 1013.3 hPa; * data of one source region not available for calculation of average concentrations; for region specific data see page 175 ff. ** sampling periods: I=winter 05/06, II=spring–early summer 06, III=early summer–late aut. 06, IV=late aut. 06–late winter 07, V=spring 07



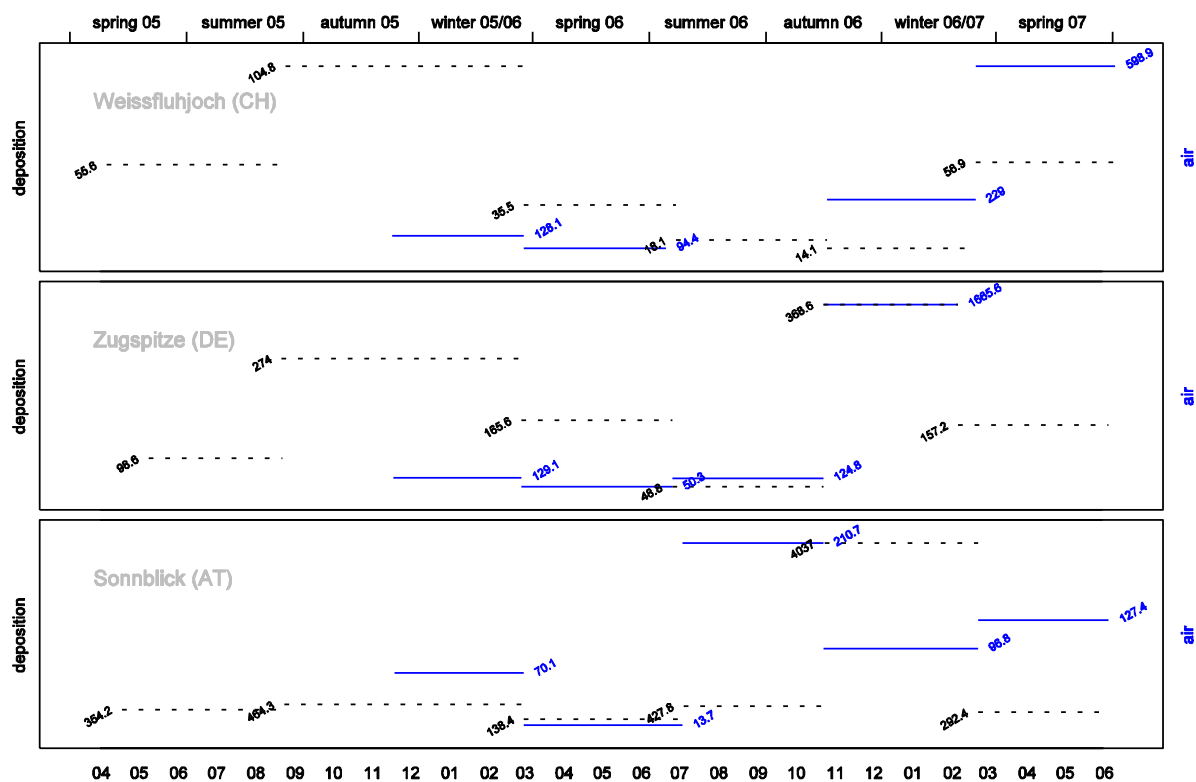
units: deposition: $\text{pg m}^{-2} \text{d}^{-1}$, air: fg m^{-3} at 0°C and 1013.3 hPa

Figure 3-174: PCDF in ambient air and deposition on three alpine summits



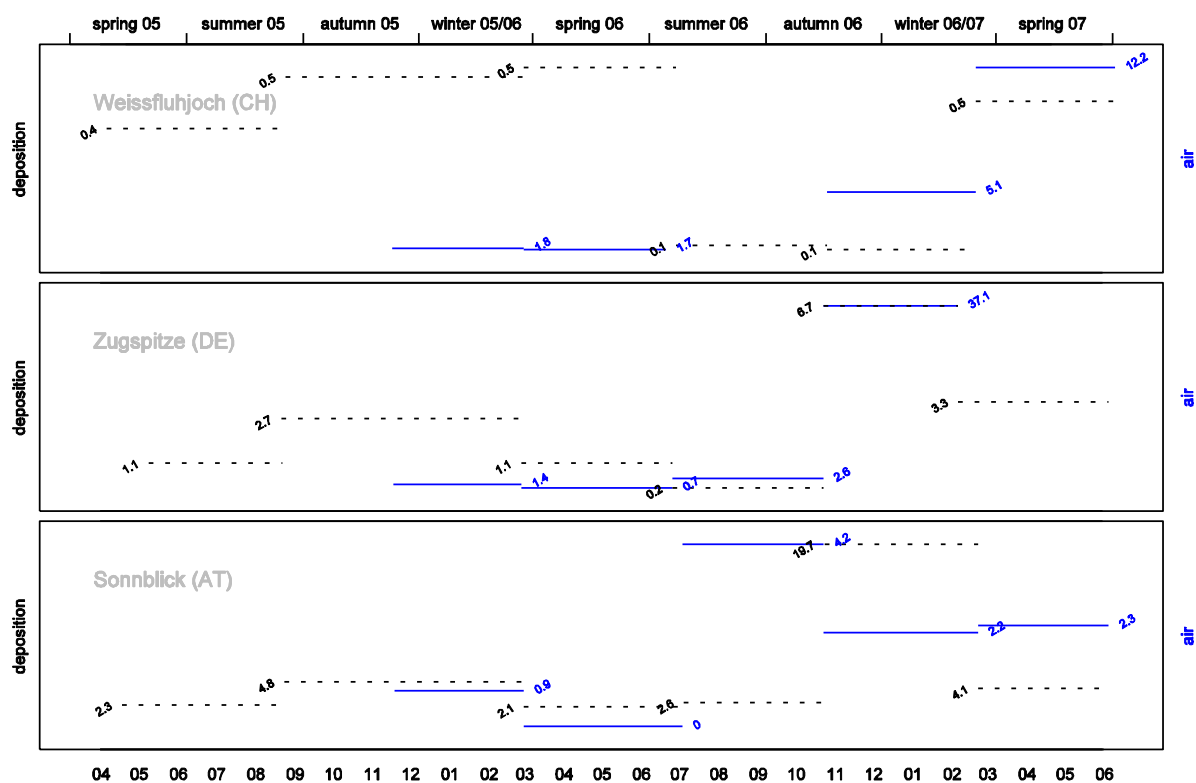
units: deposition: $\text{pg m}^{-2} \text{d}^{-1}$, air: fg m^{-3} at 0°C and 1013.3 hPa .

Figure 3-175: PCDD in ambient air and deposition on three alpine summits



units: deposition: pg m⁻² d⁻¹, air: fg m⁻³ at 0 °C and 1013.3 hPa.

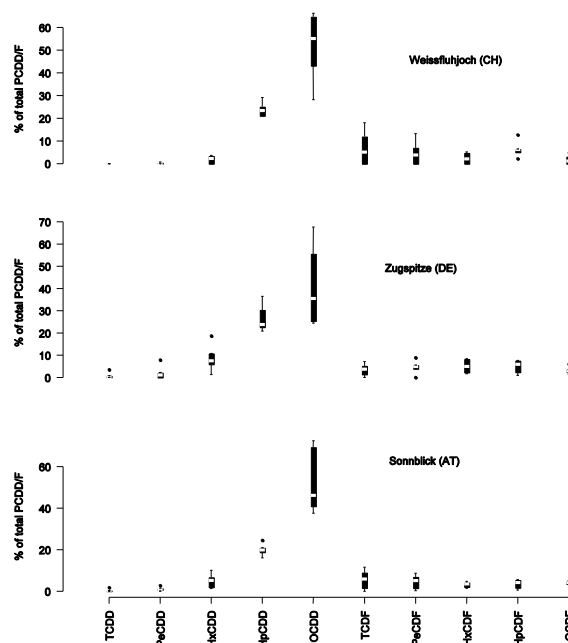
Figure 3-176: PCDD/F in ambient air and deposition on three alpine summits



units: deposition: pg TEQ_{WHO} m⁻² d⁻¹, air: fg TEQ_{WHO} m⁻³ at 0 °C and 1013.3 hPa.

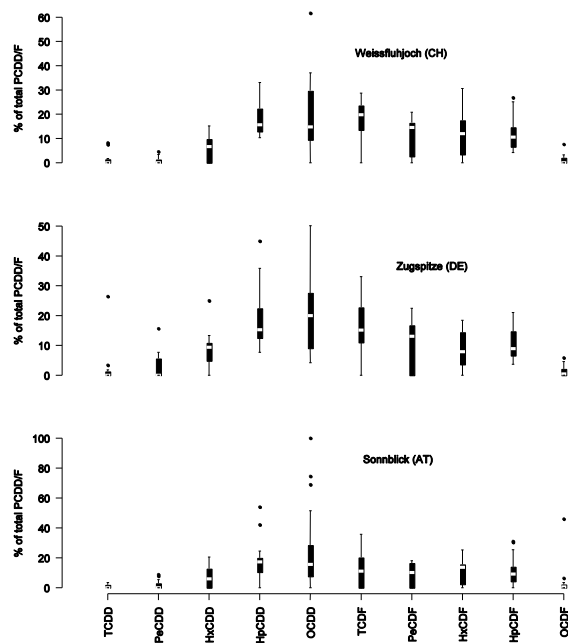
Figure 3-177: Toxic equivalents of PCDD/F in ambient air and deposition on three alpine summits

PCDD/F deposition at the three high altitude stations was dominated by the heavier dioxins, primarily by OCDD (Figure 3-178). The atmospheric homologue pattern varied stronger between sites than the PCDD/F pattern in deposition. The contribution of lower chlorinated furans to total PCDD/F content was clearly higher in air than in deposition samples (Figure 3-179).



(boxplots of six sampling periods per site)

Figure 3-178: PCDD/F pattern in deposition at three alpine summits



(boxplots of five sampling periods per site)

Figure 3-179: atmospheric PCDD/F pattern at three alpine summits

3.6.4 Spatial variation

3.6.4.1 Needles

Dioxin and furan concentrations clearly peaked in the North and South of the studied part of the Alps (Figure 3-180–Figure 3-183). These latitudinal differences were statistically significant for most homologues, the central zone of the Alps having the lowest concentrations. Remarkably, the southern fringe of the Alps was characterised by high furan concentrations, while dioxins dominated in the North.

Although this might not be so apparent from the maps, there were also significant concentration differences between the eastern, middle and western zone of the study region. Again, the middle zone of the studied area had the lowest PCDD/F levels. The highest PCDD/F loads (median concentrations) occurred in the East.

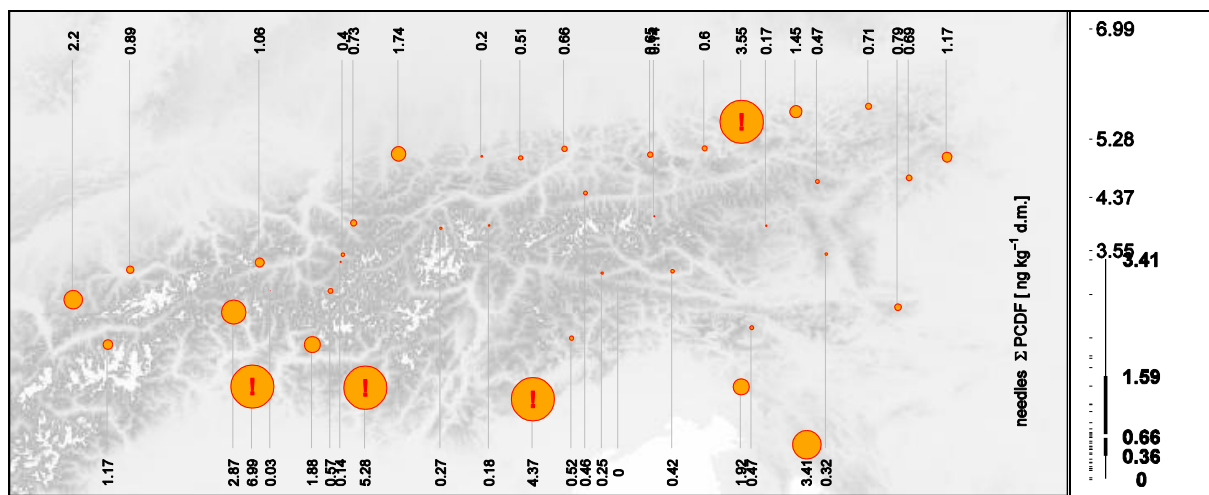


Figure 3-180: PCDF concentration in 0.5 year old Norway spruce needles

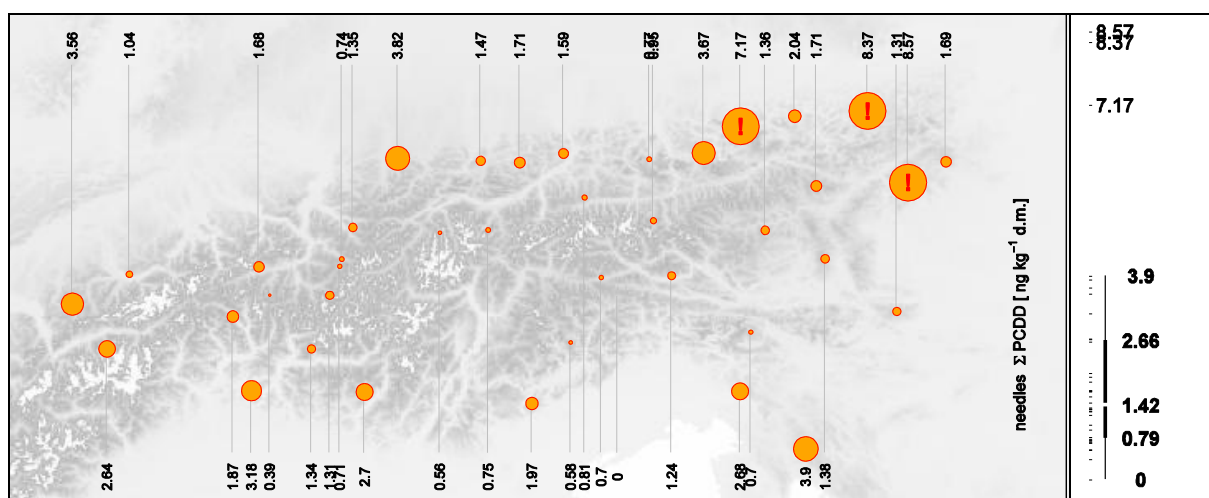


Figure 3-181: PCDD concentration in 0.5 year old Norway spruce needles

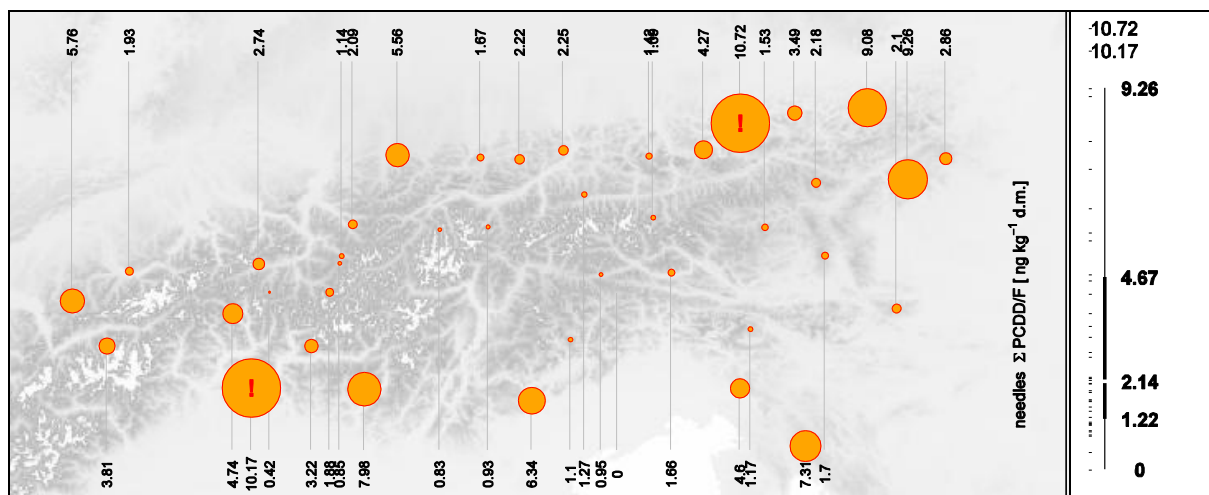


Figure 3-182: PCDD/F concentration in 0.5 year old Norway spruce needles

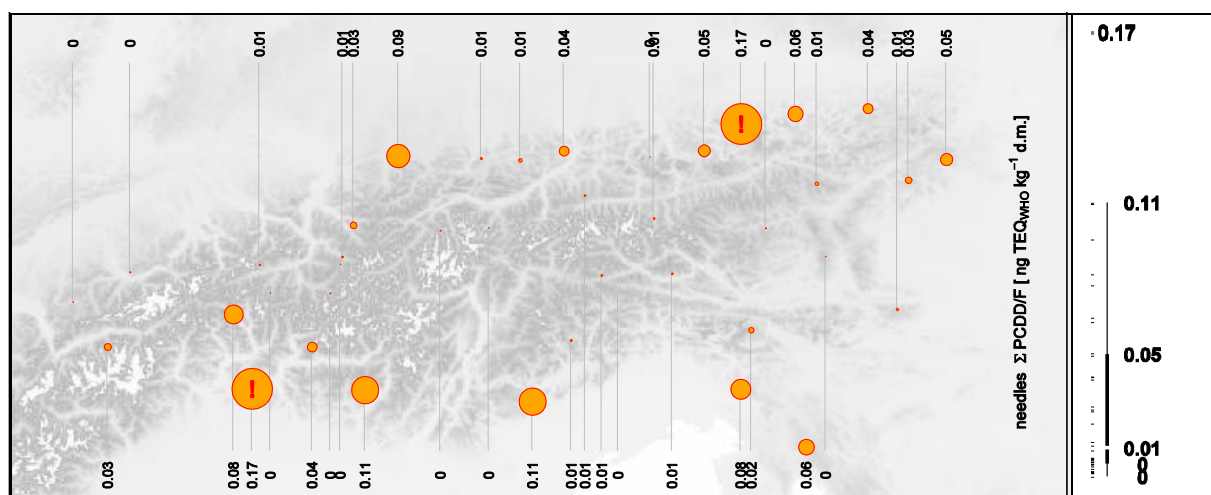


Figure 3-183: PCDD/F concentration as WHO toxic equivalents in 0.5 year old Norway spruce needles

Longitudinal differences

Significant longitude related differences were found for dioxin and furan concentrations (Σ PCDF, Σ PCDD, Σ PCDD/F), for the highly chlorinated dioxins (HpCDD, OcCDD) and for the heptachlorinated furans (Kruskal-Wallis, $\alpha \leq 0.05$).

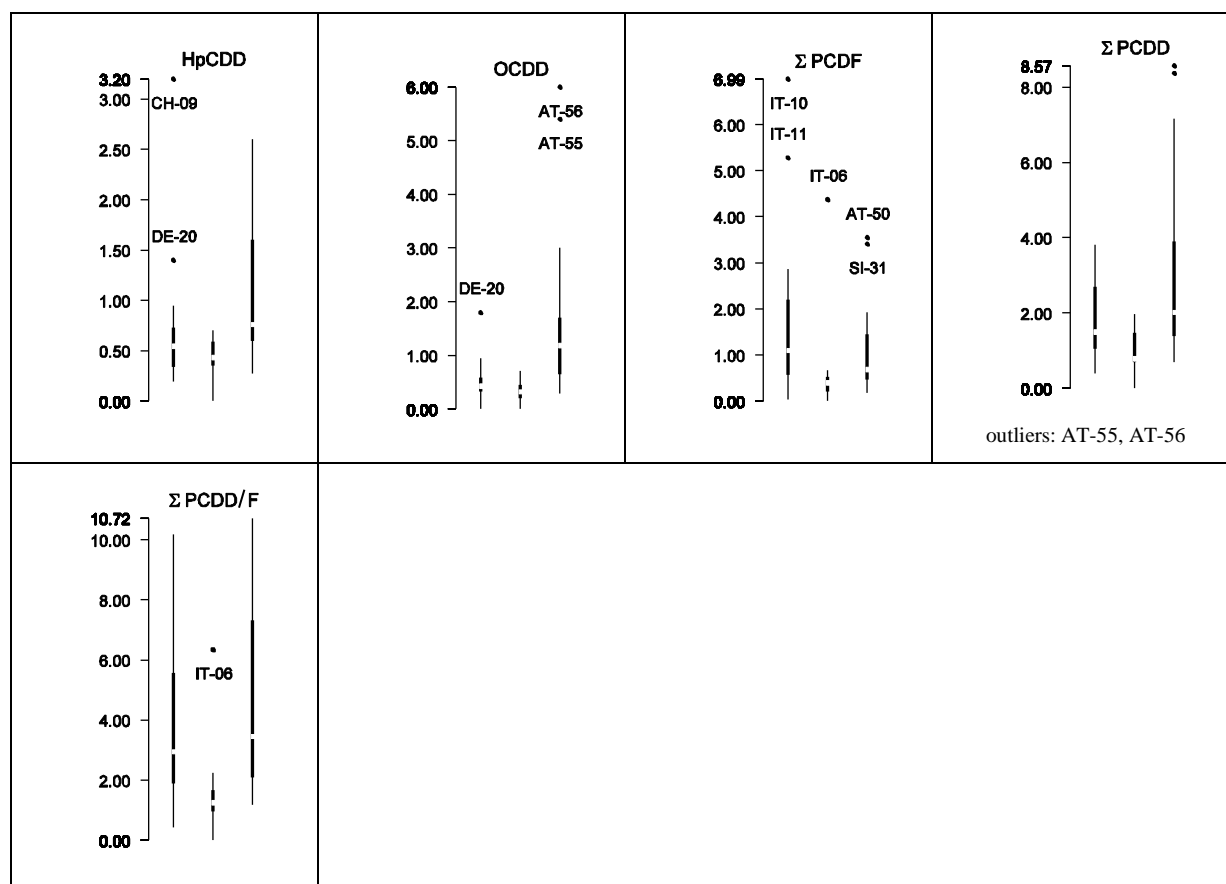


Figure 3-184: Longitudinal pollution trends of dioxins and furans in 0.5 year old Norway spruce needles

The middle study region always had the lowest concentrations (Figure 3-184). Table 3-29 lists significant differences (Mann-Whitney test, $\alpha \leq 0.05$) between pairs of site groups: again, the lower concentrations were

always found for the middle zone. Except for OCDD, there were no significant differences between the eastern and western parts of the study region.

Table 3-29: Significant differences between pairs of longitudinal site groups

	west	middle	east
HpCDD, TCDF, Σ PCDD/F in TEQ _{WHO}		lower	higher
OCDD	lower		higher
		lower	higher
HpCDF, Σ PCDF, Σ PCDD, Σ PCDD/F	higher	lower	
		lower	higher

Latitudinal differences

Except the lowly chlorinated dioxins (TCDD, PeCDD) and OCDF, all dioxin and furan homologues showed significant differences among latitudinal zones (Kruskal-Wallis, $\alpha \leq 0.05$; Figure 3-185). The central zone never had the highest median concentrations but for most parameters significantly lower values than either the northern or southern part of the study region (Mann-Whitney, $\alpha \leq 0.05$; Table 3-30). With the exception of the OCDF, the highest (median) concentrations of all furan homologues were found in the southern zone. Also median TCDD and total PCDD/F content (mass concentration and WHO toxic equivalents) was highest in the southern site group. In contrast, all dioxin homologues had the highest median values in the north (Figure 3-185).

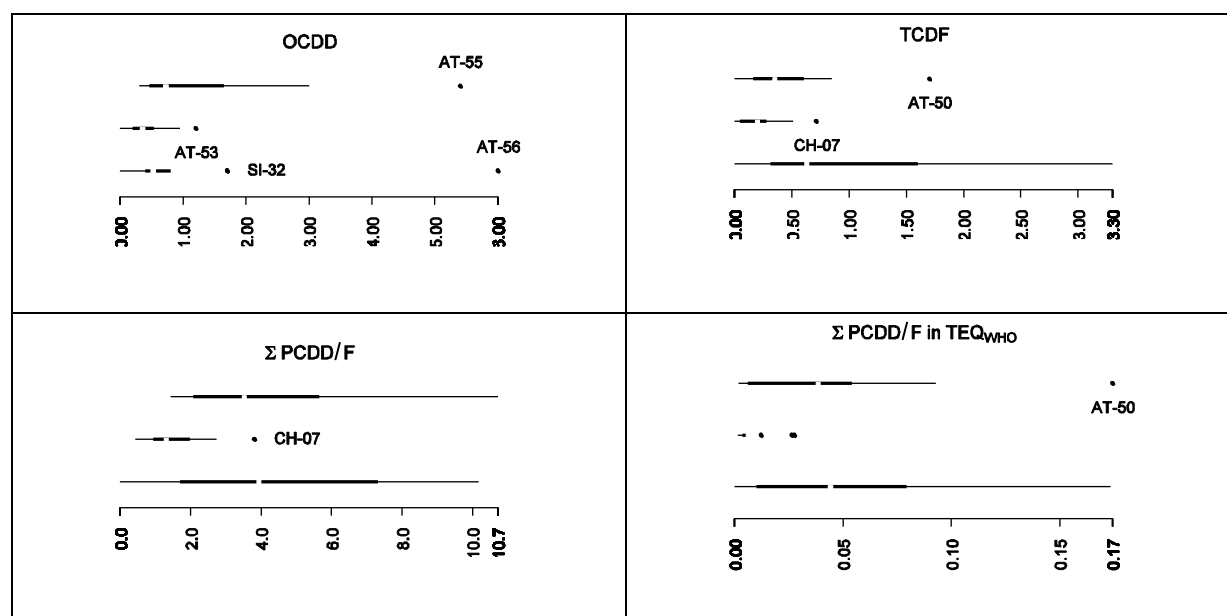


Figure 3-185: Longitudinal pollution trends of dioxins and furans in 0.5 year old Norway spruce needles.

Table 3-30: Significant differences between pairs of latitudinal site groups

OCDD	north: higher	
	central: lower	
TCDF, PeCDF, HxCDF	central: lower	
	south: higher	
HxCDD, HpCDD, HpCDF, Σ PCDD, Σ PCDF, Σ PCDD/F, Σ PCDD/F in TEQ _{WHO}	north: higher	
	central: lower	lower
	south: higher	higher

3.6.4.2 Humus

PCDD/F contamination of humus was highest in the North of the study region. Unlike observed on needle samples, there was no separation between dioxins prevailing in the northern and furans in the southern margin of the studied area. As explained below, concentration differences between latitudinal zones were significant for all dioxin and furan homologues. Longitudinal differences are even less apparent than for needle samples, and in fact were statistically insignificant. However, median PCDD/F levels were highest in the West, as opposed to the longitudinal gradient for needle samples (see above).

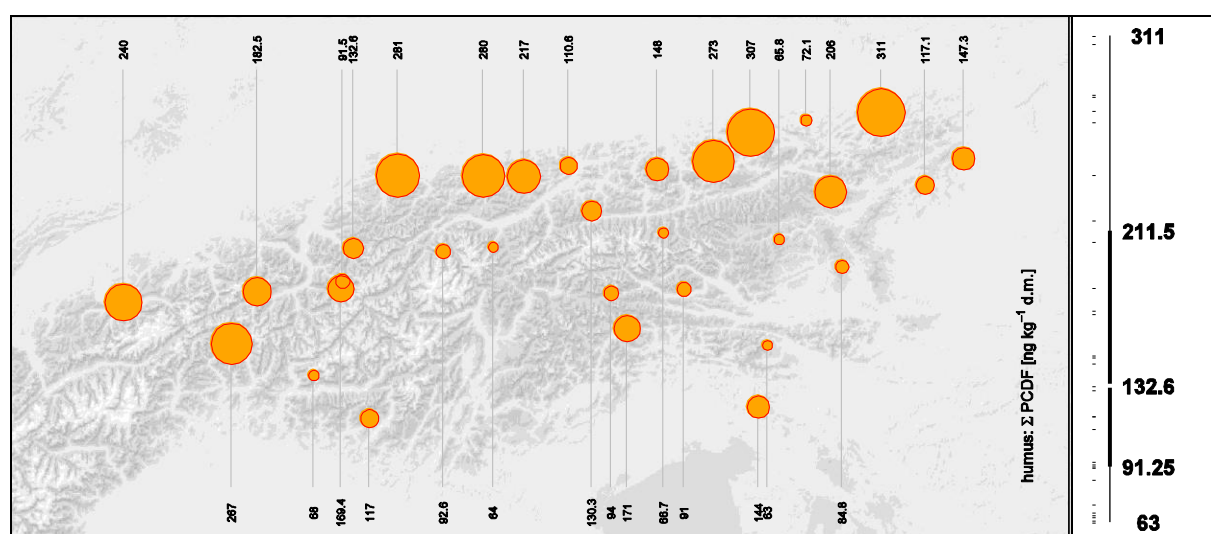


Figure 3-186: PCDF concentration in forest humus

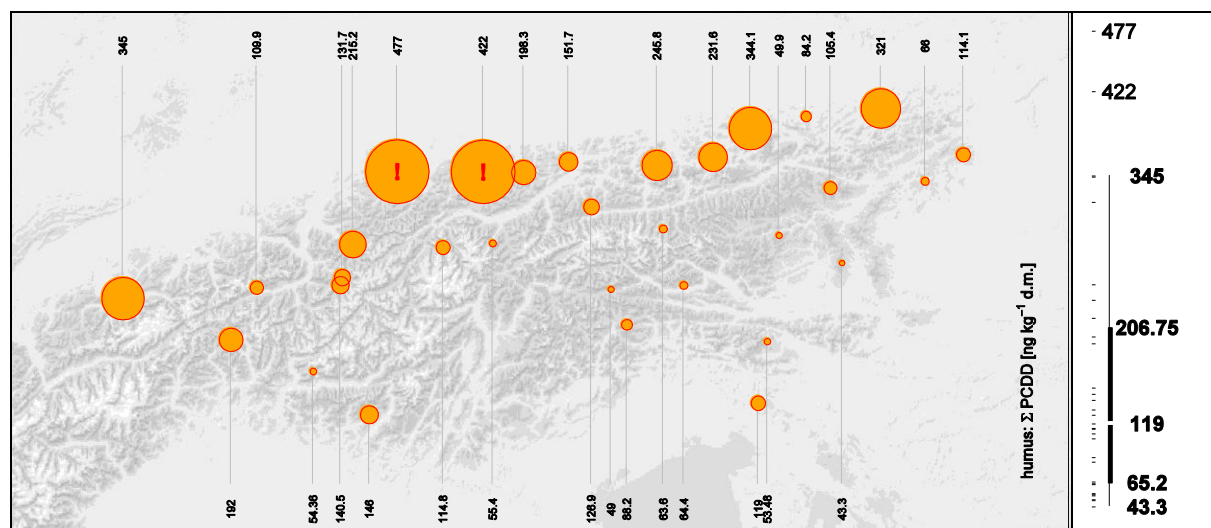


Figure 3-187: PCDD concentration in forest humus

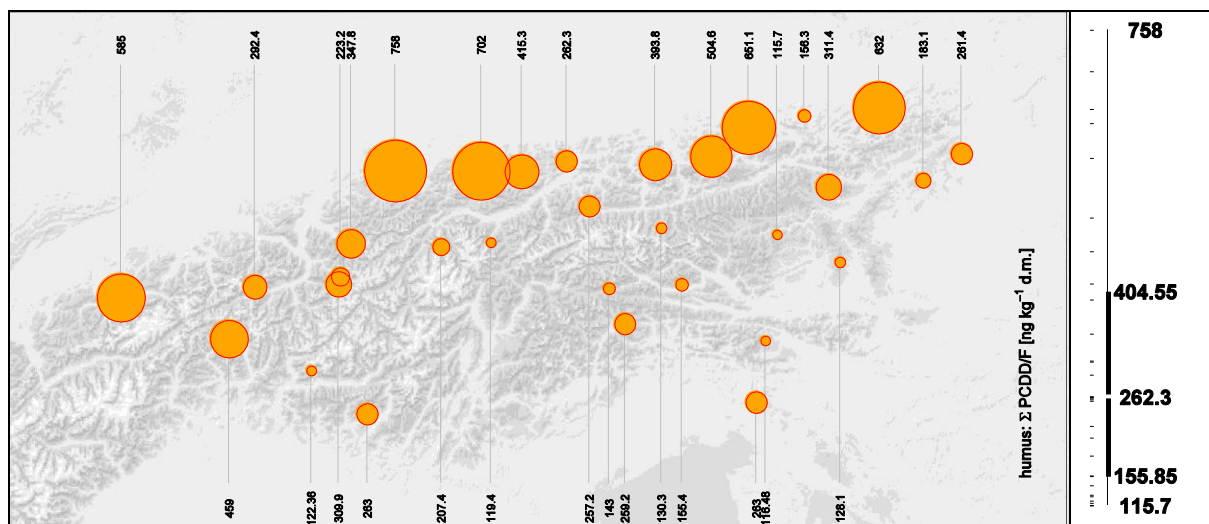


Figure 3-188: PCDD/F concentrations in forest humus

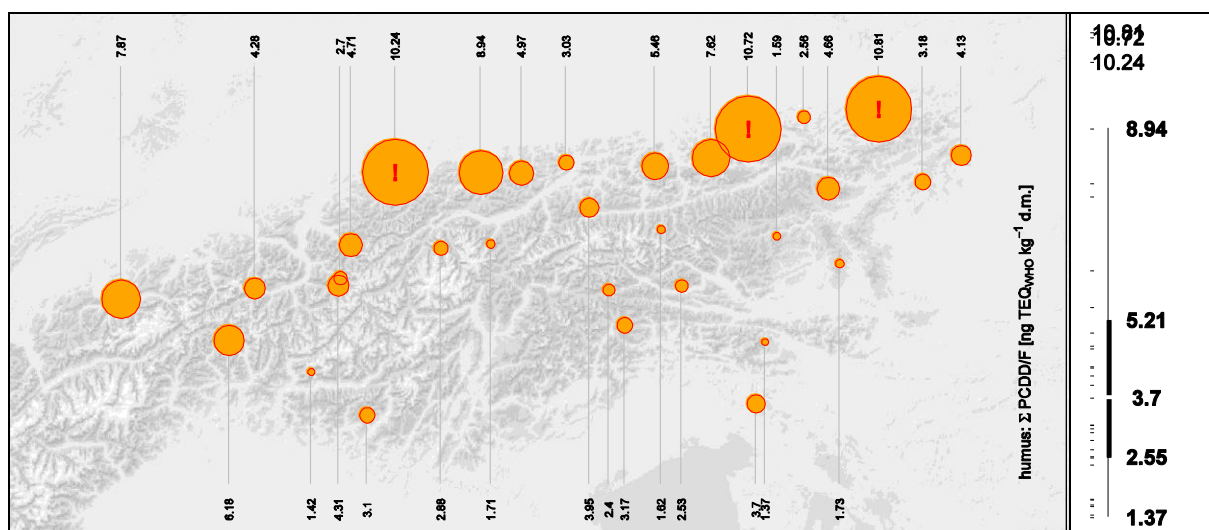


Figure 3-189: PCDD/F concentrations in WHO toxic equivalents in forest humus

Longitudinal differences

Opposite to the situation found for needles differences in humus concentrations among longitudinal site groups were never significant.

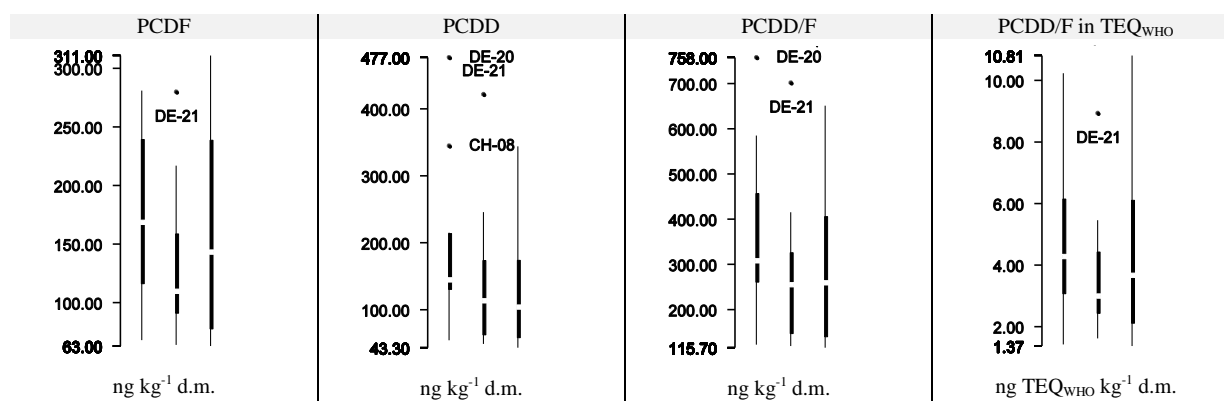


Figure 3-190: Longitudinal pollution trends of dioxins and furans in forest humus

Latitudinal differences

In contrast to the longitudinal differences, all PCDD/F homologues and cumulative parameters showed significant or (except TCDF, PeCDF and OCDF) even highly significant (Kruskal-Wallis, $p \leq 0.01$, $n=31$) differences among latitudinal site groups. Median concentrations were always highest in the northern zone. Lowest furan concentrations (median) and PCDD/F toxic equivalents were observed in the central, lowest dioxin (except OCDD) concentrations in the southern site group. Pairwise comparison of site groups showed that, for most homologues and all sum parameters, the North had significantly higher concentrations than the central and southern site group (Mann-Whitney, $\alpha \leq 0.05$: Table 3-31).

Table 3-31: Significant differences between pairs of latitudinal site groups

PeCDD, HxCDD, HpCDD, OCDD, Σ PCDD, TCDF, PeCDF, HxCDF, Σ PCDF, Σ PCDD/F, Σ PCDD/F in TEQ_{WHO}	north:	higher	higher
	central:	lower	
	south:		lower
TCDD	north:	higher	
	central:		higher
	south:	lower	lower
OCDF	north:	higher	
	central:	lower	lower
	south:		higher
HpCDF	north:	higher	
	central:	lower	

3.6.4.3 Air

A prevailing source direction for atmospheric PCDD/F levels was frequently detected. However, the dominating source direction could change from one sampling period to the next, and, in the same period, from one station to the other (Figure 3-191–Figure 3-193).

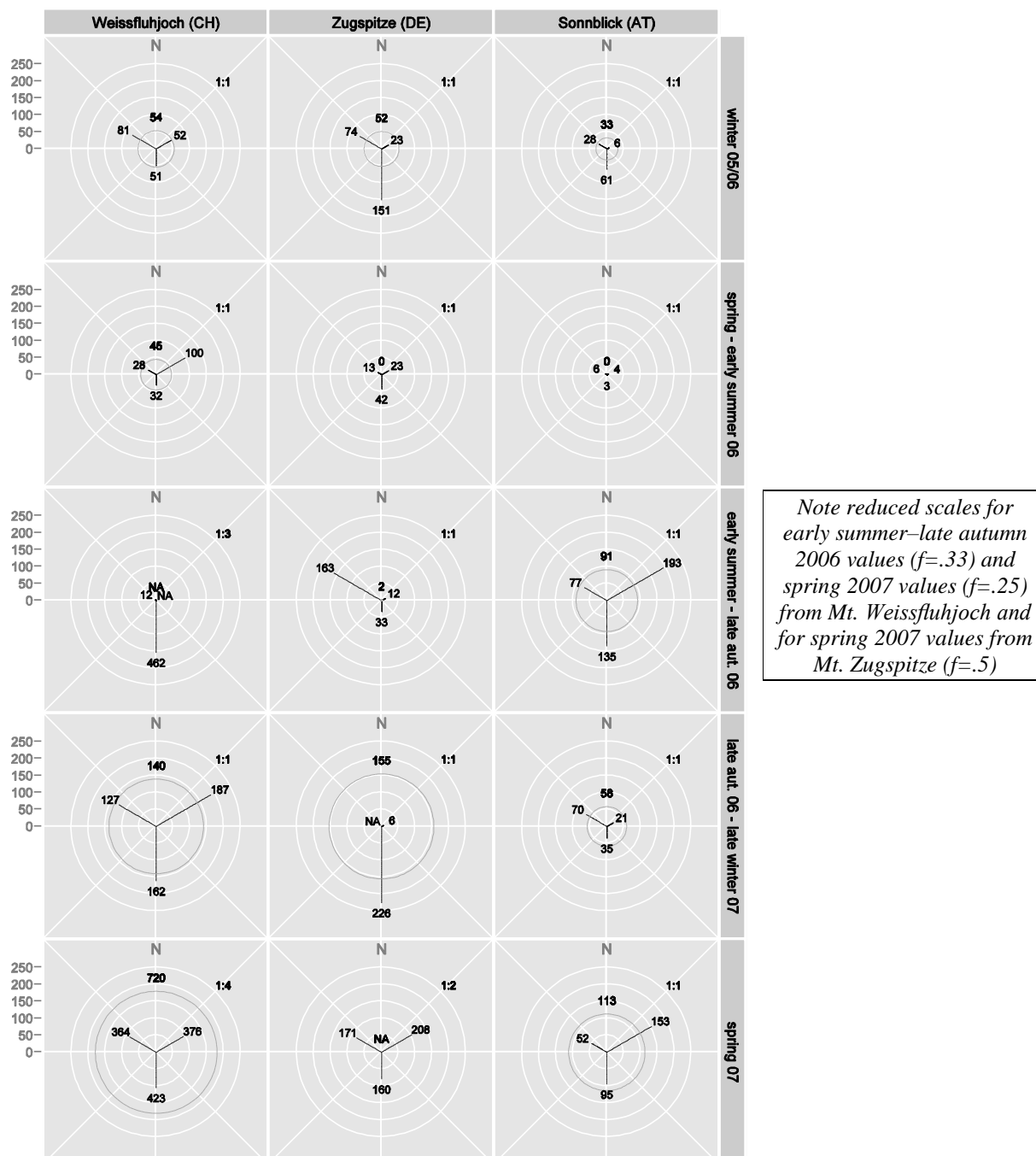
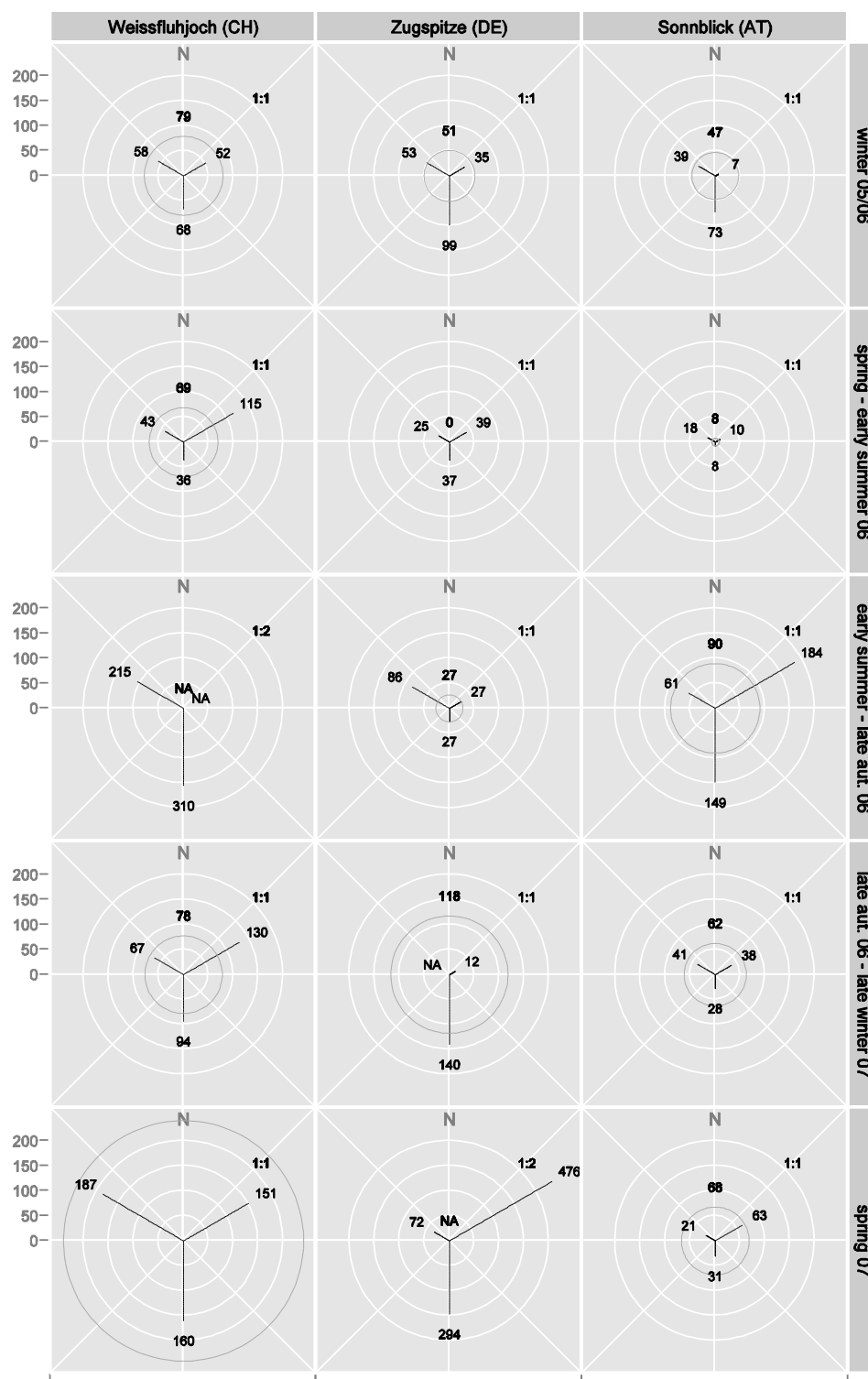


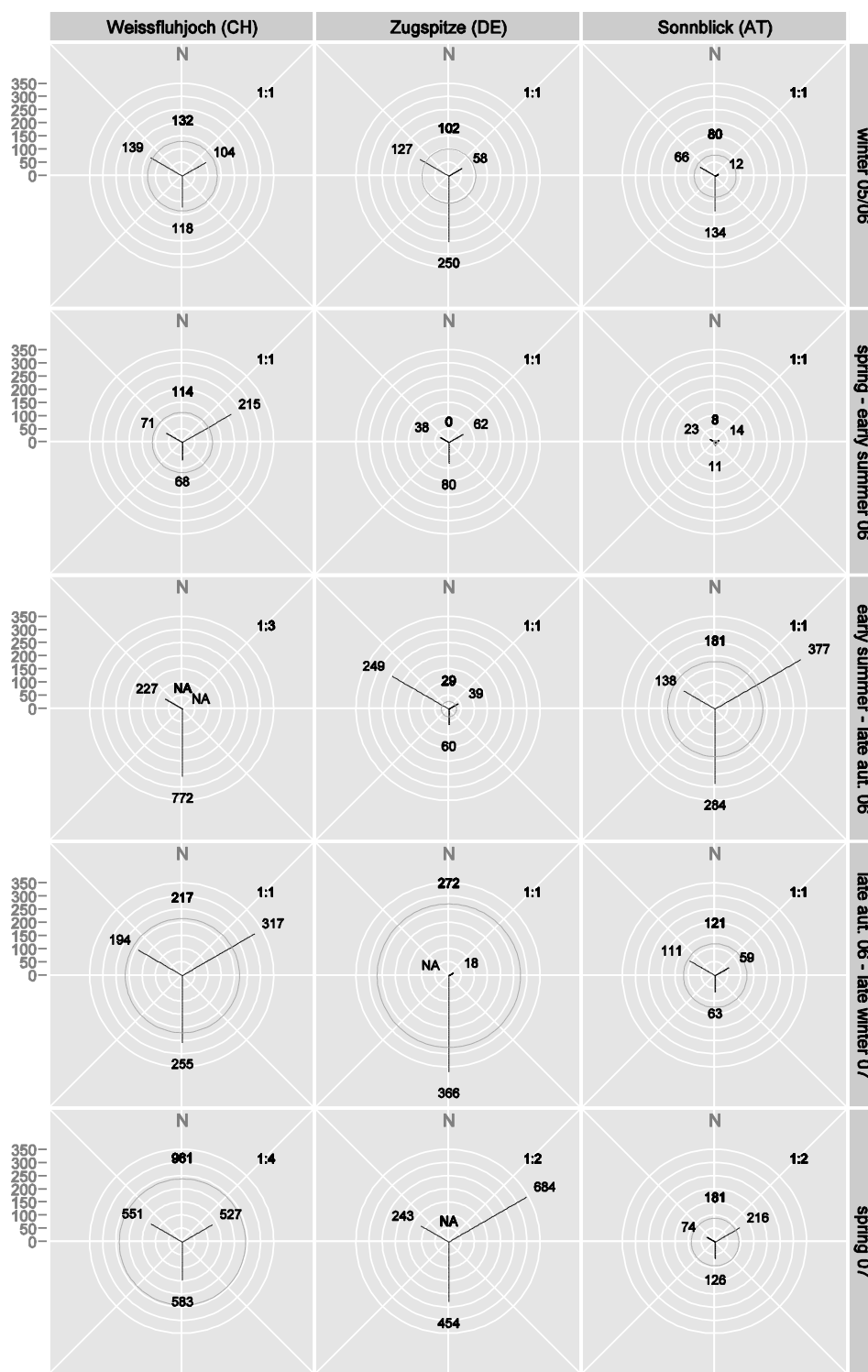
Figure 3-191: Total furan concentration [fg m^{-3}] in air from NW, NE and S (circle: trajectory not attributable to a particular sector).



Note the reduced scales ($f=.5$) for early summer-late autumn 2006 values from Mt. Weissfluhjoch and spring 2007 values from Mt. Zugspitze.

NA...data not available.

Figure 3-192: Total dioxin concentration [fg m^{-3}] in air from NW, NE and S (circle: trajectory not attributable to a particular sector).



Note the reduced scales for early summer–late autumn 2006 values ($f=.33$) and spring 2007 values ($f=.25$) from Mt. Weissfluhjoch and the reduced scale ($f=.5$) for the remaining spring 2007 observations.

NA...data not available.

Figure 3-193: Total dioxin and furan content [fg m^{-3}] of air from NW, NE and S (circle: trajectory not attributable to a particular sector).

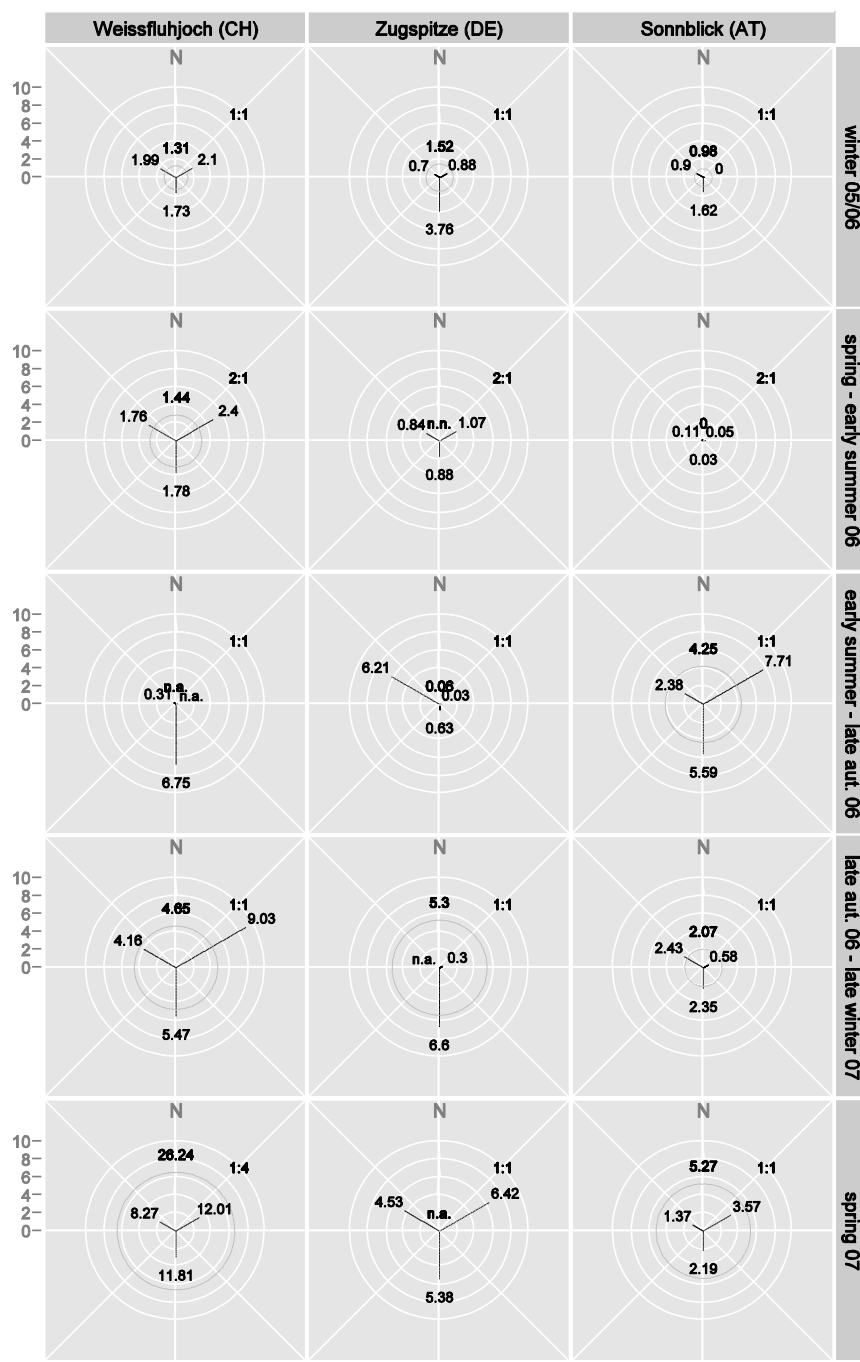


Figure 3-194: Total dioxin and furan content in WHO toxic equivalents [$\text{fg TEQ}_{\text{WHO}} \text{m}^{-3}$] of air from NW, NE and S (circle: trajectory not attributable to a particular sector).

Note reduced scale (1:4) for spring 2007 values from Mt. Weissfluhjoch and doubled scale (2:1) for all spring–early summer 2006 values.

3.6.5 Altitudinal variation

3.6.5.1 Needles

As observed with other pollutants, altitudinal concentration gradients of dioxins and furans varied considerably between height profiles. Along a height profile, concentrations could increase or decrease or show no obvious trend at all (Figures 3-195– 3-198).

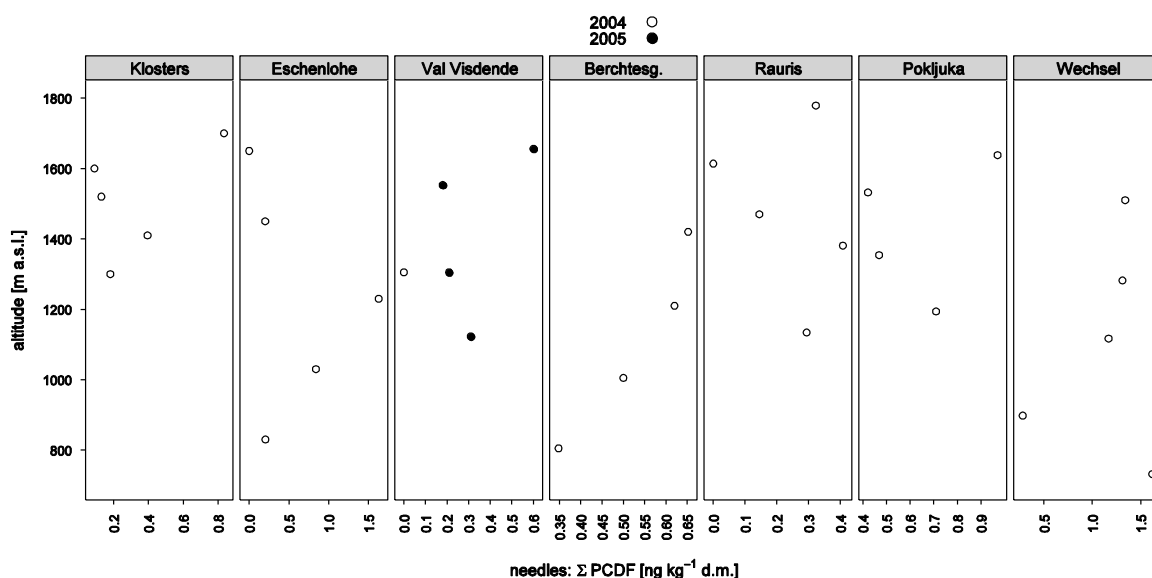


Figure 3-195: Altitudinal variation of the PCDF sum in 0.5 year old Norway spruce needles

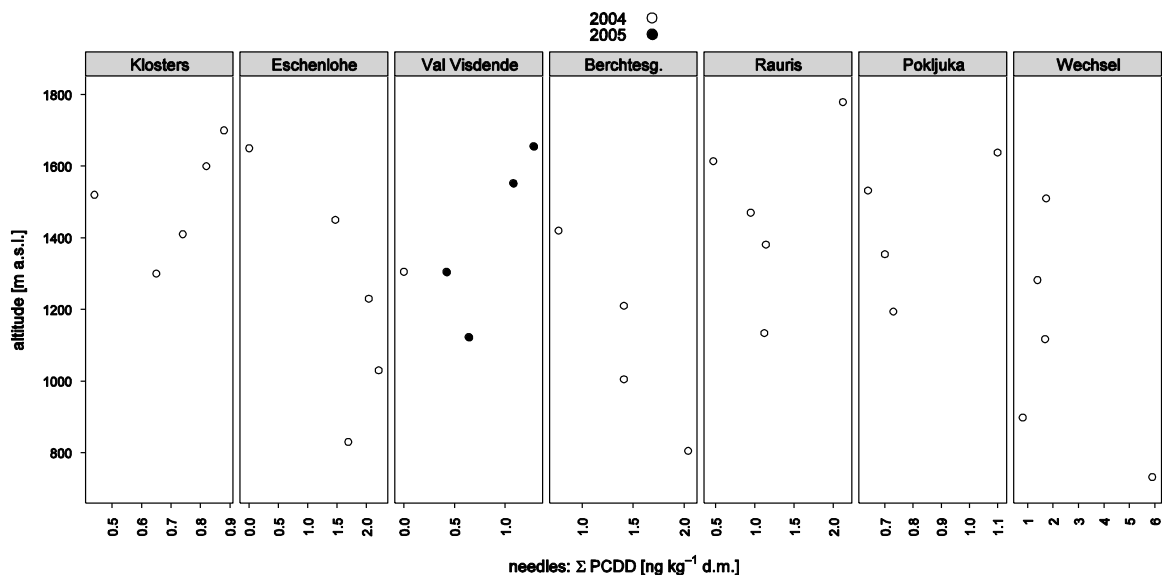


Figure 3-196: Altitudinal variation of the PCDD sum in 0.5 year old Norway spruce needles

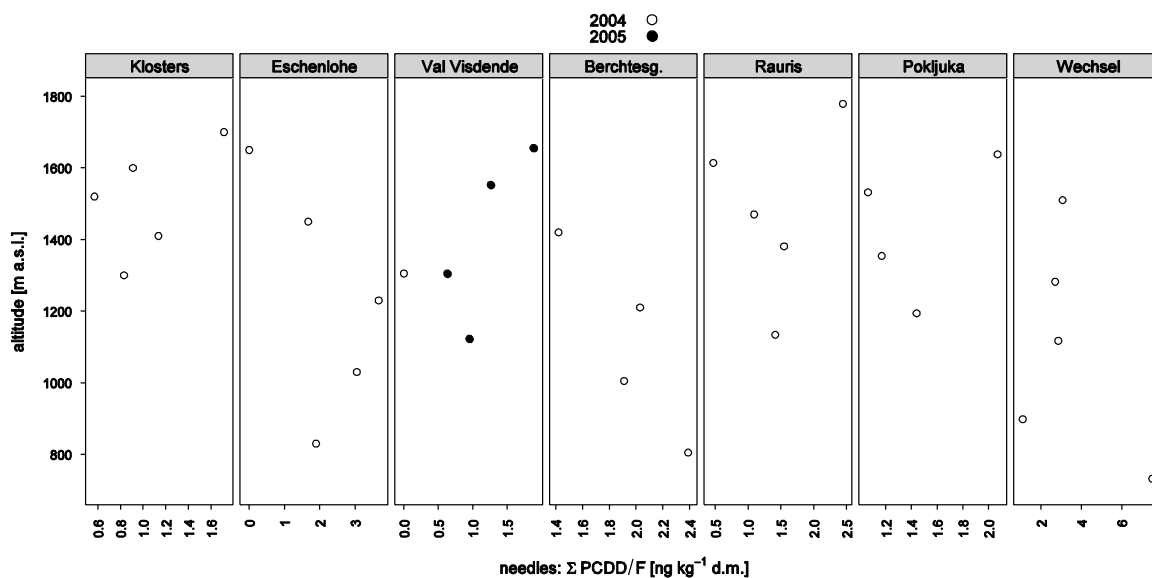


Figure 3-197: Altitudinal variation of the PCDD/F sum in 0.5 year old Norway spruce needles

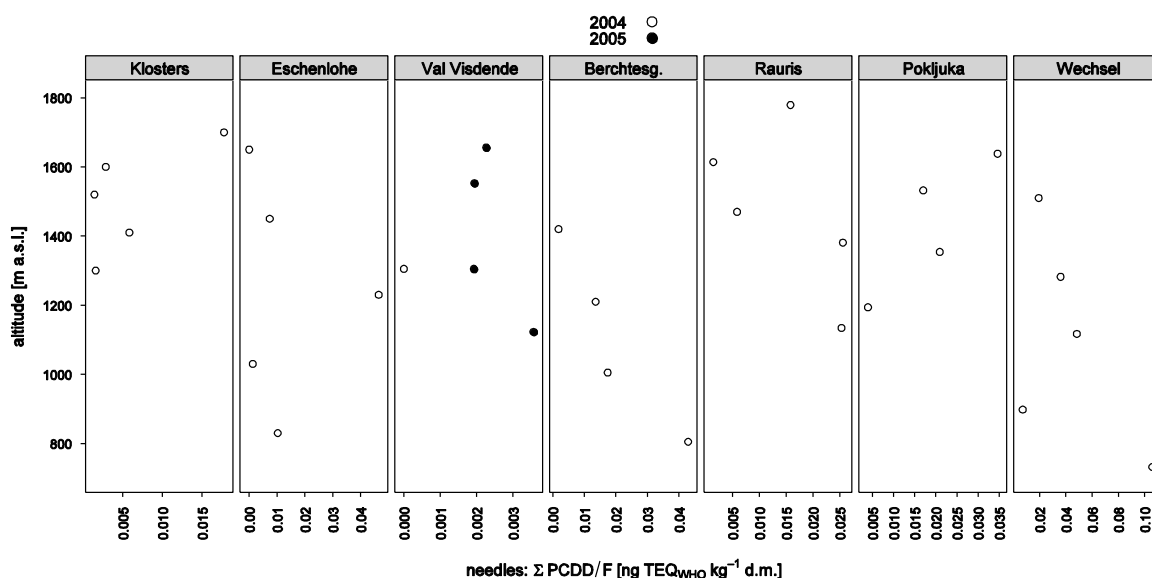


Figure 3-198: Altitudinal variation of the PCDD/F sum (in WHO toxic equivalents) in 0.5 year old Norway spruce needles

3.6.5.2 Humus

As observed earlier, altitudinal patterns varied widely between individual height profiles. As one common trend, however, the dioxin:furan ratio (Σ PCDD : Σ PCDF) decreased with height at most profiles (Figure 3-203).

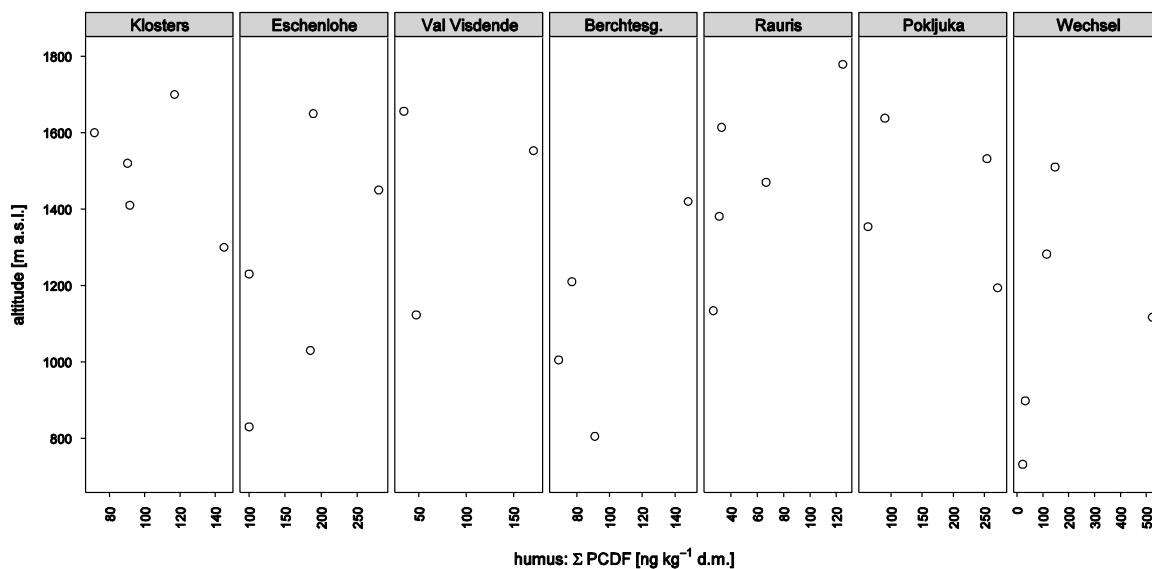


Figure 3-199: Altitudinal variation of the PCDF sum in forest humus

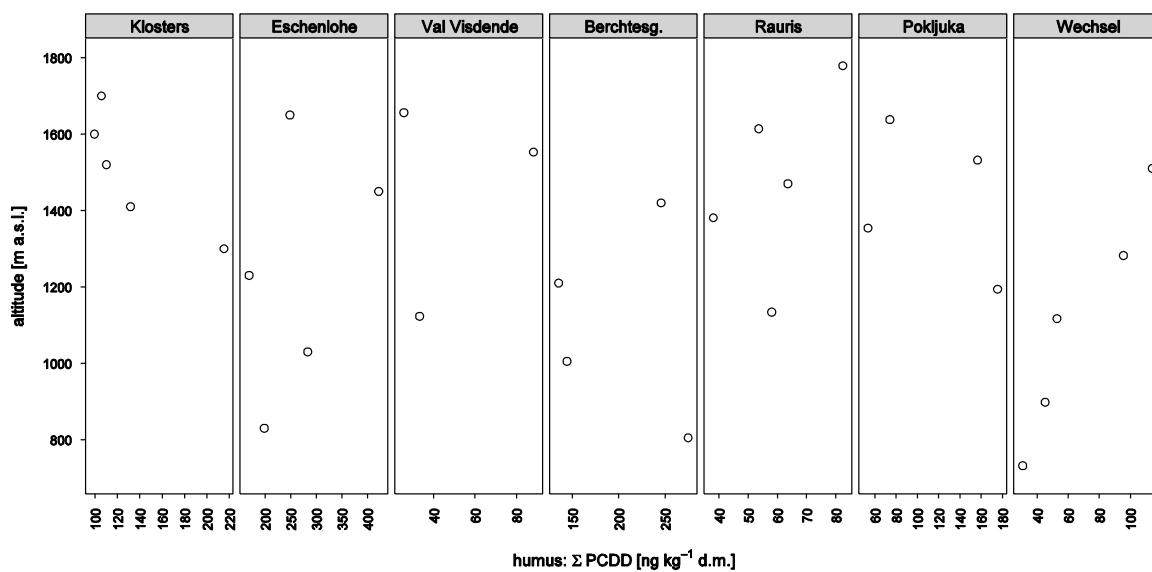


Figure 3-200: Altitudinal variation of the PCDD sum in forest humus

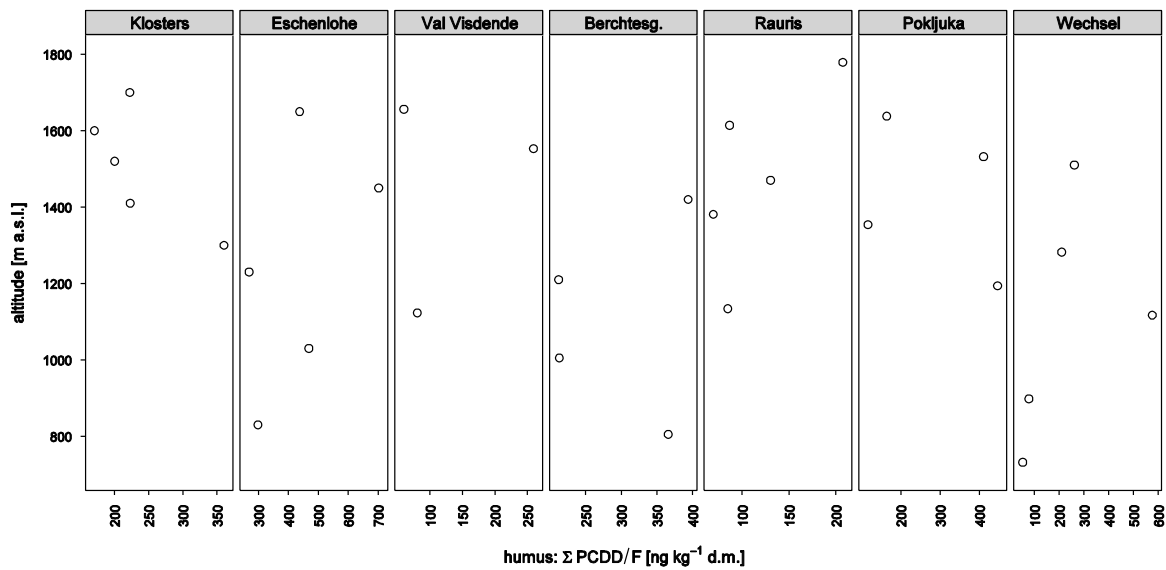


Figure 3-201: Altitudinal variation of the PCDD/F sum in forest humus

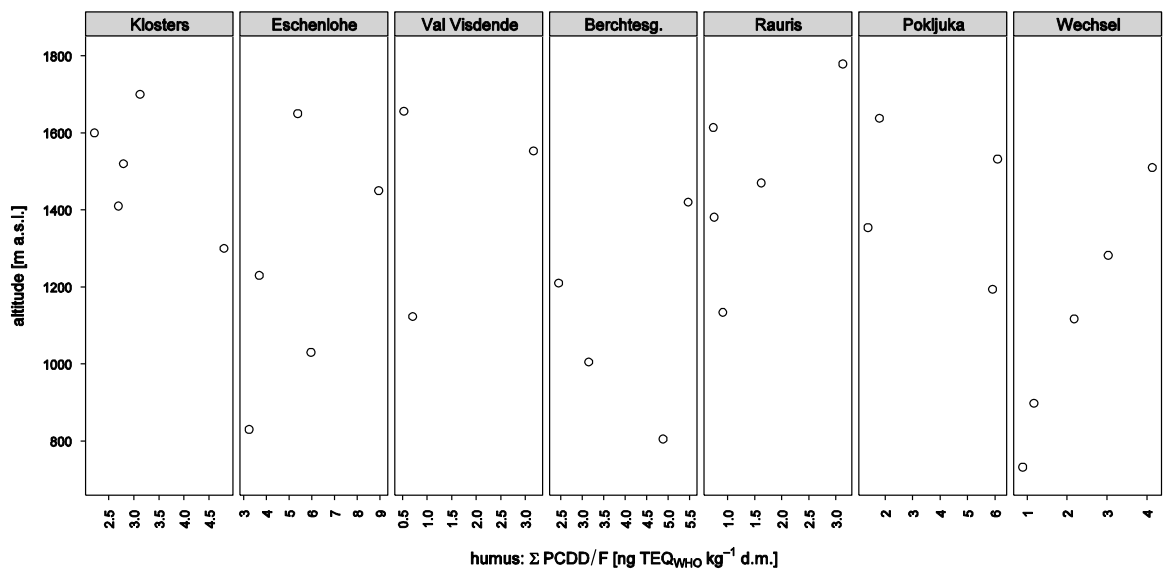


Figure 3-202: Altitudinal variation of the PCDD/F sum (in WHO toxic equivalents) in forest humus

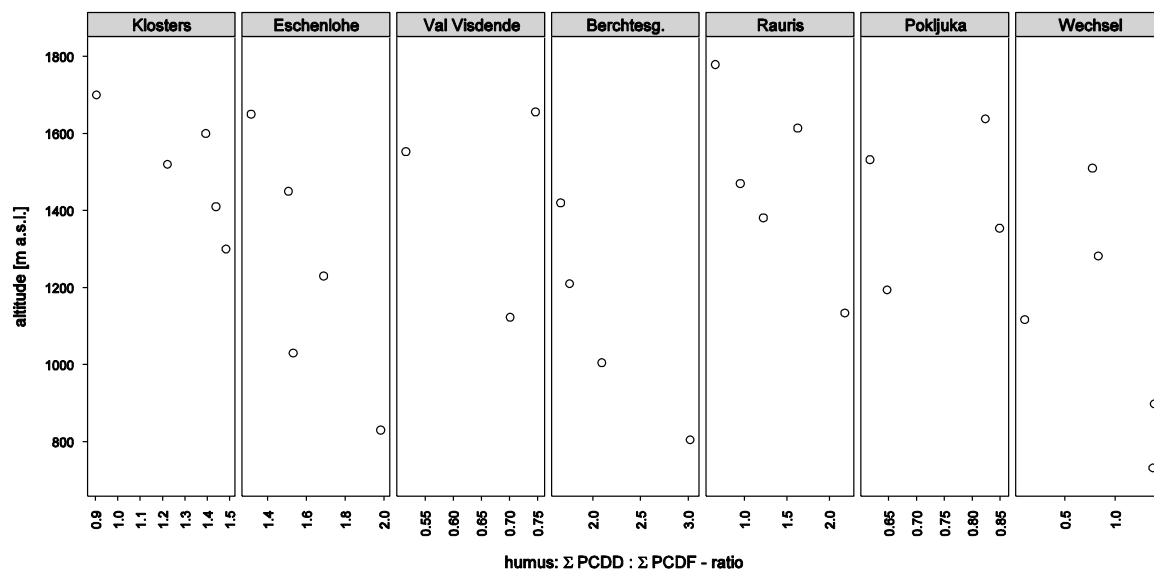
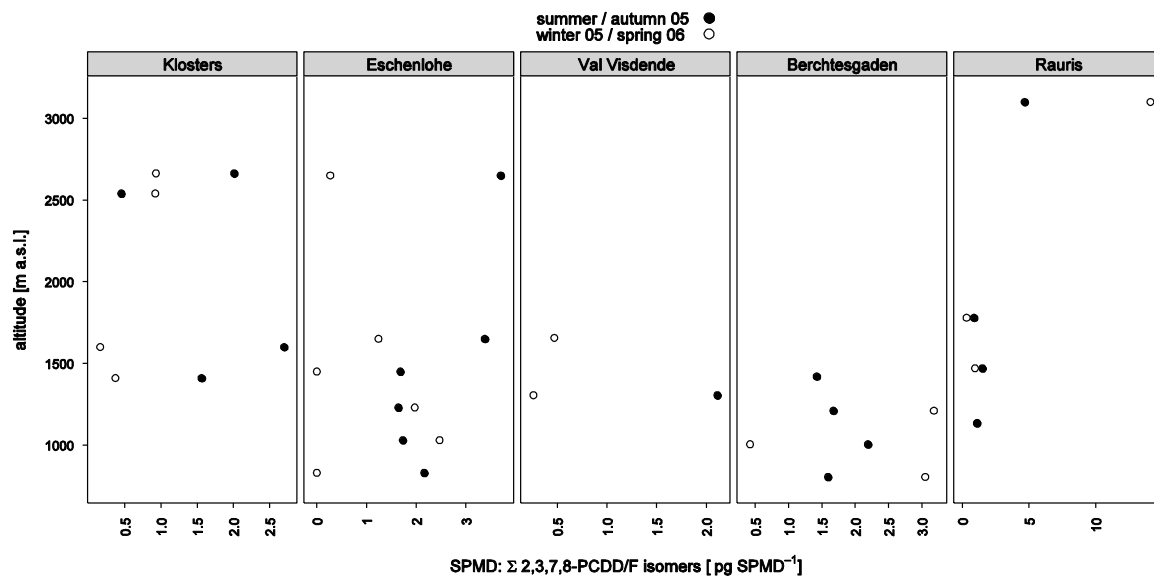


Figure 3-203: Altitudinal variation of the PCDD : PCDF ratio in forest humus.

3.6.5.3 SPMD



Extreme value of 111.9 pg SPMD⁻¹ at Berchtesgaden, 1420 m, not included in graph.

Figure 3-204: Altitudinal variation of dioxin and furan content (2,3,7,8-isomers only) in SPMD

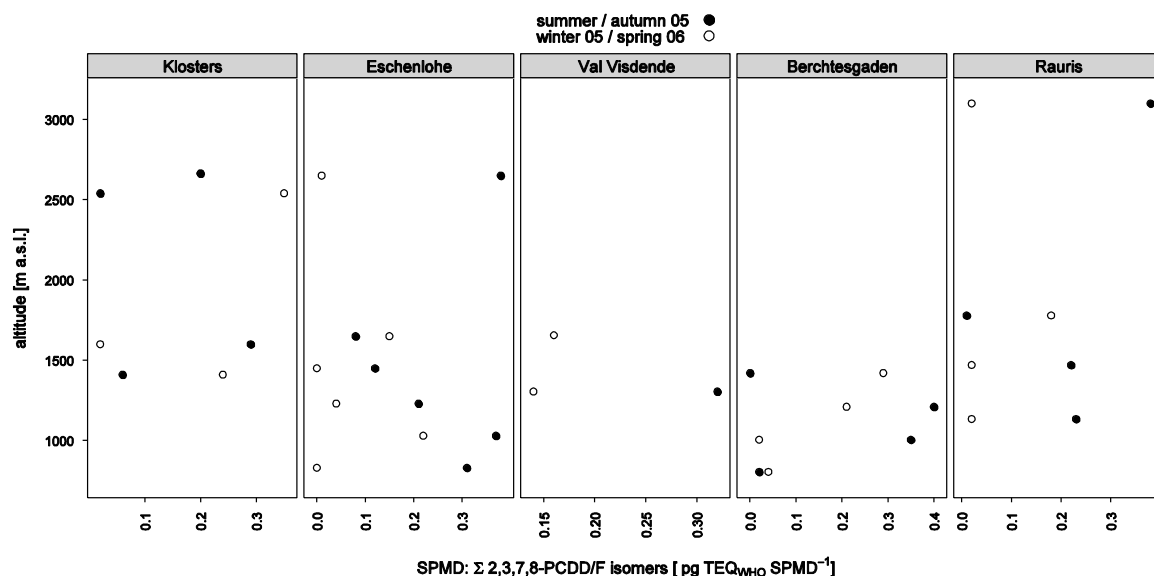


Figure 3-205: Altitudinal variation of dioxin and furan content (in WHO toxic equivalents; 2,3,7,8-isomers only) in SPMD

3.7 Polychlorinated biphenyls (PCB)

3.7.1 Characterization

3.7.1.1 Physicochemical properties

Polychlorinated biphenyls (PCBs) consist of two linked benzene rings with 1–10 chlorine substituents (Figure 3-206). 209 individual congeners are possible. Commercial PCB products are always mixtures of different congeners. PCBs are highly insoluble in water and soluble in most organic solvents. They are semi-volatile and can be therefore expected to partition into the atmosphere (WHO 2003).

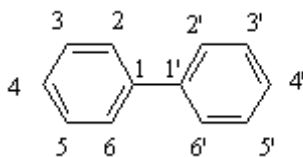


Figure 3-206: Molecular structure of PCBs. Each of the numbered positions can hold a chlorine substituent.

Table 3-32: Physical properties (range) of PCBs at 20–25°C

	monochlorobiphenyl	decachlorobiphenyl
molecular weight (g mol^{-1})	188.7	498.7
water solubility (mg l^{-1})	1.21–5.50	7.61×10^{-4}
vapour pressure (Pa)	0.9–2.5	3×10^{-4}
$\log K_{ow}$	4.30–4.60	8.26

data from Mackay et al. 1992, Vol. I

3.7.1.2 Emissions and use

PCBs have been produced since 1930 for a variety of industrial uses (e. g., dielectrics in transformers and large capacitors, heat exchange fluids). Since 1973, the 24 OECD member countries have restricted production, sales, import, export, and use of PCBs. By the end of 1980, the total world production of PCBs was higher than one million tons. Current sources of PCB include volatilization from landfills containing transformer, capacitor and other PCB waste, and improper (or illegal) disposal to open areas. Another potential source is the combustion of industrial and municipal waste. At present, the main cause for environmental PCB exposure appears to be the redistribution of previously introduced PCBs (WHO 1993).

3.7.1.3 Environmental behaviour and bioaccumulation

PCBs are ubiquitous in the environment, and residues have been detected in the arctic air, water and organisms. Due to their semi-volatility, lipophilicity and low water solubility, PCBs are highly persistent. They can be expected to partition into the atmosphere and accumulate in food chains, which predisposes them to environmental persistence and to long-range transport. They adsorb to particles in air, water, soil and sediment and accumulate in fat-containing tissue; adsorption increases with the degree of chlorination. The strong adsorption causes their mobility in soil and sediments to be negligible. Air is supposed to be the most significant compartment for environmental distribution. It has been demonstrated that PCBs can be transported by currents, wind and atmospheric diffusion over long distances from source areas (WHO 2003).

The high lipid solubility and the low water solubility lead to the retention of PCBs and their metabolites in fatty tissues. Protein binding may also contribute to their tissue retention. The rates of bioaccumulation vary with the species, duration and concentration of exposure, and the environmental conditions. The strong retention of PCBs and their metabolites means that toxic effects can also occur in organisms after and remote from the initial PCB release. The bioconcentration factor for, e. g., Arochlor 1254 in aquatic organisms ranges from 0.24 to 165 000, in birds and mammals from 5.15 to 28.5 (WHO 2003). In general, the higher chlorinated congeners accumulate more readily (WHO 1993).

3.7.1.4 Toxicology

Twelve PCB congeners with dioxin-like receptor binding activity have been assigned toxic equivalency factors (TEFs) in the dioxin TEF scheme. To date, non dioxin-like PCBs are toxicologically poorly characterised. However the available information suggests that typical effects of PCBs exposure – including carcinogenicity, immunotoxicity and neurobehavioral alterations – can be caused by all PCB congeners. Human exposure to PCBs, whether dioxin-like or not, may reach estimated LOAEL (lowest observable adverse effect levels) for neurodevelopmental effects in infants. The weight of evidence suggests an increased health risk from current exposure (WHO 2003).

3.7.2 Overview of results

Humus showed about ten times as high PCB levels as mineral soil or Norway spruce needles, the latter two matrices having comparable PCB contents. Apart from these quantitative differences, the congener profile of the six “indicator” PCB in needles was shifted towards the lighter PCB, in contrast to the PCB patterns of humus

and mineral soil which were characterised by higher shares of the heavier PCB (characteristically congener 153). This prevalence of lighter, more volatile non dioxin-like PCB was even more drastic in deposition samples from three alpine summits. No such pronounced differences were observed for the profiles of the dioxin-like congeners. Congeners 118 and 105 clearly dominated the spectra in these forest compartments – as well as in the deposition samples and ambient air samples taken at the mountain tops. In ambient air samples, however, a third congener (PCB 156) ranked second after PCB 118.

The seasonal variation of PCB levels in alpine air showed no substantial differences between different sampling sites (Mt. Weissfluhjoch, Mt. Zugspitze, Mt. Sonnblick). Deposition trends at Mt. Zugspitze and Mt. Sonnblick were comparable, but showed some deviation from the seasonal variations at Mt. Weissfluhjoch which, curiously, had the lowest deposition – and highest atmospheric – PCB levels of all three sites.

Unlike other pollutant groups, the highest atmospheric PCB concentrations repeatedly, and consistently across sites and sampling periods, were measured in air from a particular source region, namely northeastern Europe. Quite contrarily, the geographic distribution of PCB in needle samples shows a cumulation of several PCB in the southern and western parts of the studied area. Similar to PCDD/F and PAH, the highest PCB contamination of humus was generally found at the northern border of the study region. Moreover, with the exception of congener 169, the highest PCB levels (median) were never found in the central part of the investigated alpine area.

3.7.3 Summary statistics

As observed with most of the investigated pollutant classes, humus was far more contaminated with PCB than mineral soil and needles. It contained roughly ten times as much dioxin-like PCB or indicator PCB as needles and mineral soil. The PCB levels of needles and mineral soil were similar.

There were no marked differences between the congener profiles of dioxin-like PCB in either matrix (Figure 3-207). Regarding the six “indicator” PCB which were found at much higher concentrations, the congener profile found in needles was shifted towards the lighter, more volatile PCB. Humus and mineral soil were characterised by larger shares of the heavier congeners.

3.7.3.1 Needles

Table 3-33: Concentrations of polychlorinated biphenyls in 0.5 year old Norway spruce needles

PCB no.	n < LOD	mean	sd	min	P ₁₀	P ₂₅	median	P ₇₅	P ₉₀	max
77	0	12.7	7.1	3.2	7.4	9.7	11.0	13.0	17.3	40.0
81	6	0.61	0.68	<LOD	<LOD	0.36	0.48	0.62	0.99	4.20
126	12	1.07	1.33	<LOD	<LOD	<LOD	0.92	1.40	1.91	7.80
169	35	–	–					<LOD	0.10	4.10
105	0	30.0	17.8	11.0	15.9	20.8	26.0	30.3	44.6	96.0
114	5	1.52	1.05	<LOD	<LOD	1.08	1.50	1.83	2.43	5.80
118	0	64.0	31.1	29.0	40.7	48.8	56.0	67.5	91.0	180.0
123	10	2.81	4.54	<LOD	<LOD	0.00	0.94	3.00	9.57	19.00
156	0	7.56	4.10	0.28	3.69	4.80	6.80	9.03	11.40	19.00
157	0	1.85	1.39	0.37	0.92	1.20	1.60	1.95	2.67	8.60
167	0	4.19	2.72	1.20	1.97	2.73	3.50	5.00	5.77	15.00
189	1	1.03	0.90	<LOD	0.42	0.64	0.88	1.13	1.51	5.90
Σ dl-PCB	–	127.5	67.5	56.1	78.6	92.3	110.6	134.7	177.1	362.0
" in TEQ _{WHO}	–	0.125	0.145	0.008	0.010	0.015	0.108	0.156	0.212	0.868
28	0	196.8	96.5	16.0	108.6	127.5	190.0	250.0	292.0	550.0
52	0	154.7	94.0	32.0	76.2	86.5	115.0	212.5	271.0	470.0
101	0	189.3	73.3	110.0	130.0	160.0	170.0	200.0	233.0	490.0
138	0	126.6	59.8	63.0	84.8	89.0	120.0	150.0	172.0	340.0
153	7	178.1	126.3	<LOD	<LOD	127.5	180.0	242.5	283.0	560.0
180	0	59.7	35.9	19.0	29.8	33.0	51.0	71.5	84.6	200.0
Σ 6 PCB	–	905	402	394	530	652	815	1043	1276	2370

unit: ng kg⁻¹ d.m., sample size n=40, n < LOD...number of observations below the detection limit

3.7.3.2 Humus

Table 3-34: Concentrations of polychlorinated biphenyls in forest humus

PCB no.	mean	sd	min	P ₁₀	P ₂₅	median	P ₇₅	P ₉₀	max
77	75.0	36.1	22.0	42.0	48.0	67.0	91.0	130.0	170.0
81	2.72	1.18	0.81	1.20	2.05	2.60	3.30	4.30	5.70
126	20.6	9.4	6.1	10.0	13.5	18.0	27.0	32.0	44.0
169	2.3	1.1	< LOD	1.1	1.5	2.3	3.1	3.8	4.9
105	329	164	80	150	215	310	420	570	780
114	10.9	4.9	2.2	5.8	7.0	11.0	14.0	18.0	23.0
118	784	382	190	430	520	740	1000	1400	1600
123	20.4	20.8	< LOD	6.7	12.0	18.0	23.5	28.0	120.0
156	178.8	86.3	62.0	80.0	110.0	160.0	250.0	290.0	350.0
157	37.0	18.0	14.0	16.0	22.5	33.0	49.0	68.0	73.0
167	101.0	48.1	37.0	47.0	62.5	90.0	145.0	170.0	190.0
189	29.7	15.6	11.0	12.0	18.0	26.0	42.0	52.0	72.0
Σ dl-PCB	1591	748	439	807	1067	1482	1985	2635	3266
" in TEQ _{WHO}	2.32	1.06	0.70	1.13	1.51	2.06	3.01	3.59	4.92
28	239	79	100	150	175	240	295	350	420
52	654	1003	93	160	205	260	425	1600	3800
101	921	440	300	490	575	860	1150	1400	2000
138	1900	817	730	920	1200	1800	2450	2900	3600
153	3000	1250	1200	1600	1950	2800	3950	4700	5500
180	1586	797	590	740	970	1500	1950	2600	3600
Σ 6 PCB	8301	3605	3160	4380	5005	7670	11040	12700	17220

unit: ng kg⁻¹ d.m., sample size n=31; one value below detection limit for PCBs 169 and 123.

3.7.3.3 Mineral soil

Table 3-35: Concentrations of polychlorinated biphenyls in forest mineral soil.

PCB no.	n < LOD	mean	sd	min	P ₁₀	P ₂₅	median	P ₇₅	P ₉₀	max
77	0	11.82	9.93	1.90	2.98	5.05	8.90	15.75	22.20	38.00
81	5	0.39	0.40	0.00	0.00	0.12	0.31	0.55	0.70	1.60
126	1	3.69	3.68	0.00	0.47	1.18	2.05	5.15	9.20	14.00
169	0	0.78	0.66	0.18	0.23	0.33	0.54	0.98	1.94	2.30
105	0	43.2	41.3	5.1	11.3	18.5	23.5	63.3	87.5	170.0
114	2	1.40	1.33	0.00	0.28	0.53	1.10	1.93	2.61	5.40
118	0	97.7	97.1	10.0	22.8	42.8	53.5	132.5	184.0	380.0
123	0	2.37	2.17	0.24	0.71	1.28	1.50	3.13	4.53	9.70
156	0	27.8	27.3	2.0	6.5	9.9	16.0	37.3	59.8	110.0
157	0	6.13	5.70	0.40	1.82	2.35	3.65	7.93	12.30	23.00
167	0	18.24	16.92	0.78	4.65	6.40	11.50	23.75	43.20	65.00
189	0	5.14	4.74	0.34	1.38	1.78	3.10	6.95	11.20	18.00
Σ dl-PCB	–	218.6	207.3	21.3	55.8	98.0	122.0	298.0	450.9	831.4
" in TEQ _{WHO}	–	0.41	0.41	0.01	0.06	0.14	0.23	0.57	1.01	1.55
28	0	35.25	27.17	9.10	12.69	17.25	25.00	43.50	91.00	91.00
52	0	34.1	32.3	8.7	9.5	14.5	26.0	32.8	73.1	140.0
101	0	110.9	105.4	15.0	30.9	41.8	72.5	132.5	237.0	430.0
138	0	308	285	23	78	118	210	415	761	1100
153	0	433	412	36	108	165	280	583	1100	1600
180		213.0	203.7	17.0	59.7	73.3	120.0	285.0	465.0	770.0
Σ 6 PCB		1135	1017	109	313	496	747	1447	2744	4012

unit: ng kg⁻¹ d.m., sample size n=20; LOD...detection limit

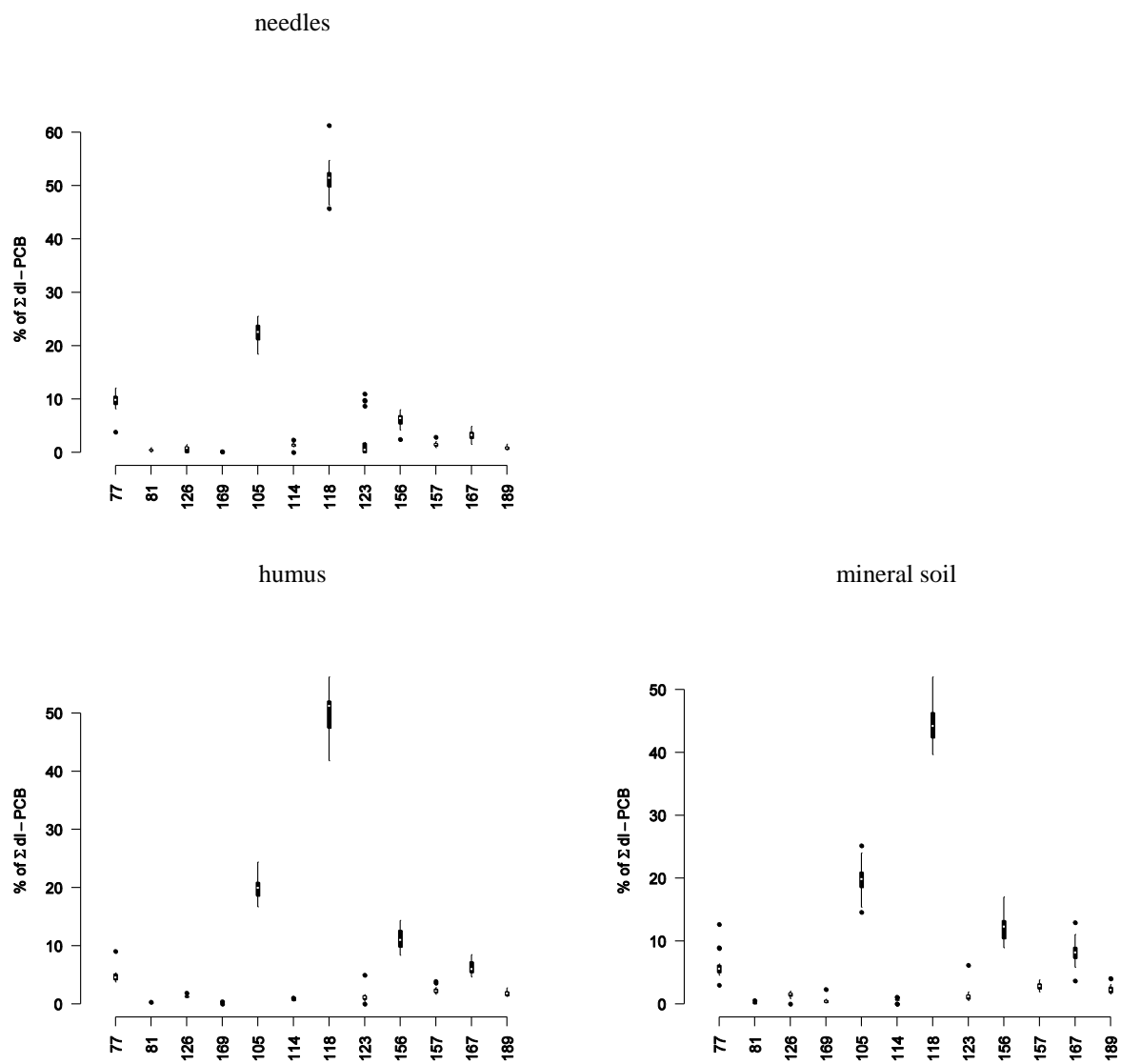


Figure 3-207: Congener pattern of dioxin-like PCB in 0.5 year old Norway spruce needles, forest humus and mineral soil

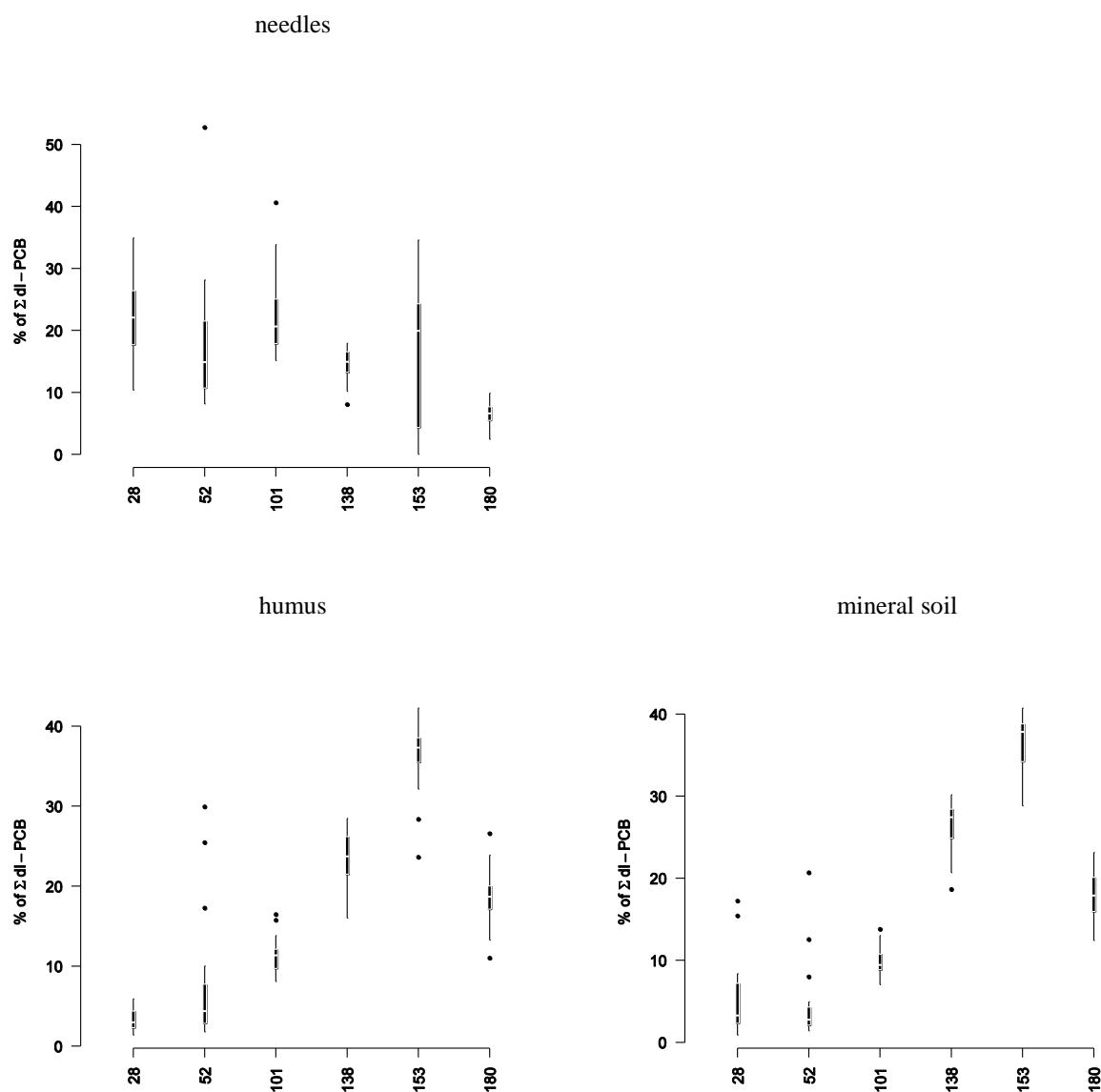


Figure 3-208: Congener pattern of 6 indicator-PCB in 0.5 year old Norway spruce needles, forest humus and mineral soil

3.7.3.4 Deposition and air

Of the dioxin-like PCB, congeners 81, 126, 114, 169 were found in only few deposition samples. Notably, the few positive samples were those from the period spring–late summer 2005, regardless of sampling site. Atmospheric PCB concentrations at the Swiss Mt. Weissfluhjoch were considerably higher than at the two other summits. (The same was observed for atmospheric PBDE concentrations: p. 138 ff). At all three sites, total PCB concentrations in air showed similar variations between sampling periods. Unlike, e. g., the temporal trends of chloropesticides in air (p. 60 ff), these variations are not easily interpreted by ambient temperature, because there are large differences between periods of low temperature (winter 2005/6 vs. late autumn 2006–late winter 2007), while different seasons had comparable atmospheric PCB levels (spring–early summer 2006 vs. spring 2007): Figure 3-228–Figure 3-230.

Table 3-36: Deposition of dioxin-like PCB on three alpine summits

	period	77	81	126	169	105	114	118	123	156	157	167	189	Σ dl-PCB	Σ dl-PCB in TEQ _{WHO}
Weissfluhjoch	A	9.3	0.29	2.6	0.37	42	1.5	86	1.5	28	5.4	14	3.9	194.9	0.296
	B	8	<LOD	<LOD	<LOD	33	<LOD	61	1.4	19	3	8.6	2.9	136.9	0.022
	C	8.4	<LOD	<LOD	<LOD	27	<LOD	52	1.2	15	2.4	7.1	2.1	115.2	0.018
	D	24	<LOD	<LOD	<LOD	68	<LOD	110	<LOD	41	4.4	15	3.6	266	0.043
	E	8.2	<LOD	<LOD	<LOD	33	<LOD	71	4.6	24	<LOD	11	6.3	158.1	0.024
	F	–	<LOD	<LOD	<LOD	62	<LOD	250	<LOD	190	13	68	19	602	0.135
Zugspitze	A	11	0.46	2.6	0.43	37	1.7	82	14	33	4.8	17	5.3	209.3	0.299
	B	9.5	<LOD	<LOD	<LOD	34	<LOD	76	<LOD	65	6.7	28	16	235.2	0.05
	C	7.2	<LOD	<LOD	<LOD	22	<LOD	64	4.7	25	4.1	17	5.2	149.2	0.025
	D	23	<LOD	<LOD	<LOD	78	<LOD	170	9.8	140	13	52	24	509.8	0.108
	E	13	<LOD	<LOD	<LOD	55	<LOD	250	<LOD	100	12	76	27	533	0.091
	F	–	<LOD	<LOD	<LOD	28	<LOD	130	<LOD	70	4.8	21	7.8	261.6	0.054
Sonnblick	A	12	0.41	2.1	0.38	31	1.3	63	1.3	24	3.9	12	3.9	155.3	0.24
	B	11	1.1	2.8	<LOD	40	1.8	59	2.2	26	4.4	13	5.7	167	0.308
	C	7.9	<LOD	<LOD	<LOD	25	<LOD	55	<LOD	21	2.2	6.7	2.7	120.5	0.021
	D	8.7	<LOD	<LOD	<LOD	75	<LOD	130	<LOD	42	<LOD	<LOD	<LOD	255.7	0.042
	E	34	<LOD	<LOD	<LOD	68	<LOD	760	43	290	17	240	<LOD	1452	0.246
	F	14	<LOD	<LOD	<LOD	50	<LOD	120	<LOD	86	<LOD	41	<LOD	311	0.061

unit: $\text{pg m}^{-2} \text{d}^{-1}$; LOD...detection limit; A...spring–late summer 2005, B...late summer 2005–late winter 2006, C...late winter–summer 2006, D...summer–autumn 2006, E...autumn 2006–late winter 07, F...late winter–spring 2007

Table 3-37: Deposition of indicator PCB on three alpine summits

	period	28	52	101	138	153	180	Σ 6 PCB
Weissfluhjoch	A	81	63	160	230	390	180	1104
	B	110	59	91	160	210	130	760
	C	84	54	94	100	150	100	582
	D	210	160	240	350	480	280	1720
	E	160	99	200	290	360	250	1359
	F	220	200	760	980	1700	1300	5160
Zugspitze	A	140	94	190	250	420	230	1324
	B	260	130	220	420	540	560	2130
	C	110	76	200	270	400	230	1286
	D	300	240	650	1200	1800	1000	5190
	E	140	300	1500	1100	3900	1200	8140
	F	98	120	370	470	580	440	2078
Sonnblick	A	120	70	140	200	280	180	990
	B	170	80	120	230	270	200	1070
	C	130	65	110	150	200	140	795
	D	240	160	330	430	700	390	2250
	E	210	350	2300	3400	12000	4600	22860
	F	160	130	430	590	930	860	3100

unit: $\text{pg m}^{-2} \text{d}^{-1}$; A...spring–late summer 2005, B...late summer 2005–late winter 2006, C...late winter–summer 2006, D...summer–autumn 2006, E...autumn 2006–late winter 07, F...late winter–spring 2007

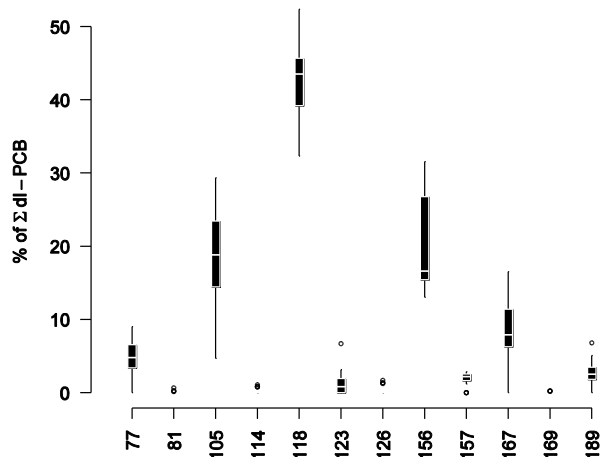


Figure 3-209: Congener pattern of dioxin-like PCB in deposition on three alpine summits

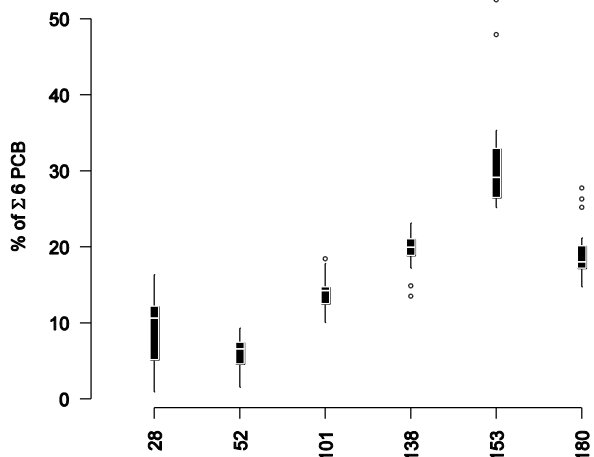


Figure 3-210: Congener pattern of indicator PCB in deposition on three alpine summits

Table 3-38: PCB concentrations in ambient air at three alpine summits

	period	77	81	126	169	105	114	118	123	156	157	167	189	Σ dl-PCB	Σ dl-PCB as TEQ _{WHO}
Weissfluh	I	142.1	9.11	6.50	1.42	409	22.45	1090	138.73	240.2	32.36	112.57	26.63	2231	0.99
	II	359.5	–	–	–	1380	50.40	3938	172.17	411.3	52.15	187.98	29.35	6581	0.85
	III	472.9	0.99	0.91	0.40	982	8.08	2201	113.54	529.1	19.74	115.83	21.90	4467	0.75
	IV	80.6	8.82	–	1.68	317	4.56	814	11.92	112.0	16.42	43.36	15.25	1426	0.21
	V	443.6	–	13.53	–	1765	60.25	5290	96.68	870.8	60.47	309.32	44.00	8954	2.62
Zugspitze	I	137.5	7.50	9.93	1.02	425	22.61	1152	142.33	314.8	36.64	141.92	37.81	2429	1.38
	II	114.2	2.61	–	1.04	425	17.47	1223	41.19	189.2	25.79	93.89	16.08	2150	0.31
	III	111.0	3.26	–	–	291	8.10	640	7.76	101.7	15.77	52.92	11.96	1243	0.17
	IV	67.8	3.74	0.71	1.13	199	4.84	519	13.31	102.3	9.14	35.32	12.34	969	0.22
	V	90.6	0.29	–	–	344	0.81	1108	9.30	290.1	34.17	104.66	22.65	2005	0.32
Sonnblick	I	97.2	6.74	–	–	264	19.51	653	60.44	171.1	24.24	72.01	19.99	1388	0.22
	II	69.5	–	–	–	222	3.43	599	70.53	90.5	11.34	38.19	6.47	1111	0.15
	III	74.6	2.68	–	–	184	4.13	398	5.50	62.1	6.85	25.48	7.12	771	0.10
	IV	24.6	–	–	–	65	1.39	188	12.43	31.8	2.07	6.35	2.79	334	0.05
	V	55.2	0.82	–	–	185	–	619	31.27	170.0	7.44	50.63	9.53	1129	0.18

unit: fg m^{-3} at 0 °C and 1013 hPa; sampling periods: I...winter 05/06, II...spring–early summer 06, III...early summer–late aut. 06, IV...late aut. 06–late winter 07, V...spring 07

Table 3-38 (continued) PCB concentrations in ambient air at three alpine summits

	period	28	52	101	138	153	180	Σ 6 PCB
Weissfluh	I	12.11	6.00	2.98	1.99	3.08	1.23	27.39
	II	33.80	20.24	12.82	4.55	7.34	2.15	80.91
	III	29.56	13.73	6.31	3.09	4.96	2.04	59.70
	IV	5.66	5.29	3.21	1.38	2.24	0.87	18.65
	V	63.08	28.49	15.89	6.82	10.98	3.28	128.54
Zugspitze	I	16.23	5.57	3.83	2.44	3.50	1.39	32.95
	II	14.30	5.16	4.13	1.81	3.03	0.83	29.26
	III	6.34	3.50	2.29	1.01	1.83	0.49	15.46
	IV	5.68	2.99	2.09	0.99	1.68	0.57	14.00
	V	15.89	7.27	4.46	2.03	3.47	1.08	34.20
Sonnblick	I	7.83	3.30	1.64	1.35	2.38	0.74	17.24
	II	8.13	3.45	1.90	0.81	1.46	0.50	16.24
	III	3.62	2.17	1.25	0.59	1.13	0.31	9.07
	IV	1.90	1.14	0.54	0.28	0.44	0.19	4.50
	V	11.11	4.51	2.01	1.14	1.66	0.61	21.05

unit: $\mu\text{g m}^{-3}$ at 0 °C and 1013 hPa; sampling periods: I...winter 05/06, II...spring - early summer 06, III...early summer - late aut. 06, IV...late aut. 06 - late winter 07, V...spring 07

Congeners 118 and 156 dominated the pattern of dioxin-like PCB in ambient air (Figure 3-211), while the congener pattern of the six indicator PCB was conspicuously shifted towards the lighter, more volatile congeners (Figure 3-212).

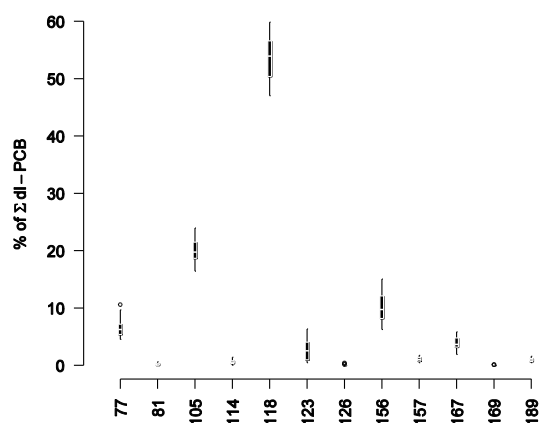


Figure 3-211: Congener pattern of dioxin-like PCB in ambient air at three alpine summits

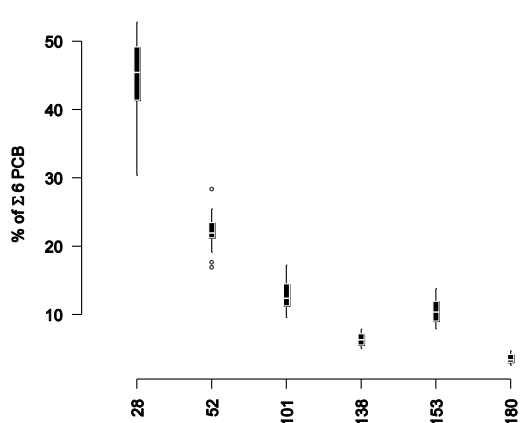
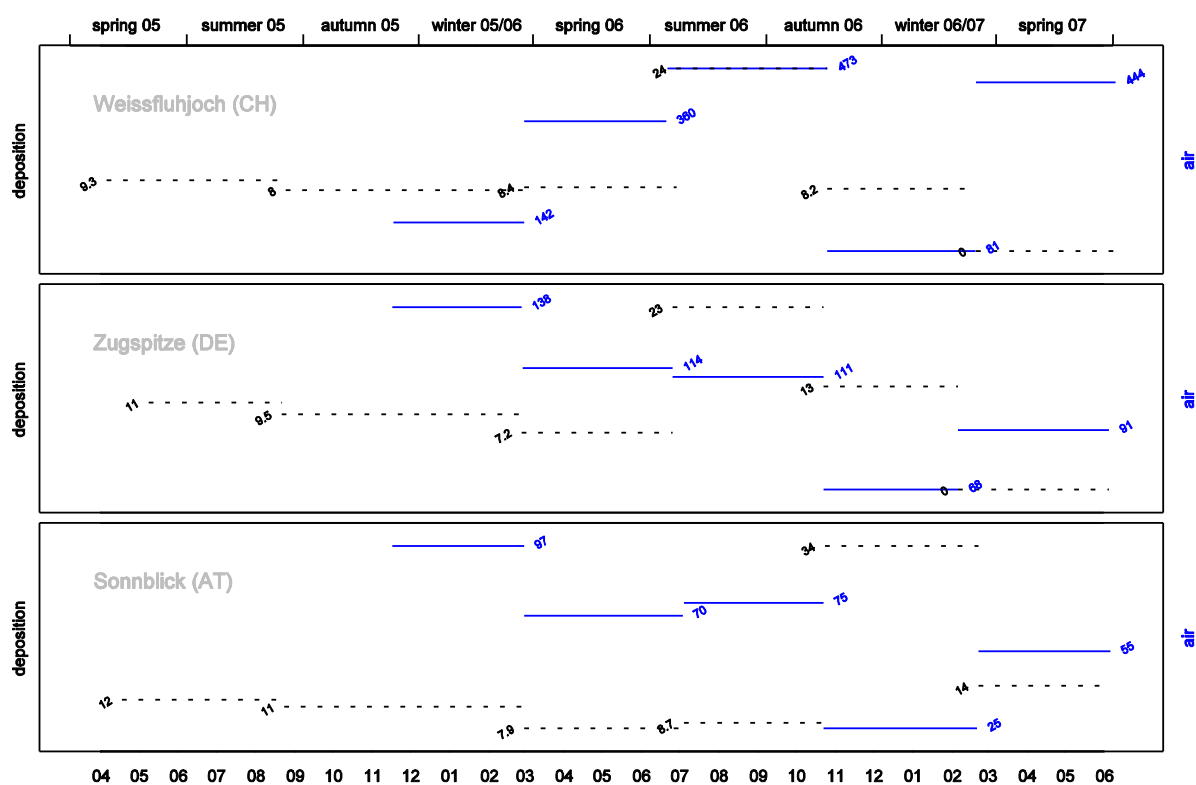
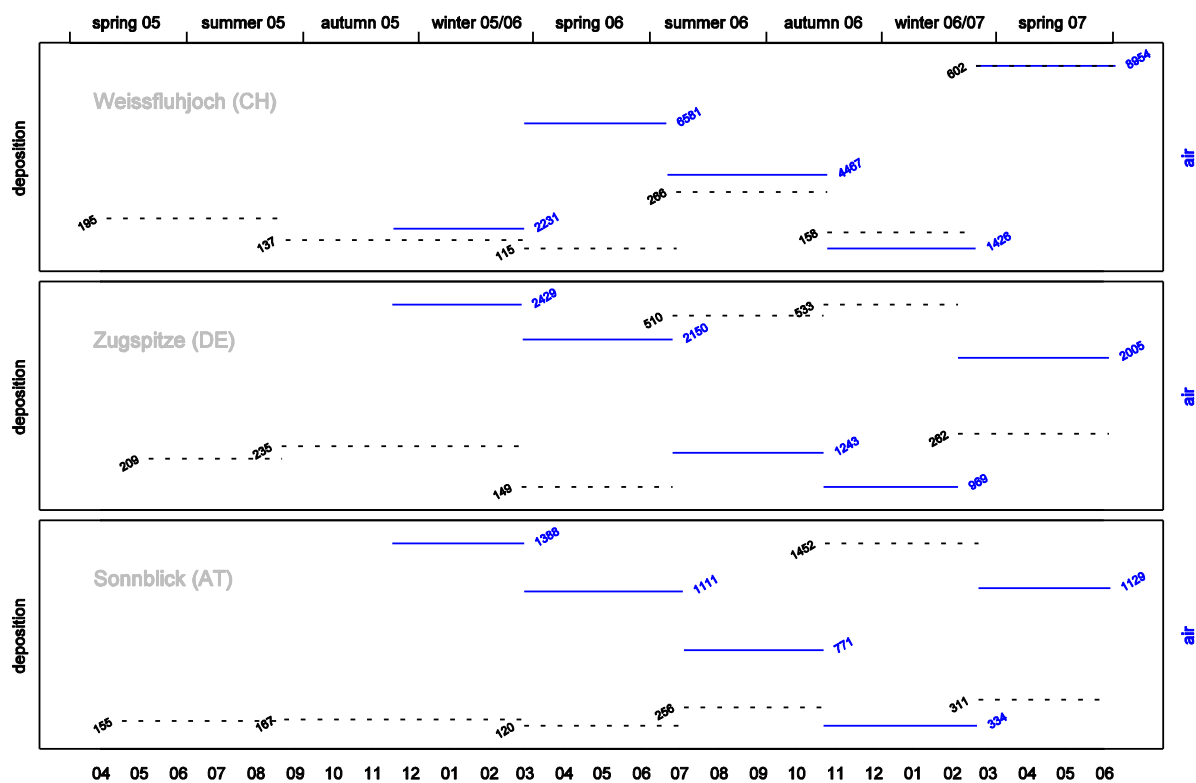


Figure 3-212: Congener pattern of six "indicator" PCB in ambient air at three alpine summits



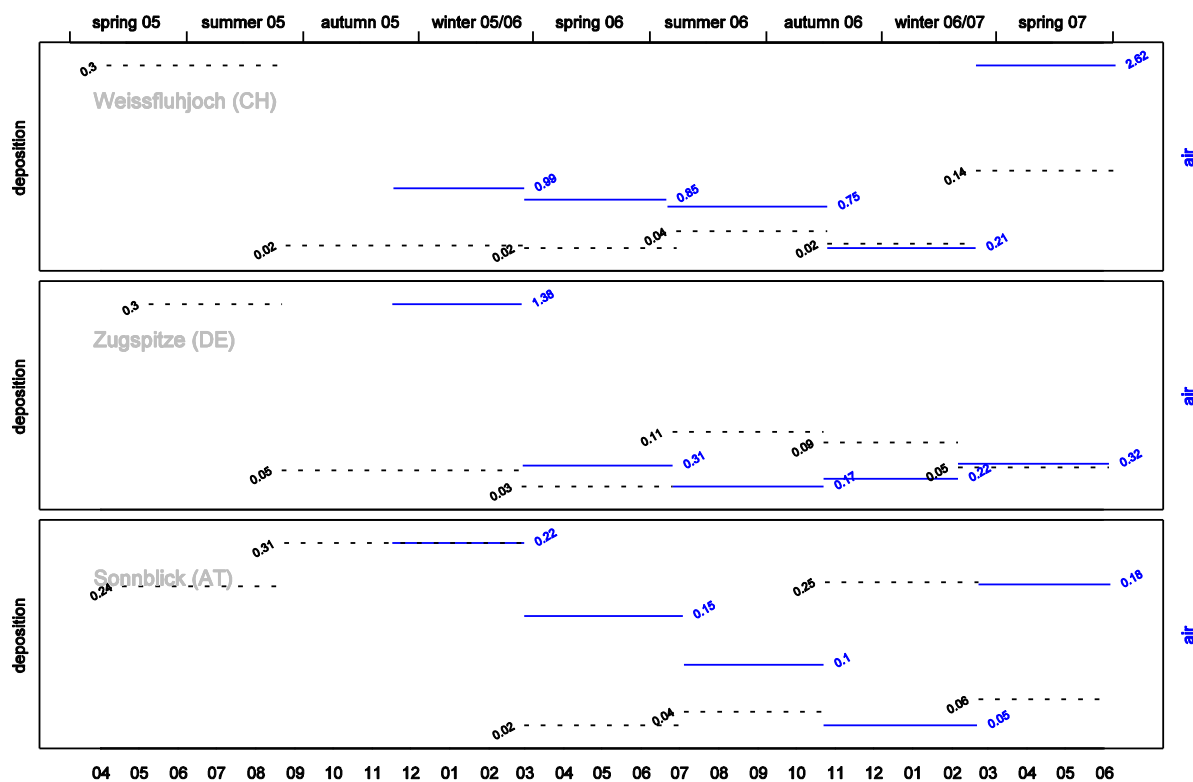
units: deposition: $\text{pg m}^{-2} \text{d}^{-1}$, air: fg m^{-3} at 0 °C and 1013.3 hPa.

Figure 3-213: Concentration of PCB 77 in deposition (---) and ambient air (—) on three alpine summits.



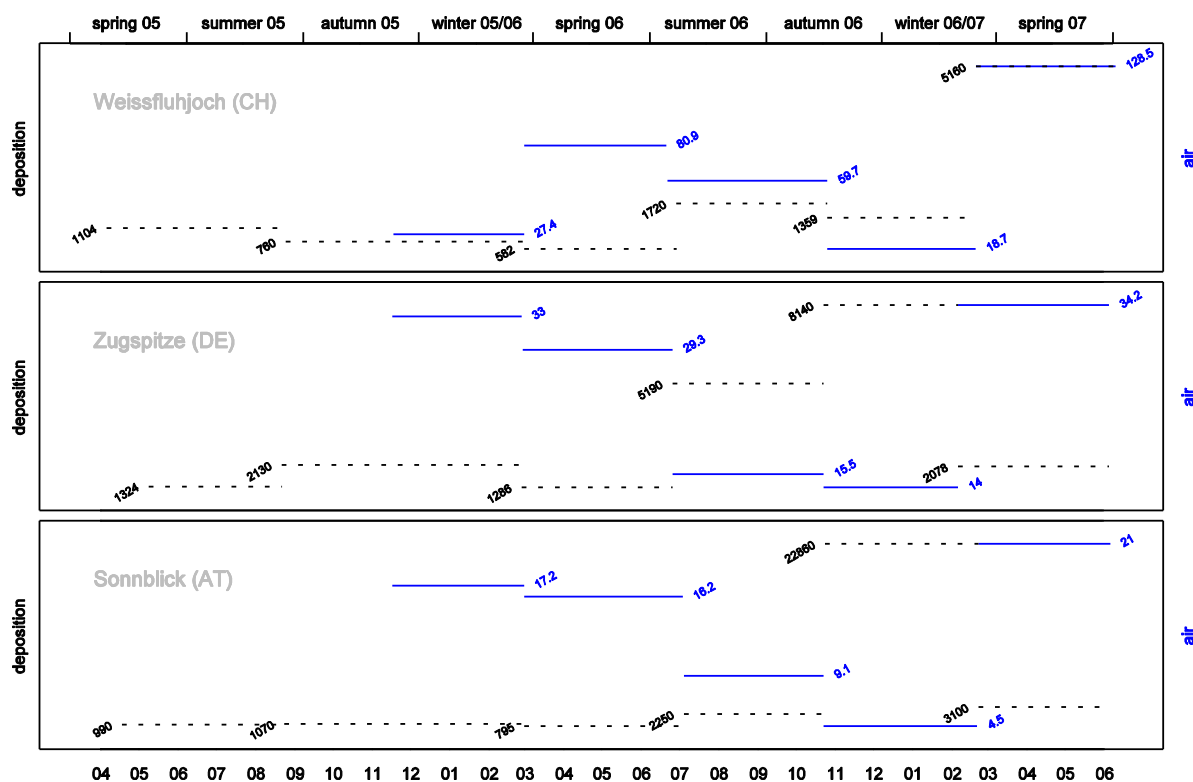
units: deposition: $\text{pg m}^{-2} \text{d}^{-1}$, air: fg m^{-3} at 0 °C and 1013.3 hPa.

Figure 3-214: Total concentration of dioxin-like PCB in deposition (---) and ambient air (—) on three alpine summits.



units: deposition: pg TEQ_{WHO} m⁻² d⁻¹, air: fg TEQ_{WHO} m⁻³ at 0 °C and 1013.3 hPa.

Figure 3-215: Total concentration of dioxin-like PCB in WHO toxic equivalents in deposition (---) and ambient air (—) on three alpine summits.



units: deposition: pg m⁻² d⁻¹, air: pg m⁻³ at 0 °C and 1013.3 hPa.

Figure 3-216: Total concentration of six indicator PCB in deposition (---) and ambient air (—) on three alpine summits.

3.7.4 Spatial variation

A few sites of conspicuously high content of dioxin-like PCB in needles appeared in the western part of the study region (Figure 3-219), and indeed this zone had significantly higher concentrations of dl-PCB than the middle (but not the eastern) zone: Table 3-39. The needle contamination with dioxin-like PCB was significantly higher in the North than in the central part of the investigated region (Table 3-40).

3.7.4.1 Needles

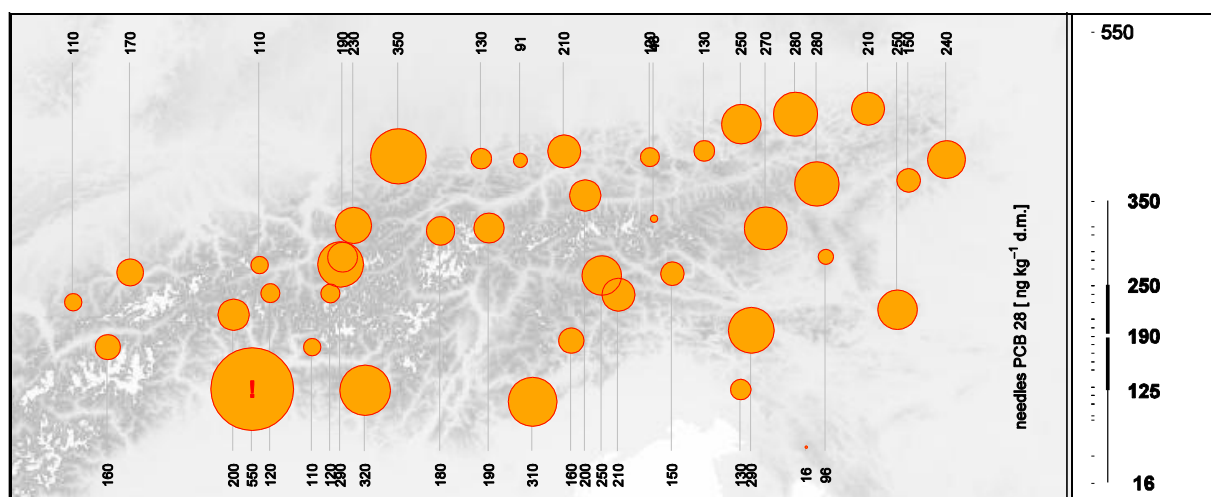


Figure 3-217: PCB 28 concentration in 0.5 year old Norway spruce needles

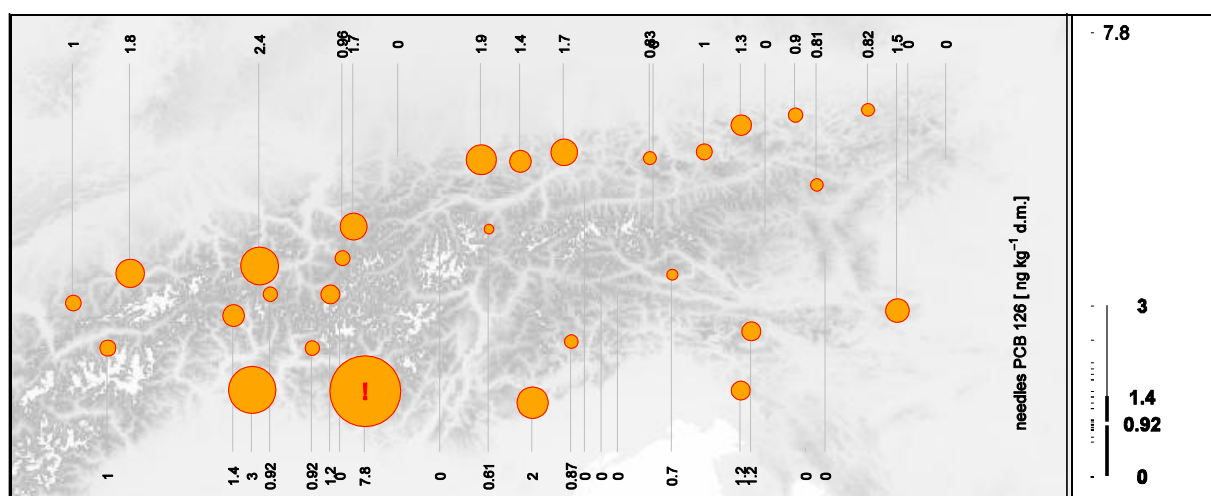


Figure 3-218: PCB 126 concentration in 0.5 year old Norway spruce needles

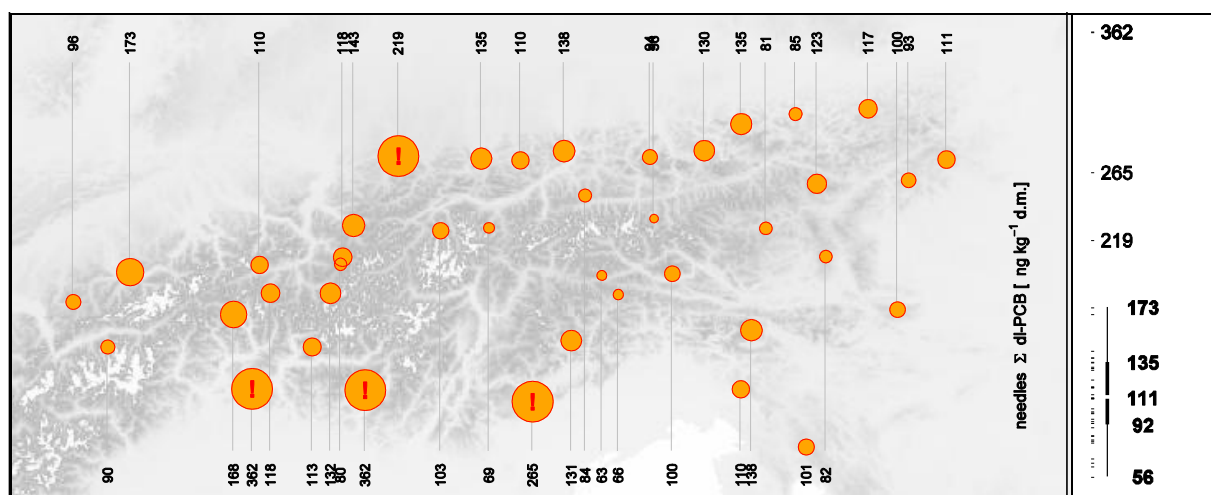


Figure 3-219: Concentration of twelve dioxin-like PCB in 0.5 year old Norway spruce needles

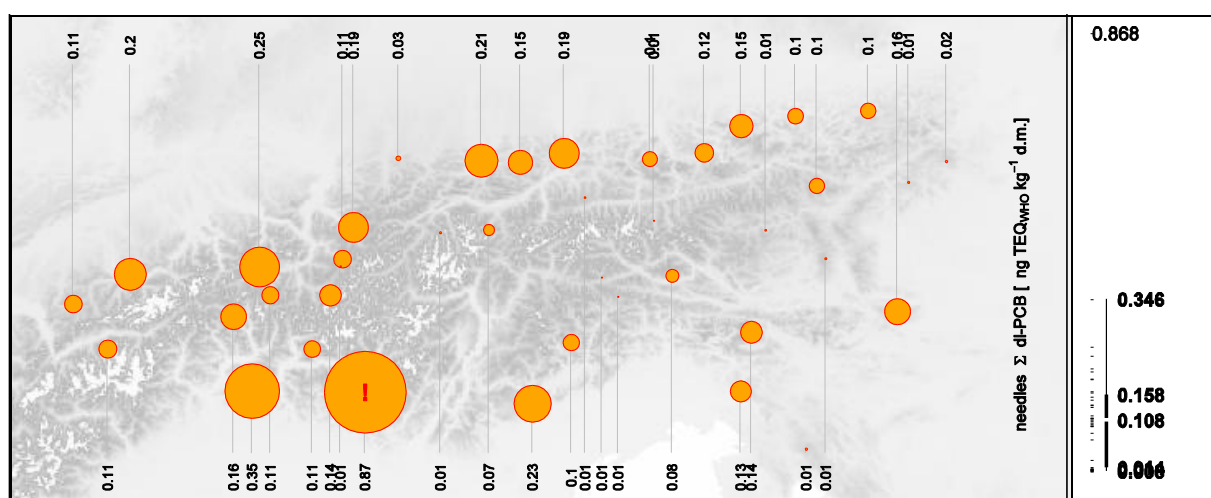


Figure 3-220: WHO toxic equivalents of twelve dioxin-like PCB in 0.5 year old Norway spruce needles

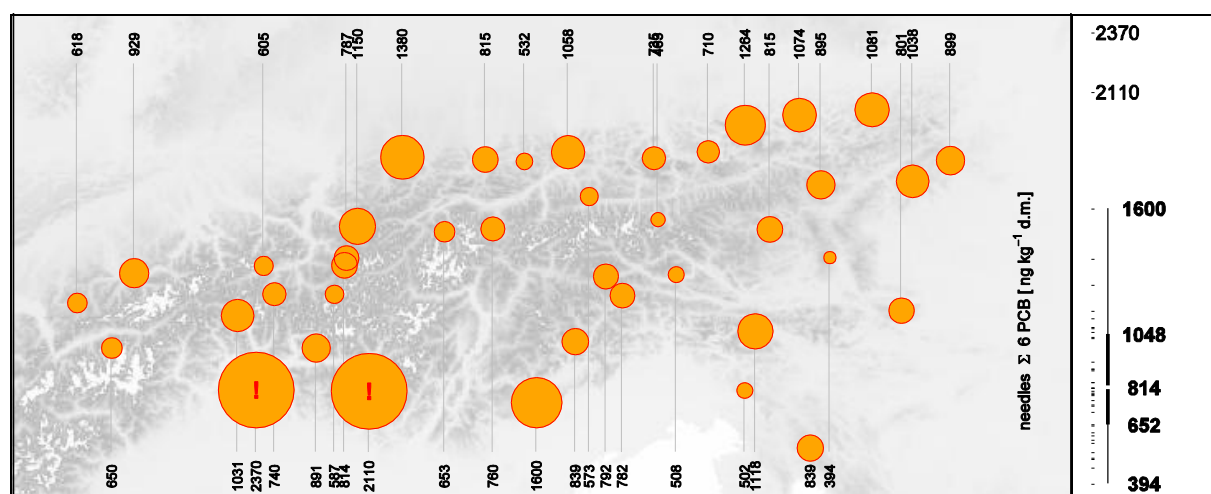


Figure 3-221: Concentration of six indicator PCB in 0.5 year old Norway spruce needles

Longitudinal differences

Congeners (126, 105, 114, 118, 156) and the sum of dioxin-like PCB as well as its WHO toxic equivalents had the highest median concentrations in the west, while congeners 52, 77, 123, 128, 153, 169, 180 and the sum of the six indicator PCB peaked in the east (Table 3-29).

Table 3-39: Significant differences between pairs of longitudinal site groups

	west	middle	east
PCB 114, 156, Σ dl-PCB	higher	lower	
PCB 126	higher		lower
PCB 105, 118, Σ dl-PCB in TEQ _{WHO}	higher	lower	
	higher		lower

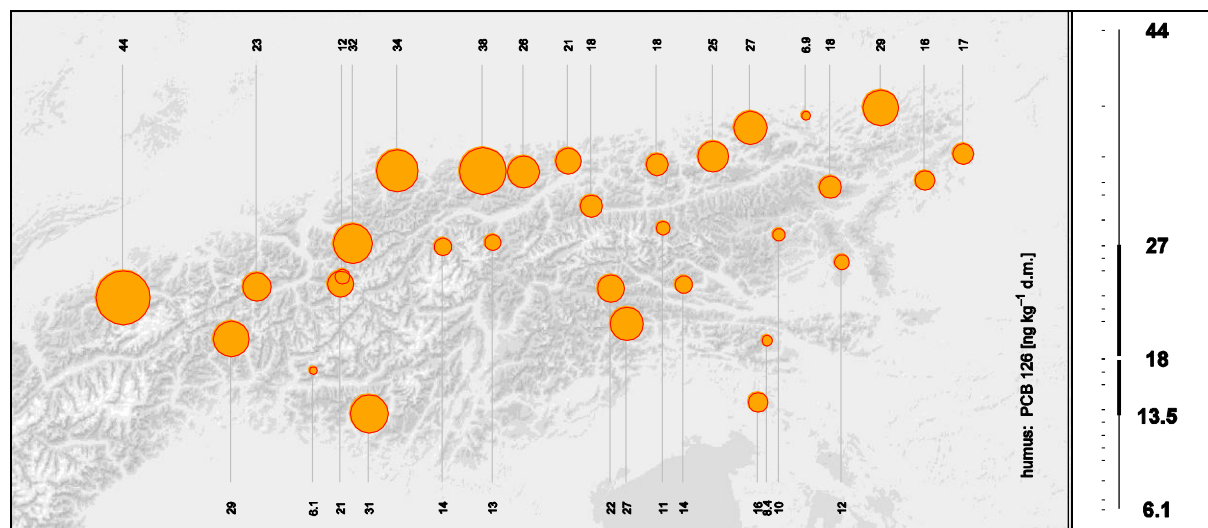
Latitudinal differences

Significant differences between latitudinal sitegroups were observed for the concentrations of congeners 52, 77, 101, 105, 138, 157, 167, 180, and for the sum of six indicator PCB. Highest median concentrations of the other congeners and sum parameters were observed, to about equal parts, in the northern and southern band.

Pairwise comparison of site groups showed that in most cases the northern zone had significantly higher concentrations than the central and/or southern site group (Table 3-40).

Table 3-40: Significant differences between pairs of latitudinal site groups

PCB 101, 105, 118, 126, 138, 153, 156, 157, Σ dl-PCB (concentration and in TEQ _{WHO})	north: higher	
	central: lower	
Σ 6 PCB	central: lower	
	south: higher	
PCB 52, 77, 167, 180	north: higher	
	central: lower	lower
	south: higher	higher

3.7.4.2 Humus*Figure 3-222: PCB 126 concentration in forest humus.*

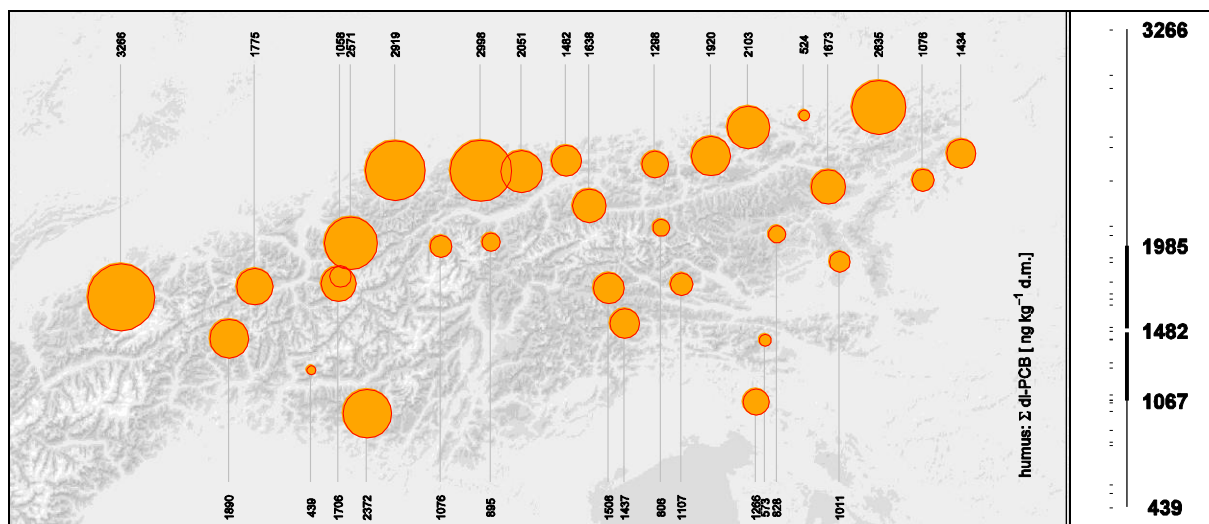


Figure 3-223: Concentration of twelve dioxin-like PCB in forest humus.

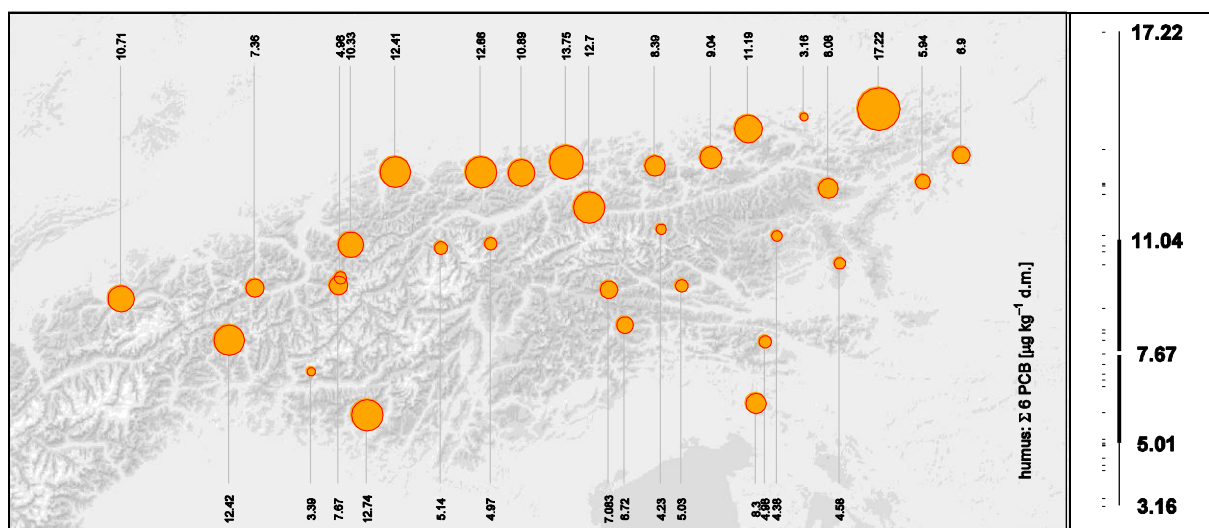


Figure 3-224: Total concentration of six "indicator" PCB in forest humus (note high concentration units of $\mu\text{g kg}^{-1} \text{ d.m.}$)

Longitudinal differences

Only for PCB congener no. 105, differences among longitudinal site groups were significant (Kruskal-Wallis, $\alpha = 0.05$). Pairwise comparison showed significant differences between the lateral zones (east and west) for the congeners 77, 105 and 157 (Figure 3-225).

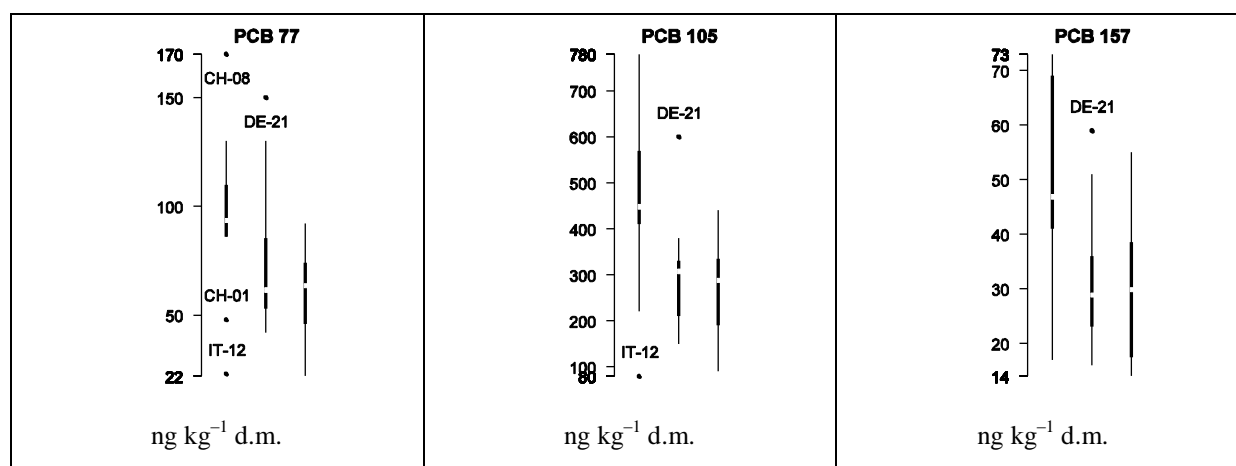
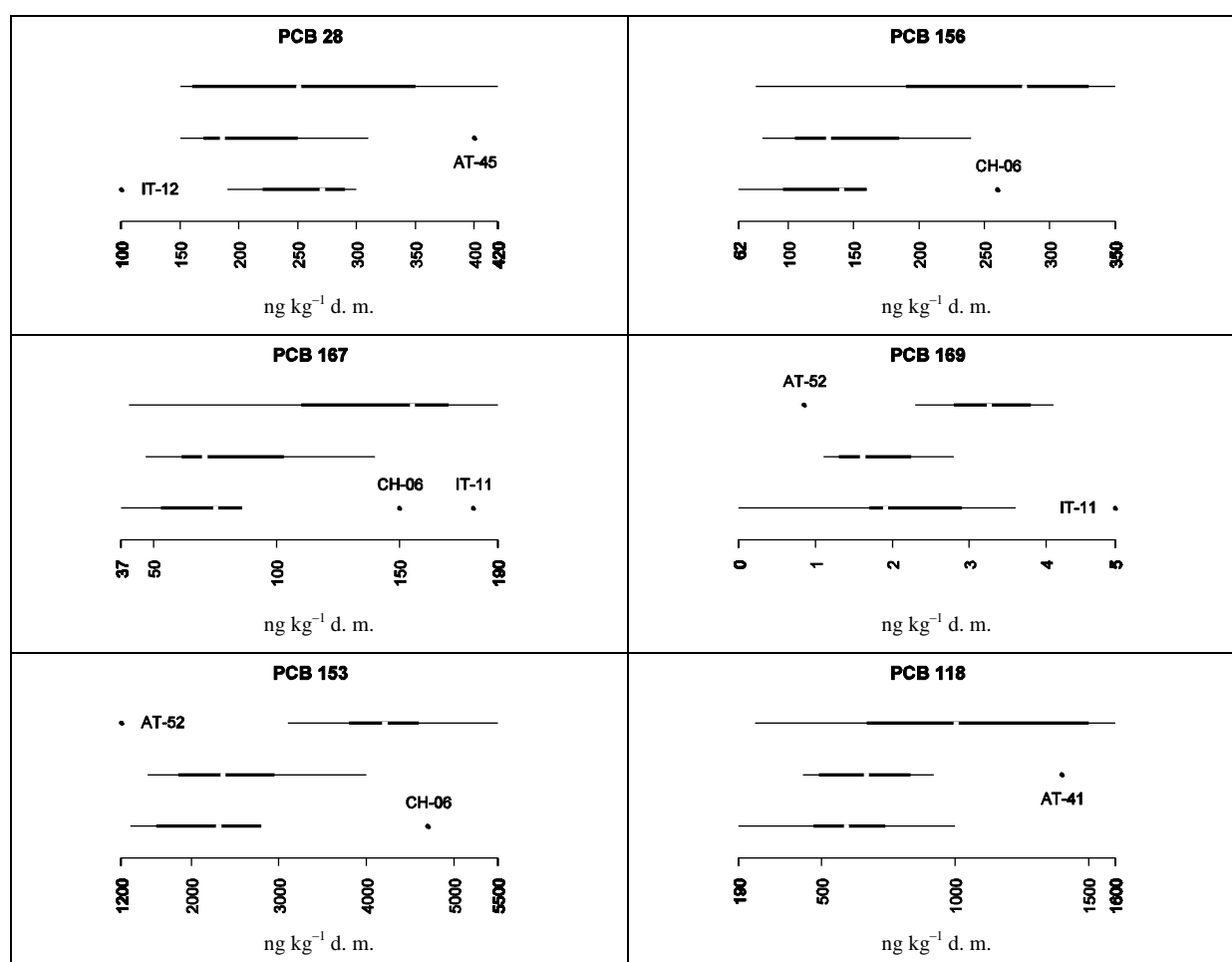
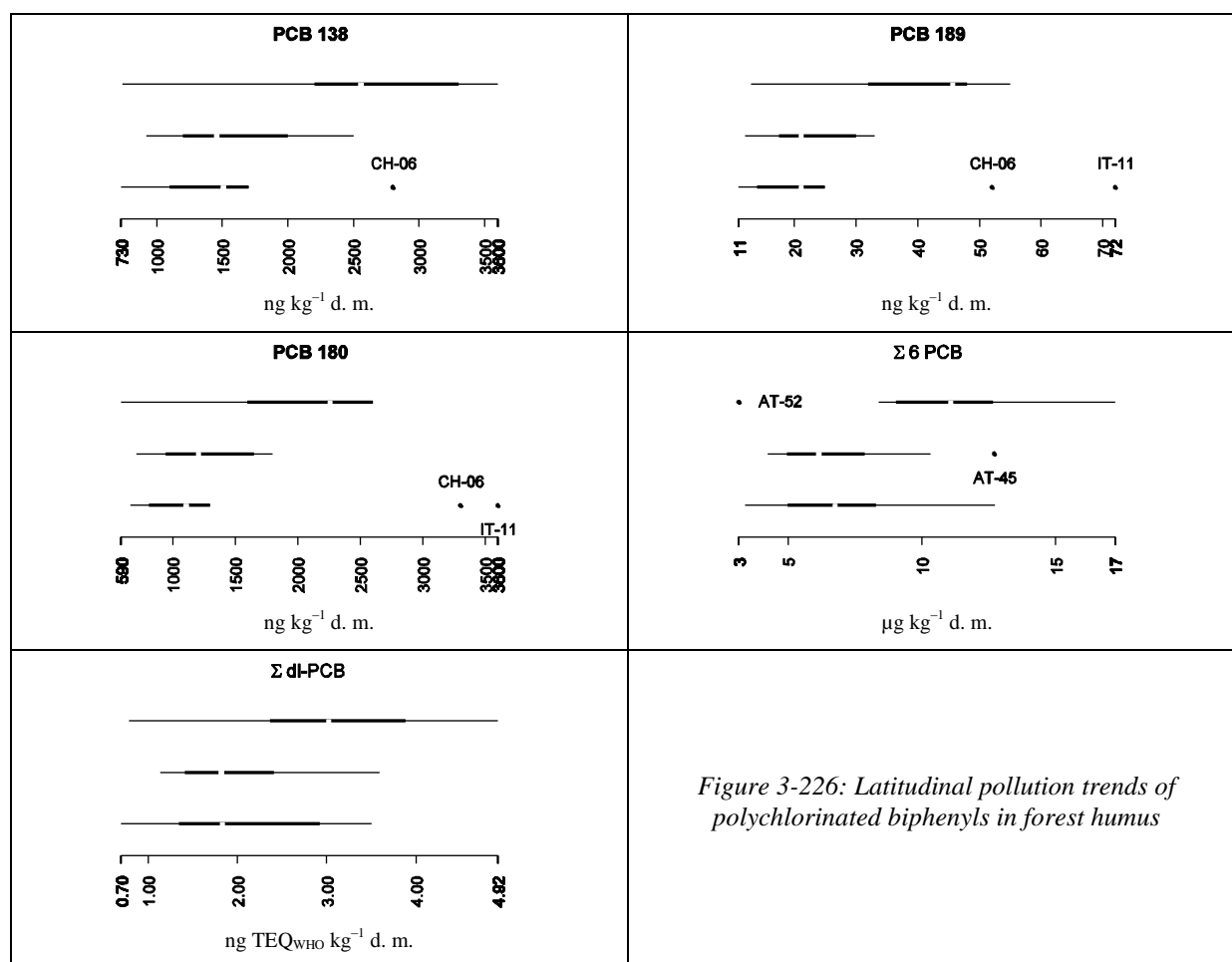


Figure 3-225: Longitudinal pollution trends of polychlorinated biphenyls in forest humus.

Latitudinal differences

About half of the measured congeners showed significant concentration differences among the latitudinal site groups (congeners 156, 167, 169, 153, 138, 189, 118, 180 and the cumulative parameters $\Sigma 6 \text{ PCB}$, $\Sigma \text{ dl-PCB}$ and $\Sigma \text{ dl-PCB}$ in TEQ_{WHO}). The lowest PCB concentrations (medians) were usually in the central zone, except congeners 114, 118, 123, 153, 180 and the WHO toxic equivalents, which had the lowest medians in the south (Figure 3-226). As already observed for dioxins (p. 172), the highest median concentrations were always found in the northern zone.

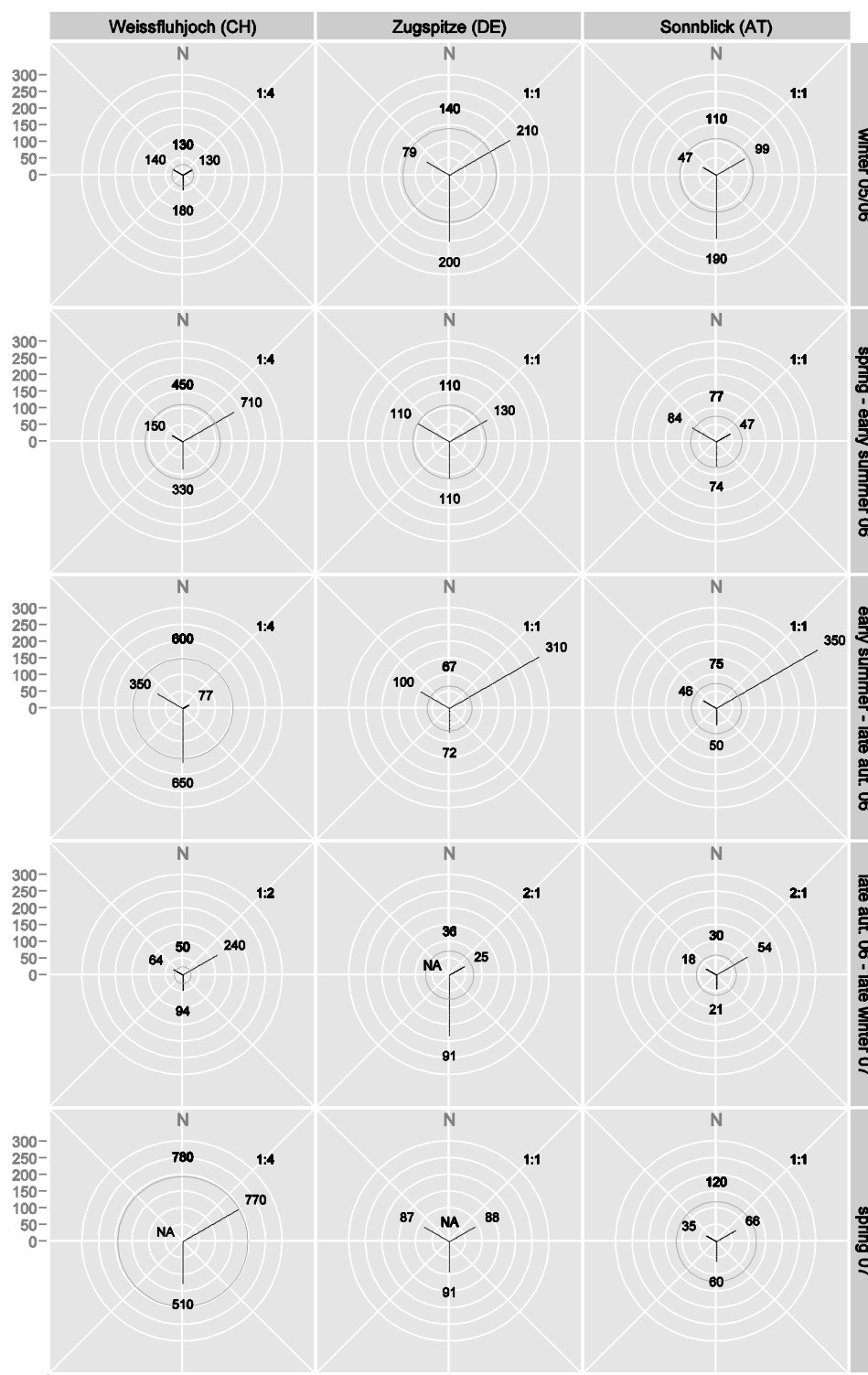




3.7.4.3 Air

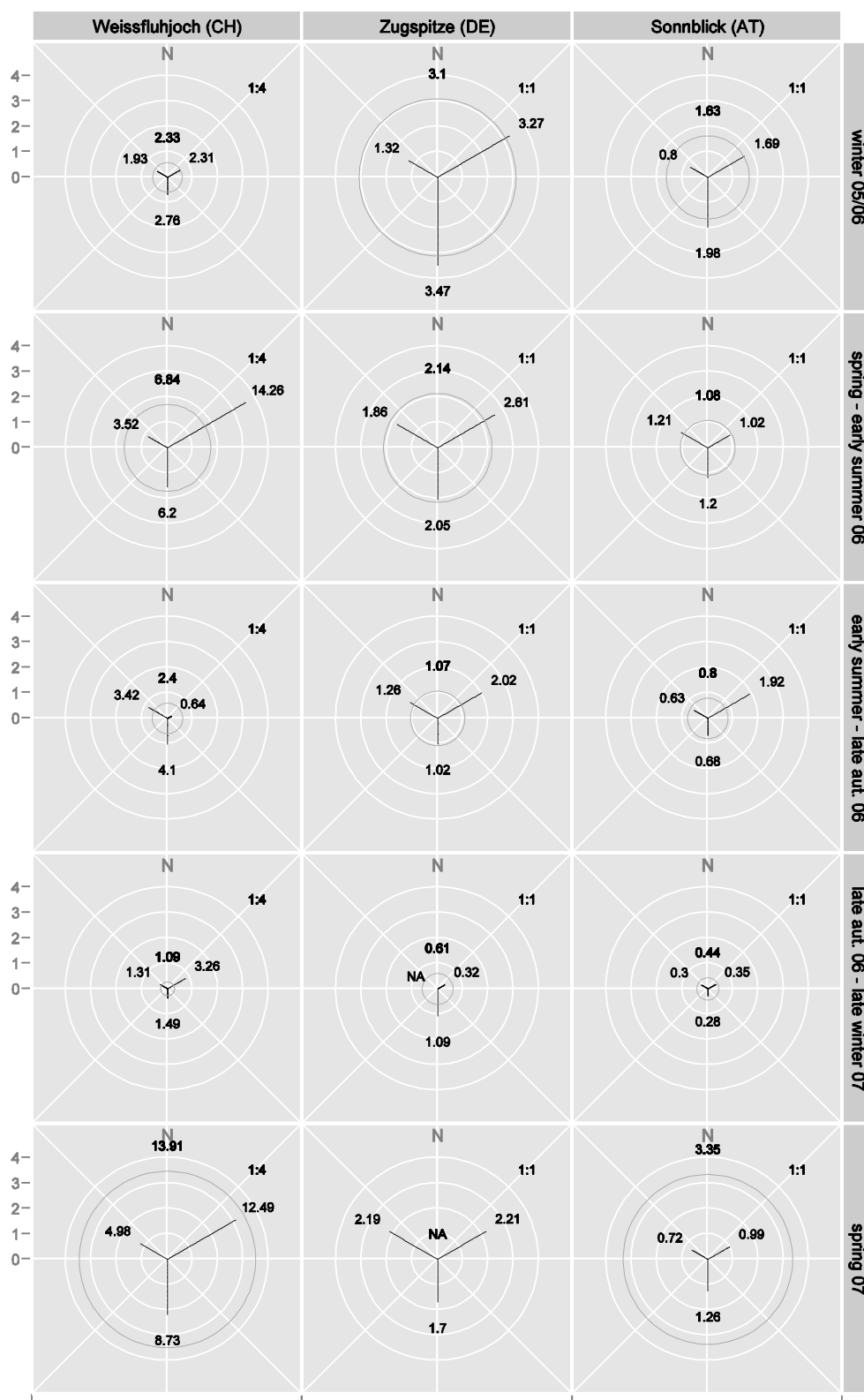
At Mt. Zugspitze, exceedingly high PCB (and PBDE and PCDD/F) contents appeared to accumulate in the filter cartridge reserved for air masses from NW-Europe during autumn and winter 2005/06. However, a series of instrument failures during this period suggests that also the volume readings underestimated the actual filtered volume by far (60 m³ at an average volume of 1000 m³ for the other filters), resulting in calculation of unusually high air concentrations. These data have therefore been omitted in the corresponding plots (row 4 column 2 in figures 3-191–3-193).

The highest PCB concentrations were often found in air that had travelled across the northeastern or the southern European regions. Figure 3-227 illustrates the prevalence of a given source region for pollutant loads arriving at a station. Similar to the findings for other environmental media, atmospheric PCB concentrations decreased from west (Weißfluhjoch) to east (Sonnblick).



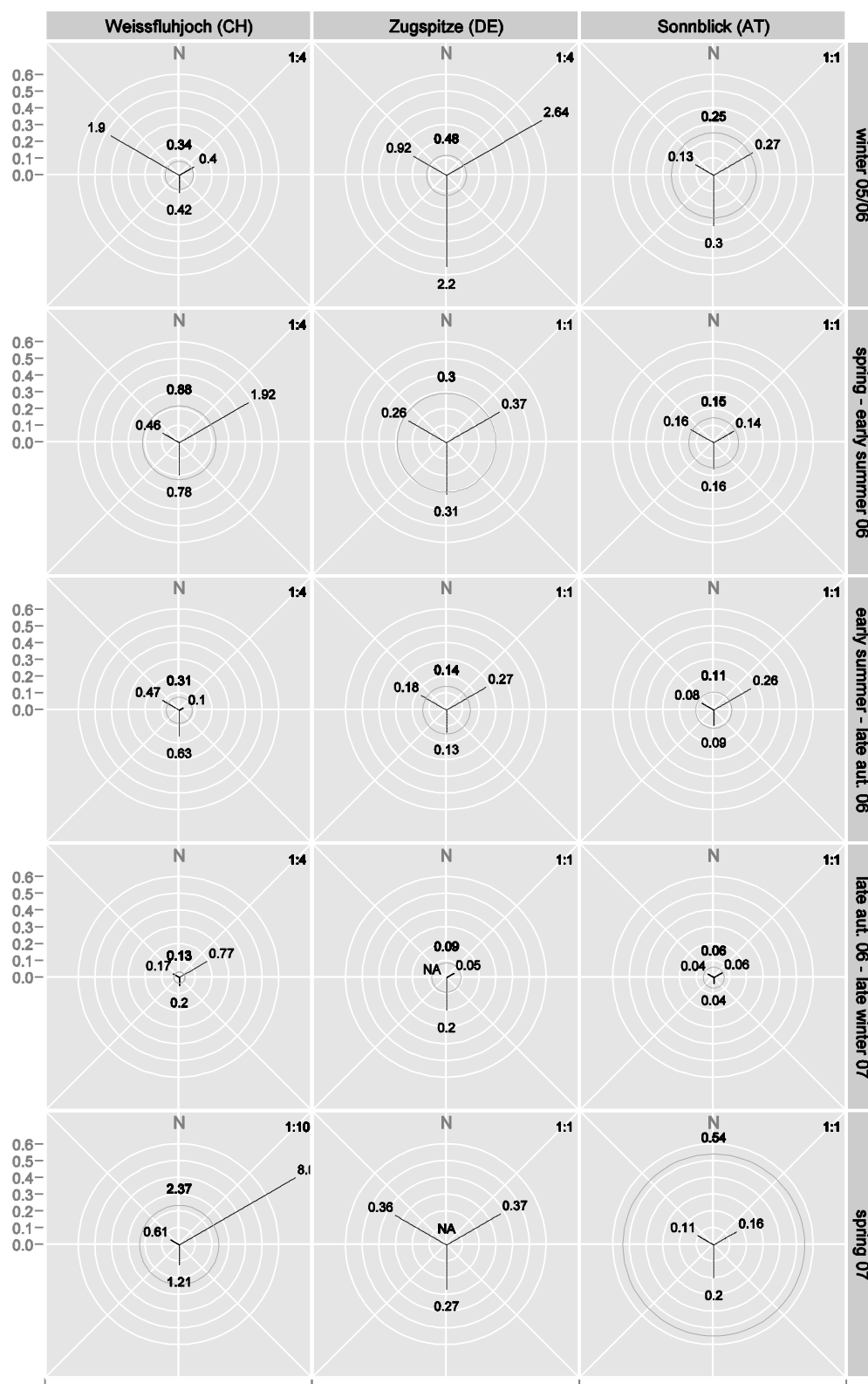
This plot illustrates the prevalence of particular source regions for the comparatively volatile PCB 77. See, e. g., the high loads from the northeastern source region during early summer–late autumn 2006. Note the varying scales (indicated in the top right corner of each panel).

Figure 3-227: Total content [fg m^{-3}] of PCB congener 77 in air from NW, NE and S (circle: trajectory not attributable to a particular sector).



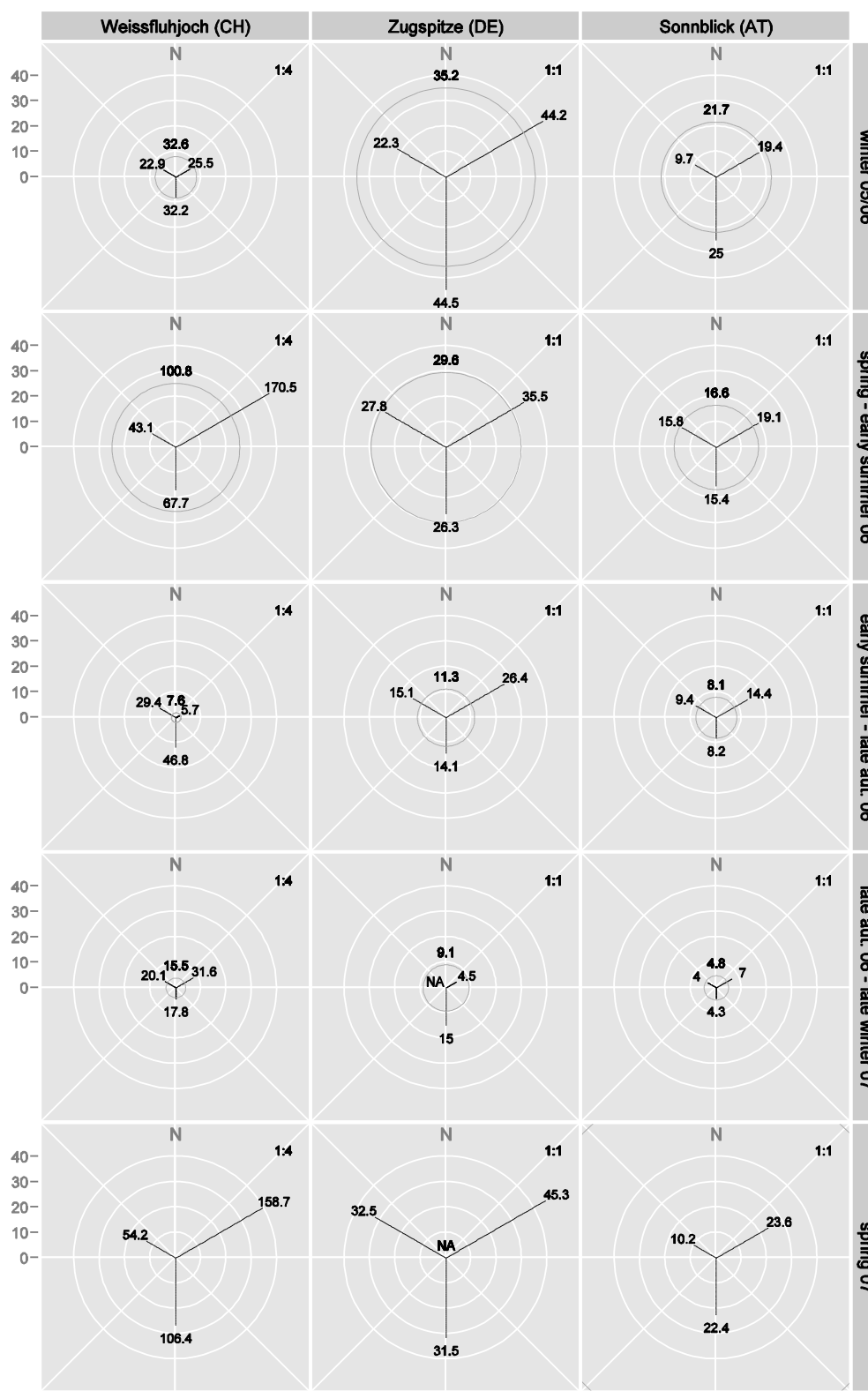
Note the reduced scale (1:4) for values from Mt. Weissfluhjoch.

Figure 3-228: Total content [pg m^{-3}] of twelve dioxin-like PCB in air from NW, NE and S (circle: trajectory not attributable to a particular sector).



Note the reduced scales (1:4; spring 2007: 1:10) for values from Mt. Weissfluhjoch and for winter 2005/6 values from Mt. Zugspitze (1:4).

Figure 3-229: Total content [$\text{fg TEQ}_{\text{WHO}} \text{m}^{-3}$] of twelve dioxin-like PCB in air from NW, NE and S (circle: trajectory not attributable to a particular sector).



Note the reduced scale (1:4) for values from Mt. Weissfluhjoch.

Figure 3-230: Total concentration [pg m^{-3}] of six indicator PCB used for routine analysis in air from NW, NE and S (circle: trajectory not attributable to a particular sector).

3.7.5 Altitudinal variation

No consistent (across height profiles) vertical trend of PCB concentrations in needles was detected.

3.7.5.1 Needles

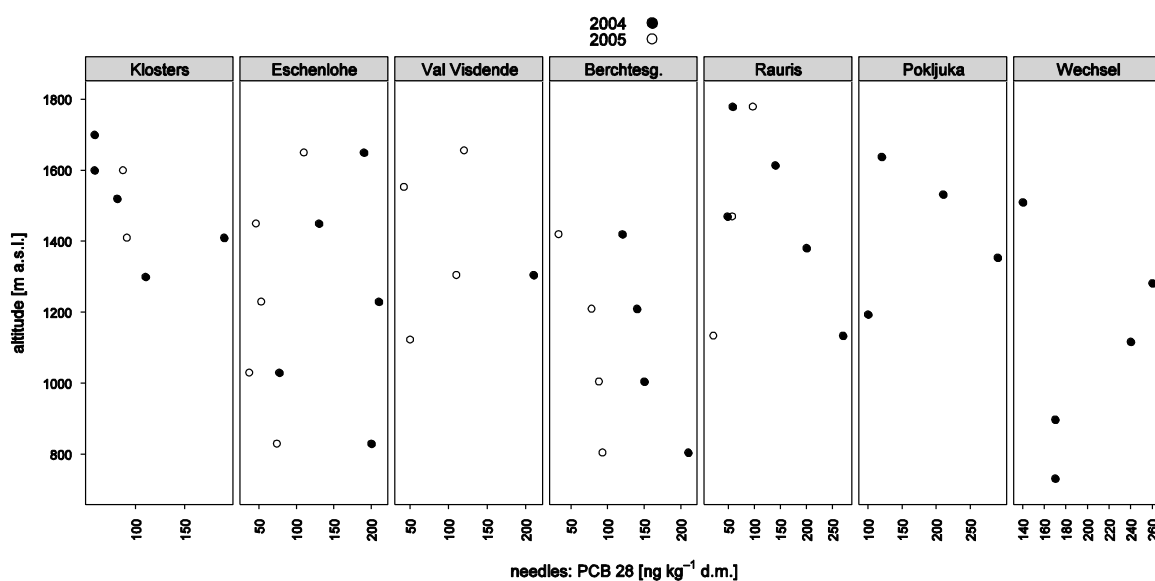


Figure 3-231: Altitudinal variation of PCB 28 in 0.5 year old Norway spruce needles

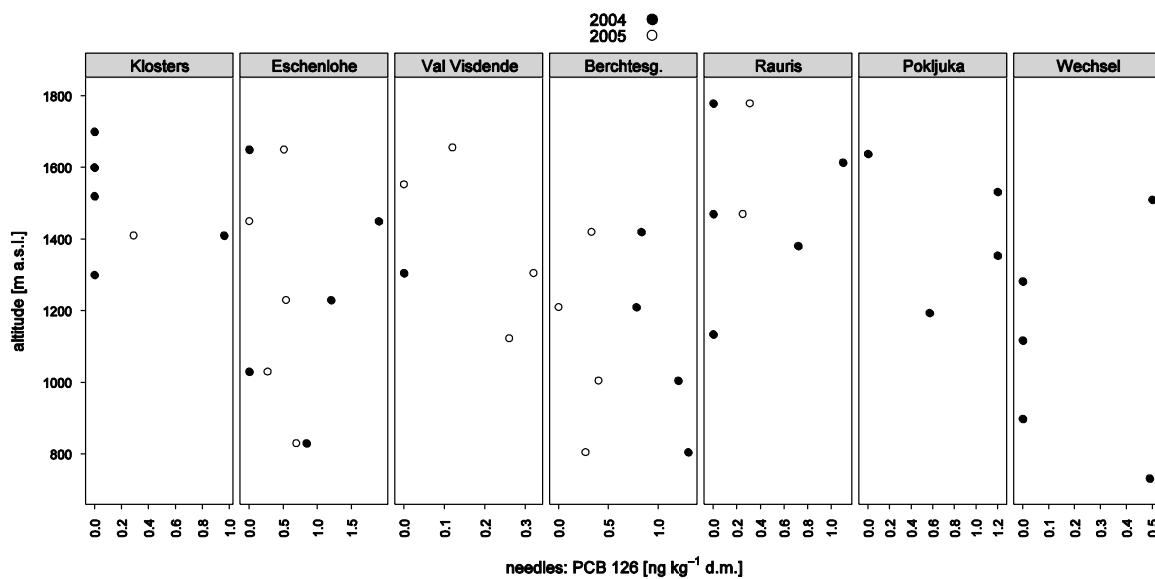


Figure 3-232: Altitudinal variation of PCB 126 in 0.5 year old Norway spruce needles

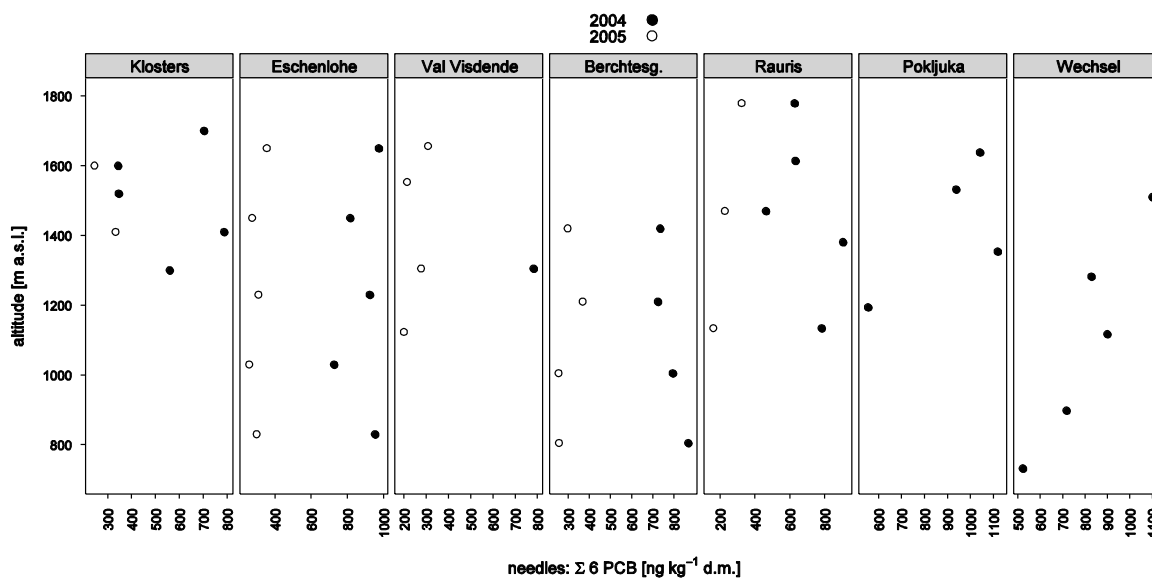


Figure 3-233: Altitudinal variation of the sum of six indicator PCB in 0.5 year old Norway spruce needles

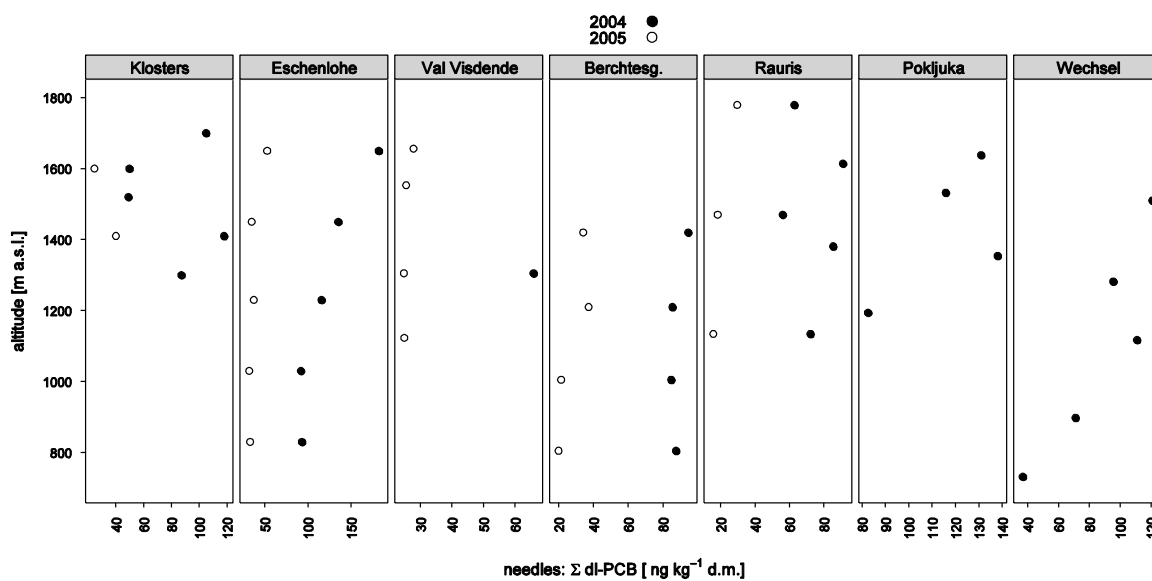


Figure 3-234: Altitudinal variation of dioxin-like PCB in 0.5 year old Norway spruce needles

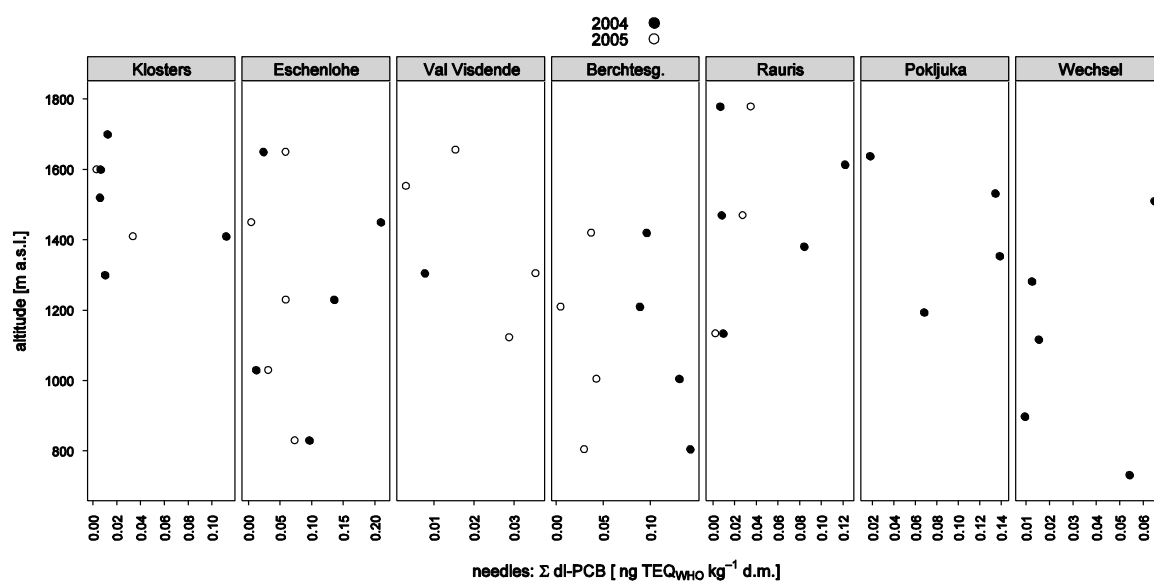


Figure 3-235: Altitudinal variation of WHO toxic equivalents of dioxin-like PCB in 0.5 year old Norway spruce needles

3.7.5.2 Humus

Again, the altitudinal pattern varied strongly between height profiles. Physicochemical properties of the congener did not seem to have much influence on the site-specific pattern: the vertical distribution of the relatively volatile congener 28 (Figure 3-236) did not differ consistently from that of the heavier congener 126 (the most toxic for mammals; Figure 3-237). Like with most other of the investigated POPs, the Wechsel profile showed an increase of (in this case: PCB) pollution with altitude.

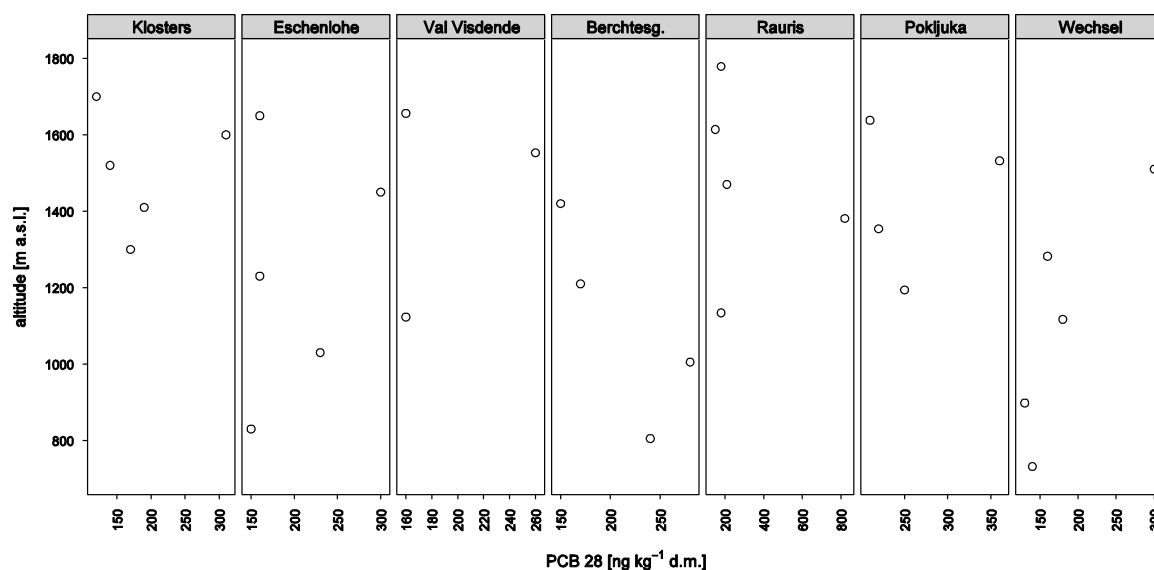


Figure 3-236: Altitudinal variation of PCB 28 in forest humus

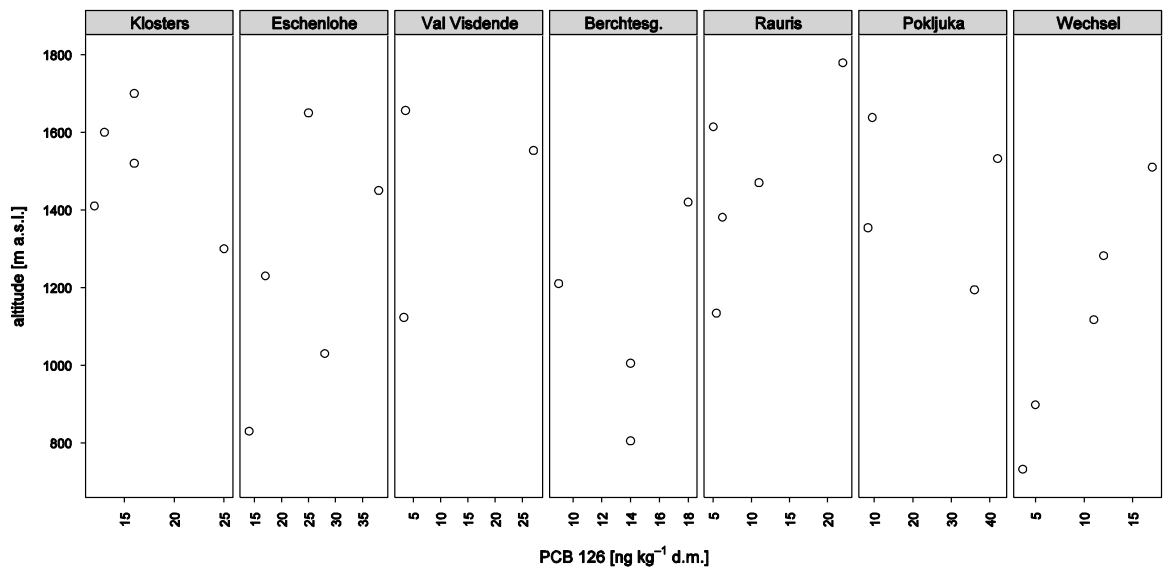


Figure 3-237: Altitudinal variation of PCB 126 in forest humus

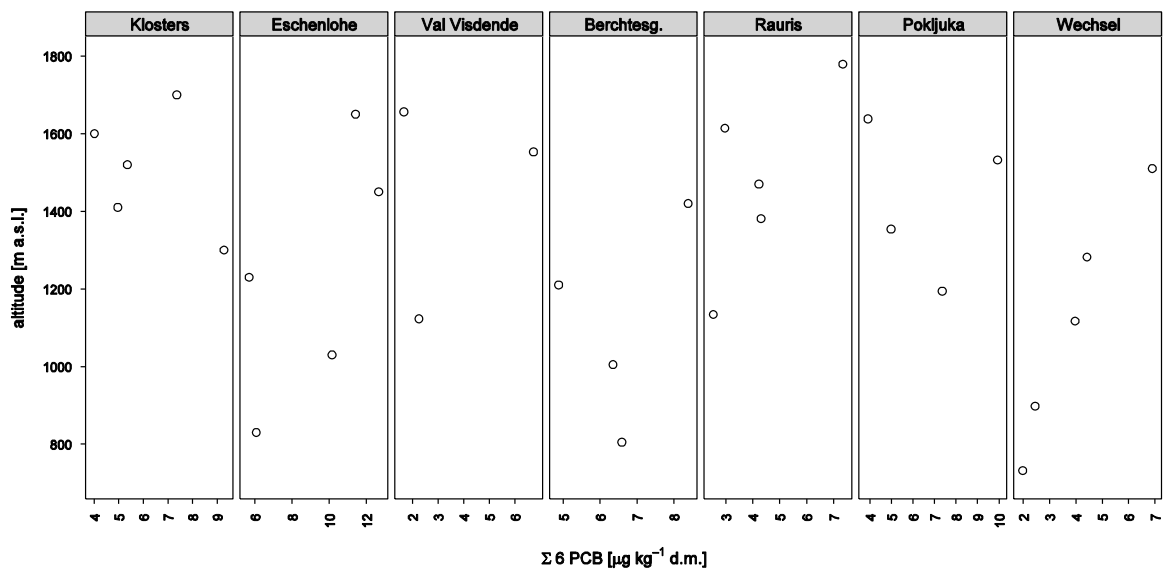


Figure 3-238: Altitudinal variation of the sum of six indicator PCB in forest humus

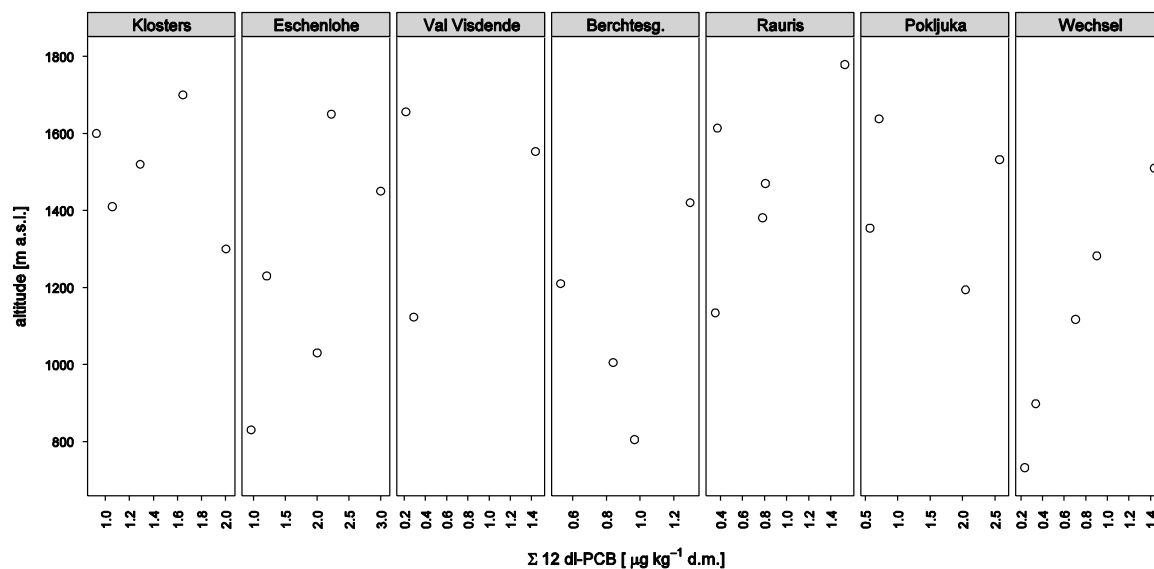


Figure 3-239: Altitudinal variation of the sum of twelve dioxin-like PCB in forest humus

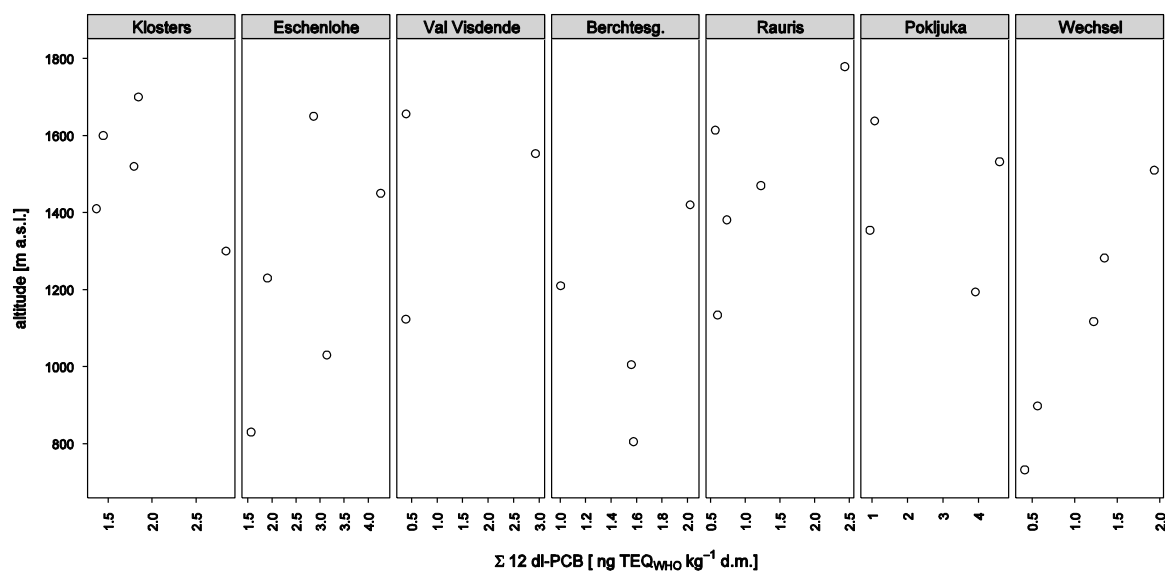


Figure 3-240: Altitudinal variation of the sum of twelve dioxin-like PCB (in WHO toxic equivalents) in forest humus

3.7.5.3 SPMD

Different from the needles, SPMD indicated an increase of PCB concentration with altitude.

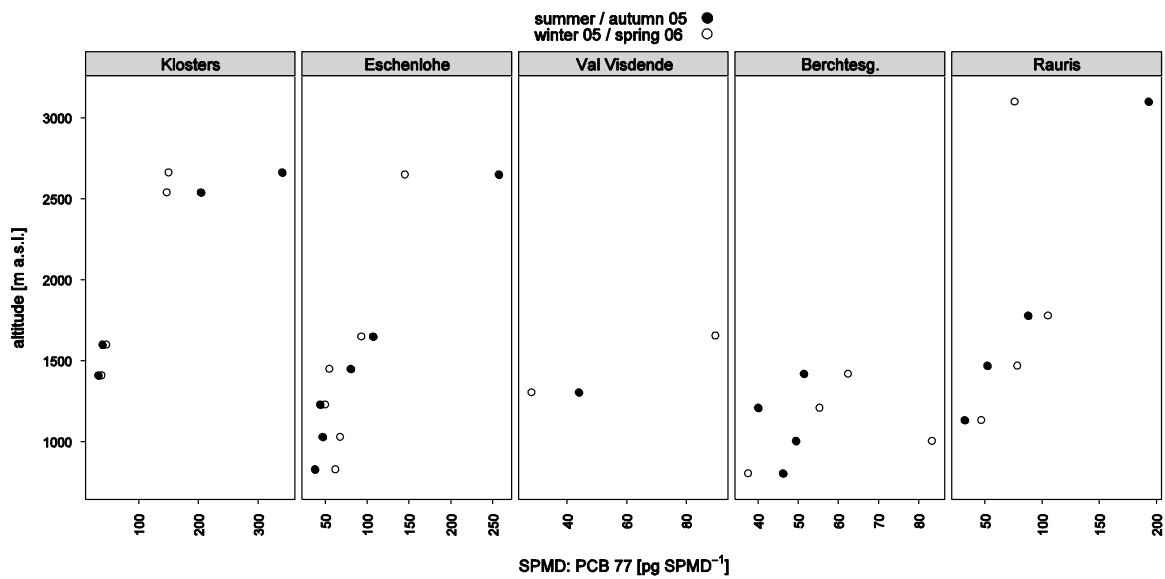


Figure 3-241: Altitudinal variation of the PCB 77 in SPMD

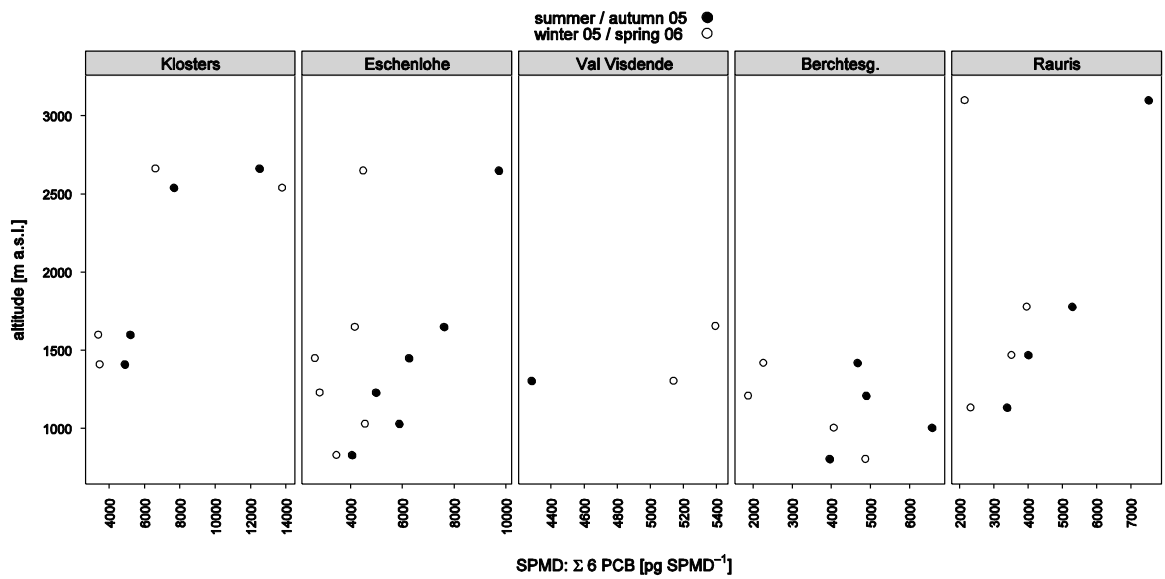


Figure 3-242: Altitudinal variation of the sum of six PCB in SPMD

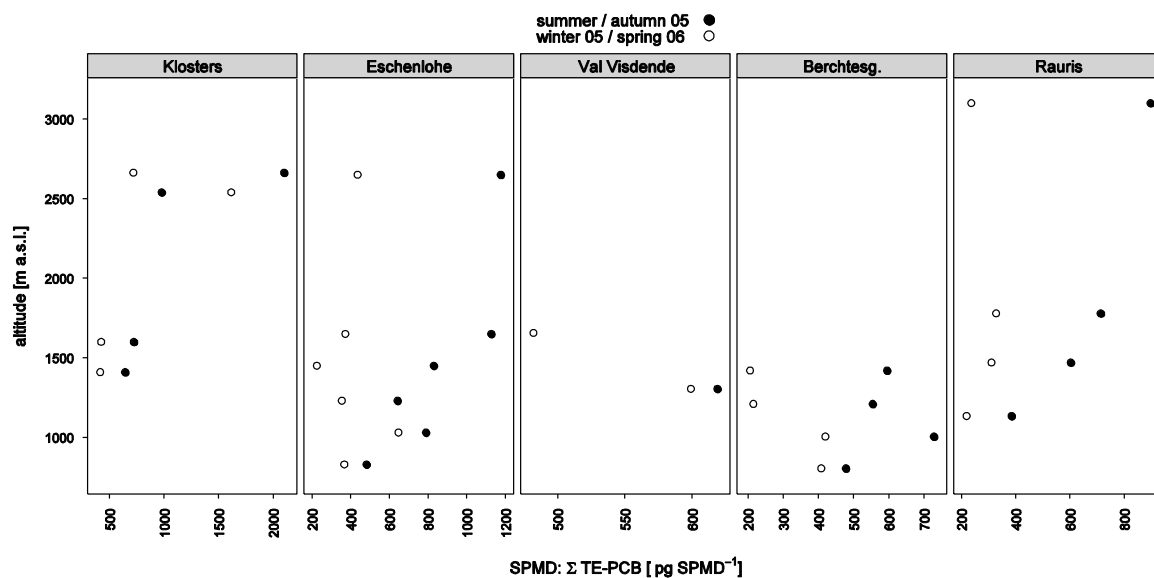


Figure 3-243: Altitudinal variation of the sum of twelve dioxin-like PCB in SPMD

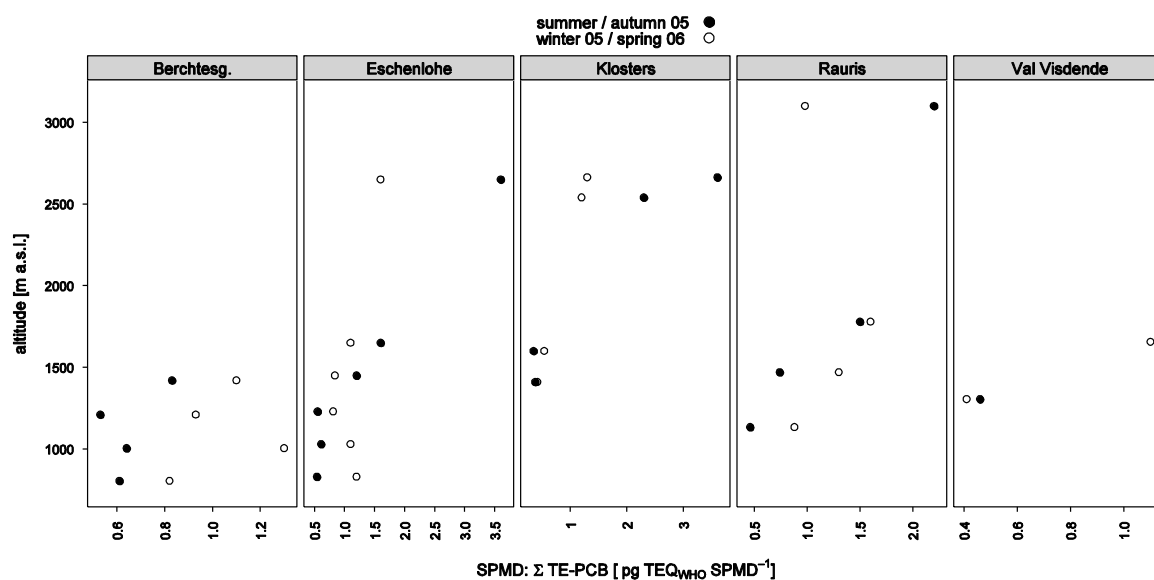


Figure 3-244: Altitudinal variation of the sum of twelve dioxin-like PCB (in WHO toxic equivalents) in SPMD

3.8 Nitrophenols

3.8.1 Characterization

3.8.1.1 Physicochemical properties

Figure 3-245 shows the structure of 2- and 4-nitrophenol. Other nitrophenols may contain additional NO₂- and/or CH₃-moieties.

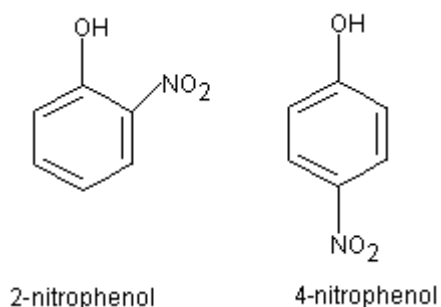


Figure 3-245: Molecular structure of 2- and 4-nitrophenol

Table 3-41: Physicochemical properties of 2- and 4-nitrophenols

	2-nitrophenol	4-nitrophenol
molecular weight (g mol ⁻¹)	139.11	139.11
boiling point (°C)	214	279
water solubility @ 20 °C (g l ⁻¹)	1.26	12.4
vapour pressure (kPa)	6.8×10 ⁻³	3.2×10 ⁻⁶
log K _{ow}	1.77	2.04

source: WHO (2000)

3.8.1.2 Emissions and use

There are no known natural sources of the nitrophenol isomers. Both 2- and 4-nitrophenol are intermediates in the synthesis of azo dyes and a number of pesticides, mainly insecticides and, to a lesser extent, herbicides. In the 1980s, the production volumes for 2- and 4-nitrophenol showed a decreasing tendency in Germany as a result of changes in and termination of the production of some organophosphorus pesticides. 2- and 4-nitrophenol have been detected in the exhaust gases of light-duty gasoline and diesel vehicles (WHO 2000).

Significant releases of 4-nitrophenol into the hydrosphere may occur from the hydrolytic degradation of the insecticides parathion and parathion-methyl and to a lesser extent from the photolytic degradation of the herbicides nitrofen and bifenox. A considerable portion of airborne nitrophenols, especially 4-nitrophenol, can be released to the hydrosphere and the geosphere by wet and dry deposition (WHO 2000).

3.8.1.3 Environmental behaviour and bioaccumulation

Environmental releases of nitrophenols are mostly received by ambient air, surface waters, and to a smaller extent by soil. Nitrophenols are classified as substances with a low to moderate potential for soil sorption. Nitrophenols emitted to soil are expected to be biodecomposed under aerobic conditions. Infiltration into groundwater is expected only under unfavourable conditions for biodegradation (e.g., anaerobic conditions; WHO 2000).

Bioconcentration factors ranging from 14.6 to 24.4 were reported for 2-nitrophenol in zebra fish (*Brachydanio rerio*), and from 30 to 76 for common carp (*Cyprinus carpio*; WHO 2000).

3.8.2 Summary statistics

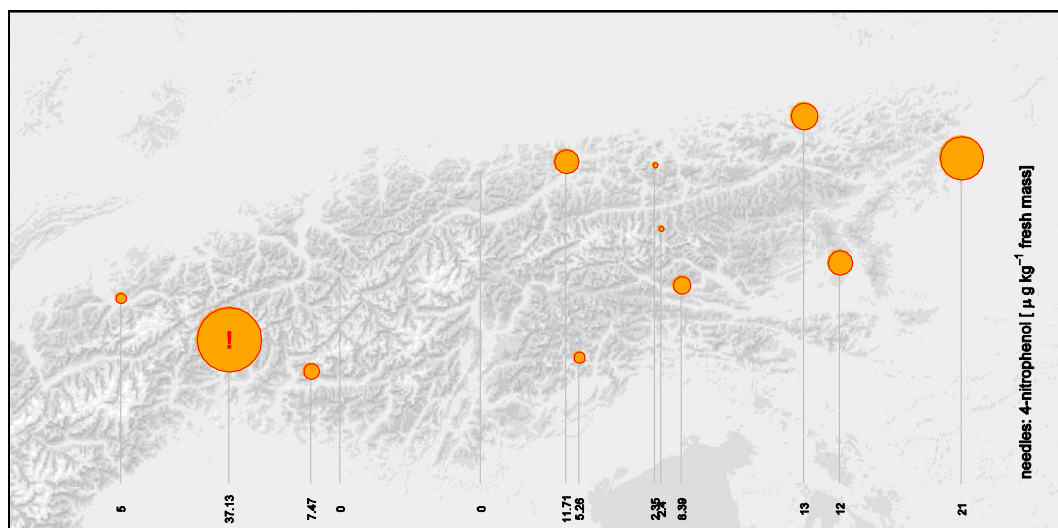
Nitrophenols were examined with a focus on their vertical distribution. Samples were thus taken from height profiles and eight additional standard plots.

3.8.2.1 Needles

4-NP was the only nitrophenol which was detected at a larger number of sites (0–37.1 $\mu\text{g kg}^{-1}$ fresh weight, median: 8.39, sample size $n=13$). The other isomers were entirely below the detection limit, or exceeded the limit of quantification (4.2–4.9 $\mu\text{g kg}^{-1}$ fresh mass) only at few sites.

3.8.3 Spatial variation

3.8.3.1 Needles

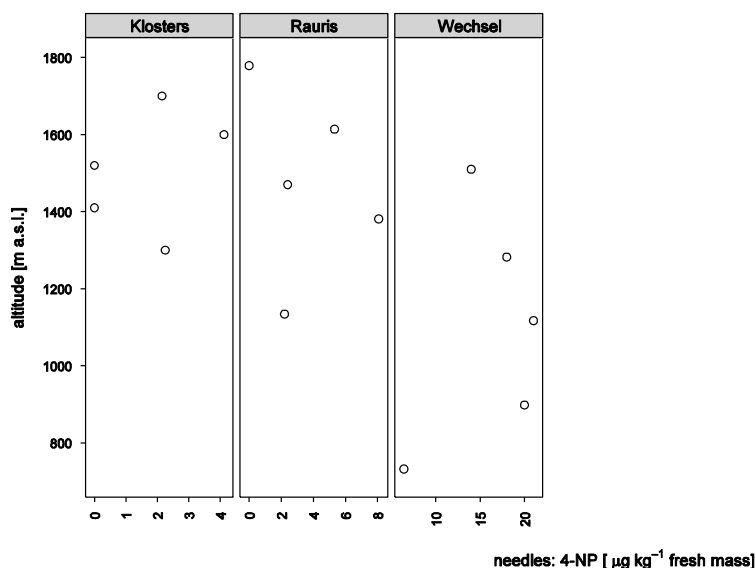


Two values below quantification limit replaced by half quantification limit (2.4 $\mu\text{g kg}^{-1}$ fresh mass). Note that there are no samples from the inner study area, so conclusions on spatial gradients are of limited validity.

Figure 3-246: Concentration of 4-nitrophenol in 0.5 year old Norway spruce needles

3.8.4 Altitudinal variation

Figure 3-247 shows the altitudinal variation of 4-nitrophenol – the only nitrophenol with a substantial number of observations above the quantification limit – at three height profiles (height profiles Berchtesgaden, Val Visdende and Pokljuka were not investigated, profile Eschenlohe had only values below the quantification limit).



Values below the quantification limit of $4.4 \mu\text{g kg}^{-1}$ fresh weight replaced by the half quantification limit.

Figure 3-247: Altitudinal variation of 4-nitrophenol in 0.5 year old Norway spruce needles

3.9 Short chain chlorinated hydrocarbons (CHCs) and trichloroacetic acid (TCA)

3.9.1 Characterization

These compounds are short chain aliphatic chlorinated hydrocarbons: i.e. trichloroacetic acid (TCA), trichloromethane (TCM) and trichloroethane (TCE).

3.9.1.1 Physicochemical properties

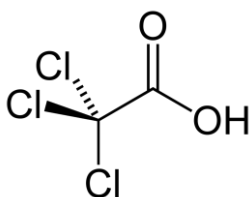


Figure 3-248: Molecular structure of trichloroacetic acid

Table 3-42: Physicochemical properties of some CHC

	TCA	TCM	TCE
molecular weight (g mol^{-1})	163.4	119.38	133.4
boiling point ($^{\circ}\text{C}$)	198	61.2	74
water solubility	very high	7.710 mg l^{-1} at 25°C	insoluble in water
vapour pressure (kPa)	133 @ 51°C	26.26 @ 25°C	13 @ 20°C
$\log K_{ow}$	1.7	1.97	

sources: ICSC (1998), IPCS (1992), HSDB (2005)

3.9.1.2 Emissions and use

TCM is mainly used as a precursor for the other materials, principally fluorocarbons (for example, chlorodifluoromethane) used in the synthesis of tetrafluoroethylene and polytetrafluoroethylene, and as a refrigerant and propellant. TCM is also widely employed as an organic solvent in industry and in analytical laboratories. It has also been used as an ingredient of pharmaceuticals, drugs, cosmetics, grain fumigants, dyes and pesticides (IPCS 1990).

In 1993, Germany produced 1000 tons of TCA. TCA is mostly used as a herbicide in the form of sodium salts. TCA is also used as an auxiliary in textile dyeing processes (OECD SIDS I).

3.9.1.3 Environmental behaviour and bioaccumulation

TCM resides in the atmosphere for several months and is removed from the atmosphere through chemical transformation. Biodegradation may only occur under anaerobic conditions. Local exposure to high TCA emissions from textile dyeing and washing, electroplating and pulp mills, together with the high toxicity for algae pose a risk to aquatic compartments. TCA is classified as “non biodegradable” and having a “low bioaccumulation” potential for fish and a “high bioaccumulation potential” for terrestrial plants. The highest sensitivity to TCA has been found for the alga *Chlorella pyrenoidosa* and pine (OECD SIDS I). 1,1,2-trichloroethane is a stable liquid and is not readily biodegraded. Its measured bioconcentration factor is 0.7–4.0 (OECD TG 305C).

3.9.1.4 Toxicology

In general the target organ of short chain chlorinated hydrocarbons toxicity is the nervous system, leading to irreversible and severe liver damage after sufficiently strong occupational or unintended exposure.

3.9.2 Summary statistics

3.9.2.1 Needles

The following short-chain CHC were not detected in any needle sample: tetrachloromethane, trichloroethene and tetrachloroethene. 1,1,1-trichloroethane was found in only one sample at the highest plot (i.e. no standard site) of height profile Rauris (35 µg kg⁻¹ fresh mass).

Table 3-43: Concentrations of short chain chlorinated hydrocarbons in Norway spruce needles

	mean	sd	min	P ₁₀	P ₂₅	median	P ₇₅	P ₉₀	max
TCA	1476	1546	279	362	459	764	1600	4229	4608
trichloromethane	688	860	39	122	159	330	833	1678	3319

unit: µg kg⁻¹ fresh mass, sample size n=13

3.9.2.2 Air

Table 3-44: Atmospheric CHC concentration on three alpine summits

	sampling period	TCM	RSD	TCE	RSD	TETRA	RSD	TRI	RSD	TETRE	RSD
Weissfluhjoch (CH)	06/01/02–06/02/03	140	23	130	18	470	3	< 21		28	30
	06/02/03–06/03/06	160	77	130	52	440	4	< 21		36	52
	06/03/06–06/04/06	220	42	130	41	440	4	37	47	31	35
	06/04/06–06/05/06	540	15	240	22	520	4	85	18	59	7
	06/05/06–06/06/05	100	71	40	28	350	11	< LOD		65	
	06/06/05–06/07/05	190	72	81	50	450	2	< 21		46	11
	06/07/05–06/08/07	91	14	90	4	380	11	< 21	3	50	16
	06/08/07–06/09/07	210		140		400		33		42	
	06/09/07–06/10/07	140	21	120	13	410	1	31	31	100	3
	06/10/07–06/11/10	120	26	120	16	450	5	55		65	22
	06/11/10–06/12/10	80	5	82	10	390	5	< LOD		24	6
Zugspitze (DE)	06/12/10–07/01/10	58	67	64	58	220	24	< LOD		<5,2	
	07/01/10–07/02/10	83	30	80	15	210	32	< LOD		31	81
	06/01/23–06/03/14	120	48	84	13	390	10	< 21		28	4
	06/03/14–06/04/27	81	4	79	0	370	1	< LOD		37	12
	06/04/27–06/05/31	120	27	72	35	400	5	< LOD		42	24
	06/05/31–06/07/11	45	10	49	1	380	0	< LOD		18	18
	06/07/11–06/08/22	130	11	110	18	380	3	< LOD		50	51
	06/08/22–06/09/12	65		100		440		< LOD		43	
	06/09/12–06/10/09	200	15	140	2	450	2	< 21		74	1
	06/10/09–06/11/07	230	11	160	9	470	1	< LOD		92	5
	06/11/07–06/12/08	360	20	220	4	400	27	27	14	130	20
	06/12/08–07/01/10	140	13	130	2	450	1	< LOD		44	12
Sonnblick (AT)	07/01/10–07/02/21	100	21	95	9	370	2	< LOD		42	50
	06/01/09–06/02/01	170	24	140	16	530	5	< LOD		<10	
	06/02/01–06/03/02	160	48	100	16	430	1	< LOD		23	28
	06/03/02–06/04/11	120	8	82	2	420	2	< 21		47	9
	06/04/11–06/05/03	180	78	95	71	470	11	< 21		33	22
	06/05/03–06/06/07	120	6	89	7	420	2	< 21		25	16
	06/06/07–06/07/02	180	85	99	67	460	10	24		20	24
	06/07/02–06/08/01	160	44	92	34	410	8	< LOD		34	10
	06/09/11–06/10/08	99		100		400		< LOD		71	
	06/10/08–06/11/08	91	2	96	3	440	3	< LOD		37	31
	06/11/08–06/12/18	99	5	99	7	410	2	< LOD		37	25
	06/12/18–07/01/15	88	6	96	5	440	3	< LOD		29	34
	07/01/15–07/02/20	81	13	81	10	410	2	< LOD		39	12

unit: ng m^{-3} ; LOD...detection limit, RSD...relative standard deviation (%); TCM...trichloromethane (chloroform), TCE...1,1,1-trichloroethane, TETRA...tetrachloromethane, TETRE...tetrachloroethene, TRI...trichloroeth(yl)ene

3.9.3 Spatial variation

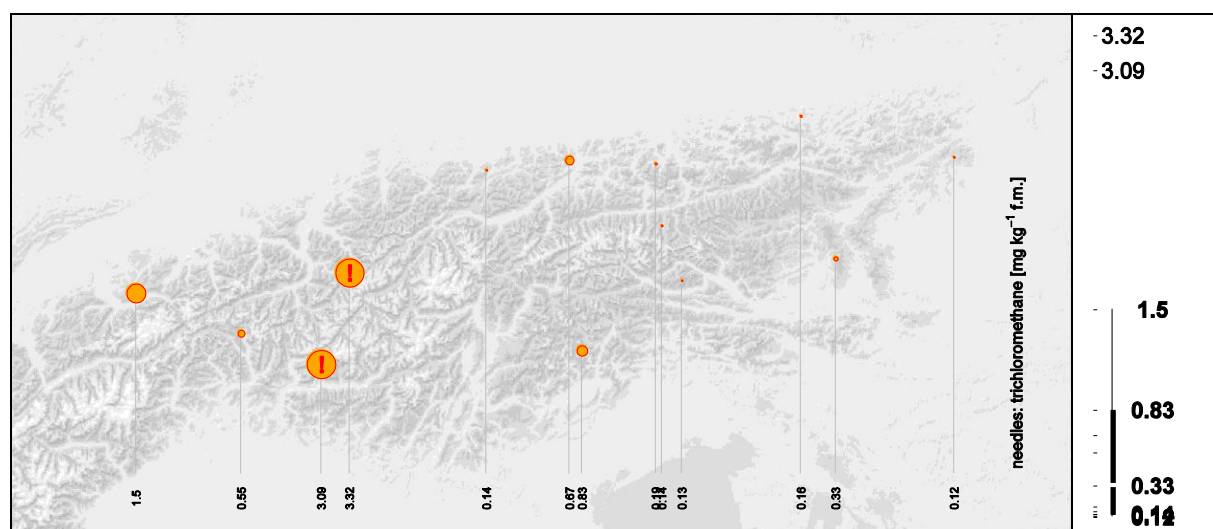


Figure 3-249: Trichloromethane concentrations in 0.5 year old Norway spruce needles.

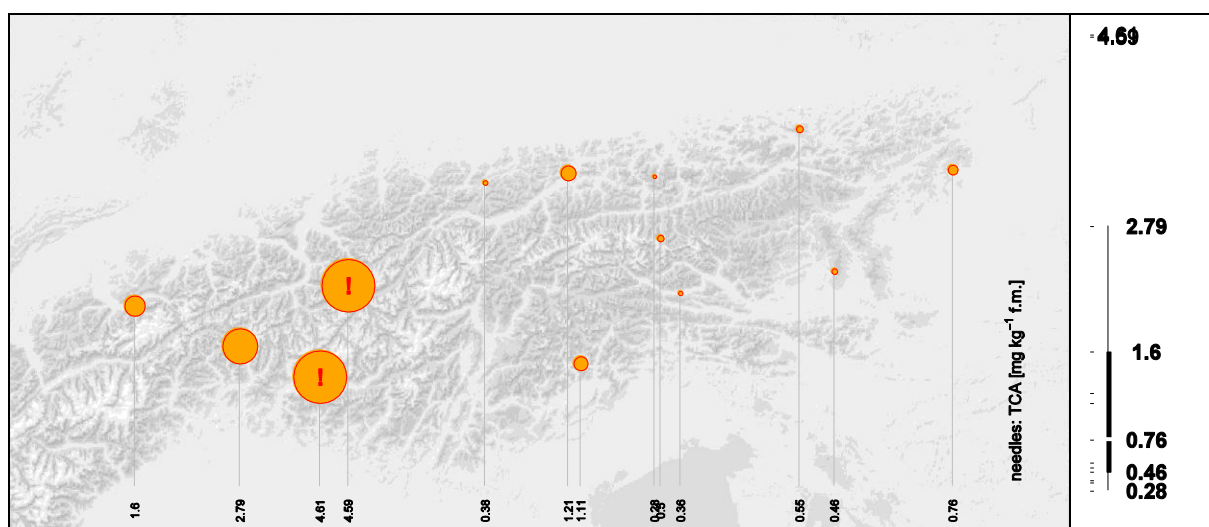


Figure 3-250: Concentrations of trichloroacetic acid in 0.5 year old Norway spruce needles.

3.9.4 Longitudinal variation

Due to the small sample size per longitudinal zone, the observed longitudinal differences were not tested for significance. However, the highest concentrations of trichloromethane and -acetic acid were found in the western part of the study region (Figure 3-249, Figure 3-250).

3.9.5 Latitudinal variation

The corresponding sample sizes were too small to conclude on the latitudinal variation. Figure 3-249 and Figure 3-250 do not suggest a substantial latitudinal gradient, but there are too few observations from the central zone to substantiate this assumption.

3.9.6 Altitudinal variation

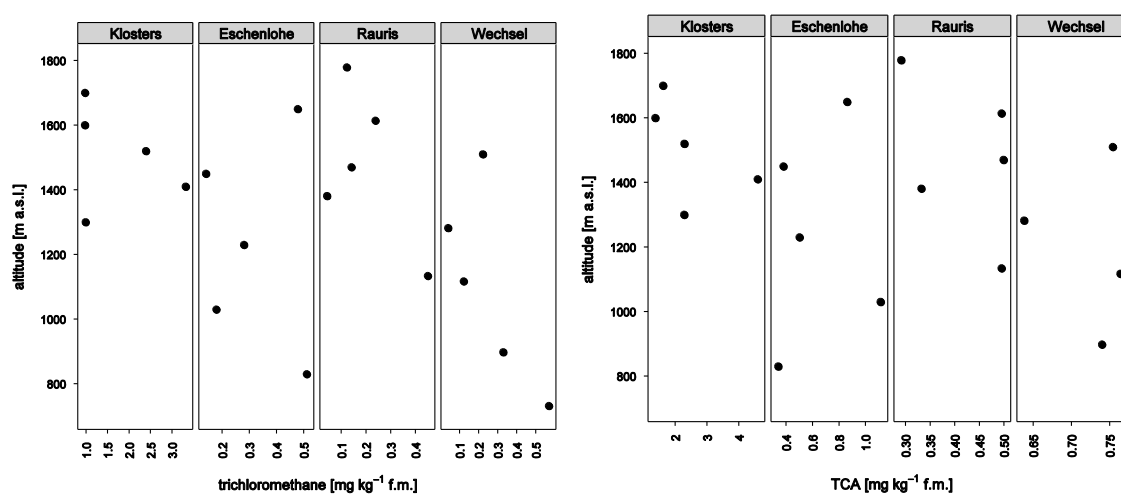


Figure 3-251: Altitudinal variation of trichloromethane and TCA in 0.5 year old Norway spruce needles.

3.10 Chlorinated paraffins (CP)

3.10.1.1 Physicochemical properties

Chlorinated paraffins (CPs), also known as polychlorinated *n*-alkanes (PCAs) or chloroparaffins, are subdivided into short chain (SCCPs, C_{10–13}), medium chain (MCCPs, C_{14–17}), and long chain compounds (LCCPs, C_{>17}) with chlorine contents between 30 and 70% (MUIR et al. 2000) consisting of several thousands of congeners (homologues, isomers and stereoisomers). Technical CPs are colourless to yellowish, low to highly viscous oils or waxy to glassy solids (GDCh, 1992) chemically stable up to >200 °C (WHO 1996). Due to varying chain length and chlorine content of CPs, physico-chemical parameters such as water solubility, vapour pressure, and octanol-water partition coefficients (K_{OW}) span large ranges (Table 3-45).

Table 3-45: Environmentally relevant physical properties (range) of CP mixtures at 20–25 °C

CP mixture	chlorine content [%]	vapour pressure ^{a,b,c} [mPa]	water solubility ^{a,d,e} [µg l ⁻¹]	log K _{OW} ^{a,b,e,f}
SCCPs	48–71	2.8×10 ⁻⁴ –5.4	0.49–975	4.39–8.69
MCCPs	37–58	1.7×10 ⁻⁵ –2.27	2.9×10 ⁻² –14	5.47–8.01
LCCPs	34–54	6.3×10 ⁻¹² –7.9×10 ⁻⁴	1.6×10 ⁻⁶ –8.6×10 ⁻²	8.70–12.68

a) Tomy et al. (1998), b) European Commission (2000), c) Drouillard et al. (1998b), d) Drouillard et al. (1998a), e) POPRC (2007), f) Sijm and Sinnige (1995)

3.10.1.2 Emissions and use

CPs are industrial chemicals introduced in the 1930ies with a current annual production of approx. 300 000 t worldwide (MUIR et al. 2000). Based on the most recently available production data (WHO 1996), a total amount of more than 7 000 000 tons of CPs has been produced since. CPs are mainly used as additives in metal working fluids, and as flame retardants and plasticizers in sealants, paints and coatings (CAMPBELL & McCONNELL 1980). CPs may be released into the environment during production, storage, transportation, industrial and consumer usage of CP containing products, disposal and waste burning, and land filling of products such as PVC, textiles, painted materials, and cutting oils. However, the major releases are supposed to occur during production and industrial usage (TOMY et al. 1998).

3.10.1.3 Environmental behaviour and bioaccumulation

Based on similar physico-chemical properties of other environment related substances, CPs are supposed to adsorb to soil, sediment particles and to atmospheric particles (ENVIRONMENT CANADA 1993, WHO 1996). Few data have been identified on the transport and mobility of CP residues from sites of industrial/manufacturing, use, or disposal. Nevertheless, calculated Henry's Law constants of some CPs are similar to those of chlorinated aliphatic pesticides, such as toxaphene, chlordane, and aldrin, which are known to be transported in the atmosphere (ENVIRONMENT CANADA 1993). However, the high adsorption of CPs to atmospheric particulates at low temperatures may limit the atmospheric degradation pathway (POPRC 2007). Long-range atmospheric transport of CPs is documented by the occurrence of CPs in remote areas like the Arctic (TOMY et al. 1999, BORGÉN et al. 2000, RETH et al. 2006) and increasing CP levels in the environment in the last decades are illustrated by a substantial rise of CP levels in a sediment core from Lake Thun, Switzerland, in the 1980ies (IOZZA et al. 2008).

Despite a high bioaccumulation potential, only few studies on bioconcentration factors (BCFs) have been published. Measurement of BCFs is demanding due to the low water solubility of CPs and subsequent slow uptake rates. Depending on animal species and CP mixture BCFs vary between < 1 and 138 000 (WHO 1996).

3.10.1.4 Toxicology

Acute toxicity of CPs is low (WHO 1996). Nevertheless, SCCPs showed chronic toxicity in aquatic organisms and are carcinogenic in rats and mice (OSPAR COMMISSION 2001). Therefore, SCCPs were categorized as group 2B possibly carcinogenic to humans” by the International Agency for Research on Cancer (WHO 1996). Due to their higher bioaccumulation tendency (WHO 1996) and higher toxicity than MCCPs and LCCPs, SCCPs have also been included in the list of priority hazardous substances of the European Water Framework Directive (EU 2000). For the same reasons, SCCPs are now under discussion to be included in the Stockholm Convention on POPs (PERSISTENT ORGANIC POLLUTANTS REVIEW COMMITTEE 2004).

3.10.2 Summary statistics

Total CP content was high in comparison with other POPs considered in this study.

Remarkably, median and extreme concentrations were higher in needles than in humus. This is a rare exception for the spectre of POPs investigated in this study: concentrations in humus were usually markedly higher than in needles.

3.10.2.1 Needles

The concentration of chlorinated paraffines was studied at the height profiles and at one additional site. At the standard height plots of these profiles and the additional standard plot, CP content varied between 35 and 450 $\mu\text{g kg}^{-1}$ d. m. (median: 55.5, sample size $n=8$). The vertical CP gradients are shown below (Figure 3-252).

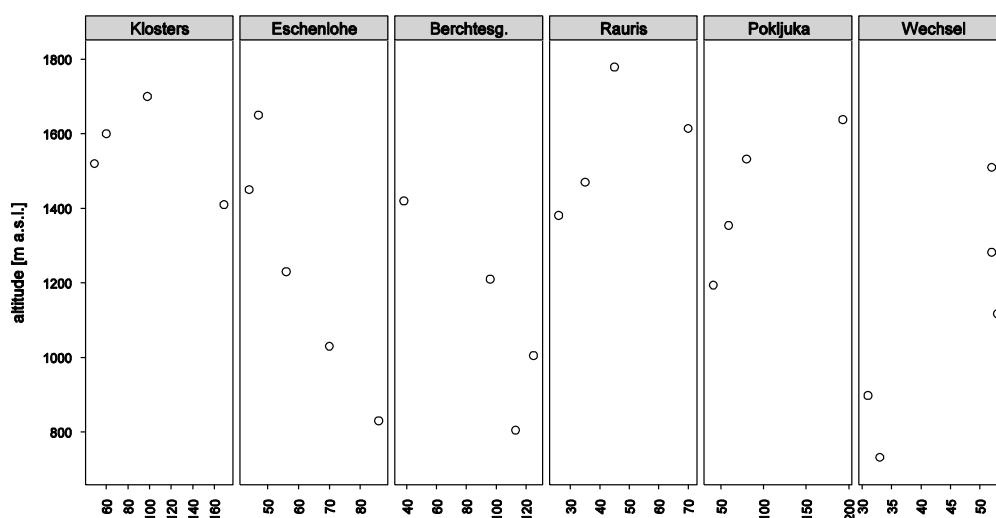
3.10.2.2 Humus

The concentration of chlorinated paraffines was studied at the height profiles. At the standard height plots of these profiles plus two additional standard plots, CP content varied between 20.55 and 95.54 $\mu\text{g kg}^{-1}$ d. m. (median: 37.6, sample size $n=9$). The vertical CP gradients are shown below (Figure 3-253).

3.10.3 Altitudinal variation

No common trend for altitudinal CP gradients was detected; CP content could increase or decrease with height.

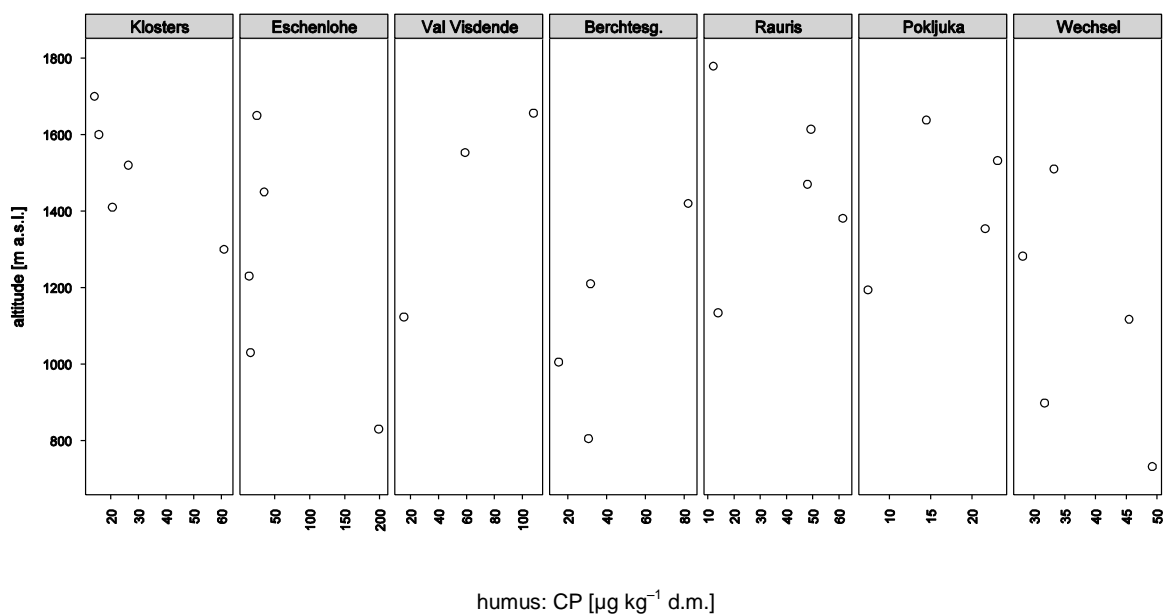
3.10.3.1 Needles



unit: $\mu\text{g kg}^{-1}$ d.m.

Figure 3-252: Altitudinal variation of chlorinated paraffins in Norway spruce needles

3.10.3.2 Humus



humus: CP [$\mu\text{g kg}^{-1}$ d.m.]

Figure 3-253: Altitudinal variation of chlorinated paraffins in forest humus

3.11 Perfluorinated tensides (PFT)

3.11.1 Characterisation

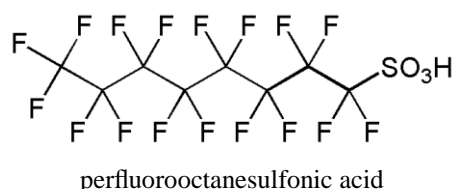
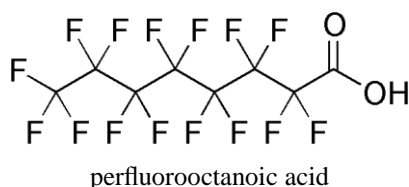
Perfluooctane sulfonate is a fully fluorinated moiety which is found in a large family of PFOS related substances such as perfluorinated tensides. Most members of this group are polymers of high molecular weights in which PFOS constitutes only a small fraction of the total polymer molecule and of the final product (SCHER, 2005).

3.11.1.1 Physicochemical properties

Table 3-46: Physicochemical properties of PFOS

molecular weight (g mol ⁻¹)	500
boiling point (°C)	214
water solubility @ 20 °C, mg l ⁻¹	519
vapour pressure (Pa)	3.31×10 ⁻⁴
log Kow	not measurable

source: EA, UK (2004)



3.11.1.2 Emissions and use

Main categories of use of PFOS related chemicals are surface treatments, paper protection, and performance chemicals. They are used in a wide variety of applications e.g. in textiles and leather products; metal plating; food packaging; fire fighting foams; floor polishes; denture cleansers; shampoos; coatings and coating additives; in the photographic and photolithographic industry; and in hydraulic fluids in the aviation industry. Estimated annual use within the EU, before the largest producer 3M ceased production, was approximately 500 tons (EUROPEAN ENVIRONMENT AGENCY, 2004).

3.11.1.3 Environmental behaviour and bioaccumulation

Perfluorooctane sulfonate is extremely persistent in the environment. Perfluorooctane sulfonate does not accumulate in fatty tissue, due to its hydro- and lipophobic properties. Perfluorooctane sulfonate binds to proteins in blood and liver. The octanol-water partition coefficient (Kow) is not measurable for perfluorooctane sulfonate. PFOS has been shown to bioconcentrate in fish (UNECE, 2005). PFOS is subject to long range trans-boundary air pollution.

3.11.1.4 Toxicology

PFOS has been shown to cause developmental effects in mammals at low levels. It is also toxic to aquatic organisms (UNECE 2005). The half-life of PFOS in organisms depends on species: 100 days in rats, 200 days in monkeys, and years in humans. The toxicity profile of PFOS is similar for rats and monkeys. Repeated exposure results in hepatotoxicity and increased mortality; the dose-response curve is very steep for mortality, with specific sensitivity of the neonate. Exposure to PFOS resulted in hepatocellular adenomas and thyroid follicular cell adenomas in a two year bioassay study. Epidemiologic studies have shown an association between PFOS exposure and the incidence of bladder cancer (OECD 2002).

3.11.2 Summary statistics

Some PFT were not detected or did at least not exceed the quantification limit in humus. Not detectable were perfluoro(PF)-decane sulfonate and PF-octanyl sulfonamide. Entirely below the quantification limit were PF-heptanoic acid and (with half the observations even below detectability) PF-dodecanoic acid (Table 3-47).

Table 3-47: Concentrations of perfluorates in forest humus

	n<LOD	n<LOQ	mean	sd	min	P ₂₅	median	P ₇₅	max
PF-hexanoic acid	5	6			< 0.13		< 0.43		0.557
PF-heptanoic acid	2	12			< 0.12		< 0.39		< 0.39
PF-octanoic acid	0	0	0.867	0.336	0.464	0.573	0.772	1.124	1.448
PF-nonanoic acid	0	4	0.431	0.188	< 0.40	0.253	0.439	0.509	0.839
PF-decanoic acid	0	4	0.454	0.228	0.185	0.231	0.425	0.631	0.832
PF-undecanoic acid	0	3	0.678	0.404	< 0.34	0.448	0.607	0.946	1.581
PF-dodecanoic acid	8	6			< 0.09		< 0.09		< 0.29
PF-octane sulfonate	0	0	2.804	1.157	1.636	1.919	2.593	3.132	6.153
PF-decane sulfonate	14	0							< 0.34
PF-octanesulfonamide	14	0							< 0.26

unit: $\mu\text{g kg}^{-1}$ d. m.; sample size n=14; LOD/LOQ...limit of detection/quantification

3.11.3 Longitudinal variation

PFT were analysed in samples from three height profiles, spatial coverage is thus confined. However, the selected height profiles approximately span the study area from the western “Klostern” profile (Switzerland) to the intermediate German “Berchtesgaden” to the easternmost profile and site “Wechsel” (Austria).

Unlike observed with other pollutants, the contamination levels of the following PFT were remarkably similar between the three height profiles: perfluoro(PF-)hexanoic acid (Figure 3-254), PF-nonaonic acid (Figure 3-257), and PF-dedaonic acid (Figure 3-258). Further, the western and the intermediate profile (Klostern and Berchtesgaden) had comparable levels of PF-octaonic acid and its sulfonate, while the eastern profile Wechsel was half (acid) or twice (sulfonate) as contaminated with these octanyl perfluorates.

3.11.4 Altitudinal variation

As observed earlier, there was no common altitudinal trend to all three height profiles: concentrations could increase or decrease with height or vary without apparent dependence on altitude.

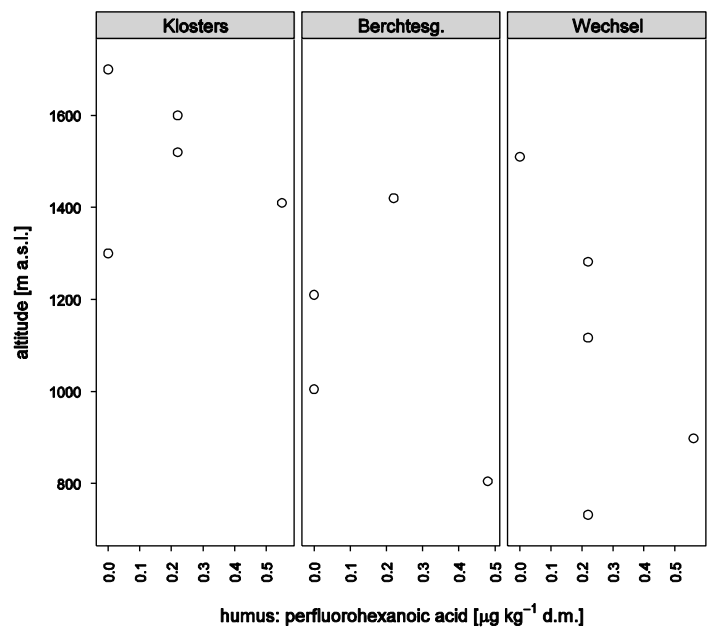


Figure 3-254: Altitudinal variation of perfluorohexanoic acid (PF6C) in forest humus

Perfluoroheptaonic acid (PF7C): twelve out of 14 samples contained PF7C below the quantification limit of $0.4 \mu\text{g kg}^{-1}$ d. m., and two samples fell below the detection limit.

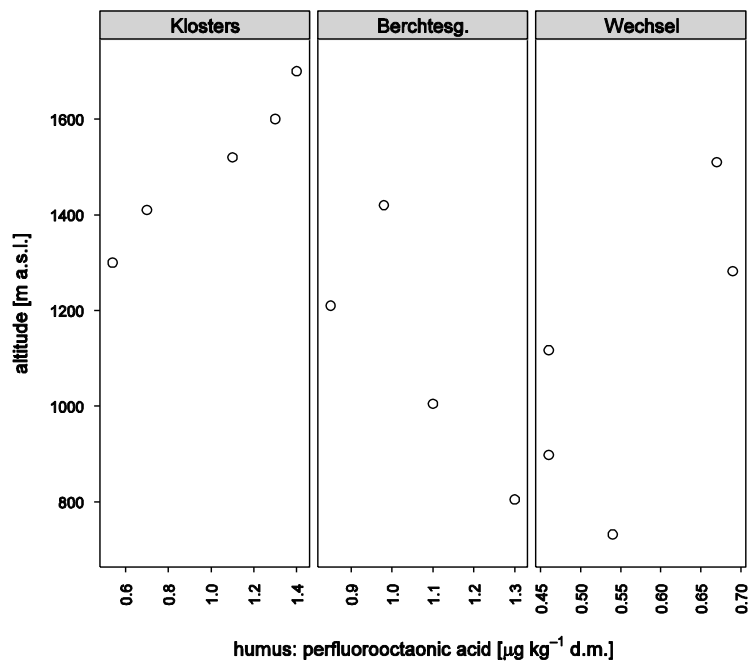


Figure 3-255: Altitudinal variation of perfluorooctaonic acid (PF8C) in forest humus

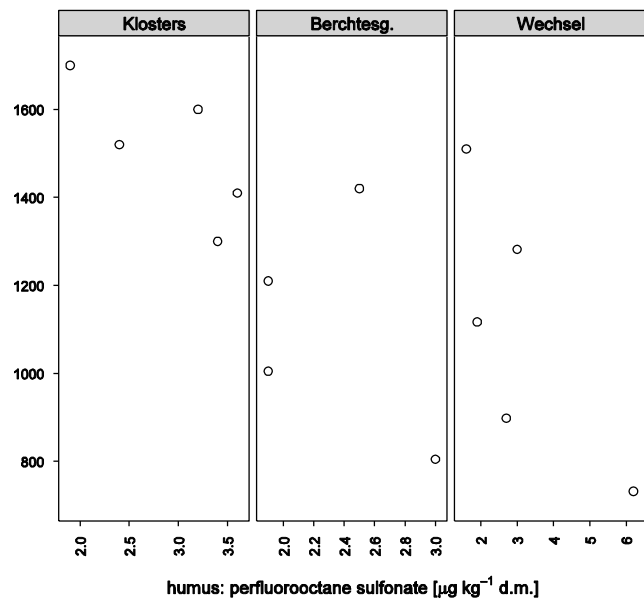


Figure 3-256: Altitudinal variation of perfluorooctane sulfonate (PF8S) in forest humus

Perfluorooctanesulfonamide (PFOSA) was not detected in any humus sample.

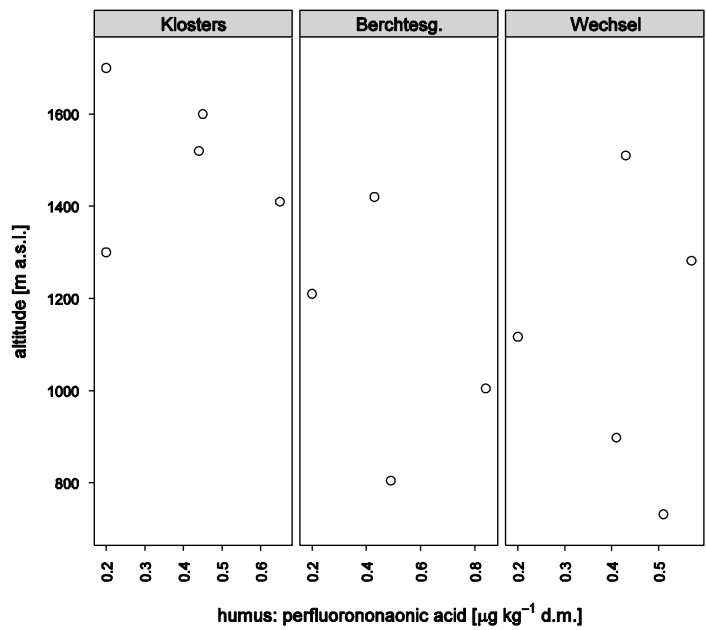


Figure 3-257: Altitudinal variation of perfluorononaonic acid (PF9C) in forest humus

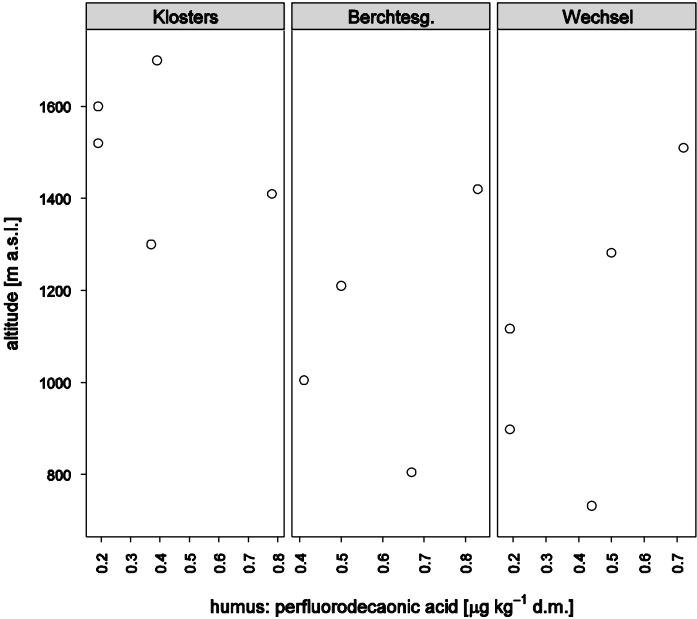


Figure 3-258: Altitudinal variation of perfluorodecaonic acid (PF9C) in forest humus

Perfluorodecaonic sulfonate was not detected in any humus sample.

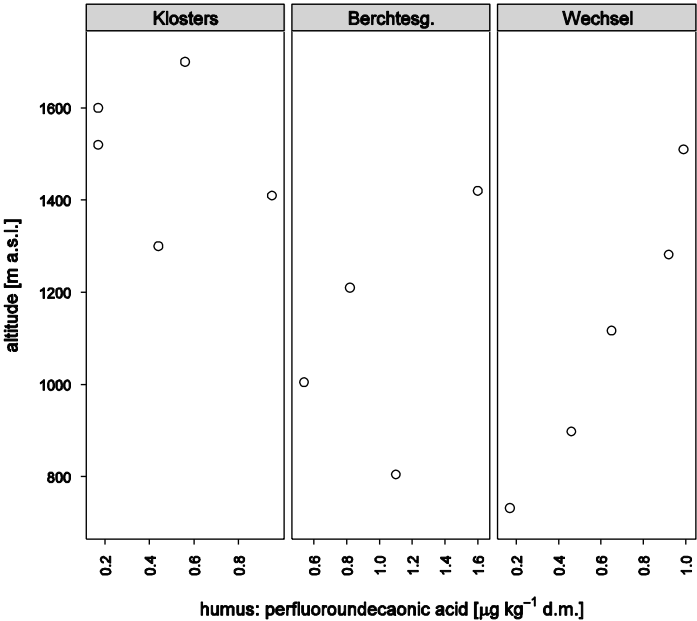


Figure 3-259: Altitudinal variation of perfluoroundecaonic acid (PF11C) in forest humus

Perfluorododecaonic acid was not detected in eight and below the quantification limit ($0.29 \mu\text{g kg}^{-1} \text{ d. m.}$) in six out of 14 samples.

3.12 Nonylphenol

3.12.1 Characterisation

3.12.1.1 Physicochemical properties

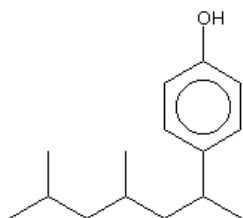


Figure 3-260: Structure of 4-nonylphenol

Table 3-48: Physicochemical properties of nonylphenol

Melting point.....	ca. -8 °C
Relative density:	0.95 at 20°C
Vapour pressure:	ca. 0.3 Pa at 25°C
Water solubility:.....	ca. 6 mg l ⁻¹ @ 20°C and pH 7
log K _{OW}	4.48

source: JRC (2002)

3.12.1.2 Emissions and use

Four companies within the EU produced nonylphenol with a total production volume of 73 500 tonnes in 1997. In the same year exports from the EU were 3,500 and imports into the EU were 8 500 tonnes, giving the total tonnage used in the EU as 78 500 tonnes.

The main uses of nonylphenol are the production of nonylphenol ethoxylates and the production of resins plastics and stabilisers. Minor uses include the production of phenolic oximes. The breakdown of nonylphenol ethoxylates in the environment may give rise to significant quantities of nonylphenol, therefore their use is considered in the risk assessment. The main use of nonylphenol ethoxylates is in products for industrial and institutional cleaning (30% total use). This is followed by use in emulsion polymerisation, as a textile auxiliary, captive use by the chemical industry, as a leather auxiliary, agricultural use, use in paints and other niche market uses. (All information on emissions and use taken from: JRC 2002).

3.12.1.3 Environmental behaviour and bioaccumulation

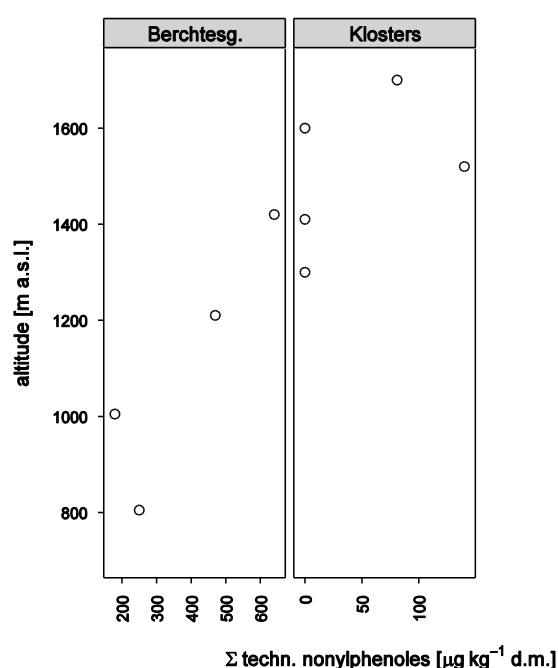
Nonylphenol can be released to the environment during production and use, or through the degradation of products containing nonylphenol groups. Atmospheric nonylphenol has a very low half life of ca. 0.3 days because it is rapidly broken down in the presence of hydroxyl radicals. Due to its physicochemical properties, the substance can be expected to adsorb strongly to soils, sludges and sediments. Significant volatilisation from water is unlikely, significant bioconcentration in aquatic systems can be expected (JRC 2002).

3.12.1.4 Toxicology

4-Nonylphenol is highly toxic in aquatic environments. It can induce liver damage and irritate skin and mucous membranes. Nonylphenol affects the endocrine system (reported are reduction of sperm count or alterations of sexual development and menstrual cycle). It can enter the placenta. There is *in vitro* evidence of immunotoxicity.

3.12.2 Altitudinal variation

Nonylphenols have been analysed in humus samples from three height profiles. Nonylphenol concentrations at profile Berchtesgaden (DE) increased with height and were much higher than at the other profiles, approaching the mg kg^{-1} range (Figure 3-261).



Limit of quantification: $69 \mu\text{g kg}^{-1}$ d. m. At the Wechsel height profile, only one sample exceeded the detection limit but remained below the limit of quantification.

Figure 3-261: Altitudinal variation of nonylphenole content in forest humus

3.13 Physiological parameters

3.13.1 Micro-EROD Bioassay

EROD bioassays confirmed the presence of conventionally (i.e. through chemical analysis) detectable, and presumably additional unidentified, toxic substances in humus and needle samples. Extracts of air and Norway spruce samples elicited low dioxin-specific responses. Humus samples, however, triggered pronounced activities which also were related to the altitude at which the samples were retrieved.

3.13.1.1 Summary statistics

Table 3-49: Dioxin-like activity of humus and mineral soil samples

	n	n < LOQ	min	median	mean	max
humus	29	0	2.1	5.2	6.5	17.7
mineral soil	9	2	< 1	4.6	7.3	21.8

unit: ng TEQ_{WHO} kg⁻¹ d.m.; LOQ: 0.6; incubation time: 72 h

Dioxin-like activity of humus samples as indicated by (the response of the Ah-receptor in) the bioassays was tendentially higher than the toxic equivalents of the measured (HRMS/GC) dioxin and PCB concentrations (Figure 3-262).

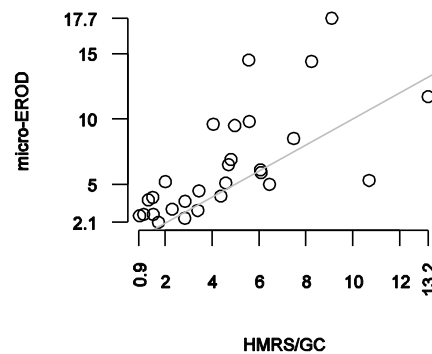
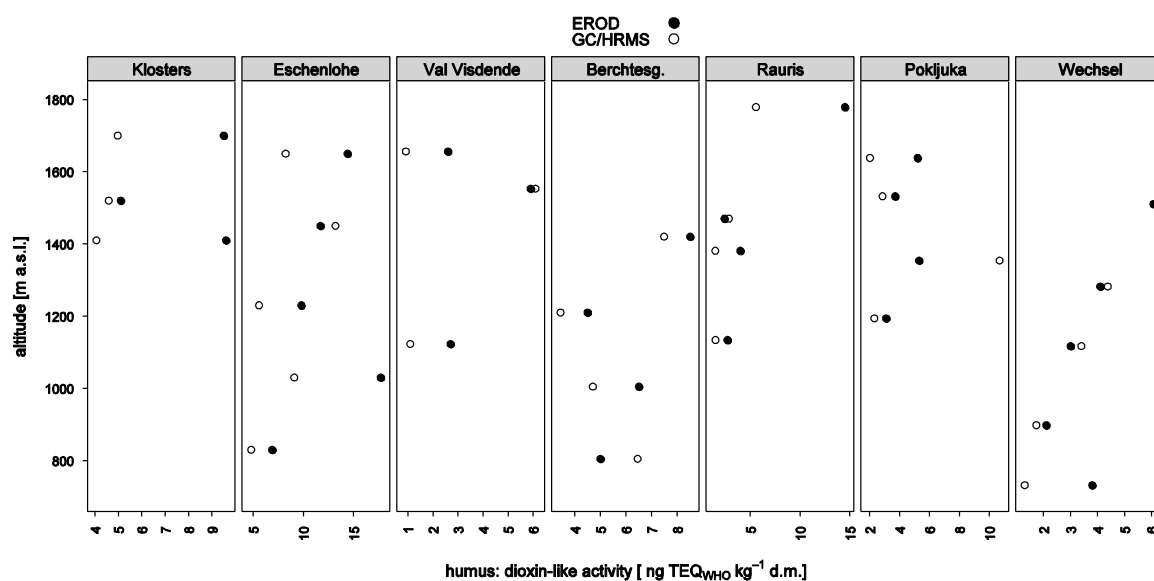


Figure 3-262: WHO toxic equivalents [ng TEQ_{WHO} kg⁻¹ d.m.] of humus samples measured with HMRS/GC vs. bioassay results (grey line indicates 1:1 ratio).

3.13.1.2 Altitudinal variation

Humus

The altitudinal variation of dioxin-like activities in humus, as indicated by the EROD bioassays, was – both qualitatively and quantitatively – at good agreement with the values calculated from measured dioxin/furan and PCB concentrations (Figure 3-263). The bioassays gave tendentially higher estimates. This could be explained by the presence of other (than PCDD/F and PCB) contaminants with dioxin-like toxicity and would confirm the value of bioassays to assess the biological effects of environmental POP pollution.



“EROD” is the dioxin-like activity of humus samples observed in the bioassays. “GC/HRMS” is the dioxin-like activity calculated from the measured concentrations of PCDD/F and dl-PCB in the corresponding humus samples.

Figure 3-263: Altitudinal variation of dioxin-like activity of forest humus extracts

SPMD

Bioassays were also tried with SPMD samples from the Eschenlohe height profile. However, SPMD extracts elicited no dioxin-specific response.

3.13.2 Enzyme activity

The pigment patterns of the analysed needles did not indicate elevated stress or disease (data not shown). All samples showed GST activity for the conjugation of chlorinated benzenes, e.g. chlorodinitrobenzene (CDNB), and dichloronitrobenzene (DCNB). CDNB was metabolized ten times as fast as DCNB (Figure 3-264 and Figure 3-266).

As observed with a number of other pollutants, height profiles showed no common trend. The relation between height and GST activity changed between individual profiles (Figure 3-265-Figure 3-267). The altitudinal gradient also varied between GST activities invoked by different substrates (CDNB or DCNB), which suggests that the involved enzyme proteins are not (fully) identical.

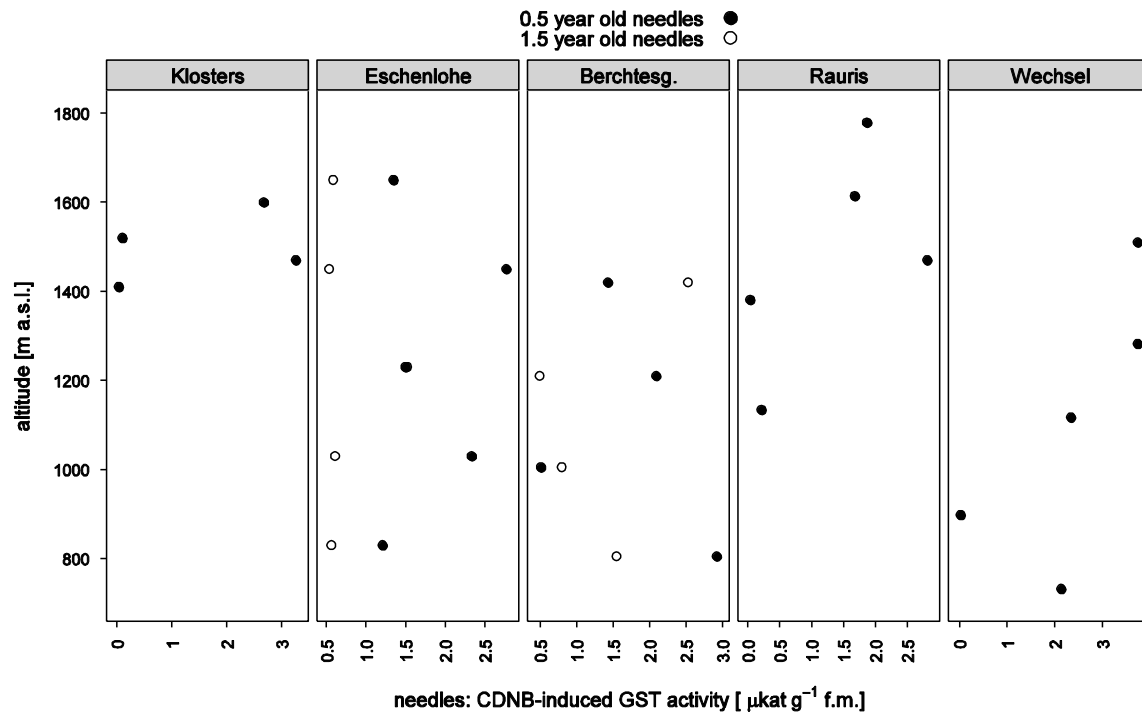


Figure 3-264: Altitudinal variation of CDNB-induced GST activity in 0.5 year and 1.5 year old Norway spruce needles

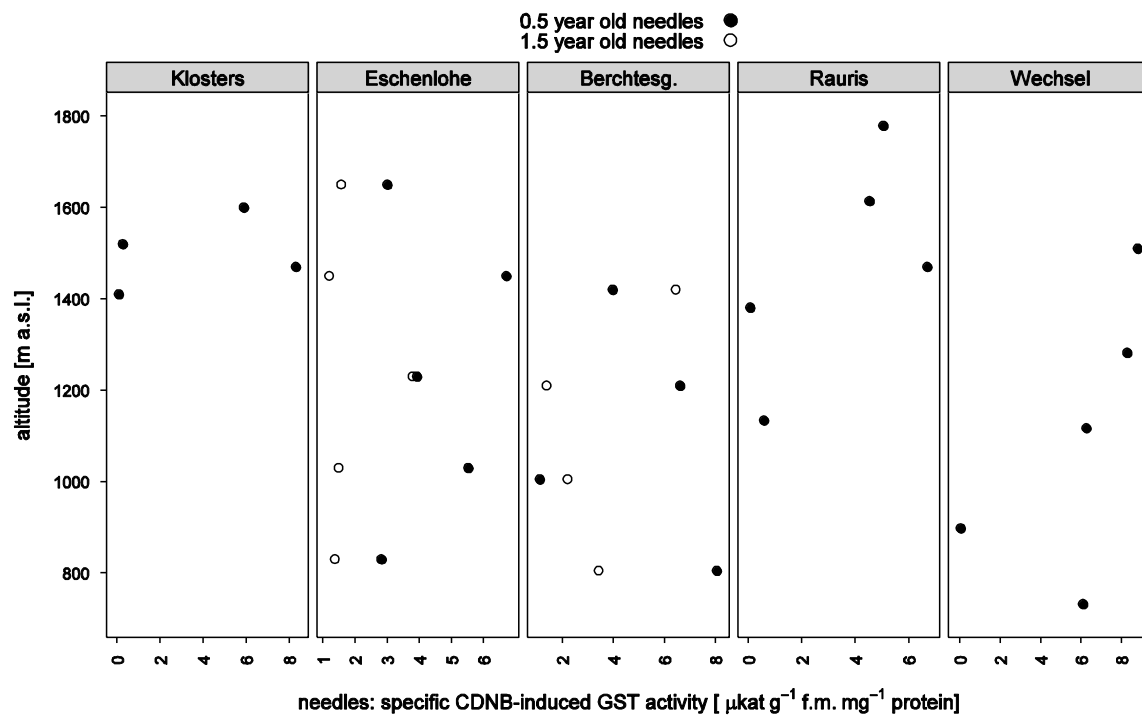


Figure 3-265: Altitudinal variation of specific CDNB-induced GST activity in 0.5 year and 1.5 year old Norway spruce needles

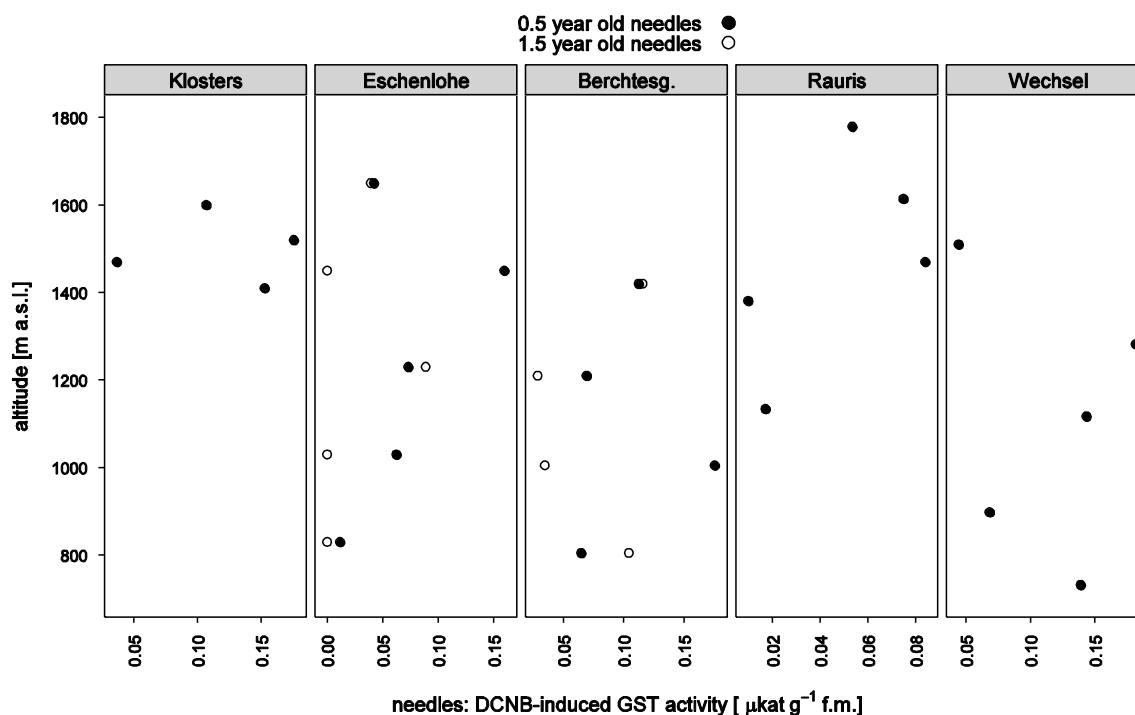


Figure 3-266: Altitudinal variation of DCNB-induced GST activity in 0.5 year and 1.5 year old Norway spruce needles

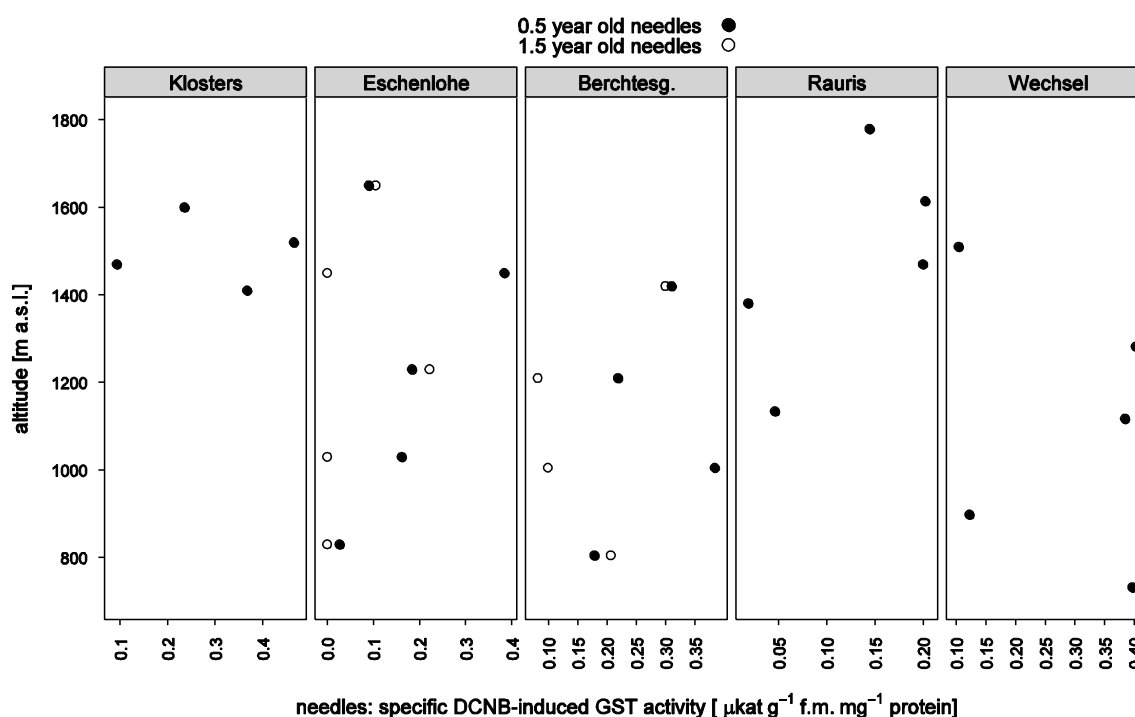


Figure 3-267: Altitudinal variation of specific DCNB-induced GST activity in 0.5 year and 1.5 year old Norway spruce needles

3.14 Correlations between different pollutants / effect parameters

Note that this section presents only the strongest associations between different compound groups (see 1.8.3 on page 28 for explanation).

3.14.1 Needles

The situation observed for 0.5 year old needles was very different from that in humus (see 3.14.2; p. 235 ff): the association between pollutants of different properties and origin was generally weak. Significant correlations between members of different compound classes were comparably sparse and usually of lower coefficient than those found for humus.

3.14.1.1 OCP

Strong correlations between organochloropesticides and other POPs in needles were sparse. Some of the few high correlations occurred between DDX, TCA and trichloromethane. DDT (which degrades a. o. into DDD) shares, as a structural similarity, a trichloroalkylic group with TCA and trichloromethane.

Table 3-50: Important correlations between OCP and other parameters in 0.5 year old Norway spruce needles

		HCH		o,p'-DDT	DDX		p,p'-DDE	cyclodiens Dieldrin
		δ -HCH	ϵ -HCH		p,p'-DDT	p,p'-DDD		
CKW	TCA			.649		.804		
	trichloromethane			.834	.673	.862		.609
CP	CP	-.937						
NP	3-methyl-2-nitrophenol						.615	

number of paired observations of OCP and ...TCA, trichloromethane, NP: n=13, ...CP: n=7

3.14.1.2 PAH

Generally, PAH concentrations in needles were only loosely associated with other POPs. Tighter correlations were only observed for the smaller (3-4 rings, except the pentacyclic DBahA) species. Given these circumstances, the association between chloroparaffine and PAH content was remarkably strong (Table 3-51).

Table 3-51: Important correlations between PAH and other parameters in 0.5 year old Norway spruce needles

		NAPH	ANA	FLU	PHEN	FLA	PYR	DBahA	Σ 16 PAH
PBDE	BDE 154					.747			
	TCA			.643	.610				
	trichloromethane	.613							
CP	CP	.880	.757	.778	.938	.964	.964		.929
NP	3-methyl-2-nitrophenol							.630	

number of paired observations: n=13 (except PAH and CP: n=7)

3.14.1.3 PCDD/F

Correlations between dioxins / furans and other POPs in needles were far less pronounced than in humus (compare Table 3-52 with Table 3-58, p. 238). Only the hexachlorinated homologues showed a stronger coupling to the heavier (six or more chlorines), less volatile and more lipophilic PCB congeners. There was a noteworthy relationship between high needle concentrations of 4-nitrophenol and dioxins/furans.

Table 3-52: Important correlations between PCDD/F and other parameters in 0.5 year old Norway spruce needles

		TCDF	PeCDF	HxCDF	HpCDF	PCDF	HxCDD	HpCDD	PCDD	PCDD/F	in TEQ
PBDE	BDE 154	.651									
CHC	TCA			.670							
CP	CP										.778
NP	4-nitrophenol				.647	.693	.631	.646	.628	.757	.619
PCB	52										.635
	138			.600			.751				
	153						.612				
	180		.618	.640			.776			.645	
	Σ 6 PCB						.667				
dl-PCB	156			.606			.703				
	157			.623			.611				
	167			.704			.690				

number of paired observations of PCDD/F and ...PCB: n=40, ... PBDE: n=14, ...NP: n=13, ...CP: n=7

3.14.1.4 PCB

Apart from the association with the hexachlorinated dioxins and furans (see previous point), PCB concentrations showed only few stronger correlations with -among all remaining parameters- PBDE (Table 3-57).

Table 3-53: Important correlations between PCB and other parameters in 0.5 year old Norway spruce needles

		PCB 153	PCB 105	PCB 156	PCB 167	PCB 189
PBDE	BDE 99		.653	.689	.605	.616
	BDE 100		.652	.622	.647	.679
	BDE 209	.600				

14 paired observations

3.14.1.5 PBDE

Apart from the few and relatively weak associations with one PAH (fluoranthene), single PCB and TCDF mentioned earlier, needle PBDE content showed no tight coupling to any of the other parameters.

3.14.1.6 CP

As described above, total chloroparaffine content showed a conspicuous association to the lighter PAH species and to the total content of 16 EPA-PAH. There was also a high correlation with WHO toxic equivalents (arising from the dioxin and furan contents) and TCA concentration (for the five sites available for comparison). One of the rare *negative* correlations was found for CP and δ -HCH content (Table 3-50).

3.14.1.7 Short-chain chloroalkanes

Table 3-54 summarizes the association between short-chain chloroalkanes and other parameters, some of which have already been mentioned earlier. High correlations were only found for TCA and trichloromethane. Remarkably, high trichloromethane (=chloroform) levels were accompanied by low activities of the potentially detoxifying GST isoenzyme (Table 3-54).

Table 3-54: Important correlations between short-chain chloroalkanes and other parameters in 0.5 year old Norway spruce needles.

	TCA	trichloromethane
PAH	NAPH	.613
	FLU	.643
	PHEN	.610
CP	CP	.955
GST	CDNB	-.670
	sCDNB	-.683
OCP	Dieldrin	.609
	o,p'-DDT	.649
	p,p'-DDD	.804
	p,p'-DDT	.673
PCDD/F	HxCDF	.670

number of paired observations of TCA/trichloromethan and ...PCDD/F: n=13, ...OCP, FLU:n=12, ...GST: n=11 ...CP: n=5

3.14.1.8 NP

The correlations between needle nitrophenol contents and other parameters have already been listed in the preceeding tables. To recapitulate, NP levels were only loosely associated to other POP concentrations, except the coupling between 4-nitrophenol and various dioxins / furans (Table 3-52).

3.14.2 Humus

To allow an overview over the most important associations between various parameters, only significant correlations with an absolute coefficient ≥ 0.6 are presented here, coefficients ≥ 0.7 are shown in bold type. Polyfluorinated tensides are not considered in the following, because observations focused on height profiles which leaves too few data to describe the situation at standard height. Table 3-55 illustrates the association between various pollutants and other parameters in humus. Note that Table 3-55 is a simplified scheme. For a more detailed description and the underlying correlation tables, consult the following subsections.

Table 3-55: Strongly correlated compound classes in forest humus.

	OCP	PAH	PCDD	PCDF	PCB	PBDE	CP	EROD	CPh
OCP		+	+	+	+	+	-	+	-
PAH	+		+++	++	-	+	-	++	-
PCDD	+	+++		-	+++	++	-	+++	-
PCDF	+	++	-		+++	+	-	++	-
PCB	+	-	+++	+++		++	-	+++	-
PBDE	+	+	++	+	++		-	-	-
CP	-	-	-	-	-	-		-	-
EROD	+	++	+++	++	+++	-	-		-

[illegible]

CPh...chlorophenols, EROD...dioxinlike activity of humus samples in EROD-bioassays

3.14.2.1 OCP

Table 3-56: Important correlations between organochloropesticides and other parameters in forest humus

		γ -HCH	Aldrin	Dieldrin	Endrin	HCB	Mirex	o,p'-DDT	o,p'-DDD	p,p'-DDD	o,p'-DDE	p,p'-DDE	Σ DDX
PBDE	28	.710		.678	.627		.603						
	47	.630		.630									
	99	.611		.630									
	100	.600		.612									
	Σ 6 BDE	.600							-.606				
PAH	ANY			.663									
	FLU			.606									
	PHEN			.698									
	FLA	.631		.674		.628	.704						
	PYR			.643									
	BaP			.601			.681						
	BkF						.625						
	DBahA			.690		.628	.714						
	BghiP			.760		.669	.720						
	IND			.661									
	DBaePYR			.633									
	DBaiPYR	.612		.677		.600	.765	.653		.655	.688	.641	
DBalPYR			.709		.603	.701							
PCB	101						.610						
	138			.808			.690						
	153			.778			.648						
	180			.790			.607						
	Σ 6 PCB			.706			.620						
	dl-PCB	105			.670								
114				.727									
118				.719			.694						
123				.696									
126				.676									
156				.799			.662						
157				.773									
167				.781			.606						
169				.624									
189				.790									
Σ dl-PCB				.744			.638						
in TEQ				.690									
PCDF	TCDF			.633			.651						
	PeCDF			.735			.672						
	HxCDF			.737			.693						
	HpCDF			.716									
	PCDF			.754			.652						
PCDD	TCDD						.641						
	PeCDD			.652			.692						
	HxCDD			.733			.740						
	HpCDD			.695			.649						
	OCDD			.679			.600						
	PCDD			.704			.627						
PCDD/F	PCDD/F			.823			.687						
	in TEQ			.721			.717						
EROD	EROD		.821					-.867	.955				

number of paired observations: n=31 (except EROD: n=7)

3.14.2.2 PAH

Humus contamination with PAH was strongly associated with dioxin contents and to a slightly smaller extent (fewer and lower significant correlations) with furan concentrations. For dioxin homologues, the association with PAH increased with the degree of chlorination.

fluorene, phenanthrene, fluoranthene and pyrene showed particularly tight correlation with PCDD/F and PCB, and fluorene was also the PAH species with notable coupling to several investigated PBDE. Naphthalene, in turn, did not vary consistently with any other compound group (neither did DBahPYR which, however, was detected in only one quart of all observations).

Table 3-57: Important correlations between PAH species and other parameters in forest humus

	NAPH	ANA	ANT	ANY	FLU	PHEN	BaA	CHR	FLA	PYR	BaP	BbF	BkF	DBahA	BghiP	IND	DBahPYR	DBahPYR	DBahPYR	DBahPYR
PBDE	28				.613															
	47				.652															
	99			.649	.722	.631														.602
	100				.657															
	154				.622															
	Σ 6 BDE				.659															
PCB	101				.653	.649			.615	.658					.615		.656			.648
	138	.616	.680	.705	.760	.819	.661	.603	.752	.742	.657		.619	.716	.728	.687	.662		.684	.714
	153		.682	.654	.733	.790	.654	.623	.719	.733	.655		.615	.698	.683	.688	.664		.654	.670
	180		.659	.638	.736	.799	.684	.636	.690	.749	.646	.625	.611	.669	.683	.693	.660		.662	.672
	Σ 6 PCB		.636		.739	.737	.643		.653	.689	.626		.626	.664	.637	.660			.637	.669
dl-PCB	77				.684				.616	.661										
	81				.619	.695			.613	.644										
	105		.656	.626	.714	.787	.601		.668	.756						.643	.633			
	114		.653	.633	.739	.798	.668		.700	.788					.631	.663	.684			.642
	118		.608	.679	.657	.766			.747	.690				.638	.700	.609			.610	.664
	126		.649	.602	.661	.783			.701	.748					.610	.654	.612			
	156	.610	.707	.739	.723	.846	.678	.625	.825	.817	.666	.607	.626	.742	.767	.728	.700		.689	.750
	157		.708	.680	.742	.824	.673	.616	.730	.810	.610	.638		.664	.672	.722	.708			.669
	167		.703	.709	.731	.842	.670	.616	.787	.805	.641	.605	.606	.701	.708	.708	.680		.626	.687
	169		.644		.710	.755	.649	.645		.713		.670			.620	.695	.663			.640
	189		.699	.716	.764	.830	.706	.648	.740	.781	.672	.648	.638	.714	.722	.721	.689		.620	.705
	Σ 12 PCB		.661	.690	.714	.811	.622		.751	.749				.652	.690	.660	.625		.602	.665
	in TEQ		.656	.616	.672	.792			.711	.754				.606	.627	.662	.621			.607
	TCDF	.635	.611	.690		.701			.801	.708				.727	.656	.628	.602		.699	.656
	PeCDF	.625	.733	.750	.742	.770	.645	.646	.838	.793	.678	.605	.643	.779	.723	.719	.693		.691	.770
	HxCDF		.786	.783	.721	.792	.608	.641	.807	.764	.670	.669	.678	.814	.825	.811	.767	.602	.685	.844
PCDD/F	HpCDF		.746	.701	.694	.708		.609	.647	.675	.600	.677	.649	.725	.714	.772	.744			.718
	PCDF		.745	.757	.717	.775	.605	.621	.820	.791	.644	.613	.624	.768	.750	.749	.714		.688	.776
	TCDD	.654		.650		.633			.779	.631				.615	.649				.606	.606
	PeCDD		.720	.767	.618	.789			.853	.752	.627			.758	.814	.702	.622		.620	.777
	HxCDD		.790	.815	.772	.798	.614	.616	.851	.751	.700	.623	.706	.815	.812	.754	.686		.627	.826
	HpCDD	.618	.792	.805	.742	.800	.638	.610	.796	.703	.718	.656	.712	.818	.834	.768	.685			.819
	OCDD		.836	.784	.772	.819	.665	.633	.764	.724	.713	.717	.738	.801	.826	.803	.718			.791
	PCDD	.601	.824	.813	.759	.834	.662	.631	.820	.748	.721	.685	.725	.822	.832	.796	.714			.811
	PCDD/F		.835	.851	.790	.852	.661	.664	.852	.813	.709	.707	.733	.840	.841	.821	.763		.660	.838
	in TEQ	.617	.744	.810	.690	.802	.616	.619	.852	.763	.682	.607	.654	.815	.823	.762	.690		.700	.813
	EROD	.870	.852	.887	.846	.834	.800							.794	.786					

number of paired observations: n=31, except dioxinlike activity in EROD bioassays (n=7)

3.14.2.3 PCDD/F

The tight connection between humus PCDD/F (particularly dioxin-) contents and PAH levels has already been mentioned above. Even stronger was the coupling between PCDD/F and PCB concentrations (Table 3-58).

OCDF was an exception from all PCDD/F homologues in that it was only loosely correlated (coefficients < 0.6) with other compounds (Table 3-57, Table 3-58). Dioxinlike activity of the humus samples (as measured with EROD bioassays) varied much stronger with dioxin than with furan concentrations.

Table 3-58: Important correlations between PCDD/F and other parameters in forest humus

		TCDF	PeCDF	HxCDF	HpCDF	OCDF	PCDF	TCDD	PeCDD	HxCDD	HpCDD	OCDD	PCDD	Σ PCDD/F	in TEQ
PBDE	28										.620				
	47			.635							.621				
	99			.684	.605					.635	.698	.652	.664	.631	.636
	100			.642						.600	.642		.603	.602	
	154			.670	.637						.640				.625
	Σ 6 BDE			.662	.603						.643		.602	.606	.623
PCB	101	.648	.646	.632		.668		.613	.730	.633	.635	.660	.724	.643	
	138	.829	.875	.863	.743	.871	.724	.857	.842	.851	.831	.866	.906	.887	
	153	.744	.827	.839	.735	.828	.624	.783	.811	.836	.824	.845	.871	.841	
	180	.687	.791	.780	.697	.805		.691	.737	.740	.742	.764	.837	.783	
	Σ 6 PCB	.682	.749	.762	.681	.751		.741	.766	.771	.757	.782	.799	.770	
	77	.691	.803	.668	.643	.809	.697	.708	.742	.665	.696	.713	.801	.710	
	81	.705	.795	.685	.629	.787	.713	.707	.718	.660	.668	.696	.766	.733	
	105	.704	.810	.698	.661	.816	.663	.718	.744	.690	.726	.739	.833	.732	
	114	.705	.767	.707	.625	.765	.657	.713	.739	.695	.722	.739	.796	.736	
	118	.807	.853	.767	.680	.847	.790	.855	.835	.813	.805	.840	.880	.834	
	123	.611	.614										.636	.602	
	126	.735	.815	.765	.700	.833	.688	.764	.768	.759	.783	.797	.852	.796	
	156	.837	.889	.861	.744	.889	.778	.847	.850	.836	.810	.857	.921	.905	
	157	.739	.828	.822	.735	.835	.649	.749	.764	.773	.783	.805	.872	.829	
	167	.786	.844	.833	.728	.849	.725	.806	.816	.820	.809	.844	.895	.867	
	169		.740	.758	.778	.604	.790		.633	.702	.735	.770	.755	.821	.729
	189	.725	.831	.820	.741	.837	.628	.736	.786	.796	.792	.816	.892	.839	
	Σ 12 PCB	.806	.864	.794	.709	.865	.758	.844	.825	.814	.817	.845	.892	.844	
	in TEQ	.746	.823	.775	.706	.840	.695	.776	.776	.771	.793	.808	.861	.807	
EROD	EROD			.807				.795	.884	.873	.907	.915	.918		.850

number of paired observations: n=31, except dioxinlike activity in EROD bioassays (n=7)

3.14.2.4 PCB

As described above, humus PCB levels were tightly associated with PCDD/F concentrations and, slightly less, with PAH contents. In addition to these, high PCB concentrations were also associated by elevated PBDE contents, at least those routinely analysed indicator PCB which are more abundant than the dioxinlike congeners. However, correlations with PBDE were generally weaker than with PCDD/F or PAH (compare coefficients in Table 3-58 with those in the previous subsections). As expectable, humus with higher levels of dioxinlike PCB congeners developed higher dioxinlike activities in the EROD bioassays (Table 3-59).

Table 3-59: Important correlations between PCB congeners and other parameters in forest humus

		BDE28	BDE47	BDE99	BDE 100	BDE154	Σ 6 BDE	EROD
PCB	101	.643	.608	.611				
	138	.692	.665	.698	.652	.643	.672	.788
	153	.672	.659	.704	.651	.640	.666	.776
	180			.628				.830
	Σ 6 PCB	.727	.686	.719	.678	.644	.682	.755
dl-PCB	28	.649	.614				.611	
	52							
	118							.769
	123							.793
	156	.603		.624				.836
	157							.834
	167			.623				.833
	169			.619				
	189			.639				.869
	Σ dl-PCB							.768

number of paired observations: n=31, except dioxinlike activity in EROD bioassays (n=7)

3.14.2.5 PBDE

The association between PBDE and other compound groups was weaker than, e.g., the coupling of PAH, PCB or PCDD/F with different pollutant classes (see above). Only in few cases, correlation coefficients exceeded 0.7 (Table 3-60). Only the heavier (highly chlorinated) PCDD/F homologues showed tighter coupling to PBDE levels -in contrast to the PAH, of which the lighter three-ring members (except DBaP_{YR}) tended to correlate with PBDE. PBDE congener 99 stood out by its comparably tight and frequent association with members of other compound classes (Table 3-60). On the other hand, the PAH fluorene, the PCB congeners 138 and 153 (as well as the sum of six abundant indicator PCB) and HpCDD were associated with a set of PBDE.

Table 3-60: Important correlations between PBDE congeners and other parameters in forest humus

		BDE 28	BDE 47	BDE 99	BDE 100	BDE 154	Σ 6 BDE
PAH	ANY			.649			
	FLU	.613	.652	.722	.657	.622	.659
	PHEN			.631			
	DBaP _{YR}			.602			
PCB	101	.643	.608	.611			
	138	.692	.665	.698	.652	.643	.672
	153	.672	.659	.704	.651	.640	.666
	180			.628			
	Σ 6 PCB	.727	.686	.719	.678	.644	.682
	28	.649	.614				.611
	156	.603		.624			
	167			.623			
	169			.619			
	189			.639			
PCDF	HxCDF		.635	.684	.642	.670	.662
	HpCDF			.605		.637	.603
PCDD	HxCDD			.635	.600		
	HpCDD	.620	.621	.698	.642	.640	.643
	OCDD			.652			
	PCDD			.664	.603		.602
PCDD/F	PCDD/F			.631	.602		.606
	in TEQ			.636		.625	.623

number of paired observations: n=31

3.14.2.6 EROD

As apparent from the previous subsections, dioxinlike activity of humus samples (as indicated by the response of EROD bioassays) was strongly correlated to most PCB congeners and dioxin (but, except HxCDF, not furanes)

homologues. High correlations were also found for the smaller (fewer rings) PAH species which, as aromatic hydrocarbons, also bind to the cellular Ah-receptor, triggerpoint of the bioassays.

3.14.2.7 Chloroparaffines, chlorophenols

Humus chloroparaffine and chlorophenol (most of which were not detected in humus) concentrations did not show any significant high (i. e. absolute value of corr. coefficient ≥ 0.6) correlations to other POPs.

3.14.3 Air

Since air measurements had been conducted on three summits with presumably different pollution cocktails, the data of the three stations (Weissfluhjoch, Zugspitze, Sonnblick) have been analysed separately. Results of four different sectors (NE, NW, S, “undefined”) and five sampling periods were pooled per region.

3.14.3.1 Zugspitze

Among the measured EPA-PAH, acenaphthene (ANA) and anthracene (ANT) showed conspicuous association with other pollutant groups. ANA was strongly correlated with most chloropesticides, including HCH isomers, DDT-related compounds and cyclodiens - but not with HCB which, although HCB was coupled with a number of other PAH species. ANT concentrations were tightly associated with dioxin and furan levels. OCDF, of the dioxin/furan group, was highly correlated with a number of PAH species (Table 3-61; only significant correlations > 0.6 displayed).

Table 3-61: Important correlations between the concentrations of PAH and other POPs in air at Mt. Zugspitze

	NAPH	ANY	ANA	FLU	PHEN	ANT	FLA	PYR	BaA	BbF	BaP	BghiP	IND	Σ EPA-PAH
α-HCH			0.720											
β-HCH			0.674											
γ-HCH			0.686	0.600										
ε-HCH			0.611											
o,p'-DDT			0.832											
p,p'-DDT			0.871											
o,p'-DDE			0.760						0.605					0.610
p,p'-DDE			0.705						0.631					0.605
Dieldrin			0.734											
Endrin			0.672											0.691
Heptachlor			0.786											0.622
HCB				0.762	0.614	0.609	0.662	0.629	0.653		0.611			
Mirex	0.677													
PCB 126			-0.638											
PCB 180												0.671	0.630	
PCB 189										0.615		0.749	0.746	
TCDF		0.614				0.726								
PeCDF						0.732								0.681
HxCDF						0.698								
HpCDF		0.637				0.626								
OCDF				0.835	0.742	0.807	0.671	0.676				0.698	0.640	0.675
PCDF		0.651				0.733								
PeCDD	0.624													0.627
HxCDD						0.678								0.731
HpCDD						0.705								0.651
PCDD						0.657								
PCDD/F						0.689								
PCDD/F in TEQ _{WHO}						0.708								
BDE 209			-0.657											

sample size n = 16-20; Spearmans rank correlation, all coefficients significant at the 0.05 level

Interestingly, pronounced correlations of organochloropesticides (OCP) with compound groups other than PAH (see above) were generally negative: Table 3-62 (only significant coefficients > 0.6 displayed). Similarly, polybrominated diphenylethers (PBDE) were negatively correlated with dioxins and furans, while high PBDE levels (especially of the congener 28) were positively associated with increased PCB concentrations (Table 3-63).

Table 3-62: Important correlations between the concentrations of OCP and other POPs in air at Mt. Zugspitze

	α -HCH	β -HCH	δ -HCH	ϵ -HCH	p,p'-DDT	o,p'-DDT	p,p'-DDD	o,p'-DDD	p,p'-DDE	o,p'-DDE	Dieldrin	Endrin	Heptachlor
BDE 28								-.645					
BDE 47		-.634				-.629	-.622	-.636					
BDE 99								-.614					
BDE 100								-.703					
BDE 154						-.665							
Σ 6 BDE		-.608				-.650	-.603	-.633					
BDE 209					-.644	-.674				-.609		-.614	
HxCDF								.602					
PCB 123					-.719	-.742	-.695		-.616	-.641		-.738	-.647
PCB 126					-.604								
Σ dl-PCB in TEQ _{WHO} *	-.637	-.710	-.730	-.684	-.727	-.727				-.608	-.670		-.690

sample size n = 16-20; Spearmans rank correlation, all coefficients significant at the 0.05 level; *upper boundary, i.e. values below detection limit replaced with detection limit

Table 3-63: Important correlations between the concentrations of PBDE and other POPs in air at Mt. Zugspitze

	BDE 28	BDE 47	BDE 99	BDE 100	BDE 153	BDE 154	Sum 6 BDE	BDE 209
TCDD		-.684	-.604	-.708		-.655	-.684	
PeCDD		-.677	-.604	-.654		-.674	-.665	
HxCDD		-.616						
HpCDD		-.643						
TCDF		-.616		-.605				
PeCDF		-.652						
HxCDF		-.687	-.669	-.703			-.640	
PCDF		-.664		-.626				
PCDD/F		-.628						
PCB 28	.634							
PCB 77	.693		.693	.645		.723	.703	
PCB 105	.725		.691	.625		.737	.696	
PCB 114			.692	.630	.608	.740	.704	
PCB 118	.649							
PCB 123		.628				.723	.722	.777
PCB 138	.606							
PCB 180	.624							
Σ dl-PCB	.670							

sample size n = 16-20; Spearmans rank correlation, all coefficients significant at the 0.05 level

Atmospheric concentrations of dioxins/furans and PCB were weakly associated. Only OCDF showed significant correlations (coefficients between 0.612 and 0.651) with the PCB congeners 156, 157 and the sum of six indicator PCB.

3.14.3.2 Weissfluhjoch

Table 3-64 shows that at the Swiss Weissfluhjoch the association between PAH and other POPs was different from that at the German Zugspitze (see above). As an example, there were no such pronounced couplings

between single PAH species and organochloropesticides (OCP) or dioxins. Instead, two PAH species were - negatively - correlated with a number of PCB.

At Mt. Weissfluhjoch - again in contrast to the situation found at Zugspitze - there was a noteworthy association between various OCP and PCB (Table 3-65). High PCB levels were also tightly linked to elevated concentrations of PBDE congener 100 (Table 3-66) and to the heptachlorinated furans (HpCDF: Table 3-67).

Table 3-64: Important correlations between the concentrations of PAH and other POPs in air at Mt. Weissfluhjoch

	ANY	FLU	ANT	BaA	CHR	FLA	BbF	IND
δ-HCH			.614	.811	-.626		-.582	
o,p'-DDT		.608						
p,p'-DDT		.613						
o,p'-DDE		.614						
BDE 28					-.642			
BDE 209	-.730							
TCDD							.646	
PeCDD						.578		
PCB 52 *					-.644		-.610	
PCB 101 *					-.677		-.682	
PCB 105					-.602		-.611	
PCB 118					-.625			
Σ 6 PCB					-.601			

sample size n = 16-20; * Spearmans rank correlation, all other: Pearsons correlation coefficient; all coefficients significant at the 0.05 level; the following parameters were log₁₀-transformed before correlation: ANT, BaA, IND

Table 3-65: Important correlations between the concentrations of OCP and other POPs in air at Mt. Weissfluhjoch

	α-HCH	β-HCH	γ-HCH	δ-HCH	ε-HCH	Dieldrin	HCB	Mirex	p,p'-DDT	o,p'-DDT	p,p'-DDD	p,p'-DDE	o,p'-DDE
BDE 100					.601								
BDE 183		-.638									-.639	-.612	
TCDD	-.592						-.677	-.726	-.725	-.687	-.644		
PCB 28		.667	.618										
PCB 52 *	.741	.839	.834			.765	.687		.717	.726	.739	.635	
PCB 77	.662					.664	.749		.627	.731	.650	.714	.680
PCB 101 *		.731	.711	.640					.678	.681	.690		
PCB 105		.833	.780			.610			.656	.654	.723		
PCB 118		.789	.732	.606							.691		
PCB 138		.656	.610	.669									
PCB 153		.706	.641	.698									
PCB 180				.629									
Σ 6 PCB		.718	.665										
Σ dl-PCB		.783	.739							.607	.692		
Σ dl-PCB in TEQ_{WHO} **	.603	.635	.626										

sample size n = 16-20; * Spearmans rank correlation, all other: Pearsons correlation coefficient; ** upper boundary, i.e. all values below the detection limit replaced with the detection limit; all coefficients significant at the 0.05 level; the following parameters were log₁₀-transformed before correlation: δ- and ε-HCH, Endrin, BDE 100, BDE 183, TCDD, PCB congeners 28, 77, 105, 118, 138, 153 and 180, Σ 6 PCB, Σ dl-PCB, Σ dl-PCB in TEQ_{WHO}

Table 3-66: Important correlations between the concentrations of PBDE and other POPs in air at Mt. Weissfluhjoch

	BDE 28	BDE 47	BDE 99	BDE 100	BDE 154	Σ 6 BDE	BDE 183
HxCDF		-.657					
HpCDD	.780			.611	.818		
PCDD	.725			.648	.822		
TCDF		-.620					
PeCDF		-.675	-.606				
HpCDF					.629		
PCDF		-.642					
PCDD/F					.750		
PCDD/F in TEQ _{WHO} **		-.675				-.628	
PCB 28				.629			-.616
PCB 52 *				.661			-.723
PCB 81	-.614						
PCB 138				.647			
PCB 153				.666			
PCB 180	.667			.678	.614		
Σ 6 PCB				.622			-.604
PCB 105	.611			.653			-.669
PCB 118				.637			-.649
PCB 156	.723			.742	.642		
Σ dl-PCB	.614			.679			-.638
Σ dl-PCB in TEQ _{WHO} **	.627						

sample size n = 16-20; * Spearmans rank correlation, all other: Pearsons correlation coefficient; ** upper boundary, i.e. all values below the detection limit replaced with the detection limit; all coefficients significant at the 0.05 level; all parameters were log₁₀-transformed, except those (*) for which Spearmans coefficient was computed

Table 3-67: Important correlations between the concentrations of PCDD/F and PCB in air at Mt. Weissfluhjoch

	TCDD	OCDD	HpCDF
PCB 28			.619
PCB 77	-.616		
PCB 101 *		.655	.655
PCB 138			.601
PCB 153			.650
PCB 180			.613
Σ 6 PCB			.661
PCB 105			.650
PCB 118			.640
Σ dl-PCB			.617

sample size n = 16-20; * Spearmans rank correlation, all other: Pearsons correlation coefficient; all coefficients significant at the 0.05 level; all parameters were log₁₀-transformed, except those (*) for which Spearmans coefficient was computed

3.14.3.3 Sonnblick

Unlike on the other two summits Mt. Weissfluhjoch and Mt. Zugspitze, there were only few tight correlations between atmospheric concentrations of chemically different pollutant classes on Mt. Sonnblick (Table 3-68).

Table 3-68: Important correlations between the concentrations of various POPs in air at Mt. Sonnblick

	FLU	ANT	FLA	BaA	Heptachlor	p,p'-DDT	p,p'-DDD	o,p'-DDD	o,p'-DDE	BDE 28	BDE 154	PCB 101	Σ 6 PCB	PCB 81	PCB 114	PCB 157
FLU														.760		
ANT						.636								.822	.783	
FLA					.603											
BaA					.760			.656	-.622							
Heptachlor			.603	.760												
p,p'-DDT												.722	.717			
p,p'-DDD		.636														
o,p'-DDD														.655		
o,p'-DDE				.656												
BDE 28				-.622												
BDE 154																-.637
PCB 101						.722										
Σ 6 PCB						.717										
PCB 81	.760	.822					.655									
PCB 114		.783														
PCB 157											-.637					

sample size n = 5-20; Spearmans rank correlation; all coefficients significant at the 0.05 level; correlations with BDE congeners greyed out, due to suspected local influence on PBDE levels; the following parameters were log₁₀-transformed before correlation: FLU, p,p'-DDT, BDE 154, Σ 6 PCB

3.15 Correlations between concentrations of the same substance in different media

3.15.1 Humus and needle concentrations

Among the examined pollutant groups (PCDD/F, PBDE, PAH, PCB, OCP), significant correlations between humus and needle contents were sparse. Significant coupling between both media's pollutant contents was almost exclusively observed for PCB. Associations were generally weak (Table 3-69).

Table 3-69: Significant correlations between pollutant contents in forest humus and 0.5 year old Norway spruce needles

		coefficient			coefficient
PCB	PCB 138	.654	PCDD/F	HpCDF	.480
	PCB 153	.505		PCDF	.402
	PCB 180	.661		PCDD/F	.438
	Σ 6 PCB	.438	OCP	p,p'-DDD	.399
dl-PCB	PCB 77	.581			
	PCB 81	.456			
	PCB 105	.698			
	PCB 114	.478			
	PCB 118	.634			
	PCB 126	.529			
	PCB 156	.657			
	PCB 157	.637			
	PCB 169	.482			
	PCB 167	.627			
	PCB 189	.459			
	Σ dl-PCB	.696			
	Σ dl-PCB in	.576			
	TEQ _{WHO}				

28 paired observations

3.15.2 Needle and SPMD concentrations

Parallel needle and SPMD sampling focused on the height profiles (15 plots). Although sharing a similar accumulation mechanism (passive uptake of airborne pollutants by lipophilic matrix), needles and SPMD hardly showed correlating pollutant concentrations after six or twelve months of parallel exposition (Table 3-70) – except the amount of several PCB congeners that had accumulated over twelve months.

Table 3-70: Exposition dates of parallel needle and SPMD samples

	needles	SPMD
six months	budburst 05-october 05	2 nd half of April 05-begin Nov. 05 growing season 2005
twelve months	budburst 05-mid June 06	2 nd half of April 05-mid June 06 includes heating period 2005/06

3.15.2.1 PAH

PAH concentrations in simultaneously exposed 0.5 year old needles and SPMD were uncorrelated. This is partly due to a lack of observations (seven out of 16 PAH species had less than four observations above the detection limit in either needle or SPMD samples). As an exception, phenanthrene contents of needles and SPMD were tightly coupled (Figure 3-268).

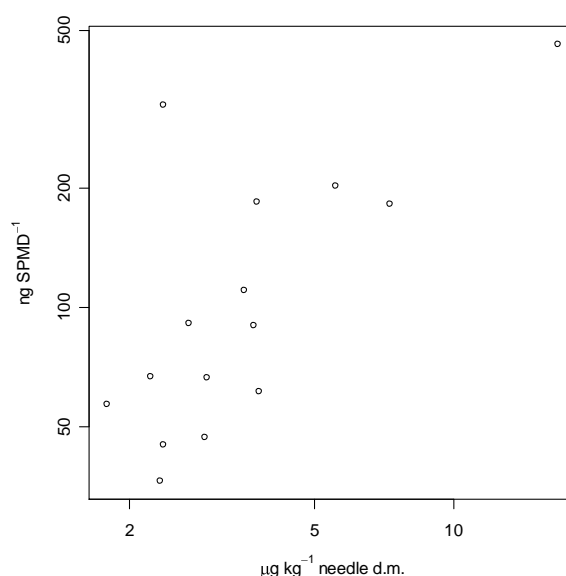


Figure 3-268: Association of needle and SPMD phenanthrene contents

3.15.2.2 PCDD/F

SPMD and needle concentrations of dioxins or furans varied as independently from each other as observed for PAH, regardless whether six or twelve months exposed samples were considered.

3.15.2.3 PCB

Six months exposure: needle and SPMD concentrations were not significantly correlated for most PCB except congeners no. 105 ($r=.717$) and 118 ($r=.640$). PCB concentrations after twelve months exposure showed, in contrast to the remaining pollutant classes and exposure times, rather good agreement between SPMD and needle concentrations (Table 3-71).

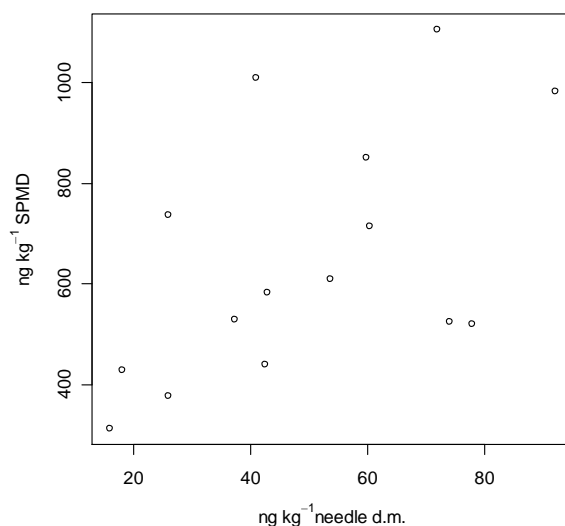
Table 3-71: Significant correlations between PCB contents in SPMD and Norway spruce needles

congener / parameter	correlation coefficient
138	.641
153	.543
180	.730
77	.736
126	.588 (Spearman)
157	.696
167	.660
Σ 12	.599

15 paired observations

3.15.2.4 OCP

Six and twelve months exposition: correlations between needle and SPMD contents were generally weak and not significant. Exceptions were the concentration of p,p'-DDT after six months exposition (correlation coefficient $r=0.546$; Figure 3-269) and δ -HCH after twelve months exposition ($r=.571$)

*Figure 3-269: Association of needle and SPMD p,p'-DDT contents.*

3.16 General descriptives

3.16.1 Humus

The depth of the humus layer and the humus mass per area increased from East to West and from North to South in the study region (Figure 3-270 and Figure 3-271).

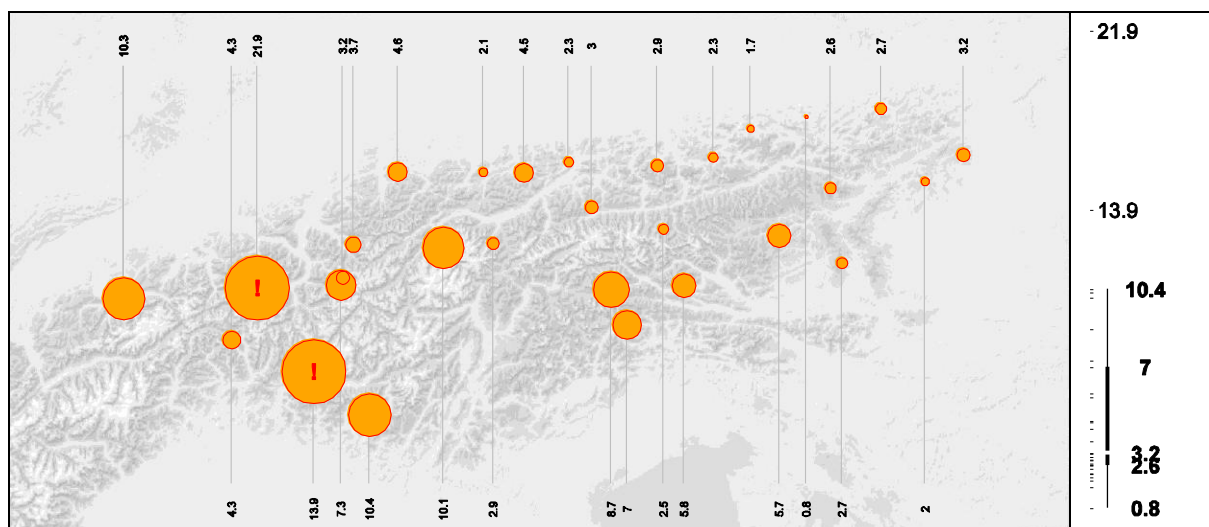


Figure 3-270: Geographic variation of humus depth

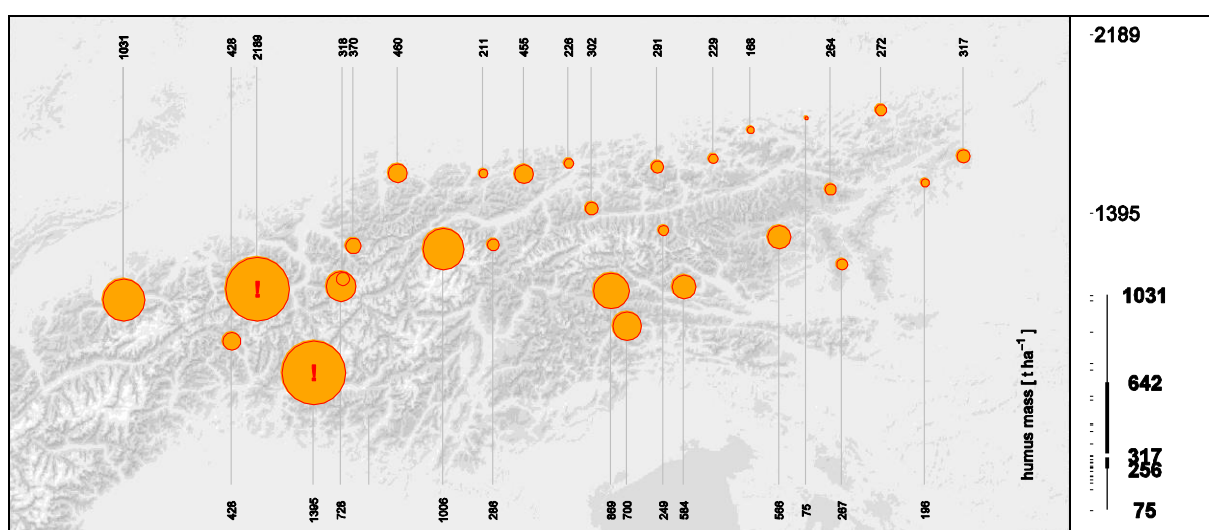


Figure 3-271: Geographic variation of humus mass

In those cases in which humus mass showed vertical trends, it tended to increase with altitude (except at the German height profile Eschenlohe: Figure 3-272).

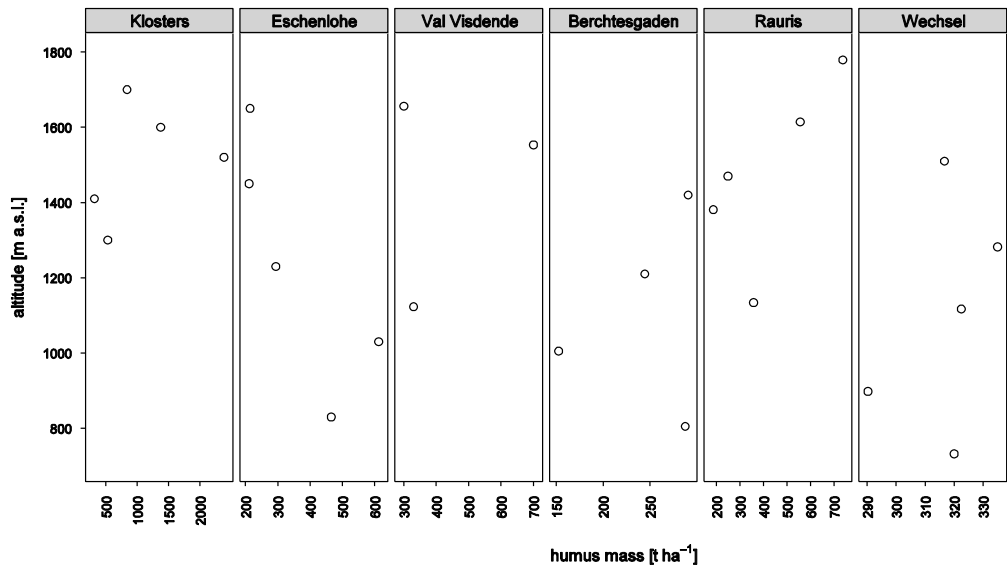


Figure 3-272: Altitudinal variation of humus mass

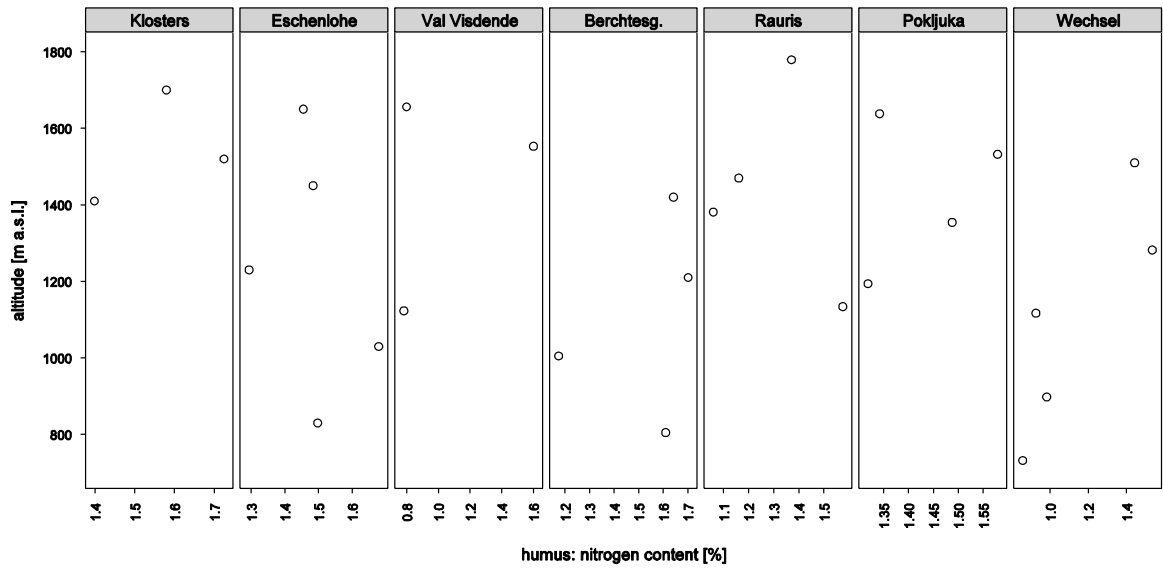


Figure 3-273: Altitudinal variation of forest humus nitrogen content

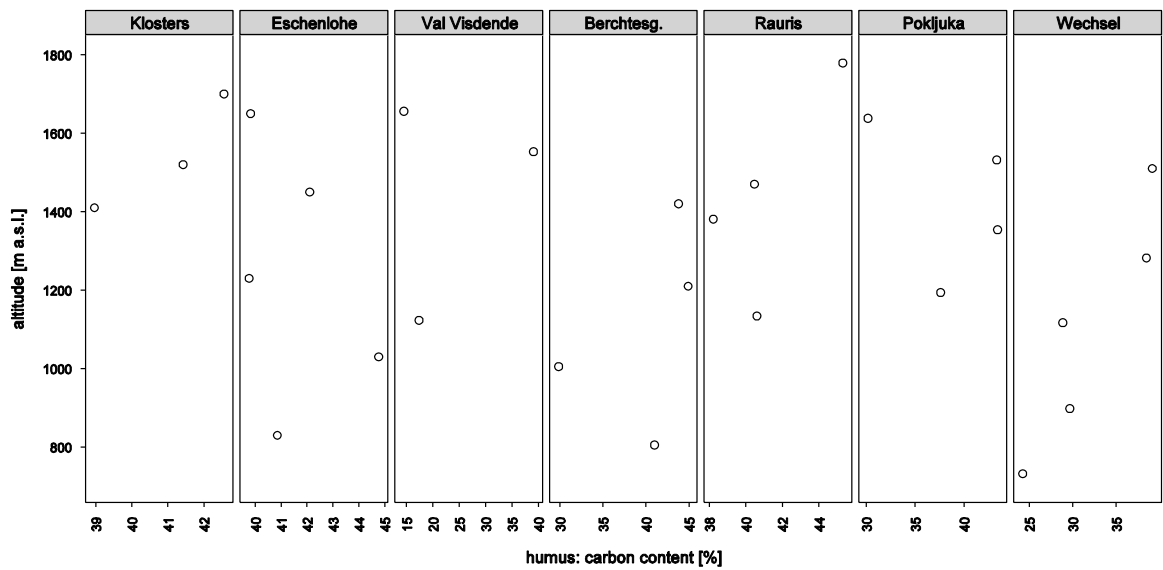


Figure 3-274: Altitudinal variation of forest humus carbon content

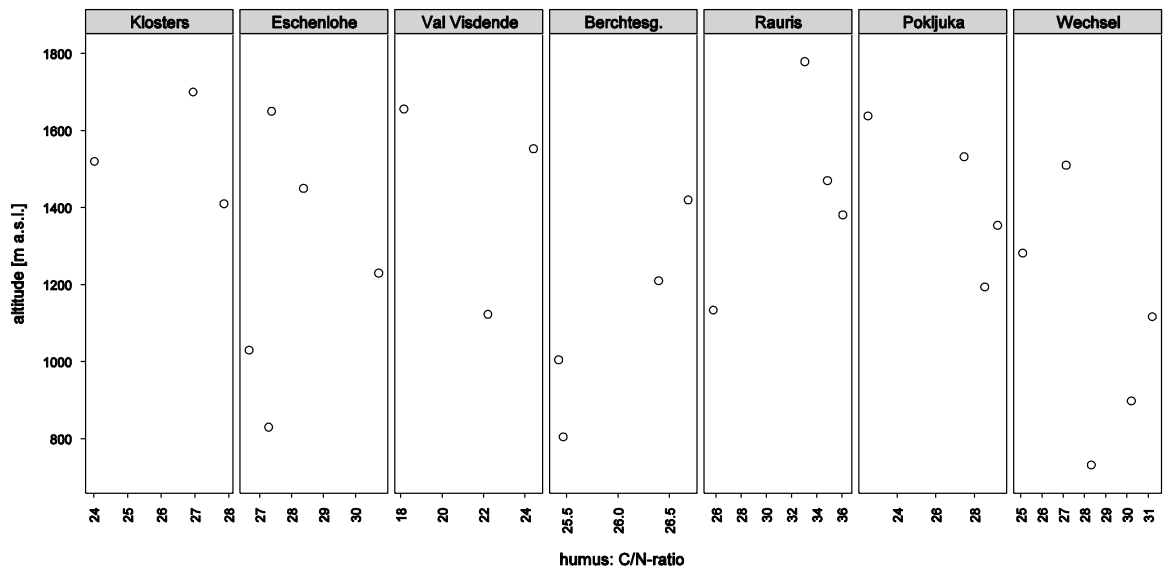


Figure 3-275: Altitudinal variation of the C/N ratio in forest humus

3.16.2 Needles

Table 3-72: 100-needle weight and wax content of 0.5 year old Norway spruce needles

	min	median	mean	s.d.	max
100-needle-wt [g]	0.27	0.56	0.55	0.12	0.83
wax content [% d.m.]	0.51	1.02	1.07	0.20	1.50

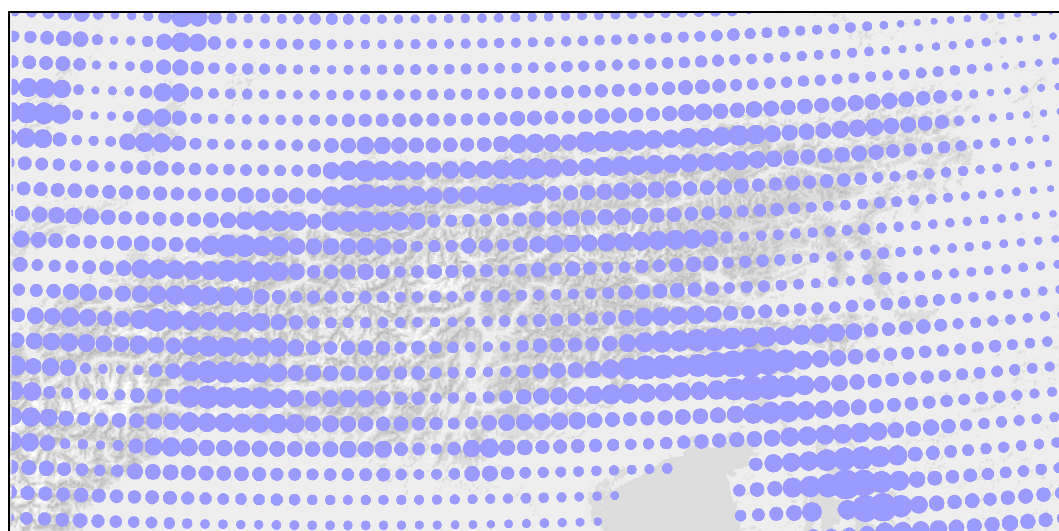
sample size: 40; s.d....standard deviation

3.17 Meteorology

All climate regions were characterized by a decline of temperature and an increase of precipitation with altitude. Judging from annual averages, the vertical temperature decrease is similar in all Alpine regions, and ranges between -0.6 and -0.4 °C per 100 m. This range depends on the frequency of temperature inversions, occurring particularly during nighttime and winter. GARTEN & HANSON (2006) found similar annual temperature declines with altitude (0.46 °C per 100 m) along a 1.3 km ascend in the southern Appalachian Mountains. We found that the correlation between temperature and height was generally stronger than between precipitation and height.

The Central Alps receive less precipitation than the Northern and Eastern Alps. The Slovenian Alps, which are strongly influenced by the Adriatic Sea, belong to the Central European regions with the highest precipitation. The altitudinal increase of precipitation is stronger at the Alpine fringes than in the Central Alps (Graubünden), which is a barrier effect. Due to the low number of suitable stations and the special climate of inneralpine dry valleys, the calculated dependency of precipitation on altitude was not always significant. In some regions, precipitation seemed to increase logarithmically with height at higher altitudes. The weaker correlation between precipitation (as compared to temperature) and altitude can partly be ascribed to local lee effects and the difficulty to measure snowfall at elevated sites. Mean precipitation and temperature at every site were estimated as linear regressions. Our modelled dependency of precipitation on altitude was lower than the gradients found for other regions, e. g. the Appalachian Mountains (56 mm per 100 m altitudinal increase; GARTEN AND HANSON, 2006).

Figure 3-276 shows the spatial distribution of annual precipitation from an independent model (observation period 1994-2003; see methods section). Figure 3-278 illustrates the situation specifically for MONARPOP: the sampling sites at the northern and southern margins, particularly in the southeast (Slovenia) receive more precipitation than those in the central part of the study region.



data from Efthymiadis et al. (2006)

Figure 3-276: Distribution of precipitation in the study region

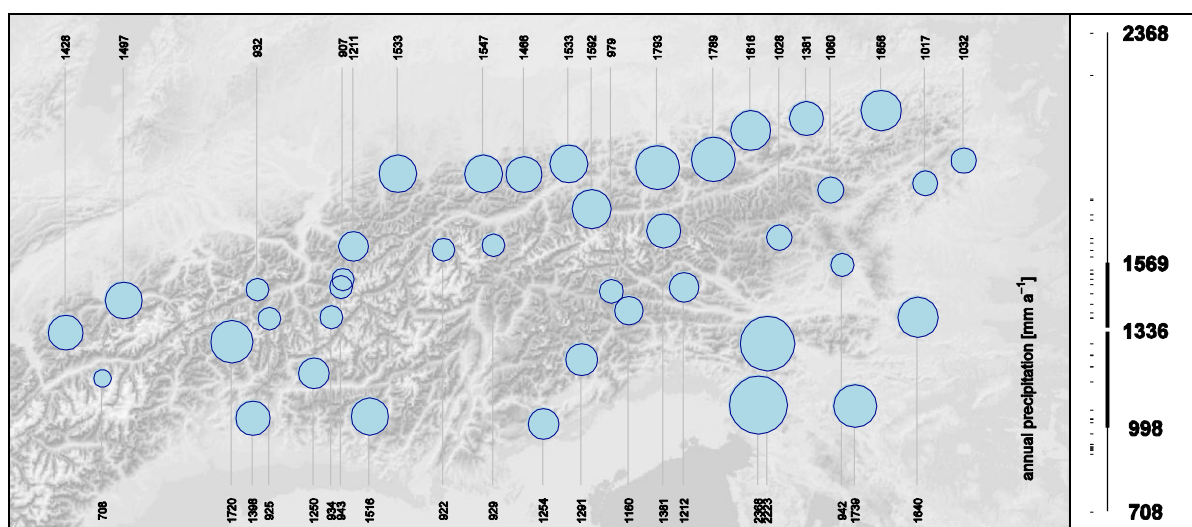


Figure 3-277: Annual precipitation at the sampling sites

Not surprisingly, the southern sites have higher annual temperature means. The span of average temperatures across all sites was five degrees (Figure 3-278).

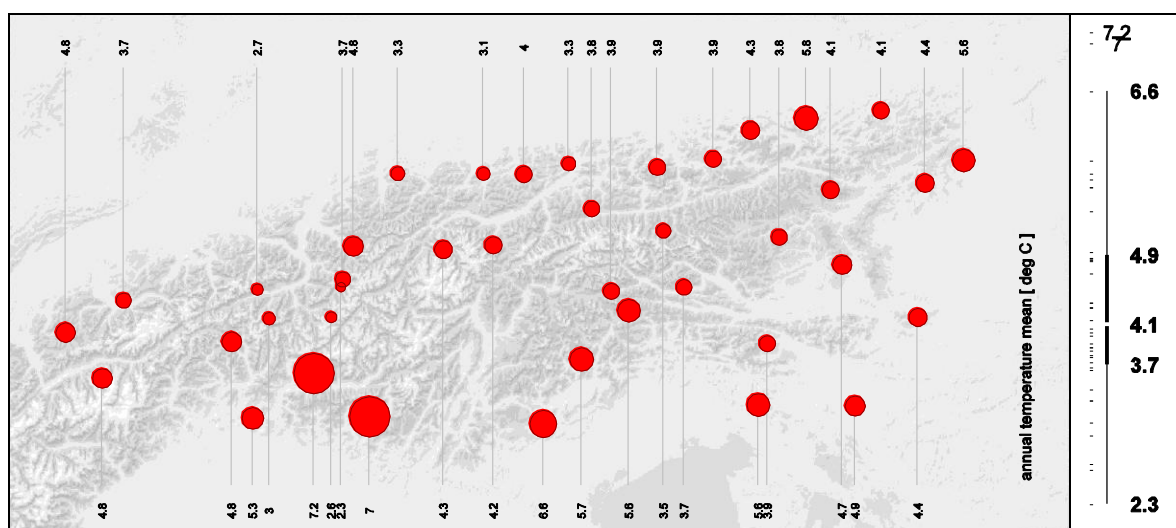


Figure 3-278: Annual temperature average at the sampling sites

3.18 Correlations between pollutant concentrations and climatic parameters

3.18.1 Needles

Several significant correlations between the concentrations of the 0.5 year old needles and the average temperature and precipitation of the standard sites have been detected (Table 3-73). These climatic parameters represent an average for 30 years. So, the identified association is not based on a coincidence of the represented time period. It needs to be tested if a comparison of the needle results with average temperature and precipitation during the exposure period of the needles would improve the fit.

Table 3-73: Significant correlation coefficients between average annual temperature or precipitation and pollutant concentrations 0.5 year old Norway spruce needles

temperature		r	precipitation		r
PCDD/F	PeCDD, TCDF, 0.3 to 0.6		PAH	ANA, DBahA, NAPH, -0.3 to -0.4 PeCDF, HxCDF, Σ PHEN, PYR, PCDD/F (conc. and in TEQ) Σ EPA-PAH	
			PCB	77, 81, 105, 118, 156, 0.3 to 0.4 157, 167, 138, 180, Σ dl- PCB (conc.)	
			PCDD/F	HxCDD, HpCDD, TCDF, 0.3 to 0.5 PeCDF, HxCDF, HpCDF, Σ PCDD/F (conc. and in TEQ)	
			OCP	OCP: β -HCH	0.5

sample size n=40

3.18.2 Humus

Several significant positive correlations between average precipitation and concentrations in the humus layer were observed. The more pronounced were detected for the PBDEs (table ..). It is remarkable that the higher chlorinated PCDD/F were positively correlated with the precipitation, while the lower chlorinated homologues were negatively associated with temperature. Likely, these meteorological parameters had an impact on the observed concentration differences in the humus layer.

Table 3-74: Significant correlation coefficients between average annual temperature or precipitation and pollutant concentrations in forest humus

temperature		r	precipitation		r
PCDD/F	TCDD, PeCDD	-0.4 to -0.5	PAH	BaA, BkF, BghiP, BaP, CHR, DBahA, FLU, IND, NAPH, PHEN, DBaP, DBaP, Σ EPA-PAH	0.4 to 0.6
			PCB	169, 123, 156, 167, 189, 52, 0.4 to 0.6 101, 138, 153, 180, Σ dl PCB (conc.), Σ 6 PCB	
			PCDD/F	HxCDD, HpCDD, OCDD, 0.4 to 0.6 HxCDF, HpCDF, OCDF, Σ PCDD/F (conc. and in TEQ)	
			PBDE	28, 47, 99, 100, 154, 209	0.5 to 0.7
			OCP	Dieldrin, Mirex	0.4 to 0.5

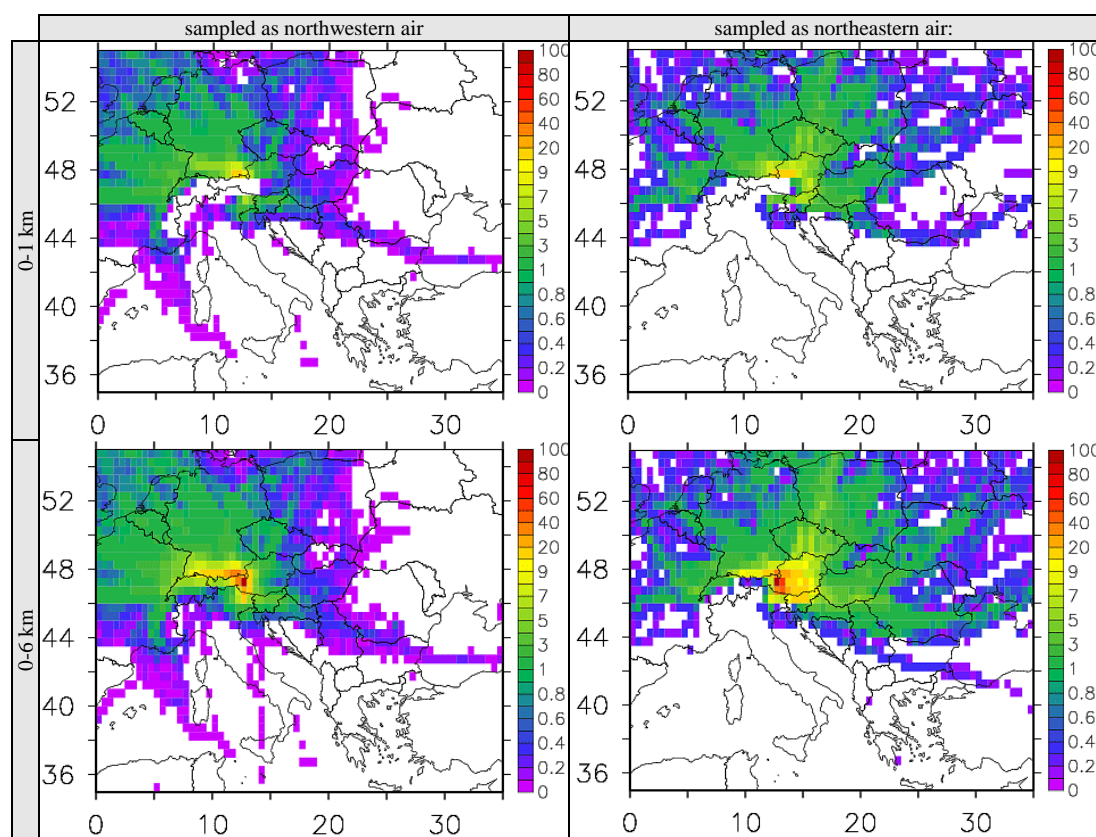
sample size n=31

4 Appendix

4.1 Accuracy of trajectory prognoses

As explained in 1.5.2 (page 9), active air sampling was distributed among four separate filter units to obtain information on the geographic origin of the collected pollutants. Daily trajectory forecasts were used to switch between filters corresponding to northwest, northeast, and south (an additional unit being reserved for not attributable air masses of “undefined” origin: these were mainly fast moving air masses from the Atlantic or the Arctic or such air that had rapidly descended from great heights). The figures below illustrate the actual trajectories along which the air masses arrived during the operative (only) periods of a given filter unit. The relative scale (0-100) indicates the frequency each cell (of a 0.5° grid) had been visited by an infinitesimal air parcel during three days before the parcel arrived at the sampler. For each predefined source region there are two graphs, one depicting trajectories below one kilometre, the other including trajectories of up to six kilometres above ground. maps: August Kaiser (www.zamg.ac.at)

Figure 4-1 shows, for example, that the “northwest” filter unit was indeed mainly loaded with air masses of northwestern origin, while the unit assigned to air of “undefined” origin actually received a relatively stronger input from the west.



maps: August Kaiser (www.zamg.ac.at)

Figure 4-1: Origin of air masses arriving sampled by each dedicated filter unit; high volume sampler.

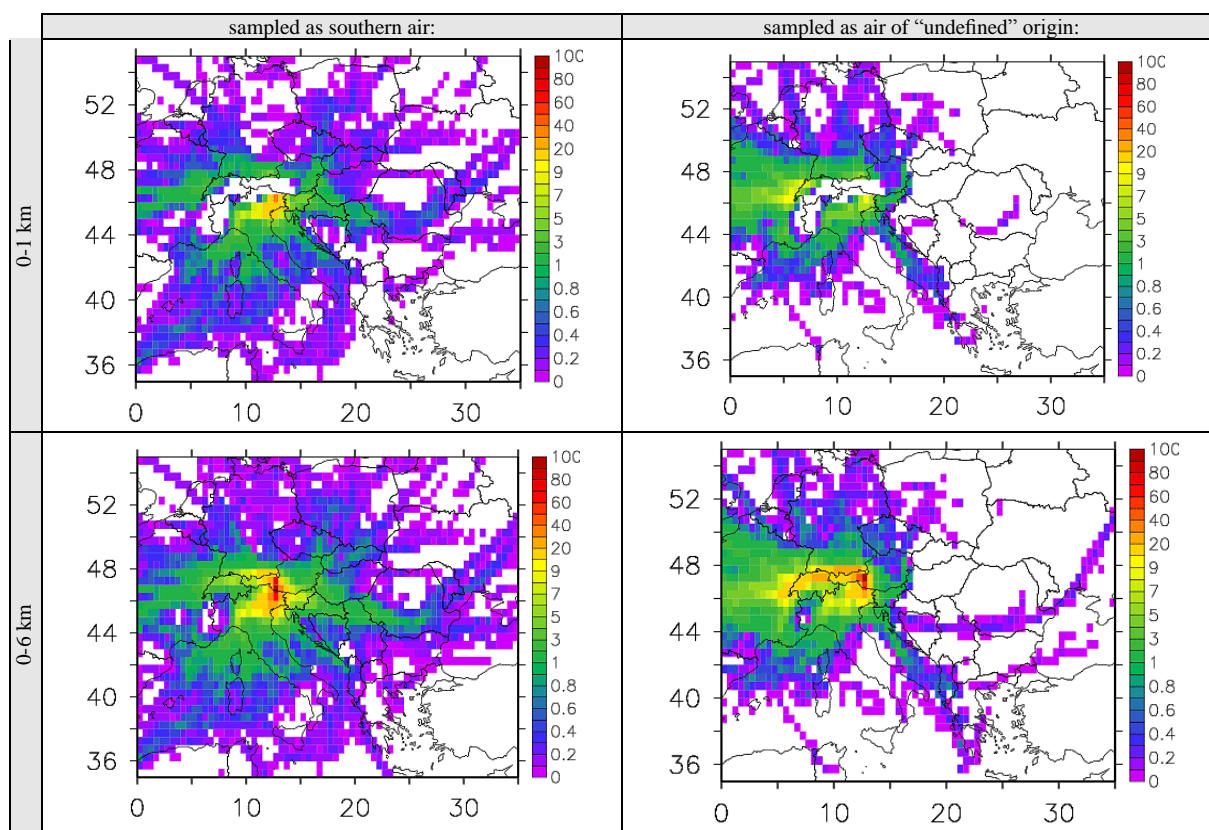


Figure 4-1 (continued): Origin of air masses arriving sampled by each dedicated filter unit; high volume sampler.

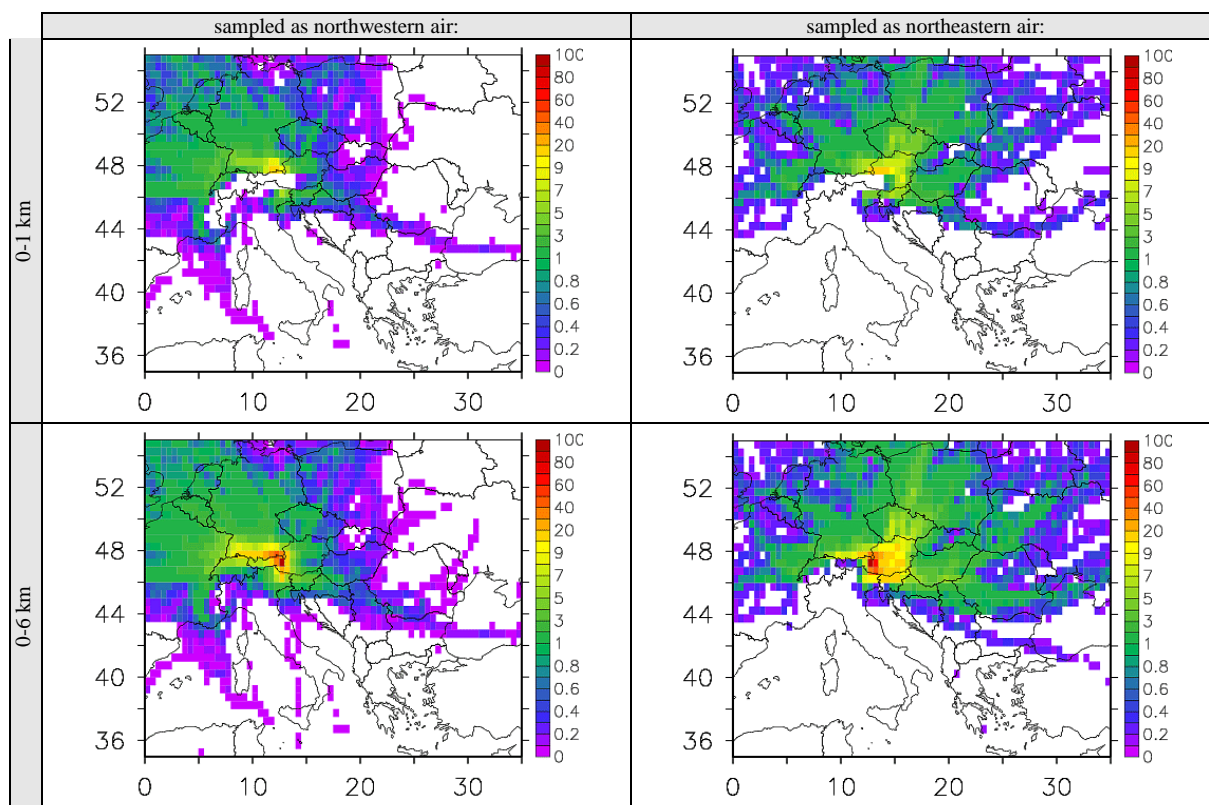
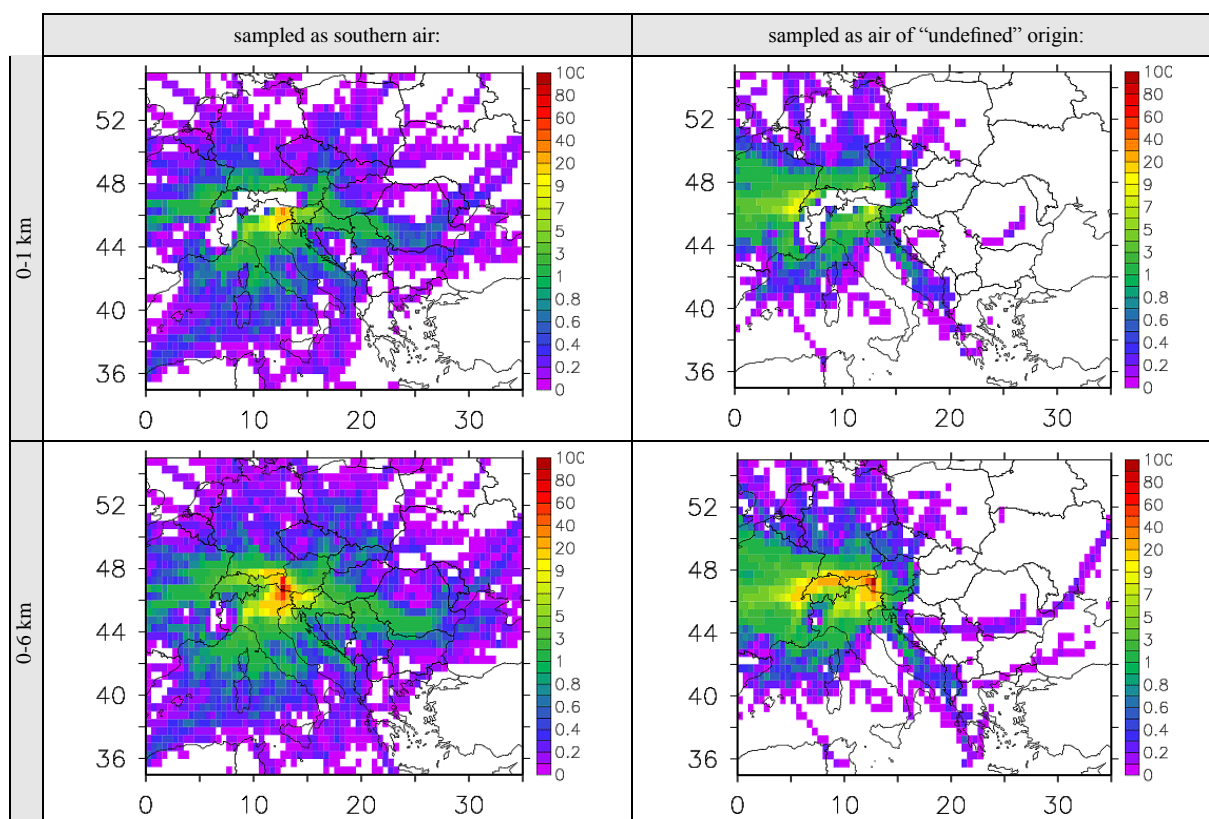


Figure 4-2: Origin of air masses arriving sampled by each dedicated filter unit; low volume sampler.



maps: August Kaiser (www.zamg.ac.at)

Figure 4-2 (continued) Origin of air masses arriving sampled by each dedicated filter unit; low volume sampler.

5 Literature

- BELIS, C. A., OFFENTHALER, I., UHL, M., NURMI-LEGAT J., BASSAN, R., JAKOBI G., KIRCHNER, M., KNOTH, W., KRAEUCHI, N., MAGNANI, T., MOCHE, W., RACCANELLI, S., SCHRAMM, K.-W., SIMONCIC, P. & P. WEISS (2008): A comparison of emissions vs masses of SVOCs in the Alps. *Env. Poll. (in press)*
- BORGEN, A.; SCHLABACH, M. & H. Gundersen (2000): Polychlorinated alkanes in Arctic air. *Organohalogen Compounds* 47, 272–275.
- BRADFORD M. M. (1976): A rapid and sensitive method for the quantification of microgram quantities of protein utilizing the principle of protein dye binding. *Anal. Bioch.* 72: 248–255.
- BSEF (2008): Bromine science and environmental forum. <http://www.bsef.com/> (Febr. 18, 2008).
- CAMPBELL, I. & G. MCCONNELL (1980): Chlorinated Paraffins and the Environment. 1. Environmental Occurrence. *Environmental Science and Technology* 14, 1209–1214.
- CEN (2007): CEN/TC BT TF 151 “Horizontal” WI CSS 99044: Soil and sludge–Determination of selected polybrominated diphenylethers (PBDE)–Gaschromatographic method with mass spectrometric detection. [http://www.ecn.nl/docs/society/horizontal/BT_TF151_WI_CSS99044_PBDE_\(E\)_2762007.pdf](http://www.ecn.nl/docs/society/horizontal/BT_TF151_WI_CSS99044_PBDE_(E)_2762007.pdf) (Nov. 07, 2007)
- DE WIT, C. A. (2002): An overview of brominated flame retardants in the environment. *Chemosphere* 46, 583–624.
- DIN 19739-1 (2002–03): Measurement of atmospheric deposition of organic trace substances; Funnel adsorber method – Part 1: Sampling devices; Requirements, installation, application. Beuth Verlag, Berlin.
- DONATO, M.T.; GOMEZ-LECHON, M. J. & J. V. CASTELL (1993): A micro assay for measuring cytochrome P450IA1 and P450IIB1 activities in intact human and rat hepatocytes cultured on 96-well plates. *Analytical Biochemistry*. 213 (1):29–33.
- DROUILLARD, K.G.; HIEBERT, T.; TRAN, P.; TOMY, G.T.; MUIR, D.C.G. & K. J. FRIESEN (1998a): Estimating the aqueous solubilities of individual chlorinated n-alkanes (C₁₀–C₁₂) from measurements of chlorinated alkane mixtures. *Environmental Toxicology and Chemistry* 17, 1261–1267.
- DROUILLARD, K.G.; TOMY, G.T.; MUIR, D.C.G. & K. J. FRIESEN (1998b): Volatility of chlorinated n-alkanes (C₁₀–C₁₂): Vapor pressures and Henry’s law constants. *Environmental Toxicology and Chemistry* 17, 1252–1260.
- EBFRIP (European brominated flame retardant industry panel, 2005): Decabromodiphenyl ether (Deca-BDE) usage in EU countries in 2004 in metric tons.
- ECJ (European Court of Justice, 2008). Judgment of 1 April 2008 on joined cases C-14/06 and C-295/06. <http://curia.europa.eu/en/actu/communiqués/index.htm> (April 29, 2008).
- EFTHYMIADIS, D.; JONES, P. D.; BRIFFA, K. R.; AUER, I.; BÖHM, R.; SCHÖNER, W.; FREI, C. & J. SCHMIDLI (2006): Construction of a 10-min-gridded precipitation data set for the Greater Alpine Region for 1800–2003. *Journal of Geophysical Research* 110.

- EA ENVIRONMENT AGENCY (2004): Environmental risk evaluation report Perfluorooctanesulphonate (PFOS) Environment Agency Science group, UK, 2004.
- ENVIRONMENT CANADA (1993): Priority Substances List Assessment Report. Chlorinated Paraffins, Canadian Environmental Protection Act (CEPA). Minister of Supply and Services Canada, Ottawa, Ontario, Canada, pp.1–32.
- EU (2000): Directive 2000/60/EC of the European parliament and the council of 23 October 2000 establishing a framework for Community action in the field of water policy. Official Journal of the European Communities L 327, 1–72.
- EU (2003): Directive 2003/11/EC of the European Parliament and of the Council of 6 February 2003 amending for the 24th time Council Directive 76/769/EEC relating to restrictions on the marketing and use of certain dangerous substances and preparations (pentabromodiphenyl ether, octabromodiphenyl ether). Official Journal of the European Union L 42, 45–46.
- EU (2004): Update of the risk assessment of bis(pentabromophenyl)ether (decabromodiphenyl ether). Final environmental draft of May 2004. CAS No. 1163-19-5, EINECS No. 214-604-9, 114 pp.
- EUROPEAN COMMISSION (2000): European Union risk assessment report: alkanes C10-13, chloro, 1st Priority Listed. Office for Official Publications of the European Communities, Luxembourg.
- GARTEN JR., C.T. & P. J. HANSON (2006). Measured forest soil C stocks and estimated turnover times along an elevation gradient. *Geoderma* 136, 342–352.
- GDCH-ADVISORY COMMITTEE ON EXISTING CHEMICALS OF ENVIRONMENTAL RELEVANCE (1992): Chlorinated Paraffins - BUA Report 93 (June 1992). Hirzel, Stuttgart.
- HABIG, W. H.; PABST, J. & W. B. JAKOBY (1974): Glutathione S-transferases, the first step in mercapturic acid formation. *J. Biol. Chem.* 249: 7130–7139.
- HALE, R. C.; LA GUARDIA, M. J.; HARVEY, E.; GAYLOR, M. O. & T. M. MAINOR (2006): Brominated flame retardant concentrations and trends in abiotic media. *Chemosphere* 64, 181–186.
- HITES, R. A. (2004): Polybrominated diphenyl ethers in the environment and in people: A meta-analysis of concentrations. *Env. Sci. Techn.* 38, 945–956.
- HSDB: Hazardous Substances Data Bank: U.S. National Library of Medicine, National Institutes of Health, Health & Human Services: <http://toxnet.nlm.nih.gov/cgi-bin/sis/htmlgen?HSDB>
- IOMC (1995): POPs Assessment Report, Dec. 1995: Chapter 6
<http://www.chem.unep.ch/pops/indxhtmls/asses6.html> POLYDIOX (Nov. 22, 2007).
- IOZZA, S.; MÜLLER, C.E.; SCHMID, P.; BOGDAL, C. & M. OEHME (2008): Historical Profiles of Chlorinated Paraffins and Polychlorinated Biphenyls in a Dated Sediment Core from Lake Thun (Switzerland). *Environmental Science and Technology* 42, 1045-1050.
- ICSC 1998; International chemical safety card 0586, trichloroacetic acid
<http://www.inchem.org/documents/icsc/icsc/eics0586.htm> (Jan 14, 2008).

- IPCS INCHEM (1990): International Programme on Chemical Safety, Poison Information Monograph, 121.
Chloroform <http://www.inchem.org/documents/pims/chemical/pim121.htm>
- IPCS INCHEM (1991): International Programme on Chemical Safety, Poison Information Monograph, Trichloroethane. <http://www.inchem.org/documents/pims/chemical/trichlor.htm>
- JRC (2002): 4-nonylphenol (branched) and nonylphenol. Summary Risk Assessment Report. Joint Research Centre Special Publication I.02.69, Ispra 2002.
- KEITH L. H. (1997): Environmental Endocrine Disruptors. A handbook of property data. Interscience Ed., Wiley 1997, New York.
- LETCHER, R. J. & P. A. BEHNISCH (Eds.) (2003): The state-of-the-science and trend of BFRs in the environment. Environment International 29, 1–885.
- MACKAY, D.; SHIU, W. Y. & K. C. MA (1992): Illustrated handbook of physical-chemical properties and environmental fate for organic chemicals. Volume I, Monoaromatic hydrocarbons, chlorobenzenes, and PCBs. Lewis Publishers, Chelsea, Michigan, USA.
- MACKAY, D.; SHIU, W. Y. & K. C. MA (1992): Illustrated handbook of physical-chemical properties and environmental fate for organic chemicals. Volume II, Polynuclear aromatic hydrocarbons, polychlorinated dioxins, and dibenzofurans. Lewis Publishers, Chelsea, Michigan, USA.
- MARIUSSEN, E.; STEINNES, E.; GUNDERSEN, H.; BORGES, A. & SCHLABACH, M. (2005): Analysis of polybrominated diphenyl ethers in moss (*Hylocomium splendens*) from the Norwegian environment. Organohalogen Compounds 67, 591–593.
- MUIR, D.C.G.; STERN, G.A. & G. T. TOMY (2000): Chlorinated Paraffins, in: Paasivirta, J. (Ed.), The Handbook of Environmental Chemistry. Springer, Berlin Heidelberg New York, pp. 203–236.
- OECD (2002) Environment directorate joint meeting of the chemicals committee and the working party on chemicals, pesticides and biotechnology . Co-operation on existing chemicals, Hazard assessment of perfluorooctane sulfonate (PFOS) and its salts. Organisation for Economic Co-operation and Development. <http://www.oecd.org/dataoecd/23/18/2382880.pdf>
- OECD SIDS I; UNEP Publications Trichloroacetic acid
Cas-Nr: 76-03-9; <http://www.inchem.org/documents/sids/sids/76039.pdf> (Jan 14, 2008).
- OSPAR COMMISSION (2001): OSPAR Background document on Short Chain Chlorinated Paraffins. OSPAR, London, United Kingdom.
- PERSISTENT ORGANIC POLLUTANTS REVIEW COMMITTEE (POPRC, 2004): Stockholm Convention on Persistent Organic Pollutants (POPs).
- R DEVELOPMENT CORE TEAM (2008). R: A language and environment for statistical computing. R Foundation for Statistical Computing, Vienna, Austria. <http://www.R-project.org>.
- RETH, M. & M. OEHME (2004): Limitations of low resolution mass spectrometry in the electron capture negative ionization mode for the analysis of short- and medium-chain chlorinated paraffins. Analytical and Bioanalytical Chemistry 378, 1741–1747.

- RETH, M.; ZENCAK, Z. & M. OEHME (2005): New quantification procedure for the analysis of chlorinated paraffins using electron capture negative ionization mass spectrometry. *Journal of Chromatography A* 1081, 225–231.
- RETH, M.; CIRIC, A.; CHRISTENSEN, G.N.; HEIMSTAD, E.S. & M. OEHME (2006): Short- and medium-chain chlorinated paraffins in biota from the European Arctic – differences in homologue group patterns. *Science of the Total Environment* 367, 252–260.
- SCHER (SCIENTIFIC COMMITTEE ON HEALTH AND ENVIRONMENTAL RISKS 2004): Scientific committee on health and environmental risks. Opinion on RPA's report "Perfluorooctane Sulphonates Risk reduction strategy and analysis of advantages and drawbacks" European Commission: Health consumer protection directorate-general.
- SCHRÖDER, P.; G. L. LAMOUREX, D. G. RUSNESS & H. RENNEBERG (1990): Glutathione S-transferase activity in spruce needles. *Pestic. Biochem. Physiol.* 37, 211–218.
- SCHRÖDER, P. & C. GÖTZBERGER (1997): Partial purification and characterization of glutathione S-transferase isozymes from the leaves of *Juniperus communis*, *Larix decidua* and *Taxus baccata*. *J. Appl. Bot. Food Qual.* 71: 31–37.
- SCHWIRZER, S.M.G.; HOFMAIER, A.M.; KETTRUP, A.; NERDINGER, P.E.; SCHRAMM, K.-W.; THOMA, H.; WEGENKE, M. & F. J. WIEBEL (1996): Establishment of a simple cleanup procedure and bioassay for determining 2,3,7,8-Tetrachlorodibenzo-p-dioxin toxicity equivalents of environmental samples. *Ecotoxicology and Environmental Safety* 41:77–82.
- SIJM, D. T. H. M. & T. L. SINNIGE (1995): Experimental octanol/water partition coefficients of chlorinated paraffins. *Chemosphere* 31, 4427–4435.
- SILLER-CEPEDA J. H.; CHEN T. H. H. & L. H. FUCHIGAMI (1991) High performance liquid chromatography analysis of reduced and oxidized glutathione in woody plant tissues. *Plant CellPhysiol.* 32(8): 1179–1185.
- SITTIG, M. (1985). Handbook of toxic and hazardous chemicals and carcinogens. 2nd Edition. N. D. Corporation. Park Ridge, NJ, USA: 487–488.
- TOMY, G. T.; fiSK, A. T.; WESTMORE, J. B. & D. C. G. MUIR (1998): Environmental chemistry and toxicology of polychlorinated n-alkanes. *Reviews of Environmental Contamination and Toxicology* 158, 53–128.
- TOMY, G. T.; STERN, G. A.; LOCKHART, W. L. & D. C. G. MUIR (1999): Occurrence of C₁₀-C₁₃ Polychlorinated n-Alkanes in Canadian Midlatitude and Arctic Lake Sediments. *Environmental Science and Technology* 33, 2858–2863.
- TROITZSCH, J. (2004): International plastics flammability handbook. Principles-regulations-testing and approval. ISBN: 978-3-446-21308-1. 727 pp.
- UNEP/POPS/POPRC.3/INF/22 (2007) : Detailed additional information provided by the intersessional working group on short-chained chlorinated paraffins. Persistent Organic Pollutants Review Committee (POPRC), United Nations Environment Programme (UNEP), Geneva, Switzerland, pp. 1–53.
- VDLUFA (2007) : Die chemische Untersuchung von Futtermitteln. Methodenbuch Band III. VDLUFA Verlag, Speyer 2007.
- VON MEYERINCK, L.; HUFNAGEL, B.; SCHMOLDT, A. & H. F. BENTHE (1990): Induction of rat liver microsomal cytochrome P-450 by pentabromo diphenyl ether bromkal 70 and half-lives of its components in adipose tissue. *Toxicology* 61, 259–274.

- WANG, Y.; JIANG, G. ; LAM, P. K. S. & A. LI (2007): Polybrominated diphenyl ether in the East Asian environment: A critical review. *Environment International* 33, 963–973.
- WANIA, F. & C. B. DUGANI (2003) : Assessing the long-range transport potential of polybrominated diphenyl ethers: A comparison of four multimedia models. *Environ. Toxicol. Chem.* 22, 1252–1261 and supplementary material.
- WEISS, P.; LORBEER, G. & S. Scharf (2001): Regional aspects and statistical characterisation of the load with semivolatile organic compounds at remote Austrian forest sites. *Chemosphere* 40:1159–1171.
- WHO (1987): EHC 71 Environmental health criteria for pentachlorophenol. <http://www.inchem.org/documents/ehc/ehc/ehc71.htm> (Dec 07, 2007).
- WHO (1989): Environmental Health Criteria, 88. Polychlorinated Dibenzo-para dioxins and dibenzo furans <http://www.inchem.org/documents/pims/chemical/pim121.htm> (Dez 07, 2007)
- WHO (1989): EHC 93 Environmental health criteria for chlorophenols other than pentachlorophenol. <http://www.inchem.org/documents/ehc/ehc/ehc093.htm> (Dec 12, 2007).
- WHO (1993): EHC 140 Environmental health criteria for polychlorinated biphenyls and terphenyls (2nd ed.) <http://www.inchem.org/documents/ehc/ehc/ehc71.htm> (Dec 10, 2007).
- WHO (1996): Environmental Health Criteria 181–Chlorinated Paraffins. WHO, Geneva, Switzerland.
- WHO (1998): Environmental Health Criteria 202–Selected non-heterocyclic polycyclic aromatic compounds. WHO, Geneva, Switzerland. <http://www.inchem.org/documents/ehc/ehc/ehc202.htm>
- WHO (2000): CICAD 20, Concise International Chemical Assessment Document 20, mononitrophenols. http://www.inchem.org/documents/cicads/cicads/cicad_20.htm#PartNumber:2 (Jan 08, 2008).
- WHO (2003): Health risks of persistent organic pollutants from long-range transboundary air pollution, <http://www.euro.who.int/Document/e78963.pdf> (Nov 22, 2007).
- WICKHAM, H. (2008) : ggplot2. <http://had.co.nz/ggplot2/book/ggplot2-book.pdf>